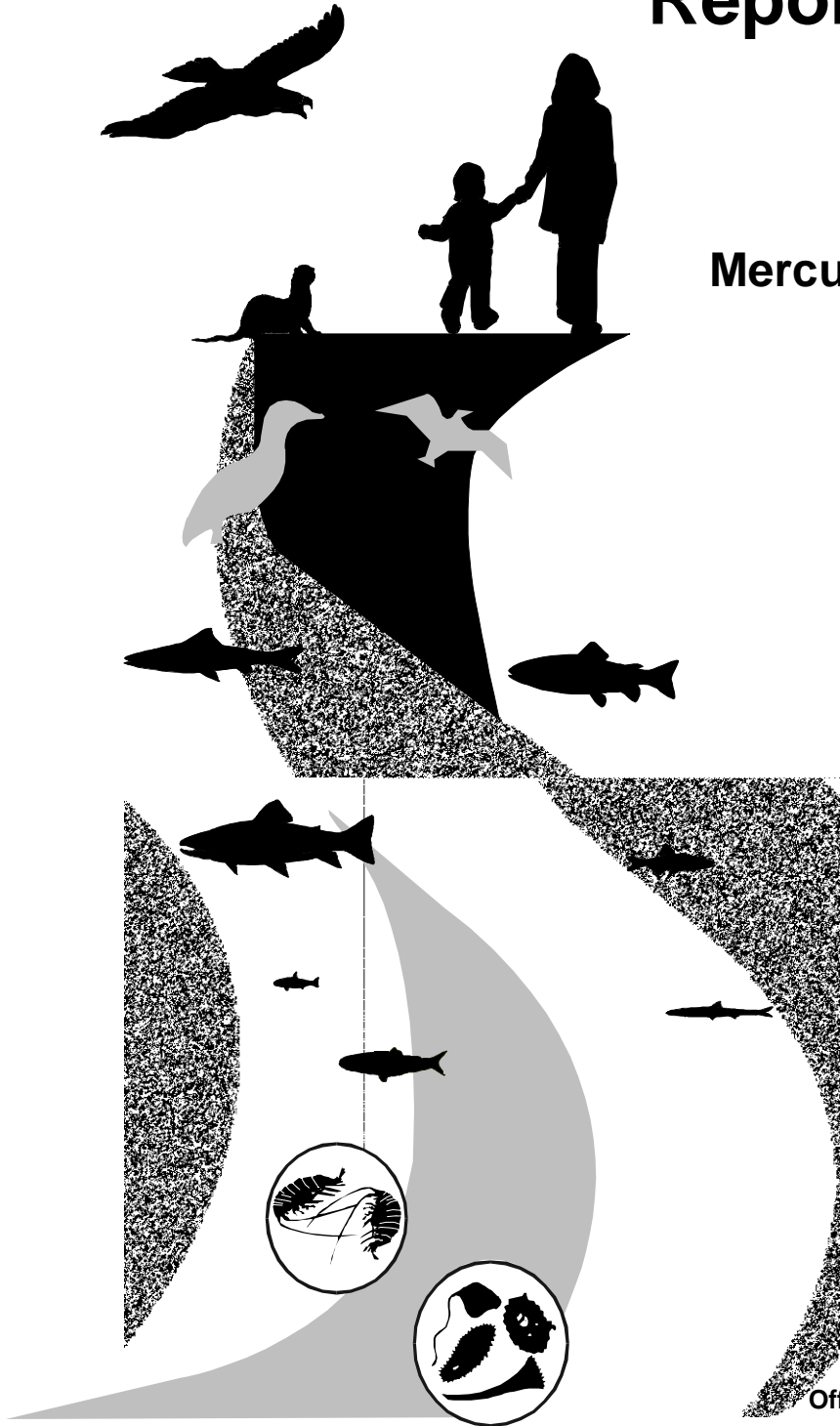


Mercury Study Report to Congress

Volume III: Fate and Transport of Mercury in the Environment



Office of Air Quality Planning & Standards
and
Office of Research and Development

MERCURY STUDY REPORT TO CONGRESS

VOLUME III:

FATE AND TRANSPORT OF MERCURY IN THE ENVIRONMENT

December 1997

**Office of Air Quality Planning and Standards
and
Office of Research and Development
U.S. Environmental Protection Agency**

TABLE OF CONTENTS

	<u>Page</u>
U.S. EPA AUTHORS	v
SCIENTIFIC PEER REVIEWERS	vi
WORK GROUP AND U.S. EPA/ORD REVIEWERS	ix
LIST OF TABLES	x
LIST OF FIGURES	xiii
LIST OF SYMBOLS, UNITS AND ACRONYMS	xiv
EXECUTIVE SUMMARY	ES-1
1. INTRODUCTION	1-1
1.1 Long Range Atmospheric Transport Modeling	1-4
1.2 Local Atmospheric Transport Modeling	1-4
1.3 Modeling Terrestrial and Aquatic Fate of Mercury	1-5
1.4 Exposure Modeling Rationale	1-6
1.5 Factors Important in Modeling of Mercury Exposure	1-7
1.6 Definition of Terms	1-9
2. OVERVIEW OF MERCURY FATE AND TRANSPORT	2-1
2.1 Mercury in the Environment	2-1
2.1.1 Chemistry of Mercury	2-2
2.1.2 The Mercury Cycle	2-2
2.1.2.1 The Global Mercury Cycle	2-3
2.1.2.2 Regional and Local Mercury Cycles	2-4
2.2 Atmospheric Processes	2-6
2.2.1 Emissions of Mercury	2-6
2.2.2 Mercury Transformation and Transport	2-7
2.2.3 Deposition of Mercury	2-9
2.2.4 Re-emissions of Mercury into the Atmosphere	2-11
2.3 Terrestrial and Aquatic Fate of Mercury	2-11
2.3.1 Mercury in Soil	2-11
2.3.2 Plant and Animal Uptake of Mercury	2-12
2.3.3 Mercury in the Freshwater Ecosystem	2-12
2.4 Fate of Mercury in Marine Environments	2-14
2.4.1 Models of Mercury in the Oceans	2-15
2.4.2 Modeling Estuaries and Coastal Regions	2-16
2.4.3 Mercury Budget for a Coastal Waterbody in U.S.A.	2-18
3. MEASURED CONCENTRATIONS	3-1
3.1 Analytic Measurement Methods	3-1
3.2 Measurement Data	3-1
3.2.1 Mercury Air Concentrations	3-1
3.2.2 Mercury Concentrations in Precipitation	3-4
3.2.3 Mercury Deposition Rates	3-5
3.2.4 Mercury Concentrations in Water	3-8

TABLE OF CONTENTS (continued)

		<u>Page</u>
	3.2.5	Mercury Concentrations in Soil/Sediment 3-10
	3.2.6	Mercury Concentrations in Biota 3-13
3.3		Measurement Data from Remote Locations 3-30
	3.3.1	Elevated Atmospheric Mercury Concentrations over Remote Locations . . . 3-30
	3.3.2	Elevated Soil Mercury Concentrations in Locations Remote from Emission Sources 3-30
	3.3.3	Elevated Mercury Concentrations in Aquatic Sediments and Fish from Remote Water Bodies 3-31
3.4		Measurement Data Near Anthropogenic Sources of Concern 3-31
	3.4.1	Municipal Waste Combustors 3-32
	3.4.2	Chlor-Alkali Plants 3-33
	3.4.3	Coal-Fired Utilities 3-33
	3.4.4	Mercury Mines 3-34
	3.4.5	Mercury Near Multiple Local Sources 3-34
4.		MODEL FRAMEWORK 4-1
	4.1	Models Used 4-1
	4.2	Modeling of Long-Range Fate and Transport of Mercury 4-1
	4.2.1	Objectives 4-1
	4.2.2	Estimating Impacts from Regional Anthropogenic Sources of Mercury 4-2
	4.2.3	Description of the RELMAP Mercury Model 4-2
		4.2.3.1 Physical Model Structure 4-3
		4.2.3.2 Mercury Emissions 4-3
		4.2.3.3 Carbon Aerosol Emissions 4-9
		4.2.3.4 Ozone Concentration 4-9
		4.2.3.5 Lagrangian Transport and Deposition 4-10
	4.2.4	Model Parameterizations 4-10
		4.2.4.1 Chemical Transformation and Wet Deposition 4-10
		4.2.4.2 Dry Deposition 4-12
		4.2.4.3 Vertical Exchange of Mass with the Free Atmosphere 4-15
	4.3	Modeling the Local Atmospheric Transport of Mercury in Source Emissions 4-16
	4.3.1	Phase and Oxidation State of Emitted Mercury 4-16
	4.3.2	Modeling the Deposition of Mercury 4-17
	4.3.3	Rationale and Utility of Model Plant Approach 4-21
	4.3.4	Development and Description of Model Plants 4-21
	4.3.5	Hypothetical Locations of Model Plants 4-22
	4.4	Modeling Mercury in a Watershed 4-24
	4.4.1	Overview of the Watershed Model 4-24
	4.4.2	Description of the Watershed Soil Module 4-26
		4.4.2.1 Development of Soil Mass Balance Equations 4-28
		4.4.2.2 Loads to Watershed Soils 4-30
		4.4.2.3 Equilibrium Speciation Reactions 4-31
		4.4.2.4 Transformation Processes in Watershed Soils 4-32
		4.4.2.5 Transport and Transfer Processes in Watershed Soils 4-32
	4.4.3	Description of the Water Body Module 4-34

TABLE OF CONTENTS (continued)

		<u>Page</u>
	4.4.3.1 The Water Body Equations	4-35
	4.4.3.2 The Solids Balance Equations	4-39
	4.4.3.3 Loads to the Water Body	4-40
	4.4.3.4 Equilibrium Speciation Reactions	4-42
	4.4.3.5 Transformation Processes in the Water Body	4-43
	4.4.3.6 Transport and Transfer Processes in the Water Body	4-44
5.	ATMOSPHERIC FATE AND TRANSPORT MODELING RESULTS	5-1
5.1	Long Range Atmospheric Fate/Transport Modeling	5-1
5.1.1	Mass Balances of Mercury within the Long-range Model Domain	5-1
5.1.2	Qualitative Description of Mercury Concentration Results	5-2
5.1.3	Description of Mercury Wet Deposition Simulation Results	5-8
5.1.4	Qualitative Description of Mercury Dry Deposition Results	5-19
5.1.5	Qualitative Description of Total Mercury Deposition Results	5-24
5.1.6	General Data Interpretations of the RELMAP Modeling	5-26
5.2	Overview of Local Scale Analysis: Background Concentrations	5-27
5.2.1	Introduction	5-27
5.2.2	The “Pre-anthropogenic” Mercury Cycle	5-28
5.2.3	Estimating Current Background Mercury Concentrations	5-30
5.3	Local Atmospheric Transport Modeling	5-36
5.3.1	Air Concentrations	5-40
5.3.2	Deposition Rates	5-40
5.3.3	Mass Balances within the Local-Scale Domain	5-41
5.3.4	Uncertainty and Sensitivity Analyses	5-47
5.3.4.1	Dry Deposition	5-47
5.3.4.2	Wet Deposition	5-53
5.3.4.3	Sensitivity to Emissions Speciation	5-53
5.3.4.4	Effect of Terrain on Results of Local Scale Modeling	5-54
6.	WATERSHED FATE AND TRANSPORT MODELING	6-1
6.1	Overview	6-1
6.2	Watershed and Waterbody Results for Pre-anthropogenic Mercury Cycle and the Current Mercury Cycle	6-1
6.3	Watershed/Waterbody Model Results for Local Scale Analysis	6-2
6.4	Variability and Sensitivity Analysis	6-8
6.4.1	Variability and Parameter Sensitivity Analysis for IEM-2M	6-9
6.4.1.1	Description of Base Simulation and Analysis of Variability	6-9
6.4.1.2	Sensitivity of Soil Mercury to Model Parameters	6-13
6.4.1.3	Sensitivity of Water Column Mercury to Model Parameters	6-15
6.4.1.4	Sensitivity of Fish Mercury to Model Parameters	6-15
6.4.2	Variability and Parameter Sensitivity Analysis for R-MCM	6-18
6.4.2.1	Overview of R-MCM	6-18
6.4.2.2	Analysis of In-Lake Variability in Mercury Levels	6-19
6.4.2.3	Sensitivity of Water Column Mercury to Model Parameters	6-26
6.4.2.4	Sensitivity of Fish Mercury to Model Parameters	6-28
6.4.3	Summary and Conclusions	6-30

TABLE OF CONTENTS (continued)

	<u>Page</u>
7. CONCLUSIONS	7-1
8. RESEARCH NEEDS	8-1
9. REFERENCES	9-1
APPENDIX A ATMOSPHERIC MODELING PARAMETERS	A-1
APPENDIX B WATERSHED AND WATERBODY MODELING PARAMETERS	B-1
APPENDIX C DESCRIPTION OF MODEL PLANTS	C-1
APPENDIX D AQUATIC BIOACCUMULATION FACTOR DEVELOPMENT AND UNCERTAINTY ANALYSIS	D-1

U.S. EPA AUTHORS

Principal Authors:

Glenn E. Rice
National Center for Environmental Assessment-
Cincinnati
Office of Research and Development
Cincinnati, OH

Robert B. Ambrose, Jr., P.E.
Ecosystems Research Division
National Exposure Research Laboratory
Athens, GA

O. Russell Bullock, Jr.
Atmospheric Sciences Modeling Division
Air Resources Laboratory
National Oceanic and Atmospheric
Administration
Research Triangle Park, NC
on assignment to the
U.S. EPA National Exposure Research Laboratory

Jeff Swartout
National Center for Environmental Assessment-
Cincinnati
Office of Research and Development
Cincinnati, OH

Contributing Authors:

William G. Benjey, Ph.D.
Atmospheric Sciences Modeling Division
Air Resources Laboratory
National Oceanic and Atmospheric
Administration
Research Triangle Park, NC
on assignment to the
U.S. EPA National Exposure Research Laboratory

Terry Clark, Ph.D.^a
Atmospheric Sciences Modeling Division
Air Resources Laboratory
National Oceanic and Atmospheric
Administration
Research Triangle Park, NC

David H. Cleverly
National Center for Environmental Assessment
Office of Research and Development
Washington, DC

Stanley Durkee
Office of Research and Science Integration
Washington, DC

Martha H. Keating
Office of Air Quality Planning and Standards
Research Triangle Park, NC

James D. Kilgroe, Ph.D.
National Environmental Research Laboratory
Office of Research and Development
Research Triangle Park, NC

Kathryn R. Mahaffey, Ph.D.
National Center for Environmental Assessment-
Cincinnati
Office of Research and Development
Cincinnati, OH

John W. Nichols, Ph.D.
Mid-Continent Ecology Division
Office of Research and Development
Duluth, MN

Rita Schoeny, Ph.D.
National Center for Environmental Assessment-
Cincinnati
Office of Research and Development
Cincinnati, OH

^a Deceased

SCIENTIFIC PEER REVIEWERS

Dr. William J. Adams*
Kennecott Utah Corporation

Dr. Brian J. Allee
Harza Northwest, Incorporated

Dr. Thomas D. Atkeson
Florida Department of Environmental
Protection

Dr. Donald G. Barnes*
U.S. EPA Science Advisory Board

Dr. Steven M. Bartell
SENES Oak Ridge, Inc.

Dr. David Bellinger*
Children's Hospital, Boston

Dr. Nicolas Bloom*
Frontier Geosciences, Inc.

Dr. Mike Bolger
U.S. Food and Drug Administration

Dr. Peter Botros
U.S. Department of Energy
Federal Energy Technology Center

Thomas D. Brown
U.S. Department of Energy
Federal Energy Technology Center

Dr. Dallas Burtraw*
Resources for the Future

Dr. Thomas Burbacher*
University of Washington
Seattle

Dr. James P. Butler
University of Chicago
Argonne National Laboratory

Elizabeth Campbell
U.S. Department of Energy
Policy Office, Washington DC

Dr. Rick Canady
Agency for Toxic Substances and Disease
Registry

Dr. Rufus Chaney
U.S. Department of Agriculture

Dr. Joan Daisey*
Lawrence Berkeley National Laboratory

Dr. John A. Dellinger*
Medical College of Wisconsin

Dr. Kim N. Dietrich*
University of Cincinnati

Dr. Tim Eder
Great Lakes Natural Resource Center
National Wildlife Federation for the
States of Michigan and Ohio

Dr. Lawrence J. Fischer*
Michigan State University

Dr. William F. Fitzgerald
University of Connecticut
Avery Point

A. Robert Flaak*
U.S. EPA Science Advisory Board

Dr. Katherine Flegal
National Center for Health Studies

Dr. Bruce A. Fowler*
University of Maryland at Baltimore

Dr. Steven G. Gilbert*
Biosupport, Inc.

Dr. Cynthia C. Gilmour*
The Academy of Natural Sciences

Dr. Robert Goyer
National Institute of Environmental Health
Sciences

SCIENTIFIC PEER REVIEWERS (continued)

Dr. George Gray
Harvard School of Public Health

Dr. Terry Haines
National Biological Service

Dr. Gary Heinz*
Patuxent Wildlife Research Center

Joann L. Held
New Jersey Department of Environmental
Protection & Energy

Dr. Robert E. Hueter*
Mote Marine Laboratory

Dr. Harold E. B. Humphrey*
Michigan Department of Community Health

Dr. James P. Hurley*
University of Wisconsin
Madison

Dr. Joseph L. Jacobson*
Wayne State University

Dr. Gerald J. Keeler
University of Michigan
Ann Arbor

Dr. Ronald J. Kendall*
Clemson University

Dr. Lynda P. Knobeloch*
Wisconsin Division of Health

Dr. Leonard Levin
Electric Power Research Institute

Dr. Steven E. Lindberg*
Oak Ridge National Laboratory

Dr. Genevieve M. Matanoski*
The Johns Hopkins University

Dr. Thomas McKone*
University of California
Berkeley

Dr. Malcolm Meaburn
National Oceanic and Atmospheric
Administration
U.S. Department of Commerce

Dr. Michael W. Meyer*
Wisconsin Department of Natural Resources

Dr. Maria Morandi*
University of Texas Science Center at Houston

Dr. Paul Mushak
PB Associates

Harvey Ness
U.S. Department of Energy
Federal Energy Technology Center

Dr. Christopher Newland*
Auburn University

Dr. Jerome O. Nriagu*
The University of Michigan
Ann Arbor

William O'Dowd
U.S. Department of Energy
Federal Energy Technology Center

Dr. W. Steven Otwell*
University of Florida
Gainesville

Dr. Jozef M. Pacyna
Norwegian Institute for Air Research

Dr. Ruth Patterson
Cancer Prevention Research Program
Fred Gutchinson Cancer Research Center

Dr. Donald Porcella
Electric Power Research Institute

SCIENTIFIC PEER REVIEWERS (continued)

Dr. Deborah C. Rice*
Toxicology Research Center

Samuel R. Rondberg*
U.S. EPA Science Advisory Board

Charles Schmidt
U.S. Department of Energy

Dr. Pamela Shubat
Minnesota Department of Health

Dr. Ellen K. Silbergeld*
University of Maryland
Baltimore

Dr. Howard A. Simonin*
NYSDEC Aquatic Toxicant Research Unit

Dennis Smith
U.S. Department of Energy
Federal Energy Technology Center

Dr. Ann Spacie*
Purdue University

Dr. Alan H. Stern
New Jersey Department of Environmental
Protection & Energy

Dr. David G. Strimaitis*
Earth Tech

Dr. Edward B. Swain
Minnesota Pollution Control Agency

Dr. Valerie Thomas*
Princeton University

Dr. M. Anthony Verity
University of California
Los Angeles

*With EPA's Science Advisory Board, Mercury
Review Subcommittee

WORK GROUP AND U.S. EPA/ORD REVIEWERS

Core Work Group Reviewers:

Dan Axelrad, U.S. EPA
Office of Policy, Planning and Evaluation

Angela Bandemehr, U.S. EPA
Region 5

Jim Darr, U.S. EPA
Office of Pollution Prevention and Toxic
Substances

Thomas Gentile, State of New York
Department of Environmental Conservation

Arnie Kuzmack, U.S. EPA
Office of Water

David Layland, U.S. EPA
Office of Solid Waste and Emergency Response

Karen Levy, U.S. EPA
Office of Policy Analysis and Review

Steve Levy, U.S. EPA
Office of Solid Waste and Emergency Response

Lorraine Randecker, U.S. EPA
Office of Pollution Prevention and Toxic
Substances

Joy Taylor, State of Michigan
Department of Natural Resources

U.S. EPA/ORD Reviewers:

Robert Beliles, Ph.D., D.A.B.T.
National Center for Environmental Assessment
Washington, DC

Eletha Brady-Roberts
National Center for Environmental Assessment
Cincinnati, OH

Annie M. Jarabek
National Center for Environmental Assessment
Research Triangle Park, NC

Matthew Lorber
National Center for Environmental Assessment
Washington, DC

Susan Braen Norton
National Center for Environmental Assessment
Washington, DC

Terry Harvey, D.V.M.
National Center for Environmental Assessment
Cincinnati, OH

LIST OF TABLES

	<u>Page</u>
1-1 Factors Potentially Important in Estimating Mercury Exposure and How They are Addressed in This Study	1-8
2-1 Annual Estimates of Mercury Release by Various Combustion and Manufacturing Source Classes	2-8
3-1 Summary of Measured Mercury Concentration in Air (U.S. EPA, 1993)	3-2
3-2 Measured Vapor- and Particulate-Phase Atmospheric Mercury Concentrations	3-3
3-3 Measured Mercury Concentrations in Precipitation	3-4
3-4 Measured Mercury Concentrations in Rain Which Include Methylmercury Estimates (ng/L) .	3-5
3-5 Mercury Wet Deposition Rates (ug/m ² /yr)	3-7
3-6 Estimated Mercury Total Deposition Rates	3-8
3-7 Measured Mercury Concentrations in Surface Fresh Water (ng/L)	3-9
3-8 Measured Mercury Concentrations in Ground/Drinking Water (ng/L)	3-9
3-9 Measured Mercury Concentrations in Ocean Water (ng/L)	3-10
3-10 Measured Mercury Concentration in Soil	3-11
3-11 Measured Mercury Concentrations in Freshwater Aquatic Sediment	3-12
3-12 Mercury Concentration in Sediments from NS&T Sites (1984-1991)	3-13
3-13 Freshwater Fish Mercury Concentrations from Nationwide Studies	3-16
3-14 Mercury Concentration in Bivalve Mollusks from Mussel Watch Sites (1986-1993)	3-17
3-15 Nationwide Geometric Mean Concentrations of Mercury in Bivalve Mollusks (1986-1993) .	3-17
3-16 Trends in Mercury Concentrations in Bivalve Mollusks (1986-1993)	3-18
3-17 Measured Mercury Concentrations Freshwater Sportfish (Total Mercury, ug/g wet wt.)	3-20
3-18 Measured Mercury Concentrations in Saltwater Commercial Fish and Shellfish (ug/g wet wt.)	3-22
3-19 Mercury Concentrations in Marine Finfish	3-23
3-20 Mercury Concentrations in Marine Shellfish	3-24
3-21 Mercury Concentrations in Marine Molluscan Cephalopods	3-25
3-22 Mercury Concentrations in Biota from the New York-New Jersey Harbor estuary (1993) . .	3-26
3-23 Measured Mercury Concentration in Meats	3-28
3-24 Measured Mercury Concentrations in Garden Produce/Crops	3-39
3-25 Mean Background Total Mercury Levels for Plants in the Netherlands	3-29
3-26 Range of Mercury Concentrations in Selected Grain Products	3-30
3-27 Mercury Concentrations in the Atmosphere and Mercury Measured in Rainwater Collected in Broward County, FL	3-35
3-28 Mercury Concentrations Measured at Two Sites in the Atmosphere Over Detroit, MI	3-35
4-1 Models Used to Predict Mercury Air Concentrations, Deposition Fluxes, and Environmental Concentrations	4-1
4-2 Mercury Emissions Inventory Used in the RELMAP Modeling	4-5
4-3 Dry Deposition Velocity (cm/s) for Divalent Mercury (Hg ²⁺)	4-14
4-4 Wind Speeds Used for Each Pasquill Stability Category in the CARB Subroutine Calculations	4-15
4-5 Roughness Length Used for Each Land-Use Category in the CARB Subroutine Calculations	4-15
4-6 Representative Particle Sizes and Size Distribution Assumed for Divalent Mercury Particulate Emissions	4-17
4-7 Parameter Values Assumed for Calculation of Dry Deposition Velocities for Divalent Mercury Vapor	4-18

LIST OF TABLES (continued)

		<u>Page</u>
4-8	Air Modeling Parameter Values Used in the Exposure Assessment: Generic Parameters	4-20
4-9	Process Parameters for Model Plants	4-23
5-1	Mercury Mass Budget in Metric Tons from RELMAP Simulation	5-1
5-2	Percentile Analysis of RELMAP Simulated Concentration Results for the Continental U. S.	5-8
5-3	Observed Mercury Deposition in Precipitation from the Transition Phase Data Report of the Mercury Deposition Network (MDN)	5-16
5-4	Estimates of 1989 Mercury Wet Deposition in Precipitation from MDN Data and Comparison to Modeled Wet Deposition	5-17
5-5	Percentile Analysis of RELMAP Simulated Wet Deposition for the Continental U. S.	5-18
5-6	Percentile Analysis of RELMAP Simulated Dry Deposition for the Continental U. S.	5-19
5-7	Percentile Analysis of RELMAP Simulated Total Depositions for the Continental U. S.	5-24
5-8	Mercury Wet Deposition Rates (ug/m ² /yr)	5-31
5-9	Estimated Mercury Total Deposition Rates	5-32
5-10	Inputs to IEM2M Model for the two time periods modeled	5-33
5-11	Predicted Air Concentrations and Deposition Rates for Eastern Site (Local + RELMAP 50th)	5-36
5-12	Predicted Air Concentrations and Deposition Rates for Eastern Site (Local + RELMAP 90th)	5-37
5-13	Predicted Air Concentrations and Deposition Rates for Western Site (Local + RELMAP 50th)	5-38
5-14	Predicted Air Concentrations and Deposition Rates for Western Site (Local + RELMAP 90th)	5-39
5-15	Mass Balance of Mercury Emissions for each Facility in the Humid Site Using the ISC3 Model	5-42
5-16	Mass Balance of Mercury Emissions for each Facility in the Arid Site Using the ISC3 Model	5-43
5-17	Area-Averaged Mercury Deposition Rates for each Facility in the Humid Site	5-45
5-18	Area-Averaged Mercury Deposition Rates for each Facility in the Arid Site	5-46
5-19	Sensitivity of Total Mercury Deposition Rate to Emissions Speciation for Municipal Waste Combustors	5-54
5-20	Ratios of Total Deposition of Mercury at Receptors at Different Elevations to Total Deposition when the Elevation is Zero	5-55
6-1	Assumed Mercury Air Concentrations and Atmospheric Deposition Rates for pre-Anthropogenic and Current Conditions	6-1
6-2	Total Mercury Concentrations Predicted by IEM-2M Model for the Pre-Anthropogenic Time Period	6-2
6-3	Total mercury concentrations predicted by IEM-2M Model for the Current (Post-Industrial) Time Period	6-2
6-4	Predicted Values for Eastern Site (Local + RELMAP 50th)	6-4
6-5	Predicted Values for Eastern Site (Local + RELMAP 90th)	6-5
6-6	Predicted Values for Western Site (Local + RELMAP 50th)	6-6
6-7	Predicted Values for Western Site (Local + RELMAP 90th)	6-7
6-8	General Properties of the IEM-2M Eastern Lake	6-10
6-9	Effect of Watershed Size on Total Mercury Concentrations	6-11
6-10	Effect of Watershed Erosion on Total Mercury Concentrations	6-12

LIST OF TABLES (continued)

	<u>Page</u>
6-11	Effect of Soil Mercury Retention on Total Mercury Concentrations 6-13
6-12	IEM-2M Parameter Sensitivity for Total Soil Mercury 6-14
6-13	IEM-2M Parameter Sensitivity for Total Water Column Mercury 6-16
6-14	IEM-2M Parameter Sensitivity for Predatory Fish Mercury 6-17
6-15	General Properties of the Four R-MCM Lakes 6-21
6-16	Variable Properties of the Four R-MCM Lakes 6-22
6-17	Partition Coefficients and First-order Rate Constants for Simulations 6-23
6-18	Simulation Results, No Watershed 6-24
6-19	Simulation Results with Standard Watershed 6-24
6-20	Simulation Results with Hypolimnion, No Watershed 6-25
6-21	Simulation Results for 5 Combinations of Watershed and Hydrology 6-25
6-22	R-MCM Parameter Sensitivity for Total Water Column Mercury 6-27
6-23	R-MCM Parameter Sensitivity for Upper Trophic Level Fish Mercury 6-29

LIST OF FIGURES

		<u>Page</u>
1-1	Fate, Transport and Exposure Modeling Conducted in the Combined ISC3 and RELMAP Local Impact Analysis	1-2
2-1	The Mercury Cycle	2-1
2-2	Comparison of Current and Pre-Industrial Mercury Budgets and Fluxes	2-5
3-1	Mercury Fish Consumption Advisories of the U.S.	3-14
4-1	Hg(0) Emissions from All Anthropogenic Sources (Base)	4-6
4-2	Hg ²⁺ Emissions from All Anthropogenic Sources (Base)	4-7
4-3	Hg(p) Emissions from All Anthropogenic Sources (Base)	4-8
4-4	Wet Deposition Scavenging Ratios Used in Local Scale Air Modeling for Particulate-Bound Mercury (Jindal and Heinold 1991)	4-19
4-5	Configuration of Hypothetical Water Body and Watershed Relative to Local Source	4-24
4-6	Overview of the IEM-2M Watershed Modules	4-25
4-7	Overview of the IEM2 Soils Processes	4-27
5-1	Average Hg(0) Concentration Excluding Background	5-4
5-2	Average Hg ²⁺ Concentration	5-5
5-3	Average Hg(p) Concentration	5-6
5-4	Hg(0) Wet Deposition Excluding Background	5-9
5-5	Hg(0) Wet Deposition (Background Only)	5-10
5-6	Hg ²⁺ Wet Deposition	5-12
5-7	Hg(p) Wet Deposition	5-13
5-8	Total Hg Wet Deposition	5-14
5-9	Hg ²⁺ Dry Deposition	5-21
5-10	Hg(p) Dry Deposition	5-22
5-11	Total Hg Dry Deposition	5-23
5-12	Total Hg Wet+Dry Deposition	5-25
5-13	IEM-2M results for pre-industrial and industrial periods for Eastern site	5-34
5-14	IEM-2M results for pre-industrial and industrial periods for Western site	5-35
5-15	Influence of the Compensation Point on the Dry Deposition of Elemental Mercury: 2,500 Meters NE of a Chlor-alkali Plant at the Eastern Site	5-48
5-16	Influence of the Compensation Point on the Dry Deposition of Elemental Mercury: 10,000 Meters NE of a Chlor-alkali Plant at the Eastern Site	5-49
5-17	Influence of the Compensation Point on the Dry Deposition of Elemental Mercury: 25,000 Meters NE of a Chlor-alkali Plant at the Eastern Site	5-50
5-18	Comparison of Sensitivity of Total Deposition Rate to Divalent Mercury Reactivity	5-52

LIST OF SYMBOLS, UNITS AND ACRONYMS

AIRS	Automatic Information Retrieval System
ANC	Acid Neutralizing Capacity
APCD	Air Pollution Control Device
BAF	Bioaccumulation Factor
BCF	Bioconcentration Factor
BW	Body Weight
CAA	Clean Air Act as Amended in 1990
CAP	Chlor-Alkali Plants
CARB	California Air Resources Board
CMWI	Continuous MWI Model Plant
COMPDEP	COMPLex terrain and DEPosition air dispersion model
DIC	Dissolved Inorganic Carbon
DOC	Dissolve Organic Carbon
EMAP	Environmental Monitoring and Assessment Program
EMEP	European Monitoring and Evaluation Programme
EPA	U.S. Environmental Protection Agency
EPRI	Electric Power Research Institute
ESP	Electrostatic Precipitator
FWS	U.S. Fish and Wildlife Service
Hg	Mercury
Hg ⁰	Elemental mercury
Hg ²⁺	Divalent or mercuric mercury
Hg ₂ ²⁺	Mercurous mercury
Hg(II)	Divalent or mercuric mercury
HgCl ₂	Mercuric chloride
HgI	Mercury iodide
Ht	Height
IED	Indirect Exposure Document (U.S. EPA, 1990. Methodology for Assessing Health Risks Associated with Indirect Exposure to Combustor Emissions, EPA 600/6-90/003)
IEM2	Modified version of U.S. EPA's Indirect Exposure Methodology
IEM-2M	The aquatic and terrestrial fate, transport, and exposure model
IMWI	Intermittent Medical Waste Incinerator Model Plant
ISC3	Industrial Source Code Dispersion Model
LCUB	Large Coal-Fired Utility Boiler
LMWC	Large Municipal Waste Combustor
MCUB	Medium Coal-Fired Utility Boiler
MHg	Methylmercury
Mg	Megagram
MMHg	MonoMethylmercury
MOUB	Median Oil-Fired Utility Boiler
MW	MegaWatt
MWC	Municipal Waste Combustors
MWI	Medical Waste Incinerators
NAPAP	National Acidic Precipitation Assessment Program
ng	Nanogram (1 x 10 ⁻⁹ gram)
NGM	Nested Grid Model
NIEHS	National Institute of Environmental Health and Safety
NJDEPE	New Jersey Department of Environmental Protection

LIST OF SYMBOLS, UNITS AND ACRONYMS (continued)

NMFS	National Marine Fisheries Science
NOAA	National Oceanic and Atmospheric Administration
NS&T	National Status and Trends
O ₃	Ozone
OAQPS	Office of Air Quality Planning and Standards
PBL	Planetary Boundary Layer
PCS	Primary Copper Smelter
pg	Picogram (1 x 10 ⁻¹² gram)
PLS	Primary Lead Smelter
ppb	Parts Per Billion
ppm	Parts Per Million
RADM	Regional Acid Deposition Model
RELMAP	Regional Lagrangian Model of Air Pollution
RHG	Rural Home Gardener
R-MCM	Regional Mercury Cycling Model
RSF	Rural Subsistence Farmer
SCRAM	Support Center for Regulatory Air Models
SCUB	Small Coal-Fired Utility Boiler
SMWC	Small Municipal Waste Combustor
SWMC	Solid Waste Management Council
TOC	Total Organic Carbon
µg	Microgram (1x10 ⁻⁶ gram)
UR	Urban Resident
USFDA	United States Food and Drug Administration
USGS	United States Geological Survey
V/P ratio	Vapor/Particle Ratio

EXECUTIVE SUMMARY

Section 112(n)(1)(B) of the Clean Air Act (CAA), as amended in 1990, requires the U.S. Environmental Protection Agency (EPA) to submit a study on atmospheric mercury emissions to Congress. The sources of emissions that must be studied include electric utility steam generating units, municipal waste combustion units and other sources, including area sources. Congress directed that the Mercury Study evaluate many aspects of mercury emissions, including the rate and mass of emissions, health and environmental effects, technologies to control such emissions, and the costs of such controls.

In response to this mandate, U.S. EPA has prepared an eight-volume Mercury Study Report to Congress. This document is a review of mercury fate and transport (Volume III of the Report). The fate and transport assessment is one component of the risk assessment of U.S. anthropogenic mercury emissions. The modeling summarized in this volume is paired with an assessment of exposure to human and wildlife populations (Volume IV). Conclusions drawn from these analyses are then integrated with information in Volumes V and VI relating to human and wildlife health impacts of mercury in the Risk Characterization Volume (Volume VII) of the Report.

Assessment Approach for Fate of Mercury

This assessment addresses atmospheric mercury emissions from selected, major anthropogenic combustion and manufacturing source categories: municipal waste combustors (MWCs), medical waste incinerators (MWIs), coal- and oil-fired utility boilers, and chlor-alkali plants. It does not address all anthropogenic emission sources.

Extant mercury monitoring data for particular sources indicate that there is a relationship between emissions and increased mercury concentrations in environmental media. Available mercury monitoring data around these sources are extremely limited, however, and no comprehensive data base describing environmental concentrations has been developed. To determine if there is a connection between the above sources and increased environmental levels, EPA utilized exposure modeling techniques to address many major scientific uncertainties.

The individual exposure assessment in this Report (Volume IV), which relies on the modeling results presented in this volume, is considered to be a qualitative study based partly on quantitative analyses; it is considered qualitative because of inherent uncertainties. The exposure assessment draws upon the available scientific information and develops two quantitative transport analyses, a long range transport analysis and a local impact analysis. It was intended that these two types of analyses would provide a more complete estimate of the nation-wide impact of anthropogenic emission sources than either analysis could provide individually.

The assessment of Volume III draws upon the available scientific information and presents quantitative modeling analyses which examine the following: (1) the long range transport of mercury from emissions sources through the atmosphere; (2) the transport of mercury from emission sources through the local atmosphere; and (3) the aquatic and terrestrial fate and transport of mercury at hypothetical sites. The results from these analyses are then applied in the exposure assessment of Volume IV to determine the resulting exposures to hypothetical humans and animals that inhabit these sites.

Long Range Atmospheric Transport Analysis

The long range transport modeling was undertaken to estimate the regional and national impacts of mercury emissions. It focusses on the long range atmospheric transport of mercury and estimates the impact of mercury across the continental U.S. This type of modeling was conducted based on the atmospheric chemistry of emitted elemental mercury (Petersen et al., 1995) and the numerous studies linking increased mercury concentrations in air, soil, sediments, and biota at remote sites to distant anthropogenic mercury release followed by long range transport. Details of several studies which demonstrate the long range transport of mercury are presented in Chapter 2. These provide ample evidence to justify this assessment of long range mercury transport.

The long range transport of mercury was modeled using site-specific, anthropogenic emission source data (presented in Volume II of this Report) to generate mean, annual atmospheric mercury concentrations and deposition values across the continental U.S. The Regional Lagrangian Model of Air Pollution (RELMAP) atmospheric model was utilized to model cumulative mercury emissions from multiple mercury emission sources. Assumptions were made concerning the form and species of mercury emitted from each source class. The results of the RELMAP modeling were combined with a local scale atmospheric model to assess average annual atmospheric mercury concentrations in air and annual deposition rates. The continental U.S. was divided into Western and Eastern halves along the line of 90 degrees west longitude. The 50th and 90th percentiles of the predicted atmospheric concentrations and deposition rates were then used.

Analysis of Local-Scale Fate of Atmospheric Mercury

The local atmospheric transport of mercury released from anthropogenic emission sources was undertaken to estimate the impacts of mercury from selected, individual sources. The Industrial Source Code air dispersion model (ISC3) was utilized to model these processes. Model plants, defined as hypothetical facilities which were developed to represent actual emissions from existing industrial processes and combustion sources, were located in hypothetical locations intended to simulate a site in either the Western or Eastern U.S. This approach was selected because some environmental monitoring studies suggest that measured mercury levels in environmental media and biota may be elevated in areas around stationary industrial and combustion sources known to emit mercury.

Assessment of Watershed Fate and Transport

Atmospheric concentrations and deposition rates were used as inputs to a series of terrestrial and aquatic models referred to as IEM-2M. IEM-2M is composed of two integrated modules that simulate mercury fate using mass balance equations describing watershed soils and a shallow lake. The results of these terrestrial and aquatic models were used to predict mercury exposure to hypothetical humans through inhalation, consumption of drinking water, and ingestion of soil, farm products (e.g., beef products and vegetables), and fish. These models were also used to predict mercury exposure in hypothetical piscivorous (i.e., fish-eating) birds and mammals through their consumption of fish. The results of these models are utilized in the exposure assessment completed in Volume IV.

Conclusions

- The present study in conjunction with available scientific knowledge supports a plausible link between mercury emissions from anthropogenic combustion and industrial sources and mercury concentrations in air, soil, water and sediments. The critical variables contributing to this linkage are these:
 - a) the species of mercury that are emitted from the sources;
 - b) the overall amount of mercury emitted from a combustion source;
 - c) atmospheric and climatic conditions;
 - d) reduction rates in the soil and water body;
 - e) erosion rates within the watershed; and
 - f) solids deposition and burial in the water body.
- The present study, in conjunction with available scientific knowledge, supports a plausible link between mercury emissions from anthropogenic combustion and industrial sources and methylmercury concentrations in freshwater fish. The additional critical variables contributing to this linkage are the following:
 - a) the extent (magnitude) of mercury methylation and demethylation in the water body; and
 - b) the degree of complexation of mercury with DOC and solids.
- Mercury is a natural constituent of the environment; concentrations of mercury in many environmental media appear to have increased over the last 500 years.
- There is a lack of adequate mercury measurement data near the anthropogenic atmospheric mercury sources considered in this report. The lack of such measured data preclude a comparison of the modeling results with measured data around these sources. This shortage of data includes measured mercury deposition rates as well as measured concentrations in the local atmosphere, soils, water bodies, and biota.
- From the atmospheric modeling analyses of mercury deposition and on a comparative basis, a facility located in a humid climate has a higher annual rate of mercury deposition than a facility located in an arid climate. The critical variables are the estimated washout ratios of elemental and divalent mercury as well as the annual amount of precipitation. Precipitation removes various forms of mercury from the atmosphere and deposits mercury to the surface of the earth. Of the species of mercury that are emitted, divalent mercury is predicted to generally deposit to local environments near sources. Elemental mercury is predicted to generally remain in the atmosphere until atmospheric conversion to divalent species or uptake and retention by plant leaves and the subsequent deposition as divalent species in litter fall.

- On a national scale, an apportionment between specific sources of mercury and mercury in environmental media and biota at particular locations cannot be described in quantitative terms with the current scientific understanding of the environmental fate of mercury.
- From the modeling analysis and a review of field measurement studies, it is concluded that mercury deposition appears to be ubiquitous across the continental U.S. and at, or above, detection limits when measured with current analytic methods.
- Based on the RELMAP modeling analysis and a review of recent measurement data published in peer-reviewed scientific literature, there is predicted to be a wide range of mercury deposition rates across the continental U.S. The highest predicted rates (i.e., above 90th percentile) are about 20 times higher than the lowest predicted rates (i.e., below the 10th percentile). Three principal factors contribute to these modeled and observed deposition patterns:
 - a) emission source locations;
 - b) amount of divalent and particulate mercury emitted or formed in the atmosphere; and
 - c) climate and meteorology.
- Based on the modeling analysis of the transport and deposition of stationary point source and area source air emissions of mercury from the continental U.S., it is concluded that the following geographical areas have the highest annual rate of deposition of mercury in all forms (above the levels predicted at the 90th percentile):
 - a) the southern Great Lakes and Ohio River Valley;
 - b) the Northeast and southern New England; and
 - c) scattered areas in the South with the most elevated deposition occurring in the Miami and Tampa areas.

Measured deposition estimates are limited, but are available for certain geographic regions. The data that are available corroborate the RELMAP modeling results for specific areas.

- Based on modeling analysis of the transport and deposition of stationary point source and area source air emissions of mercury from the continental U.S., it is concluded that the following geographical areas have the lowest annual rate of deposition of *mercury in all forms* (below the levels predicted at the 10th percentile):
 - a) the less populated areas of the Great Basin, including southern Idaho, southeastern Oregon, most of southern and western Utah, most of Nevada, and portions of western New Mexico; and
 - b) Western Texas other than near El Paso, and most of northeastern Montana.
- Based on limited monitoring data, the RELMAP model predictions of atmospheric mercury concentrations and wet deposition across the U.S. are comparable with typically measured data.

- A number of factors appear to affect the local-scale atmospheric fate of mercury emitted by/from major anthropogenic sources as well as the quantity of mercury predicted to deposit. These factors include the following:
 - a) the amounts of divalent and particulate mercury emitted;
 - b) parameters that influence the plume height, primarily the stack height and stack exit gas velocity;
 - c) meteorology; and
 - d) terrain.

- From the analysis of deposition and on a comparative basis, the deposition of divalent mercury close to an emission source is greater for receptors in elevated terrain (i.e., terrain above the elevation of the stack base) than for receptors located in flat terrain (i.e., terrain below the elevation of the stack base). The critical variables are parameters that influence the plume height, primarily the stack height and stack exit gas velocity.

- Modeling estimates of the transport and deposition of stationary point source and area source air emissions of mercury from the continental U.S. have revealed the following partial mass balance.
 - Of the total amount of elemental mercury vapor that is emitted, about 1 percent (0.9 metric tons/yr) may be atmospherically transformed into divalent mercury by tropospheric ozone and adsorbed to particulate soot in the air and subsequently deposited in rainfall and snowfall to the surface of the continental U.S. The vast majority of emitted elemental mercury does not readily deposit and is transported outside the U.S. or vertically diffused to the free atmosphere to become part of the global cycle.
 - Nearly all of the elemental mercury vapor emitted from other sources around the globe also enters the global cycle and can be deposited slowly to the U.S. Over 30 times as much elemental mercury vapor is deposited from these other sources than from stationary point sources and area sources within the continental U.S.
 - Of the total amount of divalent mercury vapor that is emitted, about 70 percent (36.8 metric tons/year) deposits to the surface through wet or dry processes within the continental U.S. The remaining 30 percent is transported outside the U.S. or is vertically diffused to the free atmosphere to become part of the global cycle.
 - Of the total amount of particulate mercury that is emitted, about 38 percent (10.0 metric tons/year) deposits to the surface through wet or dry processes within the continental U.S. The remaining 62 percent is transported outside the U.S. or is vertically diffused to the free atmosphere to become part of the global cycle.

- Given the simulated deposition efficiencies for each form of mercury air emission (namely; elemental mercury - 1 percent, divalent mercury vapor - 70 percent, and particulate mercury - 38 percent) the relative source contributions to the total anthropogenic mercury deposited to the

continental U.S. are strongly and positively correlated to the mass of emissions in oxidized form. This oxidized mercury occurs in both gaseous (Hg^{2+}) and particulate (Hg_p) forms. While coal combustion is responsible for more than half of all emissions of mercury in the inventory of U.S. anthropogenic sources, the fraction of coal combustion emissions in oxidized form is thought to be less than that from waste incineration and combustion. The true speciation of mercury emissions from the various source types modeled is still uncertain and is thought to vary, not only among source types, but also for individual plants as feed stock and operating conditions change. With further research, it may be possible to make a confident ranking of relative source contributions to mercury deposition in the continental U.S. However, no such confident ranking is possible at this time. Given the total mass of mercury thought by EPA to be emitted from all anthropogenic sources and EPA's modeling of the atmospheric transport of emitted mercury, coal combustion and waste disposal most likely bear the greatest responsibility for direct anthropogenic mercury deposition to the continental U.S.

- Based on the local scale atmospheric modeling results in flat terrain, at least 75 percent of the emitted mercury from each facility is predicted to be transported more than 50 km from the facility.
- The models used in the analysis as well as the assumptions implemented concerning the species of mercury emitted and the wet and dry deposition velocities associated with atmospheric mercury species indicate that deposition within 10 km of a facility may be dominated by emissions from the local source rather than from emissions transported from regional mercury emissions sources, with some exceptions. Specifically, the models predict that in the Eastern U.S., individual large anthropogenic sources dominate predicted mercury deposition within 2.5 km; chlor-alkali facilities are predicted to dominate up to 10 km from the source. In the western site, the models predict that the dominance of local source mercury deposition in emissions extends beyond the predicted range of the eastern site.
- Of the mercury deposited to watershed soils, a small fraction is ultimately transported to the water body. Deposition to and evasion from soils as well as the amount of reduction in upper soil layers are important factors in the determining soil concentration of mercury. In forested watersheds canopy interactions can provide significant fluxes both to and from the atmosphere. Mercury from litter fall may be an important source of mercury to some soils and water bodies, but the magnitude of the contribution from this source is uncertain at this time.
- The net mercury methylation rate (the net result of methylation and demethylation) for most soils appears to be quite low with much of the measured methylmercury in soils potentially resulting from wet fall. A significant and important exception to this appears to be wetlands. Wetlands appear to convert a small but significant fraction of the deposited mercury into methylmercury; which can be exported to nearby water bodies and potentially bioaccumulated in the aquatic food chain.
- Both watershed erosion and direct atmospheric deposition can be important sources of mercury to the water body depending on the relative sizes of the water body and the watershed.
- There appears to be a great deal of variability in the processing of mercury among bodies of water. This variability extends to water bodies that have similar and dissimilar physical characteristics. Important properties influencing the levels of total mercury and methylmercury in a water body include: pH, anoxia, DOC, productivity, turbidity, and the presence of wetlands.

- Some of the mercury entering a water body is methylated predominately through biotic processes forming methylmercury (predominately monomethylmercury). Methylmercury is accumulated and retained by aquatic organisms. Important factors influencing bioavailability of methylmercury to aquatic organisms include DOC and solids, which complex methylmercury and reduce the bioavailable pool.
- Methylmercury is bioaccumulated in predatory species of the aquatic food chain. The concentrations of methylmercury in fish muscle tissue are highly variable across water bodies. Within a given body of water methylmercury concentrations generally increase with fish size and position within the trophic structure.

To improve the quantitative environmental fate component of the risk assessment for mercury and mercury compounds, U.S. EPA would need more and better mercury emissions data and measured mercury data near sources of concern, as well as a better quantitative understanding of mercury chemistry in the emissions plume, the atmosphere, soils, water bodies and biota. Specific needs include these.

Mercury in the Atmosphere

- aqueous oxidation-reduction kinetics in atmospheric water droplets
- physical adsorption and condensation of divalent mercury gas to ambient particulate matter
- photolytic reduction of particle-bound divalent mercury by sunlight
- convincing evidence that gas-phase oxidation of mercury is insignificant

Mercury in Soils and Water Bodies

- uptake and release kinetics of mercury from terrestrial and aquatic plants
- biogeochemical mercury transport and transformation kinetics in benthic sediments
- methylation, demethylation, and reduction kinetics in water bodies
- sorption coefficients to soils, suspended solids, and benthic solids
- complexation to organic matter in water bodies
- more data to better discern seasonal trends
- reduction kinetics in soils
- mercury mass balance studies in wetlands

Information Leading to an Improved Quantitative Understanding of Aquatic Bioaccumulation Processes and Kinetics

- uptake kinetics by aquatic plants and phytoplankton
- partitioning and binding behavior of mercury species within organisms
- metabolic transformations of mercury, and the effect on uptake, internal distribution, and excretion
- more measurements of methylmercury concentrations in fish for better identification of the range in fish species.
- more measurements of methylmercury concentrations in other biotic components of the aquatic environment such as benthic and macro invertebrates and aquatic macrophytes

1. INTRODUCTION

Section 112(n)(1)(B) of the Clean Air Act (CAA), as amended in 1990, requires the U.S. Environmental Protection Agency (EPA) to submit a study on atmospheric mercury emissions to Congress. The sources of emissions that must be studied include electric utility steam generating units, municipal waste combustion units, and other sources, including area sources. Congress directed that the Mercury Study evaluate many aspects of mercury emissions, including the rate and mass of emissions, health and environmental effects, technologies to control such emissions, and the costs of such controls.

In response to this mandate, EPA has prepared an eight-volume Mercury Study Report to Congress. The eight volumes are as follows:

- I. Executive Summary
- II. An Inventory of Anthropogenic Mercury Emissions in the United States
- III. Fate and Transport of Mercury in the Environment
- IV. An Assessment of Exposure to Mercury in the United States
- V. Health Effects of Mercury and Mercury Compounds
- VI. An Ecological Assessment for Anthropogenic Mercury Emissions in the United States
- VII. Characterization of Human Health and Wildlife Risks from Mercury Exposure in the United States
- VIII. An Evaluation of Mercury Control Technologies and Costs

This document, which constitutes Volume III of the Report to Congress, is a review of processes involving the environmental fate of mercury. This analysis is one element of the human health and ecological risk assessment of U.S. anthropogenic mercury (Hg) emissions. The fate and transport of mercury in the atmosphere as well as through watershed compartments is modeled here; the model results are paired with an assessment of exposure to humans and wildlife in Volumes IV and VI, respectively. The information in these two documents is then integrated with information relating to human and wildlife health impacts of mercury in Volume VII of the report.

This assessment addresses the atmospheric fate and transport of atmospheric mercury emissions from selected, major anthropogenic combustion and manufacturing sources: municipal waste combustors (MWC), medical waste incinerators (MWI), coal- and oil-fired utility boilers, and chlor-alkali plants (CAP). This volume does not address all anthropogenic emission sources discussed in Volume II.

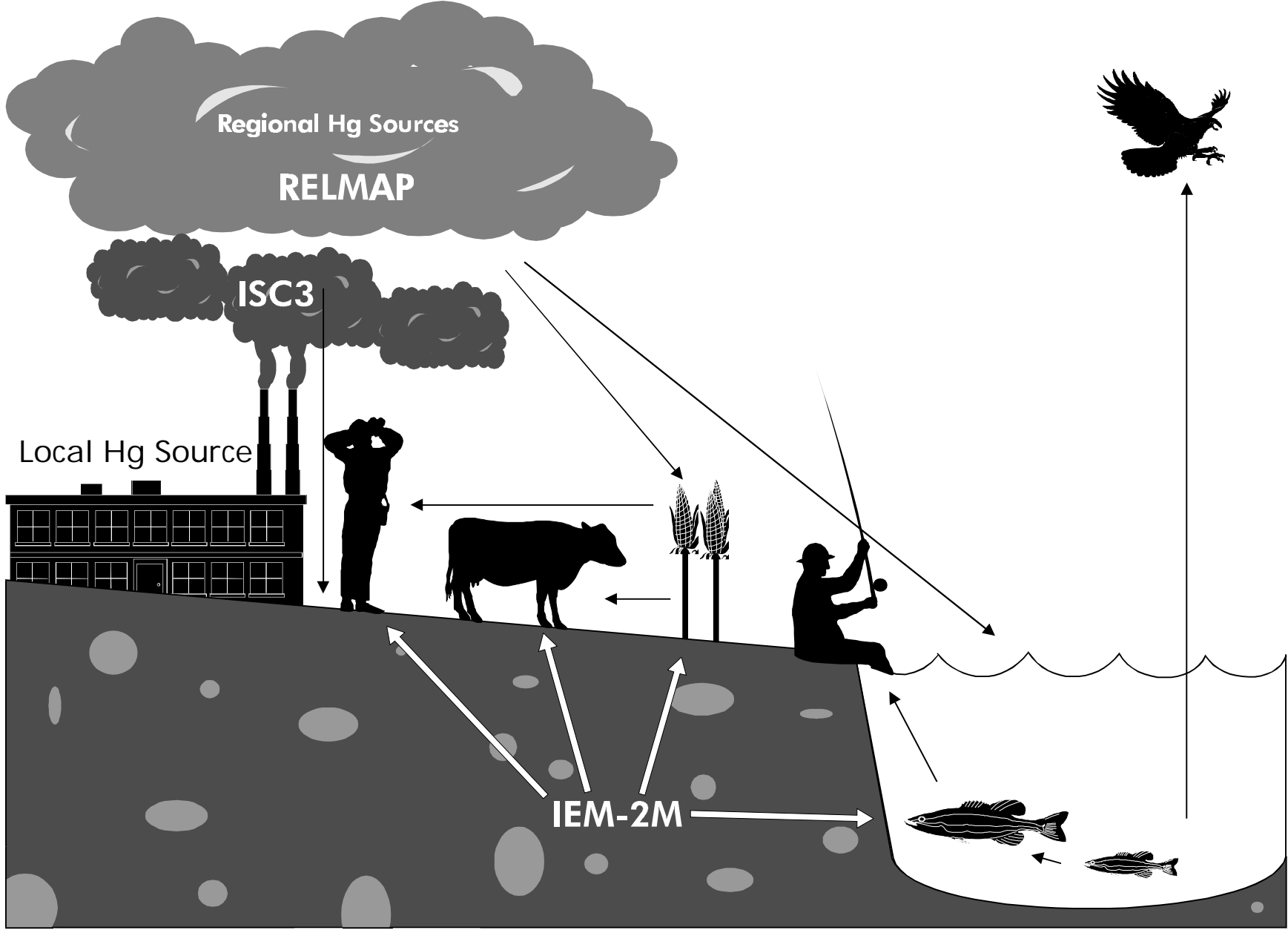
Volume III is composed of nine chapters and four appendices. The Introduction is followed by Chapter 2, which summarizes the natural environmental fate processes that comprise the mercury cycle and lead to the dispersion of anthropogenic mercury in environmental media (i.e., air, rain water, soil and surface waters and benthic sediments) and biota (i.e., plants and animals). Chapter 3 briefly describes the measured mercury concentrations in these media.

The fate and transport modeling of mercury is presented in Chapters 4, 5 and 6. Chapter 4 describes the models and modeling approach utilized in this analysis. Figure 1-1 provides an overview of the fate and transport models used and the exposure routes considered. These models include the long range atmospheric transport model (RELMAP), the local scale atmospheric transport model (ISC3) and the aquatic and terrestrial fate, transport, and exposure models (IEM-2M).

Figure 1-1

Fate, Transport and Exposure Modeling Conducted in the Combined ISC3 and RELMAP Local Impact Analysis

Figure 1-1
Fate, Transport and Exposure Modeling Conducted in the Combined ISC3 and RELMAP Local Impact Analysis



Results obtained from modeling the local and long range atmospheric dynamics of mercury using ISC3 and RELMAP are discussed in Chapter 5. Chapter 6 describes the results of the fate of mercury as modeled in terrestrial and aquatic environments. To accomplish this, model plants were developed to represent major anthropogenic combustion and manufacturing sources: MWCs, MWIs, coal- and oil-fired utility boilers, and CAPs. The atmospheric fate and transport processes of the mercury emissions from these representative model plants were modeled on a local scale by the ISC3 model. The 50th and 90th percentiles of atmospheric mercury concentrations and the deposition rates that were predicted by the RELMAP model for the Eastern and Western halves of the U.S. were added to the predicted mercury air concentrations and deposition rates that result from individual model plants at 2.5, 10, and 25 kilometers. These sums were used as inputs to the aquatic and terrestrial fate models (IEM-2M) at the hypothetical Western and Eastern U.S. sites (see Figure 1-1).

Chapter 7 summarizes the conclusions of this volume, including the extent to which the analysis demonstrates a plausible link between anthropogenic mercury sources and mercury contamination in the environment. Further research needs are specified in Chapter 8. Chapter 9 lists all references cited in this volume.

The four appendices to Volume III are as follows: Atmospheric Modeling Parameters, Watershed and Waterbody Modeling Parameters, Model Plant Descriptions, and Bioaccumulation Factor Development and Uncertainty Analysis.

Extant mercury monitoring data for particular sources indicate that there is a relationship between emissions and increased mercury in environmental media. Available mercury monitoring data around these sources are extremely limited, however, and no comprehensive data base describing environmental concentrations has been developed. To determine if there is a connection between the above sources and increased environmental mercury concentrations, EPA utilized current modeling techniques to address many major scientific uncertainties. Because of the major uncertainties inherent to these techniques, the modeling component of this report is essentially a qualitative study based partly on quantitative analyses. Uncertainties include the following:

- Comprehensive emission data for various anthropogenic and natural sources are not available. This reflects the current developmental nature of emission speciation methods, resulting in few data on the various species and proportions of mercury in vapor and solid forms emitted. Both elemental and divalent mercury species as well as gaseous and particulate forms are known to be emitted from point sources.
- Atmospheric chemistry data are incomplete. Some atmospheric reactions of mercury, such as the oxidation of elemental mercury to divalent mercury in cloud water droplets have been reported. There may exist other chemical reactions in the atmosphere that reduce divalent species to elemental mercury that have not been reported.
- There is inadequate information on the atmospheric processes that affect wet and dry deposition of mercury. Atmospheric particulate forms and divalent species of mercury are thought to wet and dry deposit more rapidly than elemental mercury; however, the relative rates of deposition are uncertain.
- There is no validated local air pollution model that estimates wet and dry deposition of vapor-phase compounds.

- There is significant uncertainty regarding the reduction and revolatilization of deposited mercury in soils and water bodies.
- There is a lack of information concerning the movement of mercury from watershed soils to water bodies.
- More data are needed quantifying the kinetics of mercury methylation and demethylation in different types of water bodies.
- There is a lack of data on the transfer of mercury between environmental compartments and biologic compartments; for example, the link between the amount of mercury in the water body and the levels in fish appears to vary from water body to water body.

The assessment draws upon the available scientific information and presents quantitative modeling analyses that examine: (1) the long range transport of mercury through the atmosphere; (2) the transport of mercury through the local atmosphere; (3) the aquatic and terrestrial fate and transport of mercury at hypothetical sites; and finally (4) the resulting exposures to hypothetical humans and animals that inhabit these sites. It was intended that these analyses would provide a more complete estimate of the impact of anthropogenic emission sources than an individual analysis.

1.1 Long-Range Atmospheric Transport Modeling

The long range transport modeling was undertaken to estimate the regional and national impacts of mercury emissions. It focusses on the long range atmospheric transport of mercury and estimates the impact of mercury across the continental U.S. This type of modeling was conducted based on the atmospheric chemistry of emitted elemental mercury (Petersen et al., 1995) and the numerous studies linking increased mercury concentrations in air, soil, sediments, and biota at remote sites to distant anthropogenic mercury release followed by long-range transport. Details of several studies that demonstrate the long range transport of mercury are presented in Chapter 2. These provide ample evidence to justify this assessment of long-range mercury transport.

The long range transport of mercury was modeled using site-specific, anthropogenic emission source data (presented in Volume II of this Report) to generate mean, annual atmospheric mercury concentrations and deposition values across the continental U.S. The Regional Lagrangian Model of Air Pollution (RELMAP) atmospheric model was utilized to model cumulative mercury emissions from multiple mercury emission sources. Assumptions were made concerning the form and species of mercury emitted from each source class. The results of the RELMAP modeling were combined with a local scale atmospheric model to assess average annual atmospheric mercury concentrations in air and annual deposition rates. The continental U.S. was divided into Western and Eastern halves along the line of 90° west longitude. The 50th and 90th percentile of the predicted atmospheric concentrations and deposition rates were then used.

1.2 Local Atmospheric Transport Modeling

The local atmospheric transport of mercury released from anthropogenic emission sources was undertaken to estimate the impacts of mercury from selected, individual sources. The Industrial Source Code air dispersion model (ISC3) was utilized to model these processes. Model plants, defined as hypothetical facilities that were developed to represent actual emissions from existing industrial processes and combustion sources, were located in hypothetical locations intended to simulate a site in

either the Western or Eastern U.S. This approach was selected because some environmental monitoring studies suggest that measured mercury levels in environmental media and biota may be elevated in areas around stationary industrial and combustion sources known to emit mercury.

1.3 Modeling Terrestrial and Aquatic Fate of Mercury

Chapter 6 uses atmospheric concentrations and deposition rates from this volume as inputs to a series of terrestrial and aquatic models. These were initially described in U.S. EPA's (1990) Methodology for Assessing Health Risks to Indirect Exposure from Combustor Emissions and a 1994 Addendum. In response to reviewer comments, these models have been updated and are now identified collectively as IEM-2M. IEM-2M is composed of two integrated modules that simulate mercury fate using mass balance equations describing watershed soils and a shallow lake. IEM-2M simulates three chemical components: elemental mercury (Hg^0), divalent mercury (HgII), and methyl mercury (MHg). The mass balances are performed for each mercury component, with internal transformation rates linking Hg^0 , HgII , and MHg. Sources include wetfall and dryfall loadings of each component to watershed soils and to the water body as well as diffusion of atmospheric Hg^0 vapor to watershed soils and the water body. Sinks include leaching of each component from watershed soils, burial of each component from lake sediments, volatilization of Hg^0 and MHg from the soil and water column, and advection of each component out of the lake.

At the core of IEM-2M are 9 differential equations describing the mass balance of each mercury component in the surficial soil layer, in the water column, and in the surficial benthic sediments. The equations are solved for a specified interval of time, and predicted concentrations are output at fixed intervals. For each calculational time step, IEM-2M first performs a terrestrial mass balance to obtain mercury concentrations in watershed soils. Soil concentrations are used along with vapor concentrations and deposition rates to calculate concentrations in various food plants. These are used, in turn, to calculate concentrations in animals. IEM-2M simultaneously performs an aquatic mass balance driven by direct atmospheric deposition along with runoff and erosion loads from watershed soils. MHg concentrations in fish are derived from dissolved MHg water concentrations using bioaccumulation factors (BAF).

Mercury residues in fish were estimated by making the simplifying assumption that aquatic food chains can be adequately represented using four trophic levels. These trophic levels are the following: level 1 - phytoplankton (algal producers); level 2 - zooplankton (primary herbivorous consumers); level 3 - small forage fish (secondary consumers); and level 4 - larger, piscivorous fish (tertiary consumers). This type of food chain typifies the pelagic assemblages found in large freshwater lakes, and has been used extensively to model bioaccumulation of hydrophobic organic compounds. It is recognized, however, that food chain structure can vary considerably among aquatic systems resulting in large differences in bioaccumulation in a given species of fish. In addition, this simplified structure ignores several important groupings of organisms, including benthic detritivores, macroinvertebrates, and herbivorous fishes. A second simplifying assumption utilized in this effort was that methylmercury concentrations in fish are directly proportional to dissolved methylmercury concentrations in the water column. It is recognized that this relationship can vary widely among both physically similar and dissimilar water bodies. Methylmercury concentrations in fish were derived from predicted water column concentrations of dissolved methylmercury by using BAFs for trophic levels 3 and 4. The BAFs selected for these calculations were estimated from existing field data. Respectively, these BAFs (dissolved methylmercury basis) are 1.6×10^6 and 6.8×10^6 .

The results of these terrestrial and aquatic models were used to predict mercury concentrations in environmental media and biota.

1.4 Exposure Modeling Rationale

The results of these modeling efforts are used in Volumes IV and VI to predict exposures to hypothetical humans and wildlife. This section explains the decision to estimate mercury exposure based on the results of environmental fate modeling of stack emissions from anthropogenic sources rather than attempting an assessment based on monitoring data.

Exposure to mercury for the purpose of this assessment may be broadly defined as chemical contact with the outer boundary of an organism (also called a receptor). An organism's contact with mercury may occur through several different exposure routes, including dermal, inhalation, and oral. The assessment of mercury exposure is complicated by the physical and chemical properties of this naturally occurring element; factors include the different physical forms manifested in the environment, the different oxidative states exhibited, and the duality of its environmental behavior as both a metallic and an organic compound. Mercury is present in many different potential contact media. In addition, the uncertain accuracy of analytical techniques, particularly at low environmental concentrations, and problems with contamination during environmental sampling complicate an assessment of exposure.

Mercury is generally present as a low-level contaminant in combustion materials such as coal, medical wastes, and municipal solid wastes. Unlike dioxin it is not created during the combustion process but is released by it. At temperatures typical of many combustion and manufacturing processes, mercury is emitted in a gaseous form rather than a particulate form; therefore, it is difficult to control mercury emissions from the source.

Anthropogenic mercury emissions are not the only source of mercury to the atmosphere. Mercury, under certain conditions, may be introduced into the atmosphere through volatilization from natural sources such as lakes and soils; for example, some areas in the western U.S. appear to have naturally elevated mercury levels. Consequently, it is difficult to trace the source(s) of the mercury in environmental media and biota and estimate the impact of any one source type.

Existing environmental concentrations are a potential source of mercury exposure to both humans and animal species. These existing environmental concentrations, often referred to as background mercury concentrations, were estimated and included in this effort.

Mercury has always been present at varying levels in environmental media and biota, and all mercury is, in a sense, naturally occurring; that is, mercury is not a substance of human origin. Anthropogenic activities are thought to redistribute mercury from its original matrix through the atmosphere to other environmental media. Numerous studies indicate that the amount of mercury being deposited from the atmosphere has increased since the onset of the industrial age (Nater and Grigal, 1992; Johansson et al., 1991; Swain et al., 1992). Some of the deposited mercury arises from natural sources and some from anthropogenic activities.

Many different yet valid approaches may be used to obtain estimates of mercury exposure. These include: direct measurement of mercury concentrations in source emissions (e.g., stack monitoring data), environmental media (e.g., air, soil or water monitoring), and biota (e.g., fish and flora); direct measurement of mercury concentrations at the expected points of receptor contact (e.g., house or office air monitoring data, measurement of receptor food sources or drinking water); and direct measurements

of mercury concentrations in the tissues of human and wildlife receptors (e.g., hair samples, feather samples, muscle samples and leaf samples).

It was decided to model the emissions data from the stacks of combustion sources and industrial processes rather than use the existing measurement data alone. Extant measured mercury data alone were judged insufficient to assess adequately the impact of anthropogenic mercury releases on human and wildlife exposures, the primary goal of the study. The discomfort with the available data arose from the lack of extensive measurement data near U.S. anthropogenic sources of concern. It is likely that these data will be available in the near future.

This assessment utilizes the results of measured mercury emissions from selected anthropogenic sources to estimate exposure. The emissions inventory used in this assessment is found in Volume II of the Report to Congress. Using a series of environmental fate models and hypothetical scenarios, the mercury concentrations in environmental media and pertinent biota were estimated. Ultimately in Volume IV and VI mercury contact with human and wildlife receptors was estimated. In Volume IV of this document an effort was made to estimate the amount of contact with mercury as well as the oxidative state and form of mercury contacted. No attempt was made to estimate an internal dose for either the animal or human receptors.

There is a great deal of uncertainty in the modeling approach selected to estimate exposure. There is uncertainty in both the predicted fate and transport of this metal and the ultimate estimates of exposure. This uncertainty can be divided into modeling uncertainty and parameter uncertainty. Parameter uncertainty can be further subdivided into uncertainty and variability depending upon the degree to which a particular parameter is understood. Research needs are identified toward reducing these key uncertainties and are presented in Chapter 8.

1.5 Factors Important in Modeling of Mercury Exposure

Factors important in the estimation of mercury exposures modeled in this study are listed in Table 1-1. This table briefly describes the possible effects of these factors on the fate, transport and exposure to mercury and the means by which these were addressed. More details are provided in subsequent sections describing the modeling analyses.

**Table 1-1
Factors Potentially Important in Estimating Mercury Exposure and
How They Are Addressed in This Study**

Factor	Importance and Possible Effect on Mercury Exposure	Means of Addressing in this Study
Type of anthropogenic source of mercury	Different combustion and industrial process sources are anticipated to have different local scale impacts due to physical source characteristics (e.g., stack height), the method of waste generation (e.g., incineration or mass burn) or mercury control devices and their effectiveness.	Four main source categories, with a total of 11 different source types, selected based on their estimated annual mercury emissions or potential to be localized point sources of concern.
Mercury emission rates from stack	Increased emissions will result in a greater chance of adverse impacts on environment.	Emissions of model plants based on emissions inventory.
Mercury species emitted from stack	More soluble species will tend to deposit closer to the source.	Two species considered to be emitted from source: elemental and divalent mercury
Form of mercury emitted from stack	Transport properties can be highly dependent on form.	Both vapor and particle-bound fractions considered.
Deposition differences between vapor and particulate-bound mercury	Vapor-phase forms may deposit significantly faster than particulate-bound forms.	Deposition (wet and dry) of vapor-phase forms calculated separately from particulate-bound deposition.
Transformations of mercury after emission from source	Relatively nontoxic forms emitted from source may be transformed into more toxic compounds.	Equilibrium fractions estimated in all environmental media for three mercury species: elemental mercury, divalent species, and methylmercury.
Transformation of mercury in watershed soil	Reduction and revolatilization of mercury in soil limits the buildup of concentration.	Rate constants are estimated from measured evasion fluxes at three locations, as reported in scientific literature.
Transport of mercury from watershed soils to water body	Mercury in watershed soils can be a significant source to water bodies and subsequently to fish.	Runoff and erosion rates are calculated as a function of average meteorological and watershed characteristics.
Transformation of mercury in water body	Reduction, methylation, and demethylation of mercury in water bodies affect the overall concentration and the MHg fraction, which is bioaccumulated in fish.	Rate constants are estimated from the scientific literature, and are calibrated to give the average observed MHg fraction.
Facility locations	Effects of meteorology and terrain may be significant.	Both a humid and less humid site considered. Effect of terrain on results addressed separately.
Location relative to local mercury source	Receptors located downwind are more likely to have higher exposures. Influence of distance depends on source type.	Three distances in downwind direction considered.
Contribution from non-local sources of mercury	Important to keep predicted impacts of local sources in perspective.	Results of local mercury source are combined with estimate of impact from non-local sources from RELMAP.
Uncertainty	Reduces confidence in ability to estimate exposure accurately.	Probabilistic capabilities possible for any combination of sources and scenarios. In the current study, limited uncertainty analyses conducted for major aspects of atmospheric transport modeling .

1.6 Definition of Terms

Definitions for the following terms related to the fate and transport of mercury were largely adapted from the Expert Panel on Mercury Atmospheric Processes (1994), and EPA (1975, 1976).

Anthropogenic Mercury Emissions

The mobilization or release of mercury by human activity that results in a mass transfer of mercury to the atmosphere.

Bioaccumulation Factor

The equilibrium concentration of a chemical in a biological medium divided by the equilibrium concentration of a chemical in an environmental medium. While similar to a bioconcentration factor, a bioaccumulation factor is designed not only to predict chemical uptake through direct contact with or uptake from an environmental medium, but also to account for any food chain pathways that may in some manner connect the environmental medium to the biological medium of interest.

Bioavailability

The state of being capable of being absorbed and available to interact with the metabolic processes of an organism. Bioavailability is typically a function of chemical properties, the physical state of the material to which an organism is exposed, and the ability of the individual organism to physiologically take up the chemical.

Bioconcentration Factor

The equilibrium concentration of a chemical in a biological medium divided by the equilibrium concentration of a chemical in an environmental medium. The parameter is typically used to predict chemical uptake through contact with or uptake from an environmental medium.

Biotransfer Factor

The equilibrium concentration of a chemical in animal tissue divided by the daily intake of the chemical.

Contact Rate

The frequency of an exposure. Generally expressed as the product of an amount of a medium per event and the number of events per a given unit of time.

Current Background Mercury Concentrations

Concentrations of mercury in the abiotic and biotic components of the environment that have resulted from natural mercury concentrations and anthropogenic activities.

Erosion

The removal of soil particles by wind and water. Water erosion is usually characterized by one or more of the following types of erosion: raindrop erosion, sheet erosion, rill erosion, gully erosion, and streambank erosion. Raindrops start soil erosion by detaching soil particles. They aggravate soil erosion by compacting the soil surface and reducing its ability to infiltrate water. Sheet erosion is the removal of a thin layer of soil resulting from sheet flow of water. It has a high transport capability. Rill erosion is on steeper slopes where channels with depths of up to one foot are formed. Gully erosion represents an advanced form of soil erosion from

concentrated storm runoff. Streambank erosion is the erosion of soil from stream channels, both on the banks and on the stream beds.

Exposure

Contact of a chemical, physical or biological agent with the outer boundary of an organism. Exposure is quantified as the concentration of the agent in the medium in contact, integrated over the time duration of the contact.

Exposure Scenario

A set of facts, assumptions, and inferences about how exposure takes place that aids the exposure assessor in evaluating estimating, or quantifying exposures.

Natural Background Mercury Concentrations

Concentrations of mercury in the abiotic and biotic components of the environment that resulted from natural mercury concentrations. These concentrations existed prior to the onset of anthropogenic activities.

Natural Mercury Emissions

The mobilization or release of mercury from environmental sources by natural biotic or abiotic activities that results in a mass transfer of mercury to the atmosphere.

Pathway

The physical course a chemical or pollutant takes from the source to the exposed organism.

Re-emitted Mercury

Mass transfer of mercury to the atmosphere by biotic and geological processes drawing on a pool of mercury that was deposited to the earth's surface after initial mobilization by either anthropogenic or natural activities.

Mercury Dry Deposition

Mass transfers of gaseous, aerosol or particulate mercury species from the atmosphere to the earth's surface (either aquatic or terrestrial, including vegetation) in the absence of precipitation.

Mercury Wet Deposition

Mass transfers of dissolved gaseous or suspended particulate mercury species from the atmosphere to the earth's surface (either aquatic or terrestrial) by precipitation.

Local Scale

A relative term, used to describe the area within which emissions travel within one diurnal cycle (generally 100 Km from source but for this analysis 50 Km from the source). Local influences are characterized by measurable pollutant concentration gradients with relatively large fluctuations in air concentrations caused by meteorological factors such as wind direction.

Regional Scale

A relative term, used to describe the area within which emissions travel in more than one diurnal cycle (generally 100 to 2000 Km from a source). The regional scale describes areas sufficiently remote or distant from large emission sources so that concentration fields are rather homogeneous, lacking measurable gradients.

Runoff

That portion of the precipitation that appears in surface streams. Surface runoff (or overland flow) is water that travels over the ground surface. Subsurface runoff (interflow, storm seepage) is water that has infiltrated the surface soil and moved laterally through the upper soil horizons. Groundwater runoff is water that has infiltrated the surface soil, percolated to the general groundwater table, and then moved laterally to the water body.

2. OVERVIEW OF ENVIRONMENTAL FATE OF MERCURY

This chapter summarizes information about the mercury cycle as it directly relates to the present study: anthropogenic source release to the atmosphere and the resulting exposure to humans and wildlife from the inhalation and ingestion pathways. It is important to note that it is not possible to know exactly what will happen to stack-released mercury, but enough is known about the speciation and cycling of mercury in the environment at this time to propose a plausible scenario.

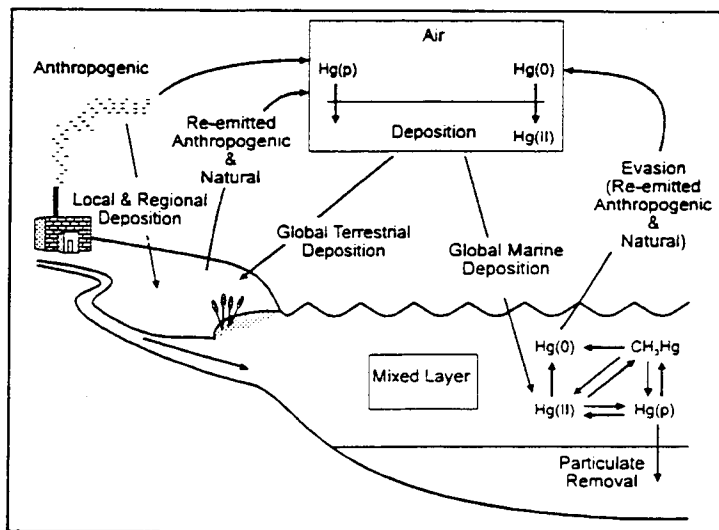
The chapter is organized into four main sections. Section 2.1 provides an overview of mercury in the environment, including the environmental chemistry of mercury and the mercury cycle. Section 2.2 summarizes major atmospheric processes, including mercury emissions, transformation and transport, deposition, and re-emissions. Section 2.3 describes the terrestrial and aquatic fate of mercury, and Section 2.4 describes the fate of mercury in marine environments.

2.1 Mercury in the Environment

Mercury is emitted by both anthropogenic and natural processes. Due to its chemical properties, environmental mercury is thought to move through various environmental compartments, possibly changing form and species during this process. Like other elements such as nitrogen, these movements are conceptualized as a cycle.

The mercury cycle has been studied and described in several reports (Swedish EPA, 1991; Mitra, 1986; Fitzgerald and Clarkson, 1991; Fitzgerald, 1994), and its understanding continues to undergo refinement. The movement and distribution of mercury in the environment can be confidently described only in general terms. There has been increasing consensus on many, but not all, of the detailed behaviors of mercury in the environment (Brosset and Lord, 1991; Expert Panel on Mercury Atmospheric Processes, 1994). The depiction of the mercury cycle in Figure 2-1 attempts to illustrate mercury release by both natural and anthropogenic sources into environmental media: air, soil, and water. The figure also illustrates the various transport and transformation processes that are expected to occur and includes a number of infinite and/or indefinite loops.

Figure 2-1
The Mercury Cycle



2.1.1 Chemistry of Mercury

Elemental mercury is a heavy, silvery-white liquid metal at typical ambient temperatures and pressures. The vapor pressure of mercury metal is strongly dependent upon temperature, and it vaporizes readily under ambient conditions. Its saturation vapor pressure of 14 mg/m^3 greatly exceeds the average permissible concentrations for occupational (0.05 mg/m^3) or continuous environmental exposure (0.015 mg/m^3) (Nriagu, 1979; WHO, 1976). Elemental mercury partitions strongly to air in the environment and is not found in nature as a pure, confined liquid. Most of the mercury encountered in the atmosphere is elemental mercury vapor.

Mercury can exist in three oxidation states: Hg^0 (metallic), Hg_2^{2+} (mercurous), and Hg^{2+} (mercuric-Hg(II)). The properties and chemical behavior of mercury strongly depend on the oxidation state. Mercurous and mercuric mercury can form numerous inorganic and organic chemical compounds; however, mercurous mercury is rarely stable under ordinary environmental conditions. Mercury is unusual among metals because it tends to form covalent rather than ionic bonds. Most of the mercury encountered in water/soil/sediments/biota (all environmental media except the atmosphere) is in the form of inorganic mercuric salts and organomercurics. Organomercurics are defined by the presence of a covalent C-Hg bond. The presence of a covalent C-Hg bond differentiates organomercurics from inorganic mercury compounds that merely associate with the organic material in the environment but do not have the C-Hg bond. The compounds most likely to be found under environmental conditions are these: the mercuric salts HgCl_2 , $\text{Hg}(\text{OH})_2$ and HgS ; the methylmercury compounds, methylmercuric chloride (CH_3HgCl) and methylmercuric hydroxide (CH_3HgOH); and, in small fractions, other organomercurics (i.e., dimethylmercury and phenylmercury).

Mercury compounds in the aqueous phase often remain as undisassociated molecules, and the reported solubility values reflect this. Solubility values for mercury compounds which do not disassociate are not based on the ionic product. Most organomercurics are not soluble and do not react with weak acids or bases due to the low affinity of the mercury for oxygen bonded to carbon. CH_3HgOH , however, is highly soluble due to the strong hydrogen bonding capability of the hydroxide group. The mercuric salts vary widely in solubility. For example HgCl_2 is readily soluble in water, and HgS is as unreactive as the organomercurics due to the high affinity of mercury for sulfur. A detailed discussion of mercury chemistry can be found in Nriagu (1979) and Mason et al. (1994).

2.1.2 The Mercury Cycle

Given the present understanding of the mercury cycle, the flux of mercury from the atmosphere to land or water at any one location is comprised of contributions from:

- The natural global cycle,
- The global cycle perturbed by human activities,
- Regional sources, and
- Local sources.

Recent advances allow for a general understanding of the global mercury cycle and the impact of anthropogenic sources. It is more difficult to make accurate generalizations of the fluxes on a regional or local scale due to the site-specific nature of emission and deposition processes.

2.1.2.1 The Global Mercury Cycle

As a naturally occurring element, mercury is present throughout the environment in both environmental media and biota. Nriagu (1979) estimated the global distribution of mercury and concluded that by far the largest repository is ocean sediments. Nriagu estimated that the ocean sediments may contain about 10^{17} g of mercury, mainly as HgS. Nriagu also estimated that ocean waters contain around 10^{13} g, soils and freshwater sediments 10^{13} g, the biosphere 10^{11} g (mostly in land biota), the atmosphere 10^8 g and freshwater on the order of 10^7 g. This budget excludes "unavailable" mercury in mines and other subterranean repositories. A more recent estimate of the global atmospheric repository by Fitzgerald (1994) is 25 Mmol or approximately 5×10^9 g. The estimate of Fitzgerald (1994) is 50 times the previous estimate of Nriagu (1979) and illustrates how rapidly the scientific understanding of environmental mercury has changed in recent years.

Several authors have used a number of different techniques to estimate the pre-industrial mercury concentrations in environmental media before anthropogenic emissions became a part of the global mercury cycle. It is difficult to separate current mercury concentrations by origin (i.e., anthropogenic or natural) because of the continuous cycling of the element in the environment. For example, anthropogenic releases of elemental mercury may be oxidized and deposit as divalent mercury far from the source; the deposited mercury may be reduced and re-emitted as elemental mercury only to be deposited again continents away. Not surprisingly, there is a broad range of estimates and a great deal of uncertainty with each. When the estimates are combined, they indicate that between 40 and 75 percent of the current atmospheric mercury concentrations are the result of anthropogenic releases. The Expert Panel on Mercury Atmospheric Processes (1994) concluded that pre-industrial atmospheric concentrations constitute approximately one-third of the current atmospheric concentrations. The panel estimated that anthropogenic emissions may currently account for 50 - 75 percent of the total annual input to the global atmosphere (Expert Panel on Mercury Atmospheric Processes, 1994). The estimates of the panel are corroborated by Lindqvist et al., (1991), who estimated that 60 percent of the current atmospheric concentrations are the result of anthropogenic emissions and Porcella (1994), who estimated that this fraction was 50 percent. Horvat et al., (1993b) assessed the anthropogenic fraction as constituting 40 to 50 percent of the current total. This overall range appears to be in agreement with the several fold increase noted in inferred deposition rates (Swain et al., 1992; Engstrom et al., 1994; Benoit et al., 1994). The percentage of current total atmospheric mercury which is of anthropogenic origin may be much higher near mercury emissions sources.

A better understanding of the relative contribution of mercury from anthropogenic sources is limited by substantial remaining uncertainties regarding the level of natural emissions as well as the amount and original source of mercury that is re-emitted to the atmosphere from soils, watersheds, and ocean waters. Recent estimates indicate that of the approximately 200,000 tons of mercury emitted to the atmosphere since 1890, about 95 percent resides in terrestrial soils, about 3 percent in the ocean surface waters, and 2 percent in the atmosphere (Expert Panel, 1994). More study is needed before it is possible to accurately differentiate natural fluxes from these soils, watersheds, and ocean waters from re-emissions of mercury which originated from anthropogenic sources. For instance, approximately one-third of total current global mercury emissions are thought to cycle from the oceans to the atmosphere and back again to the oceans, but a major fraction of the emissions from oceans consists of recycled anthropogenic mercury. According to the Expert Panel on Mercury Atmospheric Processes (1994) 20 to 30 percent of the current oceanic emissions are from mercury originally mobilized by natural sources (Fitzgerald and Mason, 1996). Similarly, a potentially large fraction of terrestrial and vegetative emissions consists of recycled mercury from previously deposited anthropogenic and natural emissions (Expert Panel, 1994).

Comparisons of contemporary (within the last 15-20 years) measurements and historical records indicate that the total global atmospheric mercury burden has increased since the beginning of the industrialized period by a factor of between two and five (see Figure 2-2). For example, analysis of sediments from Swedish lakes shows mercury concentrations in the upper layers that are two to five times higher than those associated with pre-industrialized times. In Minnesota and Wisconsin, an investigation of whole-lake mercury accumulation indicates that the annual deposition of atmospheric mercury has increased by a factor of three to four since pre-industrial times. Similar increases have been noted in other studies of lake and peat cores from this region, and results from remote lakes in southeast Alaska also show an increase, though somewhat lower than found in the upper midwest U.S. (Expert Panel, 1994).

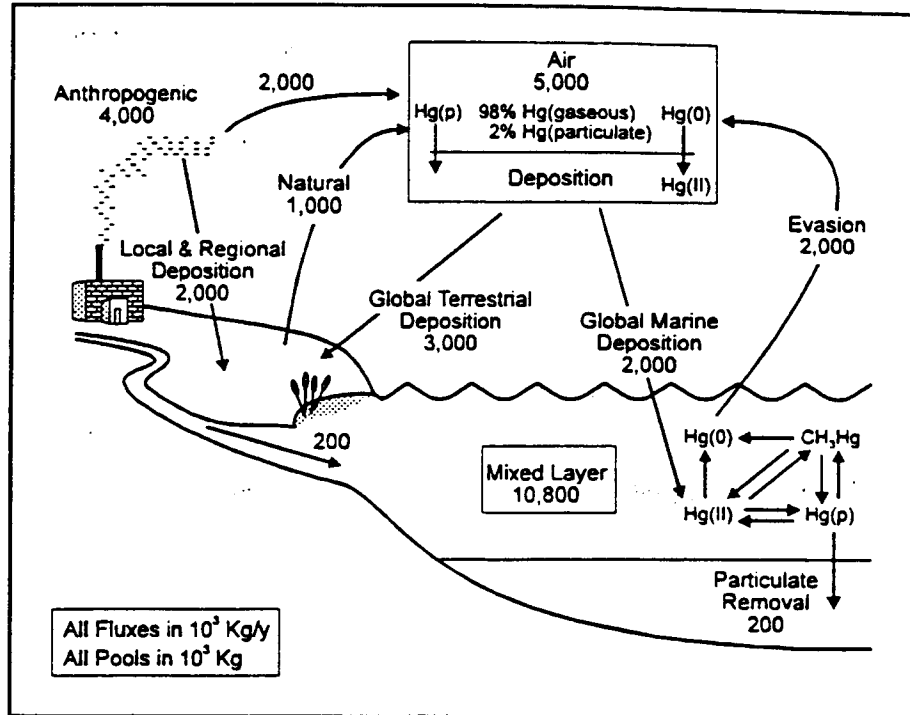
Although it is accepted that atmospheric mercury burdens have increased substantially since the preindustrial period, it is uncertain whether overall atmospheric mercury levels are currently increasing, decreasing, or remaining stable. Measurements over remote areas of the Atlantic Ocean show increasing levels up until 1990 and a decrease for the period 1990-1994 (Slemr, 1996). Measurements of deposition rates suggest decreased deposition at some localities formerly subject to local or regional deposition (see Section 2.1.2.2 below). However, other measurements at remote sites in northern Canada and Alaska show deposition rates that continue to increase (Lucotte et al., 1995; Engstrom and Swain, 1997). Since these sites are subject to global long-range sources and few regional sources, these measurements may indicate a still increasing global atmospheric burden. More research is necessary; a multi-year, world-wide atmospheric mercury measurement program may help to better determine current global trends (Fitzgerald, 1995).

2.1.2.2 Regional and Local Mercury Cycles

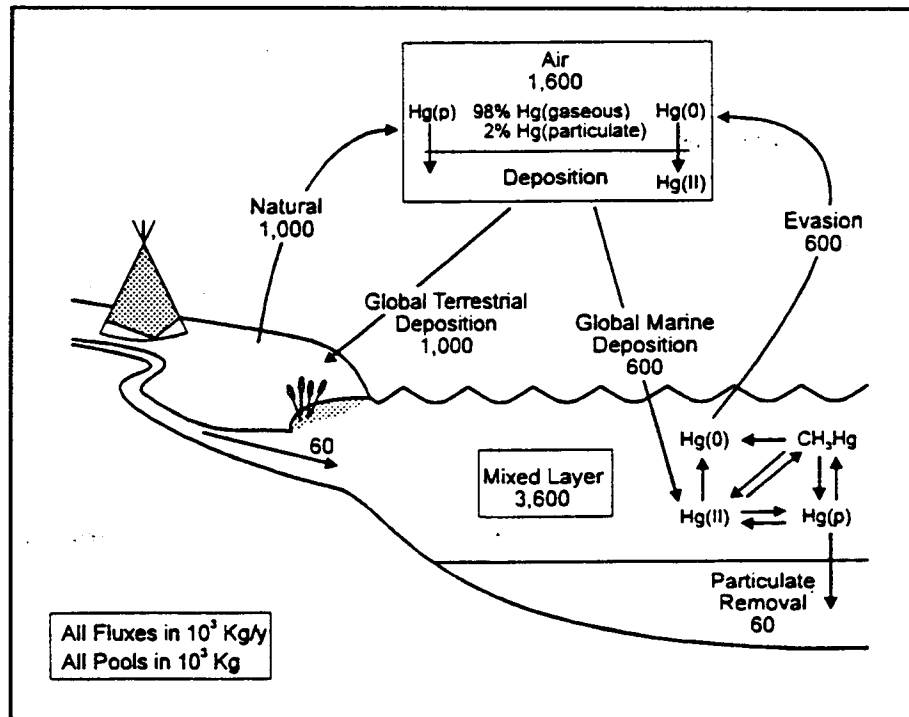
According to one estimate, about half of total anthropogenic mercury emissions eventually enter the global atmospheric cycle (Mason et al., 1994); the remainder is removed through local or regional cycles. An estimated 5 to 10 percent of primary Hg(II) emissions are deposited within 100 km of the point of emission and a larger fraction on a regional scale. Hg(0) that is emitted may be removed on a local and regional scale to the extent that it is oxidized to Hg(II). Some Hg(0) may also be taken up directly by foliage; most Hg(0) that is not oxidized will undergo long-range transport due to the insolubility of Hg(0) in water. In general, primary Hg(II) emissions will be deposited on a local and regional scale to the degree that wet deposition processes remove the soluble Hg(II). Dry deposition may also account for some removal of atmospheric Hg(II). Assuming constant emission rates, the quantity of mercury deposited on a regional and local scale can vary depending on source characteristics (especially the species of mercury emitted), meteorological and topographical attributes, and other factors (Expert Panel, 1994). For example, deposition rates at some locations have been correlated with wind trajectories and precipitation amounts (Jensen and Iverfeldt, 1994; Dvonch et al., 1995). Although these variations prohibit generalizations of local and regional cycles, such cycles may be established for specific locations. For example, unique mercury cycles have been defined for Siberia on a regional scale (Sukhenko and Vasiliev, 1996) and for the area downwind of a German chlor-alkali plant on a local scale (Ebinghaus and Kruger, 1996). Mercury cycles dependent on local and regional sources have also been established for the Upper Great Lakes region (Glass et al., 1991; Lamborg et al., 1995) and the Nordic countries (Jensen and Iverfeldt, 1994).

Figure 2-2
Comparison of Current and Pre-Industrial
Mercury Budgets and Fluxes

Current Mercury
Budgets and
Fluxes



Pre-Industrial
Mercury Budgets
and Fluxes



Source: Adapted from Mason et al., 1994.

While the overall trend in the global mercury burden since pre-industrial times appears to be increasing, there is some evidence that mercury concentrations in the environment in certain locations have been stable or decreasing over the past few decades. For example, preliminary results for eastern red cedar growing near industrial sources (chlor-alkali, nuclear weapons production) show peak mercury concentrations in wood formed in the 1950s and 1960s, with stable or decreasing concentrations in the past decade (Expert Panel, 1994). Some results from peat cores and lake sediment cores also suggest that peak mercury deposition in some regions occurred prior to 1970 and may now be decreasing (Swain et al., 1992; Benoit et al., 1994; Engstrom et al., 1994; Engstrom and Swain, 1997). Data collected over 25 years from many locations in the United Kingdom on liver mercury concentrations in two raptor species and a fish-eating grey heron indicate that peak concentrations occurred prior to 1970. The sharp decline in liver mercury concentrations in the early 1970s suggests that local sources, such as agricultural uses of fungicides, may have led to elevated mercury levels two to three decades ago (Newton et al., 1993). Similar trends have been noted for mercury levels in eggs of the common loon collected from New York and New Hampshire (McIntyre et al., 1993). The downward trend in mercury concentrations observed in the environment in some geographic locations over the last few decades generally corresponds to regional mercury use and consumption patterns over the same time frame (consumption patterns are discussed in Volume II).

2.2 Atmospheric Processes

Basic processes involved in the atmospheric fate and transport of mercury include: (1) emissions to the atmosphere; (2) transformation and transport in the atmosphere; (3) deposition from the air; and then (4) re-emission to the atmosphere. Each of these processes is briefly described below.

2.2.1 Emissions of Mercury

As discussed fully in Volume II, mercury is emitted to the atmosphere through both naturally occurring and anthropogenic processes. Natural processes include volatilization of mercury in marine and aquatic environments, volatilization from vegetation, degassing of geologic materials (e.g., soils) and volcanic emissions. The natural emissions are thought to be primarily in the elemental mercury form. Conceptually, the current natural emissions can arise from two components: mercury present as part of the pre-industrial equilibrium and mercury mobilized from deep geologic deposits and added to the global cycle by human activity. Based on estimates of the total annual global input to the atmosphere from all sources (i.e., 5000 Mg from anthropogenic, natural, and oceanic emissions), U.S. sources are estimated to contribute about 3 percent, based on 1995 emissions estimates as described below.

Anthropogenic mercury releases are thought to be dominated on the national scale by industrial processes and combustion sources that release mercury into the atmosphere. Stack emissions are thought to include both gaseous and particulate forms of mercury. Gaseous mercury emissions are thought to include both elemental and oxidized chemical forms, while particulate mercury emissions are thought to be composed primarily of oxidized compounds due to the relatively high vapor pressure of elemental mercury. The analytic methods for mercury speciation of exit gasses and emission plumes are being refined, and there is still controversy in this field. Chemical reactions occurring in the emission plume are also possible. The speciation of mercury emissions is thought to depend on the fuel used (e.g., coal, oil, municipal waste), flue gas cleaning and operating temperature. The exit stream is thought to range from almost all divalent mercury to nearly all elemental mercury. Most of the mercury emitted at the stack outlet is found in the gas phase although exit streams containing soot can bind up some fraction of the mercury. The divalent fraction is split between gaseous and particle bound phases (Lindqvist et al.,

1991, Chapter 4). Much of this divalent mercury is thought to be HgCl_2 (Michigan Environmental Science Board, 1993).

An emission factor-based approach was used to develop the nationwide emission estimates for the source categories presented in Table 2-1. The emission factors presented are estimates based on ratios of mass mercury emissions to measures of source activities and nation-wide source activity levels. Details of the emission factor approach are described in Volume II of this Report to Congress. The reader should note that the data presented in this table are estimates; uncertainties include the precision of measurement techniques and the calculation of emission factors, estimates of pollutant control efficiency, and nation-wide source class activity levels. The estimates may also be based on limited information for a particular source class, thereby increasing the uncertainty in the estimate further. Due to these and other uncertainties, other sources have calculated different total emissions estimates using similar methods (for example, see Porcella et al., 1996).

Some anthropogenic processes no longer used still result in significant environmental releases from historically contaminated areas which continue to release mercury to surface water runoff, groundwater and the atmosphere. It is estimated that the mercury content of typical lakes and rivers has been increased by a factor of two to four since the onset of the industrial age (Nriagu, 1979). More recently, researchers in Sweden estimate that mercury concentrations in soil, water and lake sediments have increased by a factor of four to seven in southern Sweden and two to three in northern Sweden in the 20th century (Swedish EPA 1991). It is estimated that present day mercury deposition is two to five times greater now than in preindustrial times (Lindqvist et al., 1991).

2.2.2 Mercury Transformation and Transport

$\text{Hg}(0)$ has an average residence time in the atmosphere of about one year and will thus be distributed fairly evenly in the troposphere. Oxidized mercury ($\text{Hg}(\text{II})$) may be deposited relatively quickly by wet and dry deposition processes, leading to a residence time of hours to months. Longer residence times are possible as well; the atmospheric residence time for some $\text{Hg}(\text{II})$ associated with fine particles may approach that of Hg^0 (Porcella et al., 1996).

The transformation of $\text{Hg}^0(\text{g})$ to $\text{Hg}(\text{II})(\text{aq})$ and $\text{Hg}(\text{II})(\text{p})$ in cloud water demonstrates a possible mechanism by which natural and anthropogenic sources of Hg^0 to air can result in mercury deposition to land and water. This deposition can occur far from the source due to the slow rate of $\text{Hg}^0(\text{g})$ uptake in cloud water. It has been suggested that this mechanism is important in a global sense for mercury pollution, while direct wet deposition of anthropogenic $\text{Hg}(\text{II})$ is the most important locally (Fitzgerald, 1994; Lindqvist et al., 1991, Chapter 6). Gaseous $\text{Hg}(\text{II})$ is expected to deposit at a faster rate after release than particulate $\text{Hg}(\text{II})$ assuming that most of the particulate matter is less than $1 \mu\text{m}$ in diameter. An atmospheric residence time of $\frac{1}{2}$ - 2 years for elemental mercury compared to as little as hours for some $\text{Hg}(\text{II})$ species (Lindqvist and Rodhe, 1985) is expected. This behavior is observed in the modeling results presented in this effort as well. It is possible that dry deposition of Hg^0 can occur from ozone mediated oxidation of elemental mercury taking place on wet surfaces, but this is not expected to be comparable in magnitude to the cloud droplet mediated processes.

This great disparity in atmospheric residence time between Hg^0 and the other mercury species leads to very much larger scales of transport and deposition for Hg^0 . Generally, air emissions of Hg^0 from anthropogenic sources, fluxes of Hg^0 from contaminated soils and water bodies and natural fluxes of Hg^0 all contribute to a global atmospheric mercury reservoir with a holding time of $\frac{1}{2}$ to 2 years. Global atmospheric circulation systems can take Hg^0 emissions from their point of origin and carry them

Table 2-1
Annual Estimates of Mercury Release by Various Combustion and
Manufacturing Source Classes (U.S. EPA, 1997)

Source	Annual Mercury Emission Rate
Combustion Sources - Total	125.2 Mg/yr (137.9 tons/yr)
Electric utilities	
Oil- and Gas-fired	0.2 Mg/yr (0.2 tons/yr)
Coal-fired	46.9 Mg/yr (51.6 tons/yr)
Incinerators	
Municipal waste combustors	26.9 Mg/yr (29.6 tons/yr)
Medical waste incinerators	14.6 Mg/yr (16.0 tons/yr)
Commercial/Industrial boilers	25.8 Mg/yr (28.4 tons/yr)
Chlor-alkali production	6.5 Mg/yr (7.1 tons/yr)
Primary lead smelting	0.1 Mg/yr (0.1 tons/yr)
Primary copper smelting	0.06 Mg/yr (0.06 tons/yr)
Other combustion sources	10.8 Mg/yr (11.9 tons/yr)
Other sources	12.1 Mg/yr (13.3 tons/yr)

anywhere on the globe before transformation and deposition occur. Emissions of all other forms of mercury are likely to be deposited to the earth's surface before they thoroughly dilute into the global atmosphere. Continental-scale atmospheric modeling, such as that performed for this study using the RELMAP, can explicitly simulate the atmospheric lifetime of gaseous and particulate Hg(II) species, but not Hg⁰. Although Hg⁰ is included as a modeled species in the RELMAP analysis, the vast majority of Hg⁰ emitted in the simulation transports outside the spatial model domain without depositing, and the same is generally thought to happen in the real atmosphere. Natural Hg⁰ emissions and anthropogenic Hg⁰ emissions from outside the model domain are simulated in the form of a constant background Hg⁰ concentration of 1.6 ng m⁻³, approximating conditions observed in remote oceanic regions (Fitzgerald, 1994). This background Hg⁰ concentration is subject to simulated wet deposition by the same process as explicitly modeled anthropogenic sources of Hg⁰ within the model domain.

Explicit numerical models of global-scale atmospheric mercury transport and deposition have not yet been developed. As our understanding of the global nature of atmospheric mercury pollution develops, numerical global-scale atmospheric models will surely follow.

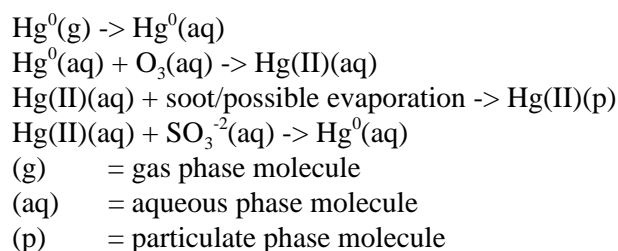
2.2.3 Deposition of Mercury

The divalent species emitted, either in the vapor or particulate phase, are thought to be subject to much faster atmospheric removal than elemental mercury (Lindberg et al., 1991, Shannon and Voldner, 1994). Both particulate and gaseous divalent mercury are assumed to dry deposit (this is defined as deposition in the absence of precipitation) at significant rates when and where measurable concentrations of these mercury species exist. The deposition velocity of particulate mercury is dependent on atmospheric conditions and particle size. Particulate mercury is also assumed to be subject to wet deposition due to scavenging by cloud microphysics and precipitation. The gaseous divalent mercury emitted is also expected to be scavenged readily by precipitation. Divalent mercury species have much lower Henry's law constants than elemental mercury, and thus are assumed to partition strongly to the water phase. Dry deposition of gas phase divalent mercury is thought to be significant due to its reactivity with surface material. Overall, gas phase divalent mercury is more rapidly and effectively removed by both dry and wet deposition than particulate divalent mercury (Lindberg et al., 1992; Petersen et al., 1995; Shannon and Voldner, 1994), a result of the reactivity and water solubility of gaseous divalent mercury.

In contrast, elemental mercury vapor is not thought to be susceptible to any major process of direct deposition to the earth's surface due to its relatively high vapor pressure and low water solubility. On non-assimilating surfaces elemental mercury deposition appears negligible (Lindberg et al., 1992), and though elemental mercury can be formed in soil and water due to the reduction of divalent mercury species by various mechanisms, this elemental mercury is expected to volatilize into the atmosphere (Expert Panel on Mercury Atmospheric Processes 1994). In fact, it has been suggested that *in-situ* production and afflux of elemental mercury could provide a buffering role in aqueous systems, as this would limit the amount of divalent mercury available for methylation (Fitzgerald, 1994). Water does contain an amount of dissolved gaseous elemental mercury (Fitzgerald et al., 1991), but it is minor in comparison to the dissolved-oxidized and particulate mercury content.

There appears to be a potential for deposition of elemental mercury via plant-leaf uptake. Lindberg et al. (1992) indicated that forest canopies could accumulate elemental mercury vapor, via gas exchange at the leaf surface followed by mercury assimilation in the leaf interior during the daylight hours. This process causes a downward flux of elemental mercury from the atmosphere, resulting in a deposition velocity. Recent evidence (Hanson et al., 1994) indicates that this does occur but only when air concentrations of elemental mercury are above an equilibrium level for the local forest ecosystem. At lower air concentration levels, the forest appears to act as a source of elemental mercury to the atmosphere, with the measured mercury flux in the upward direction. Lindberg et al. (1991) noted this may be explained by the volatilization of elemental mercury from the canopy/soil system, most likely the soil. Hanson et al. (1994) stated that "dry foliar surfaces in terrestrial forest landscapes may not be a net sink for atmospheric elemental mercury, but rather a dynamic exchange surface that can function as a source or sink dependent on current mercury vapor concentrations, leaf temperatures, surface condition (wet versus dry) and level of atmospheric oxidants." Similarly, Mosbaek et al. (1988) convincingly showed that most of the mercury in leafy plants is due to air-leaf transfer, but that for a given period of time the amount of elemental mercury released from the plant-soil system greatly exceeds the amount collected from the air by the plants. It is also likely that many plant/soil systems accumulate airborne elemental mercury when air concentrations are higher than the long-term average for the particular location, and release elemental mercury when air concentrations fall below the local long-term average. On regional and global scales, dry deposition of elemental mercury does not appear to be a significant pathway for removal of atmospheric mercury, although approximately 95% or more of atmospheric mercury is elemental mercury (Fitzgerald, 1994).

There is an indirect pathway, however, by which elemental mercury vapor released into the atmosphere may be removed and deposited to the earth's surface. Chemical reactions occur in the aqueous phase (cloud droplets) that both oxidize elemental mercury to divalent mercury and reduce the divalent mercury to elemental mercury. The most important reactions in this aqueous reduction-oxidation balance are thought to be oxidation of elemental mercury with ozone, reduction of divalent mercury by sulfite (SO_3^{2-}) ions, or complexation of divalent mercury with soot to form particulate divalent mercury:



The Hg(II) produced from oxidation of Hg^0 by ozone can be reduced back to Hg^0 by sulfite; however, the oxidation of Hg^0 by ozone is a much faster reaction than the reduction of Hg(II) by sulfite. Thus, a steady state concentration of Hg(II)(aq) is built up in the atmosphere and can be expressed as a function of the concentrations of $\text{Hg}^0(\text{g})$, $\text{O}_3(\text{g})$, H^+ (representing acids) and $\text{SO}_2(\text{g})$ (Lindqvist et al., 1991, Chapter 6). Note that H^+ and $\text{SO}_2(\text{g})$, although not apparent in the listed atmospheric reactions, control the formation of sulfite.

The Hg(II)(aq) produced would then be susceptible to atmospheric removal via wet deposition. The third reaction, however, may transform most of the Hg(II)(aq) into the particulate form, due to the much greater amounts of soot than mercury in the atmosphere. The soot concentration will not be limiting compared to the concentration of Hg(II)(aq), and S atoms in the soot matrix will bond readily to the Hg(II)(aq). The resulting Hg(II)(p) can then be removed from the atmosphere by wet deposition (if the particle is still associated with the cloud droplet) or dry deposition (following cloud droplet evaporation). It is possible that dry deposition of Hg^0 can occur from ozone mediated oxidation of elemental mercury taking place on wet surfaces, but this is not expected to be comparable in magnitude to the cloud droplet mediated processes (Lindberg, 1994).

Mercury released into the atmosphere from natural and anthropogenic sources deposits mainly as Hg(II), from either direct deposition of emitted Hg(II) or from conversion of emitted elemental Hg^0 to Hg(II) through ozone-mediated reduction. The former process may result in elevated deposition rates around atmospheric emission sources and the latter process results in regional/global transport followed by deposition.

There is still a great deal of uncertainty with respect to the amount of dry deposition of mercury. Once deposited, mercury appears to bind tightly to certain soil components. The deposited Hg(II) may revolatilize through reduction and be released back to the atmosphere as Hg^0 . Soil Hg(II) may also be methylated to form methylmercury; these two forms may remain in the soil or be transported through the watershed to a water body via runoff and leaching. Mercury enters the water body through direct deposition on the watershed, and mercury in water bodies has been measured in both the water column and the sediments. Hg(II) in the waterbody may also be methylated to form methylmercury; both Hg(II) and methylmercury may be reduced to form Hg^0 which is reintroduced to the atmosphere.

2.2.4 Re-emissions of Mercury into the Atmosphere

Re-emission of deposited mercury results most significantly from the evasion of elemental mercury from the oceans. In this process, anthropogenically emitted mercury is deposited to the oceans as Hg(II) and then reduced to volatile Hg(0) and re-emitted. According to one estimate, this process accounts for approximately 30% (10 Mmol/year) of the total mercury flux to the atmosphere (Mason et al., 1994). Overall, 70 to 80 % of total current mercury emissions may be related to anthropogenic activities (Fitzgerald and Mason, 1996). By considering the current global mercury budget and estimates of the preindustrial mercury fluxes, Mason et al. (1994) estimate that total emissions have increased by a factor of 4.5 since preindustrial times, which has subsequently increased the atmospheric and oceanic reservoirs by a factor of 3. The difference is attributed to local deposition near anthropogenic sources. Although the estimated residence time of elemental mercury in the atmosphere is about 1 year, the equilibrium between the atmosphere and ocean waters results in a longer time period needed for overall change to take place for reservoir amounts. Therefore, by substantially increasing the size of the oceanic mercury pool, anthropogenic sources have introduced long term perturbations into the global mercury cycle. Modeled results from Fitzgerald and Mason (1996) estimate that if all anthropogenic emissions were ceased today, it would take about 15 years for mercury pools in the oceans and the atmosphere to return to pre-industrial conditions. The Science Advisory Board, in its review of this study, concluded that it could take significantly longer. The slow release of mercury from terrestrial sinks to freshwater and coastal waters will likely persist for much longer, though, effectively increasing the lifetime of anthropogenic mercury further (Fitzgerald and Mason, 1996). This may be particularly significant considering that surface soils currently contain most of the pollution-derived mercury of the industrial period. Recently published studies, however, indicate that mercury in soil may be reduced and revolatilized, in that the capacity of soils to sequester airborne mercury must be reconsidered (Kim et al., 1995; Lindberg, 1996). Thus, re-emissions of anthropogenic mercury will contribute to long term influences on the global biogeochemical cycle for mercury.

2.3 **Terrestrial and Aquatic Fate of Mercury**

2.3.1 Mercury in Soil

Once deposited, the Hg(II) species are subject to a wide array of chemical and biological reactions. Soil conditions (e.g., pH, temperature and soil humic content) are typically favorable for the formation of inorganic Hg(II) compounds such as HgCl₂, Hg(OH)₂ and inorganic Hg(II) compounds complexed with organic anions (Schuster 1991). Although inorganic Hg(II) compounds are quite soluble (and, thus, theoretically mobile) they form complexes with soil organic matter (mainly fulvic and humic acids) and mineral colloids; the former is the dominating process. This is due largely to the affinity of Hg(II) and its inorganic compounds for sulfur-containing functional groups. This complexing behavior greatly limits the mobility of mercury in soil. Much of the mercury in soil is bound to bulk organic matter and is susceptible to elution in runoff only by being attached to suspended soil or humus. Some Hg(II), however, will be absorbed onto dissolvable organic ligands and other forms of dissolved organic carbon (DOC) and may then partition to runoff in the dissolved phase. Currently, the atmospheric input of mercury to soil is thought to exceed greatly the amount leached from soil, and the amount of mercury partitioning to runoff is considered to be a small fraction of the amount of mercury stored in soil. The results of Appendix C, which detail the calibration of soil-water partition coefficients in the watershed model, are consistent with these observations. The affinity of mercury species for soil results in soil acting as a large reservoir for anthropogenic mercury emissions (Meili et al., 1991 and Swedish EPA 1991). For example, note the mercury budget proposed by Meili et al., 1991. Even if anthropogenic emissions were to stop entirely, leaching of mercury from soil would not be expected to diminish for many years (Swedish EPA, 1991). Hg⁰ can be formed in soil by reduction of Hg(II)

compounds/complexes mediated by humic substances (Nriagu, 1979) and by light (Carpi and Lindberg, 1997). This Hg^0 will diffuse through the soil and re-enter the atmosphere. Methylmercury can be formed by various microbial processes acting on Hg(II) substances. Approximately 1-3% of the total mercury in surface soil is methylmercury, and as is the case for Hg(II) species, it will be bound largely to organic matter. The other 97-99% of total soil mercury can be considered largely Hg(II) complexes, although a small fraction of Mercury in typical soil will be Hg^0 (Revis et al., 1990). The methylmercury percentage exceeded 3% (Cappon, 1987) in garden soil with high organic content under slightly acidic conditions. Contaminated sediments may also contain higher methylmercury percentages compared to ambient conditions (Wilken and Hintelmann, 1991; Parks et al., 1989).

2.3.2 Plant and Animal Uptake of Mercury

The Hg(II) and methylmercury complexes in soil are available theoretically for plant uptake and translocation, potentially resulting in transfer through the terrestrial food chain. In reality plant uptake from ordinary soils, especially to above-ground parts of plants, appears to be insignificant (Schuster, 1991; Lindqvist et al., 1991, Chapter 9). Mosbaek et al. (1988) determined (by spiking soil with Hg^{203}) that the atmospheric contribution of the total mercury content of the leafy parts of plants is on the order of 90-95% and for roots 30-60%. The concentrations of mercury in leafy vegetables generally exceeds that of legumes and fruits (Cappon 1981, 1987), where it is not clear whether the mercury content results from air and/or soil uptake. Most plant uptake studies do not explicitly measure both the surrounding soil and air concentrations as performed in Mosbaek et al., 1988. Even when this is performed there is no way to determine whence the mercury in the plant originated. Speciation data do not provide much information; apparently any Hg^0 absorbed from the air is readily converted to Hg(II) in the plant interior, since even leafy vegetables do not appear to contain any Hg^0 (Cappon, 1987). Plants also have some mercury methylation ability (Fortmann et al., 1978), so the percentage of methylmercury in plants may not originate from root uptake. Studies which report plant uptake from soil have typically been conducted on heavily polluted soils near Chlor-alkali plants (Lenka et al., 1992; Temple and Linzon 1977; Lindberg et al., 1979), where the formation of Cl^- complexes can increase Hg(II) movement somewhat. Overall, mercury concentrations in plants, even those whose main uptake appears to be from the air, are small (see ambient mercury concentrations tables). Accordingly, livestock typically accumulates little mercury from foraging or silage/grain consumption, and mercury content in meat is low (see tables in the ambient mercury concentrations section). Due to these factors, the terrestrial pathway is not expected to be significant in comparison to the consumption of fish by humans and wildlife as an exposure pathway of concern for mercury.

2.3.3 Mercury in the Freshwater Ecosystem

There are a number of pathways by which mercury can enter the freshwater environment: Hg(II) and methylmercury from atmospheric deposition (wet and dry) can enter water bodies directly; Hg(II) and methylmercury can be transported to water bodies in runoff (bound to suspended soil/humus or attached to dissolved organic carbon); or Hg(II) and methylmercury can leach into the water body from groundwater flow in the upper soil layers. Once in the freshwater system, the same complexation and transformation processes that occur to mercury species in soil will occur along with additional processes due to the aqueous environment. Mercury concentrations are typically reported for particular segments of the water environment, the most common of which are the water column (further partitioned as dissolved or attached to suspended material), the underlying sediment (further divided into surface sediments and deep sediments); and biota (particularly fish). Discussion of several detailed studies on the movement of mercury between soil/water/sediment and how modeling results compare to these data are presented in Appendix B.

Partition coefficients have been calculated for the relative affinity of Hg(II) and methylmercury for sediment or soil over water. Values of the partition coefficient K_d (concentration of mercury in dry sediment, soil or suspended matter divided by the dissolved concentration in water) on the order of 10-100,000 ml/g soil, 100,000 ml/g sediment and 100,000+ ml/g suspended material are typically found for Hg(II) and methylmercury (Appendix B), indicating a strong preference for Hg(II) and methylmercury to remain bound to soil, bottom sediment or suspended matter (increasing affinity in that order). Of course, a river or lake freshwater system has a larger volume of water than sediment, and a significant amount of Hg(II) entering a water system may partition to the water column, especially if there is a high concentration of suspended material in the water column. It is often unclear whether the mercury in sediment will be HgCl_2 or $\text{Hg}(\text{OH})_2$ organic complexes, which can be considered more susceptible to methylation, or will be the more unreactive HgS and HgO forms.

Most of the mercury in the water column (Hg(II) and methylmercury) will be bound to organic matter, either to dissolved organic carbon (DOC; consisting of fulvic and humic acids, carbohydrates, carboxylic acids, amino acids and hydrocarbons; (Lindqvist et al., 1991, (Chapter 2)) or to suspended particulate matter. In most cases, studies that refer to the dissolved mercury in water include mercury complexes with DOC. Studies indicate that about 25%-60% of Hg(II) and methylmercury organic complexes are particle-bound in the water column. The rest is in the dissolved and DOC-bound phase (Nriagu, 1979; Bloom et al., 1991; NAS 1977). Typically, total mercury and methylmercury concentrations are positively correlated with DOC concentrations in lake waters (Driscoll et al., 1994; Mierle and Ingram, 1991). Hg^0 is produced in freshwater by humic acid reduction of Hg(II) or demethylation of methylmercury mediated by sunlight. An amount will remain in the dissolved gaseous state while most will volatilize. As noted previously, Hg^0 constitutes very little of the total mercury in the water column but may provide a significant pathway for the evolution of mercury out of the water body via Hg(II) or methylmercury \rightarrow Hg^0 \rightarrow volatilization. For many lakes, however, sedimentation of the Hg(II) and methylmercury bound to particulate matter is expected to be the dominant process for removal of mercury from the water column (Sorensen et al., 1990; Fitzgerald et al., 1991).

Generally, no more than 25% of the total mercury in a water column exists as a methylmercury complex; typically, less than 10% is observed (see Appendix B). The water column methylmercury concentration is a result of methylation of Hg(II) which occurs in the bottom sediment and the water column by microbial action and abiotic processes. In a number of sediment-water systems, it has been found that methylmercury concentrations in waters were independent of water column residence time or time in contact with sediments (Parks et al., 1989). Methylmercury in the water column which is lost through demethylation, exported downstream or taken up by biota is thought to be replaced by additional methylation of Hg(II) compounds to sustain equilibrium.

Once entering a water body, mercury can remain in the water column, be lost from the lake through drainage water, revolatilize into the atmosphere, settle into the sediment or be taken up by aquatic biota. After entry, the movements of mercury through any specific water body may be unique. Mercury in the water column, in the sediment, and in other aquatic biota appears to be available to aquatic organisms for uptake.

Methylation is a key step in the entrance of mercury into the food chain (Sorenson et al., 1990). The biotransformation of inorganic mercury species to methylated organic species in water bodies can occur in the sediment (Winfrey and Rudd, 1990) and the water column (Xun et al., 1987). Abiotic processes (e.g., humic and fulvic acids in solution) also appear to methylate the mercuric ion (Nagase et al., 1982). Not all mercury compounds entering an aquatic ecosystem are methylated, and demethylation reactions (Xun et al., 1987) as well as volatilization of dimethylmercury decrease the amount of

methylmercury available in the aquatic environment. There is a large degree of scientific uncertainty and variability among water bodies concerning the processes that methylate mercury.

Bacterial methylation rates appear to increase under anaerobic conditions, high temperatures (NJDEPE, 1993) and low pH (Xun et al., 1987; Winfrey and Rudd, 1990). Increased quantities of the mercuric species, the proper biologic community, and adequate suspended soil load and sedimentation rate are also important factors (NJDEPE, 1993). Anthropogenic acidification of lakes appears to increase methylation rates as well (Winfrey and Rudd, 1990).

Methylmercury is very bioavailable and accumulates in fish through the aquatic food web; nearly 100% of the mercury found in fish muscle tissue is methylated (Bloom et al., 1991). Methylmercury appears to be primarily passed to planktivorous and piscivorous fish via their diets. Larger, longer-lived fish species at the upper end of the food web typically have the highest concentrations of methylmercury in a given water body. A relationship exists between methylmercury content in fish and lake pH, with higher methylmercury content in fish tissue typically found in more acidic lakes (Winfrey and Rudd, 1990; Driscoll et al., 1994). The mechanisms for this behavior are unclear. Most of the total methylmercury production ends up in biota, particularly fish (Swedish EPA, 1991). In fact, bioconcentration factors (BCFs) for accumulation of methylmercury in fish (dry weight basis, compared with the water methylmercury concentration) are on the order of 10^5 - 10^6 (Bloom, 1992; Appendix D). Overall, methylmercury production and accumulation in the freshwater ecosystem places this pollutant into a position to be ingested by fish-eating organisms.

This bioaccumulation of methylmercury in fish muscle tissue occurs in water bodies that are remote from emission sources and seemingly pristine as well as in water bodies that are less isolated. Methylmercury appears to be efficiently passed through the aquatic food web to the highest trophic level consumers in the community (e.g., piscivorous fish). At this point it can be contacted by fish-consuming wildlife and humans through ingestion. Methylmercury appears to pass from the gastrointestinal tract into the bloodstream more efficiently than the divalent species.

2.4 Fate of Mercury in Marine Environments

This section describes the environmental fate of mercury in the marine environment. Two models are presented here: a composite conceptual model of the whole ocean, largely based on the data and modeling presented in the literature by Fitzgerald and coworkers; and a model developed for ocean margins by Cossa et al. (1996). Ocean margins occur at the convergence of continents and oceans; they include geologic features such as estuaries, inland seas, and continental shelves and are characterized by high productivity. These models are very general in nature and reflect only a basic understanding of the movements of mercury in marine environments. Examples of data collected from U.S. coastal waters are also included here. The arctic marine system is not examined in this section.

As noted earlier, mercury is an atmophilic element and, as such, its global transport occurs primarily through the atmosphere. Elemental mercury, the principle species found in the atmosphere, has a high vapor pressure and a low solubility in water. As a result of these properties, the half-life of atmospheric mercury is thought to be a year or longer. Elemental mercury appears to be deposited to ocean waters primarily through wet deposition. Oxidizing reactions in the atmosphere may also play a role in the conversion of elemental mercury to more reactive atmospheric species which are subsequently deposited.

Mercury found in ocean waters and sediments comprises a large reservoir of the total mercury on the planet. The conceptualization of oceans as reservoirs of mercury is fitting for they serve both as

sources of mercury to the atmosphere as well as environmental mercury sinks (Mason and Fitzgerald, 1993; 1996; Cossa et al., 1996). The forms and species of mercury present in the ocean waters and sediments may be transformed as a result of both biotic and abiotic factors within the ocean. The most significant species of mercury from an ecologic and human health perspective is monomethylmercury (MHg). Both monomethyl- and dimethylmercury have been measured in ocean waters (Mason and Fitzgerald, 1990). MHg shows strong evidence of bioaccumulation and biomagnification in the marine food web, potentially posing risks to consumer species (particularly apex marine predators and piscivores).

2.4.1 Models of Mercury in the Oceans

Rolfus and Fitzgerald (1995) employed a simple ocean model to examine mercury deposition and concentrations in fish. This model is largely derived from data collected by Fitzgerald and collaborators. In the model, the ocean is divided into 3 compartments: coastal zones, areas of upwelling, and open ocean. The open ocean accounts for roughly 90 percent of the total area of the oceans but very little fish production; the coastal and upwelling regions account for roughly 10 percent and 0.1 percent of the total area, respectively, but almost all fish production (each area accounted for about 50 percent of the total production). Mercury inputs to their model include atmospheric deposition, flow from riverine systems, and flow from upwelling regions of the ocean.

Mercury inputs are assumed to occur to the mixed layer. Corroborating this assumption, Mason and Fitzgerald (1996) have suggested that there is a relationship between increased concentrations of reactive mercury in surface waters and predicted atmospheric deposition rates in the North Atlantic. From the mixed upper layer of the ocean waters, reactive mercury is transported through attachment to particulates (i.e., scavenging) to regions or layers of the ocean where methylation occurs (those areas naturally lower in oxygen). Particles containing mercury are predicted to deteriorate as they descend, releasing the mercury. The model assumes that monomethylmercury is produced in these low oxygen regions below the thermocline in the open ocean and upwelling compartments. The mercury is then transported to the mixed layer at a depth of less than 100 meters where it is incorporated into the lower levels of the food web (Mason and Fitzgerald, 1990; 1993; 1996). Specifically, after transport from the mixed layer, most of the reactive mercury is assumed to become methylated to form dimethylmercury in the subthermocline waters, although direct formation of monomethylmercury from reactive mercury is also possible. Dimethylmercury is unstable in marine waters, and most dimethylmercury formed there is assumed to decompose to form monomethylmercury (Mason and Fitzgerald, 1996). Some of the monomethylmercury is then converted to Hg^0 , which is assumed to be transported to the surface resulting in a supersaturation of the elemental species in surface waters. Elemental mercury thus may evade back to the atmosphere from the surface waters. It is hypothesized that the transport of reactive mercury from the mixed layer controls the rate of methylmercury formation; this rate appears to be related positively to primary productivity (Mason and Fitzgerald, 1996).

In the model, reduction of reactive species to Hg^0 in the mixed layer and subsequent evasion from the mixed layer is a significant mechanism by which mercury is eliminated from marine waters, with rates of up to one percent per day reported in the open ocean. Reduction is associated with both abiotic and biotic components of the marine environment (Mason et al., 1995). Roughly 10 to 30 percent of the reduction has been attributed to abiotic factors. Abiotic reduction may be mediated by sunlight; Xiao et al. (1994) showed in an experimental aquatic system that the combination of fulvic and humic acids with synthetic sunlight resulted in reduction of dissolved divalent species. Weber (1993) has suggested that abiotic reduction may be mediated by the presence of methyltin compounds and humic acid. The remainder of the reduction of reactive species is the result of biologic activities. Evidence presented by Mason et al. (1995) indicates that bacteria and cyanobacteria are responsible for much of

the biologic reduction of mercury in the mixed layer.

Mercury methylation in the coastal compartment of the model (which includes estuarine regions) is assumed to occur both in the sediments and in the water column near the oxycline (Rolfus and Fitzgerald, 1995). It is assumed that methylmercury in this compartment is transported to the mixed layer and incorporated into the lower trophic levels of the marine food web. The total deposition of mercury was estimated at 10 Mmoles/year; the input from rivers and estuaries was estimated to be approximately 10 percent of this value (about 1 Mmole/year). The inputs to the upwelling zone from cooler, deeper waters is assumed to be 0.5 Mmoles/year.

To sustain fish methylmercury concentrations, Rolfus and Fitzgerald (1995) predict that in the open ocean 0.02 percent of the total mercury deposited is methylated and transferred via the food web to fish. Fractions of the total mercury deposited that are necessary for sustaining levels in fish from the upwelling and coastal regions of the oceans are estimated to be 5.4 percent and 20 percent, respectively. Overall, approximately 2 percent of the deposited mercury is needed to maintain fish concentrations of 0.2 ppm. The differences in necessary fractions between the three areas are related to trophic structure, deposition, and methylmercury production.

The cycling of mercury proposed by Mason et al. (1994) was reexamined and revised by Hudson et al. (1995). In this model, the yearly deposition of mercury to the oceans was assumed to be roughly the same as that of Mason et al., 1994 (approximately 10 Mmol/yr); oceanic emissions were reduced by 10 to 25 percent of the Mason value. Oceanic burial fluxes were assumed by Hudson et al. (1995) to be about half of the value assumed by Mason et al. (1994) (approximately 0.4 vs 1 Mmol/yr, respectively). Hudson et al. (1995) also accounted for mixing into the ocean interior, which was neglected by Mason et al. (1994).

Several authors, including Rolfus and Fitzgerald (1995), conclude that increases in the deposition of mercury that result from increases in anthropogenic emissions will result in enhanced food chain bioaccumulation and higher concentrations of mercury in marine fish.

2.4.2 Modeling Estuaries and Coastal Regions

Estuaries and coastal regions may be more highly affected by anthropogenic mercury sources. These regions are directly affected by mercury transported from freshwater rivers as well as direct oceanic discharges. These regions are also potentially affected to a greater degree by reactive mercury species and particulate-bound mercury released to the atmosphere from nearby anthropogenic sources. Reactive mercury species in the vapor-phase are assumed to deposit more rapidly than vapor-phase Hg⁰. The atmosphere above these coastal waters may also have higher concentrations of oxidants. For some mercury-contaminated estuaries, the primary source of mercury contamination appears to be aquatic discharges rather than atmospheric deposition.

Cossa et al. (1996) have reviewed data collected in coastal regions and constructed a mercury mass balance model specifically for these areas. In this model, fluxes from river systems to ocean margins were determined to be the largest input of total mercury to coastal systems. Annually, about 4.8 Mmol of mercury are assumed to be added via riverine systems. Cossa et al. (1996) noted that measured concentrations of total mercury are highly variable, with the highest measured concentrations found in rivers passing through urban and industrialized areas. Over 90% of the total mercury transported from river systems is bound to particles. Much of this transported particle bound mercury appears to be unreactive and is assumed to be buried in near shore sediments. However, Cossa et al. (1996) also note the potentially important lack of data describing mercury concentrations in tropical river systems.

Atmospheric deposition to coastal waters was estimated to be approximately 2 Mmol/yr. Much of the deposited mercury in the model is assumed to be chemically reactive, participating in chemical reactions in the marine environment. Atmospheric deposition of mercury to other parts of the oceans followed by transport via upwelling to the coastal regions was also thought to be an important source of total mercury into these areas, accounting for between 2.5 and 3.5 Mmol/yr. The movement of mercury from sediments to coastal waters is considerably less important than the other inputs for this model. In total, approximately 3.3 Mmol of mercury is estimated to be present in the coastal waters.

Fluxes of total mercury from coastal waters include (listed in approximate order of significance): sedimentation of particle bound mercury derived from both riverine and upwelling regions; export to the open ocean; and evasion to the atmosphere. On a global scale, evasion is speculated to be balanced by deposition to the oceans; regional imbalances may occur with deposition exceeding evasion in the northern latitudes and the converse occurring in the southern latitudes.

Cossa et al. (1996) have used this model to describe methylmercury in coastal waters. Inputs to coastal waters occur through upwelling from other parts of the ocean (0.1-0.2 Mmol/yr), atmospheric deposition (0.02 Mmol/yr), river systems (0.01 Mmol/yr), and sediments (0.001 Mmol/yr). An unknown quantity is assumed to pass back to the atmosphere through evasion after undergoing demethylation. Approximately 0.05 Mmol/yr was predicted to deposit to the sediments and less than 0.04 Mmol/yr was predicted to pass to deep ocean. The model indicates that more than half of the methylmercury in coastal aquatic species originated in waters of the deep ocean; the remainder is the result of methylation of reactive mercury in coastal waters and methylmercury from other sources. Cossa et al. (1996) noted general agreement between their model and the model proposed by Mason and Fitzgerald (1993) and Rolfus and Fitzgerald (1995).

Mercury (particularly methylmercury) clearly accumulates in coastal marine food webs. Two general food webs can be conceptualized: a benthic sediment community which includes macroinvertebrates; and a community that resides primarily in the water column, which includes phytoplankton and zooplankton as well as planktivorous and piscivorous fishes. For mercury species to accumulate within members of these food webs, they must be bioavailable and retained within the tissues.

Mercuric ions in anoxic sediments are transformed to monomethylmercury primarily through biotic processes. The bulk of this activity appears to occur in the top layers of the sediment. Compeau and Bartha (1985) showed that sulfate-reducing bacteria such as *Desulfovibrio desulfuricans* are the primary group of organisms responsible for this reaction. The organic matter content of the sediment appears to be a factor controlling mercury methylation rates (Choi and Bartha, 1994). Production of methylmercury in sediments would enable benthic organisms to accumulate this species. Gagnon and Fisher (1997) have examined bioavailability of particle-bound inorganic divalent mercury and particle-bound monomethylmercury to a species of marine mussel and concluded that the assimilation of particle-bound methylmercury is greater than particle-bound inorganic mercury. Furthermore, dissolved methylmercury and divalent mercury are both assimilated in mussels to a greater degree than particle-bound species. However, because particulate mercury species dominate dissolved mercury in coastal waters, Gagnon and Fisher (1997) have concluded that particle-bound methylmercury is likely the major source of this chemical species to mussels. Other organisms that dwell in the benthos may share these characteristics with the mussel. Of particular concern are benthic worms (Bryan and Langston, 1992) and higher invertebrates as well as some species of carnivorous fish (such as *Cynoglossus macrostomas*) (Joseph and Srivastava, 1993) and terrestrial vertebrates (such as carnivorous birds) which consume these benthic organisms. Mercury species may also impact detritivores, as high mercury concentrations have been associated with decomposing plant materials (Bryan and Langston, 1992). Some benthic

invertebrates also have been reported to contain elevated levels of inorganic mercury species.

The food web that exists primarily in the water column may be impacted by methylation of reactive mercury species. Concentrations of methylmercury in predatory piscivorous marine fishes that inhabit coastal waters (such as sharks) may exceed 1 ppm (see Volume IV of this Report). Much of this methylmercury is thought to be transferred through the food web.

2.4.3 Mercury Budget for a Coastal Waterbody in U.S.A.

Mercury fluxes may be defined more precisely for a specific body of water. For example, Vandell and Fitzgerald (1995) have developed a preliminary mercury budget for Narragansett Bay in Rhode Island. The average residence time for waters within this estuary was determined to be 24 days. River waters which drained into the bay had higher concentrations of total mercury than water in the bay; a major component of total mercury in the freshwaters was the strongly-bound fraction. Concentrations of the strongly-bound fraction appeared to decline as the salinity increased. The estimated mercury flux from the rivers which drain into the bay was 61 g/day (69% of the total flux). Point sources such as waste water treatment facilities were estimated to contribute 18.5 g/day (21% of total flux), and atmospheric deposition was estimated to be 10 g/day (10% of total flux). Approximately half of the mercury entering the bay was predicted to be retained within the estuarine sediments; the remainder of the mercury is transported to the ocean through tidal exchange.

3. MEASURED CONCENTRATIONS

This chapter first presents available measurement data for mercury in environmental media and biota. This is followed by a discussion of efforts to collect measurement data from remote locations and near anthropogenic sources of concern. Note that this chapter does include measured mercury concentrations in wildlife that function as vectors to humans but does not include measured concentrations in final receptors of concern (i.e., humans and selected wildlife receptors). Measurement data for people and wildlife are presented in Volumes IV and VI, respectively.

3.1 Analytic Measurement Methods

A number of methods can be employed to determine mercury concentrations in environmental media. The concentrations of total mercury, elemental mercury, organic mercury compounds (especially methylmercury) and chemical properties of various mercuric compounds can be measured, although speciation among mercuric compounds is not usually attempted. Recent, significant improvements and standardizations in analytical methodologies enable reliable data on the concentration of methylmercury, elemental mercury and the mercuric fraction to be separated from the total mercury in environmental media. It is possible to speciate the mercuric fraction further into reactive, non-reactive and particle-bound components. It is generally not possible to determine which mercuric species is present in environmental media (e.g., HgS or HgCl₂).

One of the significant advances in mercury analytical methods over the past decade or so has been in the accurate detection of mercury at low levels (less than 1 µg/g). Over the past two decades mercury determinations have progressed from detection of µg levels of total mercury to picogram levels of particular mercury species (Mitra, 1986 and Hovart et al., 1993a and 1993b). Typical detection limits for data used or presented in this study are on the order of 1 to 2 ng/L for water samples (Sorensen et al., 1994), 0.1 ng/g for biota (Cappon, 1987; Bloom, 1992) and 0.1 ng/m³ for atmospheric samples (Lindberg et al., 1992). Mercury contamination of samples has been shown to be a significant problem in past studies. The use of ultra-clean sampling techniques is critical for the more precise measurements required for detection of low levels of mercury.

3.2 Measurement Data

Based on the current understanding of the mercury cycle, mercury is thought to be transported primarily through the atmosphere and distributed to other compartments of the environment (Chapter 2). The primary source of mercury in terrestrial, aquatic and oceanic environments appears to be the wet or dry deposition of atmospheric mercury. Once deposited, the mercury may be revolatilized back to the atmosphere, incorporated into the medium of deposit or transferred to other abiotic or biotic components of these environments.

Elemental mercury vapor is the most common form of mercury in the atmosphere and divalent mercury the most common in soils, sediments and the water column. The most common form in most biota is Hg(II); the exception is fish in which the most common form is methylmercury.

3.2.1 Mercury Air Concentrations

As noted in section 2.3.1 anthropogenic emissions are currently thought to account for between 40-75% of the total annual input to the global atmosphere (Expert Panel on Mercury Atmospheric

Processes, 1994; Hovart et al., 1993b). Current air concentrations are thought to be 2 - 3 times pre-industrial levels. This is in agreement with the several fold increase noted in inferred deposition rates (Swain et al., 1992; Engstrom et al., 1994; Benoit et al., 1994).

As shown in Tables 3-1 and 3-2, measured U.S. atmospheric mercury concentrations are generally very low. The dominant form in the atmosphere is vapor-phase elemental mercury, although close to emission sources, higher concentrations of the divalent form may be present. Small fractions of particulate mercury and methylmercury may also be measured in ambient air. In rural areas, airborne particulate mercury is typically 4% or less of the total (particulate + gas phase) mercury in air (U.S. EPA, 1993; WHO, 1990). Particulate mercury comprises a greater fraction of the total in urban areas U.S. EPA (1993), and will consist primarily of bound Hg(II) compounds.

There is a substantial body of recent data pertaining to the atmospheric concentrations and deposition rates of atmospheric mercury collected at specific sites across the U.S. Most of the collected deposition data are from sites located some distance from large emission sources. The data have been collected by several different groups of researchers. These data are briefly summarized here.

Keeler et al., (1994) measured vapor- and particulate-phase atmospheric mercury concentrations from a site in Chicago, IL, two sites in Detroit, MI and a Lake Michigan site. The mean values are presented along with the range of measurement data. The collection period for these sites was generally less than one month; for example, the Detroit data were collected during a 10-day period.

Keeler et al., (1995) reported the results of several short-term atmospheric particulate mercury measurements in Detroit, MI and longer-term (1-year) particulate measurements at rural sites in Michigan and Vermont. In the Detroit measurements the particulates sampled were divided into two categories: fine (<2.5 µm) and coarse (>2.5 µm). The average size of the fine particles was 0.68 µm, and the average size of the coarse particles was 3.78 µm. Most (mean=88%) of the particulate mercury at the Detroit, MI site was measured on fine particles; the range for individual samples was 60-100% of total particulate.

Fitzgerald et al., (1991) reported measured mercury concentrations at Little Rock Lake, WI from May of 1988 through September of 1989 and particulate mercury concentrations at Long Island Sound (Avery Point, CT).

Table 3-1
Summary of Measured Mercury Concentration
in Air (U.S. EPA, 1993)

Total Atmospheric Mercury (ng/m³)	%Hg(II)	% Methylmercury
Rural areas: 1 - 4 Urban areas: 10 - 170	1-25% ^a	0-21% ^b

^a Higher fractions in urban areas

^b Generally % methylmercury on low end of this range

Table 3-2
Measured Vapor- and Particulate-Phase Atmospheric Mercury Concentrations

Site	Vapor-Phase Mercury Conc. in ng/m ³ Mean (Range)	Particulate-Phase Mercury Conc. in ng/m ³ Mean (Range)	Reference
Chicago, IL	8.7 (1.8-62.7)	0.098 (0.022-0.52)	Keeler et al., (1994)
Lake Michigan	2.3 (1.3-4.9)	0.028 (0.009-0.054)	Keeler et al., (1994)
South Haven, MI	2.0 (1.8-4.3)	0.019 (0.009-0.029) 0.022 (max 0.086)	Keeler et al., (1994) Keeler et al., (1995)
Ann Arbor, MI	2.0 (max 4.4)	0.10 (max 0.21) 0.022 (max 0.077)	Keeler et al., (1994) Keeler et al., (1995)
Detroit, MI Site A	>40.8 (max >74)	0.34 (max 1.09) 0.094 (0.022-0.23)	Keeler et al., (1994) Keeler et al., (1995)
Detroit, MI Site B	3.7 (max 8.5)	0.30 (max 1.23)	Keeler et al., (1994)
Pellston, MI		0.011 (max 0.032)	Keeler et al., (1995)
Underhill Center, VT	2.0 (1.2-4.2)	0.011 (0.001-0.043)	Burke et al., (1995)
Broward County, FL ^a Background Site near Atlantic Ocean (Site 1)	1.8	0.034	Dvonch et al., (1995)
Broward County, FL Inland (Site 2)	3.3	0.051	Dvonch et al., (1995)
Broward County, FL Inland (Site 3)	2.8	0.049	Dvonch et al., (1995)
Little Rock Lake, WI	1.6 (1.0-2.5)	0.022 (0.007-0.062)	Fitzgerald et al., (1991)
Long Island Sound, Avery Pt., CT ^b	(1.4-5.3): 95-100% elemental; 0-1% methylmercury	0.062 (0.005-0.18)	Particulate: Fitzgerald et al., (1991) Vapor: Bloom and Fitzgerald et al., (1988)
Crab Lake, WI	1.7	Winter 0.006 Summer 0.014	Lamborg et al., (in press)

^a Diurnal variations were also noted; elevated concentrations were measured at night. For example at site 2 the average nighttime vapor-phase concentration was 4.5 ng/m³. This was attributed to little vertical mixing and lower mixing heights that occur in this area at night.

^b 99% of Total Gaseous Mercury is Hg⁰. During 1 month (October) the mean methylmercury concentration was measured to be 12 pg/m³ with a range of 4-38 pg/m³; 0.7% of the total gaseous mercury was methylmercury. During November it was measured as <10 pg/m³ and from December through August it was measured below the detection limit (<5 pg/m³).

3.2.2 Mercury Concentrations in Precipitation

Mercury concentrations in precipitation are shown in Table 3-3. Total mercury concentrations in rainwater are typically higher than in surface water. This is thought to be the result of efficient scavenging of divalent mercury by rain droplets and the oxidation of elemental mercury to divalent mercury, while mercury in surface waters can be lost by revolatilization from the water body and sequestration in the sediment.

**Table 3-3
Measured Mercury Concentrations in Precipitation**

Site	Mean Mercury Concentration in precipitation, ng/L Mean (Range)	Reference
Ely, MN	20 in 1988 51 in 1989 13 in 1990	1988-89 data: Glass et al., (1992) 1990 data: Sorensen et al., (1992)
Duluth, MN	23 in 1988 11 in 1989 13 in 1990	1988-89 data: Glass et al., (1992) 1990 data: Sorensen et al., (1992)
Marcell, MN	18 in 1988 18 in 1989	Glass et al., (1992)
Bethel, MN	13 in 1990	Sorensen et al., (1992)
Cavalier, ND	19 in 1990	Sorensen et al., (1992)
International Falls, MN	9 in 1990	Sorensen et al., (1992)
Lamberton, MN	15 in 1990	Sorensen et al., (1992)
Raco, MN	10 in 1990	Sorensen et al., (1992)
Little Rock Lake, WI	11 (3.2-15) in rain 6 in snow	Fitzgerald et al., (1991)
Crab Lake, WI	7.9 in rain 3.3 in snow	Lamborg et al., (1995)
Underhill Center, VT ^a	8.3	Burke et al., (1995)
Broward County, FL Background Site near Atlantic Ocean (Site 1)	Total: 35 (15-56) Reactive: 1.0 (0.5-1.4)	Dvonch et al., (1995)
Broward County, FL Inland (Site 2)	Total: 40 (15-73) Reactive: 1.9 (0.8-3.3)	Dvonch et al., (1995)
Broward County, FL Inland (Site 3)	Total: 46 (14-130) Reactive: 2.0 (1.0-3.2)	Dvonch et al., (1995)
Broward County, FL 300 m from MWC (Site 4)	Total: 57 (43-81) Reactive: 2.5 (1.7-3.7)	Dvonch et al., (1995)

^a Both the concentrations of mercury in precipitation and the amount of precipitation deposited/event increased in spring and summer. Most (66%) of the mercury in the spring and fall precipitation samples (only ones tested) was dissolved. The mean concentration of reactive mercury was 1.0 ng/L. Higher particulate concentrations were observed in the winter.

Total mercury concentrations in precipitation are generally less than 100 ng/L in areas not directly influenced by an emissions source, including suburban and urban locations. Levels much higher (greater than 1000 ng/L) however, have been reported for precipitation downwind of anthropogenic mercury sources (NJDEPE 1993; see also "Measured Mercury Levels from Point Sources" section below). Areas downwind of mercury sources also show the greatest variability in precipitation concentrations. Mercury concentrations do not vary much among different precipitation types (snow, rain, and ice; NJDEPE 1993, Fitzgerald et al., 1991). Mercury precipitation concentrations show a seasonal pattern, with average concentrations several times higher during the summer than during the winter months, even in areas with a warm climate (Pollman et al., 1994). Current average precipitation mercury levels are on the order of 2-4 times greater than pre-industrial levels, based on information on the increases in mercury deposition rates (Swain et al., 1992; Expert Panel on Mercury Atmospheric Processes, 1994). The concentration of methylmercury in rain is minor, and its origins are uncertain (see Table 3-4).

Table 3-4
Measured Mercury Concentrations in Rain Which Include Methylmercury Estimates (ng/L)

Study Description	Total Mercury (ng/L)	Methylmercury (ng/L)	% Methylmercury	Reference
Swedish rain: 9 samples and 4 sites.	7.5-89.8	0.04-0.59	0.1-3.7	Lee and Iverfeldt (1991)
6 Samples at Little Rock Lake, WI.	3.5-15	0.06-0.22	0.4-6.3	Fitzgerald et al. (1991)

N.B. The difference between Total mercury and methylmercury can be considered Hg(II) species (Brosset 1981; U.S. EPA 1988). This is assumed for all water samples.

3.2.3 Mercury Deposition Rates

Environmental mercury is widely thought to be transported primarily through the atmosphere. The primary source of mercury in terrestrial, aquatic and oceanic environments appears to be the wet or dry deposition of atmospheric mercury. Once deposited, the mercury may be revolatilized back to the atmosphere, incorporated into the medium of deposit or transferred to abiotic or biotic components of these environments.

Intensive, site-specific studies of environmental mercury fluxes have been done at only a handful of U.S. sites. Watras et al., (1994) summarize the collected data and present a conceptualization of mercury fluxes between abiotic and biotic components of the environment in 7 Northern Wisconsin seepage Lakes, including Little Rock Lake. Most of the mercury was thought to enter the lakes through atmospheric deposition with wet deposition of mercury contributing the most to the total. The total amount deposited was approximately 10 µg/m²/yr. Most of the mercury deposited was thought to deposit into the sediment or volatilize back into the atmosphere. There was a net production of methylmercury in the lakes with most of the produced methylmercury being stored in the tissues of fish. The behavior of

mercury at most U.S. sites is not characterized to the same degree as at Little Rock Lake, WI. It should be noted that Little Rock Lake is a rather remote seepage lake and that atmospheric mercury may behave differently closer to emission sources. Mercury may also behave differently in different types of watersheds and waterbodies.

Measured wet deposition rates are given in Table 3-5. Similar measurements of dry deposition are rare due to limitations of analytical methods. In particular, dry deposition of divalent mercury vapor has not been measured to date. This is a major source of uncertainty because its high reactivity implies that it may be efficiently removed from the atmosphere via dry deposition.

Burke et al., (1995) measured mercury concentrations on a precipitation event basis for one year at a rural site in Vermont. Underhill Center, VT is located near Lake Champlain and was 200 Km away from a major urban or industrial area.

Dvonch et al., (1995) conducted a 4-location, 20 day mercury study in Broward County, FL. Broward county contains the city of Ft. Lauderdale as well as an oil-fired utility boiler and a municipal waste combustion facility. Daily measurements of atmospheric particulate and vapor-phase mercury were collected at 3 of the 4 sites, and daily precipitation samples were collected at all sites.

Hoyer et al., (1995) conducted a 2-year study of mercury concentrations in precipitation (by event) at 3 rural sites (Pellston, South Haven, and Dexter) in the state of Michigan.

Several authors have estimated mercury total deposition (wet and dry) rates by sample coring of various media. For example, Engstrom et al., (1994) used lake core sediments to estimate a current deposition rate of $12.5 \mu\text{g}/\text{m}^2/\text{yr}$ and a preindustrial (natural) deposition rate $3.7 \mu\text{g}/\text{m}^2/\text{yr}$ for remote lakes located in Minnesota and northern Wisconsin. Benoit et al., (1994) analyzed mercury concentrations in a peat bog at a Minnesota site. The estimated pre-1900 deposition rate at this site was $7.0 \mu\text{g}/\text{m}^2/\text{yr}$, and the current mean deposition rate was estimated to be $24.5 \mu\text{g}/\text{m}^2/\text{yr}$. Estimates of total deposition are given in Table 3-6.

Table 3-5
Mercury Wet Deposition Rates (ug/m²/yr)

Site	Wet Mercury Deposition Rates (ug/m ² /yr), Means	Reference
Ely, MN	17 in 1988 42 in 1989 6.7 in 1990	1988-89 data: Glass et al., (1992) 1990 data: Sorensen et al., (1992)
Duluth, MN	20 in 1988 6.5 in 1989 9.3 in 1990	1988-89 data: Glass et al., (1992) 1990 data: Sorensen et al., (1992)
Marcell, MN	17 in 1988 14 in 1989	Glass et al., (1992)
Bethel, MN	13 in 1990	Sorensen et al., (1992)
Cavalier, ND	6.1 in 1990	Sorensen et al., (1992)
International Falls, MN	5.5 in 1990	Sorensen et al., (1992)
Lamberton, MN	9.3 in 1990	Sorensen et al., (1992)
Raco, MN	8.9 in 1990	Sorensen et al., (1992)
Little Rock Lake, WI	4.5 from rain 2.3 from snow	Fitzgerald et al., (1991)
Crab Lake, WI	4.4 from rain 0.8 from snow	Lamborg et al., (1995)
Nothern MN	10-15	Sorensen et al., (1990)
Pellston, MI	5.8 in year 1 5.5 in year 2 0.07 ug/m ² (max 0.51) per rainfall event	Hoyer et al., (1995)
South Haven, MI	9.5 in year 1 13 in year 2 0.12 ug/m ² (max 0.85) per rainfall event	Hoyer et al., (1995)
Dexter, MI	8.7 in year 1 9.1 in year 2 0.10 ug/m ² (max 0.98) per rainfall event	Hoyer et al., (1995)
Underhill Center, VT	9.3 0.07 ug/m ² per rainfall event	Burke et al., (1995)

Table 3-6
Estimated Mercury Total Deposition Rates

Site	Estimate of Pre-industrial Annual Deposition Rates $\mu\text{g}/\text{m}^2/\text{yr}$	Estimate of Current Annual Deposition Rates $\mu\text{g}/\text{m}^2/\text{yr}$	Reference
Minnesota and northern Wisconsin	3.7	12.5	Swain et al. (1992); Engstrom et al., (1994) Lake core sediments
Minnesota	7.0	24.5	Benoit et al., (1994) Peat bog core sampling
Little Rock Lake, WI ^a		10	Fitzgerald et al., (1991)
Crab Lake, WI ^a		7.0 (86% estimated to deposit in summer)	Lamborg et al., (1995)

^a Data includes previously tabled values of wet deposition plus particulate deposition. Fitzgerald et al., 1991 did not collect particulate size data. Assuming a particulate deposition velocity of 0.5 cm/s, a yearly average particulate deposition flux of $3.5 \pm 3 \mu\text{g}/\text{m}^2/\text{yr}$ was estimated. Lamborg et al., (1995) noted the smaller particle sizes in the winter and assumed a deposition velocity 0.1 cm/s for the average winter concentrations ($7 \text{ pg}/\text{m}^3$) and a deposition velocity of 0.5 cm/s for average summer concentrations ($26 \text{ pg}/\text{m}^3$).

3.2.4 Mercury Concentrations in Water

Tables 3-7 through 3-9 show measured data in surface water, groundwater and ocean water. There is a great deal of variability in these data, some of which may be due to the seasonality of the water concentrations.

Table 3-7
Measured Mercury Concentrations in Surface Fresh Water (ng/L)

Study Description	Total Mercury (ng/L)	Methyl-mercury (ng/L)	% Methyl-mercury	Reference
Swedish lakes: 8 sites, 2-4 samples each.	1.35-15	0.04-0.8	1.0-12	Lee and Iverfeldt (1991)
Swedish mires: 8 sites, 4 samples each.	2.9-12	0.08-0.73	2-14	Westling (1991)
Lake Crescent, WA	0.163	<0.004	<2.5	Bloom and Watras (1989)
Swedish runoff: 7 sites, 3 samples each.	2-12	0.04-0.64	1-6	Lee and Iverfeldt (1991)
Little Rock Lake: reference basin.	1.0-1.2	0.045-0.06	mean of 5	Watras and Bloom (1992)
Lake Michigan (total)	7.2 microlayer 8.0 at 0.3m 6.3 at 10m			Cleckner et al. (1995)
Lake Champlain (filtered)	3.4 microlayer 3.2 at 0.3m 2.2 at 15m			Cleckner et al. (1995)
Lakes Rivers and Streams	0.04 - 74 1 - 7	NA	NA	NJDEPE (1993)

Table 3-8
Measured Mercury Concentrations in Ground/Drinking Water (ng/L)

Study Description	Total Mercury	Reference
Southern New Jersey domestic wells	Up to and exceeding 2000	Dooley (1992)
Drinking/Tap water in U.S.	0.3-25	NJDEPE (1993)
Washington State well	0.3	Bloom (1989)

**Table 3-9
Measured Mercury Concentrations in Ocean Water (ng/L)**

Study Description	Total Mercury (ng/L)	Reference
Review on concentrations of dissolved mercury: Open ocean	0.5 - 3.0	WHO (1989)
Review on concentrations of dissolved mercury: Coastal sea water	2 - 15	WHO (1989)
Hg along the Italian coast	Dissolved: 1.7-12.2 Particulate: 0.3 - 80	Seritti et al. (1982)
Puget Sound near-shore sea water	0.72	Hovert et al. (1993b)

Total mercury levels in lakes and streams generally are lower than mercury levels found in precipitation, with levels typically well under 20 ng/L (NJDEPE 1993). Elevated levels may be found in lakes and streams thought to be impacted by anthropogenic mercury sources but not to the extent that precipitation levels appear to be. Total lake water mercury concentrations tend to increase with lower pH and higher humic content (U.S. EPA, 1993). Present-day mercury levels in freshwater are thought to be 2 - 7 times greater than pre-industrial levels (Swedish EPA, 1991). Methylmercury percentages are higher than those in precipitation, ranging from 5 - 20%, with levels around 10% being the most common. Mercury levels continue to increase in many lakes (Swedish EPA, 1991).

It is important to note that much of the data on mercury in drinking water and ground water report levels as below detection limits (U.S. EPA, 1988), although the detection limit was a somewhat dated 100 ng/L. Lindqvist and Rodhe (1985) report that the concentration range for mercury in drinking water is the same as in rain, with an average estimate for total mercury of 25 ng/L. It seems reasonable to assume similar speciation as no speciation data could be found. Dooley (1992) states that mercury concentrations in pristine wells are likely to be below that of unpolluted surface waters.

Table 3-9 shows published values for mercury concentrations in ocean water. Limited speciation data are available. Hovert et al. (1993b) reported that 2.8% of total mercury was methylmercury, which is not much different from the speciation in fresh water. Total mercury concentrations in ocean and sea water vary from undetectable to over 1000 ng/l (Nriagu, 1979).

3.2.5 Mercury Concentrations in Soil/Sediment

Table 3-10 presents reported mercury concentrations in soil. The relatively high concentrations illustrate the strong partitioning of mercury to soils. Based on the soil data presented, it can be inferred that soil, while not as important as the atmosphere, is a significant reservoir for environmental mercury. The concentrations are presented as total mercury and methylmercury. Most of the soil mercury is thought to be Hg(II).

Table 3-10
Measured Mercury Concentration in Soil

Study Description	Total Mercury (ng/g dry weight)	Methylmercury (ng/g dry weight)	% Methylmercury	Reference
Discovery Park, Seattle, WA	29 - 133	0.3-1.3	0.6-1.5	Lindqvist et al. (1991)
Wallace Falls, Cascades (WA)	155 - 244	1.0-2.6	0.5-1.2	Lindqvist et al. (1991)
Control Soil, New York State	117	4.9	4.2	Cappon (1981)
Compost, New York State	213	7.3	3.3	Cappon (1987)
Garden soil, New York State	406	22.9	5.3	Cappon (1987)
Typical U.S. Soils	8 - 117	NA	NA	NJDEPE (1993)

N.B. As in water samples the fraction of Hg^0 , if present at all, will be very small compared to $Hg(II)$ (Revis et al., 1990), and the difference between Total mercury and methylmercury can be considered to be $Hg(II)$ to be species.

Soil mercury levels are usually less than 200 ng/g in the top soil layer, but values exceeding this level are not uncommon, especially in areas affected by anthropogenic activities (see section 2.6). Soil mercury levels vary greatly with depth, with nearly all the mercury found in the top 20 cm of soil. Mercury levels are also positively correlated with the percentage of organic matter in soil (Nriagu 1979). Top soil mercury concentrations are estimated to be a factor of 4-6 (Swedish EPA, 1991) higher now as compared to pre-industrial concentrations. Methylmercury percentages in soil are typically on the order of a few percent. Soil mercury levels are continuing to rise (Fitzgerald 1994), and most (up to 95%) of the anthropogenic mercury released over the past 100 years resides in surface soil (Fitzgerald, 1994; Expert Panel on Mercury Atmospheric Processes, 1994). Mercury from soil provides in most cases (depending on watershed characteristics) the main source of mercury to water bodies and fish. Mercury is very slowly removed from soil, and long after anthropogenic emissions are reduced, soil and water concentrations can be expected to remain elevated.

Sediment mercury levels are typically higher than soil levels, and concentrations exceeding 200 ng/g are not unusual (see Table 3-11). Sediment mercury levels follow the same trends as soil in regards to depth, humic matter, and historical increases, and methylmercury percentage. There is some evidence suggesting that the methylmercury percentage increases with increasing total mercury contamination (Parks et al., 1989).

Two large-scale monitoring projects have measured mercury levels in coastal sediments: the National Oceanic and Atmospheric Administration's (NOAA's) National Status and Trends (NS&T) Program and EPA's Environmental Monitoring and Assessment Program (EMAP) for estuaries. These programs and their findings are discussed below.

Table 3-11
Measured Mercury Concentrations in Freshwater Aquatic Sediment

Study Description	Total Mercury (ng/g dry weight)	Reference
80 MN Lakes	34-753; mean 174	Sorensen et al. (1990)
North Central WI Lakes	90-190	Rada et al. (1989)
Little Rock Lake, WI	10-170	Wiener et al. (1990)
U.S. Lake sediment mean ranges	70-310	NJDEPE (1993)

NOAA's NS&T Program was initiated in 1984 to determine the status of, and detect changes in, the environmental quality of our Nation's estuarine and coastal waters. Currently, the NS&T Program conducts periodic chemical monitoring for more than 70 organic chemicals and trace elements in benthic (bottom-dwelling) fish, sediments and bivalve mollusks (mussels and oysters) at more than 300 sites throughout the United States. The Mussel Watch Project and the Benthic Surveillance Project, which are components of the NS&T Program, have measured concentrations of mercury in sediments. These data, collected during the period 1984-1991, are summarized on a regional basis in Table 3-12.

Concentrations along the North Atlantic, Middle Atlantic, and Pacific coasts (0.14, 0.12, and 0.08 µg/g dry weight, respectively) are higher relative to those along the South Atlantic and Eastern and Western Gulf coasts (0.03, 0.05, and 0.04 µg/g dry weight, respectively). The highest concentrations measured exceed 2.0 µg/g dry weight along the North Atlantic and Pacific coasts (5.00 and 2.20 µg/g dry weight, respectively). Information on temporal trends is not available.

EMAP is a national program initiated in 1989 in response to the EPA Science Advisory Board's recommendation to monitor the status and trends of U.S. ecological resources -- terrestrial, freshwater and marine. The program is directed by EPA's Office of Research and Development, with participation by other federal agencies (e.g., NOAA, U.S. Forest Service, U.S. Fish and Wildlife Service). One of the original goals of EMAP was to quantitatively evaluate the condition of coastal estuaries by monitoring environmental conditions, including sediment contamination. More recently, the goals of EMAP have been refined to emphasize "indicator development" and other methods for translating monitoring data into assessments of ecological condition. There will be diminished emphasis on large-scale monitoring. Nevertheless, sediment contamination levels were measured in the Virginia Province (Cape Cod to Chesapeake Bay) during the period 1990-1993. For the 1992 samples, the median mercury concentrations in Chesapeake Bay and Long Island Sound sediments were 0.054 and 0.088 µg/g dry weight, respectively (Strobel et al. 1994).

Table 3-12
Mercury Concentration in Sediments from NS&T Sites (1984-1991)

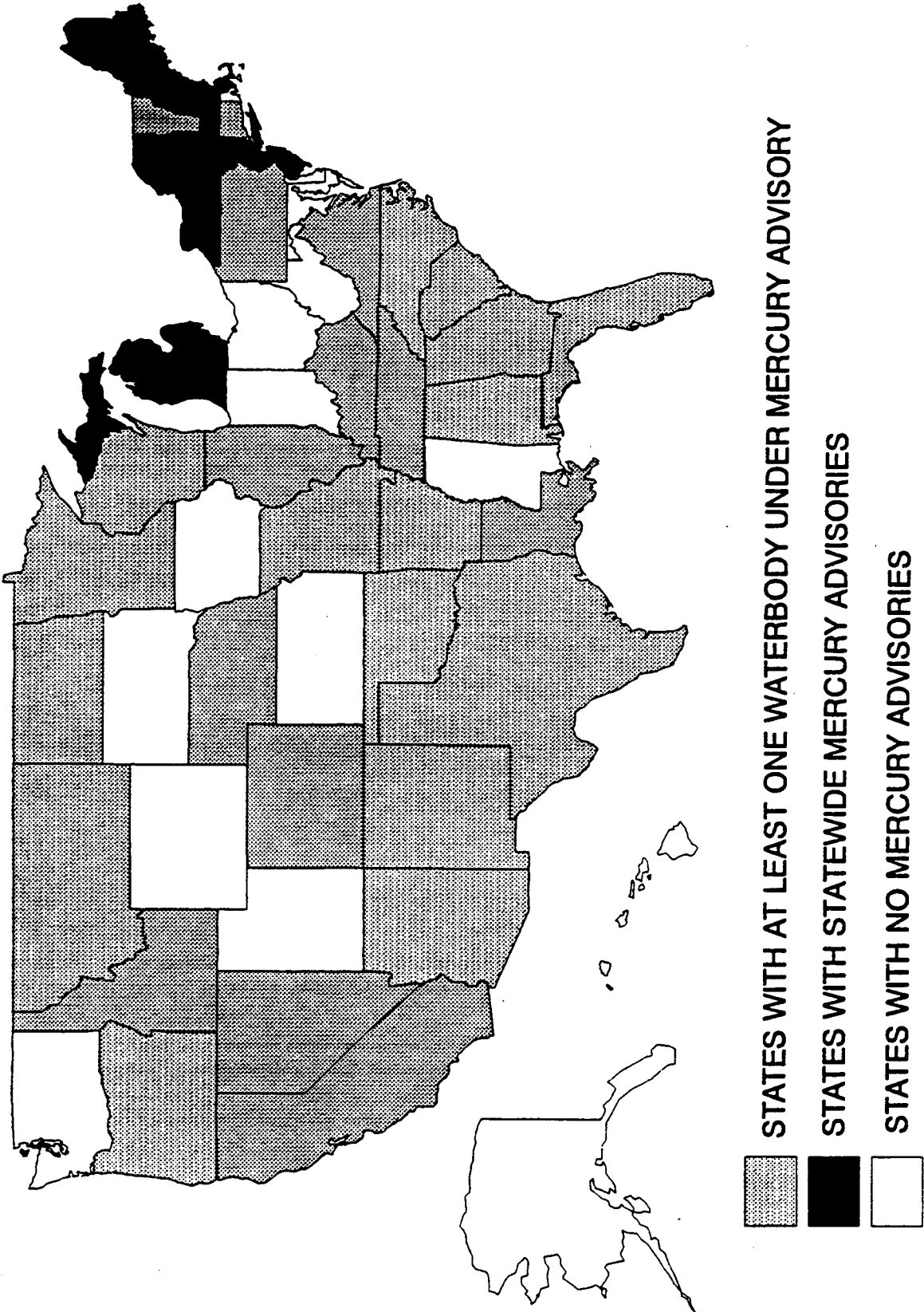
Region	States	Concentration Range ($\mu\text{g/g-dry weight}$)	Median Concentration ($\mu\text{g/g-dry weight}$)
North Atlantic	ME, MA , RI, CT, NY, NJ	0.007-5.00	0.14
Middle Atlantic	DE, MD, VA	0.010-0.84	0.12
South Atlantic	NC, SC, GA, FL (east coast)	0.002-0.27	0.03
Eastern Gulf of Mexico	FL (west coast), AL, MS	0.007-0.98	0.05
Western Gulf of Mexico	LA, TX	0.009-0.34	0.04
Pacific	CA, OR, WA, HI, AK	0.009-2.20	0.08

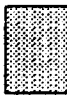


3.2.6 Mercury Concentrations in Biota

Elevated mercury concentrations in fish have been measured across the U.S. As seen in Figure 3-1, 35 states have at least one waterbody under mercury advisory, including six states with statewide mercury advisories. There are differences in the action levels for advisories from state to state. Fish mercury concentrations are the single greatest concern in regards to the effects of mercury pollution. Fish in lakes seemingly far removed from anthropogenic sources have been found to have mercury levels of concern to human health. Mercury levels in fish vary greatly, often showing little correlation to proximity to mercury emission sources. In Sweden, fish mercury concentrations in 1 kg pike have risen from 0.05 - 0.3 $\mu\text{g/g}$ to 0.5 - 1.0 $\mu\text{g/g}$ in southern and central Sweden over the last 100 years. Fish mercury concentrations in most cases strongly correlate with pH (lower pH resulting in higher methylmercury concentrations). Other lake characteristics have been found to correlate with fish mercury levels, but not as strongly as pH, with some factors showing a positive correlation in some lakes and a negative correlation in others (U.S. EPA, 1993).

It has been so well established that most (>95%) of the total mercury content of fresh and saltwater fish is methylmercury (Bloom, 1992) that currently some researchers no longer speciate fish samples (NJDEPE 1994). Thus, only total mercury concentrations are reported here. Approximately 90% of the mercury in shrimp, mussels and copepods from IAEA standards contain other forms of mercury (only about 10% of total mercury is methylmercury), but rather about 90% of the mercury total concentration is ethylmercury (Bloom, 1992). (It should be noted that ethylmercury exposure was not assessed in this document.)

Figure 3-1
Mercury Fish Consumption Advisories of the U.S.



-  STATES WITH AT LEAST ONE WATERBODY UNDER MERCURY ADVISORY
-  STATES WITH STATEWIDE MERCURY ADVISORIES
-  STATES WITH NO MERCURY ADVISORIES

SOURCE: USEPA FISH ADVISORY DATABASE.

The data from two studies national in scope are summarized in Table 3-13. Lowe et al. (1985) reported mercury concentrations in fish from the National Contaminant Biomonitoring Program. The fresh-water fish data were collected between 1978-1981 at 112 stations located across the United States. Mercury was measured by a flameless cold vapor technique, and the detection limit was 0.01 $\mu\text{g/g}$ wet weight. Most of the sampled fish were taken from rivers (93 of the 112 sample sites were rivers); the other 19 sites included larger lakes, canals, and streams. Fish weights and lengths were consistently recorded. A wide variety of types of fishes were sampled; most commonly carp, large mouth bass, and white sucker. The geometric mean mercury concentration of all sampled fish was 0.11 $\mu\text{g/g}$ wet weight; the minimum and maximum concentrations reported were 0.01 and 0.77 $\mu\text{g/g}$ wet weight, respectively. The highest reported mercury concentrations (0.77 $\mu\text{g/g}$ wet weight) occurred in the northern squawfish of the Columbia River.

"A National Study of Chemical Residues in Fish" was conducted by U.S. EPA (1992) and also reported by Bahnick et al. (1994). In this study mercury concentrations in fish tissue were analyzed. Five bottom feeders (e.g., carp) and five game fish (e.g., bass) were sampled at each of the 314 sampling sites in the U.S. The sites were selected based on proximity to either point or non-point pollution sources. Thirty-five "remote" sites among the 314 were included to provide background pollutant concentrations. The study primarily targeted sites that were expected to be impacted by increased dioxin levels. The point sources proximate to sites of fish collection included the following: pulp and paper mills, Superfund sites, publicly owned treatment works, and other industrial sites. Data describing fish age, weight, and sex were not consistently collected. Whole body mercury concentrations were determined for bottom feeders, and mercury concentrations in fillets were analyzed for the game fish. Total mercury levels were analyzed using flameless atomic absorption; the reported detection limits were 0.05 $\mu\text{g/g}$ early in the study and 0.0013 $\mu\text{g/g}$ as analytical technique improved later in the analysis. Mercury was detected in fish at 92% of the sample sites. The maximum mercury level detected was 1.8 $\mu\text{g/g}$, and the mean across all fish and all sites was 0.26 $\mu\text{g/g}$. The highest measurements occurred in walleye, large mouth bass, and carp. The mercury concentrations in fish around publicly owned treatment works were highest of all point source data; the median value measured were 0.61 $\mu\text{g/g}$. Paper mills were located near many of the sites where mercury-laden fish were detected.

The mean mercury concentrations in all fish sampled differ by approximately a factor of 2 for each study. The mean mercury concentration reported by Lowe et al. was 0.11 $\mu\text{g/g}$, whereas the mean mercury concentration reported by Bahnick et al. was 0.26 $\mu\text{g/g}$. This is difference which can be extended to the highest reported mean concentrations in fish species. Note that the average mercury concentrations in bass and walleye reported by Bahnick's data are higher than the northern squawfish, which is the species with the highest mean concentration of mercury identified by Lowe et al. (1985).

The bases for these differences in methylmercury concentrations are not immediately obvious. The trophic positions of the species sampled, the sizes of the fish, or ages of fish sampled could significantly increase or decrease the reported mean mercury concentration. Older and larger fish, which occupy higher trophic positions in the aquatic food chain, would, all other factors being equal, be expected to have higher mercury concentrations. The sources of the fish will also influence fish mercury concentrations. Most of the fish obtained by Lowe et al. (1985) were from rivers. The fate and transport of mercury in river systems is less well characterized than in small lakes. Most of the data collected by Bahnick et al. (1994) were collected with a bias toward more contaminated/industrialized sites, although not sites specifically contaminated with mercury. It could be that there is more mercury available to the aquatic food chains at the sites reported by Bahnick et al. (1994). Finally, the increase in the more recent data as reported in Bahnick et al., 1994 could be the result of temporal increases in mercury concentrations.

Table 3-13
Freshwater Fish Mercury Concentrations from Nationwide Studies

Species	Mean Mercury Concentration $\mu\text{g/g}$ (fresh weight)	
	Lowe et al., (1985)	U.S.EPA (1992c) and Bahnick et al., (1994)
Bass	0.157	0.38 ¹
Bloater	0.093	
Bluegill	0.033	
Smallmouth Buffalo	0.096	
Carp, Common	0.093	0.11
Catfish	0.088 ²	0.16 ³
Crappie (black, white)	0.114	0.22
Fresh-water Drum	0.117	
Northern Squawfish	0.33	
Northern Pike	0.127	0.31
Perch (white and yellow)	0.11	
Sauger	0.23	
Sucker	0.114 ⁴	0.167 ⁵
Trout (brown, lake, rainbow)	0.149	0.14 ⁶
Walleye	0.100	0.52
Mean of all measured fish	0.11	0.26

¹ Average concentration found in white, largemouth and smallmouth bass.

² Channel, largemouth, rock, striped, white catfish.

³ Channel and flathead catfish.

⁴ Bridgelip, carpsucker, klamath, largescale, longnose, rivercarpsucker, tahoe sucker.

⁵ Mean of average concentrations found in white, redhorse and spotter sucker.

⁶ Brown trout only.

Another national study of pollutant contamination in biota is the Mussel Watch Project, which is a component of NOAA's NS&T Program. The Mussel Watch Project measures concentrations of organic and trace metal contaminants in fresh whole soft-parts of bivalve mollusks (i.e., mussels and oysters) at over 240 coastal and estuarine sites. These data, which are available for 1986-1993, are summarized in Table 3-14. Concentrations along the North Atlantic, Eastern Gulf, and Pacific coasts (0.15, 0.14, and 0.11 $\mu\text{g/g}$ dry weight, respectively) are higher relative to those along the Middle Atlantic, South Atlantic, and Western Gulf coasts (0.06, 0.09, and 0.08 $\mu\text{g/g}$ dry weight, respectively). The highest concentrations measured exceed 1.0 $\mu\text{g/g}$ dry weight along the Western Gulf and Pacific coasts (1.80 and 1.01 $\mu\text{g/g}$ dry weight, respectively).

Table 3-14
Mercury Concentration in Bivalve Mollusks from Mussel Watch Sites (1986-1993)

Region	States	Concentration Range ($\mu\text{g/g-dry weight}$)	Median Concentration ($\mu\text{g/g-dry weight}$)
North Atlantic	ME, MA , RI, CT, NY, NJ	0.005-0.72	0.15
Middle Atlantic	DE, MD, VA	0.003-0.33	0.06
South Atlantic	NC, SC, GA, FL (east coast)	0.012-0.98	0.09
Eastern Gulf of Mexico	FL (west coast), AL, MS	0.005-0.72	0.14
Western Gulf of Mexico	LA, TX	0.002-1.80	0.08
Pacific	CA, OR, WA, HI, AK	0.002-1.01	0.11

For the purpose of temporal analysis, annual Mussel Watch data on mercury concentrations in bivalve mollusks at specific sites have been aggregated to national geometric means (O’Conner and Beliaeff 1995). The national means, which are shown in Table 3-15, do not show any temporal trend in mercury concentrations in mussels and oysters for the period 1986-1993.

Table 3-15
Nationwide Geometric Mean Concentrations of Mercury in Bivalve Mollusks (1986-1993)

	1986	1987	1988	1989	1990	1991	1992	1993
Mean Mercury Concentration ($\mu\text{g/g-dry weight}$)	0.11	0.11	0.11	0.12	0.09	0.11	0.11	0.12

Temporal trend analysis was also conducted on a site-by-site basis for 154 Mussel Watch sites that had data for at least six years during the period 1986-1993 (O’Conner and Beliaeff 1995). Seven sites exhibited an increasing trend in mercury concentrations, and eight sites exhibited a decreasing trend in mercury concentrations, with 95% statistical confidence. The sites with increasing and decreasing trends are shown in Table 3-16.

Table 3-16
Trends in Mercury Concentrations in Bivalve Mollusks (1986-1993)

Site Name	State
Increasing Trend	
Mobile Bay - Hollingers Island Channel	AL
Lake Borgne - Malheureux Point	LA
Galveston Bay - Confederate Reef	TX
Point Loma - Lighthouse	CA
San Francisco Bay - Emeryville	CA
Point Arena - Lighthouse	CA
Crescent - Point St. George	CA
Decreasing Trend	
Charlotte Harbor - Bord Island	FL
Mississippi Sound - Pascagoula Bay	MS
Sabine Lake - Blue Buck Point	TX
Mission Bay - Ventura Bridge	CA
Marina Del Rey - South Jetty	CA
Elliott Bay - Four-Mile Rock	WA
Sinclair Inlet - Waterman Point	WA
Whidbey Island - Possession Point	WA

The studies reported by Lowe et al. (1985) and by Bahnick et al. (1994) and the Mussel Watch Project are systematic, national examinations of pollutant concentrations in biota. Higher mercury concentrations in biota have been found in other studies that focused on specific locations. These data, which are presented below, indicate wide variations in mercury levels in biota.

Table 3-17 summarizes measured mercury concentrations in freshwater sportfish as reported by a number of researchers, and Table 3-18 summarizes available data on measured mercury concentrations in saltwater commercial fish. In general, the mercury levels in freshwater fish appear to be higher than the levels in saltwater fish. Several authors report mercury levels that are higher than 1 ug/g (1 µg/g) in the muscle of freshwater fish: NJDEPE (1994); Wren, et al. (1991); Lathrop et al. (1989); MacCrimmon et al. (1983); Lange et al. (1993); Glass et al. (1990); Sorensen et al. (1990); U.S. EPA (1992a), U.S. EPA (1992b); Simonin et al. (1994); and Florida DER (1990). Due to the importance of fish mercury levels, discussions of several of the mercury studies referenced in the tables are summarized here.

The New Jersey Department of Environmental Protection and Energy collected individual fish samples throughout the state (NJDEPE 1994). Generally larger fish were sampled from New Jersey rivers, lakes and reservoirs known to be contaminated with mercury or at risk for mercury contamination.

Samples were prepared as skin-off fillets, and clean protocols were used throughout the analysis. Mercury levels in fish exceeded the FDA Criterion of 1.0 ug/g (wet weight) in 50 of the 313 sampled fish and at 15 of the 55 sample locations. It is noted that the FDA criterion is applicable to fish sold through interstate commerce in the United States under the Food, Drug and Cosmetic Act (21 U.S.C. 301). Levels of greater than 0.5 ug/g (wet weight) occurred in 108 of the 313 fish. The highest reported concentration occurred in a largemouth bass taken from the Atlantic City Reservoir at a concentration of 8.94 ug/g. The mercury levels in all six of the largemouth bass sampled from this site were elevated. At the Atlantic City site the range of mercury concentrations was 3.05 to 8.94 and the mean was 4.5 ug/g. The overall study range for largemouth bass was 0.05 to 8.94 ug/g. High levels were also noted in chain pickerel particularly those obtained from a series of low pH waterbodies. The range of mercury concentrations reported for chain pickerel was 0.09 to 2.82 ug/g. Levels of greater than 1 ug/g were also reported in yellow bullheads (maximum reported 1.47 ug/g). Acidity of these waterbodies was also measured, and reported in Table 3-17 are the ranges of mean fish mercury concentrations for 9 pH categories.

Simonin et al. (1994) collected yellow perch from 12 drainage lakes located in Adirondack Park, New York State, during the fall of 1987. The age of the fish was determined from acetate impressions of the scales, and filets (including the skin and ribs) were analyzed for total mercury. Lake water samples were taken late in the summer of 1987 and included analysis of pH, dissolved inorganic and organic carbon (DIC and DOC), conductance, color, acid neutralizing capacity (ANC) and a number of metals and ligands. A total of 372 fish were collected, with 7 to 53 fish taken per lake. Fish ranged from 2+ to 11+ years of age, with 4+ year old fish being the most common; fish of this age were used in making comparisons among lakes. It was found that air-equilibrated pH was the best predictor of mercury concentrations, with lower lake pH resulting in higher mercury levels in perch. This was clear despite large variations in mercury concentrations from the same lake. Perch mercury concentrations from the highest pH lake (considering all ages) ranged from 0.07 - 0.27 $\mu\text{g/g}$ wet wt., the corresponding range for the lowest pH lake was 0.63 - 2.28 $\mu\text{g/g}$. Other variables that were highly correlated ($p < 0.0001$) with fish mercury levels included ANC, DIC, Ca, conductivity, Mg and field pH. Variables less strongly correlated ($p < 0.05$) include DOC, Na, SO_4 , lake area and watershed area. Variables not correlated with 4+ year old yellow perch include color, total phosphorus, Al, Cl-, lake depth, ratio of watershed area to lake area, ratio of watershed area to lake volume, fish length and fish weight. For a given lake, fish age was most strongly correlated with mercury concentrations; older fish had the highest concentrations. Fish length and weight were also significantly correlated.

Table 3-17
Measured Mercury Concentrations Freshwater Sportfish (Total Mercury, ug/g wet wt.)

Study	Pike/Pickereel	Walleye	Bass	Bottom Feeders	Panfish	Trout	Reference	
12 Adirondack Lakes					2 year old: 0.23 4 year old: 0.36 6 year old: 0.41 8 year old: 0.46 10+ year old: 1.65		Simonin et al. (1994)	
16 New York Lakes					Yellow Perch: 0.01 - 0.64 Punkin Seed: 0.01 - 0.19		Mills et al., (1994)	
42 New Jersey Lakes and Rivers, averages of 9 pH categories	0.15-1.45		0.15-1.16	0.07-0.72	0.10-0.32	0.05-0.64	NJDEPE (1994)	
Historical trends in mean fish concentrations in NE Minnesota Lakes	1930s (museum): 0.08-0.29 1980s: 0.12-0.37	1930s: 0.08-0.20 1980s: 0.07-0.73					Swain and Helwig (1989)	
Mean concentrations in 65 northern MN lakes	0.14-1.52	0.13-1.75					Sorensen et al. (1990)	
Ashtabula River, OH; Means			LMouth: 0.15 Smouth: 0.12	Carp: 0.05	Bluegill:0.07-0.17		U.S. EPA (1992a)	
Saginaw River, MI; Means		Fillets: .12		Carp: 0.07			U.S. EPA (1992b)	
Northern Michigan Lakes	0.10-1.64		0.11-1.00				Gloss et al. (1990)	
Large fish above dams in 3 Michigan rivers	0.11 - 0.28	< 0.05 to 0.72		< 0.05 to 0.23	< 0.05 to 0.73	0.20 - 0.45	Giesy et al., (1994)	
Mean Concentrations (and ranges) in Fish from the St. Louis River, MN	0.28 (0.25-0.31)	0.29 (0.20-0.37)	S. Mouth: 0.25 (0.12-0.43) Rock: 0.35 (0.14-0.61)	Channel Cat: 0.39 (0.20-0.74) Red H. Sucker: 0.41 (0.32-0.55) W. Sucker: 0.27 (0.12-0.37)			Sorensen et al. (1991)	
Historical trends in Onondaga lake Smallmouth Bass, Syracuse, NY			1970: 1.96 1972: 1.26 1974: 0.81	1975: 1.09 1977: 0.87 1978: 0.68	1979: 0.68 1981: 1.23 1983: 1.08	1984: 1.04 1985: 1.20 1986: 1.05	1987: 1.75 1988: 1.43 1989: 1.71	Sloan et al. (1990)
38 Wisconsin Lakes		0.16-1.74					Lathrop et al. (1989)	
34 Northern Wisconsin Lakes		0.19 - 0.999					Gerstenberger et al., (1993)	
53 Florida lakes			0.04-1.90				Lange et al. (1993)	

Table 3-17 (continued)
Measured Mercury Concentrations Freshwater Sportfish (Total Mercury, $\mu\text{g/g}$ wet wt.)

Study	Pike/Pickereel	Walleye	Bass	Bottom Feeders	Panfish	Trout	Reference
Florida Surface Waters			Lakes: 0.07 - 0.85 Streams: 0.22 - 2.37				Florida DER (1990)
Mean Concentrations (and ranges) in Maine Predatory Fishes	0.92 (0.58-1.22)		LMouth: 0.57 (0.26-0.95) SMouth: 0.67 (0.31-1.12)		Yellow Perch: 0.28 (0.18-0.81)	Brook: 0.30 (0.05-0.79) Brown: 0.29 (0.12-0.45)	Stafford (1991)
St. Lawrence River Drainage at Massena, NY.	0.21-0.97	0.24-0.93	SMouth: 0.37-0.71 Rock: 0.34-0.76	W. Sucker: 0.12-0.55 B. Bullhead: 0.08-0.32	Punkinseed: 0.10-0.35 Y. Perch: 0.18-0.59	Rainbow: 0.12-0.13	New York DEC (1990)
9 Canadian Shield Lakes						0.24-3.44	MacCrimmon et al. (1983)
Ontario Lakes	0.07-1.28	0.09-3.24					Wren et al. (1991)

Table 3-18
Measured Mercury Concentrations in Saltwater Commercial Fish and Shellfish (ug/g wet wt.)

Fish	Mean Hg-tot			References
	U.S. EPA (1992c)	Cramer (1992)	USDOC (1978)	
Cod	0.03		0.13	
Canned Tuna		0.17	0.24	
Fish Sticks			0.21	
Shrimp		0.18	0.46	
Crabs/Lobsters		0.03-0.08	0.25	
Salmon	0.05-0.32	.005		
Flounder	0.03	0.06		
Clams	0.02		0.05	
Boston Mackerel (2 samples)		0.03-0.05		NJDEPE (1994)
Porgy (3 samples)		0.08-0.14		NJDEPE (1994)
Spot (5 samples)		0.02-0.06		NJDEPE (1994)
Scallops		0.05		NOAA (1978)

Ocean fish are an important source of mercury exposure. Although these fish appear to have lower mercury concentrations, humans typically consume higher quantities of these types of fish. Wildlife, depending on location, also may typically consume ocean fish species. Data on mercury concentrations in marine finfish obtained from the National Marine Fisheries Service are summarized in Table 3-19. Tables 3-20 and 3-21 summarize data from the National Marine Fisheries Service on mercury concentrations in marine shellfish and molluscan cephalopods.

Table 3-19
Mercury Concentrations in Marine Finfish

Fish	Mercury Concentration ($\mu\text{g/g}$, wet weight)	Source of Data
Anchovy ¹	0.047	NMFS
Barracuda, Pacific ²	0.177	NMFS
Cod ³	0.121	NMFS
Croaker, Atlantic	0.125	NMFS
Eel, American	0.213	NMFS
Flounder ⁴	0.092	NMFS
Haddock	0.089	NMFS
Hake ⁵	0.145	NMFS
Halibut ⁶	0.25	NMFS
Herring ⁷	0.013	NMFS
Kingfish ⁸	0.10	NMFS
Mackerel ⁹	0.081	NMFS
Mullet ¹⁰	0.009	NMFS
Ocean Perch ¹¹	0.116	NMFS
Pollack	0.15	NMFS
Pompano	0.104	NMFS
Porgy	0.522	NMFS
Ray	0.176	NMFS
Salmon ¹²	0.035	NMFS
Sardines ¹³	0.1	NMFS
Sea Bass	0.135	NMFS
Shark ¹⁴	1.327	NMFS
Skate ¹⁵	0.176	NMFS
Smelt, Rainbow	0.1	NMFS
Snapper ¹⁶	0.25	NMFS
Sturgeon ¹⁷	0.235	NMFS
Swordfish	0.95	FDA Compliance Testing
Tuna ¹⁸	0.206	NMFS
Whiting (silver hake)	0.041	NMFS

¹ This is the average of NMFS mean mercury concentrations for both striped anchovy (0.082 $\mu\text{g/g}$) and northern anchovy (0.010 $\mu\text{g/g}$).

² USDA data base specified the consumption of the Pacific Barracuda and not the Atlantic Barracuda.

³ The mercury content for cod is the average of the mean concentrations in Atlantic Cod (0.114 $\mu\text{g/g}$) and the Pacific Cod (0.127 $\mu\text{g/g}$).

⁴ The mercury content for flounder is the average of the mean concentrations measured in 9 types of flounder: Gulf (0.147 $\mu\text{g/g}$), summer (0.127 $\mu\text{g/g}$), southern (0.078 $\mu\text{g/g}$), four-spot (0.090 $\mu\text{g/g}$), windowpane (0.151 $\mu\text{g/g}$), arrowtooth (0.020 $\mu\text{g/g}$), witch (0.083 $\mu\text{g/g}$), yellowtail (0.067 $\mu\text{g/g}$).

μg/g), and winter (0.066 μg/g).

⁵ The mercury content for Hake is the average of the mean concentrations measured in 6 types of Hake: silver (0.041 μg/g), Pacific (0.091 μg/g), spotted (0.042 μg/g), red (0.076 μg/g), white (0.112 μg/g), and blue (0.405 μg/g).

⁶ The mercury content for Halibut is the average of the mean concentrations measured in 3 types of Halibut: Greenland, Atlantic, and Pacific.

⁷ The mercury content for Herring is the average of the mean concentrations measured in 4 types of Herring: blueback (0.0 μg/g), Atlantic (0.012 μg/g), Pacific (0.030 μg/g), and round (0.008 μg/g).

⁸ The mercury content for Kingfish is the average of the mean concentrations measured in 3 types of Kingfish: Southern, Gulf, and Northern.

⁹ The mercury content for Mackerel is the average of the mean concentrations measured in 3 types of Mackerel: jack (0.138 μg/g), chub (0.081 μg/g), and Atlantic (0.025 μg/g).

¹⁰ The mercury content for Mullet is the average of the mean concentrations measured in 2 types of Mullet: striped (0.011 μg/g) and silver (0.007 μg/g).

¹¹ The mercury content for Ocean Perch is the average of the mean concentrations measured in 2 types of Ocean Perch: Pacific (0.083 μg/g) and Redfish (0.149 μg/g)

¹² The mercury content for Salmon is the average of the mean concentrations measured in 5 types of Salmon: pink (0.019 μg/g), chum (0.030 μg/g), coho (0.038 μg/g), sockeye (0.027 μg/g), and chinook (0.063 μg/g).

¹³ Sardines were estimated from mercury concentrations in small Atlantic Herring.

¹⁴ The mercury content for Shark is the average of the mean concentrations measured in 9 types of Shark: spiny dogfish (0.607 μg/g), (unclassified) dogfish (0.477 μg/g), smooth dogfish (0.991 μg/g), scalloped hammerhead (2.088 μg/g), smooth hammerhead (2.663 μg/g), shortfin mako (2.539 μg/g), blacktip shark (0.703 μg/g), sandbar shark (1.397 μg/g), and thresher shark (0.481 μg/g).

¹⁵ The mercury content for skate is the average of the mean concentrations measured in 3 types of skate: thorny skate (0.200 μg/g), little skate (0.135 μg/g) and the winter skate (0.193 μg/g).

¹⁶ The mercury content for snapper is the average of the mean concentrations measured in types of snapper:

¹⁷ The mercury content for sturgeon is the average of the mean concentrations measured in 2 types of sturgeon: green sturgeon (0.218 μg/g) and white sturgeon (0.251 μg/g).

¹⁸ The mercury content for tuna is the average of the mean concentrations measured in 3 types of tuna: albacore tuna (0.264 μg/g), skipjack tuna (0.136 μg/g) and yellowfin tuna (0.218 μg/g)

Table 3-20
Mercury Concentrations in Marine Shellfish

Shellfish	Mercury Concentration (μg/g, wet weight)	Source of Data
Abalone ¹	0.016	NMFS
Clam ²	0.023	NMFS
Crab ³	0.117	NMFS
Lobster ⁴	0.232	NMFS
Oysters ⁵	0.023	NMFS
Scallop ⁶	0.042	NMFS
Shrimp ⁷	0.047	NMFS

¹ The mercury content for abalone is the average of the mean concentrations measured in 2 types of abalone: green abalone (0.011 μg/g) and red abalone (0.021 μg/g).

² The mercury content for clam is the average of the mean concentrations measured in 4 types of clam: hard (or quahog) clam (0.034 μg/g), Pacific littleneck clam (0 μg/g), soft clam (0.027 μg/g), and geoduck clam (0.032 μg/g).

³ The mercury content for crab is the average of the mean concentrations measured in 5 types of crab: blue crab (0.140 μg/g), dungeness crab (0.183 μg/g), king crab (0.070 μg/g), tanner crab (*C.opilio*) (0.088 μg/g), and tanner crab (*C.bairdi*) (0.102 μg/g).

⁴ The mercury content for lobster is the average of the mean concentrations measured in 3 types of lobster: spiny (Atlantic) lobster (0.108 μg/g), spiny (Pacific) lobster (0.210 μg/g) and northern (American) lobster (0.378 μg/g).

⁵ The mercury content for oyster is the average of the mean concentrations measured in 2 types of oyster: eastern oyster (0.022 μg/g) and Pacific (giant) oyster (0.023 μg/g).

⁶ The mercury content for scallop is the average of the mean concentrations measured in 4 types of scallop : sea (smooth) scallop (0.101 μg/g), Atlantic Bay scallop (0.038 μg/g), calico scallop (0.026 μg/g), and pink scallop (0.004 μg/g).

⁷ The mercury content for shrimp is the average of the mean concentrations measured in 7 types of shrimp : royal red shrimp (0.074 μg/g), white shrimp (0.054 μg/g), brown shrimp (0.048 μg/g), ocean shrimp (0.053 μg/g), pink shrimp (0.031 μg/g), pink northern shrimp (0.024 μg/g) and Alaska (sidestripe) shrimp (0.042 μg/g).

Table 3-21
Mercury Concentrations in Marine Molluscan Cephalopods

Mercury Concentrations in Marine Molluscan Cephalopods		
Cephalopod	Mercury Concentration ($\mu\text{g/g}$ wet wt.)	Source of Data
Octopus	0.029	NMFS
Squid ¹	0.026	NMFS

¹ The mercury content for squid is the average of the mean concentrations measured in 3 types of squid: Atlantic longfinned squid (0.025 $\mu\text{g/g}$), short-finned squid (0.034 $\mu\text{g/g}$), and Pacific squid (0.018 $\mu\text{g/g}$)

The New York State Department of Environmental Conservation has investigated chemical residues found in a wide variety of edible aquatic organisms from the New York-New Jersey Harbor Estuary. In 1993, 23 fish species, six bivalve species, two crustacean species and one cephalopod species were collected from six areas of the Harbor estuary (Skinner et al. 1996). Average total mercury concentrations in these samples did not equal or exceed 1 $\mu\text{g/g}$ -wet weight for any species; however, two individual striped bass samples did exceed 1 $\mu\text{g/g}$ -wet weight (1.046 and 1.252 $\mu\text{g/g}$ -wet weight). An average mercury concentration exceeding 0.5 $\mu\text{g/g}$ -wet weight was found only in striped bass larger than 762 mm, and an average mercury concentration exceeding 0.25 $\mu\text{g/g}$ -wet weight was found in striped bass and tautog. In striped bass, there was a significant ($p < 0.05$) correlation between size (i.e., age) and mercury concentration (Skinner et al. 1996). Non-detectable mercury concentrations were most prevalent in the six bivalve species, butterfish, winter flounder, the hakes and American eel. Mercury concentrations in fish, bivalves, crustaceans and cephalopods exhibited no consistent spatial variations within the harbor estuary (Skinner et al. 1996). The data are presented in Table 3-22.

Table 3-22
Mercury Concentrations in Biota from the New York-New Jersey Harbor estuary (1993)

Species	Mercury Concentration ($\mu\text{g/g-wet weight}$): Mean \pm Standard Deviation						
	Upper Bay Area 1	East River Area 2	The Kills Area 3	Jamaica Bay Area 4	Lower Bay Area 5	New York Bight Apex Area 6	All Areas Areas 1-6
Fish							
American eel	0.202 \pm 0.115	0.025	0.338 \pm 0.208	0.059 \pm 0.047	0.260 \pm 0.231	NA	0.167 \pm 0.178
Atlantic herring	0.127 \pm 0.049	NA	NA	NA	0.170	76 \pm 52	0.119 \pm 0.059
Atlantic tomcod	0.059 \pm 0.059	0.119 \pm 0.046	0.283 \pm 0.138	NA	NA	NA	0.154 \pm 0.128
Bluefish <305 mm	0.126 \pm 0.024	NA	0.527	0.130 \pm 0.025	NA	0.055	0.151 \pm 0.112
305-559 mm	NA	0.095	NA	0.151 \pm 0.097	0.184 \pm 0.049	0.242 \pm 0.081	0.183 \pm 0.083
\geq 559 mm	0.414 \pm 0.182	0.338 \pm 0.066	NA	0.276 \pm 0.033	0.162	0.233 \pm 0.076	0.312 \pm 0.122
Butterfish	0.073 \pm 0.049	0.025	0.043 \pm 0.031	NA	0.035 \pm 0.017	0.025	0.041 \pm 0.030
Cuner	0.256 \pm 0.036	0.185 \pm 0.083	0.209 \pm 0.061	0.275 \pm 0.133	0.164 \pm 0.011	0.389 \pm 0.166	0.246 \pm 0.112
Kingfish	0.056	NA	NA	0.038 \pm 0.023	NA	0.025	0.039 \pm 0.020
Northern sea robin	0.025	NA	NA	0.141	NA	0.196	0.139 \pm 0.111
Porgy	NA	0.071	0.060	0.094 \pm 0.040	0.044 \pm 0.027	0.037 \pm 0.016	0.060 \pm 0.035
Rainbow smelt	0.106 \pm 0.034	NA	NA	NA	NA	NA	0.106 \pm 0.34
Red hake	NA	NA	NA	NA	NA	0.078 \pm 0.065	0.078 \pm 0.065
Sea bass	0.151	NA	NA	NA	NA	0.097 \pm 0.041	0.106 \pm 0.043
Silver hake	NA	NA	NA	NA	NA	0.025	0.025
Spot	0.042 \pm 0.029	NA	0.025	NA	0.045 \pm 0.035	0.025	0.039 \pm 0.026
Spotted hake	0.106 \pm 0.026	NA	0.077 \pm 0.046	NA	0.044	0.025	0.065 \pm 0.042
Striped bass <457 mm	0.163 \pm 0.076	0.295 \pm 0.211	0.377 \pm 0.130	0.129 \pm 0.068	NA	NA	0.258 \pm 0.160
457-610 mm	0.289 \pm 0.122	0.391 \pm 0.199	0.325 \pm 0.110	0.198 \pm 0.050	0.340 \pm 0.169	0.150 \pm 0.054	0.284 \pm 0.150
610-762 mm	0.435 \pm 0.359	0.648 \pm 0.368	NA	0.299 \pm 0.130	0.242 \pm 0.163	0.241 \pm 0.021	0.389 \pm 0.288
\geq 762 mm	0.534 \pm 0.104	0.524 \pm 0.296	NA	0.578	0.437	0.572	0.528 \pm 0.261
Striped sea robin	NA	NA	NA	0.209	0.105 \pm 0.072	0.357	0.176 \pm 0.122
Summer flounder	0.094 \pm 0.039	NA	NA	0.125 \pm 0.038	0.122 \pm 0.076	0.065 \pm 0.016	0.102 \pm 0.050
Tautog	0.337 \pm 0.319	0.353 \pm 0.120	NA	0.203 \pm 0.087	0.133 \pm 0.044	0.320 \pm 0.307	0.267 \pm 0.197
Weakfish	0.250 \pm 0.209	NA	0.177 \pm 0.078	0.096	0.154 \pm 0.08	0.025	0.167 \pm 0.120

Species	Mercury Concentration ($\mu\text{g/g}$ -wet weight): Mean \pm Standard Deviation						
	Upper Bay Area 1	East River Area 2	The Kills Area 3	Jamaica Bay Area 4	Lower Bay Area 5	New York Bight Apex Area 6	All Areas Areas 1-6
White perch	0.207 \pm 0.054	0.281 \pm 0.11	0.397 \pm 0.179	0.025	NA	NA	0.230 \pm 0.172
Windowpane flounder	0.127 \pm 0.062	NA	0.105 \pm 0.04	NA	0.124 \pm 0.047	0.093 \pm 0.017	0.112 \pm 0.041
Winter flounder	0.070 \pm 0.068	0.033 \pm 0.016	0.035 \pm 0.018	0.092 \pm 0.022	0.056 \pm 0.034	0.036 \pm 0.019	0.061 \pm 0.04
Bivalves							
Blue mussel	NA	0.025	NA	0.064 \pm 0.041	0.025	0.025	0.036 \pm 0.026
Eastern oyster	0.059	0.025	0.091 \pm 0.021	NA	0.025	NA	0.049 \pm 0.031
Hard clam	NA	NA	NA	0.025	0.025	NA	0.025
Horse mussel	0.082 \pm 0.021	0.051 \pm 0.046	0.042 \pm 0.029	NA	0.025	NA	0.055 \pm 0.034
Softshell clam	0.025	0.071 \pm 0.03	0.101 \pm 0.011	0.025	0.025	NA	0.052 \pm 0.035
Surf clam	NA	NA	NA	NA	Na	0.025	0.025
Crustaceans							
American lobster -muscle	NA	NA	NA	NA	0.246	0.162 \pm 0.06	0.170 \pm 0.062
-hepatopancreas	NA	NA	NA	NA	0.068	0.061 \pm 0.029	0.062 \pm 0.028
Blue crab -muscle	0.112 \pm 0.068	0.134 \pm 0.087	0.199 \pm 0.068	0.132 \pm 0.148	0.253 \pm 0.169	NA	0.166 \pm 0.119
-hepatopancreas	0.074 \pm 0.035	0.140 \pm 0.149	0.084 \pm 0.068	0.066 \pm 0.044	0.100 \pm 0.031	NA	0.093 \pm 0.077
Cephalopod							
Longfin squid	NA	NA	NA	NA	0.096 \pm 0.075	0.035 \pm 0.017	0.065 \pm 0.059

The detection limit was 0.050 $\mu\text{g/g}$; a reported value of 0.025 $\mu\text{g/g}$ represents one-half the detection limit.
NA = No samples available or none analyzed

By comparing the mercury concentration in fish with concentrations in other biota (Tables 3-23 through 3-24), it is noted that fish appear to have the highest concentrations of methylmercury in the environment.

The little recent data available on mercury in meat products show concentrations to be very low (near the detection limits) for both Hg(II) and methylmercury. It is not thought that meat consumption is a major concern with regards to mercury exposure, especially in comparison to concentration in fish tissues. Surprisingly few data, however, are available on meat mercury levels.

Plant mercury levels are generally very low and of little concern, as with meats (see Tables 3-25 and 3-26). Levels tend to be highest in leafy vegetables, and plants grown in mercury contaminated conditions (in air and/or soil) do accumulate more mercury than plants in background areas. There are no other noticeable trends in plant concentrations, with mercury levels varying widely among plants and studies. For further information, see plant BCFs in Appendix B.

Table 3-23
Measured Mercury Concentration in Meats

Study Description	Total Mercury (ng/g wet weight)	Approx. Total Mercury (ng/g dry weight) ¹	% Methylmercury	Reference
6 Saginaw River, MI "roaster" ducks	48	124.7	NA	U.S. EPA (1992b)
Japan background levels				
Chicken	12	31.2	NA	Shitara and Yasumasa (1976)
Beef	5	13.0	NA	Shitara and Yasumasa (1976)
Pork	21	54.5	NA	Shitara and Yasumasa (1976)
Wild Deer (Northern Wisconsin)	5-14	13 -36	11-57 %	Bloom and Kuhn (1994)
Beef				
Raw	< 1	< 2.6	> 10%	Bloom and Kuhn (1994)
Lunch Meat	21	54.5	4%	Bloom and Kuhn (1994)
Frank	<1	< 2.6	> 60%	Bloom and Kuhn (1994)
Beef Muscle - Control group	2-3	5.2 - 7.8	NA	Vreman et al. (1986)*
Beef Muscle - Exposed group	1-4	2.6 - 10.4	NA	Vreman et al. (1986)*
Beef Liver - Control group	3000 - 7000	7800 - 18000	NA	Vreman et al. (1986)*
Beef Liver - Exposed group	9000 - 26000	23400- 67000	NA	Vreman et al. (1986)*
Pork (raw and sausage)	< 1	< 2.6	0-70%	Bloom and Kuhn (1994)
Chicken (raw and lunch meat)	< 1 to 29	< 2.6 to 75.4	20-67%	Bloom and Kuhn (1994)
Turkey (lunch meat)	< 1	< 2.6	>20%	Bloom and Kuhn (1994)

* See Appendix A for a more complete discussion of this study.

¹ Based on an assumed water content of 0.615, which is average for beef (Baes et al., 1984)

Table 3-24
Measured Mercury Concentrations in Garden Produce/Crops

Study Description	Total Mercury (ng/g dry weight)	Methyl-mercury	% Methyl-mercury	Reference
NY Garden conditions: Leafy vegetables	64-139	9.5-30	15-23	Cappon (1987)
NY Garden conditions: Tuberous plants	11-36	0.3-6.6	11-36	Cappon (1987)
NY Garden conditions: Cole	50-64	8.8-12	18	Cappon (1987)
NY Garden conditions: Fruiting vegetables	2.9-27	0-2.4	0-9.1	Cappon (1987)
NY Garden conditions: Beans	4.3	0	0	Cappon (1987)
Herbs; Garden samples from Belgium background	130 ^a			Temmerman et al. (1986)

N.B. No Hg⁰ was detected in plants (Cappon, 1987).

^aConversion to dry wt. assuming 90% water by wt.

Table 3-25
Mean Background Total Mercury Levels for Plants in the Netherlands
(Wiersma et al., 1986)

Plant	Total Mercury Concentration (ng/g wet weight)	Approximate Water Content (from Baes et al., 1984)	Total Mercury Concentration (ng/g dry weight)
Lettuce, greenhouse	2	0.948	38.5
Tomato, greenhouse	1.3	0.941	22.0
Cucumber, greenhouse	0.3	0.961	7.7
Spinach	5	0.927	68.5
Carrot	2	0.882	16.9
Potato	3	0.778	13.5
Wheat	5	0.125	5.7
Barley	6	0.111	6.7
Oats	8	0.083	8.7
Apples	1	0.841	6.3

Table 3-26
Range of Mercury Concentrations in Selected Grain Products

Grain product	Range (ng/g wet weight)	Range (ng/g dry weight) ¹	Reference
Wheat	< 0.1 - 30	< 0.1 - 34	Wiersma et al., (1986)
Barley	1 - 30	1.1 - 34	
Oats	<0.1 - 20	< 0.1 - 22	
Maize	1.5 - 6.5	1.7 - 7.3	Szymczak and Grajeta (1992)

¹ Calculated assuming water content of 0.112 (Baes et al., 1984).

3.3 Measurement Data from Remote Locations

The Long Range Transport Analysis (Chapter 5) focusses on the long range atmospheric transport of mercury and estimates its impact at remote sites. This type of analysis was selected based on the atmospheric chemistry of emitted elemental mercury (Petersen et al., 1995) and the numerous studies linking increased mercury levels in air, soil, sediments, and biota at remote sites to distant anthropogenic mercury release followed by long-range transport. Details of several of the many studies which demonstrate the long range transport of mercury follow. These provide evidence to support this assessment of long-range mercury transport.

3.3.1 Elevated Atmospheric Mercury Concentrations over Remote Locations

Olmez et al. (1994) correlated elevated atmospheric levels of particulate mercury at rural U.S. sites to long range transport from distant sources. Briefly, Olmez et al. (1994) collected ambient particulates of two sizes (< 2.5µm and between 2.5µm and 10µm) for two years at five rural sites in New York State and measured levels of numerous pollutants. Using a pollutant fingerprinting technique, the collected data were evaluated to identify the pollutant sources. Mercury was considered to be a tracer pollutant for mixed industry and coal combustion. There were no local anthropogenic mercury sources at these sites. At the five sites the average sub- 2.5µm particulate mercury concentrations ranged from 0.051 to 0.089 ng/m³, and the 90th percentile particulate mercury levels ranged from 0.21 to 0.10 ng/m³. The highest values reported were 0.63 ng/m³. Elevated mercury levels were attributed to long-range transport from industrial sources in Canada as well as parts of New York State and occasionally the midwest U.S. The authors noted that only 1-10% of the total mercury in remote areas is generally thought to be found on particles. Preliminary vapor-phase analysis (on samples collected for months) indicated that the mercury attached to these small particulates accounted for only 1.8% of the total mercury at these rural sites.

Glass et al. (1991) reported that mercury released from distant sources (up to 2500 km distant) contribute to mercury levels in rain water deposited on remote sites in northern Minnesota.

3.3.2 Elevated Soil Mercury Concentrations in Locations Remote from Emission Sources

Increased concentrations of mercury have been reported in both remote U.S. (Nater and Grigal, 1992) and Swedish soils (as reviewed in Johansson et al., 1991 and by the Swedish Environmental

Protection Agency, 1991). These elevated concentrations have been correlated with regional transport and deposition of mercury to soil. Nater and Grigal (1992) found an increasing mercury gradient from west to east in soils across the upper midwest U.S. This increase was also found to correlate with increasing regional industrialization. Briefly, soils were sampled in 155 different forest stands representing five types of forested stands. Mercury levels were measured in three layers: the surface detritus, surface soil (0-25 cm) and deep mineral soil (75-100 cm). Increases were observed along the west-east gradient in the upper two layers. The highest values reported for the detritus layer and the surface soil layer were >150 ng Hg/g detritus and >200 ng Hg/g soil, respectively. Differences in the ability of various soil types to bind mercury was discounted as a possible reason for the range of mercury values. The authors felt that their results implicated regional source contributions. Data summarized in Johansson et al. (1991) and the Swedish Environmental Protection Agency (1991) indicates that mercury levels in remote soils of southern Sweden are elevated when compared to those in the north. The increase observed in the soils of southern Sweden is related to emissions from regional Swedish industry and East European industry (Hakanson et al., 1990).

3.3.3 Elevated Mercury Concentrations in Aquatic Sediments and Fish from Remote Water Bodies

Elevated mercury levels in remote water body bed sediments have been widely reported and well characterized in many different parts of the world. These elevated levels are related to increased levels of atmospheric mercury which have been linked to anthropogenic activities. For example Swain et al. (1992) showed that, based on the vertical distribution of mercury in sediment, mercury deposition from the atmosphere over Wisconsin and Minnesota had increased from approximately 3.7 to 12.5 $\mu\text{g}/\text{m}^2$ since 1850 causing increases in sediment levels. For similar data from remote Wisconsin lakes, remote lakes in Ontario (Canada) and from remote Scandinavian bogs see Rada et al. (1989), Evans (1986), and Jensen and Jensen (1991), respectively. Some of the sediment analysis data for Sweden is presented in the report on mercury by the Swedish Environmental Protection Agency (1991).

The regional and widespread nature of mercury pollution was first identified when elevated levels of mercury in fish were discovered. These elevated levels in fish were evidence of the efficient transfer of mercury from prey to predator through the aquatic food chain (Watras and Bloom, 1992). In fact, the bioaccumulative nature of the mercury in fish has generated much of the interest in the measurement of mercury in other environmental media. It should be noted that the data of Hakanson et al. (1990) indicate that mercury levels in Swedish piscivorous fish continue to increase.

Elevated mercury concentrations in fish, particularly higher trophic level fish (e.g., northern pike) have been measured at sites distant from anthropogenic sources in Sweden (Hakanson et al., 1988; Swedish Environmental Protection Agency, 1991) and across the U.S. (e.g., Grieb et al., 1990; Sorensen et al., 1990 and Weiner et al., 1990). The report by Cunningham et al. (1994) illustrates the widespread nature of mercury fish advisories across the U.S.

3.4 **Measurement Data Near Anthropogenic Sources of Concern**

Measured mercury levels in environmental media around a single anthropogenic source are briefly summarized in this section. These data are not derived from a comprehensive study for mercury around the sources of interest. Despite the obvious needs for such an effort, such a study does not appear to exist. The quality of the following studies has not been assessed in this Report. The data do not appear to be directly comparable among themselves because of differences in analytic techniques and collection methods used. Finally, some of these studies are dated and may not reflect current mercury emissions from the sources described below.

These data collectively indicate that mercury concentrations near these anthropogenic sources are generally elevated when compared with data collected at greater distances from the sources. However, because these data do not conclusively demonstrate or refute a connection between anthropogenic mercury emissions and elevated environmental levels, a modeling exercise was undertaken to examine further this possible connection. This exercise is described in Chapters 4,5, and 6 of this document. The conclusions are discussed in Chapter 7. Materials in Appendices A-G support the modeling effort.

3.4.1 Municipal Waste Combustors

Bache et al. (1991) measured mercury concentrations in grasses located upwind and downwind from a modular mass-burn municipal waste combustor located in a rural area. The facility reportedly had no pollution control equipment and had been operating for about seven years when the grasses were sampled. Mercury levels were measured in air-dried grass samples by the flameless atomic absorption method developed by Hatch and Ott (1968). The sensitivity and detection limit of the method were not reported. Mercury levels in grass located downwind (along the prevailing wind direction) from the stack decreased with distance beginning at 100 m and continuing through 900 m. The highest value recorded downwind of the facility was 0.2 μg mercury/g grass (dry weight) at 100 m. The highest reported value upwind (225 meters in the opposite direction from the prevailing wind direction) of the facility was 0.11 $\mu\text{g}/\text{g}$ (dry weight). All other upwind values including measurements closer to the facility were 0.05 $\mu\text{g}/\text{g}$ or less.

In response to a Congressional mandate, U.S. EPA assessed the "environmental impact of municipal waste incineration facilities" (U.S. EPA, 1991). Background levels of mercury were measured in air, soil, water and biota in the area around an MWC in Vermont. The facility, which had a 50 m stack, was not yet operational when the initial set of measurements were made. Pollution control equipment included an electrostatic precipitator (ESP) and a wet scrubber. After the facility had begun operating, pollutant levels were again measured. After the start-up of operations mercury emissions were measured at approximately 2×10^{-4} g/s. Mercury levels above the analytical detection limits or above background levels were not observed in this analysis. Problems were noted with some of the analytical equipment used for ambient air monitoring. The MWC was also not operational during some of the time after start-up, and there was a short time (10 months) between operation start-up and environmental measurement data collection.

Greenberg et al. (1992) measured mercury levels in rainwater near a rural New Jersey municipal resource recovery facility (MWC). The measurement protocols developed by Glass et al. (1990) were employed in the analysis. The 2-stack MWC had a 400-ton/day capacity, and pollution control included a dry fabric filter. The maximum allowable mercury emissions were 0.05 pounds/hour/stack (22.7 grams/hour/stack). During one collection period, state-mandated stack testing indicated that the facility was emitting mercury at levels slightly lower than the maximum allowable emission rates. Rain water was collected and analyzed on three separate 2-day time periods; the facility was not operating during one collection period. Collection sites were generally located in the prevailing wind directions. Mercury concentrations in rain water appeared to be elevated near the facility in the prevailing wind directions when compared with measurements taken when the facility was not operating and with measurements at more remote sites (>2 km). Mercury concentrations in rain water measured up to 2 km from the facility while it was not operating exhibited a range of 26 - 62 ng mercury/L rainwater (26-62 ppt). Mercury measurements at sites 3 - 5 km downwind did not exceed 63 ng mercury/L rain water. During facility operation the highest measured mercury concentration was 606 ng/L. The measurement was taken 2 km in the prevailing wind direction. Several other measurements of greater than 100 ng mercury/L rain water were also collected within 2 km of the facility.

Carpi et al. (1994) measured mercury levels in moss and grass samples around a MWC in rural New Jersey (same facility as Greenberg et al., 1992 studied). Pollution control equipment on the MWC reportedly included a spray dryer and a fabric filter. Samples were collected at sites up to 5 km from the source and mercury levels measured by a cold vapor atomic absorption spectroscopy method described in U.S. EPA (1991). Statistically significant elevations in mercury concentrations were measured in moss samples located within 1.7 km of the facility with the highest mercury measured levels exceeding 240 parts per billion (ppb). Oven-dried moss samples had lower levels of mercury than those samples that were not oven-dried. This was attributed to the loss of volatile mercury species during drying. The decrease in total mercury was most notable in moss samples at more distant sites (beyond 2 km from the facility). The authors felt that this might indicate the uptake and retention of different species during drying. The results of the analysis of grass samples were not presented. They were termed "inconclusive" in that they did not appear to exhibit point source influence.

3.4.2 Chlor-Alkali Plants

Temple and Linzon (1977) sampled the mercury content of foliage, soil, fresh fruits, vegetables and snow around a large chlor-alkali plant in an urban-residential area. This facility produced 160 tons of chlorine/day, resulting in approximately 0.8 kg/day of mercury emissions. Resulting mercury concentrations were compared to background levels from an urban area 16 km to the west. Mercury levels averaged 15 $\mu\text{g/g}$ (300 times the background level of 0.05 $\mu\text{g/g}$) in maple foliage up to 260 m downwind, and concentrations 10 times background were found 1.8 km downwind. Mercury levels in soil averaged 3 $\mu\text{g/g}$ (75 times the background level of 0.04 $\mu\text{g/g}$) within 300 m of the plant, and soil concentrations averaged 6 times background 1.8 km downwind. The mercury levels in snow ranged from 0.9-16 $\mu\text{g/L}$ within 500 m of the plant dropping to 0.10 $\mu\text{g/L}$ 3 km downwind. The background level was found to average 0.03 $\mu\text{g/L}$. Leafy crops were found to accumulate the highest mercury among garden produce. One lettuce sample contained 99 ng/g (wet w.) of mercury (background: <0.6 ng/g), and a sample of beet greens contained 37 ng/g (wet w.) (background: 3 ng/g). Tomatoes and cucumbers within 400 m averaged 2 and 4.5 ng/g (wet w.) of mercury. Background levels in each case measured 1 ng/g.

In one of the earliest reports which measured mercury levels around an industrial emission source, Jernelov and Wallin (1973) found elevated levels of mercury in the snow around five chlor-alkali facilities in Sweden. As distance from the facility increased, the amount of mercury detected decreased. They linked the elevated levels to source emissions.

Tamura et al. (1985) measured mercury concentrations in plant leaves and humus from areas with and without mercury emission sources in Japan. Data on total mercury concentrations were determined by cold flameless atomic absorption. Mercury concentrations were determined at four sites within 2 km of a currently operating chlor-alkali electrolysis plant. This facility was estimated to release 10-20 kg of mercury per year. Mercury concentrations at the four sites near this area ranged from 0.04-0.71 $\mu\text{g/g}$ in woody plant leaves, 0.05-0.59 $\mu\text{g/g}$ in herbaceous plants, and 0.11-2.74 $\mu\text{g/g}$ in humus. In contrast, mercury levels for identical species of plants in the uncontaminated area (three sites) ranged from 0.02-0.07 $\mu\text{g/g}$ in woody plant leaves, 0.02-0.08 $\mu\text{g/g}$ in herbs, and 0.02-0.59 $\mu\text{g/g}$ in humus. Values are typically on the order of 5-10 times less than mercury levels from the contaminated area, showing significant mercury contamination of plant biota can result from local point sources.

3.4.3 Coal-Fired Utilities

Crockett and Kinnison (1979) sampled the arid soils around a 2,150 megawatt (MW) coal-fired power plant in New Mexico in 1974. The four stack (two stacks 76 m high and two 91 m high) facility

had been operational since 1963 with an estimated mercury release rate of 850 kg/year. The rainfall in the area averaged 15-20 cm/year. Although a mercury distribution pattern was noted, soil mercury levels near the facility did not differ significantly from background. Given the high amounts of mercury released by the facility and the insignificant amounts detected, the authors speculated that much of the mercury emitted was transported over a large area, rather than depositing locally.

Anderson and Smith (1977) measured mercury levels in environmental media and biota around a 200 MW coal-fired power plant in Illinois. The facility used two 152 m high smokestacks and was equipped with an electrostatic precipitator. Commercial operations at the facility had been ongoing for 6 years when sampling was conducted (from 1973 through 1974). Elevated levels of mercury detected in atmospheric particulate samples collected 4.8 and 9.6 km downwind of the facility were not statistically significant when compared with samples collected 4.8 km upwind of the site. Elevated mercury levels detected in samples from the upper 2 cm of downwind agricultural soils (sample mean 0.022 ug/g mercury) were statistically significantly elevated when compared with upwind samples (0.015 ug/g mercury). Core sediment sampling from a nearby lakebed showed statistically significant elevations in sediment mercury concentrations after plant operations began (sample mean 0.049 ug/g mercury) when compared with sediment deposits prior to operation (0.037 ug/g mercury). No increases were observed in mercury levels in fish from the nearby lake when compared with fish from remote lakes. Mercury levels in local duck muscle samples and aquatic plant samples were also reported but not compared to background or data from remote areas.

3.4.4 Mercury Mines

Lindberg et al. (1979) compared soil concentrations and plant uptake of mercury in samples taken one Km west of a mine/smelter operation in Almaden, Spain, to levels found in control soils (20 Km east of the smelter). The most significant mercury release from the Almaden complex was from the ore roaster via a 30 m high stack; however, estimates of annual mercury releases were unavailable. Mine soils contained 97 $\mu\text{g/g}$ of mercury compared to the control soil level of 2.3 $\mu\text{g/g}$, a 40 fold increase. Alfalfa was grown on these soils under controlled conditions. Comparing plant mercury concentrations (grown under conditions of no fertilizer or lime treatment), the above ground parts of alfalfa contained 1.4 and 2.3 $\mu\text{g/g}$ of mercury in the control and mine soils, respectively. The roots of alfalfa contained 0.53 and 9.8 $\mu\text{g/g}$ of mercury in the control and mine soils, respectively. The control levels in this experiment were found to exceed the worldwide average for grass crops by about 10 times; perhaps not surprising, since the control soil mercury content is also quite high. Nevertheless, additional mercury from the mine was found to elevate mercury content in surrounding soil and plant material significantly.

3.4.5 Mercury Near Multiple Local Sources

There are two recent reports of atmospheric mercury measurements in the vicinity of multiple anthropogenic emissions sources. Both are of studies are of short duration but show elevated mercury concentrations in the local atmosphere or locally collected rain.

Dvonch et al., (1994) conducted a 4-site, 20 day mercury study during August and September of 1993 in Broward County, FL. This county contains the city of Ft. Lauderdale as well as an oil-fired utility boiler and a municipal waste combustion facility. One of the sample collection sites (site 4) was located 300 m southwest of the municipal waste combustion facility. Daily measurements of atmospheric particulate and vapor-phase mercury were collected at 3 of the 4 sites; (daily atmospheric concentrations were not collected at the site near the municipal waste combustor (site 4)), and daily precipitation samples were collected at all sites. As shown in Table 3-27, the average vapor and particulate phase atmospheric mercury concentrations were higher at the inland sites than at the site near

the Atlantic Ocean, which was considered by the authors to represent background site. Diurnal variations were also noted; elevated concentrations were measured at night. For example at site 2, an inland site, the average nighttime vapor-phase concentration was 4.5 ng/m³. This was attributed to little vertical mixing and lower mixing heights that occur in this area at night. Particulate mercury comprised less than 5% of the total (vaporous + particulate) atmospheric mercury. Mercury concentrations in precipitation samples at the 4 sites were variable; the highest mean concentrations were measured at the inland sites. Given the high levels of precipitation in this area of the U.S. and short collection period, it is not appropriate to extend these analysis beyond the time frame measured. These mercury concentrations are nonetheless elevated.

Table 3-27
Mercury Concentrations in the Atmosphere and Mercury Measured in Rainwater Collected in Broward County, FL

Site Description	Avg. Vapor-phase Mercury Conc., ng/m ³	Avg. Particulate Mercury Conc. pg/m ³	Avg. Total Mercury conc. in rain, ng/L (Range)	Avg. Reactive Mercury conc. in rain, ng/L (Range)
Background Near Atlantic Ocean (Site 1)	1.8	34	35 (15-56)	1.0 (0.5-1.4)
Inland (Site 2)	3.3	51	40 (15-73)	1.9 (0.8-3.3)
Inland (Site 3)	2.8	49	46 (14-130)	2.0 (1.0-3.2)
Inland (Site 4), 300 m from MWC	-	-	57 (43-81)	2.5 (1.7-3.7)

Keeler et., al. (1994) and Lamborg et al., (1994) reported results of a 10-day atmospheric mercury measurement at 2 sites (labeled as sites A and B) in Detroit, MI (see Table 3-28). There is a large MWC 9 Km from site A and a sludge combustor 5 Km from site B. It should be noted that other mercury emission sources such as coal-fired utility boiler and steel manufacturing occur in the city as well. The vapor-phase mercury concentration encountered at site B during the first days of the experiment exceeded the capacity of the measurement device. Subsequent analyses indicated that the concentrations of mercury encountered were significantly higher than other reported U.S. observations.

Table 3-28
Mercury Concentrations Measured at Two Sites in the Atmosphere Over Detroit, MI

Site	Mean Vapor-Phase Mercury Concentrations in, ng/m ³ (Maximum Measured Value)	Mean Particulate-Phase Mercury Concentrations in pg/m ³ , (Maximum Measure Value)
Detroit, MI Site A	>40.8, (>74)	341 (1086)
Detroit, MI Site B	3.7, (8.5)	297 (1230)

4. MODEL FRAMEWORK

This section describes the models and modeling scenarios used to predict the environmental fate of mercury. Measured mercury concentrations in environmental media were used when available to parameterize these models. Human and wildlife exposures to mercury were predicted based on modeling results.

4.1 Models Used

The extant measured mercury data alone were judged insufficient for a national assessment of mercury exposure for humans and wildlife. Thus, the decision was made to model the mercury emissions data from the stacks of combustion sources. In this study, there were three major types of modeling efforts: (1) modeling of mercury atmospheric transport on a regional basis; (2) modeling of mercury atmospheric transport on a local scale (within 50 km of source); and (3) modeling of mercury fate in soils and water bodies into biota, as well as the resulting exposures to human and selected wildlife species. The models used for these aspects of this study are described in Table 4-1.

Table 4-1
Models Used to Predict Mercury Air Concentrations, Deposition Fluxes,
and Environmental Concentrations

Model	Description
RELMAP	Predicts average annual atmospheric mercury concentration and wet and dry deposition flux for each 40 km ² grid in the U.S. due to all anthropogenic sources of mercury in the U.S.
ISC3	Predicts annual average atmospheric concentrations and deposition fluxes within 50 km of mercury emission source
IEM-2M	Predicts environmental mercury concentrations based on air concentrations and deposition rates to watershed and water body.

4.2 Modeling of Long-Range Fate and Transport of Mercury

4.2.1 Objectives

The goal of this analysis was to model the emission, transport, and fate of airborne mercury over the continental U.S. using the meteorologic data for the year of 1989 and the most current emissions data. The results of the simulation were intended to be used to answer a number of fundamental questions. Probably the most general question was "How much mercury is emitted to the air annually over the United States, and how much of that is then deposited back to U.S. soils and water bodies over a typical year?" It is known that year-to-year variations in accumulated precipitation and wind flow patterns affect the observed quantity of mercury deposited to the surface at any given location. Meteorological data for the year of 1989 was used since most of the continental U.S. experienced near

normal average weather conditions during that year. A secondary question was that of the contribution by source category to the total amount of mercury emitted and the amount deposited within the U.S. In order to answer the questions about the source relative depositions, information on chemical and physical forms of the mercury emissions from the various source categories was needed since these characteristics determine the rate and location of the wet and dry deposition processes for mercury.

The intent of the analysis was to determine which geographical areas of the United States have the highest and lowest amounts of deposition from sources using the overall results of the long-range transport modeling effort nation-wide. This analysis was expected to contribute understanding of the key variables, such as source location, chemical/physical form of emission, or meteorology, that might contribute to the outcomes. These long-range modeling efforts were also intended to be used for comparison with local impact modeling results, essentially to estimate the effects of hypothetical new local sources in relation to the estimated effects from long-range transport.

4.2.2 Estimating Impacts from Regional Anthropogenic Sources of Mercury

The impact of mercury emissions from stationary, anthropogenic U.S. sources is not entirely limited to the local area around the facility. To account for impacts of mercury emitted from many of these other non-local sources on the area around a specific source, the long-range transport of mercury from all selected sources has been modeled using the RELMAP (Regional Lagrangian Model of Air Pollution) model. The RELMAP model was used to predict the average annual atmospheric mercury concentration and the wet and dry deposition flux for each ½ degree longitude by ⅓ degree latitude grid cell (approximately 40 km square) in the continental U.S. The emission, transport, and fate of airborne mercury over the continental U.S. was modeled using meteorological data for the year of 1989. Over 10,000 mercury emitting cells within the U.S. were addressed; the emission data used were those presented in Volume II, *Inventory of Anthropogenic Mercury Emissions*.

The RELMAP model was originally developed to estimate concentrations of sulfur and sulfur compounds in the atmosphere and rainwater in the eastern U.S. The primary modification of RELMAP for this study was the handling of three species of mercury (elemental, divalent, and particulate) and carbon soot (or total carbon aerosol). Carbon soot was included as a modeled pollutant because carbon soot concentrations are important in the modeling estimates of the wet deposition of elemental mercury (Iverfeldt, 1991; Brosset and Lord, 1991; Lindqvist et al., 1991).

4.2.3 Description of the RELMAP Mercury Model

Previous versions of the RELMAP are described and evaluated in Eder et al. (1986) and Clark et al. (1992) and a separate description of the initial development of the RELMAP mercury modeling is provided in Bullock et al. (1997a). Modifications to the RELMAP for atmospheric mercury simulation were heavily based on recent Lagrangian model developments in Europe (Petersen et al., 1995). The mercury version of the RELMAP was developed to handle three species of mercury: elemental vapor (Hg^0), divalent vapor (the mercuric ion, Hg^{2+}) and particulate Hg (Hg_p), and also aerosol carbon soot. Recent experimental work indicates that ozone (Munthe, 1992) and carbon soot (Iverfeldt, 1991; Brosset and Lord, 1991; Lindqvist et al., 1991) are both important in determining the wet deposition of Hg^0 . Carbon soot, or total carbon aerosol, was included as a modeled pollutant in the mercury version of RELMAP to provide necessary information for the Hg^0 wet deposition parameterization. Observed ozone (O_3) air concentration data for the simulation period were obtained from EPA's Aerometric Information Retrieval System (AIRS) data base. Thus, it was not necessary to include O_3 as an explicitly modeled pollutant. Methyl mercury was not included in the mercury version of RELMAP because it is

not yet known if it has a primary natural or anthropogenic source, or if it is produced in the atmosphere. Unless specified otherwise in the following sections, the modeling concepts and parameterizations described in the EPA users' guide (Eder et al., 1986) were preserved for the RELMAP mercury modeling study.

4.2.3.1 Physical Model Structure

RELMAP simulations were originally limited to the area bounded by 25 and 55 degrees north latitude and 60 and 105 degrees west longitude, and had a minimum spatial resolution of 1 degree in both latitude and longitude. For this study, the western limit of the RELMAP modeling domain was moved out to 130 degrees west longitude, and the modeling grid resolution was reduced to ½ degree longitude by ⅓ degree latitude (approximately 40 km square) to provide high-resolution coverage over the entire continental U.S.

The original 3-layer puff structure of the RELMAP has been replaced by a 4-layer structure. The following model layer definitions were used for the RELMAP mercury simulations to account for the development of deeper nocturnal inversion layers during autumn and winter and higher convective mixing heights in the spring and summer:

Layer 1 top	-	30 to 50 meters above the surface (season-dependent)
Layer 2 top	-	200 meters above the surface
Layer 3 top	-	700 meters above the surface
Layer 4 top	-	700 to 1500 meters above the surface (month-dependent)

4.2.3.2 Mercury Emissions

Area source emissions were introduced into the model in the lowest layer. Point source emissions were introduced into model layer 2 to account for the effective stack height of the point source type in question. Effective stack height is the actual stack height plus the estimated plume rise. The layer of emission is inconsequential during the daytime when complete vertical mixing is imposed throughout the 4 layers. At night, since there is no vertical mixing, area source emissions to layer 1 are subject to dry deposition while point source emissions to layer 2 are not. Large industrial emission sources and sources with very hot stack emissions tend to have a larger plume rise, and their effective stack heights might actually be larger than the top of layer 2. Since, however the layers of the pollutant puffs remain vertically aligned during advection, the only significant process effected by the layer of emission is nighttime dry deposition.

Mercury emissions data were grouped into eleven different point-source types and a general area-source type. The area source emissions data describe those sources that are too small to be accounted for individually in pollutant emission surveys. For the RELMAP mercury modeling study, area sources were assumed to emit mercury entirely in the form of Hg^0 gas, while ten of the point source types were each assigned mercury speciation profiles based on previous European research (Petersen et al., 1995) and the results of stack testing at a medical waste incinerator in Dade County, Florida (Stevens et al., 1996). These speciation profiles defined the estimated fraction of mercury emitted as Hg^0 , Hg^{2+} , and Hg_p . For medical waste incinerator speciation estimates, it was assumed that one-quarter of the Hg^{2+} emissions measured in the hot stack exhaust would quickly convert to Hg_p form upon cooling and dilution in ambient air. Municipal waste combustors and medical waste incinerators were further grouped by the types of air pollution control devices (APCDs) indicated for each plant in the inventory and separate speciation profiles were assumed for each group based on the assumption that Hg^{2+} and Hg_p

are preferentially extracted from the waste stream and that Hg^0 is extracted only after all Hg^{2+} and Hg_p is removed. The total mercury extraction efficiency for each APCD configuration was based on information presented in Volume II, *Inventory of Anthropogenic Mercury Emissions*. The mercury emissions inventory for hazardous waste combustors included estimates of the emission speciation for each plant and no general assumption of speciation profile was required.

There remains considerable uncertainty as to the actual speciation factors for each point source type. A wide variety of alternate emission speciations have been simulated for important groups of atmospheric mercury sources in order to test the sensitivity of the RELMAP results to the speciation profiles used (Bullock et al., 1997b). This work showed that the RELMAP modeling results are very strongly dependent on the assumed emission speciations. The emission speciation profiles used for this study are shown in Table 4-2. The total (non-speciated) mercury emissions inventory used is that described in Volume II of this Report. Figures 4-1, 4-2 and 4-3 show the total mercury emissions from all anthropogenic sources in the form of Hg^0 , Hg^{2+} and Hg_p , respectively. Speciated data derived from actual monitoring of sources are a critical research need. These data are needed to establish a clear causal link between mercury originating from anthropogenic sources and mercury concentrations (projected or actual) in environmental media and/or biota.

Global-scale natural emissions, recycled anthropogenic emissions and current emissions from anthropogenic sources outside the RELMAP model domain were accounted for by superimposing an ambient atmospheric concentration of Hg^0 gas of 1.6 ng/m^3 . This use of a constant background concentration to account for global-scale and external anthropogenic emissions is the same technique used by Petersen et al. (1995). Functional limitations of Lagrangian pollutant parcel modeling prevent any explicit treatment of emission sources located outside the spatial domain of the RELMAP as no external starting point for parcel trajectories can be defined. Natural and recycled emissions from soils and water bodies within the model domain cannot be treated explicitly due to the number of simulated pollutant parcels that would originate from all locations. Even if these natural and recycled parcels were explicitly modeled, the prevailing west-to-east atmospheric flow of the mid-latitude northern hemisphere would produce an artificial west-to-east gradient in the simulated effects from these pollutant parcels. The deposition parameterizations described in section 4.2.4.1 were used to simulate the scavenging of Hg^0 from the constant background concentration throughout the entire RELMAP model domain. The result was used as an estimate of the deposition of mercury from all natural sources and anthropogenic sources outside the model domain.

**Table 4-2
Mercury Emissions Inventory Used in the RELMAP Modeling**

Mercury Emission Source Type		Emissions (kg/yr)	Speciation Percentages		
			Hg ⁰ ^a	Hg ²⁺ ^b	Hg _p ^c
Electric Utility Boilers (coal, oil and gas)		46,183	50	30	20
Municipal Waste Combustors	Standard	17,393	20	60	20
	50% Control	9,099	40	45	15
	85% Control	219	100	0	0
	Total	26,711			
Commercial and Industrial Boilers		25,650	50	30	20
Medical Waste Incinerators	Standard	13,177	2	73	25
	94% Control	1,365	33	50	17
	Total	14,542			
Chlor-Alkali Factories		6,482	70	30	0
Hazardous Waste Incinerators		6,435	58 [†]	20 [†]	22 [†]
Portland Cement Manufacturing		4,355	80	10	10
Residential Boilers		3,244	50	30	20
Pulp and Paper Plants		1,651	50	30	20
Sewage Sludge Incinerators		799	20	60	20
Other Point Sources		3,072	80	10	10
Area Sources		2,721	100	0	0

^a Hg⁰ represents elemental mercury gas

^b Hg²⁺ represents divalent mercury gas

^c Hg_p represents particulate mercury

[†] The inventory included emissions speciation for each plant. Speciation percentages shown are cumulative for all hazardous waste incinerators in the inventory.

Figure 4-1
Hg(0) Emissions from All Anthropogenic Sources (Base)
(Megagrams per year)

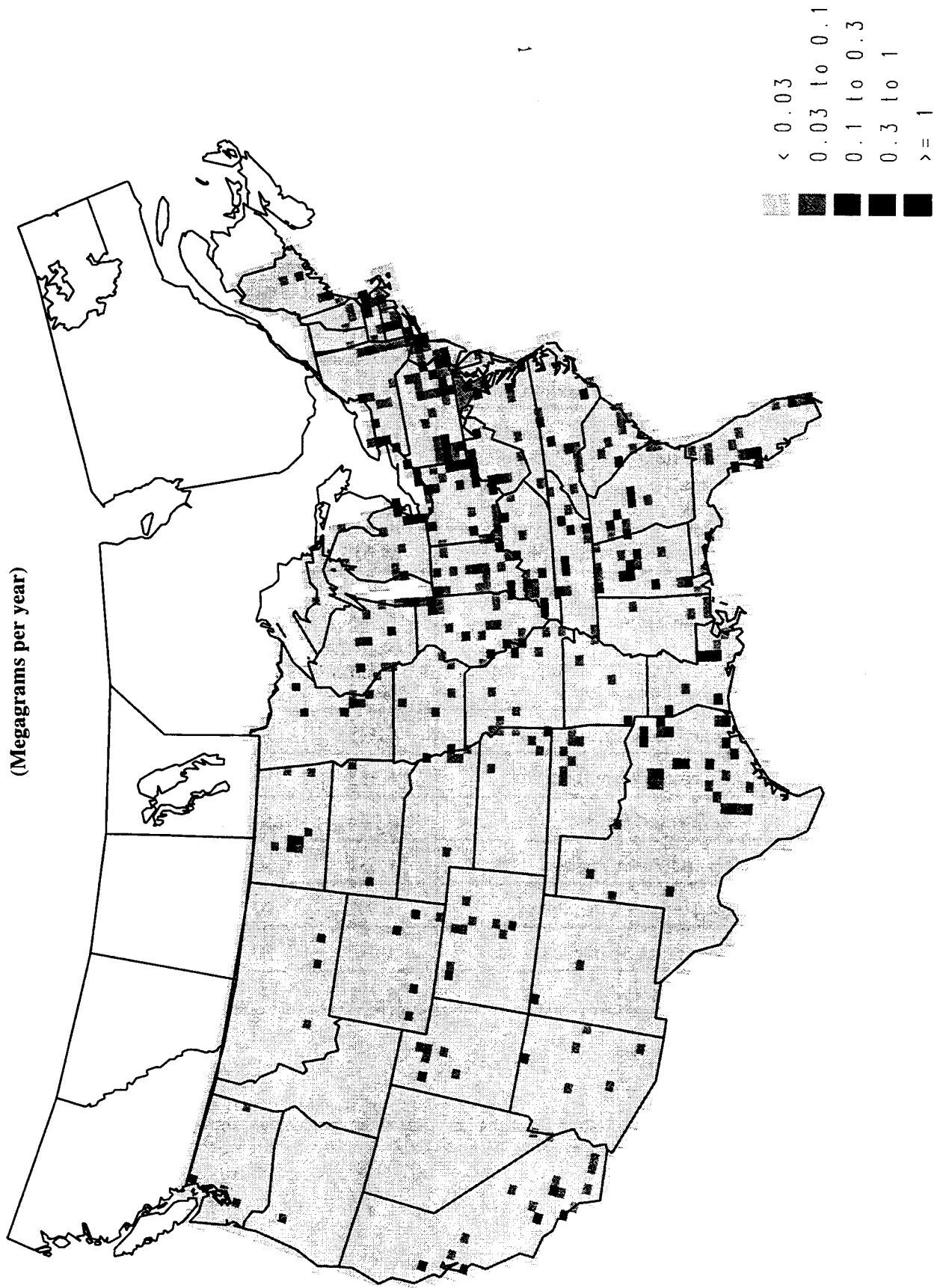


Figure 4-2
Hg²⁺ Emissions from All Anthropogenic Sources (Base)

(Megagrams per year)

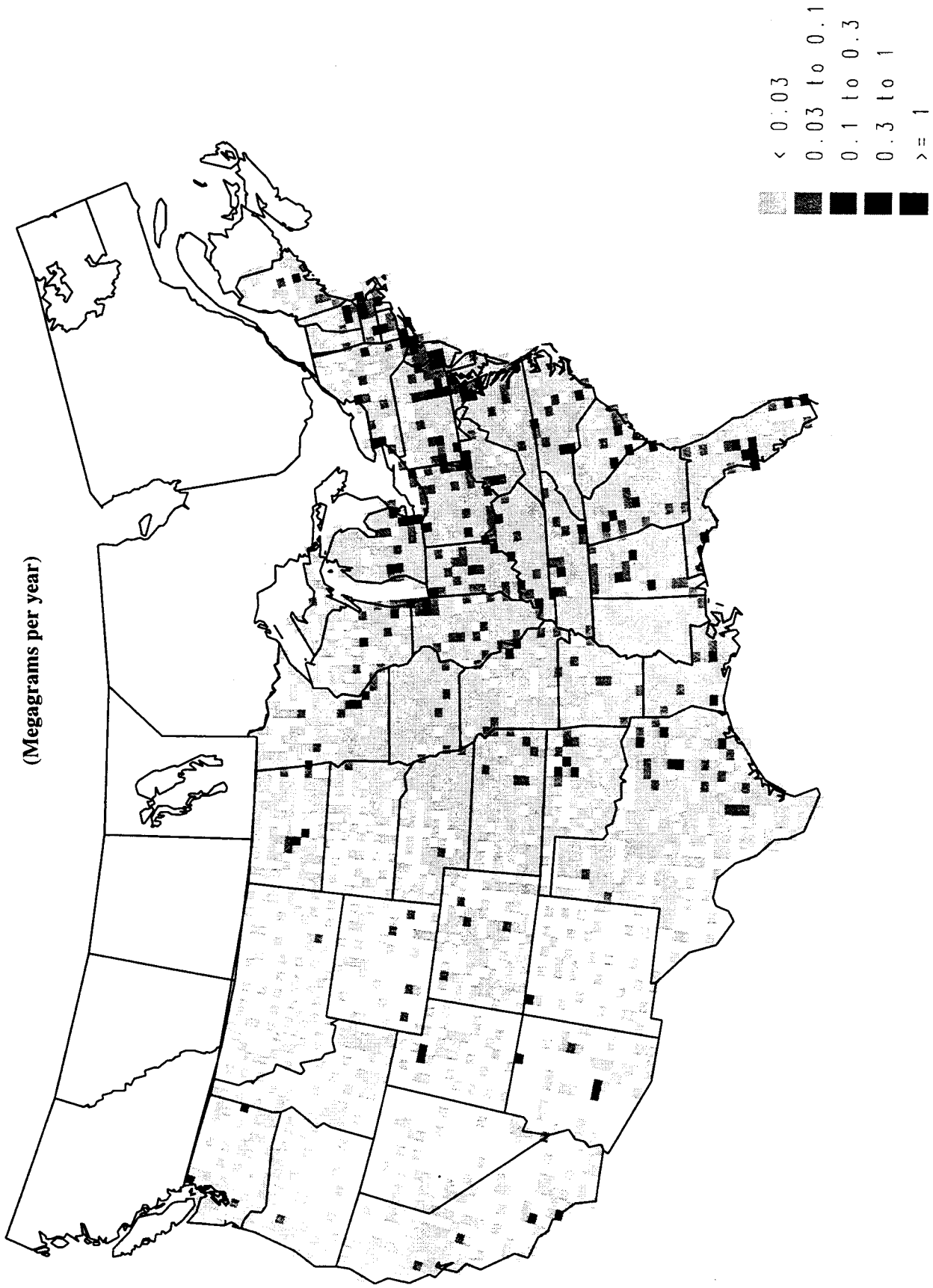
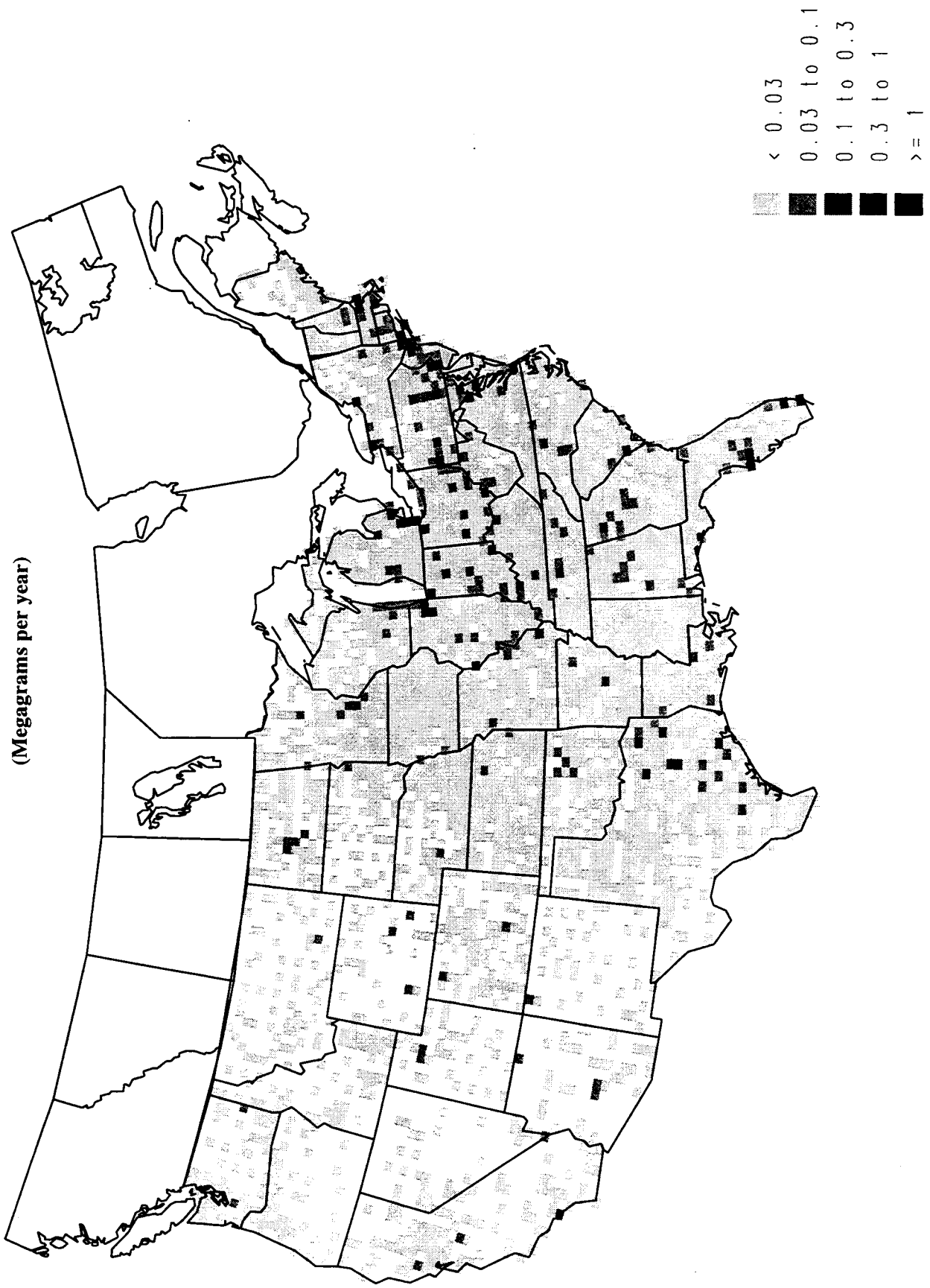


Figure 4-3
Hg(p) Emissions from All Anthropogenic Sources (Base)

Figure 4-3
Hg(p) Emissions from All Anthropogenic Sources (Base)

(Megagrams per year)



4.2.3.3 Carbon Aerosol Emissions

Penner et al. (1993) concluded that total carbon air concentrations are highly correlated with sulfur dioxide (SO₂) air concentrations from minor sources. They concluded that the emissions of total carbon and SO₂ from minor point sources are correlated as well, since both pollutants result from the combustion of fossil fuel. Their data indicate a 35% proportionality constant for total carbon air concentrations versus SO₂ air concentrations. The RELMAP mercury model estimated total carbon aerosol emissions using this 35% proportionality constant and SO₂ emissions data for minor sources obtained by the National Acidic Precipitation Assessment Program (NAPAP) for the year 1988. Much of these SO₂ emissions data had been previously analyzed for use by the Regional Acid Deposition Model (RADM). For the portion of the RELMAP mercury model domain not covered by the RADM domain, state by state totals of SO₂ emissions were apportioned to the county level on the basis of weekday vehicle-miles-traveled data since recent air measurement studies have indicated that aerosol elemental carbon can be attributed mainly to transportation source types (Keeler et al., 1990). The county level data were then apportioned by area to the individual RELMAP grid cells. Total carbon soot was assumed to be emitted into the lowest layer of the model.

4.2.3.4 Ozone Concentration

Ozone concentration data were obtained from U.S. EPA's Aerometric Information Retrieval System (AIRS) and the Acidmodes experimental air sampling network. AIRS and Acidmodes data were available hourly. For each observation site in the AIRS database, the ozone concentrations were computed for the two mid-day RELMAP time steps by using the mean concentration value during the two corresponding time periods (1000-1300 and 1400-1600 local time). The mean of these two mid-day values was used to estimate the ozone concentration for the time steps after 1600 local time and before 1000 local time the next morning. This previous-day average was used at night since ground-level ozone data are not valid for the levels aloft where the wet removal of elemental mercury was assumed to be occurring. Finally, an objective interpolation scheme using $1/r^2$ weighted averaging was used to produce complete ozone concentration grids from observational data for each time step, with a minimum value of 20 ppb imposed.

It is recognized that, by estimating nighttime elevated ozone concentrations from observed ground-level ozone concentrations of the previous day, we do not resolve any possible advection of ozone concentration gradients during the nighttime hours. Since it is well documented that ground level observations of ozone concentration do not correlate well with actual elevated concentrations at night, we opted not to use nighttime surface-level data. Since observations of elevated ozone concentration were not available except in rare instances, we believe that estimation based on previous-day observations were our only recourse short of explicit modeling of ozone advection and chemistry within the RELMAP which is not currently possible. By not resolving the advection of ozone gradients, it is possible that nighttime precipitation could co-locate with erroneous estimates of ozone concentration. Given that high ozone concentrations do not normally occur with precipitation, these erroneous estimates of ozone concentration would most likely be too high, leading to an artificial bias toward high simulated Hg⁰ oxidation and subsequent wet deposition. Since there remains considerable uncertainty about the true nature of Hg⁰ oxidation in cloud water and its controlling effect on wet deposition, the risk of modeling errors related to nighttime ozone concentration estimates from previous-day observations was deemed acceptable.

4.2.3.5 Lagrangian Transport and Deposition

In the model, each pollutant puff begins with an initial mass equal to the total emission rate of all sources in the source cell multiplied by the model time-step length. For mercury, as for most other pollutants previously modeling using RELMAP, emission rates for each source cell were defined from emission inventory data, and a time step of three hours was used. The initial horizontal area of each puff was set to 1200 km², instead of the standard initial size of 2500 km², in order to accommodate the finer grid resolution used for the mercury modeling study; however, the standard horizontal expansion rate of 339 km² per hour was not changed. Although each puff was defined with four separate vertical layers, each layer of an individual puff was advected through the model cell array by the same wind velocity field. Thus, the layers of each puff always remained vertically stacked. Wind field initialization data for a National Weather Service prognostic model, the Nested Grid Model (NGM), were obtained for each 0000 and 1200 GMT initialization time during the year of 1989. Wind analyses for the $\sigma_p=0.897$ vertical level of the NGM were used to define the translation of the puffs across the model grid, except during the months of January, February, and December, when the $\sigma_p=0.943$ vertical level was used to reflect a more shallow mixed layer. σ_p is a pressure-based vertical coordinate equal to $(p-p_{top})/(p_{surface}-p_{top})$. The $\sigma_p=0.897$ and $\sigma_p=0.943$ levels approximate elevations above ground level of 1000 m and 500 m, respectively. These wind fields at 12-h intervals were linearly interpolated in time to produce the wind fields used to define puff motion for each 3-h RELMAP time step.

Pollutant mass was removed from each puff by the processes of wet deposition, dry deposition, diffusive air exchange between the surface-based mixed layer and the free atmosphere, and, in the case of reactive species, chemical transformation. The model parameterizations for these processes are discussed in Section 4.2.4. Hourly precipitation data for the entire year of 1989 from the TD-3240 data set of the U.S. National Climatic Data Center were used to estimate the wet removal of all pollutant species modeled. A spatial and temporal sub-grid-scale analysis of these hourly observations was performed using a process previously developed for sulfur wet deposition modeling (Bullock, 1994). This process provides resolution of precipitation variability not obtainable by simple numerical averaging of all observations within each grid cell and time step. Wet and dry deposition mass totals were accumulated and average surface-level concentrations were calculated on a monthly basis for each model cell designated as a receptor. Except for cells in the far southwest and eastern corners of the model domain where there were no wind data, all cells were designated as receptors for the mercury simulation. When the mass of pollutant in a puff declines through deposition, vertical diffusion or transformation to a user-defined minimum value, or when a puff moves out of the model grid, the puff and its pollutant load is no longer tracked. The amount of pollutant in the terminated puff is taken into account in monthly mass balance calculations so that the integrity of the model simulation is assured. Output data from the model includes monthly wet and dry deposition totals and monthly average air concentration for each modeled pollutant, in every receptor cell.

4.2.4 Model Parameterizations

4.2.4.1 Chemical Transformation and Wet Deposition

The simplest type of pollutant to model with RELMAP is the inert type. To model inert pollutants, one can simply omit chemical transformation calculations for them, and not be concerned with chemical interactions with the other chemical species in the model. In the mercury version of RELMAP, particulate mercury and total carbon were each modeled explicitly as inert pollutant species. Reactive pollutants are normally handled by a chemical transformation algorithm. RELMAP was originally developed to simulate sulfur deposition, and the algorithm for transformation of sulfur dioxide

to sulfate was independent of wet deposition. For gaseous mercury, however, the situation is more complex. Since there are no gaseous chemical reactions of mercury in the atmosphere which appear to be significant (Petersen et al., 1995), for this modeling study mercury was assumed to be reactive only in the aqueous medium. Elemental mercury has a very low solubility in water, while oxidized forms of mercury and particle bound mercury readily find their way into the aqueous medium through dissolution and particle scavenging, respectively. Worldwide observations of atmospheric mercury, however, indicate that particulate mercury is generally a minor constituent of the total mercury loading (Iverfeldt, 1991) and that gaseous elemental mercury (Hg^0) is, by far, the major component. Swedish measurements of large north-to-south gradients of mercury concentration in rainwater without corresponding gradients of atmospheric mercury concentration suggest the presence of physical and chemical interactions with other pollutants in the precipitation scavenging process (Iverfeldt, 1991). Aqueous chemical reactions incorporated into the mercury version of RELMAP were based on research efforts in Sweden (Iverfeldt and Lindqvist, 1986; Lindqvist et al., 1991; Munthe et al., 1991; Munthe and McElroy, 1992; Munthe, 1992) and Canada (Schroeder and Jackson, 1987; Schroeder et al., 1991).

Unlike other pollutants that have been modeled with RELMAP, mercury has wet deposition and chemical transformation processes that are interdependent. A combined transformation/wet-removal scheme proposed by Petersen et al. (1995) was used. In this scheme, the following aqueous chemical processes were modeled when and where precipitation is present:

- 1) oxidation of dissolved Hg^0 by ozone yielding Hg^{2+}
- 2) catalytic reduction of this Hg^{2+} by sulfite ions
- 3) adsorption of Hg^{2+} onto carbon soot particles suspended in the aqueous medium

Petersen et al. (1995) shows that these three simultaneous reactions can be considered in the formulation of a scavenging ratio for elemental mercury gas as follows:

$$W(Hg^0) = \frac{k_1}{k_2} \cdot \frac{1}{H_{Hg}} \cdot [O_3]_{aq} \cdot \left(1 + K_3 \cdot \frac{c_{soot}}{r}\right)$$

where,

k_1 is the second order rate constant for the aqueous oxidation of Hg^0 by O_3 equal to $4.7 \times 10^7 \text{ M}^{-1}\text{s}^{-1}$,

k_2 is the first order rate constant for the aqueous reduction of Hg^{2+} by sulfite ions equal to $4.0 \times 10^{-4} \text{ s}^{-1}$,

H_{Hg} is the dimensionless Henry's Law coefficient for Hg^0 (0.18 in winter, 0.22 in spring and autumn, and 0.25 in summer as calculated from Sanemasa (1975)),

$[O_3]_{aq}$ is the aqueous concentration of ozone,

K_3 is a model specific adsorption equilibrium constant ($5.0 \times 10^{-6} \text{ m}^4\text{g}^{-1}$),

c_{soot} is the total carbon soot aqueous concentration, and

r is the assumed mean radius of soot particles ($5.0 \times 10^{-7} \text{ m}$).

$[O_3]_{aq}$ is obtained from this equation:

$$[O_3]_{aq} = \frac{[O_3]_{gas}}{H_{O_3}}$$

where H_{O_3} is the dimensionless Henry's Law coefficient for ozone (0.448 in winter, 0.382 in spring and autumn, and 0.317 in summer as calculated from Seinfeld (1986)). c_{soot} is obtained from the simulated atmospheric concentration of total carbon aerosol using a scavenging ratio of 5.0×10^5 .

The model used by Petersen et al. (1995) defined one-layer cylindrical puffs, and the Hg^0 scavenging layer was defined as the entire vertical extent of the model. The RELMAP defines 4-layer puffs to allow special treatment of surface-layer and nocturnal inversion-layer processes. It was believed that, due to the low solubility of Hg^0 in water, the scavenging process outlined above would only take place effectively in the cloud regime, where the water droplet surface-area to volume ratio is high, and not in falling raindrops. Thus the Hg^0 wet scavenging process was applied only in the top two layers on RELMAP, which extends from 200 meters above the surface to the model top.

For the modeling study described in Petersen et al. (1995), the wet deposition of Hg^{2+} was treated separately from that of Hg^0 . Obviously, any Hg^{2+} dissolved into the water droplet directly from the air could affect the reduction-oxidation balance between the total concentration of Hg^0 and Hg^{2+} in the droplet. Since the solubility and scavenging ratio for Hg^{2+} is much larger than that for Hg^0 , and since air concentrations of Hg^0 are typically larger than those of Hg^{2+} , separate treatment of Hg^{2+} wet deposition was deemed acceptable for this modeling study also. Thus, process 2 above was only considered as a moderating factor for the oxidation of dissolved Hg^0 .

In the exposure analysis in Volume III, there was no attempt to develop a new interacting chemical mechanism for simultaneous Hg^0 and Hg^{2+} wet deposition. Although Hg^{2+} was recognized as a reactive species in aqueous phase redox reactions, it was, in essence, modeled as an inert species just like particulate mercury and total carbon soot. With the rapid rate at which the aqueous Hg^{2+} reduction reaction is believed to occur in the presence of sulfite, it is possible that an interactive cloud-water chemical mechanism might produce significant conversion of scavenged Hg^{2+} to Hg^0 , with possible release of that Hg^0 into the gaseous medium.

Wet deposition of Hg^{2+} , particulate mercury, and total carbon soot in the mercury version of RELMAP were modeled with the same scavenging ratios used by Petersen et al. (1995). The gaseous nitric acid scavenging ratio of 1.6×10^{-6} has been applied for Hg^{2+} since the water solubilities of these two pollutant species are similar. For particulate mercury, a scavenging ratio of 5.0×10^{-5} was used, based on experiences in long-range modeling of lead in northern Europe. As previously mentioned, a scavenging ratio of 5.0×10^{-5} was also used for total carbon soot. These scavenging ratios for Hg^{2+} , particulate mercury, and total carbon soot were applied to all four layers of the RELMAP in the calculation of pollutant mass scavenging by precipitation.

4.2.4.2 Dry Deposition

Recent experimental data indicate that elemental mercury vapor does not exhibit a net dry depositional flux to vegetation until the atmospheric concentration exceeds a rather high compensation point well above the global background concentration of 1.6 ng m^{-3} (Hanson et al., 1994). This

compensation point is apparently dependent on the surface or vegetation type and represents a balance between emission from humic soils and dry deposition to leaf surfaces (Lindberg et al., 1992). Since the emission of mercury from soils was accounted for with a global-scale ambient concentration and not an actual emission of Hg^0 , for consistency, there was no explicit simulation of the dry deposition of Hg^0 .

For Hg^{2+} during daylight hours, a dry deposition velocity table previously developed based on HNO_3 data (Walcek et al., 1985; Wesely, 1986) was used. The dry deposition characteristics of HNO_3 and Hg^{2+} should be similar since their water solubilities are similar and gaseous dry deposition to vegetation involves solution into moist plant tissue. This dry deposition velocity data, shown in Table 4-3, provided season-dependent values for 11 land-use types under six different Pasquill stability categories. Based on the predominant land-use type and climatological Pasquill stability estimate of each RELMAP grid cell, and the season for the month being modeled, the dry deposition velocity values shown in Table 4-3 were used for the daytime only. For nighttime, a value of 0.3 cm/s was used for all grid cells since the RELMAP does not have the capability of applying land-use dependent dry deposition at night. Since the nighttime dry deposition was applied only to the lowest layer of the model and no vertical mixing is assumed for nighttime hours, all Hg^{2+} modeled would be quickly depleted from the lowest model layer by larger dry deposition velocities.

For Hg_p , Petersen et al. (1995) used a dry deposition velocity of 0.2 cm/s at all times and locations. Lindberg et al. (1991) suggests that the dry deposition of Hg_p seems to be dependent on foliar activity. In the RELMAP mercury model, daytime dry deposition velocities for Hg_p were calculated using a FORTRAN subroutine developed by the California Air Resources Board (CARB, 1987). A particle density of 2.0 g cm^{-3} and diameter of $0.3 \text{ }\mu\text{m}$ was assumed. Table 4-4 shows the wind speed (u) used for each Pasquill stability category in the calculation of deposition velocity from the CARB subroutine, while Table 4-5 shows the roughness length (z_0) used for each land-use category. During simulated night, all cells used 0.02 cm/s as the dry deposition velocity for Hg_p . Lindberg et al. (1991) suggested a value of 0.003 cm/s for non-vegetated land, but since the RELMAP can not model land-use dependent dry deposition at night, the value of 0.02 cm/s was used for these cells by necessity.

For total carbon soot, daytime dry deposition velocities were also calculated using the CARB subroutine. A particle density of 1.0 g/cm^3 and radius of $0.5 \text{ }\mu\text{m}$ was assumed. For nighttime, a dry deposition velocity of 0.07 cm/s was used for all seasons and land-use types.

Petersen et al. (1995) used local dry deposition factors for Hg^{2+} and Hg_p in addition to the normal model treatments to remedy an assumed underestimation of the dry deposition rate for mercury species emitted near the ground due to an underestimation of the ground-level concentration from instantaneous complete vertical mixing in their model. This local deposition factor was the fraction of the emissions from a grid cell that were assumed to dry deposit within that grid cell by processes not otherwise simulated by the dry deposition parameterization. In the RELMAP mercury model, we compensated for this underestimation of local deposition by simulating all depositions before pollutant parcel transport in each model timestep. In essence, the parcel was held over its location of origin for 3 h before being transported away by the horizontal wind. Thus, no use of a local deposition factor in the RELMAP modeling was deemed necessary.

Table 4-3
Dry Deposition Velocity (cm/s) for Divalent Mercury (Hg²⁺)

Season	Land-Use Category	Pasquill Stability Category					
		A	B	C	D	E	F
Winter	Urban	4.83	4.80	4.61	4.30	2.79	0.36
	Agricultural	1.32	1.30	1.20	1.05	0.46	0.15
	Range	1.89	1.86	1.73	1.52	0.73	0.19
	Deciduous Forest	3.61	3.57	3.34	3.02	1.68	0.29
	Coniferous Forest	3.61	3.57	3.34	3.02	1.68	0.29
	Mixed Forest/Wetland	3.49	3.46	3.27	2.99	1.77	0.29
	Water	1.09	1.07	0.98	0.85	0.38	0.13
	Barren Land	1.16	1.14	1.06	0.92	0.39	0.31
	Non-forested Wetland	2.02	2.00	1.89	1.70	0.96	0.21
	Mixed Agricultural/Range	1.62	1.60	1.48	1.30	0.60	0.17
	Rocky Open Areas	1.98	1.95	1.81	1.58	0.73	0.20
Spring	Urban	4.59	4.54	4.35	4.05	2.49	0.36
	Agricultural	1.60	1.56	1.46	1.28	0.53	0.18
	Range	1.49	1.46	1.36	1.19	0.48	0.17
	Deciduous Forest	3.42	3.36	3.13	2.81	1.42	0.29
	Coniferous Forest	3.42	3.36	3.13	2.81	1.42	0.29
	Mixed Forest/Wetland	3.28	3.23	3.05	2.78	1.55	0.29
	Water	0.98	0.96	0.89	0.77	0.31	0.13
	Barren Land	1.05	1.04	0.97	0.85	0.30	0.13
	Non-forested Wetland	1.85	1.82	1.73	1.56	0.84	0.21
	Mixed Agricultural/Range	1.60	1.56	1.46	1.28	0.53	0.18
	Rocky Open Areas	1.84	1.81	1.67	1.46	0.58	0.20
Summer	Urban	4.47	4.41	4.12	3.73	2.07	0.36
	Agricultural	2.29	2.25	2.04	1.76	0.72	0.24
	Range	1.67	1.64	1.48	1.26	0.41	0.19
	Deciduous Forest	3.32	3.26	2.95	2.57	1.04	0.29
	Coniferous Forest	3.32	3.26	2.95	2.57	1.04	0.29
	Mixed Forest/Wetland	3.17	3.12	2.86	2.53	1.27	0.29
	Water	0.92	0.90	0.81	0.69	0.22	0.13
	Barren Land	0.98	0.98	0.89	0.76	0.23	0.13
	Non-forested Wetland	1.91	1.88	1.73	1.52	0.77	0.22
	Mixed Agricultural/Range	1.90	1.87	1.69	1.44	0.52	0.21
	Rocky Open Areas	1.95	1.91	1.71	1.46	0.42	0.21
Autumn	Urban	4.64	4.59	4.35	4.05	2.49	0.36
	Agricultural	2.02	1.98	1.81	1.60	0.73	0.21
	Range	1.78	1.74	1.59	1.40	0.60	0.19
	Deciduous Forest	3.46	3.40	3.13	2.81	1.42	0.29
	Coniferous Forest	3.46	3.40	3.13	2.81	1.42	0.29
	Mixed Forest/Wetland	3.32	3.27	3.05	2.78	1.55	0.29
	Water	1.00	0.98	0.89	0.77	0.31	0.13
	Barren Land	1.07	1.06	0.97	0.85	0.30	0.13
	Non-forested Wetland	1.88	1.86	1.73	1.56	0.84	0.21
	Mixed Agricultural/Range	1.93	1.90	1.74	1.53	0.68	0.20
	Rocky Open Areas	1.97	1.94	1.76	1.54	0.63	0.20

Table 4-4
Wind Speeds Used for Each Pasquill Stability Category
in the CARB Subroutine Calculations

Stability Category	Wind Speed (m/s)
A	2.0
B	3.0
C	4.0
D	5.0
E	3.0
F	2.0

Table 4-5
Roughness Length Used for Each Land-Use Category
in the CARB Subroutine Calculations

Land-Use Category	Roughness Length (meters)	
	spring-summer	autumn-winter
Urban	0.5	0.5
Agricultural	0.15	0.05
Range	0.12	0.1
Deciduous Forest	0.5	0.5
Coniferous Forest	0.5	0.5
Mixed Forest/Wetland	0.4	0.4
Water	10 ⁻⁶	10 ⁻⁶
Barren Land	0.1	0.1
Non-forested Wetland	0.2	0.2
Mixed Agricultural/Range	0.135	0.075
Rocky Open Areas	0.1	0.1

4.2.4.3 Vertical Exchange of Mass with the Free Atmosphere

Due to the long atmospheric lifetime of mercury, the RELMAP was adapted to simulate a continuous exchange of mass between the surface-based mixed layer and the free atmosphere above. In the modeling of Petersen et al. (1995), a depletion of pollutant from the mixed layer was simulated at the end of the day based on estimates of the subsidence of the mixed-layer top due to the horizontal divergence of the wind field. For the RELMAP modeling, a pollutant depletion rate of 5 percent per 3-hour timestep was chosen to represent this diffusive mass exchange. When compounded over a 24-hour period, this depletion rate removes 33.6% of an inert, non-depositing pollutant. This compares to an average diffusive mass loss of 30-40% per day in the European modeling study (Petersen, personal communication). Since a portion of all modeled species of mercury can deposit to the surface before this

diffusive mass loss is calculated in the RELMAP, the effective mass loss is somewhat less than 33.6% per day from this process.

4.3 Modeling the Local Atmospheric Transport of Mercury in Source Emissions

The program used to model the transport of the anthropogenic mercury within 50 km of an emissions source was the ISC3 gas deposition model, obtained from USEPA's Support Center for Regulatory Air Models (SCRAM) website (the program is called GDISCDFT). This model has a gas dry deposition model that was applied in this study.

4.3.1 Phase and Oxidation State of Emitted Mercury

Reports describe several forms of mercury detected in the emissions from the selected sources. Primarily, these include elemental mercury (Hg^0) and inorganic mercuric (Hg^{2+}). Generally, only total mercury has been measured in emission analyses. The reports of MHg in emissions are imprecise. It is believed that, if MHg is emitted from industrial processes and combustion sources, the quantities emitted are much smaller than emissions of Hg^0 and Hg^{2+} . Only Hg^0 and Hg^{2+} were considered in the air dispersion modeling.

The two types of mercury species considered in the emissions are expected to behave quite differently once emitted from the stack. Hg^0 , due to its high vapor pressure and low water solubility, is not expected to deposit close to the facility. In contrast, Hg^{2+} , because of differences in these properties, is expected to deposit in greater quantities closer to the emission sources.

At the point of stack emission and during atmospheric transport, the contaminant is partitioned between two physical phases: vapor and particle-bound. The mechanisms of transport of these two phases are quite different. Particle-bound contaminants can be removed from the atmosphere by both wet deposition (precipitation scavenging) and dry deposition (gravitational settling, Brownian diffusion). Vapor phase contaminants may also be depleted by these processes, although historically their main impacts were considered to be through absorption into plant tissues (air-to-leaf transfer) and human exposure occurred through inhalation.

For the present analysis, the vapor/particle (V/P) ratio was assumed to be equal to the V/P ratio as it would exist in the emissions plume. It is recognized that this is a simplification of reality, as the ratio when emitted from the stack is likely to change as the distance from the stack increases. It was assumed that 25% of the divalent emissions from an individual source would attach to particles in the plume. The uncertainty in this estimate is acknowledged. Essentially, particulate mercury is not measured at stack tip but has been measured in plumes downwind from local sources. It is assumed that the divalent fraction binds to sulfur particles.

The particle-size distribution may differ from one combustion process to another, depending on the type of furnace and design of combustion chamber, composition of feed/fuel, particulate matter removal efficiency and design of air pollution control equipment, and amount of air in excess of stoichiometric amounts that is used to sustain the temperature of combustion. The particle size distribution used is an estimate of the distribution within an ambient air aerosol mass and not at stack tip. Based on this assumption, an aerosol particle distribution based on data collected by Whitby (1978) was used. This distribution is split between two modes: accumulation and coarse particles. The geometric mean diameter of several hundred measurements indicates that the accumulation mode dominates particle size, and a representative particle diameter for this mode is 0.3 microns. The coarse particles are formed

largely from mechanical processes that suspend dust, sea spray and soil particles in the air. A representative diameter for coarse particles is 5.7 microns. The fraction of particle emissions assigned to each particle class is approximated based on the determination of the density of surface area of each representative particle size relative to total surface area of the aerosol mass. Using this method, approximately 93% and 7% of the total surface area is estimated to be in the 0.3 and 5.7 micron diameter particles, respectively.

**Table 4-6
Representative Particle Sizes and Size Distribution
Assumed for Divalent Mercury Particulate Emissions**

Representative Particle Size (microns)*	Assumed Fraction of Particle Emissions in Size Category
0.3	0.93
5.7	0.07

*These values are based on the geometric means of aerosol particle distribution measurements as described in Whitby (1978).

The speciation estimates for the model plants were made from thermal-chemical modeling of mercury compounds in flue gas, from the interpretation of bench and pilot scale combustor experiments and from interpretation of available field test results. The amount of uncertainty surrounding the emission rates data varies for each source. There is also a great deal of uncertainty with respect to the species of mercury emitted.

Although the speciation may change with distance from the local source, for this analysis it was assumed that there were no plume reactions that significantly modified the speciation at the local source. Because of the differences in deposition characteristics of the two forms of mercury considered, the assumption of no plume chemistry is a particularly important source of uncertainty.

4.3.2 Modeling the Deposition of Mercury

Once emitted from a source, the mercury may be deposited to the ground via two main processes: wet and dry deposition. Wet deposition refers to the mass transfer of dissolved gaseous or suspended particulate mercury species from the atmosphere to the earth's surface by precipitation, while dry deposition refers to such mass transfer in the absence of precipitation.

The deposition properties of the two species of mercury addressed in stack emissions, elemental and divalent mercury, are considered to be quite different. Due to its higher solubility, divalent mercury vapor is thought to deposit much more rapidly than elemental mercury. However, at this time no conclusive data exist to support accurate quantification of the deposition rate of divalent mercury vapor. In this analysis, nitric acid vapor is used as a surrogate for Hg⁺⁺ vapor based on their similar solubility in water. Whether a pollutant is in the vapor form or particle-bound is also important for estimating deposition, and each is treated separately.

Dry deposition is estimated by multiplying the predicted air concentration at ground level by a deposition velocity. For particles, the dry deposition velocity is estimated using the CARB algorithms

(CARB 1986) that represent empirical relationships for transfer resistances as a function of particle size, density, surface area, and friction velocity. For the vapor phase fraction for elemental mercury, a single dry deposition velocity of 0.06 cm/s is assumed. This is based on the average of the winter and summer deposition velocities presented in Lindberg et al. (1992) for forests. Although it is generally acknowledged that elemental mercury dry deposits with a (net) rate much lower than divalent mercury vapor, the precise value is uncertain, and there can be considerable variability with season and time of day. Additionally, dry deposition of elemental mercury may not occur at all unless the air concentration is sufficiently high. Preliminary research (Hanson et al. 1995) indicates that under some experimental conditions no dry deposition occurs unless the air concentration is at least 10 ng/m³; this was termed a compensation point (the value at which dry deposition would be expected to occur is expected to depend on many factors, including time of year and the type of flora present). These preliminary results were not specifically addressed in the current study; however, sensitivity analyses were conducted in order to determine the possible impact that such a compensation point might have on the predicted dry deposition of elemental mercury (see Section 5.3.4.1 below).

In ISC-GAS, the dry deposition of divalent mercury vapor was modeled by calculating a dry deposition velocity for each hour using the assumptions usually made for nitric acid for the input parameters (see EPA 1996; User's Guide for the Gas Dry Deposition Model, page inserts to the User's Guide for the Industrial Source Complex (ISC3) Dispersion Models). Ultimately, using the assumptions here, the average predicted dry deposition velocity was about 2.9 cm/s for divalent mercury vapor, which is essentially the average of the values used in the RELMAP modeling for coniferous forests.

Table 4-7
Parameter Values Assumed for Calculation of Dry Deposition Velocities for
Divalent Mercury Vapor

Parameter	Value
Molecular diffusivity (cm ² /sec)	0.1628
Solubility enhancement factor	10 ⁹
Pollutant reactivity	800
Mesophyll resistance	0
Henry's law coefficient	2.7e ⁻⁷

Wet deposition is estimated by assuming that the wet deposition rate is characterized by a scavenging coefficient which depends on precipitation intensity and particle size. For particles, the scavenging ratios used are from Jindal and Heinold (1991) (see Figure 4-4). For the vapor phase fraction, a scavenging coefficient is also used, but it is calculated using estimates for the washout ratio, which is the ratio of the concentration of the chemical in surface-level precipitation to the concentration in surface-level air. Because of its higher solubility, divalent mercury vapor is assumed to be washed out at significantly higher rates than elemental mercury vapor. The washout ratio for divalent mercury vapor was selected based on an assumed similarity between scavenging for divalent mercury and gaseous nitric acid. This is based on Peterssen (1995), and the value used for the washout ratio for divalent vapor was

1.6×10^6 . The washout ratio for elemental mercury vapor was assumed to be 1200. This is a calculated value based on the model of Peterssen et al. (1995), with a soot concentration 0.

Figure 4-4
Wet Deposition Scavenging Ratios Used in Local Scale Air Modeling for Particulate-Bound Mercury (Jindal and Heinold 1991)

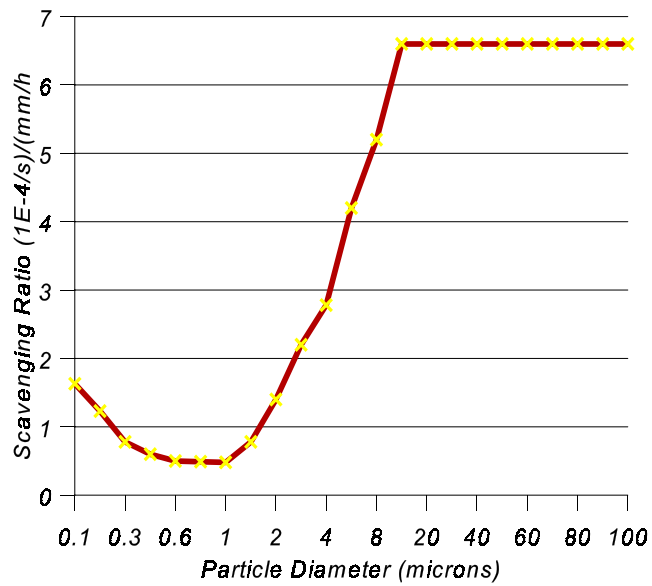


Table 4-8
Air Modeling Parameter Values Used in the Exposure Assessment: Generic Parameters

Parameter	Value Used in Study
Particle Density (g/cm ³)	1.8
Surface Roughness Length (m)*	0.30
Anemometer Height (m)	10
Wind Speed Profile Exponents	
Stability Class A	0.07
Stability Class B	0.07
Stability Class C	0.10
Stability Class D	0.15
Stability Class E	0.35
Stability Class F	0.55
Terrain Adjustment Factors	
Stability Class A	0.5
Stability Class B	0.5
Stability Class C	0.5
Stability Class D	0.5
Stability Class E	0
Stability Class F	0
Distance Limit for Plume Centerline (m)	10
Model Run Options	
Terrain Adjustment	Yes
Stack-tip Downwash	No
Building Wake Effects	No
Transitional Plume Rise	Yes
Buoyancy-induced dispersion	Yes
Calms Processing Option	No

^a This is used to estimate deposition velocities for particles.

4.3.3 Rationale and Utility of Model Plant Approach

Mercury is generally present as a low-level contaminant in combustion materials (e.g., coal or municipal solid waste) and industrial material (for more information on mercury in emissions refer to Volume II of this Report). During combustion and high-temperature industrial processes, mercury is volatilized from these materials. Because of its high volatility, it is difficult to remove mercury from the post-combustion air stream. As a consequence, mercury is released to the atmosphere. As noted previously, anthropogenic mercury emissions are not the only source of mercury to the atmosphere. Mercury may be introduced into the atmosphere through volatilization from natural sources such as lakes and soils. Consequently, it is difficult to trace the source(s) of mercury concentrations in environmental media and biota. For this reason it is also difficult to gain an understanding of contribution to those concentrations.

For this assessment it was not possible to model the emission impact of every mercury emission source in each selected industrial and combustion class. Consequently, the actual mercury emission data and facility characteristics for any specific source were not modeled. Instead, a model plant approach, as described in Appendix C, was utilized to develop facilities which represent actual sources. Model plants were developed to represent four source categories; namely municipal waste combustors, coal and oil-fired boilers, medical waste incinerators, and chlor-alkali plants. The model plants were designed to characterize the mercury emission rates as well as the atmospheric release processes exhibited by actual facilities in the source class. The modeled facilities were not designed to exhibit extreme sources (e.g., the facility with the highest mercury emission rate) but rather to serve as a representative of the industrial/combustion source class.

This assessment took as its starting point the results of measured mercury emissions from selected anthropogenic sources. Using a series of fate models and hypothetical constructs, mercury concentrations in environmental media, pertinent biota and ultimately mercury contact with human and wildlife receptors were predicted. An effort was made to estimate the amount of receptor contact with mercury as well as the oxidative state and form of mercury contacted.

In taking the model plant approach, it was realized that there would be a great deal of uncertainty surrounding the predicted fate and transport of mercury as well as the ultimate estimates of exposure. The uncertainty can be divided into modeling uncertainty and parameter uncertainty. Parameter uncertainty can be further subdivided into uncertainty and variability depending on the level to which a particular model parameter is understood. A limited quantitative analysis of uncertainty is presented. It is also hoped that the direction of future research can be influenced toward reducing the identified uncertainties which significantly impact key results.

4.3.4 Development and Description of Model Plants

Model plants representing four source classes were developed to represent a range of mercury emissions sources. The source categories were selected for the exposure assessment based on their estimated annual mercury emissions as a class or their potential to be localized point sources of concern. The categories selected were these:

- municipal waste combustors (MWCs),
- medical waste incinerators (MWIs),
- utility boilers, and
- chlor-alkali plants (CAP).

Parameters for each model plant were selected after evaluation of the characteristics of a given source category and current knowledge of mercury emissions from that source category. Important variables for the mercury risk assessment included mercury emission rates, mercury speciation and mercury transport/deposition rates. Important model plant parameters included stack height, stack diameter, stack volumetric flow rate, stack gas temperature, plant capacity factor (relative average operating hours per year), stack mercury concentration, and mercury speciation. Emission estimates were assumed to represent typical emission levels emitted from existing sources. Table 4-9 shows the process parameters assumed for each model plant considered in this analysis (for details regarding these values, see Appendix C).

4.3.5 Hypothetical Locations of Model Plants

There are a variety of geographic aspects that can influence the impacts of mercury emissions from an anthropogenic source. These aspects include factors that affect the environmental chemistry of a pollutant and the physics of plume dispersion. Environmental chemistry can include factors such as the amount of wet deposition in a given area. Factors affecting plume dispersion include terrain, wind direction and average wind speed.

Because wet deposition may be an important factor leading to mercury exposures, especially for the more soluble species emitted, the meteorology of a location was used as a selection criterion. Two different types of meteorology were deemed necessary to characterize the environmental fate and transport of mercury: an arid/semi-arid site and a humid site. The humidity of an area was based on total yearly rainfall. (See Appendix B).

Terrain features refer to the variability of the receptor height with respect to a local source. Broadly speaking, there were two main types of terrain used in the modeling: simple, and complex. Simple terrain is defined as a study area that is relatively level and well below stack top (rather, the effective stack height). Complex terrain referred to terrain that is not simple, such as source located in a valley or a source located near a hill. This included receptors that are above or below the top of the stack of the source. Complex terrain can effect concentrations, plume trajectory, and deposition. Due to the complicated nature of plume flow in complex terrain, it is probably not possible to predict impacts in complex terrain as accurately as for simple terrain. In view of the wide range of uncertainty inherent in accurately modeling the deposition of the mercury species considered, the impacts posed by complex terrain were not incorporated in the local scale analysis.

Two generic sites are considered: a humid site east of 90 degrees west longitude, and a more arid site west of 90 degrees west longitude (these are described in Appendix B). The primary differences between the two sites as parameterized were the assumed erosion characteristics for the watershed and the amount of dilution flow from the water body. The eastern site had generally steeper terrain in the watershed than for the other site. A circular drainage lake with a diameter of 1.78 km and average depth of 5 m, with a 2 cm benthic sediment depth was modeled at both sites. The watershed area was 37.3 km².

**Table 4-9
Process Parameters for Model Plants**

Model Plant	Plant Size	Capacity (% of year)	Stack Height (ft)	Stack Diameter (ft)	Hg Emission Rate (kg/yr)	Speciation Percent (Hg ⁰ /Hg ²⁺ /Hg ^p)	Exit Velocity (m/sec)	Exit Temp. (°F)
Large Municipal Waste Combustors	2,250 tons/day	90%	230	9.5	220	60/30/10	21.9	285
Small Municipal Waste Combustors	200 tons/day	90%	140	5	20	60/30/10	21.9	375
Large CommercialHMI Waste Incinerator (Wetscrubber)	1500 lb/hr capacity (1000 lb/hr actual)	88%	40	2.7	4.58	33/50/17	9.4	175
Large Hospital HMI Waste Incinerators (Good Combustion)	1000 lb/hr capacity (667 lb/hr actual)	39%	40	2.3	23.9	2/73/25	16	1500
Small Hospital HMI Waste Incinerators (1/4 sec.Combustion)	100 lb/hr capacity (67 lb/hr actual)	27%	40	0.9	1.34	2/73/27	10.4	1500
Large Hospital HMI Waste Incinerators (Wet Scrubber)	1000 lb/hr capacity (667 lb/hr actual)	39%	40	2.3	0.84	33/50/17	9.0	175
Small Hospital HMI Waste Incinerators (Wet Scrubber)	100 lb/hr capacity (67 lb/hr actual)	27%	40	0.9	0.05	33/50/17	5.6	175
Large Coal-fired Utility Boiler	975 Megawatts	65%	732	27	230	50/30/20	31.1	273
Medium Coal-fired Utility Boiler	375 Megawatts	65%	465	18	90	50/30/20	26.7	275
Small Coal-fired Utility Boiler	100 Megawatts	65%	266	12	10	50/30/20	6.6	295
Medium Oil-fired Utility Boiler	285 Megawatts	65%	290	14	2	50/30/20	20.7	322
Chlor-alkali plant	300 tons chlorine/day	90%	10	0.5	380	70/30/0	0.1	Ambient

^a Hg⁰ = Elemental Mercury

^b Hg²⁺ = Divalent Vapor Phase Mercury

^c Hg_p = Particle-Bound Mercury

4.4 Modeling Mercury in a Watershed

Atmospheric mercury concentrations and deposition rates estimated from RELMAP and ISC3 drive the calculations of mercury in watershed soils and surface waters. The soil and water concentrations, in turn, drive calculations of concentrations in the associated biota and fish, which humans and other animals are assumed to consume. The watershed model used for this report, IEM-2M, was adapted from the more general IEM-2 methodology (U.S. EPA, 1990; U.S. EPA, 1994, external review draft) to handle mercury fate in soils and water bodies.

4.4.1 Overview of the Watershed Model

IEM-2M simulates three chemical components -- elemental mercury, Hg^0 (C_1), divalent mercury, Hg^{II} (C_2), and methyl mercury, MHg (C_3). In the previous version of IEM-2, these components were assumed to be in a fixed ratio with each other as specified by the fraction elemental (f_1) and fraction methyl (f_3). This updated version calculates the fractions in each component based on specified or calculated rate constants. The equations and parameters are described below, and implemented in an Excel spreadsheet. The model is parameterized for several hypothetical scenarios as described in Chapter 5.

IEM-2M is composed of two integrated modules that simulate mercury fate using mass balance equations describing watershed soils and a shallow lake, as illustrated in Figures 4-5 and 4-6. The mass balances are performed for each mercury component, with internal transformation rates linking Hg^0 , Hg^{II} , and MHg . Sources include wetfall and dryfall loadings of each component to watershed soils and to the water body. An additional source is diffusion of atmospheric Hg^0 vapor to watershed soils and the water

Figure 4-5
Configuration of Hypothetical Water Body and Watershed Relative to Local Source

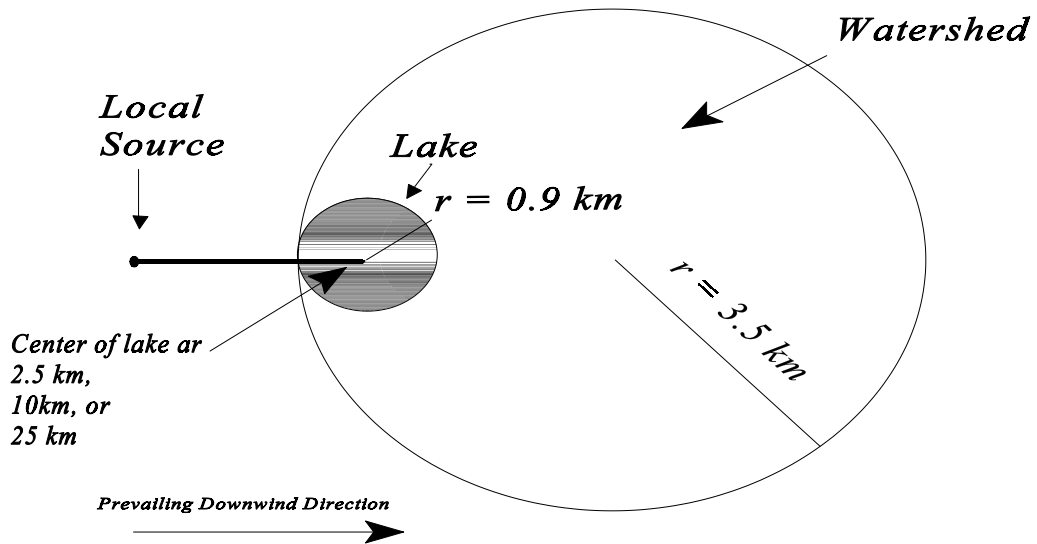
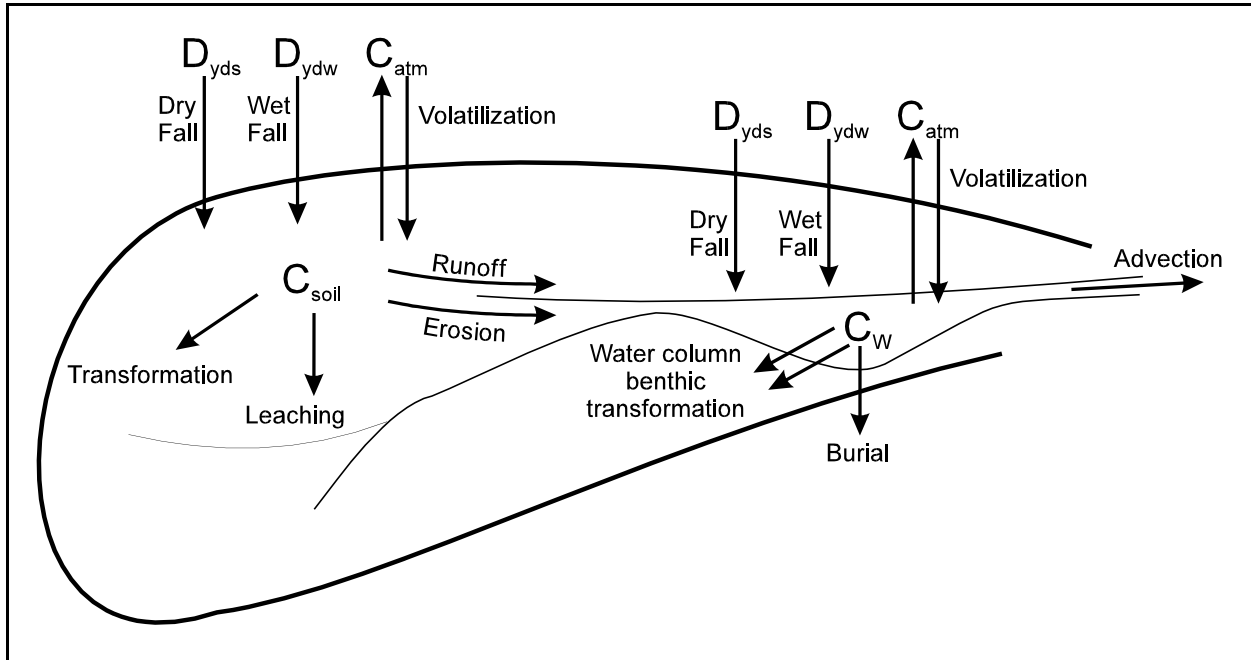


Figure 4-6
Overview of the IEM-2M Watershed Modules



Definitions for Figure 4-6

C_{soil}	total mercury concentration in upper soil	ng/g
C_w	total mercury concentration in water body	ng/L
C_{atm}	vapor phase mercury concentration in air	ng/m ³
D_{yds}	average dry deposition to watershed	μg/m ² -yr
D_{yws}	average wet deposition to watershed	μg/m ² -yr

body. Sinks include leaching of each component from watershed soils, burial of each component from lake sediments, volatilization of Hg^0 and MHg from the soil and water column, and advection of each component out of the lake.

At the core of IEM-2M are 9 differential equations describing the mass balance of each mercury component in the surficial soil layer, in the water column, and in the surficial benthic sediments. The equations are solved for a specified interval of time, and predicted concentrations are output at fixed intervals. For each calculational time step, IEM-2M first performs a terrestrial mass balance to obtain mercury concentrations in watershed soils. Soil concentrations are used along with vapor concentrations and deposition rates to calculate concentrations in various food plants. These are used, in turn, to calculate concentrations in animals. IEM-2M next performs an aquatic mass balance driven by direct atmospheric deposition along with runoff and erosion loads from watershed soils. MHg concentrations in fish are derived from dissolved MHg water concentrations using bioaccumulation factors (BAF).

IEM-2 was developed to handle individual chemicals, or chemicals linked by kinetic transformation reactions. IEM-2M is expanded to include specific kinetic transformation rates affecting mercury components in soil, water, and sediments -- oxidation, reduction, methylation, and demethylation. These transformation rates are driven by specified rate constants. Volatilization kinetics are included as a transfer reaction driven by specified chemical properties and environmental conditions.

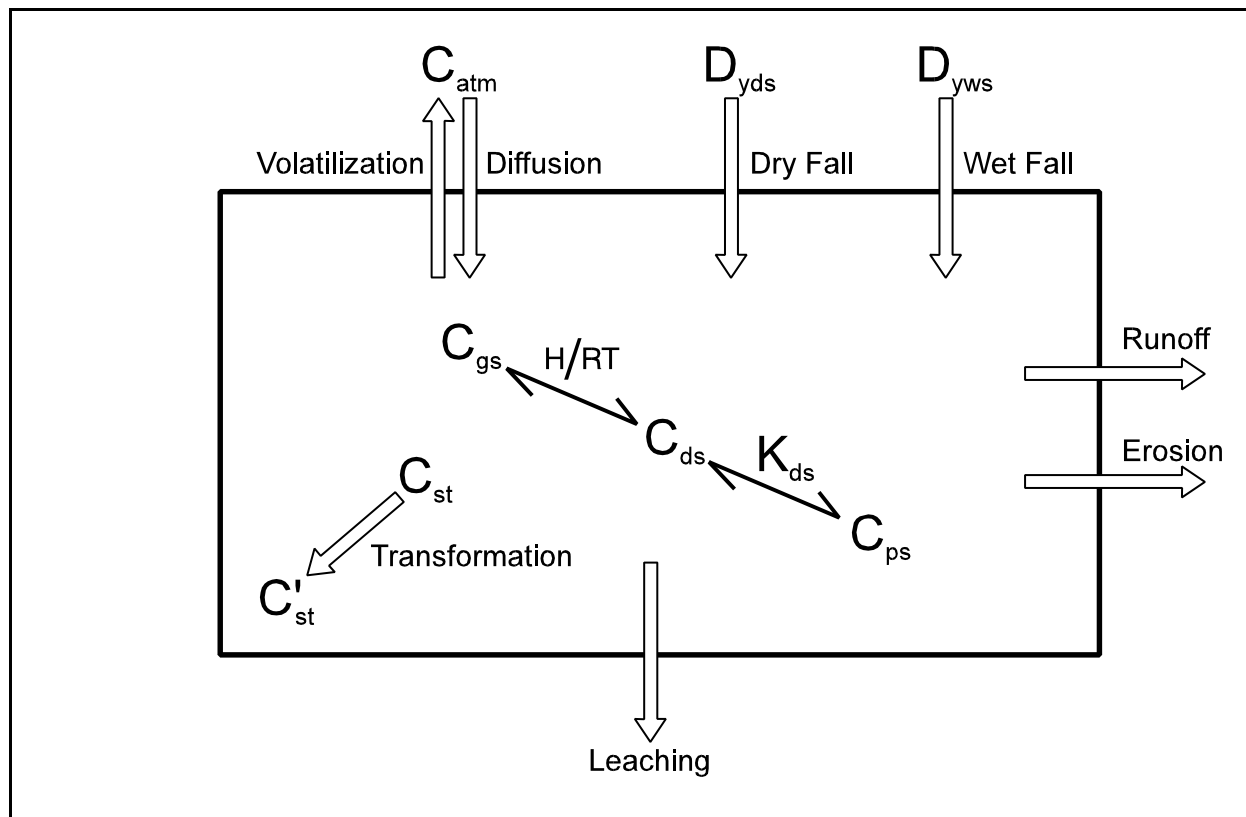
The nature of this methodology is quasi-steady with respect to time and homogeneous with respect to space. While it tracks the buildup of soil and water concentrations over the years given a steady depositional load and long-term average hydrological behavior, it does not respond to unsteady loading or meteorological events. There are, thus, limitations on the analysis and interpretations imposed by these simplifications. The model's calculations of average water body concentrations are less reliable for unsteady environments, such as streams, than for more steady environments, such as lakes.

4.4.2 Description of the Watershed Soil Module

The IEM-2M watershed soil module calculates surface soil concentrations, including dissolved, sorbed, and gas phases, as illustrated in Figure 4-7. The model accounts for three routes of contaminant entry into the soil: deposition of particle-bound contaminant through dryfall; deposition through wetfall; and diffusion of vapor phase contaminant into the soil surface. The model also accounts for four dissipation processes that remove mercury from the surface soils: volatilization (diffusion of gas phase out of the soil surface); runoff of dissolved phase from the soil surface; leaching of the dissolved phase through the soil horizon; and erosion of particulate phase from the soil surface. Key assumptions in the watershed soil module were these:

- Soil concentrations within a depositional area are assumed to be uniform within the area, and can be estimated by the following key parameters: dry and wet contaminant deposition rates, a diffusion-driven gaseous exchange rate with the atmosphere, a set of soil transformation rates, a soil bulk density, and a soil mixing depth.
- The partitioning of mercury components among soil water, soil particle, and soil gas phases can be described by partition coefficients and Henry's Law constants.

Figure 4-7
Overview of the IEM2 Soils Processes



Definitions for Figure 4-7

C_{atm}	vapor phase chemical concentration in air	$\mu\text{g}/\text{m}^3$
D_{yds}	average dry deposition to watershed	mg/yr
D_{yws}	average wet deposition to watershed	mg/yr
C_{st}	total chemical concentration in soil	mg/L
C'_{st}	reaction product concentration in soil	mg/L
C_b	background chemical concentration in soil	mg/L
C_{gs}	chemical concentration in soil gas	$\mu\text{g}/\text{m}^3$
C_{ds}	chemical concentration in soil water	mg/L
C_{ps}	chemical concentration on soil particles	$\mu\text{g}/\text{g}$
H	Henry's Law constant	$\text{atm}\cdot\text{m}^3/\text{mole}$
R	universal gas constant	$\text{atm}\cdot\text{m}^3/\text{mole}\cdot^\circ\text{K}$
T	temperature	$^\circ\text{K}$
K_{ds}	soil/water partition coefficient	L/kg

4.4.2.1 Development of Soil Mass Balance Equations

The concentration of constituent “i” in watershed soils can be expressed per unit volume (C_{si} , in mg/L) or per unit mass (Sc_i , in mg/kg), where BD is soil bulk density (dry weight basis), in kg/L:

$$C_{si} = Sc_i \cdot BD$$

Given constant steady depositional loading $L_{SD,i}$ (g/yr) onto a surficial soil layer, the following mass balance equation governs the mass response:

$$\frac{V_s dC_{si}}{dt} = L_{SD,i} + S_{Ts,i} - S_{Ls,i}$$

where:

$$\begin{aligned} V_s &= \text{watershed soil volume (m}^3\text{)} \\ S_{Ts,i} &= \text{total transformation source in the soil layer (g/yr)} \\ S_{Ls,i} &= \text{total transport and transformation loss in the soil layer (g/yr)}. \end{aligned}$$

A simple first-order transformation source from constituent C_{sj} would be given by:

$$S_{Ts,i} = +ks_T \cdot V_s \cdot C_{sj}$$

where:

$$ks_T = \text{first-order transformation rate constant (yr}^{-1}\text{)}$$

Similarly, a simple first-order loss process would be given by:

$$S_{Ls,i} = ks_x \cdot V_s \cdot C_{si}$$

where:

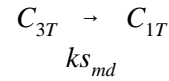
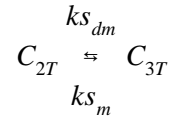
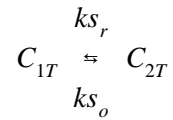
$$ks_x = \text{total first-order loss rate constant (yr}^{-1}\text{)}$$

The basic mass balance equation is applied to three interacting mercury components. For each component “i,” three phases in local equilibrium are calculated -- gas phase (C_{ig} , $\mu\text{g/m}^3$), aqueous phase (C_{iw} , mg/L), and solid phase (C_{is} , $\mu\text{g/g}$):

$$C_{ig} \rightleftharpoons C_{iw} \rightleftharpoons C_{is}$$

The fraction of each component “i” in each phase -- f_{ig} , f_{iw} , and f_{is} -- is calculated using partition coefficients and properties of the soil, as described in a section below.

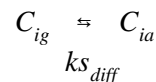
The three mercury components are linked by a set of transformation reactions, including oxidation of total elemental mercury, reduction and methylation of total divalent mercury, and demethylation of total methyl mercury by two pathways:



These are modeled as first-order processes, each a function of environmental conditions, where:

- ks_o = oxidation rate constant (yr^{-1})
- ks_r = reduction rate constant (yr^{-1})
- ks_m = methylation rate constant (yr^{-1})
- ks_{dm} = demethylation rate constant (yr^{-1})
- ks_{md} = *mer* cleavage demethylation rate constant (yr^{-1})

Each mercury component is also subject to a set of transport processes, including leaching and runoff of dissolved phase, erosion of particulate phase, and volatilization of gas phase. These are modeled as first-order processes, where ks_L is the leaching rate constant (yr^{-1}), ks_R is the runoff rate constant (yr^{-1}), and ks_e is the erosion rate constant (yr^{-1}). Each of these rate constants is a function of environmental conditions. While leaching, runoff, and erosion are strictly loss processes from the soil, volatilization is a diffusive exchange process between soil and atmosphere:



where:

- ks_{diff} = diffusive exchange volume (m^3/yr)

This diffusive exchange leads to an atmospheric loading that partially balances the volatile loss from the soil. The net loss rate is the product of ks_{diff} and the concentration gradient ($C_{ig}-C_{ia}$). For modeling purposes, it is convenient to divide this process into a diffusive loading term and a first-order loss term, where ks_v is the volatilization loss rate constant (yr^{-1}). These are developed in the sections below.

Using the calculated phase fractions, three differential equations can be written to describe the mercury mass balance in soil:

$$\frac{V_s \cdot dC_{s1}}{dt} = L_{SD,1} + [ks_r \cdot V_s] \cdot C_{s2} + [ks_{md} \cdot V_s] \cdot C_{s3} \\ - [(ks_{v,1} + ks_o + ks_{RO} + ks_L + ks_e) \cdot V_s] \cdot C_{s1}$$

$$\frac{V_s \cdot dC_{s2}}{dt} = L_{SD,2} + [ks_o \cdot V_s] \cdot C_{s1} + [ks_{dm} \cdot V_s] \cdot C_{s3} \\ - [(ks_r + ks_m + ks_{RO} + ks_L + ks_e) \cdot V_s] \cdot C_{s2}$$

$$\frac{V_s \cdot dC_{s3}}{dt} = L_{SD,3} + [ks_m \cdot V_s] \cdot C_{s2} \\ - [(ks_{v,3} + ks_{dm} + ks_{md} + ks_{RO} + ks_L + ks_e) \cdot V_s] \cdot C_{s3}$$

The major model coefficients are described in more detail in the sections below.

4.4.2.2 Loads to Watershed Soils

The total atmospheric loading term for component “i” -- $L_{SD,i}$ in the mass balance equations -- is the sum of the wetfall, dryfall, and vapor diffusion fluxes:

$$L_{SD,i} = (Dydw_i + Dyww_i + L_{DIF,i}) \cdot A_s$$

where:

$$\begin{aligned} Dydw_i &= \text{yearly-average dry depositional flux of component “i” (g/m}^2\text{-yr)} \\ Dyww_i &= \text{yearly-average wet depositional flux of component “i” (g/m}^2\text{-yr)} \\ L_{DIF,i} &= \text{yearly-average vapor diffusion flux of component “i” (g/m}^2\text{-yr)} \end{aligned}$$

The vapor diffusion flux is calculated from the diffusion volume and the atmospheric concentration, normalized to the surface area:

$$L_{DIF,i} = \frac{ks_{diff,i}}{A_s} \cdot C_{a,i} \cdot 10^{-6}$$

where:

$$\begin{aligned} ks_{diff,i} &= \text{diffusive exchange volume (m}^3\text{/yr)} \\ A_s &= \text{surface area of the watershed soil element (m}^2\text{)} \\ C_{a,i} &= \text{vapor phase atmospheric concentration for component “i” (}\mu\text{g/m}^3\text{)} \end{aligned}$$

The diffusive exchange volume is calculated from the atmospheric diffusion coefficient:

$$kS_{diff} = \frac{D_i \cdot A_s \cdot \theta_v}{z_r} \cdot 3.15 \times 10^7 \cdot 10^{-4}$$

where:

D_i	=	atmospheric diffusion coefficient for component "i" (cm ² /sec)
θ_v	=	soil void fraction
z_r	=	characteristic diffusion reference depth (m)
3.15×10^7	=	units conversion factor (sec/yr)
10^{-4}	=	units conversion factor (m ² /cm ²)

The product $A_s \cdot \theta_v$ represents the cross-sectional area within the soil through which diffusion occurs.

4.4.2.3 Equilibrium Speciation Reactions

The gas and solid phase concentrations are calculated from the aqueous phase concentration:

$$C_{ig} = (H_i / RT_K) \cdot C_{iw}$$

$$C_{is} = K_{di} \cdot C_{iw}$$

where:

H_i	=	Henry's Law constant (atm·m ³ /mole)
R	=	universal gas constant (atm·m ³ /mole·°K)
T_K	=	temperature (°K)
K_{di}	=	solids partition coefficient (L/kg)

The total amount of mercury in component "i" is the summation across all phases:

$$C_{iT} = C_{ig} \cdot \theta_v + C_{iw} \cdot \theta_w + C_{is} \cdot BD$$

where:

θ_v	=	soil void fraction (L/L)
θ_w	=	soil water fraction (L/L)
BD	=	soil bulk density (kg/L) on a dry weight basis.

From these equations, the fraction of component "i" in each phase can be calculated:

$$f_{ig} = \frac{(H_i/RT_K) \cdot \theta_v}{(H_i/RT_K) \cdot \theta_v + \theta_w + K_{di} \cdot BD}$$

$$f_{iw} = \frac{\theta_w}{(H_i/RT_K) \cdot \theta_v + \theta_w + K_{di} \cdot BD}$$

$$f_{is} = \frac{K_{di} \cdot BD}{(H_i/RT_K) \cdot \theta_v + \theta_w + K_{di} \cdot BD}$$

4.4.2.4 Transformation Processes in Watershed Soils

As described above, five transformation reactions are modeled as first-order rates. Rate constants are directly specified and applied to the bulk concentration (all phases) to give internal mass transformation loadings. The oxidation loading $ks_o \cdot V_s \cdot C_{s1}$ is subtracted from the Hg^0 mass balance equation and added to the $HgII$ equation. The reduction loading $ks_r \cdot V_s \cdot C_{s2}$ is subtracted from the $HgII$ equation and added to the Hg^0 equation. The methylation loading $ks_m \cdot V_s \cdot C_{s3}$ is subtracted from the $HgII$ equation and added to the MHg equation. The demethylation loading $ks_{dm} \cdot V_s \cdot C_{s3}$ is subtracted from the MHg equation and added to the $HgII$ equation. Finally, the *mer* demethylation loading $ks_{md} \cdot V_s \cdot C_{s3}$ is subtracted from the MHg equation and added to the Hg^0 equation.

There is evidence that reduction in soil is mediated by sunlight, is proportional to soil water content, and occurs most rapidly within the upper 5 mm of the soil surface (Carpi and Lindberg, 1997). As a result, the input reduction rate constant k_{rs} is normalized to a reference depth z_r of 5 mm and to 100% water content. The actual reduction rate constant ks_r used in the model is the product of k_{rs} , the soil water content θ_w and the ratio of the reference depth to the depth of the soil layer z_r/z_s .

4.4.2.5 Transport and Transfer Processes in Watershed Soils

The total transport loss of component “i” from the soil is the sum of the loss rates due to leaching, runoff, erosion, and volatilization. In the governing mass balance equations, these loss rates are expressed as the product of a loss rate constant, the total component concentration, and the soil volume. The runoff loss constant is a function of the runoff volume and the dissolved fraction of component “i”:

$$k_{S_{RO,i}} = \left(\frac{RO}{z_s} \right) \cdot \frac{f_{iw}}{\theta_w}$$

where:

Ro	=	average annual runoff (m/yr)
z_s	=	upper soil layer depth (m)
θ_w	=	volumetric water content (dimensionless; cm^3/cm^3)

f_{iw} = aqueous fraction of component “i” concentration.

The first term times the soil volume is the annual runoff volume in m^3/yr , while the second term times the total concentration is the aqueous concentration in the runoff in g/m^3 .

The leaching loss constant is a function of the leaching volume and the dissolved fraction of component “i”:

$$kS_{L,i} = \left(\frac{P + I - Ro - EV}{z_s} \right) \cdot \frac{f_{iw}}{\theta_s}$$

where:

P = average annual precipitation (m/yr)
 I = average annual irrigation (m/yr)
 EV = average annual evapotranspiration (m/yr).

The first term times the soil volume is the annual percolation volume in m^3/yr , while the second term times the total concentration is the aqueous concentration in percolating water, in g/m^3 .

The erosion loss constant is a function of the erosion mass and the particulate fraction of component “i”:

$$kS_{e,i} = \left(\frac{X_e \cdot SD \cdot ER}{z_s} \right) \cdot \frac{f_{is}}{1000 \cdot BD}$$

where:

X_e = unit soil loss (kg/m^2 -yr; see Eq [9-3], IED; Wischmeier and Smith, 1978)
 SD = sediment delivery ratio
 ER = particle enrichment ratio
 BD = soil dry density (g/cm^3)
 f_{is} = sorbed fraction of the total component “i” concentration .

The first term times the soil volume is the annual erosion mass in kg/yr , while the second term times the total concentration is the sorbed concentration on the eroding particles in g/kg .

The volatilization rate constant ks_v can be derived from the diffusive exchange volume and gas phase concentration:

$$ks_v \cdot V_s \cdot C_{si} = ks_{diff,i} \cdot C_{ig}$$

$$ks_v = \left(\frac{ks_{diff,i}}{V_s} \right) \cdot \frac{f_{ig}}{\theta_v}$$

where:

$ks_{diff,i}$ = diffusive exchange volume (m^3/yr)
 V_s = soil layer volume (m^3)

θ_v = void fraction.

Substituting in the expression for $k_{s_{diff,i}}$ gives the volatilization rate constant in terms of the atmospheric diffusivity and the gaseous fraction of component "i" in the soil:

$$k_{s_v} = \left(3.15 \times 10^3 \frac{D_i \cdot \theta_v}{z_s \cdot z_r} \right) \cdot \frac{f_{ig}}{\theta_v}$$

where:

D_i = atmospheric diffusivity (cm²/sec)
 z_s = soil thickness (m)
 z_r = characteristic diffusive mixing depth (m)
 3.15×10^3 = units conversion factor (sec/yr · m²/cm²)
 θ_v = soil void fraction
 f_{ig} = gaseous fraction of the total component "i" concentration.

The first term times the soil volume is the annual gas diffusion volume in m³/yr, while the second term times the total concentration is the gas phase concentration in the void space in g/m³.

4.4.3 Description of the Water Body Module

The IEM-2M water body module estimates water column as well as bed sediment concentrations in a shallow lake. Water column concentrations included dissolved, sorbed to suspended sediments and total (sorbed plus dissolved, or total contaminant divided by total water volume). This framework also provides three concentrations for the bed sediments: dissolved in pore water, sorbed to bed sediments, and total. The model accounts for five routes of contaminant entry into the water body: erosion of mercury sorbed to soil particles; runoff of dissolved mercury in runoff water; deposition of particle-bound mercury through wetfall; deposition of particle-bound mercury through dryfall; and diffusion of vapor phase Hg⁰ into the water body. The model also accounts for three dissipation processes that remove mercury from the water body: volatilization of dissolved phase Hg⁰ and MHg from the water column; removal of total mercury via "burial" from the surficial bed sediment layer; and advection of total mercury from the water column via outflow. The burial rate is a function of the deposition of biotic and abiotic solids from the water column to the bed; it accounts for the fact that much of the soil eroding into a water body annually is incorporated into bottom sediment. The impact to the water body was assumed to be uniform. This tends to be more realistic for smaller water bodies as compared to large rivers or lakes. Key features and assumptions in the surface water body module include the following.

- The partitioning of mercury components between the water column and suspended biotic and abiotic solids, and between pore water and sediment particles is in local equilibrium as described by a set of partition coefficients.
- Atmospheric mercury wetfall and dryfall loads are handled as a constant average flux.
- Surface runoff mercury loadings are estimated as a function of the dissolved concentration of mercury in the surficial soil water (calculated by the soil module as a function of time) and the specified annual water runoff.

- Soil erosion mercury loadings are calculated as a function of the sorbed concentration of mercury in the surficial soil layer (calculated by the soil module as a function of time), together with the calculated annual soil erosion, a sediment delivery ratio, and an enrichment ratio. The sediment delivery ratio serves to reduce the total potential amount of soil erosion (where the total potential erosion equals the unit erosion rate in kg/m² multiplied by the watershed area, in m²) reaching the water body. This parameter accounts for the observation that most of the eroded particles mobilized within a watershed during a year deposit prior to reaching the water body. The enrichment ratio accounts for the fact that eroding soils tend to be lighter in texture, more abundant in surface area, and higher in organic carbon. All these characteristics lead to concentrations in eroded soils that tend to be higher than those in *situ* soils.
- Diffusive mercury loadings from the atmosphere are calculated as a function of a specified atmospheric vapor concentration, the calculated dissolved water column concentration, and the calculated transfer velocity. The dissolved concentration in a water body is driven toward equilibrium with the vapor phase concentration above the water body. At equilibrium, gaseous diffusion into the water body is matched by volatilization out of the water body. This specified air concentration is an output of the atmospheric transport model.
- The rate of contaminant burial in bed sediments is estimated as a function of the rate at which biotic and abiotic solids deposit from the water column onto the surficial sediment layer minus the rate at which they resuspend to the water column. Burial represents a permanent sink of eroded soil and mercury concentrations scavenged from the water column.
- Separate transformation rate constants allow for the calculation of mercury component fractions in the water column and benthic sediments.

In the following sections, the mass balance equations and the equilibrium state equations that link the concentrations are developed.

4.4.3.1 The Water Body Equations

Given the loading of mercury from atmospheric deposition and the surrounding watershed, the following mass balance equations govern the concentration response in the water column and surficial benthic sediment layer of a shallow lake:

$$\begin{aligned} \frac{V_w dC_{wt}}{dt} = & L_T - Vf_x \cdot C_{wt} + R_{sw} \cdot (C_{db} - C_{dw}) \\ & - [v_s \cdot C_{sw} + v_{sB} \cdot C_{Bw} - v_{rs} \cdot C_{bt}] \cdot A_w \\ & + S_{wt} - k_v \cdot A_w \cdot C_{dw} \end{aligned}$$

$$\begin{aligned} \frac{V_b dC_{bt}}{dt} = & - R_{sw} \cdot (C_{db} - C_{dw}) + S_{bt} \\ & + [v_s \cdot C_{sw} + v_{sB} \cdot C_{Bw} - (v_{rs} + v_b) \cdot C_{sb}] \cdot A_w \end{aligned}$$

where:

C_{wt}	=	total water column concentration (mg/L)
C_{bt}	=	total benthic concentration (mg/L)
C_{dw}	=	dissolved water column concentration (mg/L)
C_{db}	=	dissolved benthic concentration (mg/L)
C_{sw}	=	particulate abiotic water column concentration (mg/L)
C_{bw}	=	particulate biotic water column concentration (mg/L)
C_{sb}	=	particulate (sorbed) benthic concentration (mg/L)
C_a	=	atmospheric concentration ($\mu\text{g}/\text{m}^3$)
V_w	=	water column volume (m^3)
V_b	=	benthic volume (m^3)
L_T	=	total loading (g/year)
Vf_x	=	dilution flow (m^3/year)
R_{sw}	=	pore water diffusion volume (m^3/year)
A_w	=	surface area (m^2)
v_s	=	settling velocity for abiotic solids (m/year)
v_{sB}	=	settling velocity for biotic solids (m/year)
v_{rs}	=	resuspension velocity (m/year)
v_b	=	burial velocity (m/year)
S_{wt}	=	net transformation source in the water column (g/yr)
S_{bt}	=	net transformation source in the benthic sediment layer (g/yr)

The pore water diffusion volume is calculated as:

$$R_{sw} = \frac{E_{sw} \cdot A_w \cdot \theta_{bs}}{z_b}$$

where:

E_{sw}	=	pore water diffusion coefficient (m^2/year)
θ_{bs}	=	benthic porosity (L_w/L)
z_b	=	surficial benthic layer depth (m)

The first term in the water column mass balance equation describes external loading, while the second term describes advective export. The third term covers net pore water exchange with the surficial benthic layer, and is also present in the benthic sediment equation. The fourth term gives net deposition of particulate mercury, including settling of abiotic and biotic solids and resuspension of benthic solids. These processes are also represented in the benthic sediment equation. The fifth term in the water column equation gives the net internal transformation source, while the last term gives the net volatilization loss.

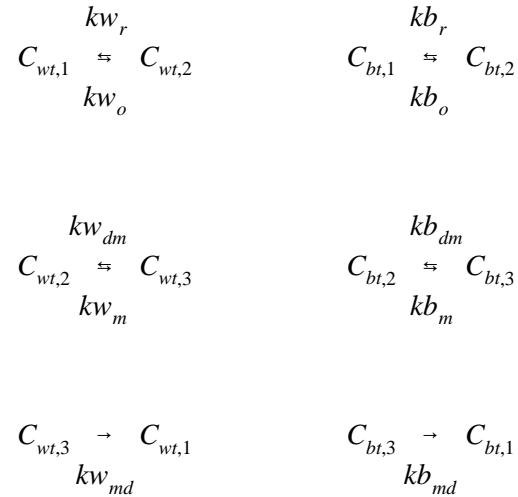
The benthic sediment mass balance equation contains terms for pore water exchange, internal transformation source, and net solids transport, which includes deposition, resuspension, and burial.

These basic equations are applied to three interacting mercury components. For each component "i" in the water column, three phases in local equilibrium are calculated -- aqueous phase (C_{iw} , mg/L), abiotic solid phase (C_{is} , $\mu\text{g}/\text{g}$), and biotic solid phase (C_{iB} , $\mu\text{g}/\text{g}$):

$$C_{is} \rightleftharpoons C_{iw} \rightleftharpoons C_{iB}$$

In the sediments, two phases in local equilibrium are calculated -- aqueous pore water phase (C_{db} , mg/L) and sediment phase (C_{sb} , $\mu\text{g/g}$). The fraction of each component "i" in each phase -- $f_{dw,i}$, $f_{sw,i}$, and $f_{Bw,i}$ in the water column and $f_{db,i}$ and $f_{sb,i}$ in the sediments -- is calculated using partition coefficients and properties of the solids and sediment, as described in a section below.

The three mercury components are linked by a set of first-order transformation reactions, including oxidation of total elemental mercury, reduction and methylation of total divalent mercury, and demethylation of total methyl mercury by two pathways:



where:

- kw_o = water column oxidation rate constant (yr^{-1})
- kb_o = benthic oxidation rate constant (yr^{-1})
- kw_r = water column reduction rate constant (yr^{-1})
- kb_r = benthic reduction rate constant (yr^{-1})
- kw_m = water column methylation rate constant (yr^{-1})
- kb_m = benthic methylation rate constant (yr^{-1})
- kw_{dm} = water column demethylation rate constant (yr^{-1})
- kb_{dm} = benthic demethylation rate constant (yr^{-1})
- kw_{md} = water column *mer* cleavage demethylation rate constant (yr^{-1})
- kb_{md} = benthic *mer* cleavage demethylation rate constant (yr^{-1})

Each of these rate constants is a function of environmental conditions. Their values are specified as input to the IEM-2M model.

Each mercury component is also subject to a set of transport processes, including advective export of all phases in the water column, volatilization and pore water exchange of dissolved phase, and settling, resuspension, and burial of particulate phase. These are modeled as first-order processes as described in the general water column and benthic sediment mass balance equations above. Volatilization is modeled as a surficial "thin-film" exchange process in which the dissolved concentration in the water column is driven toward equilibrium with the atmosphere:

$$\left. \frac{V_w \cdot dC_{w,i}}{dt} \right|_{volatilization} = K_{v,i} \cdot A_w \cdot \left(C_{dw,i} - \frac{C_{a,i} \cdot 10^{-6}}{H_i / RT_K} \right)$$

where:

$K_{v,i}$	=	conductivity of component "i" through the air-water interface (m/yr)
H_i	=	Henry's Law constant for component "i" ($\text{m}^3\text{-atm/mole}$)
R	=	Universal Gas constant ($\text{atm}\cdot\text{m}^3/\text{mole}\cdot^\circ\text{K}$)
T_K	=	water temperature ($^\circ\text{K}$)
$C_{a,i}$	=	component "i", vapor phase air concentration ($\mu\text{g}/\text{m}^3$)

For modeling purposes, it is convenient to divide this process into a diffusive loading term and a first-order loss term, where $kw_{v,i}$ is the volatilization loss rate constant (yr^{-1}). These terms are developed in the sections below.

Using the calculated phase fractions, six differential equations for the three mercury components in water column and sediments can be expressed in their mass balance form, grouping constants and model parameters within brackets:

$$\begin{aligned} \frac{V_w \cdot dC_{wt,1}}{dt} = & L_{T1} + [V_s \cdot (ks_{RO} + ks_e)] \cdot C_{s1} + [kw_r \cdot V_w] \cdot C_{wt,2} + [kw_{md} \cdot V_w] \cdot C_{wt,3} \\ & - [Vf_x + R_{sw} \cdot f_{dw,1} + (kw_{v,1} + kw_o) \cdot V_w + (v_s \cdot f_{sw,1} + v_{sB} \cdot f_{Bw,1}) \cdot A_w] \cdot C_{wt,1} \\ & + [R_{sw} \cdot (f_{db,1} / \theta_{bs}) + v_{rs} \cdot f_{sb,1} \cdot A_w] \cdot C_{bt,1} \end{aligned}$$

$$\begin{aligned} \frac{V_w \cdot dC_{wt,2}}{dt} = & L_{T2} + [V_s \cdot (ks_{RO} + ks_e)] \cdot C_{s2} + [kw_o \cdot V_w] \cdot C_{wt,1} + [kw_{dm} \cdot V_w] \cdot C_{wt,3} \\ & - [Vf_x + R_{sw} \cdot f_{dw,2} + (kw_r + kw_m) \cdot V_w + (v_s \cdot f_{sw,2} + v_{sB} \cdot f_{Bw,2}) \cdot A_w] \cdot C_{wt,2} \\ & + [R_{sw} \cdot (f_{db,2} / \theta_{bs}) + v_{rs} \cdot f_{sb,2} \cdot A_w] \cdot C_{bt,2} \end{aligned}$$

$$\begin{aligned} \frac{V_w \cdot dC_{wt,3}}{dt} = & L_{T3} + [V_s \cdot (ks_{RO} + ks_e)] \cdot C_{s3} + [kw_m \cdot V_w] \cdot C_{wt,2} \\ & - [Vf_x + R_{sw} \cdot f_{dw,3} + (kw_{v,3} + kw_{md} + kw_{dm}) \cdot V_w + (v_s \cdot f_{sw,3} + v_{sB} \cdot f_{Bw,3}) \cdot A_w] \cdot C_{wt,3} \\ & + [R_{sw} \cdot (f_{db,3} / \theta_{bs}) + v_{rs} \cdot f_{sb,3} \cdot A_w] \cdot C_{bt,3} \end{aligned}$$

$$\begin{aligned} \frac{V_b \cdot dC_{bt,1}}{dt} = & \left[R_{sw} \cdot f_{dw,1} + (v_s \cdot f_{sw,1} + v_{sB} \cdot f_{Bw,1}) \cdot A_w \right] \cdot C_{wt,1} + [kb_r \cdot V_b] \cdot C_{bt,2} \\ & + [kb_{md} \cdot V_b] \cdot C_{bt,3} - \left[R_{sw} \cdot (f_{db,1} / \theta_{bs}) + (v_{rs} + v_b) \cdot f_{sb,1} \cdot A_w + (kb_o) \cdot V_b \right] \cdot C_{bt,1} \end{aligned}$$

$$\begin{aligned} \frac{V_b \cdot dC_{bt,2}}{dt} = & \left[R_{sw} \cdot f_{dw,2} + (v_s \cdot f_{sw,2} + v_{sB} \cdot f_{Bw,2}) \cdot A_w \right] \cdot C_{wt,2} + [kb_o \cdot V_b] \cdot C_{bt,1} \\ & + [kb_{dm} \cdot V_b] \cdot C_{bt,3} - \left[R_{sw} \cdot (f_{db,2} / \theta_{bs}) + (v_{rs} + v_b) \cdot f_{sb,2} \cdot A_w + (kb_r + kb_m) \cdot V_b \right] \cdot C_{bt,2} \end{aligned}$$

$$\begin{aligned} \frac{V_b \cdot dC_{bt,3}}{dt} = & \left[R_{sw} \cdot f_{dw,3} + (v_s \cdot f_{sw,3} + v_{sB} \cdot f_{Bw,3}) \cdot A_w \right] \cdot C_{wt,3} + [kb_m \cdot V_b] \cdot C_{bt,2} \\ & - \left[R_{sw} \cdot (f_{db,3} / \theta_{bs}) + (v_{rs} + v_b) \cdot f_{sb,3} \cdot A_w + (kb_{md} + kb_{dm}) \cdot V_b \right] \cdot C_{bt,3} \end{aligned}$$

Combined with the soil mercury equations expressed in the previous section, there are nine mass balance differential equations to solve for nine state variables -- elemental, divalent, and methyl mercury in the soil, water column, and benthic sediments. These differential equations have constant parameters and can be solved for specified time intervals using a standard ODE solver. The following sections describe how the model parameters in the water body differential equations are calculated or specified.

4.4.3.2 The Solids Balance Equations

The abiotic and biotic solids must be modeled in order to predict the dissolved and particulate mercury fractions. These determine the amount of mercury lost through deposition and burial, and also influence the bioavailability of methyl mercury in the water column. The differential equations describing the fate of watershed-derived solids in the water column (S_w), internally-generated biotic solids in the water column (S_{Bio}), and total solids in the benthic sediments (S_B) are given by:

$$\frac{V_w \cdot dS_w}{dt} = + [L_{Se} \cdot A_s \cdot 10^3] - [Vf_x + v_s \cdot A_w] \cdot S_w + [v_{rs} \cdot A_w] \cdot S_B$$

$$\frac{V_w \cdot dS_{Bio}}{dt} = + [L_{SB} \cdot A_w] - [Vf_x + k_{mort} \cdot V_w + v_{sB} \cdot A_w] \cdot S_{Bio}$$

$$\frac{V_b \cdot dS_B}{dt} = + [v_s \cdot S_w + v_{sB} \cdot S_{Bio}] \cdot A_w - [(v_{rs} + v_{min} + v_b) \cdot A_w] \cdot S_B$$

where:

L_{Se}	=	watershed solids erosion load (kg/m ² -yr)
L_{SB}	=	net internal production of biotic solids (g/m ² -year)
k_{mort}	=	phytoplankton mortality rate (yr ⁻¹)
v_{min}	=	mineralization rate for upper benthic solids (m/year)

For long-term average calculations using average watershed loading and waterbody productivity, S_w , S_{Bio} , and S_B can be assumed to be at steady-state. If S_B , v_s , v_{sB} , v_{rs} , and k_{mort} are specified, then the water column solids concentrations and the burial velocity can be calculated from:

$$S_w = \frac{L_{Se} \cdot A_s \cdot 10^3 + v_{rs} \cdot A_w \cdot S_B}{Vf_x + v_s \cdot A_w}$$

$$S_{Bio} = \frac{L_{SB} \cdot A_w}{Vf_x + k_{mort} \cdot V_w + v_{sB} \cdot A_w}$$

$$v_B = \frac{v_s \cdot S_w + v_{sB} \cdot S_{Bio} - (v_{rs} + v_{min}) \cdot S_B}{S_B}$$

4.4.3.3 Loads to the Water Body

The total chemical load term L_T in the mass balance equation is the sum of the loadings for each component "i." Component loadings included wet and dry deposition, impervious and pervious runoff, erosion, and atmospheric diffusion:

$$L_{T,i} = L_{Dep,i} + L_{RI,i} + L_{R,i} + L_{E,i} + L_{Dif,i}$$

where:

$L_{T,i}$	=	total component "i" load to the water body (g/yr)
$L_{Dep,i}$	=	deposition of particle bound component "i" (g/yr)
$L_{RI,i}$	=	runoff load from impervious surfaces (g/yr)
$L_{R,i}$	=	runoff load from pervious surfaces (g/yr)
$L_{E,i}$	=	soil erosion load (g/yr)
$L_{Dif,i}$	=	diffusion load for vapor phase component "i" (g/yr)

The runoff and erosion loads required estimation of average contaminant concentration in watershed soils that comprise the depositional area. These concentrations were developed in terrestrial sections above.

Load due to direct deposition -- The load to surface waters via direct deposition is solved as follows:

$$L_{Dep,i} = (D_{yds,i} + D_{yws,i}) \cdot A_w$$

where:

$L_{Dep,i}$	=	direct component "i" deposition load (g/yr)
$D_{yds,i}$	=	yearly dry deposition rate of component "i" onto surface water body (g pollutant/m ² -yr)
$D_{yws,i}$	=	yearly wet deposition rate of component "i" onto surface water body (g pollutant/m ² -yr)
A_w	=	water body area (m ²)

Load due to impervious surface runoff -- A fraction of the wet and dry chemical deposition in the watershed will be to impervious surfaces. Dry deposition may accumulate and be washed off during rain events. If the impervious surface includes gutters, the pollutant load will be transported to surface waters, bypassing the watershed soils. The average load from such impervious surfaces is given by this equation:

$$L_{RI,i} = (D_{yww,i} + D_{ydw,i}) \cdot A_I$$

where:

$L_{RI,i}$	=	impervious surface runoff load for component "i" (g/yr)
A_I	=	impervious watershed area receiving pollutant deposition (m ²)
$D_{yww,i}$	=	yearly wet deposition flux of component "i" onto the watershed (g/m ² -yr)
$D_{ydw,i}$	=	yearly dry deposition flux of component "i" onto the watershed (g/m ² -yr)

Load due to pervious surface runoff -- Most of the chemical deposition to a watershed will be to pervious soil surfaces. These loads are accounted for in the soil mass balance equation. During periodic runoff events, dissolved chemical concentrations in the soil are transported to surface waters as given by this equation:

$$L_{R,i} = ks_{RO,i} \cdot V_s \cdot C_{si}$$

where:

$L_{R,i}$	=	pervious surface runoff load for component "i" (g/yr)
$ks_{RO,i}$	=	soil runoff rate constant for component "i" (yr ⁻¹)
C_{si}	=	component "i" concentration in watershed soils (g/m ³)
V_s	=	volume of pervious soil layer = $A_s \cdot z_s$ (m ³)
A_s	=	surface area of pervious soil layer = $WA_L - WA_I$ (m ²)
WA_L	=	total watershed area receiving pollutant deposition (m ²)
WA_I	=	impervious watershed area receiving pollutant deposition (m ²)
z_s	=	depth of surface soil layer (m)

Load due to soil erosion -- During periodic erosion events, particulate chemical concentrations in the soil are transported to surface waters as described by this relationship:

$$L_{E,i} = ks_{e,i} \cdot V_s \cdot C_{si}$$

where:

$L_{E,i}$	=	soil erosion load for component "i" (g/yr)
-----------	---	--

$ks_{e,i}$ = soil erosion loss rate constant for component "i" (yr^{-1})

Load due to gaseous diffusion -- The volatilization equation presented above is divided into a diffusive loading term and a loss term in IEM-2M. The diffusive loading term is given by:

$$L_{Dif,i} = K_{v,i} \cdot A_w \cdot \left(\frac{C_{a,i} \cdot 10^{-6}}{H_i/RT_K} \right)$$

where:

$L_{Dif,i}$ = diffusive loading rate for component "i" (g/yr)
 $K_{v,i}$ = overall transfer rate, or conductivity for component "i" (m/yr)
 A_w = surface area of water body (m^2)
 $C_{a,i}$ = component "i" vapor phase air concentration over water body ($\mu g/m^3$)
 H_i = component "i" Henry's Constant ($atm \cdot m^3/mole$)
 R = universal gas constant, $8.206 \cdot 10^{-5} atm \cdot m^3/mole \cdot ^\circ K$
 T_K = water body temperature ($^\circ K$)
 10^{-6} = units conversion factor (g/ μg)

This treatment of volatilization is based on the well-known two-film theory (Whitman, 1923), as implemented in standard chemical fate models (Burns, et al., 1982, Ambrose, et al., 1988). The equations for $K_{v,i}$ are presented in the volatilization loss section below.

4.4.3.4 Equilibrium Speciation Reactions

In the previous methodology, all mercury components and phases were assumed to be in equilibrium. The equations presented here drop the assumption of equilibrium among components and between water column and underlying sediments. For each mercury component, the fractions in the aqueous phase and on the particulate phases are calculated for the water column and for the benthic sediments from partition coefficients, solids concentrations, and porosities:

$$f_{dw,i} = \frac{1}{1 + K_{dw,i} \cdot S_w \cdot 10^{-6} + K_{Bio,i} \cdot S_{Bio} \cdot 10^{-6}}$$

$$f_{sw,i} = \frac{K_{dw,i} \cdot S_w \cdot 10^{-6}}{1 + K_{dw,i} \cdot S_w \cdot 10^{-6} + K_{Bio,i} \cdot S_{Bio} \cdot 10^{-6}}$$

$$f_{Bw,i} = \frac{K_{Bio,i} \cdot S_{Bio} \cdot 10^{-6}}{1 + K_{dw,i} \cdot S_w \cdot 10^{-6} + K_{Bio,i} \cdot S_{Bio} \cdot 10^{-6}}$$

$$f_{db,i} = \frac{\theta_{bs}}{\theta_{bs} + K_{db,i} \cdot S_b \cdot 10^{-6}}$$

$$f_{sb,i} = \frac{K_{db,i} \cdot S_b \cdot 10^{-6}}{\theta_{bs} + K_{db,i} \cdot S_b \cdot 10^{-6}}$$

where:

$f_{dw,i}$	=	aqueous phase fraction for component “i” in the water column
$f_{db,i}$	=	aqueous phase fractions for component “i” in the benthic sediments
$f_{sw,i}$	=	abiotic particulate fraction in the water column
$f_{Bw,i}$	=	biotic particulate fraction in the water column
$f_{sb,i}$	=	particulate fraction in the sediments
S_w	=	abiotic solids concentration in the water column (g/m ³)
S_{Bio}	=	biotic solids concentration in the water column (g/m ³)
S_b	=	solids concentration (dry density) in the benthic sediments (g/m ³)
$K_{dws,i}$	=	partition coefficient for abiotic solids in the water column (L _w /kg _s)
K_{Bio}	=	partition coefficient for biotic solids in the water column (L _w /kg _{Bio})
$K_{db,i}$	=	partition coefficient for benthic solids (L _w /kg _s)
θ_{bs}	=	porosity of the upper sediment bed (L _w /L).

4.4.3.5 Transformation Processes in the Water Body

As described above, five transformation reactions are modeled as first-order rates. Rate constants are directly specified and applied to the bulk concentration (all phases) in the water column and in the benthic sediments to give internal mass transformation loadings. The oxidation loadings -- $kw_o \cdot V_w \cdot C_{wt,1}$ in the water column and $kb_o \cdot V_b \cdot C_{bt,1}$ in the sediments -- are subtracted from the Hg⁰ mass balance equations and added to the HgII equations. The reduction loadings, $kw_r \cdot V_w \cdot C_{wt,2}$ and $kb_r \cdot V_b \cdot C_{bt,2}$, are subtracted from the HgII equations and added to the Hg⁰ equations. The methylation loadings, $kw_m \cdot V_w \cdot C_{wt,2}$ and $kb_m \cdot V_b \cdot C_{bt,2}$, are subtracted from the HgII equations and added to the MHg equations. The demethylation loadings, $kw_{dm} \cdot V_w \cdot C_{wt,3}$ and $kb_{dm} \cdot V_b \cdot C_{bt,3}$, are subtracted from the MHg equations and added to the HgII equations. Finally, the *mer* demethylation loadings, $kw_{md} \cdot V_w \cdot C_{wt,3}$ and $kb_{md} \cdot V_b \cdot C_{bt,3}$, are subtracted from the MHg equations and added to the Hg⁰ equations.

While the transformation rate constants are specified as input to the IEM-2M model, it is understood that their values may be affected by several environmental properties, including pH, DOC, anoxia, sulfate concentrations, and water clarity. Many of these dependencies are under investigation by the scientific community; some are built into the Regional Mercury Cycling Model (R-MCM). It was decided not to program the environmental rate dependencies into the IEM-2M, but rather to require their consideration external to the model. The rate dependencies and values for the rate constants are discussed in Appendix B, with citations to the current scientific literature. A qualitative summary is given here.

Low pH conditions should favor oxidation of Hg^0 , while high pH conditions should favor reduction of HgII . Lower pH, then, should lead to lower volatilization loss and higher levels of HgII that can be methylated. Reduction and demethylation in the water column appear to be mediated by sunlight. Low water clarity due to high concentrations of DOC and solids should lead to slower reduction and subsequent volatilization loss, and higher levels of total and methyl mercury. Methylation is mediated by anaerobic bacteria, predominantly sulfate reducers. Anoxic conditions and moderate concentrations of sulfate should lead to more rapid methylation. DOC affects mercury in several ways. High levels of DOC compete with solids in complexing HgII and MHg , thus promoting more mobility of these components from the benthic sediments to the water column. The DOC-complexed mercury does not volatilize, further promoting higher levels of mercury in the water column. Other reactions, however, may also be retarded by DOC complexation, including bioaccumulation in the aquatic food web.

4.4.3.6 Transport and Transfer Processes in the Water Body

Mercury components are transferred between the water column and benthic sediment compartments of a water body through pore water diffusion, solids deposition, and resuspension. They are lost from the water body due to advection, burial, and volatilization.

Advection -- Advective flow from the water body removes all phases of component "i" at a rate proportional to the average volumetric flow rate, Vf_x , and the water column concentration $C_{wt,i}$. An impacted water body derives its annual flow from its watershed or effective drainage area. Flow and watershed area, then, are related, and compatible values should be specified by the user. Given the area of drainage, one way to estimate annual flow volume is to multiply total drainage area (in length squared units) by a unit surface water runoff (in length per time). The *Water Atlas of the United States* (Geraghty et al., 1973) provides maps with isolines of annual average surface water runoff, which is defined as all flow contributions to surface water bodies, including direct runoff, shallow interflow, and groundwater recharge. The values ranged from 5 to 40 in/yr (0.13 to 1.0 m/yr) in various parts of the United States.

Pore Water Diffusion -- Pore water diffusion exchanges dissolved constituents between the water column and the benthic sediments. As expressed in the mass balance equations above, this exchange is the product of the pore water diffusive volume and the dissolved phase concentration gradient between the pore water and the water column:

$$R_{sw} \cdot [f_{dw,i} \cdot C_{wt,i} - (f_{db,i}/\theta_{bs}) \cdot C_{bt,i}]$$

where:

$$\begin{aligned} R_{sw} &= \text{pore water diffusive volume (m}^3\text{/yr)} \\ \theta_{bs} &= \text{benthic porosity (L}_w\text{/L)} \end{aligned}$$

The diffusive volume is calculated from the pore water diffusion coefficient:

$$R_{sw} = \frac{E_{sw} \cdot A_w \cdot \theta_{bs}}{z_b} \cdot 3.15 \times 10^7$$

where:

$$\begin{aligned} E_{sw} &= \text{pore water diffusion coefficient (m}^2\text{/sec)} \\ A_w &= \text{water body surface area (m}^2\text{)} \\ \theta_{bs} &= \text{benthic porosity (L}_w\text{/L)} \end{aligned}$$

z_b = benthic layer depth, taken as the characteristic mixing length (m)
 3.15×10^7 = units conversion factor (sec/yr)

The product $A_w \cdot \theta_{bs}$ represents the cross-sectional area within the sediment layer through which diffusion occurs.

Solids Movement -- The sorbed fraction of component "i" moves at the same velocity as its particulate carrier. The solids balance equations include the processes of abiotic and biotic deposition, resuspension, and burial. As expressed in the mercury mass balance equations above, abiotic and biotic deposition is the product of the solids deposition velocity, the particulate phase concentrations in the water column, and the surface area:

$$(v_s \cdot A_w) \cdot (f_{sw,i} \cdot C_{wt,i}) + (v_{sB} \cdot A_w) \cdot (f_{Bw,i} \cdot C_{wt,i})$$

where:

A_w = water body surface area (m²)
 v_s = abiotic solids deposition velocity (m/yr)
 v_{sB} = biotic solids deposition velocity (m/yr)
 $C_{wt,i}$ = total component "i" concentration (g/m³)
 $f_{sw,i}$ = fraction of component "i" concentration sorbed to abiotic solids
 $f_{Bw,i}$ = fraction of component "i" concentration sorbed to biotic solids

In a similar manner, resuspension is the product of the sediment resuspension velocity, the particulate phase concentration in the sediments, and the surface area:

$$(v_{rs} \cdot A_w) \cdot (f_{sb,i} \cdot C_{bt,i})$$

where:

A_w = water body surface area (m²)
 v_{rs} = sediment resuspension velocity (m/yr)
 $C_{bt,i}$ = total component "i" concentration in the sediment (g/m³)
 $f_{sb,i}$ = fraction of component "i" concentration sorbed to sediment solids

Finally, burial is the product of the sediment burial velocity, the particulate phase concentration in the sediments, and the surface area:

$$(v_b \cdot A_w) \cdot (f_{sb,i} \cdot C_{bt,i})$$

where:

A_w = water body surface area (m²)
 v_b = sediment burial velocity (m/yr)
 $C_{bt,i}$ = total component "i" concentration in the sediment (g/m³)
 $f_{sb,i}$ = fraction of component "i" concentration sorbed to sediment solids

Volatilization -- The volatilization equation presented above is divided into a diffusive loading term and a loss term in IEM-2M. The volatilization loss term is given by:

$$K_{v,i} \cdot A_w \cdot C_{dw,i} = \frac{K_{v,i}}{z_w} \cdot V_w \cdot f_{dw,i} \cdot C_{wt,i}$$

where:

$K_{v,i}$	=	overall transfer rate, or conductivity for component "i" (m/yr)
A_w	=	surface area of water body (m ²)
z_w	=	depth of water column (m)
V_w	=	volume of water column (m ³)
$C_{dw,i}$	=	dissolved concentration of component "i" in water column (g/m ³)
$f_{dw,i}$	=	dissolved fraction of component "i" in water column
$C_{wt,i}$	=	total concentration of component "i" in water column (g/m ³)

From this equation, the rate constant for volatilization loss used in the mass balance equation can be derived:

$$kw_{v,i} = \frac{K_{v,i} \cdot f_{dw,i}}{z_w}$$

where:

$kw_{v,i}$	=	water column volatilization loss rate constant for component "i" (yr ⁻¹)
$K_{v,i}$	=	overall transfer rate, or conductivity for component "i" (m/yr)
$f_{dw,i}$	=	fraction of component "i" in the water column that is dissolved
z_w	=	water body depth (m)

The overall transfer rate, $K_{v,i}$ or conductivity, was determined by the two-layer resistance model (Whitman, 1923; or see Burns, et al., 1982 or Ambrose, et al., 1988). The two-resistance method assumes that two "stagnant films" at the air-water interface are bounded on either side by well mixed compartments. Concentration differences serve as the driving force for the water layer diffusion. Pressure differences drive the diffusion for the air layer. From mass balance considerations, it is obvious that the same mass must pass through both films; thus, the two resistances combine in series, so that the conductivity is the reciprocal of the total resistance:

$$K_{v,i} = (R_{L,i} + R_{G,i})^{-1} = \left(K_{L,i}^{-1} + \left(K_{G,i} \frac{H_i}{R T_K} \right)^{-1} \right)^{-1}$$

where:

$R_{L,i}$	=	liquid phase resistance (year/m)
$K_{L,i}$	=	liquid phase transfer coefficient (m/year)
$R_{G,i}$	=	gas phase resistance (year/m)
$K_{G,i}$	=	gas phase transfer coefficient (m/year)
R	=	universal gas constant (atm-m ³ /mole-°K)
H_i	=	Henry's law constant for component "i" (atm-m ³ /mole)

T_K = water body temperature ($^{\circ}\text{K}$)

The value of $K_{v,i}$, the conductivity, depends on the intensity of turbulence in a water body and in the overlying atmosphere. As the Henry's Law constant increases, the conductivity tends to be increasingly influenced by the intensity of turbulence in water. As the Henry's Law constant decreases, the value of the conductivity tends to be increasingly influenced by the intensity of atmospheric turbulence.

Because Henry's Law constant generally increases with increasing vapor pressure of a compound and generally decreases with increasing solubility of a compound, highly volatile low solubility compounds are most likely to exhibit mass transfer limitations in water, and relatively nonvolatile high solubility compounds are more likely to exhibit mass transfer limitations in the air. Volatilization is usually of relatively less magnitude in lakes and reservoirs than in rivers and streams.

The estimated volatilization rate constant was for a nominal temperature of 20°C . It is adjusted for the actual water temperature using the equation:

$$K_{v,i,T} = K_{v,i,20} \theta^{(T-20)}$$

where:

θ = temperature correction factor, set to 1.026.
 T = water body temperature ($^{\circ}\text{C}$)

There have been a variety of methods proposed to compute the liquid ($K_{L,i}$) and gas phase ($K_{G,i}$) transfer coefficients. For a stagnant system, the transfer coefficients are controlled by wind-induced turbulence. For stagnant systems, the liquid film transfer coefficient ($K_{L,i}$) is computed using the O'Connor (1983) equations:

$$K_{L,i} = u^* \left(\frac{\rho_a}{\rho_w} \right)^{0.5} \left(\frac{k^{0.33}}{\lambda_2} \right) Sc_{w,i}^{-0.67} (3.15 \times 10^7)$$

$$K_{G,i} = u^* \left(\frac{k^{0.33}}{\lambda_2} \right) Sc_{a,i}^{-0.67} (3.15 \times 10^7)$$

where:

$$u^* = C_d^{0.5} W$$

$$Sc_{a,i} = \frac{\mu_a}{\rho_a D_{a,i}} = \frac{\nu_a}{D_{a,i}}$$

$$D_{a,i} = \frac{1.9}{MW_i^{2/3}}$$

$$v_a = (1.32 + 0.009 T_a) \times 10^{-1}$$

$$Sc_{w,i} = \frac{\mu_w}{\rho_w D_{w,i}}$$

$$D_{w,i} = \frac{22 \times 10^{-5}}{MW_i^{2/3}}$$

$$\rho_w = 1 - 8.8 \times 10^{-5} T_w$$

$$\log(\mu_w) = \left[\frac{1301}{998.333 + 8.1855(T_w - 20) + 0.00585(T_w - 20)^2} \right] - 3.0233$$

and:

u^*	=	shear velocity (m/s)
C_d	=	drag coefficient (= 0.0011)
W	=	wind velocity, 10 m above water surface (m/s)
ρ_a	=	density of air corresponding to the air temperature (g/cm ³)
ρ_w	=	density of water corresponding to the water temperature (g/cm ³)
k	=	von Karman's constant (= 0.4)
λ_2	=	dimensionless viscous sublayer thickness (= 4)
$Sc_{a,i}$	=	air Schmidt number for component "i" (dimensionless)
$Sc_{w,i}$	=	water Schmidt number for component "i" (dimensionless)
$D_{a,i}$	=	diffusivity of component "i" in air (cm ² /sec)
$D_{w,i}$	=	diffusivity of component "i" in water (cm ² /sec)
μ_a	=	viscosity of air corresponding to the air temperature (g/cm-s)
μ_w	=	viscosity of water corresponding to the water temperature (g/cm-s)
v_a	=	dynamic viscosity of air (cm ² /sec)
MW_i	=	molecular weight of component "i"
T_a	=	air temperature (°C)
T_w	=	water temperature (°C)
3.15×10^7	=	units conversion factor (sec/yr)

5. ATMOSPHERIC FATE AND TRANSPORT MODELING RESULTS

This chapter summarizes the results of the atmospheric fate and transport modeling of mercury using the long-range and local models.

5.1 Long-Range Atmospheric Fate/Transport Modeling

5.1.1 Mass Balances of Mercury within the Long-Range Model Domain

The general mass balance of elemental mercury gas, divalent mercury gas, and particle-bound mercury from the RELMAP simulation results using the assumed emission speciation profiles are shown in Table 5-1. The mass-balance accounting for the simulation using the meteorological data from the year 1989 shows a total of 141.8 metric tons of mercury emitted to the atmosphere from anthropogenic sources. This simulated emission total differs slightly from the national totals indicated in Volume II since the states of Alaska and Hawaii are not within the model domain. The RELMAP simulation indicates that 47.6 metric tons of anthropogenic mercury emissions are deposited within the model domain and 0.4 metric tons remain in the air within the model domain at the end of the simulation. The remainder, about 93.8 metric tons, is transported outside the model domain and probably diffuses into the global atmospheric reservoir. The simulation also shows 32.0 metric tons of mercury is deposited within the model domain from the global atmospheric reservoir, suggesting that about three times as much mercury is being added to the global reservoir as is being deposited from it. The total amount of mercury deposited in the model domain annually from U.S. anthropogenic emissions and from the global background concentration is estimated to be 79.6 metric tons, or slightly more than one-half of the mass of all atmospheric emissions from anthropogenic sources in the lower 48 United States.

Table 5-1
Mercury Mass Budget in Metric Tons from RELMAP Simulation

Source/Fate	Hg ⁰ ^a	Hg ²⁺ ^b	Hg _p ^c	Total Mercury
Total U.S. anthropogenic emissions	63.5	52.3	26.0	141.8
Mass advected from model domain	62.3	15.5	16.0	93.8
Dry deposited anthropogenic emissions	0.0	22.9	0.5	23.4
Wet deposited anthropogenic emissions	0.9	13.8	9.5	24.2
Remaining in air at end of simulation	0.3	<0.1	<0.1	0.4
Total deposited anthropogenic emissions	0.9	36.8	10.0	47.6
Deposition from background Hg ⁰	32.0	-	-	32.0
Mercury deposited from all sources	32.9	36.8	10.0	79.6

(All figures rounded to the nearest tenth of a metric ton)

^a Hg⁰ = Elemental Mercury

^b Hg²⁺ = Divalent Vapor-phase Mercury

^c Hg_p = Particle-Bound/Mercury

A variety of emission speciation profiles have been tested for all source types in the RELMAP mercury model to evaluate the model's sensitivity to the assumed chemical and physical forms of the mercury air emissions (Bullock et al., 1997b). The results of this study showed a strong positive correlation between the fraction of emissions in Hg^{2+} and Hg_p forms and total simulated wet deposition. A specific alternate speciation has been tested using the RELMAP where all Hg^{2+} emissions were assumed to convert to the particulate form (Bullock et al., 1997a). The results of this simulation showed that the total mass of mercury deposited in all forms was reduced by 40% compared to the base-case simulation. It is generally known that gaseous Hg^{2+} can adsorb to the surface of particulate matter, especially carbon soot. However, there exists no evidence of complete conversion to the particulate form. This case of complete Hg^{2+} -to- Hg_p transfer was modeled only as a sensitivity test for the RELMAP mercury model. There remains considerable uncertainty about the actual speciation of atmospheric mercury emissions from most anthropogenic sources. As current studies of this subject progress, our confidence in the results of atmospheric model simulations will increase. Based on the results in Bullock et al. (1997a), we estimate an emission speciation modeling uncertainty of +/- 40% for RELMAP-derived mass balance estimates.

Of the total anthropogenic mercury mass deposited to the surface in the model domain, 77% is estimated by the RELMAP simulation to come from Hg^{2+} emissions, 21% from Hg_p emissions and 2% from Hg^0 emissions. When the deposition of Hg^0 from the global background is considered in addition to anthropogenic sources in the lower 48 states, the species fractions of total deposition become 46% Hg^{2+} , 41% Hg^0 and 13% Hg_p . The vast majority of mercury already in the global atmosphere is in the form of Hg^0 and, in general, the anthropogenic Hg^0 emissions do not greatly increase the existing Hg^0 concentration. Although Hg^0 is removed from the atmosphere very slowly, the global background reservoir is large and total deposition from it is significant. It should be noted here that dry deposition of Hg^0 is thought to be significant only on the local scale and has not been included in the RELMAP simulations. Wet deposition is the only major pathway for removal of Hg^0 from the atmosphere. This removal pathway simulated by the RELMAP involves oxidation of mercury by ozone in an aqueous solution; thus, the Hg^0 that is extracted from the atmosphere by the modeled precipitation process would actually be deposited primarily in the form of Hg^{2+} .

Results from the RELMAP simulation show that of the 63.5 metric tons of anthropogenic Hg^0 emitted in the lower 48 states, only 0.9 tons (1.4%) is deposited within the model domain, while of the 52.3 metric tons of Hg^{2+} emitted, about 36.8 tons (70.4%) is deposited. Ninety-eight percent of the deposited anthropogenic mercury was emitted in the form of Hg^{2+} or Hg_p . Thus, a strong argument can be made that the combined Hg^{2+} and Hg_p component of anthropogenic mercury emissions can be used as an indicator of eventual deposition of those emissions to the lower 48 states and surrounding areas. The emission inventory and estimated chemical/physical speciation profiles indicate that of all combined Hg^{2+} and Hg_p emissions, 29% is from electric utility boilers, 25% is from municipal waste combustion, 18% is from medical waste incineration, 16% is from commercial and industrial boilers, and 12% is from all other modeled sources.

5.1.2 Qualitative Description of Mercury Concentration Results

Average surface-level concentration fields for elemental mercury, divalent mercury, and particulate mercury have been calculated from the RELMAP simulation using the meteorological data for the year 1989 and current air emission estimates. Figure 5-1 shows the annual average elemental mercury (Hg^0) concentration at ground level from anthropogenic sources obtained by using the source-based emission speciation profiles described in chapter 4, section 2. It shows that anthropogenic Hg^0

concentrations remain less than 0.1 ng/m³ over nearly all of the modeled area. The areas where the average anthropogenic Hg⁰ concentrations exceed 0.1 ng/m³ are mostly confined to the highly industrialized regions of the eastern Mid-west and the North-east. Compared to the estimated average global background concentration of 1.6 ng/m³, this 0.1 ng/m³ elevation of Hg⁰ concentration by anthropogenic emissions is rather small.

Figure 5-2 shows annual average divalent mercury vapor (Hg²⁺) air concentrations, also using the base case emissions. These values are significantly lower than for anthropogenic Hg⁰, and there are some new areas of higher concentration. The highest concentration areas have values from 0.05 to 0.1 ng/m³ and are mostly confined to the Midwest and the Northeast corridor, but two high concentration areas are also located near Tampa and Miami, Florida. The background atmospheric mercury loading is assumed to be completely in the elemental form, so there is no background contribution to the Hg²⁺ concentrations. In most areas, the anthropogenic component of the Hg⁰ concentrations shown in Figure 5-1 are at least 4 times higher than the Hg²⁺ concentrations shown in Figure 5-2. For the assumed emission speciation, Hg²⁺ vapor is a minor component of the total mercury emissions from some source types, but it is a significant part of the total mercury emissions from most waste incineration (60%) and fossil fuel combustion (30%). Since the total Hg²⁺ emissions are similar to those for Hg⁰, these much lower average annual Hg²⁺ concentrations cannot be attributed to the emissions. The lower simulated air concentrations of Hg²⁺ vapor are due to its more rapid removal from the atmosphere than for Hg⁰.

The RELMAP Hg⁰ and Hg²⁺ air concentration results taken together with the assumed background Hg⁰ concentration of 1.6 ng/m³ agree well with observations of vapor-phase Hg air concentration in Minnesota by Fitzgerald et al. (1991), in Vermont by Burke et al. (1995) and in Wisconsin by Lamborg et al. (1995). These works showed that annual average vapor-phase Hg concentrations were near the levels found over other remote locations in the northern hemisphere, from 1.6 to 2.0 ng/m³. Measurements taken for a two-week period at three sites in Broward County, Florida, (Dvonch et al., 1995) show slightly elevated vapor-phase Hg air concentrations for two of those sites downwind of industrial activities. These two sites had average vapor-phase Hg air concentrations of 3.3 and 2.8 ng/m³. The RELMAP simulation results for the Fort Lauderdale area show only about a 0.1 ng/m³ elevation of the annual average vapor-phase Hg (Hg⁰ plus Hg²⁺) concentration over the 1.6 ng/m³ background value assumed. The measurements of Dvonch et al. (1995), however, did not extend for a significant portion of the year and there was no discrimination between Hg⁰ and Hg²⁺ forms. The third site for their observations had an average vapor-phase air concentration of 1.8 ng/m³, which is much closer to the RELMAP simulation results. A more comprehensive air monitoring program is required before an evaluation of the RELMAP results in Florida can be performed.

Particulate mercury (Hg_p) emissions are thought to be a small fraction of the total for most source types. For the base-case emission speciation, 20% is the largest particulate fraction of mercury emissions for any source type. Figure 5-3 shows that the simulated annual average Hg_p concentrations were even lower than those for Hg²⁺ vapor. The maximum annual average values are around 50 pg/m³ (0.05 ng/m³) in the urban centers of the Northeast. Keeler et al. (1995) found instantaneous Hg_p concentrations in urban Detroit during March of 1992 of over 1 ng/m³ and average concentrations over an 18-day period of 94 pg/m³. Given the 40-km horizontal scale of the RELMAP computational grid, however, one cannot expect the simulation to reflect these extreme local-scale measurement results. The RELMAP simulation suggests an annual average Hg_p concentration in the Detroit area of about 40 pg/m³. Dvonch et al. (1995) found average Hg_p concentrations in Broward County, Florida, of between 34 and 51 pg/m³ at three sites

Figure 5-1
Average Hg(0) Concentration Excluding Background
(Nanograms per cubic meter)

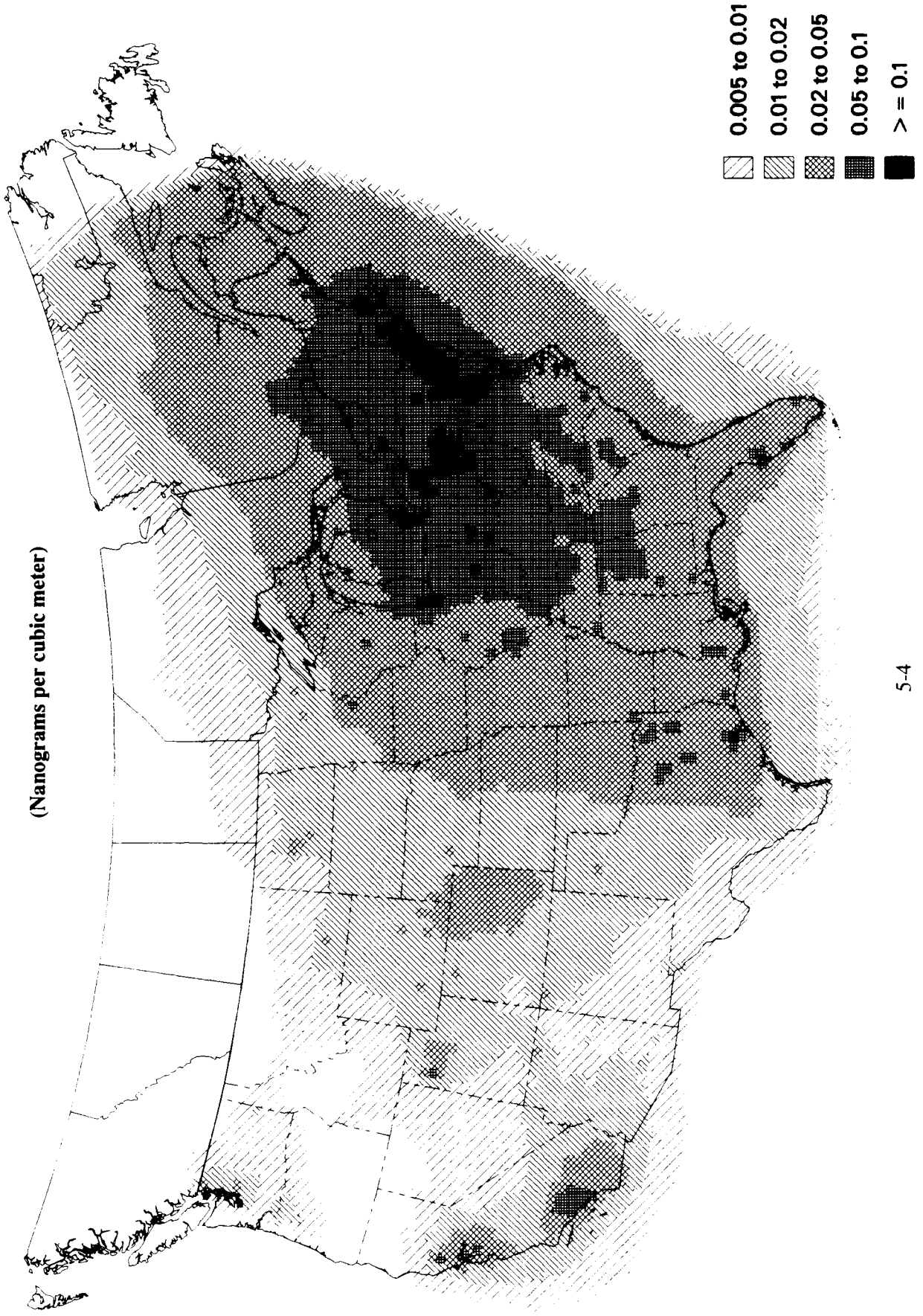


Figure 5-2
Average Hg²⁺ Concentration
(Nanograms per cubic meter)

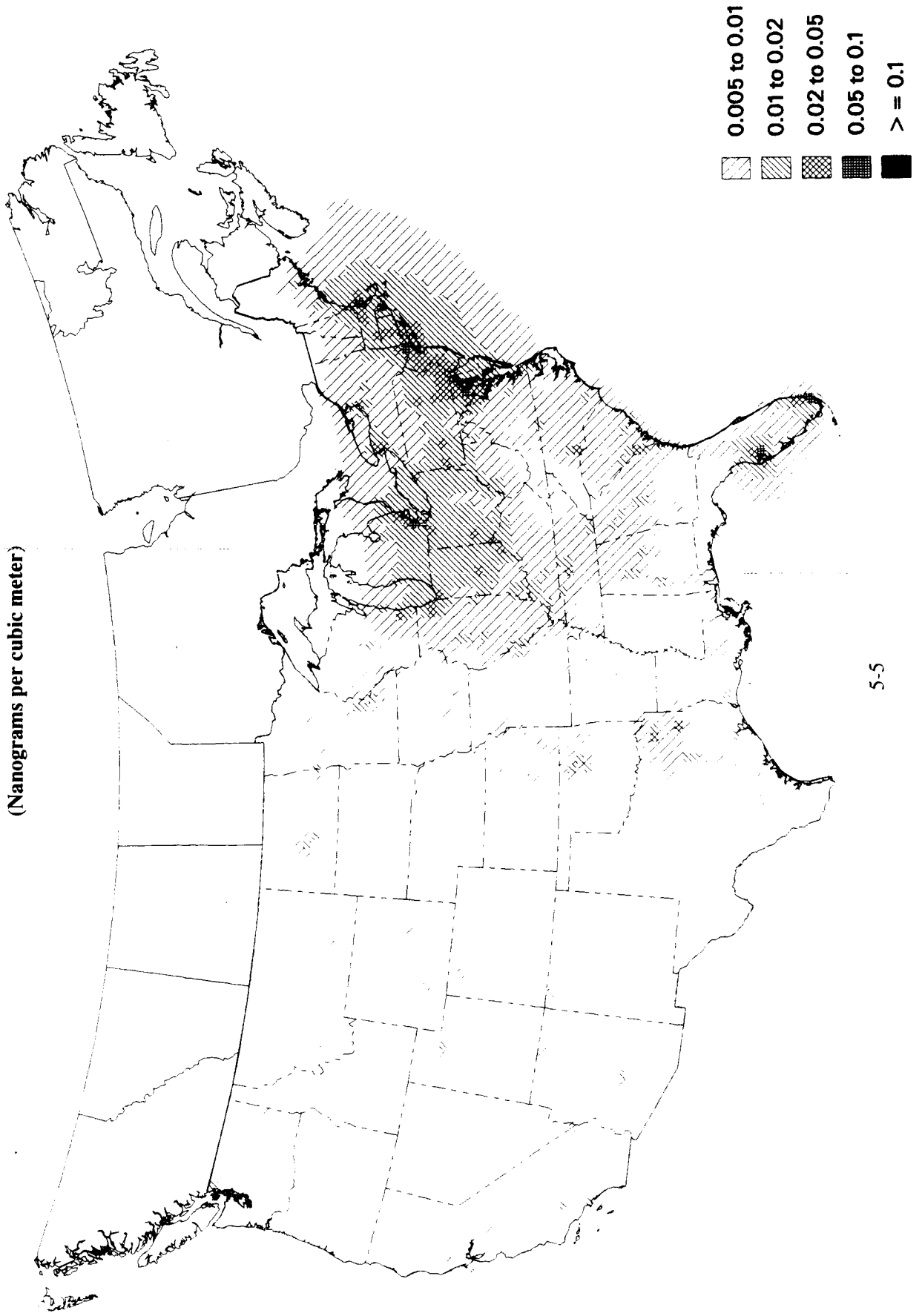
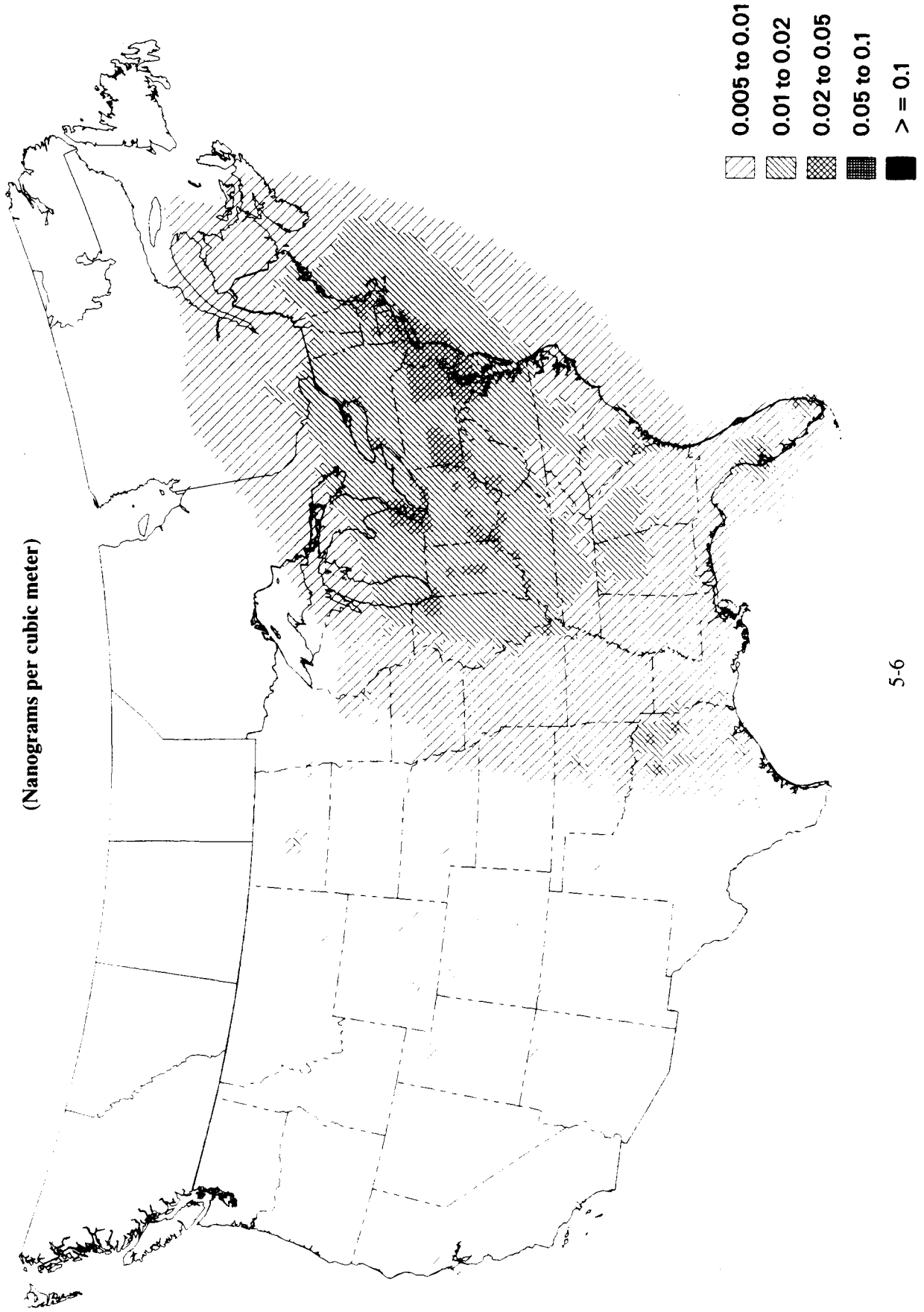


Figure 5-3
Average Hg(p) Concentration
(Nanograms per cubic meter)



from 25 August to 7 September of 1993. The RELMAP simulation resulted in a value of around 25 pg/m^3 near the city of Fort Lauderdale. Keeler et al. (1995) found annual average Hg_p air concentrations of 10.5 pg/m^3 in Pellston, Michigan, 22.4 pg/m^3 in South Haven, Michigan, and 21.9 pg/m^3 in Ann Arbor, Michigan, from April 1993 to April 1994, and 11.2 pg/m^3 in Underhill, Vermont, for the year of 1993. The RELMAP simulation showed 8.0 pg/m^3 for Pellston, Michigan, 15.2 pg/m^3 in South Haven, Michigan, 21.2 pg/m^3 in Ann Arbor, Michigan, and 10.6 pg/m^3 in Underhill, Vermont, indicating a slight tendency of the model to under-estimate particulate mercury air concentrations in these locations, but by no more than 25%.

Table 5-2 shows a percentile analysis of the simulated concentration results from the RELMAP grid cells over the entire continental United States and for two subsets of this area east and west of 90°W longitude. This table shows that the Hg^0 concentrations never exceeded the assumed background level of 1.6 ng/m^3 by a large relative amount. It also shows that Hg^{2+} and to a lesser degree Hg_p air concentrations were highly elevated in only a few grid cells. Over the entire continental U.S., there is nearly an order of magnitude difference between the modeled Hg^{2+} concentrations at the 90th percentile level and those at the maximum level, with approximately a factor of 4 difference for Hg_p .

Table 5-2
Percentile Analysis of RELMAP Simulated Concentration Results
for the Continental U. S.

Variable	Min	10th	50th	90th	Max
Full Area					
Hg ^{0a} concentration (ng/m ³)	1.602	1.606	1.619	1.662	1.903
Hg ^{2+b} concentration (pg/m ³)	0.101	0.329	1.825	9.144	72.71
Hg _p ^c concentration (pg/m ³)	0.156	0.699	3.753	13.87	51.18
Total mercury (ng/m ³)	1.602	1.607	1.624	1.685	1.995
East of 90°W longitude					
Hg ^{0a} concentration (ng/m ³)	1.612	1.629	1.651	1.687	1.903
Hg ^{2+b} concentration (pg/m ³)	0.787	2.750	6.426	14.92	72.71
Hg _p ^c concentration (pg/m ³)	2.789	6.324	10.89	19.29	51.18
Total mercury (ng/m ³)	1.616	1.640	1.668	1.720	1.995
West of 90°W longitude					
Hg ^{0a} concentration (ng/m ³)	1.602	1.605	1.613	1.632	1.702
Hg ^{2+b} concentration (pg/m ³)	0.101	0.271	1.100	3.481	26.95
Hg _p ^c concentration (pg/m ³)	0.158	0.595	2.146	6.392	27.43
Total mercury (ng/m ³)	1.602	1.606	1.616	1.642	1.743

^a Hg⁰ = Elemental Mercury

^b Hg²⁺ = Divalent Vapor-phase Mercury

^c Hg_p = Particle-Bound/Mercury

5.1.3 Description of Mercury Wet Deposition Simulation Results

Figure 5-4 shows the total simulated wet deposition of Hg⁰ from U. S. anthropogenic sources using the meteorological data for the year 1989 and current air emission estimates. Figure 5-5 shows the total simulated wet deposition of Hg⁰ assuming only a non-depleting global background concentration of 1.6 ng/m³. Both of these wet deposition results are influenced by ozone and soot concentrations due to the chemical transformations modeled by the RELMAP. Emission patterns influence the primary anthropogenic Hg⁰ wet deposition pattern, and it is obvious that total annual precipitation is a strong factor in wet deposition from the global background concentration with heaviest wet deposition in areas with the

Figure 5-4
Hg(0) Wet Deposition Excluding Background

(Micrograms per square meter)

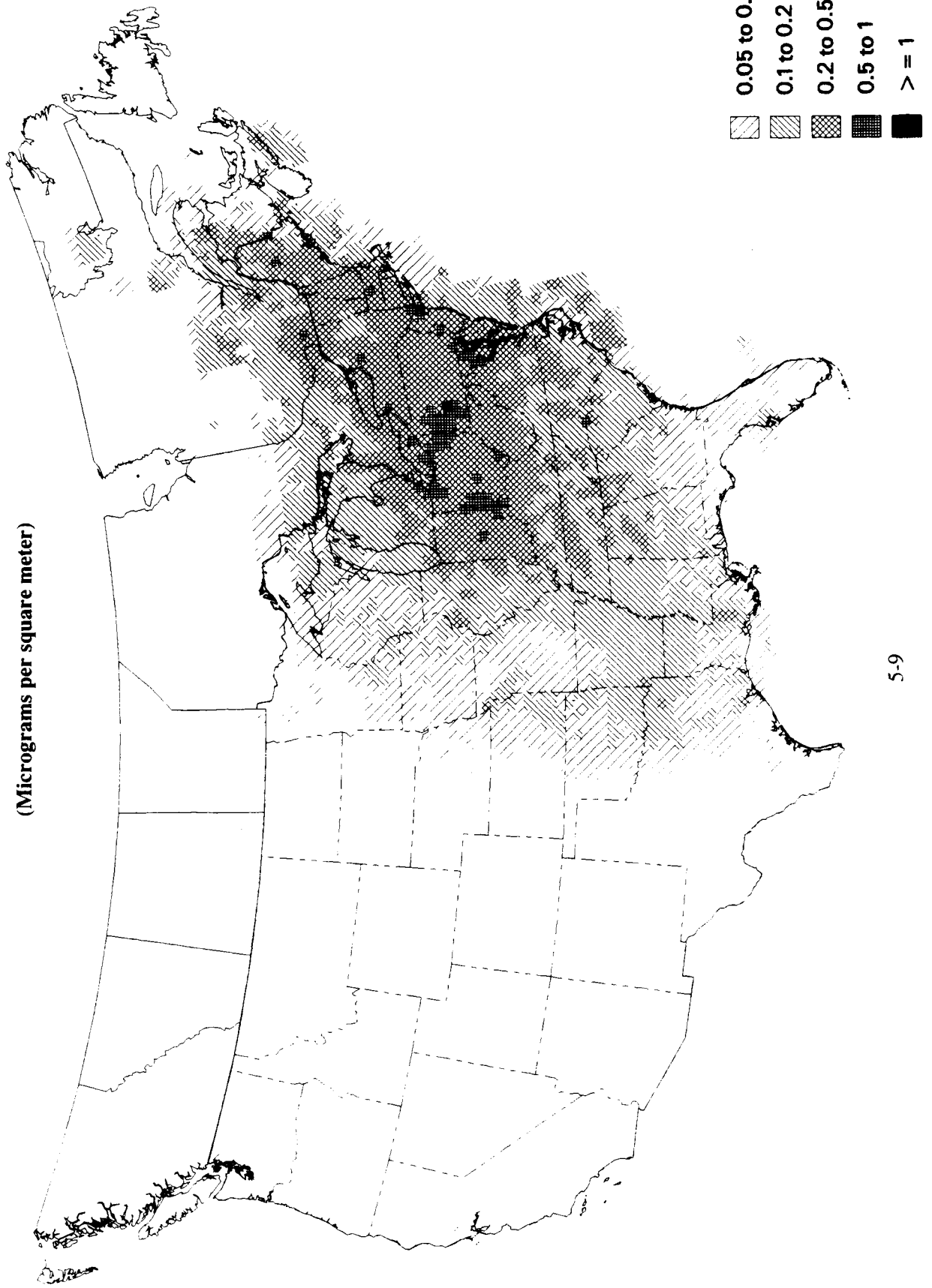
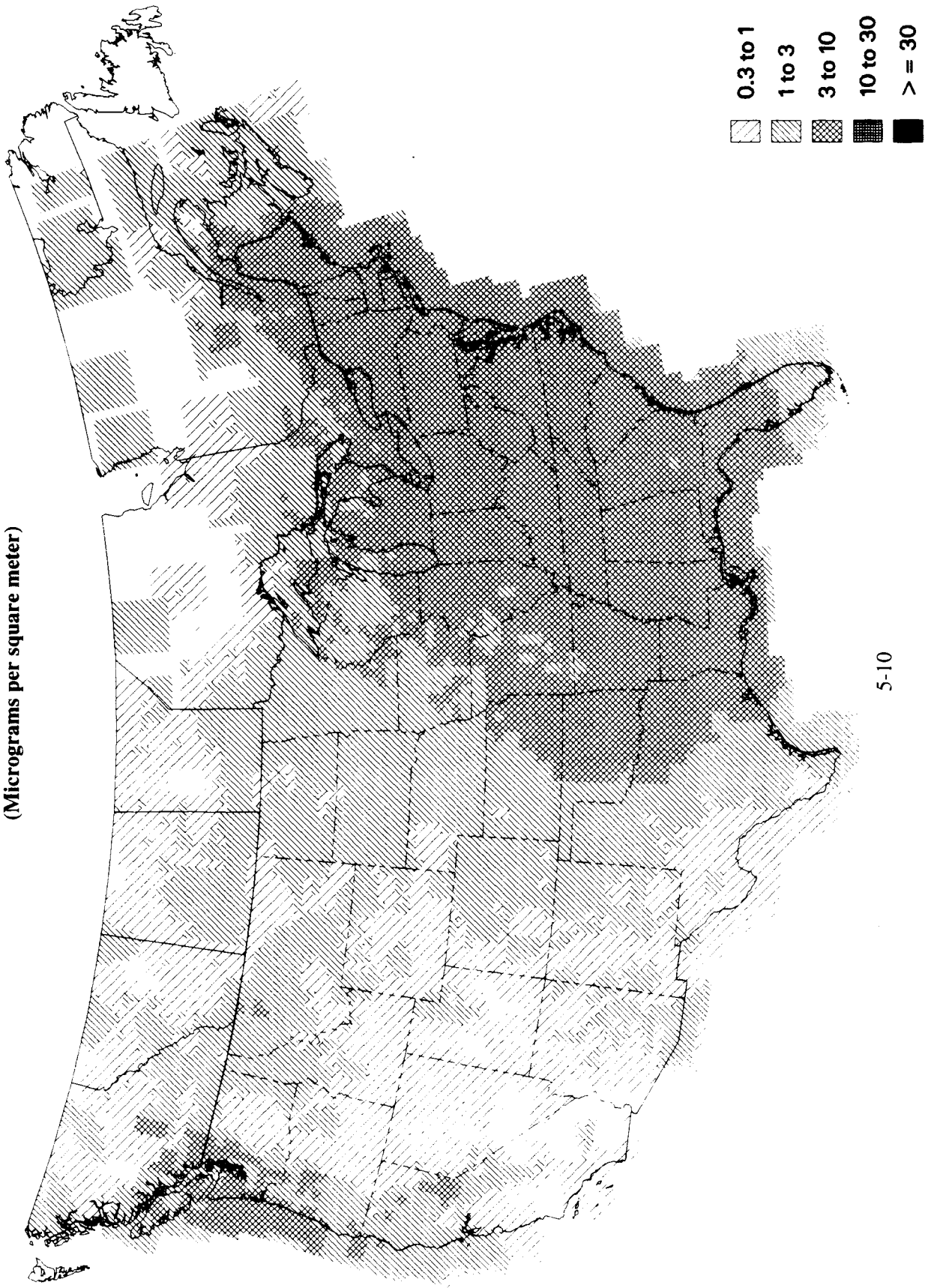


Figure 5-5
Hg(0) Wet Deposition (Background Only)
(Micrograms per square meter)



highest annual precipitation. It is widely accepted that deposition of measurable quantities of mercury occurs on continental and global scales, and the RELMAP simulation shows areas of Hg^0 wet deposition occurring in remote areas. The simulated annual wet deposition for Hg^{2+} vapor shown in Figure 5-6 show high deposition areas that are much more local to the emission source areas. There are a few model cells in urban areas with wet deposition totals of Hg^{2+} vapor over $30 \mu\text{g}/\text{m}^2$ while most of the cells in the non-urban areas have wet depositions of less than $3 \mu\text{g}/\text{m}^2$. This indicates the Hg^{2+} vapor wet deposits more on the local scale and less on regional or global scales and that its wet removal from the atmosphere is much more rapid than for Hg^0 . This is an expected result due to the higher water solubility of most mercuric salts compared to mercury in the elemental form. Figure 5-7 shows that the maximum simulated wet deposition of Hg_p is about one-third of that for Hg^{2+} vapor. This is partly due to differences in the total mass of Hg_p emitted compared to Hg^{2+} , but it is also due to the less efficient wet scavenging that is assumed for Hg_p versus Hg^{2+} . The areas of Hg_p wet deposition are also more widely distributed than for Hg^{2+} due to the slower wet scavenging of Hg_p and, thus, a greater opportunity for long-range transport.

The simulated total wet deposition of mercury from anthropogenic emissions in all three forms and from the global background is shown in Figure 5-8. This illustration shows significant wet deposition of mercury over most of the eastern half of the U.S. For the simulated meteorological year of 1989, the entire eastern half of the nation has a wet deposition total of over $3 \mu\text{g}/\text{m}^2$ and values exceed $10 \mu\text{g}/\text{m}^2$ over most of the Ohio Valley and Northeast U.S. In fact, the largest simulated wet deposition is slightly over $80 \mu\text{g}/\text{m}^2$ in the grid cell containing New York City. At this time, these highest wet deposition rates for total mercury cannot be substantiated by observations. In the RELMAP simulation the most impacted areas are subjected to wet deposition of mercury mainly from emissions of Hg^{2+} vapor. It is likely that the RELMAP model for mercury may still be significantly incomplete, and that other chemical and/or physical transformations may occur which moderate the wet deposition of Hg^{2+} vapor and possibly Hg_p .

There exist only limited data with which to compare the RELMAP simulation results. Measurements of mercury wet deposition at three locations in northeastern Minnesota during 1989 by Glass et al. (1991) indicated annual wet deposition rates of $6.5 \mu\text{g}/\text{m}^2$ at Duluth, $13.5 \mu\text{g}/\text{m}^2$ at Marcell and $41.9 \mu\text{g}/\text{m}^2$ at Ely. A later study by Sorensen et al. (1994) measuring annual wet deposition of mercury during 1990, 1991 and 1992 at Ely, Duluth and seven other sites in Minnesota, upper Michigan and northeastern North Dakota found all annual wet deposition totals to be within the range of 3.8 to $9.7 \mu\text{g}/\text{m}^2$, bringing into question the Ely observation of $41.9 \mu\text{g}/\text{m}^2$ in 1989 by Glass et al. (1991). Measurements by Fitzgerald et al. (1991) at Little Rock Lake, in northern Wisconsin, of mercury in snow during February and March, 1989, and in rain from May to August, 1989, have been used to estimate annual mercury depositions in rain and snow of 4.5 and $2.3 \mu\text{g}/\text{m}^2$, respectively. This suggests a total annual mercury wet deposition of $6.8 \mu\text{g}/\text{m}^2$ at Little Rock Lake. Measurements at Presque Isle, also in northern Wisconsin, from 1993 to 1994 by Lamborg et al. (1995) suggested a wet deposition rate for total mercury of $5.2 \mu\text{g}/\text{m}^2/\text{yr}$, somewhat less than the measurements by Fitzgerald et al. (1991). The extremely heavy rainfall during the summer of 1993 in the mid-west states to the south and west of Presque Isle may be responsible for the lower wet deposition. The RELMAP simulation results using the meteorological data for 1989 indicate around $4 \mu\text{g}/\text{m}^2$ wet deposition of total mercury over northern Minnesota and $5 \mu\text{g}/\text{m}^2$ wet deposition of total mercury over northern Wisconsin. However, due to the varying years of observation, these data cannot be used to confidently evaluate the RELMAP model performance for the 1989 simulation period.

Figure 5-6
Hg²⁺ Wet Deposition

(Micrograms per square meter)

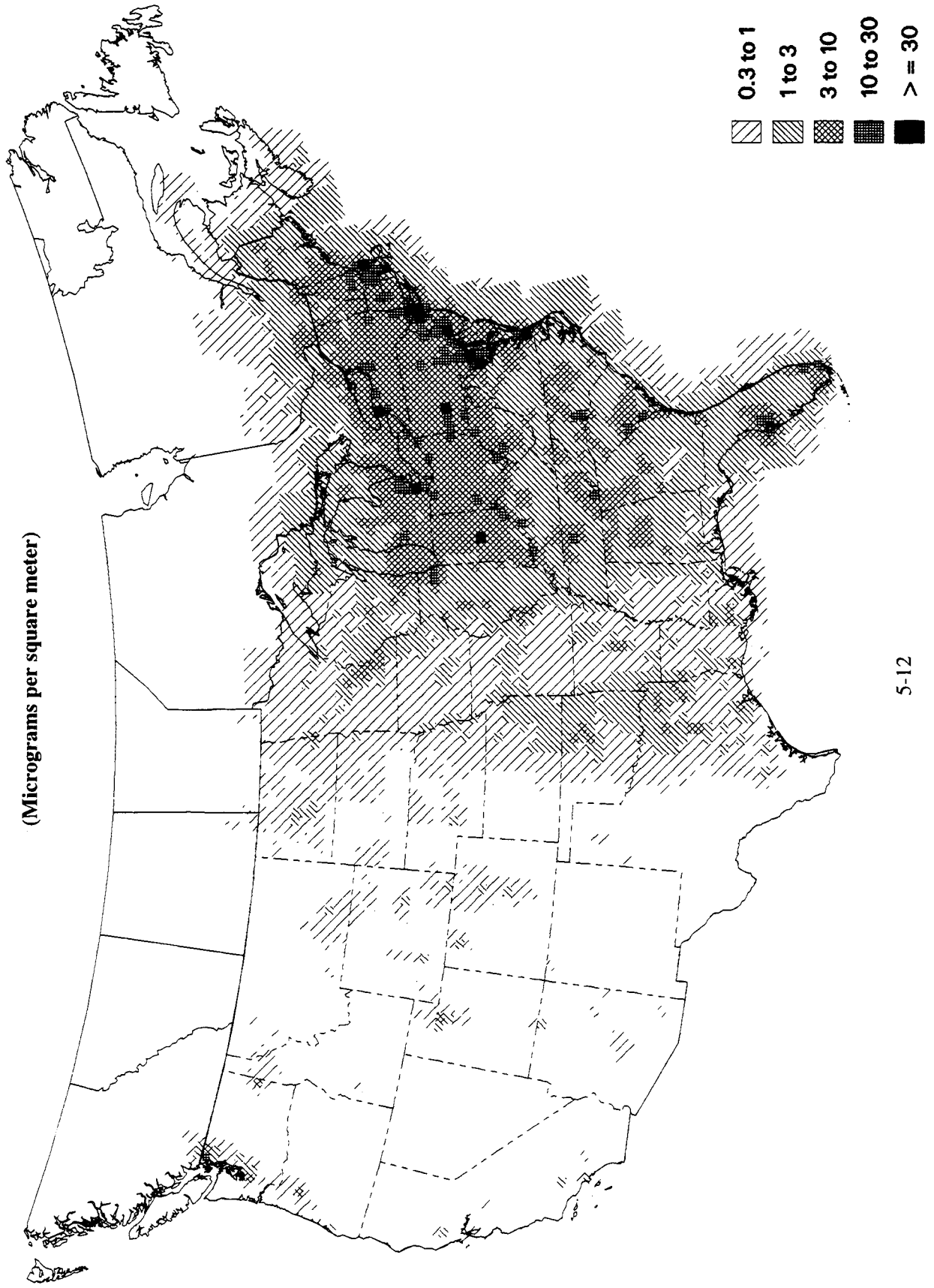


Figure 5-7
Hg(p) Wet Deposition

(Micrograms per square meter)

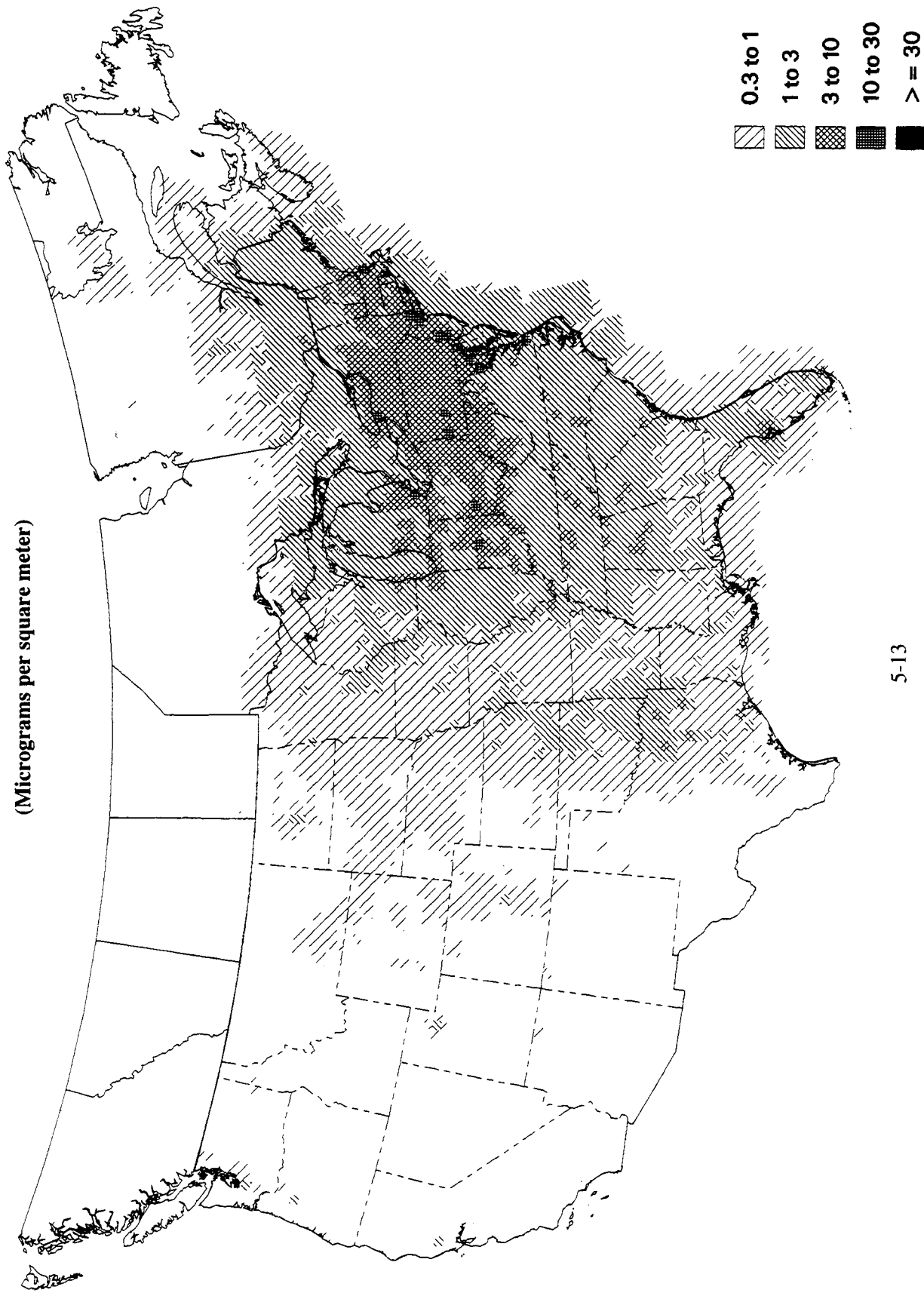
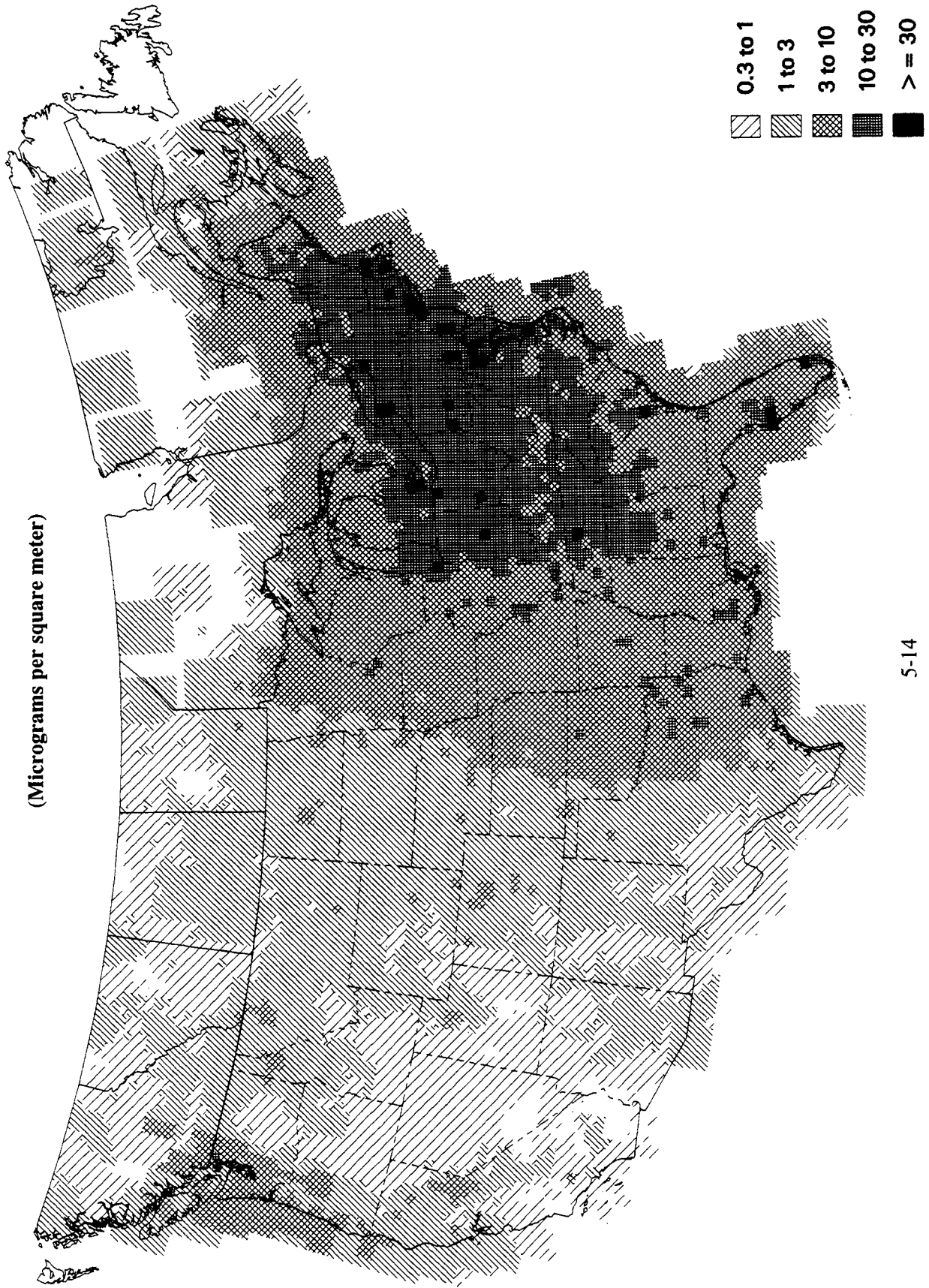


Figure 5-8
Total Hg Wet Deposition

(Micrograms per square meter)



There were also some mercury wet deposition measurement programs conducted during the early 1990's in somewhat less remote sites in Michigan and Vermont. Observations by Hoyer et al. (1995) during two years of event precipitation sampling at three sites in Michigan show evidence for a north-to-south gradient in mercury wet deposition. From March 1992 to March 1993, the total mercury wet deposition observed at South Haven, in southwest Michigan, was $9.45 \mu\text{g}/\text{m}^2$. At Pellston, in the northern part of the lower peninsula of Michigan, the wet deposition was $5.79 \mu\text{g}/\text{m}^2$. At Dexter, in southeast Michigan about 100 km west of Detroit, the wet deposition was $8.66 \mu\text{g}/\text{m}^2$. From March 1993 to March 1994, wet deposition at South Haven was $12.67 \mu\text{g}/\text{m}^2$, significantly higher than for the previous year, while measurements at Pellston and Dexter remained about constant at 5.54 and $9.11 \mu\text{g}/\text{m}^2$, respectively. Hoyer et al. (1995) attribute the higher second-year wet deposition at South Haven to an increased precipitation rate and cite the measurements by Burke et al (1995) at Underhill, Vermont, as further evidence of the importance of precipitation amount. From December 1992 to December 1993, the average volume-weighted mercury concentration at Underhill ($8.3 \text{ ng}/\text{L}$) was similar to that observed at Pellston ($7.9 \text{ ng}/\text{L}$). However, with more precipitation during that period the total mercury wet deposition at Underhill was $9.26 \mu\text{g}/\text{m}^2$, significantly higher than at Pellston. The RELMAP simulation results show $6.63 \mu\text{g}/\text{m}^2$ wet deposition of total mercury at the Pellston site, about 20% larger than the 1992 to 1994 observations. At Underhill, the RELMAP simulation indicates $11.86 \mu\text{g}/\text{m}^2$ wet deposition, about 25% larger than the observation in 1993. At the South Haven site, the RELMAP simulation showed $11.57 \mu\text{g}/\text{m}^2$ wet deposition of total mercury, which closely approximates the measurements taken there from 1992 to 1994. At Dexter, the RELMAP simulation showed $12.84 \mu\text{g}/\text{m}^2$ wet deposition of total mercury, about 40% above the observed values from 1992 to 1994. Overall, this comparison seems to indicate a slight tendency of the RELMAP mercury model to over-estimate wet deposition. However, one should not expect the RELMAP simulation using 1989 meteorology to exactly match observed wet deposition values from 1992 to 1994 due to differences in annual precipitation from year to year. Nonetheless, the agreement between simulated and observed annual wet deposition of total mercury provides some evidence that the most important atmospheric processes for deposition of mercury in precipitation are being accounted for.

The very large total mercury wet deposition values ($>30 \mu\text{g}/\text{m}^2$) from the RELMAP simulation for some of the larger urban centers in the Great Lakes, Ohio Valley and Northeast regions cannot be evaluated thoroughly due to a lack of long-term precipitation event sampling at those locations. A data report recently obtained by EPA's Great Lakes National Program Office (Keeler, 1997) showed a total mercury wet deposition of $30.3 \mu\text{g}/\text{m}^2$ at the Illinois Institute of Technology in Chicago between July 1, 1994 and October 31, 1995, a period of 16 months. The 12-month RELMAP simulation produced $37.5 \mu\text{g}/\text{m}^2$ at this location. A study by Dvonch et al. (1995) describes precipitation event sampling from 19 August to 7 September of 1993 at 4 sites in Broward County, Florida, in and around the city of Fort Lauderdale. During the 20-day sampling period, total mercury mean concentrations in precipitation were 35, 57, 40 and $46 \text{ ng}/\text{L}$ at the 4 sites. Given the average annual precipitation of 150 cm per year typical of that area, the resulting annual wet deposition estimates at these 4 sites would be 52.5, 85.5, 60 and $69 \mu\text{g}/\text{m}^2$. Since most of the annual rainfall in Broward County occurs in warm tropical conditions of the March to October wet season, this extrapolation from 20 days during the wet season to an annual estimate is not totally without basis. However, additional urban measurement studies are required to allow any credible evaluation of RELMAP wet deposition results in heavily populated, industrialized area.

Observational mercury wet deposition data obtained over the World Wide Web from the Mercury Deposition Network (Lindberg and Vermette, 1995; Vermette et al., 1995) have been used to estimate 1989 mercury wet deposition totals for 12 locations in the eastern U. S. Table 5-3 shows the data obtained from the MDN transitional data set at 17 locations during 1994 and 1995. Only those sites

with 50% or more data completeness were used to estimate 1989 wet deposition totals. The observed volume-weighted mercury concentration at the MDN site (ng/L) was multiplied by the total accumulated precipitation depth (m) as modeled for 1989 at each location to obtain estimates of total wet deposition of mercury during the 1989 simulation period ($\mu\text{g}/\text{m}^2$). These estimates of total 1989 mercury wet deposition are shown along with the RELMAP-simulated values and percent differences on Table 5-4. For all locations but two, the RELMAP simulation produced 20 to 50% less wet deposition than the estimated 1989 values. It should be noted that the Sturgeon Point (NY97) site, where the model difference is most positive, and the Mulberry Flat (KY99) site, where the model difference is most negative, are both located very close to the edge of their model cells. They are also located in areas where large point sources of atmospheric mercury are known to exist. Thus the indicated model error may be due more to horizontal resolution problems than inaccurate atmospheric process modeling. Overall, this comparison seems to contradict the previous comparison to 1993 and 1994 observations in Michigan and Vermont and indicates a tendency for the RELMAP mercury model to under-estimate wet deposition.

Table 5-3
Observed Mercury Deposition in Precipitation from the Transition Phase Data Report
of the Mercury Deposition Network (MDN)
 (from <http://nadp.nrel.colostate.edu/nadp/mdn/mdn.html>)

Station	Latitude (ddmmss)	Longitude (ddmmss)	Vol. Wt. Conc. (ng/L)	Data Completeness
Lewes (DE02)	384620	750557	8.28	94%
Everglades Nat'l Pk. (FL11)	252324	804048	7.90	42%
Bondville (IL11)	400312	882219	13.56	50%
Mulberry Flat (KY99)	365405	880049	12.56	88%
Wye (MD13)	385447	760909	8.59	46%
Acadia Nat'l Pk. (ME98)	442226	681538	3.62	40%
Marcell Exp. Forest (MN16)	473152	932807	8.40	94%
Fernberg (MN18)	475647	912946	9.0	79%
Waccamaw State Pk. (NC08)	341000	782500	9.18	96%
Pettigrew State Pk. (NC42)	354500	762200	8.79	87%
Sturgeon Point (NY97)	424100	790200	12.75	75%
Congaree Swamp (SC19)	335200	805200	12.83	94%
Longview (TX21)	322243	944242	8.13	27%
Olympic Nat'l Pk. (WA14)	475136	1235555	4.18	37%
Brule River (WI08)	464500	913000	10.04	85%
Popple River (WI09)	454747	882358	12.52	96%
Trout Lake (WI36)	460310	893911	10.53	96%

Table 5-4
Estimates of 1989 Mercury Wet Deposition in Precipitation from MDN Data
and Comparison to Modeled Wet Deposition

Station	Vol. Wt. Conc. (ng/L)	Modeled Precip. (meters)	Estimated Hg Dep. ($\mu\text{g}/\text{m}^2$)	Modeled Hg Dep. ($\mu\text{g}/\text{m}^2$)	% difference
DE02	8.28	1.525	12.63	12.47	+1
IL11	13.56	0.857	11.62	8.51	-27
KY99	12.56	1.271	15.97	7.46	-53
MN16	8.40	0.707	5.94	3.37	-43
MN18	9.00	0.683	6.15	3.52	-43
NC08	9.18	1.336	12.26	8.38	-32
NC42	8.79	2.209	19.41	11.52	-41
NY97	12.75	0.888	11.33	14.47	+28
SC19	12.83	1.257	16.12	12.91	-20
WI08	10.04	0.685	6.88	4.25	-38
WI09	12.52	0.631	7.91	4.48	-43
WI36	10.53	0.751	7.91	4.70	-41

The percentile analysis of the wet deposition simulation results in Table 5-5 shows that 50 percent of the continental U.S. had an annual wet deposition of total Hg of $2.9 \mu\text{g}/\text{m}^2$ or more, and 10 percent of the area had $12.4 \mu\text{g}/\text{m}^2$ or more. However, due to rapid wet deposition of Hg^{2+} and Hg_p there are select areas where wet deposition may be significantly higher. In the eastern U.S., east of 90 degrees west longitude, the 50th and 90th percentile levels for total Hg wet deposition are considerably higher than those for the entire continental U.S., about 10 and $18 \mu\text{g}/\text{m}^2$, respectively.

Table 5-5
Percentile Analysis of RELMAP Simulated Wet Deposition for the Continental U. S.

Variable	Min	10th	50th	90th	Max
Full Area					
Hg ^{0a} wet dep. (µg/m ² /yr)	<0.001	0.002	0.029	0.247	1.011
Hg ^{2+b} wet dep. (µg/m ² /yr)	<0.001	0.031	0.401	3.880	54.42
Hg _p ^c wet dep. (µg/m ² /yr)	<0.001	0.030	0.371	2.613	19.41
Background Hg (µg/m ² /yr)	0.022	0.584	2.111	5.994	9.722
Total mercury (µg/m ² /yr)	0.022	0.697	2.858	12.42	80.31
East of 90°W longitude					
Hg ^{0a} wet dep. (µg/m ² /yr)	0.007	0.060	0.181	0.385	1.011
Hg ^{2+b} wet dep. (µg/m ² /yr)	0.123	1.053	2.652	7.056	54.42
Hg _p ^c wet dep. (µg/m ² /yr)	0.134	0.848	1.956	4.368	19.41
Background Hg (µg/m ² /yr)	0.524	2.908	5.138	6.944	9.722
Total mercury (µg/m ² /yr)	0.795	5.455	10.26	18.42	80.31
West of 90°W longitude					
Hg ^{0a} wet dep. (µg/m ² /yr)	<0.001	0.002	0.011	0.090	0.465
Hg ^{2+b} wet dep. (µg/m ² /yr)	<0.001	0.022	0.174	0.967	10.81
Hg _p ^c wet dep. (µg/m ² /yr)	<0.001	0.022	0.175	0.855	6.306
Background Hg (µg/m ² /yr)	0.022	0.507	1.317	3.889	7.627
Total mercury (µg/m ² /yr)	0.022	0.597	1.765	5.856	21.94

^a Hg⁰ = Elemental Mercury from U.S. sources

^b Hg²⁺ = Divalent Vapor-phase Mercury from U.S. sources

^c Hg_p = Particle-Bound/Mercury from U.S. sources

5.1.4 Qualitative Description of Mercury Dry Deposition Results

As described in the section on the RELMAP mercury model parameterizations, it was assumed that Hg^0 was not effectively dry deposited due to its high vapor pressure and very low water solubility at normal atmospheric temperatures. Therefore, only Hg^{2+} vapor and Hg_p were dry deposited in the RELMAP simulation. The percentile analysis of the simulated dry deposition using the assumed emission speciation profiles is shown in Table 5-6. The statistics on this table indicate the strong local dry deposition of Hg^{2+} vapor as parameterized in the RELMAP mercury model. There is considerable uncertainty regarding the dry deposition velocity of Hg^{2+} and in the extremely high local depositions indicated from the simulation.

Table 5-6
Percentile Analysis of RELMAP Simulated Dry Deposition for the Continental U. S.

Variable	Min	10th	50th	90th	Max
Full Area					
Hg^{2+a} dry dep. ($\mu\text{g}/\text{m}^2/\text{yr}$)	0.047	0.175	0.864	5.46	62.24
Hg_p^b dry dep. ($\mu\text{g}/\text{m}^2/\text{yr}$)	<0.001	0.005	0.026	0.096	0.418
Total mercury ($\mu\text{g}/\text{m}^2/\text{yr}$)	0.050	0.183	0.887	5.56	62.61
East of 90°W longitude					
Hg^{2+a} dry dep. ($\mu\text{g}/\text{m}^2/\text{yr}$)	0.246	1.595	4.101	9.342	62.24
Hg_p^b dry dep. ($\mu\text{g}/\text{m}^2/\text{yr}$)	0.011	0.036	0.078	0.139	0.418
Total mercury ($\mu\text{g}/\text{m}^2/\text{yr}$)	0.258	1.629	4.175	9.479	62.61
West of 90°W longitude					
Hg^{2+a} dry dep. ($\mu\text{g}/\text{m}^2/\text{yr}$)	0.047	0.139	0.546	2.092	17.73
Hg_p^b dry dep. ($\mu\text{g}/\text{m}^2/\text{yr}$)	<0.001	0.004	0.016	0.047	0.210
Total mercury ($\mu\text{g}/\text{m}^2/\text{yr}$)	0.050	0.145	0.564	2.136	17.93

^a Hg^{2+} = Divalent Vapor-phase Mercury from U.S. sources

^b Hg_p = Particle-Bound/Mercury from U.S. sources

Figure 5-9 shows the simulated annual dry deposition totals for Hg^{2+} . Dry deposition of Hg^{2+} appears to occur primarily on the local scale, the majority occurring within one or two grid cells from the source (40-80 km), much like the wet deposition. The magnitude of the dry deposition of Hg^{2+} is similar to that for wet deposition, with major urban areas showing values in excess of $30 \mu\text{g}/\text{m}^2$. Simulated dry deposition of Hg^{2+} vapor in heavily industrialized urban centers is very intense, exceeding $60 \mu\text{g}/\text{m}^2$ in the model grid cell containing New York City. Again, it must be stressed that dry deposition of Hg^{2+} vapor is not well understood. The simulation used nitric acid vapor data as a surrogate for Hg^{2+} vapor based on similar water solubilities. The Agency has been unable to find observations of the dry deposition of Hg^{2+} vapor with which to compare to the RELMAP simulation results. Dry deposition rates for vapor-phase Hg have been estimated from vertical eddy flux calculations at a single site (Lindberg et al., 1992), but these calculations estimate the combined effects of both Hg^0 and Hg^{2+} vapors. The relatively high solubility and reactivity of Hg^{2+} compounds suggests that dry deposition of total vapor-phase mercury may be strongly driven by the Hg^{2+} component of the total vapor-phase mercury concentration.

Figure 5-10 shows the simulated annual dry deposition totals for Hg_p . As described in Appendix D, the dry deposition velocity estimates for Hg_p have been made based on the assumption that the particulate mass is concentrated around a $0.3 \mu\text{m}$ diameter size. The patterns show much less intense dry deposition of Hg_p than for Hg^{2+} , but the dry deposition still appears to occur primarily within a few hundred km of the source areas. This slower dry deposition combined with relatively smaller quantities of Hg_p emission result in maximum dry deposition values of only around $0.4 \mu\text{g}/\text{m}^2$. In urban areas where larger particle sizes are more prevalent, these estimates of Hg_p dry deposition are probably too low, but the RELMAP could treat only one particle size. Since the focus of this modeling was on the regional scale, $0.3 \mu\text{m}$ was chosen as the most appropriate diameter size.

Figure 5-11 shows the simulated annual dry deposition for all forms of mercury. This graphic looks nearly identical to the simulated dry deposition of Hg^{2+} shown in Figure 5-9, indicating that the simulated dry deposition is strongly driven by the Hg^{2+} component of the air concentration of total mercury. Total dry deposition of mercury in all forms would be greatly reduced if significant transfer of Hg^{2+} to Hg_p is occurring through particle adsorption or condensation. Thus, it is very important that our understanding of the physical transformations of Hg in the atmosphere be complete and accurate.

Figure 5-9
Hg²⁺ Dry Deposition

(Micrograms per square meter)

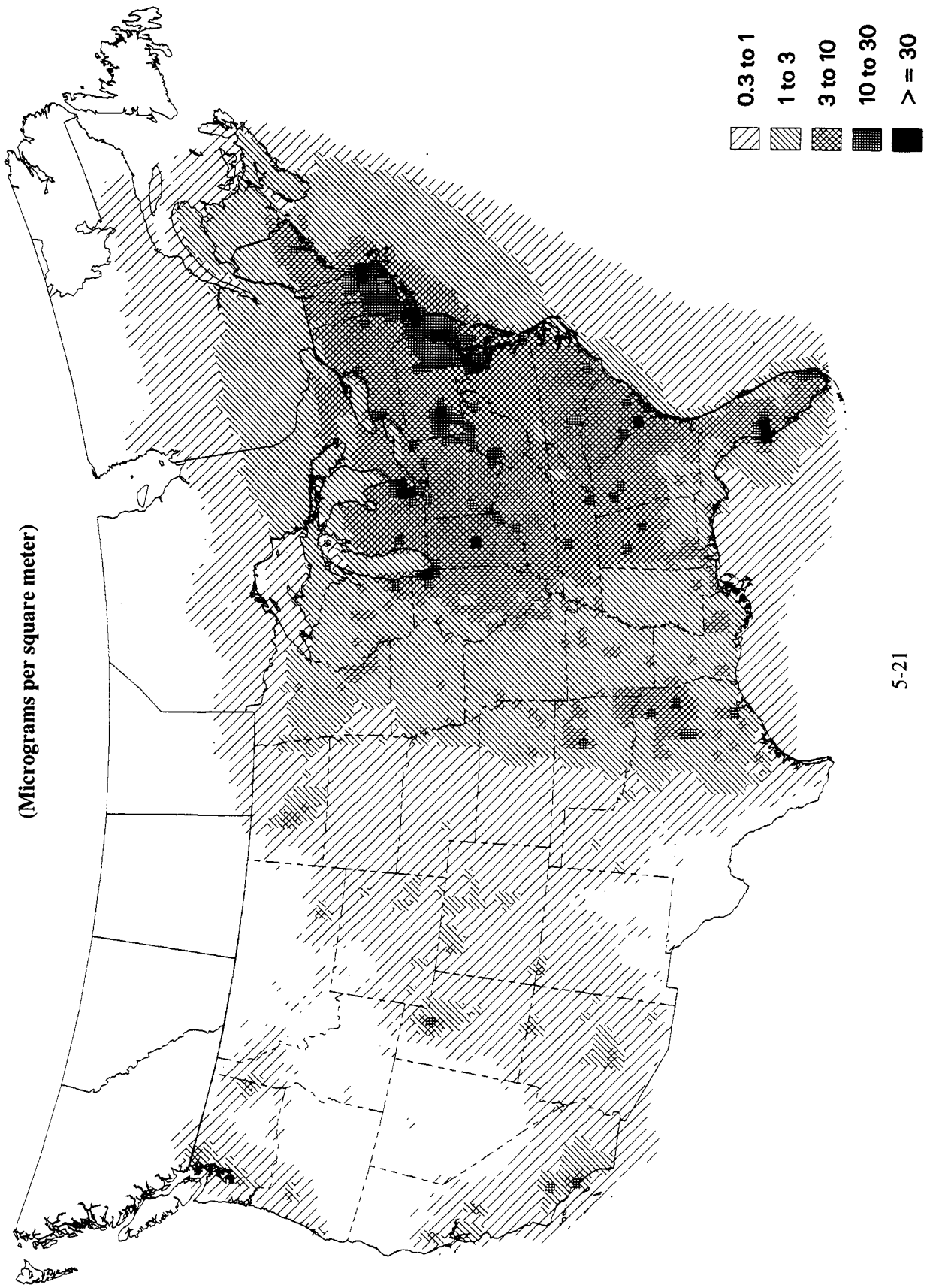


Figure 5-10
Hg(p) Dry Deposition

(Micrograms per square meter)

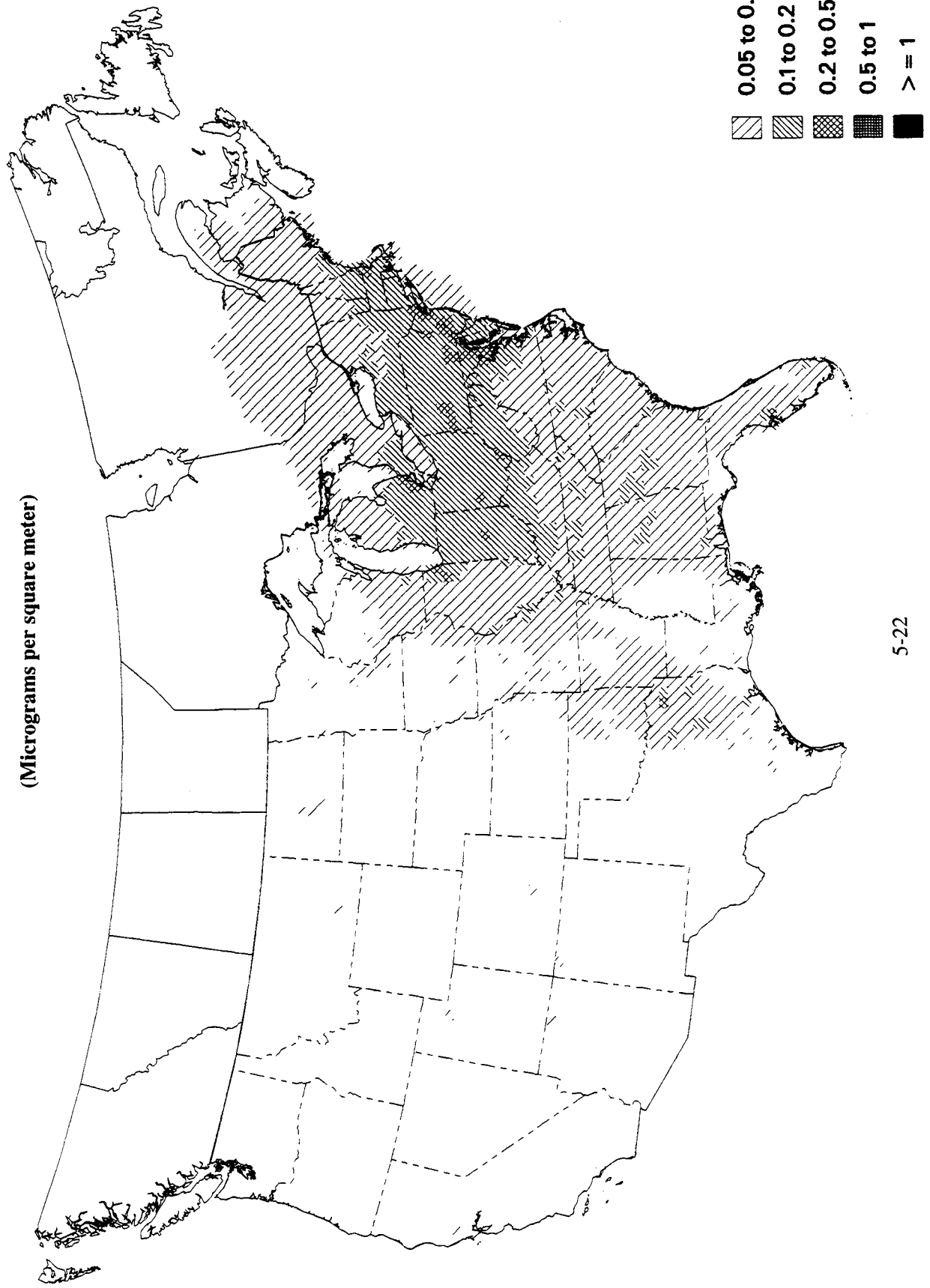
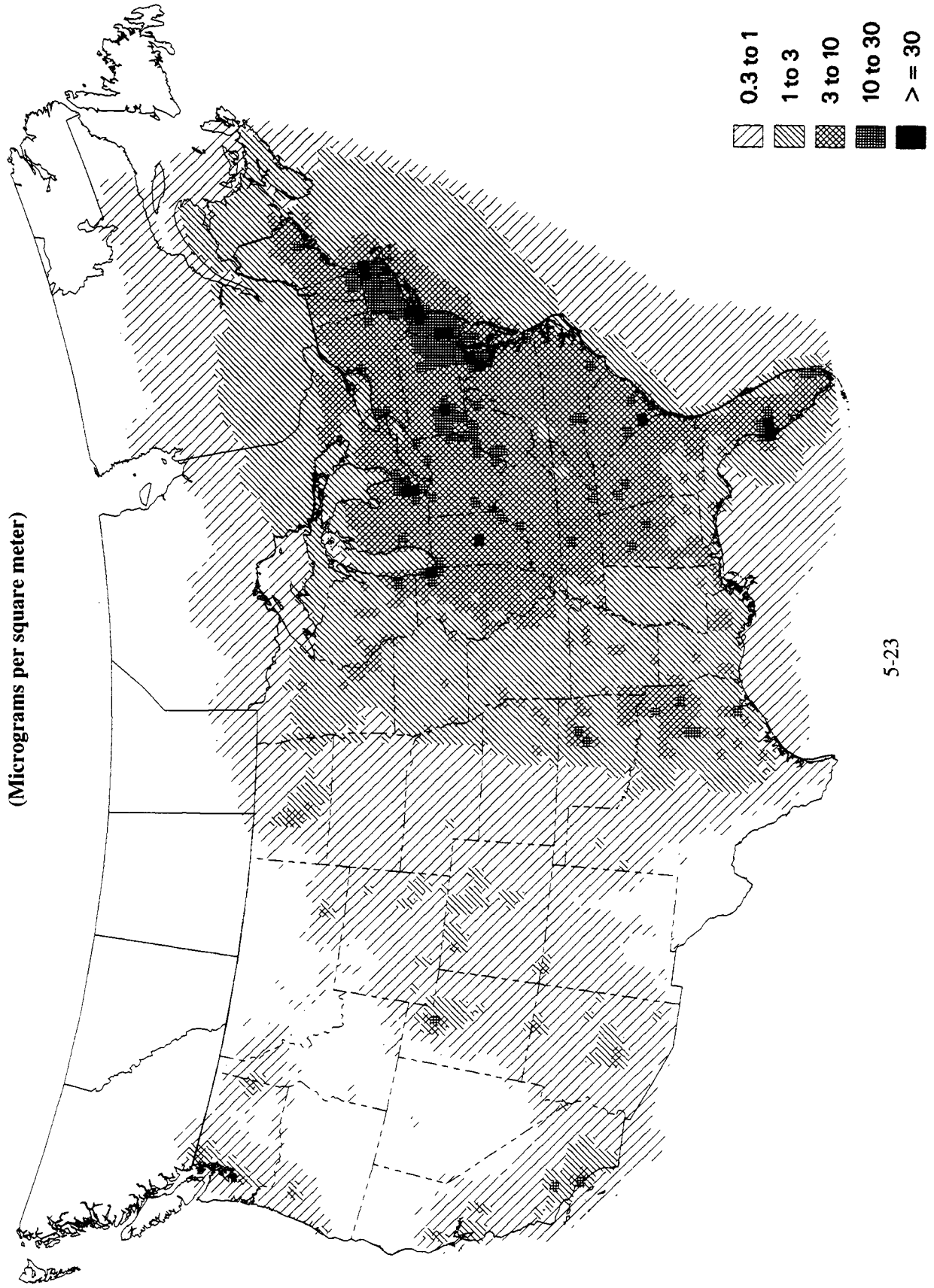


Figure 5-11
Total Hg Dry Deposition

(Micrograms per square meter)



5.1.5 Qualitative Description of Total Mercury Deposition Results

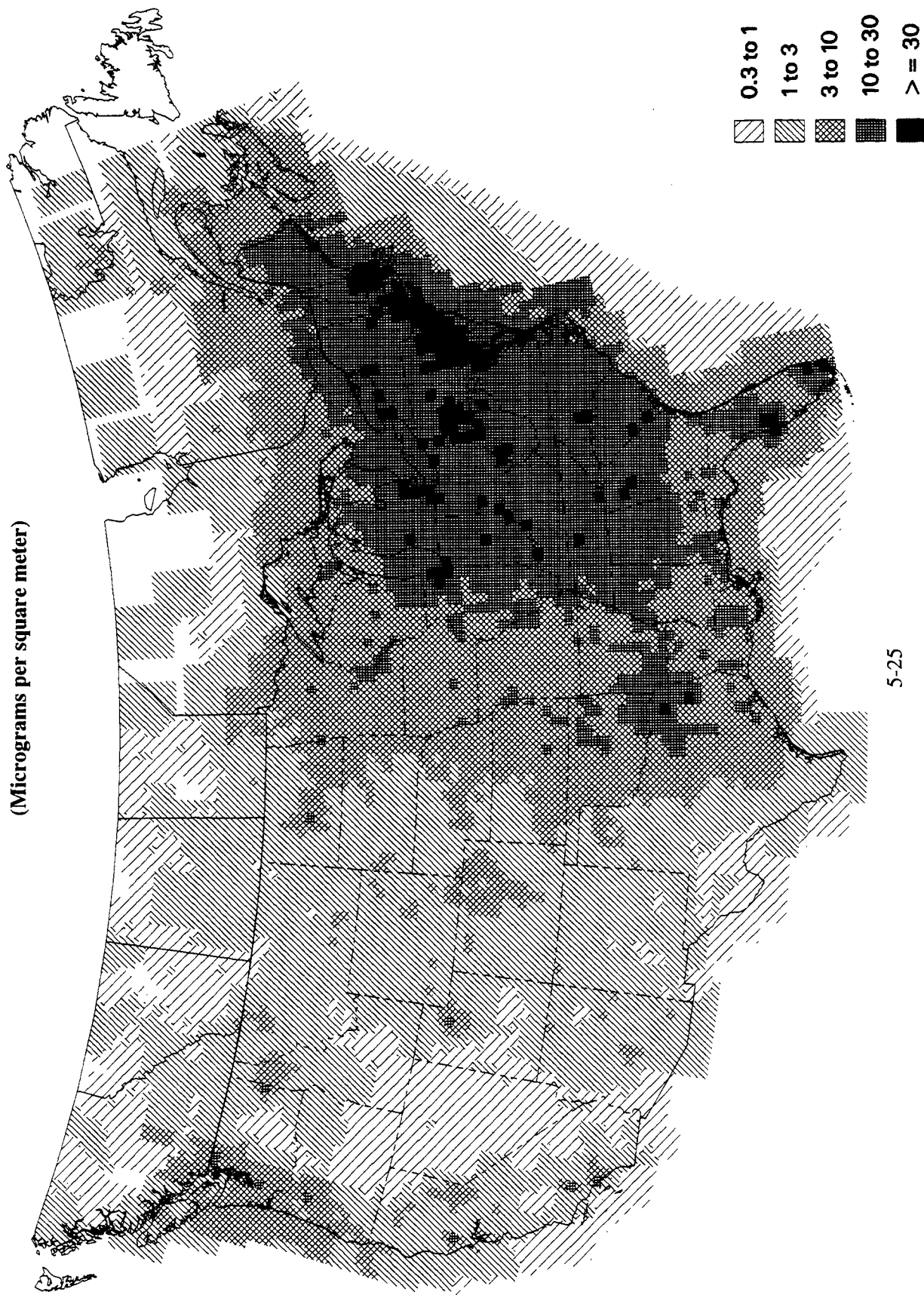
Since both wet and dry deposition of mercury can affect human and ecosystem health, an analysis of the simulated total deposition of all forms of mercury has been performed. Table 5-7 shows a percentile analysis of total deposition of mercury in all modeled forms. The strong bias toward mercury deposition in the eastern U.S. is immediately obvious. Also obvious is the order of magnitude difference between the 90th percentile level and the maximum values in the nationwide and eastern U.S. analyses. The extremely high simulated deposition totals over heavily populated urban centers cannot be substantiated by observations at this time. Due to the high degree of uncertainty regarding the emission speciations and possible rapid chemical and physical transformations immediately after emission, it is recommended that these maximum simulated deposition values should be considered highly uncertain until further research is conducted to reduce these uncertainties.

Figure 5-12 shows the RELMAP-simulated total deposition of mercury to the Earth's surface from U.S. anthropogenic sources and the global atmospheric background concentration combined. These results show deposition totals of over 10 $\mu\text{g}/\text{m}^2$ throughout most of the continental U. S. east of 90°W longitude, with values over 30 $\mu\text{g}/\text{m}^2$ for the northeast corridor and at other major urban centers.

Table 5-7
Percentile Analysis of RELMAP Simulated Total Depositions for the Continental U. S.

Area of Analysis	Min ($\mu\text{g}/\text{m}^2/\text{yr}$)	10th ($\mu\text{g}/\text{m}^2/\text{yr}$)	50th ($\mu\text{g}/\text{m}^2/\text{yr}$)	90th ($\mu\text{g}/\text{m}^2/\text{yr}$)	Max ($\mu\text{g}/\text{m}^2/\text{yr}$)
Full Area	0.310	1.024	3.718	17.94	142.9
East of 90°W longitude	1.226	7.407	14.50	27.18	142.9
West of 90°W	0.310	0.861	2.321	8.003	38.56

Figure 5-12
Total Hg Wet+Dry Deposition
(Micrograms per square meter)



5.1.6 General Data Interpretations of the RELMAP Modeling

At this time there is significant uncertainty regarding the chemical and physical forms of mercury air emissions and their chemical and physical transformations in the atmosphere. This long-range modeling effort has relied heavily on the assumptions and parameterizations of Petersen et al. (1995) regarding emission speciation and chemical and physical pathways for mercury deposition. These previous mercury modeling results were compared to measurements of Hg^0 and Hg_p air concentration and wet deposition in northern Europe. The comparison showed the European model results agreed with measurements to within a factor of 2 in nearly all cases. While the climate of northern Europe may be quite different from that of some locations in North America, it has been assumed that the predominant chemical and physical mechanisms for mercury transport, transformation and deposition should be the same for both regions.

The wet deposition results from the RELMAP simulation of atmospheric mercury also seem to agree with actual measurements within a factor of 2 in most cases. The RELMAP estimate of just over $80 \mu\text{g}/\text{m}^2$ wet deposition in the grid cell containing New York City seems extraordinarily high, but there currently are no measurement data which can be compared to these results. The simulated wet deposition in the grid cell immediately east of New York City is about $20 \mu\text{g}/\text{m}^2$. Thus, measurements taken outside the central industrial areas cannot be used to evaluate these maximum wet deposition results. Comparison of modeled mercury wet deposition to observed values during 1993 and 1994 in Michigan and Vermont suggest that the RELMAP is over-estimating wet deposition, while comparison to estimates based on observed volume-weighted average concentrations and 1989 precipitation data suggest the model is under-estimating wet deposition. Overall, the RELMAP mercury model seems to produce reasonable spatial patterns of annual wet deposition with site-specific agreement to observations to within a factor of two. A rigorous model evaluation will require better spatial coverage by a long-term observation network than is now available.

The RELMAP dry deposition results indicate that the importance of dry versus wet deposition processes may be dependent on the fraction of emitted mercury that eventually becomes particle-bound before deposition. Very few direct measurements of the dry deposition of gaseous and particulate Hg have been made to date. Vertical concentration gradients and eddy flux correlations have been used to estimate the dry flux of total gaseous mercury by Lindberg et al. (1992), but no discrimination was made between Hg^0 and Hg^{2+} forms. At this time, no scientifically credible model evaluation for dry deposition of mercury is possible. Once techniques for the measurement of gaseous dry deposition of mercury become available and observational networks employing them are developed and operated, model evaluation and subsequent refinement should rapidly follow.

Many of the measurement studies performed up until the 1980's are now suspected of having been subject to laboratory contamination. It is only recently that, by employing ultra-clean laboratory techniques, mercury measurement studies have been able to assess accurately atmospheric concentrations and deposition quantities of mercury in near-background conditions. Even now, it is very difficult to obtain an accurate assessment of the chemical forms of mercury in typical ambient air samples. The RELMAP air concentration results seem quite plausible, with the vast majority of atmospheric mercury estimated to be in the elemental vapor form, but the precise concentrations of Hg^{2+} and Hg_p cannot be simulated with much confidence until a more complete understanding is established of all pertinent chemical and physical processes in the atmosphere.

There are some limitations of the RELMAP and other Lagrangian puff models that may negatively affect the accuracy of atmospheric mercury modeling. The simulated pollutant puff must

move as an integral volume, and differences in wind direction or speed at various heights above the surface are not treated. The pollutant puff is currently simulated with a predefined vertical top, through which turbulent exchanges of air and pollutants are set at an arbitrary value. For pollutants such as Hg⁰ that remain in the atmosphere for a long time, significant transfer of mass between the PBL and the rest of the atmosphere is inevitable. These exchanges can be attributed not only to turbulent processes but also larger-scale vertical atmospheric motions, both rising and sinking. Finally, Lagrangian puff models have no straightforward way to treat the horizontal boundary flux of pollutant into the model domain. Hg⁰ vapor is known to be transported in the atmosphere on a global scale, but adequate methods are unavailable to model its transport from other parts of the earth into the model domain. The U.S. EPA is working to develop a general purpose air-quality modeling system employing an Eulerian reference frame which should prove more suitable for mercury transport and deposition simulations; completion of this model is expected in 1998.

5.2 Overview of Local Scale Analysis: Background Concentrations

5.2.1 Introduction

Background concentrations arising from numerous and varied sources are clearly of concern when evaluating contaminants such as mercury that are ubiquitous and exist as natural constituents of the environment. Some of the mercury on the planet has by virtue of its location alone been inaccessible to living things; for example, if undisturbed, mercury contained in deep crustal materials is expected to cycle extremely slowly (if at all) through the environment. Other forms of mercury, although more accessible, are tightly bound chemically and are expected to cycle slowly. By comparison, mercury in the upper layers of the soil cycles more rapidly in the environment. Some human activities have liberated mercury which was formerly sequestered; as a result, mercury concentrations in the atmosphere, soils, water bodies and sediments have increased over time due to natural and human activities. For example, the mercury concentration measured in a given soil sample is potentially the result of a combination of the “natural” constituent mercury, previous mining emissions, as well as current emissions; additionally mercury could have volatilized from other soils or bodies of water and deposited to the soil being sampled.

Hudson et al., (1995) recognized the occurrence of three separate historical periods of mercury cycling in the Americas: 1) “paleochemical” which occurred prior to 1550 AD, 2) a period of mining-related emissions which occurred roughly between 1550 - 1900 AD, and finally, 3) the period of 1900-present (which includes past anthropogenic increases from mining as well as current increases related to industrial emissions). In their model current mercury levels in the environment are influenced by all three time periods.

The purpose of this section is to estimate “existing” mercury concentrations in the U.S. over two different time periods. These estimates are used as inputs to the local dispersion analysis so that an assessment can be made of the impacts of a local anthropogenic source currently emitting mercury relative to existing background concentrations. This type of analysis enables an examination of mercury concentrations and potential exposures near emissions sources in a more comprehensive manner because both current and past releases of mercury are accounted. The reader should note that these are imprecise estimates designed to examine a typical site and perhaps typical conditions. Local concentrations of mercury in environmental compartments are highly variable, with perhaps the exception of current atmospheric mercury concentrations located distant to point sources.

Two separate estimates are presented. The first is an estimate of the mercury biogeochemical cycle in the U.S. prior to major influences from anthropogenic sources; this is prior to a period of

mining-related mercury emissions in the Americas. A representation of the “pre-anthropogenic” mercury cycle will be developed by inputting to the IEM-2M model an average atmospheric mercury concentration and average annual atmospheric mercury deposition rates for the hypothetical eastern and western sites. The estimate of the “pre-anthropogenic” atmospheric mercury concentration is based on work by Mason et. al (1994). The estimate of an average annual deposition rate from this period is derived from coring samples of geologic materials which can be correlated to specific time periods. The mercury concentrations contained in the core samples are assumed to reflect deposition patterns. Using these inputs the local dispersion model will be run until equilibrium is achieved for the model compartments. Chemical equilibrium is defined as “a steady state, in which opposing chemical reactions occur at equal rates” (Pauling, 1963). The hypothetical sites of the modeling are a shallow lake and watershed described previously as existing in the Eastern U.S. and the Western U.S.

The second estimate is an approximation of the mercury biogeochemical cycle as it currently exists at the two hypothetical U.S. sites remote from emission sources. This second estimation of the mercury cycle will roughly correspond to the current conditions. The predicted mercury concentrations from the “pre-anthropogenic” IEM-2M modeling results will be used as inputs for the approximation of the current mercury cycle. The atmospheric concentrations and the annual rate of mercury deposition are thought to have increased from the “pre-anthropogenic” period. Elevated concentration and deposition rates will be used as inputs to the IEM-2M. The deposition rate and an atmospheric air concentration will be assumed to have existed for a period of time sufficient to reach equilibrium. (This is clearly a simplifying and uncertain assumption. The current mercury cycle may not be in equilibrium). The predicted equilibrium mercury concentrations from this second approximation will be used as inputs to the IEM-2M model to estimate current exposures near emission point sources. These emissions sources will be assumed to be operational for 30 years.

5.2.2 The “Pre-anthropogenic” Mercury Cycle

The purpose of this section is to determine an approximate natural background concentration of mercury in the atmosphere and approximate atmospheric deposition rates for the hypothetical eastern and western sites prior to anthropogenic influences on the mercury cycle. The “pre-anthropogenic” atmosphere concentrations and deposition rates will be utilized as inputs to the IEM-2M model for the purposes of predicting mercury concentrations in soils and other media and biota associated with the hypothetical shallow lakes and their respective watersheds prior to anthropogenic emissions.

The Expert Panel on Mercury Atmospheric Processes (1994) described the current background mercury concentration in the atmosphere over the northern hemisphere as ranging from 1.5 - 2.0 ng/m³. Fitzgerald (1994) reported that the value used in their modeling of 25 Mmol of mercury in the atmosphere represents an average concentration of 1.6 ng/m³ which is comparable to the average measured concentration of mercury over oceans. Mason et al., 1994 estimate that pre-industrial atmospheric mercury levels were roughly one third of current levels. Assuming that 1.6 ng/m³ is a reasonable estimate of the current continental atmospheric background, an estimate of 0.5 ng/m³ is a crude estimate of a pre-anthropogenic background.

While the levels of mercury circulating in the atmosphere are directly influenced by emissions, deposition rates appear to be influenced by a number of factors including: the atmospheric mercury concentration, rainfall, particulate concentration in the atmosphere, and levels of atmospheric oxidants.

To estimate deposition rates, Mason et al. (1994) present a pre-anthropogenic global mercury budget in which the predicted atmospheric deposition to both terrestrial and marine environments is equal to the evasion of mercury from the two compartments. Given the extensive time period over which the pre-anthropogenic mercury cycle operated, it is logical when modeling this time period that the system be in chemical equilibrium.

Since there are no measured mercury concentration data from this time period, other sources of data providing indirect measurements must be examined to infer a record of mercury deposition. Core samples of sedimented materials from lake beds, ombrotrophic bogs and oceans present opportunities to evaluate the history of mercury deposition from the atmosphere. Other sources such as ice sheets and tree ring analyses may also evidence patterns of atmospheric mercury concentrations or deposition rates (Expert Panel on Mercury Atmospheric Processes, (1994). It is important to note that these types of data only provide inferred deposition rates. These data are primarily interpreted by the authors to describe trends in mercury deposition rather than precise deposition rates. They do offer one advantage to current measurement data in that they account for both wet and dry deposition of mercury.

Rada et al., (1989) analyzed sediment mercury concentrations from Wisconsin (U.S.A.) lakes and concluded that atmospheric mercury deposition to these lakes had increased significantly when compared to deposition from earlier time period. Several authors have estimated the total annual deposition (wet and dry) rates of mercury by sample coring of various media. Swain et al., (1992) and Engstrom et al., (1994) analyzed sediment cores from remote lakes in Wisconsin (U.S.A.) and Minnesota (U.S.A.). They concluded that the annual atmospheric deposition rate of mercury was $3.7 \mu\text{g}/\text{m}^2/\text{yr}$ around the year 1850 in this region of the U.S. Benoit et al., (1994) analyzed mercury concentrations in a peat bog at a Minnesota site. The estimated pre-1900 deposition rate at this site was $7 \mu\text{g}/\text{m}^2/\text{yr}$.

Meili (1995) re-evaluated these types of estimates and concluded that the inferred rates were higher than actual deposition rates. Meili speculated that lake sediment and peat profiles may overestimate atmospheric deposition rates and that this could be the result of focussing of mercury from the catchment to a comparatively smaller area of sediment bed and the movement of fine sediments to deeper zones within a lake. In re-evaluating the data of Swain et al., 1992, Meili poses that as the ratio of catchment to lake area increases, there is a smaller likelihood of mercury not being retained by the lake (i.e., it is removed through outflow). In his reevaluation Meili (1995) suggested that a total mercury deposition rate of approximately $2 \mu\text{g}/\text{m}^2/\text{yr}$ is perhaps more accurate. This estimate is similar to that inferred by Meili et al., 1991 (WASP 56:333-347) for Europe prior to mercury releases of large anthropogenic sources. Additionally, the studies of Benoit et al., as well as Swain et al., and Engstrom et al. estimate mercury deposition rates only back to 1850; these estimates would postdate mercury emissions from mining in the Americas (Hudson et al., 1995) and these inferred estimates could include an anthropogenic component. Meili's other analyses indicate a deposition rate of between 1 and $5 \mu\text{g}/\text{m}^2/\text{yr}$. Based on these data and considerations, the EPA believes a deposition rate of $3 \mu\text{g}/\text{m}^2/\text{yr}$ is a reasonable estimate of yearly pre-anthropogenic deposition rate for Eastern site (this would also be an appropriate estimate for northern U.S. sites.)

Most of the data used to infer deposition rates have been collected at sites which experience higher levels of precipitation. The "pre-anthropogenic" deposition rate of $3 \mu\text{g}/\text{m}^2/\text{yr}$ is probably more appropriate to Eastern sites rather than Western sites. Given the lower rates of precipitation in the West, a lower end value from Meili (1995) of $1 \mu\text{g}/\text{m}^2/\text{yr}$ is believed by the EPA to be an appropriate estimate of deposition for the "pre-anthropogenic" deposition at the hypothetical Western site.

Based on the studies described above, in this analysis EPA is using an atmospheric concentration of 0.5 ng/m^3 for both hypothetical sites as a model input. The deposition rate of $3 \text{ } \mu\text{g/m}^2/\text{yr}$ and $1 \text{ } \mu\text{g/m}^2/\text{yr}$ will be used for the hypothetical Eastern site and Western sites respectively as inputs to the model. The IEM-2M model will be used to estimate the equilibrium concentrations in the hypothetical shallow water bodies of the eastern and western sites. The initial quantity of mercury in soil, sediments, water column, and biota is assumed to be zero. The predicted values are EPA'S estimates of the pre-anthropogenic background concentrations.

5.2.3 Estimating Current Background Mercury Concentrations

Current environmental mercury levels are the result of both natural and human events. The mercury cycle has changed over the last 100 years. Most agree that there has been a sharp increase in the loadings of mercury to the atmosphere over this period of time as a direct result of anthropogenic activity (e.g., Expert Panel on Mercury Atmospheric Processes, 1994, Mason et al., 1994, Hudson et al., 1995). There is also some evidence indicating that recent deposition rates have declined in some areas.

As noted previously the current background mercury concentration over the northern hemisphere is considered to be between $1.5 - 2.0 \text{ ng/m}^3$ (Expert Panel on Mercury Atmospheric Processes, 1994). A background atmospheric concentration of elemental mercury gas of 1.6 ng/m^3 was put forth by Fitzgerald (1994). This value will be used as an estimate of the current background atmospheric mercury concentration across the U.S. This concentration reflects contributions from many sources: "natural" sources, volatilization and evasion of previously deposited mercury from both natural and "old" anthropogenic sources, as well as current mercury emissions and evasion of mercury from water bodies contaminated by mercury in effluents.

Current deposition rates at remote sites are difficult to assess. Most measured data are collected for only a short period of time. Measured data typically only include mercury deposited through wet deposition, although some researchers have included estimates of dry particulate-bound mercury (e.g., Fitzgerald et al., 1991). Methods to measure potential dry deposition of vapor phase mercury are still being developed. The current measured data may not include this fraction of the total mercury deposited.

Watras et al., (1994) summarized the collected data and presented a conceptualization of mercury fluxes between abiotic and biotic components of the environment in 7 Northern Wisconsin seepage Lakes, including Little Rock Lake. Most of the mercury was thought to enter the lakes through atmospheric deposition with wet deposition of mercury contributing the most to the total. The total amount deposited was approximately $10 \text{ } \mu\text{g/m}^2/\text{yr}$. Additional estimates of annual mercury deposition rates are listed in Table 5-8 below. Most of the mercury deposited at Little Rock Lake was thought to either deposit into the sediment or volatilize back into the atmosphere. The behavior of mercury at most U.S. sites is not characterized to the same degree as at Little Rock Lake. It should be noted that Little Rock Lake is a remote seepage lake and that the atmospheric chemistry of mercury may be different closer to emission sources and under different atmospheric conditions. The chemistry of mercury may also be different across a spectrum of watersheds and water bodies. Other current deposition rates measured primarily through mercury concentrations in rainfall are presented in the table below. At remote sites the primary pathway of atmospheric mercury deposition is presumed to be the result of wet deposition. The average annual deposition rate across the sites and years is roughly $11 \text{ } \mu\text{g/m}^2/\text{yr}$.

Table 5-8
Mercury Wet Deposition Rates (ug/m²/yr)

Site	Wet Mercury Deposition Rates (ug/m ² /yr). Means	Reference
Ely, MN	17 in 1988 42 in 1989 6.7 in 1990	1988-89 data: Glass et al., (1992) 1990 data: Sorensen et al., (1992)
Duluth, MN	20 in 1988 6.5 in 1989 9.3 in 1990	1988-89 data: Glass et al., (1992) 1990 data: Sorensen et al., (1992)
Marcell, MN	17 in 1988 14 in 1989	Glass et al., (1992)
Bethel, MN	13 in 1990	Sorensen et al., (1992)
Cavalier, ND	6.1 in 1990	Sorensen et al., (1992)
International Falls, MN	5.5 in 1990	Sorensen et al., (1992)
Lamberton, MN	9.3 in 1990	Sorensen et al., (1992)
Raco, MN	8.9 in 1990	Sorensen et al., (1992)
Little Rock Lake, WI	4.5 from rain 2.3 from snow	Fitzgerald et al., (1991)
Crab Lake, WI	4.4 from rain 0.8 from snow	Lamborg et al., (1995)
Northern MN	10-15	Sorensen et al., (1990)
Pellston, MI	5.8 in year 1 5.5 in year 2 0.07 ug/m ² (max 0.51) per rainfall event	Hoyer et al., (1995)
South Haven, MI	9.5 in year 1 13 in year 2 0.12 ug/m ² (max 0.85) per rainfall event	Hoyer et al., (1995)
Dexter, MI	8.7 in year 1 9.1 in year 2 0.10 ug/m ² (max 0.98) per rainfall event	Hoyer et al., (1995)
Underhill Center, VT	9.3 0.07 ug/m ² per rainfall event	Burke et al., (1995)

Several authors have estimated current mercury total deposition (wet and dry) rates by sample coring of various media (see Table 5-9). For example, Swain et al., (1992) and Engstrom et al., (1994) used lake core sediments to estimate a current deposition rate of 12.5 $\mu\text{g}/\text{m}^2/\text{yr}$ for remote lakes located in Minnesota and northern Wisconsin. Benoit et al., (1994) estimated current mean mercury deposition rate to be 24.5 $\mu\text{g}/\text{m}^2/\text{yr}$ in Minnesota. Engstrom and Swain (1997) evaluated sediment core data from lakes located in Minnesota and Alaska. They concluded that there has been a recent (over approximately the last 20 years) decline in the deposition rate of atmospheric mercury to some lakes. Specifically, they showed declines in the mercury deposition rate in four Eastern Minnesota lakes and in four lakes around Minneapolis, MN, but not in three Alaskan lakes and four lakes located in Western Minnesota. The authors suggested that the observed declines were the result of decreased regional emissions. The lakes that did not exhibit a decrease were believed to be more influenced by the global concentrations. Benoit et al., (1994) also noted a recent decline in inferred deposition rates over the last 10 year interval measured. The deposition rate of 24.5 $\mu\text{g}/\text{m}^2/\text{yr}$ is actually one third of the rate reported for the previous 10 year interval.

Table 5-9
Estimated Mercury Total Deposition Rates

Site	Estimate of Pre-industrial Annual Deposition Rates $\mu\text{g}/\text{m}^2/\text{yr}$	Estimate of Current Annual Deposition Rates $\mu\text{g}/\text{m}^2/\text{yr}$	Reference
Minnesota and northern Wisconsin	3.7	12.5	Swain et al. (1992); Engstrom et al., (1994) Lake core sediments
Minnesota	7.0	24.5	Benoit et al., (1994) Peat bog core sampling
Little Rock Lake, WI ^a		10	Fitzgerald et al., (1991)
Crab Lake, WI ^a		7.0 (86% estimated to deposit in summer)	Lamborg et al., (1995)

^a Data includes previously tabled values of wet deposition plus particulate deposition. Fitzgerald et al., 1991 did not collect particulate size data. Assuming a particulate deposition velocity of 0.5 cm/s, a yearly average particulate deposition flux of 3.5 \pm 3 $\mu\text{g}/\text{m}^2/\text{yr}$ was estimated. Lamborg et al., (1995) noted the smaller particle sizes in the winter and assumed a deposition velocity 0.1 cm/s for the average winter concentrations (7 pg/m^3) and a deposition velocity of 0.5 cm/s for average summer concentrations (26 pg/m^3).

Given these data, a reasonable estimate of annual deposition at Eastern and Northern sites remote from sources is 10 $\mu\text{g}/\text{m}^2/\text{yr}$. This value will be input into the model. It is intended that this value account for “pre-anthropogenic” mercury as well as the cycling of mercury emitted from “old anthropogenic” sources that has been previously deposited. There is a collection bias associated with these data; specifically, the data primarily examine mercury deposition at remote sites from the Northern and Eastern parts of the U.S. Mercury deposition at these sites is thought to be primarily derived by climactic

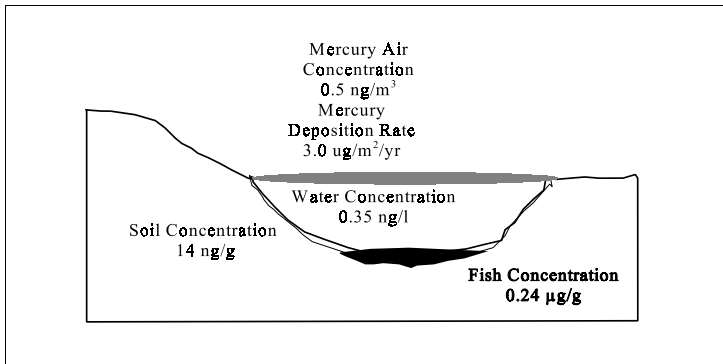
factors such as wet deposition. The total deposition in this region of the U.S. is thought to be approximately a factor of 5 lower; this is based roughly on the decrease in precipitation rates. These deposition rates and the air concentration rate will be input to the model until equilibrium is achieved. The final predicted concentrations will serve as initial inputs to the local scale modeling effort with the model plants at both hypothetical sites.

Table 5-10 summarizes the inputs to the IEM-2M model which have been derived from the data discussed above. It is important to recognize that many alternative approaches could have been developed to examine the influence of “background” mercury. This option was utilized because of the internal consistency it offered. Additionally, it conveys a more general rather than a specific or exact understanding of the influences on the mercury cycle that is more consistent with the current level of scientific understanding. Figures 5-13 and 5-14 show schematically how these inputs have been utilized to establish initial conditions for analysis.

Table 5-10
Inputs to IEM-2M Model for the two time periods modeled

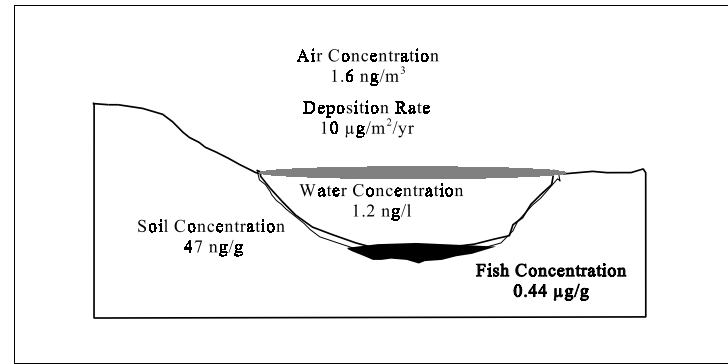
Time Period	Parameter	East	West
Pre-industrial	Air Concentration (ng/m ³)	0.5	0.5
	Deposition Rate (ug/m ² /yr)	3.0	1
	Predicted Watershed soil concentration (ng/g)	14	4
	Predicted Total Hg Water Concentration (ng/L)	0.35	0.1
	Predicted Trophic Level 4 Fish Concentration (ug/g)	0.13	0.04
Industrial	Air Concentration (ng/m ³)	1.6	1.6
	Deposition Rate (ug/m ² /yr)	10.0	2.0
	Predicted Watershed soil concentration (ng/g)	47	8.0
	Predicted Total Hg Water Concentration (ng/L)	1.2	0.2
	Predicted Trophic Level 4 Fish Concentration (ug/g)	0.44	0.09

Figure 5-13 IEM-2M results for pre-industrial and industrial periods for Eastern site



Pre-industrial Period Steady-State Conditions (used as initial conditions for industrial period)

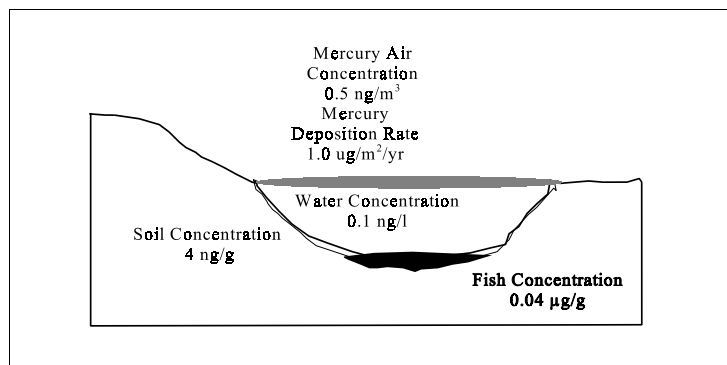
Used as Initial Conditions



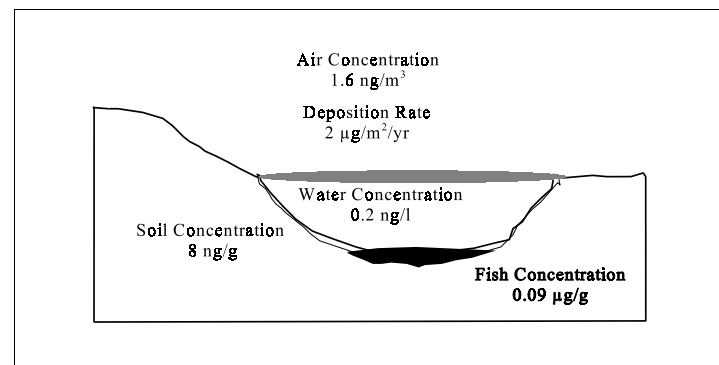
Industrial Period Steady-State Conditions (used as initial conditions for model plant analysis)

Used as Initial Conditions for Analysis

Figure 5-14 IEM-2M results for pre-industrial and industrial periods for Western site



Used as Initial Conditions



Used as Initial Conditions for Analysis

Pre-industrial Period Steady-State Conditions (used as initial conditions for industrial period)

Industrial Period Steady-State Conditions (used as initial conditions for model plant analysis)

5.3 Local Atmospheric Transport Modeling

Tables 5-11 through 5-14 show the predicted air concentrations and deposition rates for each facility in each site, for both the RELMAP 50th and RELMAP 90th percentiles. These results are discussed in sections 5.3.1 and 5.3.2 below.

**Table 5-11
Predicted Air Concentrations and Deposition Rates for**

Plant	Distance	Air Concentration (ng/m3)	%RelMap	%ISC	Total Deposition (ug/m2/yr)	%RelMap	%ISC
Variant b:Large Municipal Waste Combustor	2.5 km	1.7E+00	97%	3%	4.2E+01	34%	66%
	10 km	1.7E+00	98%	2%	2.6E+01	57%	43%
	25 km	1.7E+00	99%	1%	1.9E+01	78%	22%
Variant b:Small Municipal Waste Combustor	2.5 km	1.7E+00	99%	1%	1.9E+01	74%	26%
	10 km	1.7E+00	100%	0%	1.6E+01	90%	10%
	25 km	1.7E+00	100%	0%	1.5E+01	97%	3%
Large Commercial HMI	2.5 km	1.7E+00	99%	1%	1.9E+01	76%	24%
	10 km	1.7E+00	100%	0%	1.5E+01	95%	5%
	25 km	1.7E+00	100%	0%	1.5E+01	99%	1%
Large Hospital HMI	2.5 km	1.7E+00	97%	3%	4.4E+01	33%	67%
	10 km	1.7E+00	99%	1%	2.0E+01	74%	26%
	25 km	1.7E+00	100%	0%	1.6E+01	92%	8%
Small Hospital HMI	2.5 km	1.7E+00	100%	0%	1.6E+01	88%	12%
	10 km	1.7E+00	100%	0%	1.5E+01	98%	2%
	25 km	1.7E+00	100%	0%	1.5E+01	100%	0%
Large Hospital HMI (wet scrubber)	2.5 km	1.7E+00	100%	0%	1.5E+01	94%	6%
	10 km	1.7E+00	100%	0%	1.5E+01	99%	1%
	25 km	1.7E+00	100%	0%	1.5E+01	100%	0%
Small Hospital HMI (wet scrubber)	2.5 km	1.7E+00	100%	0%	1.5E+01	100%	0%
	10 km	1.7E+00	100%	0%	1.5E+01	100%	0%
	25 km	1.7E+00	100%	0%	1.5E+01	100%	0%
Large Coal-fired Utility Boiler	2.5 km	1.7E+00	100%	0%	3.0E+01	48%	52%
	10 km	1.7E+00	100%	0%	1.7E+01	83%	17%
	25 km	1.7E+00	100%	0%	1.6E+01	93%	7%
Medium Coal-fired Utility Boiler	2.5 km	1.7E+00	100%	0%	2.1E+01	68%	32%
	10 km	1.7E+00	100%	0%	1.6E+01	89%	11%
	25 km	1.7E+00	100%	0%	1.5E+01	94%	6%
Small Coal-fired Utility Boiler	2.5 km	1.7E+00	100%	0%	1.6E+01	90%	10%
	10 km	1.7E+00	100%	0%	1.5E+01	96%	4%
	25 km	1.7E+00	100%	0%	1.5E+01	99%	1%
Medium Oil-fired Utility Boiler	2.5 km	1.7E+00	100%	0%	1.5E+01	99%	1%
	10 km	1.7E+00	100%	0%	1.5E+01	100%	0%
	25 km	1.7E+00	100%	0%	1.5E+01	100%	0%
Chlor-alkali plant	2.5 km	4.0E+00	42%	58%	2.5E+02	6%	94%
	10 km	2.1E+00	79%	21%	4.6E+01	32%	68%
	25 km	1.8E+00	92%	8%	2.2E+01	65%	35%

**Table 5-12
Predicted Air Concentrations and Deposition Rates for**

Plant	Distance	Air Concentration (ng/m ³)	%RelMap	%ISC	Total Deposition (ug/m ² /yr)	%RelMap	%ISC
Variant b:Large Municipal Waste Combustor	2.5 km	1.8E+00	97%	3%	5.5E+01	50%	50%
	10 km	1.8E+00	98%	2%	3.8E+01	71%	29%
	25 km	1.7E+00	99%	1%	3.1E+01	87%	13%
Variant b:Small Municipal Waste Combustor	2.5 km	1.7E+00	99%	1%	3.2E+01	85%	15%
	10 km	1.7E+00	100%	0%	2.9E+01	95%	5%
	25 km	1.7E+00	100%	0%	2.8E+01	98%	2%
Large Commercial HMI	2.5 km	1.7E+00	99%	1%	3.2E+01	85%	15%
	10 km	1.7E+00	100%	0%	2.8E+01	98%	2%
	25 km	1.7E+00	100%	0%	2.7E+01	99%	1%
Large Hospital HMI	2.5 km	1.8E+00	97%	3%	5.7E+01	48%	52%
	10 km	1.7E+00	99%	1%	3.2E+01	84%	16%
	25 km	1.7E+00	100%	0%	2.8E+01	96%	4%
Small Hospital HMI	2.5 km	1.7E+00	100%	0%	2.9E+01	93%	7%
	10 km	1.7E+00	100%	0%	2.7E+01	99%	1%
	25 km	1.7E+00	100%	0%	2.7E+01	100%	0%
Large Hospital HMI (wet scrubber)	2.5 km	1.7E+00	100%	0%	2.8E+01	97%	3%
	10 km	1.7E+00	100%	0%	2.7E+01	100%	0%
	25 km	1.7E+00	100%	0%	2.7E+01	100%	0%
Small Hospital HMI (wet scrubber)	2.5 km	1.7E+00	100%	0%	2.7E+01	100%	0%
	10 km	1.7E+00	100%	0%	2.7E+01	100%	0%
	25 km	1.7E+00	100%	0%	2.7E+01	100%	0%
Large Coal-fired Utility Boiler	2.5 km	1.7E+00	100%	0%	4.3E+01	64%	36%
	10 km	1.7E+00	100%	0%	3.0E+01	90%	10%
	25 km	1.7E+00	100%	0%	2.8E+01	96%	4%
Medium Coal-fired Utility Boiler	2.5 km	1.7E+00	100%	0%	3.4E+01	80%	20%
	10 km	1.7E+00	100%	0%	2.9E+01	94%	6%
	25 km	1.7E+00	100%	0%	2.8E+01	97%	3%
Small Coal-fired Utility Boiler	2.5 km	1.7E+00	100%	0%	2.9E+01	94%	6%
	10 km	1.7E+00	100%	0%	2.8E+01	98%	2%
	25 km	1.7E+00	100%	0%	2.7E+01	99%	1%
Medium Oil-fired Utility Boiler	2.5 km	1.7E+00	100%	0%	2.7E+01	99%	1%
	10 km	1.7E+00	100%	0%	2.7E+01	100%	0%
	25 km	1.7E+00	100%	0%	2.7E+01	100%	0%
Chlor-alkali plant	2.5 km	4.0E+00	43%	57%	2.6E+02	10%	90%
	10 km	2.2E+00	79%	21%	5.9E+01	46%	54%
	25 km	1.9E+00	92%	8%	3.5E+01	77%	23%

Table 5-13
Predicted Air Concentrations and Deposition Rates for

Plant	Distance	Air Concentration (ng/m³)	%RelMap	%ISC	Total Deposition (ug/m²/yr)	%RelMap	%ISC
Variant b:Large Municipal Waste Combustor	2.5 km	1.7E+00	98%	2%	2.0E+01	11%	89%
	10 km	1.6E+00	98%	2%	1.1E+01	20%	80%
	25 km	1.6E+00	99%	1%	5.6E+00	41%	59%
Variant b:Small Municipal Waste Combustor	2.5 km	1.6E+00	99%	1%	6.2E+00	38%	62%
	10 km	1.6E+00	100%	0%	3.4E+00	68%	32%
	25 km	1.6E+00	100%	0%	2.7E+00	87%	13%
Large Commercial HMI	2.5 km	1.6E+00	99%	1%	6.0E+00	38%	62%
	10 km	1.6E+00	100%	0%	2.8E+00	83%	17%
	25 km	1.6E+00	100%	0%	2.4E+00	95%	5%
Large Hospital HMI	2.5 km	1.7E+00	98%	2%	2.7E+01	9%	91%
	10 km	1.6E+00	99%	1%	5.9E+00	39%	61%
	25 km	1.6E+00	100%	0%	3.3E+00	71%	29%
Small Hospital HMI	2.5 km	1.6E+00	100%	0%	3.9E+00	59%	41%
	10 km	1.6E+00	100%	0%	2.5E+00	92%	8%
	25 km	1.6E+00	100%	0%	2.4E+00	98%	2%
Large Hospital HMI (wet scrubber)	2.5 km	1.6E+00	100%	0%	3.0E+00	77%	23%
	10 km	1.6E+00	100%	0%	2.4E+00	96%	4%
	25 km	1.6E+00	100%	0%	2.3E+00	99%	1%
Small Hospital HMI (wet scrubber)	2.5 km	1.6E+00	100%	0%	2.4E+00	98%	2%
	10 km	1.6E+00	100%	0%	2.3E+00	100%	0%
	25 km	1.6E+00	100%	0%	2.3E+00	100%	0%
Large Coal-fired Utility Boiler	2.5 km	1.6E+00	100%	0%	5.8E+00	40%	60%
	10 km	1.6E+00	100%	0%	3.5E+00	67%	33%
	25 km	1.6E+00	100%	0%	3.3E+00	69%	31%
Medium Coal-fired Utility Boiler	2.5 km	1.6E+00	100%	0%	4.3E+00	53%	47%
	10 km	1.6E+00	100%	0%	3.7E+00	63%	37%
	25 km	1.6E+00	100%	0%	3.2E+00	73%	27%
Small Coal-fired Utility Boiler	2.5 km	1.6E+00	100%	0%	3.4E+00	69%	31%
	10 km	1.6E+00	100%	0%	2.8E+00	84%	16%
	25 km	1.6E+00	100%	0%	2.5E+00	94%	6%
Medium Oil-fired Utility Boiler	2.5 km	1.6E+00	100%	0%	2.4E+00	96%	4%
	10 km	1.6E+00	100%	0%	2.4E+00	97%	3%
	25 km	1.6E+00	100%	0%	2.3E+00	99%	1%
Chlor-alkali plant	2.5 km	3.5E+00	46%	54%	1.9E+02	1%	99%
	10 km	1.9E+00	84%	16%	2.5E+01	9%	91%
	25 km	1.7E+00	94%	6%	8.1E+00	28%	72%

Table 5-14
Predicted Air Concentrations and Deposition Rates for

Plant	Distance	Air Concentration (ng/m ³)	%RelMap	%ISC	Total Deposition (ug/m ² /yr)	%RelMap	%ISC
Variant b:Large Municipal Waste Combustor	2.5 km	1.7E+00	98%	2%	2.6E+01	31%	69%
	10 km	1.7E+00	98%	2%	1.7E+01	47%	53%
	25 km	1.7E+00	99%	1%	1.1E+01	71%	29%
Variant b:Small Municipal Waste Combustor	2.5 km	1.7E+00	99%	1%	1.2E+01	67%	33%
	10 km	1.6E+00	100%	0%	9.1E+00	88%	12%
	25 km	1.6E+00	100%	0%	8.3E+00	96%	4%
Large Commercial HMI	2.5 km	1.7E+00	99%	1%	1.2E+01	68%	32%
	10 km	1.6E+00	100%	0%	8.5E+00	94%	6%
	25 km	1.6E+00	100%	0%	8.1E+00	98%	2%
Large Hospital HMI	2.5 km	1.7E+00	98%	2%	3.2E+01	25%	75%
	10 km	1.7E+00	99%	1%	1.2E+01	69%	31%
	25 km	1.6E+00	100%	0%	8.9E+00	90%	10%
Small Hospital HMI	2.5 km	1.6E+00	100%	0%	9.6E+00	83%	17%
	10 km	1.6E+00	100%	0%	8.2E+00	98%	2%
	25 km	1.6E+00	100%	0%	8.0E+00	99%	1%
Large Hospital HMI (wet scrubber)	2.5 km	1.6E+00	100%	0%	8.7E+00	92%	8%
	10 km	1.6E+00	100%	0%	8.1E+00	99%	1%
	25 km	1.6E+00	100%	0%	8.0E+00	100%	0%
Small Hospital HMI (wet scrubber)	2.5 km	1.6E+00	100%	0%	8.0E+00	99%	1%
	10 km	1.6E+00	100%	0%	8.0E+00	100%	0%
	25 km	1.6E+00	100%	0%	8.0E+00	100%	0%
Large Coal-fired Utility Boiler	2.5 km	1.6E+00	100%	0%	1.2E+01	69%	31%
	10 km	1.6E+00	100%	0%	9.1E+00	88%	12%
	25 km	1.6E+00	100%	0%	9.0E+00	89%	11%
Medium Coal-fired Utility Boiler	2.5 km	1.6E+00	100%	0%	1.0E+01	80%	20%
	10 km	1.6E+00	100%	0%	9.4E+00	85%	15%
	25 km	1.6E+00	100%	0%	8.9E+00	90%	10%
Small Coal-fired Utility Boiler	2.5 km	1.6E+00	100%	0%	9.1E+00	88%	12%
	10 km	1.6E+00	100%	0%	8.5E+00	95%	5%
	25 km	1.6E+00	100%	0%	8.2E+00	98%	2%
Medium Oil-fired Utility Boiler	2.5 km	1.6E+00	100%	0%	8.1E+00	99%	1%
	10 km	1.6E+00	100%	0%	8.1E+00	99%	1%
	25 km	1.6E+00	100%	0%	8.0E+00	100%	0%
Chlor-alkali plant	2.5 km	3.6E+00	46%	54%	2.0E+02	4%	96%
	10 km	1.9E+00	84%	16%	3.0E+01	26%	74%
	25 km	1.7E+00	94%	6%	1.4E+01	58%	42%

5.3.1 Air Concentrations

In analyzing the air concentrations predicted by the ISC3 model, it is important to observe that in a typical year the predicted air concentration due to the local source at *any* receptor is zero a rather substantial fraction of the time. There are two basic reasons for this. First, in order to predict a non-zero air concentration for a given hour the receptor must be in the downwind direction. This means that the wind must be blowing in a direction within 90 degrees of the receptor itself. For most sites this only occurs about 50% of the time for the direction with the highest frequency. Second, even if the receptor is downwind, the predicted air concentration will be significant only if the wind is blowing in a direction within about 10 degrees of the receptor's direction relative to the facility. For most sites this occurs for the prevailing downwind direction only about 10 to 15 percent of the time. Because the air concentrations are averaged over the year, this results in (usually) low average air concentrations.

The predicted air concentrations are typically dominated by the regional values, even for the watersheds relatively close to the facility. The only exception to this is the chlor-alkali plant, for which larger air concentrations are predicted (this is due to the low stack height and assumed stack gas exit velocity). The predicted air concentrations are similar for both sites, and none of the predicted air concentrations exceed 4 ng/m³.

The differences in predicted air concentrations across source classes depend mainly on three key parameters: the total mercury emission rate, the stack height, and the exit velocity of the plume from the source. The sensitivity of the air model to the emission rate is to be expected because the predicted air concentrations are linear with the total mercury emission rate, and the model plants are assumed to have a wide range of emission rates (from less than 1 kg/yr up to 380 kg/yr). Both the stack height and exit velocity are used in calculating the effective stack height, which is the height to which the plume rises from the stack top. The importance of the effective stack height on air concentrations is well known, and is demonstrated here by the predicted air concentrations for the chlor-alkali plant, which clearly dominates the values as a whole. This is due to a combination of a low stack height (10 feet) and slow stack gas exit velocity (0.1 m/s) and a comparatively high assumed total mercury emissions rate of about 380 kg/yr. The low stack parameters result in predicted low plumes that are not as vertically dispersed at the receptor when compared with the facilities with higher stacks, thereby enhancing air concentrations.

In general, the predicted average air concentrations are quite low. The only source class for which significantly elevated air concentrations are predicted is the chlor-alkali facility. This is due to a very low stack height coupled with a high assumed mercury emission rate. The low stack height results in predicted plumes that are close to the receptors considered, and so there is less dispersion of the plume compared to the other facilities.

5.3.2 Deposition Rates

In contrast to the predicted air concentrations, the annual deposition rates are *cumulative*; they represent the sum of any deposition that occurs during the year, and hence are not affected by long periods of little deposition. Further, the ISC3 model predicts that significant deposition events occur infrequently, and it is these relatively rare events that are responsible for the majority of the annual deposition rate.

Because dry deposition is calculated by multiplying the predicted air concentration for the hour by the deposition velocity, significant dry deposition events only occur when, for the reasons discussed above, there is a "spike" of predicted high air concentration for a given hour. Annual dry deposition

tends to be dominated by these peak values when the wind is blowing within a few degrees of the receptor's direction.

For any site with appreciable precipitation, wet deposition can dominate the total deposition for receptors close to the source. Single wet deposition events can deposit 300 times more Hg than a high dry deposition event. These events are even rarer than significant dry deposition events because not only must the wind direction be within a few degrees of the receptor's direction, but precipitation must be occurring as well.

The predicted dry deposition rates depend ultimately on the predicted air concentrations. For this reason, dry deposition accounts for most of the total deposition for the facility with the highest predicted air concentrations, the chlor-alkali plant. In complex terrain, dry deposition can play a larger but uncertain role than in the results presented here.

5.3.3 Mass Balances within the Local-Scale Domain

In this section the fraction of the mercury emitted from each hypothetical facility that is predicted to deposit within 50 km is estimated. The area-averaged wet and dry deposition rates are also estimated based on the fraction from the single source that is predicted to deposit within 50 km.

Tables 5-15 and 5-16 show the results for all facilities at both sites. These results were obtained by using a total of 480 receptors for each facility and site. The receptors were placed in 16 directions around the facility and 30 distances, from 0.5 km to 50 km.

In general, 7-45 percent of the total mercury emitted is predicted to deposit within 50 km at the humid site in flat terrain, while 2-38 percent is predicted to deposit at the arid site. (The ranges represent values from the different sources considered.) This implies that at least 55 percent of the total mercury emissions is transported more than 50 km from any of the sources considered, and is consistent with the RELMAP results that predict that mercury may be transported across considerable distances.

The differences between the results for the two sites are due primarily to the differences in the frequency and intensity of precipitation. At the humid site, precipitation occurs about 12 percent of the year, with about 5 percent of this precipitation of moderate intensity (0.11 to 0.30 in/hr). At the arid site, precipitation occurs about 3 percent of the year, with about 2 percent of the precipitation of moderate intensity.

Table 5-15
Mass Balance of Mercury Emissions for each Facility in the Humid Site Using the ISC3 Model

Eastern Site		Hg Emission (kg/yr)	Speciation of Emissions				Percent of Total Mercury Emissions Deposited within 50 km							
Facility	Stack height (m)		Hg0 Vapor	Hg0 Particulate	Hg(II) Vapor	Hg(II) Particulate	Total		Hg0 Vapor		Hg(II) Vapor		Hg(II) Particulate	
							Dry Dep	Wet Dep	Dry Dep	Wet Dep	Dry Dep	Wet Dep	Dry Dep	Wet Dep
LMWC_b	70	220	60%	0%	30%	10%	6.7%	6.2%	0.5%	3.9%	6.1%	1.9%	0.1%	0.4%
SMWC_b	43	20	60%	0%	30%	10%	10.5%	6.1%	0.9%	3.9%	9.4%	1.8%	0.2%	0.4%
LCMHI	12	5	33%	0%	50%	17%	27.5%	5.2%	1.3%	2.1%	25.5%	2.3%	0.7%	0.8%
LHMHI	12	24	2%	0%	73%	25%	35.3%	5.0%	0.1%	0.1%	34.3%	3.8%	0.9%	1.1%
SHMHI	12	1	2%	0%	73%	25%	38.8%	4.5%	0.1%	0.1%	37.8%	3.3%	1.0%	1.1%
LHMHI_Scrubber	12	1	33%	0%	50%	17%	27.6%	5.2%	1.3%	2.1%	25.7%	2.3%	0.7%	0.8%
SHMHI_Scrubber	12	0	33%	0%	50%	17%	28.1%	5.0%	1.4%	2.1%	26.0%	2.1%	0.7%	0.8%
LCUB	223	230	50%	0%	30%	20%	0.8%	5.9%	0.0%	3.2%	0.8%	1.9%	0.0%	0.8%
MCUB	142	90	50%	0%	30%	20%	2.5%	6.0%	0.1%	3.3%	2.2%	1.9%	0.1%	0.8%
SCUB	81	10	50%	0%	30%	20%	7.8%	5.9%	0.5%	3.2%	7.0%	1.8%	0.3%	0.8%
MOUB	88	2	50%	0%	30%	20%	4.6%	6.0%	0.2%	3.3%	4.1%	1.9%	0.2%	0.8%
CAP	3	380	70%	0%	30%	0%	17.2%	5.5%	3.5%	4.5%	13.6%	1.0%	0.0%	0.0%

Table 5-16
Mass Balance of Mercury Emissions for each Facility in the Arid Site Using the ISC3 Model

Western Site			Speciation of Emissions				Estimated Percent of Total Mercury Emissions Deposited within 50 km							
Facility	Stack height (m)	Assumed Hg Emission (kg/yr)	Hg0 Vapor	Hg0 Particulate	Hg(II) Vapor	Hg(II) Particulate	Total		Hg0 Vapor		Hg(II) Vapor		Hg(II) Particulate	
							Dry Dep	Wet Dep	Dry Dep	Wet Dep	Dry Dep	Wet Dep	Dry Dep	Wet Dep
LMWC_b	70	220	60%	0%	30%	10%	6.7%	1.0%	0.5%	0.6%	6.1%	0.3%	0.1%	0.1%
SMWC_b	43	20	60%	0%	30%	10%	10.0%	1.0%	0.8%	0.7%	9.0%	0.3%	0.2%	0.1%
LCMHI	12	5	33%	0%	50%	17%	26.0%	0.9%	1.2%	0.4%	24.2%	0.4%	0.6%	0.1%
LHMHI	12	24	2%	0%	73%	25%	33.5%	0.8%	0.1%	0.0%	32.6%	0.6%	0.8%	0.2%
SHMHI	12	1	2%	0%	73%	25%	36.9%	0.7%	0.1%	0.0%	35.8%	0.5%	1.0%	0.2%
LHMHI_Scrubber	12	1	33%	0%	50%	17%	26.3%	0.9%	1.3%	0.4%	24.4%	0.4%	0.6%	0.1%
SHMHI_Scrubber	12	0	33%	0%	50%	17%	27.0%	0.8%	1.4%	0.4%	24.9%	0.3%	0.7%	0.1%
LCUB	223	230	50%	0%	30%	20%	1.2%	0.9%	0.0%	0.5%	1.1%	0.3%	0.0%	0.1%
MCUB	142	90	50%	0%	30%	20%	2.8%	0.9%	0.1%	0.5%	2.6%	0.3%	0.1%	0.1%
SCUB	81	10	50%	0%	30%	20%	7.5%	1.0%	0.4%	0.5%	6.8%	0.3%	0.3%	0.1%
MOUB	88	2	50%	0%	30%	20%	4.8%	1.0%	0.2%	0.5%	4.4%	0.3%	0.2%	0.1%
CAP	3	380	70%	0%	30%	0%	16.7%	1.0%	3.6%	0.8%	13.1%	0.2%	0.0%	0.0%

The percentage of mercury deposited within 50 km depends on two main factors: facility characteristics that influence effective stack height (stack height plus plume rise) and the fraction of mercury emissions that is divalent mercury. In most cases, the effective stack height affects only the air concentrations, and hence dry deposition.

The differences between the results for the LMWC and SMWC are primarily due to differences in the parameters used to estimate the effective stack height (stack height plus plume rise): stack height, stack diameter, and exit temperature. The effective stack height is used to estimate dry deposition. The lower plumes predicted for the SMWC result in higher air concentrations, and hence higher predicted dry deposition. About twice as much of the emitted mercury is predicted to dry deposit for the SMWC than for the LMWC. This difference is roughly the same as the ratio of the stack heights (LMWC stack is about twice as high as that of the SMWC). Wet deposition is only affected by differences in wind speed at stack top, and in this case the ultimate effects are minimal. The wind speed at stack top is extrapolated from the height at which it was measured using wind profile exponents.

Differences between the results for the utility boilers are due primarily to the difference in stack heights. For all utility boilers, less than 15 percent of the total mercury emitted is predicted to deposit within 50 km. Again, this is a reflection of the high effective stacks predicted for this source class.

The deposition rates averaged over the entire 50 km radius region surrounding each facility are given in Tables 5-17 and 5-18. These values are comparable to or well below typically reported deposition rates (see Section 2).

Table 5-17
Area-Averaged Mercury Deposition Rates for each Facility in the Humid Site

Eastern Site									
Facility	Stack height (m)	Hg Emission (kg/yr)	Hg0 Vapor	Speciation of Emissions			Area-Averaged Values within 50km (ug/m2/yr)		
				Hg0 Particulate	Hg(II) Vapor	Hg(II) Particulate	Total Deposition Rate	Dry Deposition Rate	Wet Deposition Rate
LMWC_b	70.1	220.0	60%	0%	30%	10%	3.6	1.9	1.7
SMWC_b	42.7	20.0	60%	0%	30%	10%	0.4	0.3	0.2
LCMHI	12.2	4.6	33%	0%	50%	17%	0.2	0.2	0.0
LHMHI	12.2	23.9	2%	0%	73%	25%	1.2	1.1	0.2
SHMHI	12.2	1.3	2%	0%	73%	25%	0.1	0.1	0.0
LHMHI_Scrubber	12.2	0.8	33%	0%	50%	17%	0.0	0.0	0.0
SHMHI_Scrubber	12.2	0.1	33%	0%	50%	17%	0.0	0.0	0.0
LCUB	223.1	230.0	50%	0%	30%	20%	2.0	0.2	1.7
MCUB	141.7	90.0	50%	0%	30%	20%	1.0	0.3	0.7
SCUB	81.1	10.0	50%	0%	30%	20%	0.2	0.1	0.1
MOUB	88.4	2.0	50%	0%	30%	20%	0.1	0.1	0.0
CAP	3.0	380.0	70%	0%	30%	0%	11.0	8.3	2.7

Table 5-18
Area-Averaged Mercury Deposition Rates for each Facility in the Arid Site

Western Site									
Facility	Stack height (m)	Assumed Hg Emission (kg/yr)	Assumed Speciation of Emissions				Area-Averaged Values within 50km (ug/m2/yr)		
			Hg0 Vapor	Hg0 Particulate	Hg(II) Vapor	Hg(II) Particulate	Total Deposition Rate	Dry Deposition Rate	Wet Deposition Rate
LMWC_b	70.1	220.0	60%	0%	30%	10%	2.2	1.9	0.3
SMWC_b	42.7	20.0	60%	0%	30%	10%	0.3	0.3	0.0
LCMHI	12.2	4.6	33%	0%	50%	17%	0.2	0.2	0.0
LHMHI	12.2	23.9	2%	0%	73%	25%	1.0	1.0	0.0
SHMHI	12.2	1.3	2%	0%	73%	25%	0.1	0.1	0.0
LHMHI_Scrubber	12.2	0.8	33%	0%	50%	17%	0.0	0.0	0.0
SHMHI_Scrubber	12.2	0.1	33%	0%	50%	17%	0.0	0.0	0.0
LCUB	223.1	230.0	50%	0%	30%	20%	0.6	0.4	0.3
MCUB	141.7	90.0	50%	0%	30%	20%	0.4	0.3	0.1
SCUB	81.1	10.0	50%	0%	30%	20%	0.1	0.1	0.0
MOUB	88.4	2.0	50%	0%	30%	20%	0.0	0.0	0.0
CAP	3.0	380.0	70%	0%	30%	0%	8.5	8.1	0.5

5.3.4 Uncertainty and Sensitivity Analyses

As has been noted previously, the behavior of atmospheric mercury close to the point of release has not been studied extensively. This alone results in a significant degree of uncertainty implicit in the preceding modeling exercises. In this section, several of these assumptions along with other possible behaviors are examined to illustrate the implications of these potential properties of atmospheric mercury in the near-field.

5.3.4.1 Dry Deposition

Impact of a Compensation Point for Dry Deposition of Elemental Mercury

It has been suggested that dry deposition of elemental mercury to plants may not occur at all unless the air concentration is above a certain threshold value, which is termed the compensation point. Results of Hanson et al. (1995) suggest that this threshold is at least about 10 ng/m^3 , although there are lingering uncertainties due to the possible dependence of the compensation point on the type of vegetation, season, and time of day. Sensitivity analyses were conducted to examine the possible impact of a compensation point on the ISC3 analysis. This analysis represents one of the first efforts ever to investigate the possible impact of a compensation point on the dry deposition of elemental mercury.

Figures 5-15, 5-16, and 5-17 show the predicted dry deposition of elemental mercury at 2.5 km, 10 km, and 25 km, respectively, northeast (the direction of maximum deposition) of the model plant chlor-alkali facility located at the eastern site. These results were generated assuming a dry deposition velocity of 0.06 cm/s for elemental mercury (the same value used in the analyses); however, if the calculated air concentration for a given hour is not above the compensation point, no dry deposition is allowed to occur. The figures show the sensitivity of the total dry deposition rate to different compensation points.

Figure 5-15

**Influence of the Compensation Point on the Dry Deposition of Elemental Mercury:
2,500 Meters NE of a Chlor-alkali Plant at the Eastern Site**

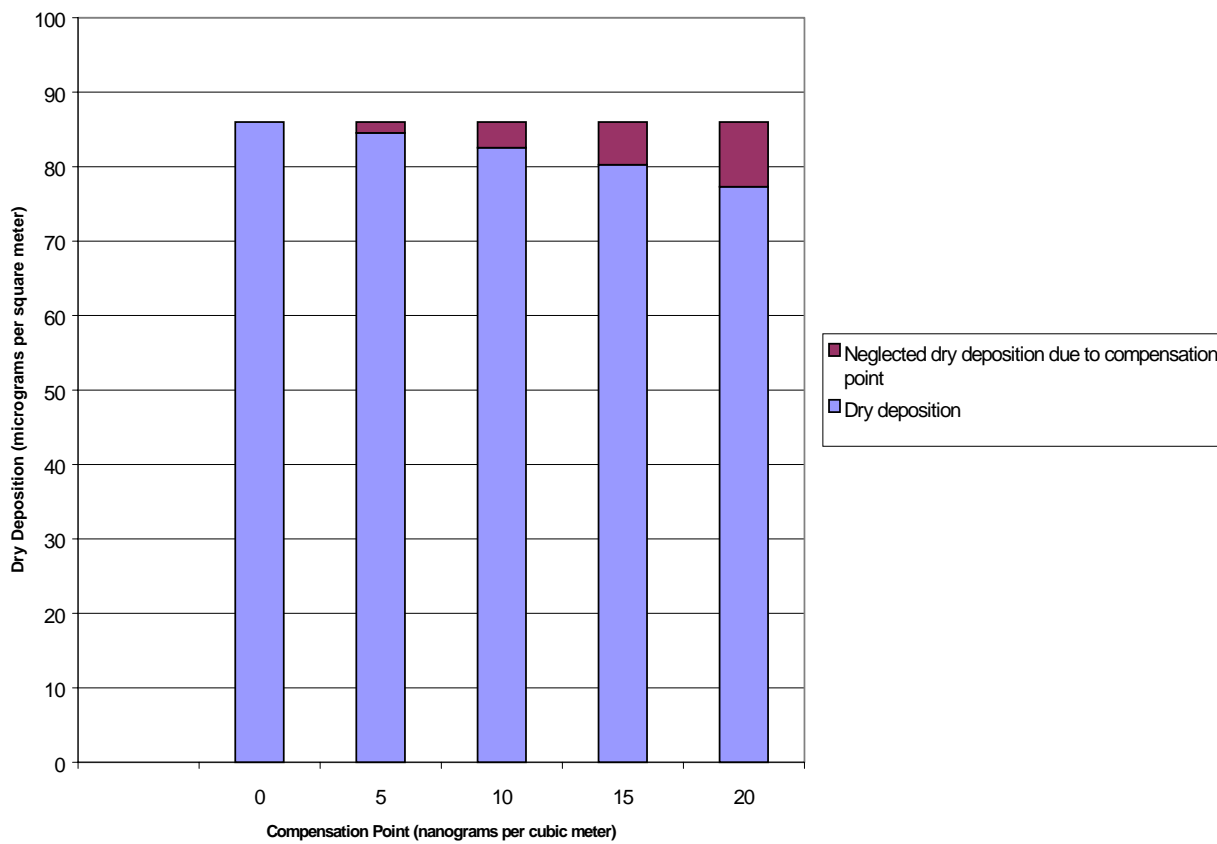


Figure 5-16

Influence of the Compensation Point on the Dry Deposition of Elemental Mercury:
10,000 Meters NE of a Chlor-alkali Plant at the Eastern Site

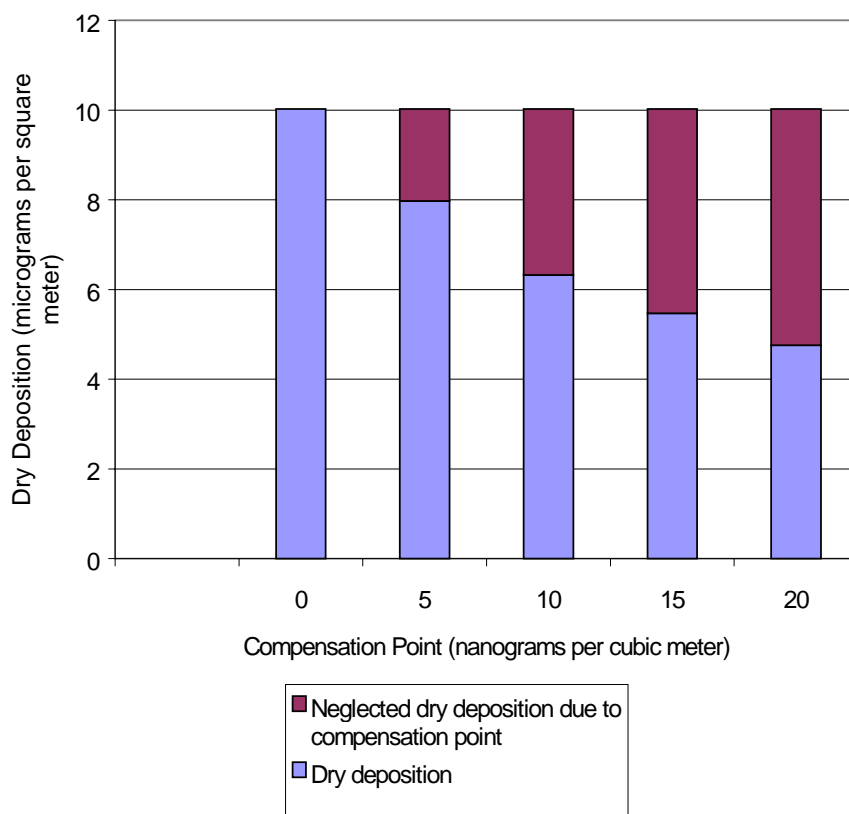
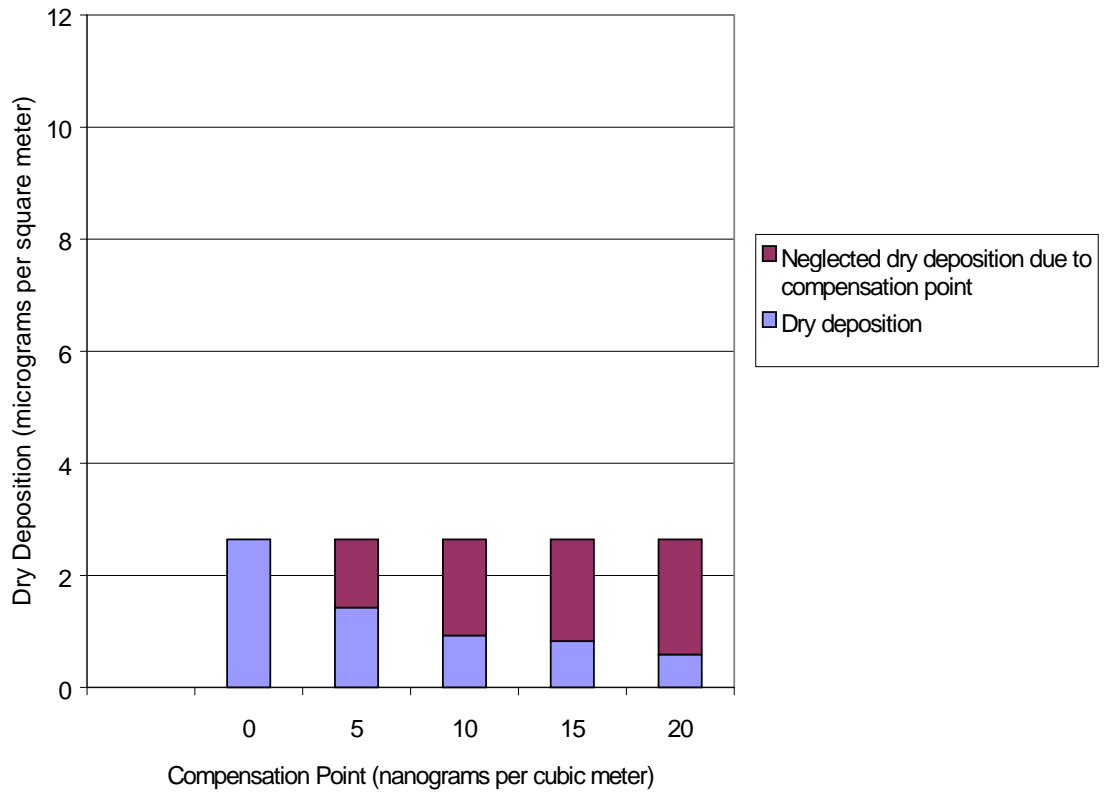


Figure 5-17

Influence of the Compensation Point on the Dry Deposition of Elemental Mercury:
25,000 Meters NE of a Chlor-alkali Plant at the Eastern Site



As a percentage of the total dry deposition, there is little impact for the receptor located at 2.5 km from the facility. This indicates that almost all of the predicted dry deposition occurs during hours when the predicted air concentration is above 20 ng/m³. This suggests that the existence of a compensation point will not have a large impact on the results for receptors close to this facility unless it is above 20 ng/m³.

For receptors farther from the facility, the compensation point is predicted to have more of an impact, in terms of the fraction of the total dry deposition. This impact indicates that most of the dry deposition is predicted to occur when the air concentration is low. However, in these cases the total dry deposition rate is then correspondingly low. For example, at 25 km, by not assuming a compensation point there is the possibility of overestimating the dry deposition of elemental mercury by up to a factor of 2, depending on what the compensation point is; however, this amounts to less than 2 µg/m²/yr.

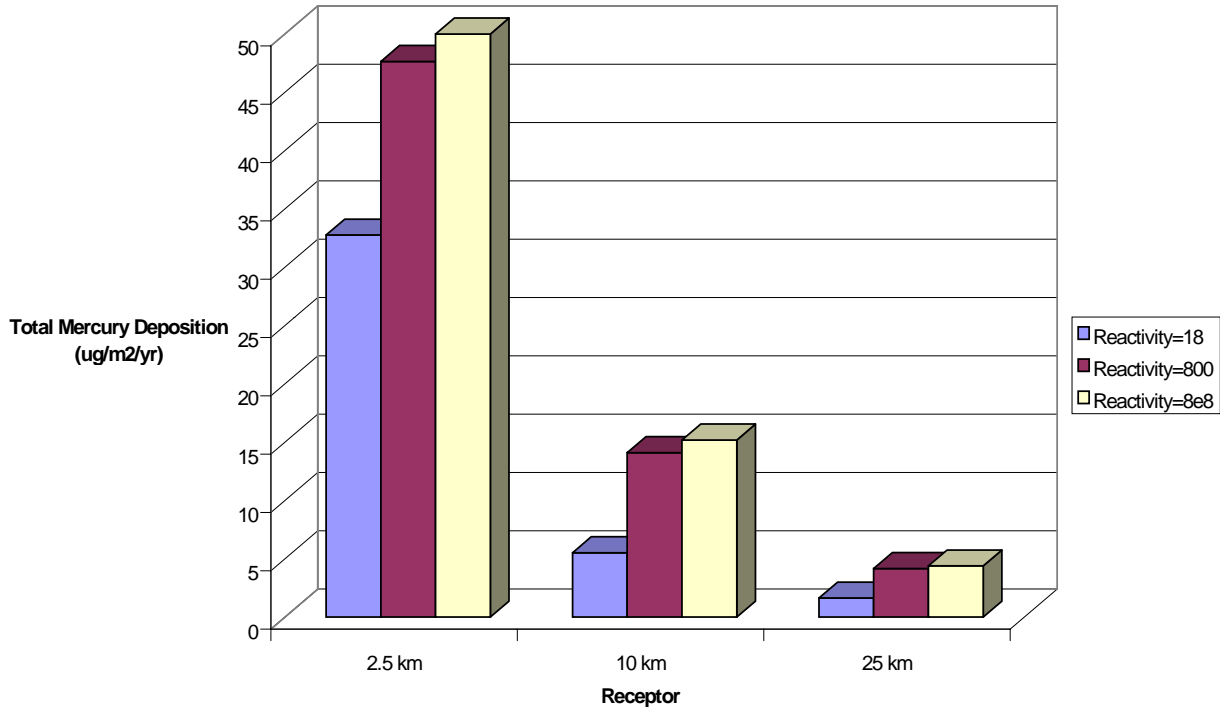
Sensitivity of Dry Deposition of Divalent Mercury to Reactivity

The gas deposition module of the ISC3 model utilizes several parameters to estimate the dry deposition velocity for gases. In this section, the sensitivity of the results to the pollutant reactivity parameter is investigated. The pollutant reactivity is used to estimate the resistance through the vegetative canopy (EPA 1996; page inserts to ISC3 Dispersion Model User's Guide). In particular, this resistance is obtained by scaling the reference resistance for SO₂ by (A_{ref}/A_{poll}), where A_{ref} is the default reference reactivity for SO₂ of 8 (EPA 1996), and A_{poll} is the reactivity for the pollutant of interest. In this analysis, nitric acid has been used as a surrogate for divalent mercury vapor, and for this reason a large value for the reactivity (i.e., a low value for canopy resistance) is assumed. A precise estimate is not available for nitric acid. Previous applications of similar models (e.g., CALPUFF) suggested a default value of 18 for the reactivity for nitric acid, although no references are available to support this value. More recent discussions with the model developers suggested that the reactivity of nitric acid should be considerably higher than 18 in order to reduce the canopy resistance. Based on discussions with the model developers, in the present analysis reactivity of 800 was assumed. This results in average dry deposition velocities of about 3 cm/s for the eastern site.

Figure 5-18 shows the predicted dry deposition assuming different reactivities for divalent mercury vapor. These results indicate that increasing the reactivity higher than 800 will have little effect on the predicted deposition. However, there is a substantial difference between the deposition results using a reactivity of 18 instead 800. Indeed, the predicted dry deposition velocities average about 0.6 cm/s if a reactivity of 18 is assumed.

Figure 5-18

Comparison of Sensitivity of Total Deposition Rate to Divalent Mercury Reactivity



The above sensitivity analysis shows that if more empirical data would show that the pollutant reactivity is 18 or less for divalent mercury vapor, then our use of the number 800 in the present analysis has led to overestimation of mercury deposition by, at most, about a factor of five. An observation in support of the use of a reactivity near 800 is that the average predicted dry deposition velocity for divalent mercury vapor of about 3 cm/s is consistent with the table of values used by RELMAP for coniferous forests.

5.3.4.2 Wet Deposition

In the local impact analysis, wet deposition of particulate mercury is estimated by calculating a scavenging coefficient that depends on particle size and precipitation intensity, while wet deposition of vapor is estimated by converting a washout ratio to a scavenging coefficient. The washout ratio is the ratio of the concentration in surface-level precipitation to the concentration in surface level air (Slinn 1984). Because most facilities are assumed to emit primarily vapor-phase mercury (elemental or divalent), in this section the possible impacts of uncertainty in wet deposition of vapor are briefly discussed.

Due to its higher solubility, divalent mercury is thought to wet deposit at much higher rates than that of elemental mercury vapor. Determination of washout ratios for divalent mercury vapor has precluded by the limitations of current analytical measurement techniques: it has not been possible to obtain measurements of divalent vapor air concentrations, and hence there are no reported values in the peer-reviewed literature. For this reason, the washout ratio used for divalent mercury vapor is based on an assumed similarity between divalent mercury and nitric acid, for which washout ratios are available (Petersen 1995). In particular, a value of 1.6×10^6 is used. Comparisons of concentrations in precipitation calculated using this value agree quite well for nitric acid. However, the applicability of this value for divalent mercury vapor is uncertain, as there may be other processes specific to mercury that would result in a smaller washout ratio.

Because the washout ratio is used to calculate a scavenging coefficient, the effect of the uncertainty in the washout ratio is not strictly linear. A larger washout ratio results in a larger scavenging coefficient, which results in more of the plume being depleted closer to the source. Thus, at larger distances from the source, the predicted wet deposition may be higher using a smaller washout ratio, and the uncertainty in the washout ratio will primarily affect predictions of deposition close to the facility. These predictions are of course the most critical, and at present cannot be validated due to a lack of available measured data near the facilities of concern. In the end, the total deposited within 50 km is actually not sensitive to the washout ratio assumed. This is indicated when the mass balance results for elemental and divalent mercury are compared: the fraction of total elemental mercury emitted that is deposited within 50 km via wet deposition is similar to that for divalent mercury (both at about 6%), despite the fact that the washout ratio for divalent mercury is 10,000 times larger than that for elemental mercury.

5.3.4.3 Sensitivity to Emissions Speciation

For the two municipal waste combustors, two additional emissions speciations were utilized to investigate the sensitivity of the deposition rates to the speciation. These results are summarized in Table 5-19.

Table 5-19
Sensitivity of Total Mercury Deposition Rate to Emissions Speciation for
Municipal Waste Combustors

Mercury Emissions Scenario	% Hg0	% Hg2 Vapor	% Hg2 Particulate	Total Hg Deposition rate at 2.5 km (ug/m ² /yr)	Total Hg Deposition rate at 10 km (ug/m ² /yr)
LMWC_A	30	50	20	46.0	18.1
LMWC_B (used in analyses)	60	30	10	26.7	11.2
LMWC_C	90	10	0	9.46	4.19
SMWC_A	30	50	20	8.15	2.47
SMWC_B (used in analyses)	60	30	10	4.98	1.54
SMWC_C	90	10	0	1.81	0.62

The results are qualitatively similar for both facilities: the predicted total mercury deposition rate is roughly proportional to the fraction of emissions that is assumed to be divalent mercury vapor. This indicates the significance of the assumption regarding emissions speciation for these facilities.

5.3.4.4 Effect of Terrain on Results of Local Scale Modeling

The ISC3 modeling in this report has assumed that the model plants were placed in simple terrain, with the receptors all located at the same elevation as the stack base. In reality, many of these emission sources may actually be located in rolling topography, which may ultimately affect the predicted media concentrations near the facility. In this section a limited analysis of the effect of terrain on the total deposition of mercury is reported.

For this analysis, the ISC3 model was run with receptors located at the following heights: same height as stack base, half the height of the stack, the same height as the stack, and 1.5 times the height of the stack. Analyses were made at 2.5 km, 10.0 km, and 25.0 km northeast of a large municipal waste combustor (variant b, with 60% elemental mercury, 30% divalent mercury vapor, and 10% divalent mercury in particulates) located at the eastern site. The direction of maximum deposition for this site is northeast of the plant, and the stack height for this model plant is 70.104 meters. At each receptor location (three distances and four elevations), the total depositions were combined for elemental mercury and for divalent mercury both in the vapor and particulate forms. It is important to realize that the total depositions evaluated in this analysis included both wet and dry depositions. Table 5-20 shows the extent of the increase observed in total deposition with increase in elevation at each of the 3 distances from the stack. This table shows the dimensionless ratio of the predicted value at a given height and the predicted value for a receptor at the same elevation as the stack base. The value for height of 0, yielding a ratio of 1.0, is included to make the meaning of the ratio explicitly clear.

Table 5-20
Ratios of Total Deposition of Mercury at Receptors at Different Elevations
to Total Deposition when the Elevation is Zero

Elevation of receptor in meters	Calculated for the following three distances		
	2.5 km from stack	10.0 km from stack	25.0 km from stack
0	1.00	1.00	1.00
35.052 (i.e. half stack height)	1.48	1.26	1.13
70.104 (i.e., stack height)	1.81	1.47	1.27
105.156 (i.e., 1.5 x stack height)	2.79	1.72	1.36

At 25 km, the difference as a function of receptor height is not as extreme because more dispersion has occurred: the vertical change in air concentrations is not as great as it is for closer receptors, thereby resulting in less deposition. The maximum increase noted, which is at 2.5 km, is less than three fold.

6. WATERSHED FATE AND TRANSPORT MODELING

6.1 Overview

The purpose of this section is to present the summary results for the watershed fate and transport modeling. In section 6.2 the watershed results are summarized for the pre-anthropogenic and current condition periods. The results of the latter analysis are used as the initial conditions for evaluating the potential impact of the model plants considered in this report that emit mercury. In section 6.3, selected watershed/waterbody output are presented for all model plants. In section 6.4, the results of sensitivity analyses conducted with the IEM-2M model are discussed.

6.2 Watershed and Waterbody Results for Pre-Anthropogenic Mercury Cycle and the Current Mercury Cycle

Mercury has always been an environmental constituent. Table 6-1 compares pre-anthropogenic and current cycle values for average air concentrations and average annual deposition rates for the hypothetical Eastern and Western U.S. Table 6-2 lists predicted total mercury concentrations in the watershed soils, grain, the water column, and trophic level 4 fish for both sites. Predicted concentrations at the eastern site are higher than those in the West. This is the result of higher estimated deposition rates due to differences in annual precipitation rates. Over 90% of the total mercury in grain and soils is predicted to be the inorganic divalent species. Over 80% of the total mercury in the water column is predicted to be inorganic divalent. All of the mercury in trophic level 4 fish is methylated.

The predictions of the IEM-2M model for the pre-anthropogenic mercury cycle were used as inputs to the current cycle. Table 6-3 lists the results for the current cycle. These values were used as inputs to the Local Scale Analysis. The predictions for the western site are much lower than those for the eastern site.

Table 6-1
Assumed Mercury Air Concentrations and Atmospheric Deposition Rates for Pre-Anthropogenic and Current Conditions

Period	Eastern Site		Western Site	
	Air Concentration ng/m ³	Annual Deposition Rate µg/m ² /yr	Air Concentration ng/m ³	Annual Deposition Rate µg/m ² /yr
pre- Anthropogenic	0.5	3	0.5	1
Current Cycle	1.6	10	1.6	2

Table 6-2
Total Mercury Concentrations Predicted by IEM-2M Model for the
Pre-Anthropogenic Time Period

Media	Eastern Site	Western Site
watershed soils (ng/g)	14	4
grain (ng/g)	0.6	0.5
Dissolved water column(ng/L)	0.3	0.1
Trophic level 4 fish ppm	0.13	0.04

Table 6-3
Total Mercury Concentrations Predicted by IEM-2M Model for the Current
(Post-Industrial) Time Period

Media	Eastern Site	Western Site
watershed soils (ng/g)	47	8
grain (ng/g)	2	1.6
Dissolved water column(ng/L)	0.9	0.2
Trophic level 4 fish ppm	0.44	0.09

6.3 Watershed/Waterbody Model Results for Local Scale Analysis

Tables 6-4 through 6-7 show selected results for all facilities at both sites, using both the RELMAP 50th and 90th percentiles. The columns labeled “background” represent the fraction of the total value that were predicted prior to modeling the facility. For example, for the eastern site the total predicted watershed soil concentration assumed before the facility was modeled was 47 ng/g (see Table 6-3 above). When the facility and RELMAP are modeled for an additional 30 years, the predicted soil concentration at 2.5 km is 102 ng/g; the “percent background” is 46 percent. Similarly, the “percent RELMAP” is the ratio of the value predicted using RELMAP for 30 years without the facility, with the total value (using the same initial conditions; i.e., Table 6-3). The “percent ISC” is the remaining fraction.

For all facilities, the contribution of the local source decreases as the distance from the facility increases. With the exception of the chlor-alkali plant, the facilities are generally predicted to contribute less than 50% to the total watershed soil concentration, with regional anthropogenic sources contributing up to 15% for the RELMAP 50th percentiles and up to 60% for the RELMAP 90th percentiles.

The results for the methylmercury water concentrations and trophic level 4 fish concentrations show a slightly higher contribution from the local sources. While the fractions are similar to those for

watershed soil since the watershed serves as a mercury source for the waterbody, these values are slightly higher due to the direct deposition onto the waterbody.

The predicted fruit, leafy vegetable, and beef concentrations are generally dominated by the background values. For plants, these products are assumed to take up most of the mercury from the air, and therefore the local source usually does not impact the local air concentrations significantly. The exception is the chlor-alkali plant for which the low stack results in higher mercury air concentrations. The results for the beef concentrations are similar; however, there is a slightly higher contribution from the local source because the cattle are exposed through the ingestion of soil.

Table 6-5
Predicted Values for Eastern Site (Local + RELMAP 90th)

	Watershed	Soil Concentration (ng/g)	%Background	%RelMap	%ISC	MHg Dissolved Water Conc.(ng/l)	Tier 4 Fish MHg Concentration (ug/g)	%Background	%RelMap	%ISC	Total Hg Fruit Concentration (ng/g)	%Background	%RelMap	%ISC	Total Hg Leafy Vegetable Concentration (ng/g)	%Background	%RelMap	%ISC	Total Hg Beef Concentration (ng/g)	%Background	%RelMap	%ISC
Variant b:Large Municipal Waste Combustor	2.5 km	1.2E+02	38%	24%	38%	2.0E-01	1.4E+00	32%	23%	45%	3.6E+01	89%	7%	4%	3.5E+01	88%	7%	4%	9.0E+00	82%	9%	9%
	10 km	9.5E+01	49%	31%	20%	1.5E-01	9.9E-01	44%	32%	23%	3.6E+01	90%	7%	3%	3.5E+01	90%	7%	3%	8.7E+00	86%	10%	5%
	25 km	8.3E+01	56%	35%	8%	1.2E-01	8.4E-01	52%	38%	9%	3.5E+01	91%	7%	1%	3.4E+01	91%	7%	2%	8.4E+00	88%	10%	2%
Variant b:Small Municipal Waste Combustor	2.5 km	8.5E+01	55%	35%	10%	1.3E-01	8.8E-01	50%	36%	13%	3.5E+01	92%	7%	1%	3.4E+01	91%	7%	1%	8.4E+00	88%	10%	2%
	10 km	7.9E+01	59%	37%	3%	1.2E-01	8.0E-01	55%	40%	4%	3.5E+01	92%	7%	1%	3.4E+01	92%	8%	1%	8.3E+00	89%	10%	1%
	25 km	7.7E+01	61%	38%	1%	1.1E-01	7.7E-01	57%	42%	1%	3.5E+01	93%	7%	0%	3.4E+01	92%	8%	0%	8.3E+00	90%	10%	0%
Large Commercial HMI	2.5 km	8.4E+01	55%	35%	9%	1.3E-01	8.9E-01	50%	36%	14%	3.5E+01	92%	7%	1%	3.4E+01	91%	7%	1%	8.4E+00	88%	10%	2%
	10 km	7.7E+01	60%	38%	2%	1.1E-01	7.8E-01	57%	41%	2%	3.5E+01	93%	7%	0%	3.4E+01	92%	8%	0%	8.3E+00	90%	10%	0%
	25 km	7.7E+01	61%	39%	0%	1.1E-01	7.7E-01	58%	42%	0%	3.5E+01	93%	7%	0%	3.4E+01	92%	8%	0%	8.3E+00	90%	10%	0%
Large Hospital HMI	2.5 km	1.3E+02	37%	23%	40%	2.3E-01	1.5E+00	29%	21%	51%	3.6E+01	89%	7%	4%	3.5E+01	88%	7%	5%	9.1E+00	82%	9%	9%
	10 km	8.5E+01	55%	35%	10%	1.3E-01	8.8E-01	50%	37%	13%	3.5E+01	92%	7%	1%	3.4E+01	91%	7%	1%	8.4E+00	88%	10%	2%
	25 km	7.8E+01	60%	38%	3%	1.2E-01	7.9E-01	56%	41%	3%	3.5E+01	92%	7%	0%	3.4E+01	92%	8%	0%	8.3E+00	89%	10%	1%
Small Hospital HMI	2.5 km	8.0E+01	59%	37%	4%	1.2E-01	8.2E-01	54%	39%	7%	3.5E+01	92%	7%	0%	3.4E+01	92%	8%	0%	8.3E+00	89%	10%	1%
	10 km	7.7E+01	61%	38%	1%	1.1E-01	7.7E-01	57%	42%	1%	3.5E+01	93%	7%	0%	3.4E+01	92%	8%	0%	8.3E+00	90%	10%	0%
	25 km	7.6E+01	61%	39%	0%	1.1E-01	7.6E-01	58%	42%	0%	3.5E+01	93%	7%	0%	3.4E+01	92%	8%	0%	8.3E+00	90%	10%	0%
Large Hospital HMI (wet scrubber)	2.5 km	7.8E+01	60%	38%	2%	1.2E-01	7.9E-01	56%	41%	3%	3.5E+01	93%	7%	0%	3.4E+01	92%	8%	0%	8.3E+00	90%	10%	0%
	10 km	7.6E+01	61%	39%	0%	1.1E-01	7.7E-01	58%	42%	0%	3.5E+01	93%	7%	0%	3.4E+01	92%	8%	0%	8.3E+00	90%	10%	0%
	25 km	7.6E+01	61%	39%	0%	1.1E-01	7.6E-01	58%	42%	0%	3.5E+01	93%	7%	0%	3.4E+01	92%	8%	0%	8.3E+00	90%	10%	0%
Small Hospital HMI (wet scrubber)	2.5 km	7.6E+01	61%	39%	0%	1.1E-01	7.6E-01	58%	42%	0%	3.5E+01	93%	7%	0%	3.4E+01	92%	8%	0%	8.3E+00	90%	10%	0%
	10 km	7.6E+01	61%	39%	0%	1.1E-01	7.6E-01	58%	42%	0%	3.5E+01	93%	7%	0%	3.4E+01	92%	8%	0%	8.3E+00	90%	10%	0%
	25 km	7.6E+01	61%	39%	0%	1.1E-01	7.6E-01	58%	42%	0%	3.5E+01	93%	7%	0%	3.4E+01	92%	8%	0%	8.3E+00	90%	10%	0%
Large Coal-fired Utility Boiler	2.5 km	1.0E+02	45%	29%	26%	1.7E-01	1.1E+00	38%	28%	34%	3.5E+01	92%	7%	0%	3.4E+01	92%	7%	1%	8.6E+00	87%	10%	3%
	10 km	8.1E+01	57%	36%	6%	1.2E-01	8.2E-01	54%	39%	7%	3.5E+01	93%	7%	0%	3.4E+01	92%	8%	0%	8.3E+00	89%	10%	1%
	25 km	7.8E+01	60%	38%	2%	1.2E-01	7.8E-01	56%	41%	3%	3.5E+01	93%	7%	0%	3.4E+01	92%	8%	0%	8.3E+00	90%	10%	0%
Medium Coal-fired Utility Boiler	2.5 km	8.8E+01	53%	34%	13%	1.4E-01	9.3E-01	48%	35%	18%	3.5E+01	92%	7%	0%	3.4E+01	92%	8%	0%	8.4E+00	88%	10%	2%
	10 km	7.9E+01	59%	37%	4%	1.2E-01	8.0E-01	55%	40%	5%	3.5E+01	93%	7%	0%	3.4E+01	92%	8%	0%	8.3E+00	89%	10%	1%
	25 km	7.8E+01	60%	38%	2%	1.1E-01	7.8E-01	57%	41%	2%	3.5E+01	93%	7%	0%	3.4E+01	92%	8%	0%	8.3E+00	90%	10%	0%
Small Coal-fired Utility Boiler	2.5 km	7.9E+01	59%	37%	3%	1.2E-01	8.0E-01	55%	40%	5%	3.5E+01	93%	7%	0%	3.4E+01	92%	8%	0%	8.3E+00	89%	10%	1%
	10 km	7.7E+01	60%	38%	1%	1.1E-01	7.8E-01	57%	41%	2%	3.5E+01	93%	7%	0%	3.4E+01	92%	8%	0%	8.3E+00	90%	10%	0%
	25 km	7.7E+01	61%	39%	0%	1.1E-01	7.7E-01	58%	42%	1%	3.5E+01	93%	7%	0%	3.4E+01	92%	8%	0%	8.3E+00	90%	10%	0%
Medium Oil-fired Utility Boiler	2.5 km	7.7E+01	61%	39%	0%	1.1E-01	7.7E-01	58%	42%	1%	3.5E+01	93%	7%	0%	3.4E+01	92%	8%	0%	8.3E+00	90%	10%	0%
	10 km	7.6E+01	61%	39%	0%	1.1E-01	7.6E-01	58%	42%	0%	3.5E+01	93%	7%	0%	3.4E+01	92%	8%	0%	8.3E+00	90%	10%	0%
	25 km	7.6E+01	61%	39%	0%	1.1E-01	7.6E-01	58%	42%	0%	3.5E+01	93%	7%	0%	3.4E+01	92%	8%	0%	8.3E+00	90%	10%	0%
Chlor-alkali plant	2.5 km	4.8E+02	10%	6%	84%	1.0E+00	7.1E+00	6%	5%	89%	8.2E+01	39%	3%	58%	8.3E+01	38%	3%	59%	2.3E+01	32%	4%	64%
	10 km	1.3E+02	36%	23%	41%	2.1E-01	1.4E+00	31%	22%	47%	4.4E+01	73%	6%	21%	4.3E+01	72%	6%	22%	1.1E+01	68%	8%	24%
	25 km	9.0E+01	52%	33%	15%	1.4E-01	9.2E-01	48%	35%	17%	3.7E+01	86%	7%	8%	3.6E+01	85%	7%	8%	9.0E+00	82%	9%	9%

**Table 6-6
Predicted Values for Western Site (Local + RELMAP 50th)**

				Watershed Soil Concentration (ng/g)	%Background	%RelMap	%ISC	MHg Dissolved Water Conc.(ng/l)	Tier 4 Fish MHg Concentration (ug/g)	%Background	%RelMap	%ISC	Total Hg Fruit Concentration (ng/g)	%Background	%RelMap	%ISC	Total Hg Leafy Vegetable Concentration (ng/g)	%Background	%RelMap	%ISC	Total Hg Beef Concentration (ng/g)	%Background	%RelMap	%ISC
Variant b:Large Combustor	Municipal Waste	2.5 km	10 km	3.8E+01	20%	1%	79%	8.8E-02	6.0E-01	15%	1%	84%	3.3E+01	96%	1%	3%	3.2E+01	96%	1%	3%	7.7E+00	92%	1%	7%
				2.3E+01	33%	2%	65%	5.5E-02	3.7E-01	24%	2%	74%	3.2E+01	97%	1%	2%	3.2E+01	97%	1%	2%	7.5E+00	95%	1%	4%
				1.3E+01	56%	4%	40%	2.7E-02	1.9E-01	48%	4%	48%	3.2E+01	98%	1%	1%	3.2E+01	98%	1%	1%	7.3E+00	97%	1%	2%
Variant b:Small Combustor	Municipal Waste	2.5 km	10 km	1.4E+01	53%	4%	44%	3.3E-02	2.3E-01	40%	3%	57%	3.2E+01	98%	1%	1%	3.2E+01	98%	1%	1%	7.3E+00	97%	1%	2%
				9.9E+00	76%	5%	18%	1.9E-02	1.3E-01	68%	6%	26%	3.2E+01	99%	1%	0%	3.1E+01	99%	1%	0%	7.2E+00	98%	1%	1%
				8.6E+00	87%	6%	6%	1.6E-02	1.1E-01	84%	7%	9%	3.2E+01	99%	1%	0%	3.1E+01	99%	1%	0%	7.2E+00	99%	1%	0%
Large Commercial HMI		2.5 km	10 km	1.4E+01	53%	4%	43%	3.4E-02	2.3E-01	39%	3%	58%	3.2E+01	98%	1%	1%	3.2E+01	98%	1%	1%	7.3E+00	97%	1%	2%
				8.9E+00	85%	6%	9%	1.7E-02	1.1E-01	80%	7%	14%	3.2E+01	99%	1%	0%	3.1E+01	99%	1%	0%	7.2E+00	99%	1%	0%
				8.3E+00	91%	6%	2%	1.5E-02	1.0E-01	89%	8%	3%	3.2E+01	99%	1%	0%	3.1E+01	99%	1%	0%	7.2E+00	99%	1%	0%
Large Hospital HMI		2.5 km	10 km	4.8E+01	16%	1%	83%	1.4E-01	9.6E-01	9%	1%	90%	3.3E+01	96%	1%	3%	3.3E+01	95%	1%	4%	7.8E+00	91%	1%	8%
				1.4E+01	54%	4%	42%	3.1E-02	2.1E-01	42%	4%	54%	3.2E+01	98%	1%	1%	3.2E+01	98%	1%	1%	7.3E+00	97%	1%	2%
				9.6E+00	79%	5%	16%	1.8E-02	1.2E-01	73%	6%	20%	3.2E+01	99%	1%	0%	3.1E+01	99%	1%	0%	7.2E+00	98%	1%	0%
Small Hospital HMI		2.5 km	10 km	1.1E+01	71%	5%	24%	2.3E-02	1.5E-01	58%	5%	37%	3.2E+01	99%	1%	0%	3.1E+01	99%	1%	0%	7.2E+00	98%	1%	1%
				8.4E+00	90%	6%	4%	1.5E-02	1.0E-01	87%	7%	6%	3.2E+01	99%	1%	0%	3.1E+01	99%	1%	0%	7.2E+00	99%	1%	0%
				8.2E+00	93%	6%	1%	1.4E-02	9.8E-02	91%	8%	1%	3.2E+01	99%	1%	0%	3.1E+01	99%	1%	0%	7.2E+00	99%	1%	0%
Large Hospital HMI (wet scrubber)		2.5 km	10 km	9.2E+00	82%	6%	12%	1.8E-02	1.2E-01	73%	6%	20%	3.2E+01	99%	1%	0%	3.1E+01	99%	1%	0%	7.2E+00	99%	1%	0%
				8.2E+00	92%	6%	2%	1.5E-02	1.0E-01	90%	8%	3%	3.2E+01	99%	1%	0%	3.1E+01	99%	1%	0%	7.2E+00	99%	1%	0%
				8.1E+00	93%	6%	0%	1.4E-02	9.8E-02	92%	8%	1%	3.2E+01	99%	1%	0%	3.1E+01	99%	1%	0%	7.2E+00	99%	1%	0%
Small Hospital HMI (wet scrubber)		2.5 km	10 km	8.2E+00	93%	6%	1%	1.5E-02	9.9E-02	91%	8%	2%	3.2E+01	99%	1%	0%	3.1E+01	99%	1%	0%	7.2E+00	99%	1%	0%
				8.1E+00	93%	6%	0%	1.4E-02	9.7E-02	92%	8%	0%	3.2E+01	99%	1%	0%	3.1E+01	99%	1%	0%	7.2E+00	99%	1%	0%
				8.1E+00	94%	6%	0%	1.4E-02	9.7E-02	92%	8%	0%	3.2E+01	99%	1%	0%	3.1E+01	99%	1%	0%	7.2E+00	99%	1%	0%
Large Coal-fired Utility Boiler		2.5 km	10 km	1.4E+01	55%	4%	42%	3.1E-02	2.1E-01	43%	4%	53%	3.2E+01	99%	1%	0%	3.1E+01	99%	1%	0%	7.2E+00	98%	1%	1%
				9.9E+00	76%	5%	19%	1.9E-02	1.3E-01	70%	6%	24%	3.2E+01	99%	1%	0%	3.1E+01	99%	1%	0%	7.2E+00	99%	1%	0%
				9.8E+00	78%	5%	17%	1.8E-02	1.2E-01	73%	6%	21%	3.2E+01	99%	1%	0%	3.1E+01	99%	1%	0%	7.2E+00	99%	1%	0%
Medium Coal-fired Utility Boiler		2.5 km	10 km	1.1E+01	66%	5%	29%	2.3E-02	1.5E-01	58%	5%	37%	3.2E+01	99%	1%	0%	3.1E+01	99%	1%	0%	7.2E+00	98%	1%	1%
				1.0E+01	73%	5%	22%	2.0E-02	1.4E-01	66%	6%	28%	3.2E+01	99%	1%	0%	3.1E+01	99%	1%	0%	7.2E+00	98%	1%	1%
				9.5E+00	79%	5%	15%	1.8E-02	1.2E-01	74%	6%	19%	3.2E+01	99%	1%	0%	3.1E+01	99%	1%	0%	7.2E+00	99%	1%	0%
Small Coal-fired Utility Boiler		2.5 km	10 km	9.8E+00	77%	5%	18%	1.9E-02	1.3E-01	70%	6%	24%	3.2E+01	99%	1%	0%	3.1E+01	99%	1%	0%	7.2E+00	99%	1%	0%
				8.8E+00	86%	6%	8%	1.6E-02	1.1E-01	81%	7%	13%	3.2E+01	99%	1%	0%	3.1E+01	99%	1%	0%	7.2E+00	99%	1%	0%
				8.3E+00	91%	6%	3%	1.5E-02	1.0E-01	88%	7%	4%	3.2E+01	99%	1%	0%	3.1E+01	99%	1%	0%	7.2E+00	99%	1%	0%
Medium Oil-fired Utility Boiler		2.5 km	10 km	8.2E+00	92%	6%	2%	1.5E-02	1.0E-01	90%	8%	2%	3.2E+01	99%	1%	0%	3.1E+01	99%	1%	0%	7.2E+00	99%	1%	0%
				8.2E+00	92%	6%	1%	1.5E-02	9.9E-02	91%	8%	2%	3.2E+01	99%	1%	0%	3.1E+01	99%	1%	0%	7.2E+00	99%	1%	0%
				8.1E+00	93%	6%	1%	1.4E-02	9.8E-02	92%	8%	1%	3.2E+01	99%	1%	0%	3.1E+01	99%	1%	0%	7.2E+00	99%	1%	0%
Chlor-alkali plant		2.5 km	10 km	3.2E+02	2%	0%	97%	1.0E+00	6.9E+00	1%	0%	99%	7.2E+01	44%	0%	56%	7.3E+01	43%	0%	57%	1.9E+01	36%	0%	63%
				4.5E+01	17%	1%	82%	1.2E-01	8.0E-01	11%	1%	88%	3.8E+01	83%	1%	16%	3.8E+01	82%	1%	17%	8.9E+00	79%	1%	20%
				1.8E+01	43%	3%	54%	3.7E-02	2.5E-01	36%	3%	61%	3.4E+01	93%	1%	6%	3.3E+01	93%	1%	6%	7.7E+00	92%	1%	7%

6.4 Variability and Sensitivity Analysis

The main thrust of this chapter has been to establish a plausible link between mercury emissions and mercury concentrations in soil, surface water bodies, and fish. It is well established, however, that watershed and water body characteristics significantly influence these concentrations as well. Several reports document variability among water bodies within a region in which atmospheric deposition is presumably constant (Watras, et al., 1995, Schofield, et al., 1994, Verta and Matilainen, 1995, Hurley et al., 1995, St. Louis et al., 1996).

To explore the effects of watershed and water body characteristics on mercury levels, a series of model variability and sensitivity analyses were performed. Variability analyses were used to determine an expected range of mercury concentrations in soil, water, and fish due to a reasonable range of watershed or water body characteristics. These analyses presented the opportunity to benchmark the IEM-2M water body module against the independently-derived R-MCM (Harris, et al., 1996), which is described below. Calculated input and output from the two models are compared in several tables. This exercise provides a degree of model verification testing for IEM-2M.

Sensitivity analyses were conducted to better understand the importance of various model parameters. First, a representative base simulation was run and calculated concentrations were noted. Next, a series of sensitivity simulations were run, each with a single model parameter increased or decreased by 50%. The resulting changes in calculated concentrations were noted. The model sensitivity to a parameter change is defined as the relative change in the mercury concentration divided by the relative change in the parameter value, and is expressed as a percentage:

$$\Delta(x,p) = 100 \cdot \frac{\left(\frac{X_{\delta p} - X_B}{X_B} \right)}{\left(\frac{p_{\delta} - p_B}{p_B} \right)}$$

where:

$\Delta(x,p)$	=	sensitivity of model output “x” to parameter “p” (percent)
x	=	model output of interest, such as total water column mercury concentration
p	=	model parameter being varied
X_B	=	calculated value of model output in base simulation
$X_{\delta p}$	=	calculated value of model output for a change in parameter “p”
p_B	=	model parameter value in base simulation
p_{δ}	=	model parameter value in sensitivity simulation

The calculated concentrations of interest are the total mercury concentration in soil, the total mercury concentration in the water column, and the predatory (trophic level 4) fish concentration. Model sensitivity results are summarized in tables, in which model parameters are presented in the order of their sensitivity and grouped into four categories: extra strongly sensitive (> 100%), strongly sensitive (50% - 99%), moderately sensitive (25% - 49%), and weakly sensitive (<25%).

6.4.1 Variability and Parameter Sensitivity Analysis for IEM-2M

6.4.1.1 Description of Base Simulation and Analysis of Variability

The IEM-2M is set up to represent a shallow drainage lake and its adjoining watershed. For the model sensitivity analysis, we used the environmental parameters for the eastern lake scenario, as summarized in Table 6-8. The atmospheric deposition flux of $10 \mu\text{g}/\text{m}^2\text{-yr}$ represents a typical preindustrial loading. Because the model is linear with respect to loading, the choice of atmospheric deposition does not affect the analysis of model sensitivity.

For the model parameters shown, IEM-2M predicts a steady-state total soil concentration of 46.8 ng/g. The total water column concentration is 1.16 ng/L, 7% of which is methyl mercury. Concentrations in prey and predator fish are 100 and 440 ng/g, respectively.

Several sets of model simulations were conducted to explore how variable watershed characteristics affect mercury concentrations in the lake. Three major watershed characteristics are expected to influence mercury levels: watershed size, watershed erosion potential, and soil mercury retention.

Variability due to watershed size -- In the first set of simulations, watershed size was varied from 10% of the lake surface area to 50 times the lake surface area ($0.25 - 125 \text{ km}^2$). The sediment delivery ratio was adjusted for watershed size following the Vanoni (1975) relationship as presented in Mills et al. (1985). Results are summarized in Table 6-9.

As watershed size increases by a factor of 500, average soil concentrations increase by a factor of 2 because smaller sediment delivery ratios from larger surface areas yield lower net erosion loss rates from the watershed. Similarly, while erosion loads of mercury from the watershed increase by a factor of 500, water body concentrations increase by a factor of just over 2. This is because the increased load of solids to the water body causes increased settling and burial loss of mercury from the water body. Furthermore, the higher solids levels cause lower dissolved MHg fractions and thus lower bioavailability of the mercury. Consequently, fish levels increase by less than a factor of 2. Large variations in watershed size, then, should cause small but significant variations in water body mercury levels.

**Table 6-8
General Properties of the IEM-2M Eastern Lake**

Water Body	
Volume	$1.245 \times 10^7 \text{ m}^3$
Surface Area	$2.49 \times 10^6 \text{ m}^2$
Average Depth	5 m
Advective Flow	$0.46 \text{ m}^3/\text{sec}$
Upper Sediment Depth	0.02 m
Solids Density	1.5 g/mL
Benthic Porosity	0.95
Primary Productivity	$100 \text{ mg-C/m}^2\text{-day}$
Biotic Solids Settling Velocity	0.2 m/day
Abiotic Solids Settling Velocity	2 m/day
Biotic Solids Concentration (calculated)	0.7 mg/L
Abiotic Solids Concentration (calculated)	1.2 mg/L
Watershed	
Atmospheric Deposition	$10 \mu\text{g/m}^2\text{-yr}$
Watershed Area	$3.74 \times 10^7 \text{ m}^2$
Watershed Soil Depth	0.01 m
Soil Dry Density	1.4 g/mL
Soil Moisture Content	0.1
Precipitation	0.8 m/yr
Runoff	0.18 m/yr
Erosivity Factor (R)	200 yr^{-1}
Erodibility Factor (K)	0.3 tons/acre
Topographic Factor (LS)	2.5
Cover Management Factor (C)	0.006
Sediment Delivery Ratio	0.2
Enrichment Ratio	2

Table 6-9
Effect of Watershed Size on Total Mercury Concentrations

Watershed Size, km²:	0.25	2.5	12.5	37.3	124.5
Sediment Delivery Ratio:	0.5	0.3	0.22	0.18	0.12
Soil, ng/g	30	39	45	49	55
Water Column, ng/L	0.65	0.73	0.95	1.18	1.55
Sediment, ng/g	51	57	72	86	106
Predatory Fish, ng/g	330	360	430	460	460

Variability due to watershed erosion -- Watershed erosion is the major pathway of mercury transport from soil to water body. IEM-2M calculates soil erosion using the Universal Soil Loss Equations (USLE), in which:

$$X_e = 1.29 \cdot (R \cdot 1.735) \cdot K \cdot LS \cdot C$$

where:

X_e	=	soil erosion (tonnes/ha-yr)
R	=	rainfall erosivity index (yr ⁻¹)
K	=	soil erosivity factor (tonnes/ha)
LS	=	topographic (slope-length) factor
C	=	cover-management factor
1.29	=	units conversion factor
1.735	=	units conversion factor for R

The default values for these parameters used in the IEM-2M eastern lake give a soil erosion value of 1.2 tonnes/ha-yr. To explore the feasible range of values for X_e , five diverse watershed types were defined:

A: Northern (R=100), sand (K=0.05), moderate slope (slope-length=3%-500 m, LS=0.66), undisturbed forest (75% cover, C=0.001); $X_e = 0.0074$ tonnes/ha-yr.

B: Mideastern (R=175), sandy loam (K=0.24), hilly (slope-length=10%-100 m, LS=1.17), undisturbed forest (75% cover, C=0.001); $X_e = 0.11$ tonnes/ha-yr.

C: Western (R=20), fine sand (K=0.16), moderate slope (slope-length=3%-500 m, LS=0.66), brush and weeds (20% cover, C=0.2); $X_e = 0.95$ tonnes/ha-yr.

D: Southeastern (R=350), clay loam (K=0.25), hilly (slope-length=10%-100 m, LS=2.47), trees, brush, and grass (80% cover, C=0.013); $X_e = 6.3$ tonnes/ha-yr.

E: Midwestern (R=175), silty loam (K=0.42), moderate slope (slope-length=3%-500 m, LS=0.66), row crops (C=0.4); $X_e = 43$ tonnes/ha-yr.

These watershed erosion characteristics were specified for the standard 12.43 km² watershed. Calculated mercury concentrations are presented in Table 6-10.

Table 6-10
Effect of Watershed Erosion on Total Mercury Concentrations

Watershed (see text):	A	B	C	D	E
Erosion Loss, tonnes/ha:	0.0072	0.11	0.95	6.3	43
Soil, ng/g	75	72	58	26	5
Water Column, ng/L	0.87	1.00	1.24	0.81	0.36
Sediment, ng/g	69	78	93	52	11
Predatory Fish, ng/g	450	510	560	190	20

As watershed erosion increases by a factor of 100 between watershed A and C, soil mercury concentrations decline only slightly. In this range, losses from soil due to reduction and volatilization are more important than losses due to erosion. Water body and fish concentrations increase slightly in response to the large loading increase. The large increases in mercury loading are partially counterbalanced by increases in settling and burial loss. As erosion losses increase by a factor of 50 between watershed C and E, soil concentrations decline by a factor of 10. In this range, mercury losses from soil due to erosion become important relative to the reduction and volatilization loss. In response to declining soil levels, water column concentrations decline by a factor of 4. Fish concentrations decline by a factor of 25 due to the lower water concentrations and the markedly lower bioavailable dissolved fraction. Variability in watershed erosion characteristics, then, is expected to cause significant variability in water body mercury levels, particularly for more disturbed watersheds with high levels of erosion.

Variability due to soil mercury retention -- Soil mercury retention in a watershed depends upon several transport and transformation processes, some of which are not well understood. The IEM-2M includes simple algorithms for leaching, runoff, and volatilization, which is driven by reduction of HgII. Erosion carries soil solids and associated mercury away from the watershed. Leaching and runoff losses of mercury are small because of its strong partitioning to solids. The soil partition coefficient itself is a relatively insensitive parameter. Changes in its value do not significantly affect the absolute amount of mercury lost from the upper soil layer.

Soil retention of mercury in IEM-2M, then, is controlled by reduction, which is formulated as a first-order reaction in the upper 5 mm that is proportional to soil water content, as described in Appendix B. Rate constants characterizing a forest and a field, derived from data presented in Carpi and Lindberg (1997) and Lindberg (1996), are 1×10^{-4} and 1.3×10^{-3} L/L_w-day, respectively. A value of 5×10^{-4} L/L_w-day was selected for the base IEM-2M simulations. To examine the water body response to variable soil

mercury retention, reduction rate constants were varied from 5×10^{-5} to 5×10^{-3} L/L_w-day. Resulting mercury concentrations are summarized in Table 6-11.

Table 6-11
Effect of Soil Mercury Retention on Total Mercury Concentrations

Reduction Rate Constant (day⁻¹):	0.00001	0.00025	0.0005	0.0025	0.005
Soil, ng/g	99	66	47	14	8
Water Column, ng/L	2.25	1.56	1.16	0.47	0.33
Sediment, ng/g	164	114	84	34	24
Predatory Fish, ng/g	880	600	440	170	110

As reduction rates increase 2 orders of magnitude, soil concentrations decrease by a factor of 10 and water body concentrations decrease by a factor of 8. Soil retention of mercury, then, is an uncertain component of watershed variability that could cause large variations in mercury response.

6.4.1.2 Sensitivity of Soil Mercury to Model Parameters

The relative sensitivity of mercury concentrations in the upper soil layer to the model parameters is summarized in Table 6-12. Total soil mercury is strongly sensitive to **total atmospheric deposition**. In these simulations, wetfall and dryfall are not separated. Increases in loading lead to increases in total mercury concentrations.

The main loss pathway for soil mercury is volatilization of Hg⁰, which is controlled by the HgII reduction rate. This rate is proportional to the **soil reduction rate constant** and the **soil moisture content**, which are both strongly sensitive parameters. Increases in the rate constant or soil moisture lead to strongly-increased loss rates and lower soil concentrations.

Soil erosion is another significant loss pathway for soil mercury. Several model parameters contribute to the calculation of bulk erosion, including **rainfall erosivity**, **soil erodibility**, the **topographic factor**, the **cover factor**, and the **sediment delivery ratio**. The **enrichment ratio** contributes to the calculation of mercury concentrations on eroded soil. Increases in these parameters lead to moderately-increased loss rates and lower soil concentrations. The soil-water partition coefficient also contributes to the calculation of mercury concentrations on eroded soil. Its value is high enough, however, so that increases or decreases lead to only slightly higher or lower particulate soil concentrations.

Mercury loss from runoff and leaching is relatively insignificant. For this reason, model parameters related to these processes, such as **runoff curve number**, are not sensitive. On the other hand, the exchange of gas phase Hg⁰ is relatively rapid. Moderate changes in model parameters contributing to this process, such as **soil void fraction** and **atmospheric diffusivity**, are insensitive.

Table 6-12
IEM-2M Parameter Sensitivity* for Total Soil Mercury

Model Parameter	Eastern Lake	
	decrease	increase
Total Atmospheric Deposition	-100	+100
Soil Water Content	+82	-74
Soil Reduction Rate Constant	+82	-45
Soil Enrichment Ratio	+46	-32
Soil Erosion Factors**	+46	-32
Soil Water Partition Coefficient	- 8	+3
Soil Demethylation Rate Constant	+2	- 1
Soil Methylation Rate Constant	0	0
Runoff Curve Number	0	0
Soil Void Fraction	0	0
Atmospheric Diffusivity	0	0

* Sensitivity is expressed as relative change in total water column mercury concentration divided by the relative change in the model parameter, in percent.

** Erosion factors include rainfall erosivity, soil erodibility, the topographic factor, the cover factor, and the sediment delivery ratio

6.4.1.3 Sensitivity of Water Column Mercury to Model Parameters

The sensitivity of total mercury concentration in the water column to the model parameters is summarized in Table 6-13. Water column mercury is strongly sensitive to **total atmospheric deposition**, which occurs over the watershed as well as directly onto the water body. In these simulations, wetfall and dryfall are not separated. Increases in loading lead to increases in total mercury concentrations.

Water column mercury is strongly sensitive to loading from the watershed, including those parameters that most influence soil mercury levels -- **soil water content**, the **soil reduction rate constant**, and the **soil enrichment ratio**. Increases in soil water content and the reduction rate constant cause strong declines in soil concentrations, erosion loads, and water concentrations. Increases in the enrichment ratio cause moderate declines in soil concentration, but moderate increases in mercury erosion loads and subsequent water concentrations. While increased **soil erosion factors** might be expected to cause higher erosion loading and water concentrations, the reduced soil concentrations and increased water column settling loss actually lead to slightly lower water column concentrations. Decreases in soil erosion lead first to small increases in water concentrations. Further large reductions in soil erosion, however, lead to small reductions in water concentrations, as summarized in Table 6-10.

Mercury is lost from the water column through settling and volatilization. Settling loss is strongly influenced by the **solids-water partition coefficient**. Increases in solids partitioning lead to greater settling loss and moderately lower concentrations. Decreases in solids partitioning are strongly sensitive. **Settling velocities** for biotic and abiotic solids are weakly sensitive parameters. The **water column reduction rate constant** controls the supply of Hg^0 , and thus the volatile loss rate. Increases in reduction lead to moderate decreases in water column mercury levels. **Wind speed** directly contributes to the volatilization rate, which is generally much faster than the reduction rate. While increases in wind speed cause almost insignificant declines in mercury levels, decreases in wind speed are more sensitive.

Benthic mercury fluxes are internal loadings that moderately affect water column concentrations. Increased **sediment-pore water partition coefficients** and decreased **pore water diffusion coefficients** cause small declines in net pore water diffusive loading to the water column, and thus slightly lower water concentrations.

6.4.1.4 Sensitivity of Fish Mercury to Model Parameters

The sensitivity of predatory fish mercury concentration to the IEM-2M model parameters is summarized in Table 6-14. The sensitivities of fish concentration and total water column concentration are virtually identical for those parameters controlling atmospheric and watershed loading -- **atmospheric deposition**, **soil water content**, **soil reduction rate constant**, and **soil enrichment ratio**. Increases in loading cause strong increases in fish levels. Increases in the **soil erosion parameters**, however, cause moderate declines in fish levels not only because water concentrations are lowered, but also because the increased solids concentrations cause lower fractions of dissolved MHg, which is bioavailable. **The watershed surface area** has a similar effect on fish levels as the soil erosion parameters because of the increased supply of solids. The **soil demethylation rate constant** affects the MHg fraction in the soil erosion loads. Increased soil demethylation leads to lower MHg concentrations and slightly lower fish concentrations.

The internal sediment-water column exchange processes can provide an important net source of MHg to the water column. The relatively low MHg partition coefficient in the upper sediment favors the mobilization of MHg in the pore water. Consequently, both the **pore water diffusion coefficient** and the

Table 6-13
IEM-2M Parameter Sensitivity* for Total Water Column Mercury

Model Parameter	Eastern Lake	
	decrease	increase
Total Atmospheric Deposition	-100	+100
Soil Water Content	+69	-64
Solids-Water Partition Coefficient	+74	-36
Soil Reduction Rate Constant	+69	-40
Soil Enrichment Ratio	-62	+41
Water Reduction Rate Constant	+14	-29
Soil Erosion Factors**	+14	-19
Sediment-Pore Water Partition Coefficient	+22	-10
Biotic Solids Settling Velocity	+12	-9
Abiotic Solids Settling Velocity	+ 14	-5
Dilution Flow	+9	- 9
Watershed Surface Area	- 10	+7
Pore Water Diffusion Coefficient	- 10	+7
Wind Speed	+12	-5
Sediment Mineralization Rate Constant	-3	+2
Sediment Resuspension Velocity	-3	+2

* Sensitivity is expressed as relative change in total water column mercury concentration divided by the relative change in the model parameter, in percent.

** Erosion factors include rainfall erosivity, soil erodibility, the topographic factor, the cover factor, and the sediment delivery ratio.

Table 6-14
IEM-2M Parameter Sensitivity* for Predatory Fish Mercury

Model Parameter	Eastern Lake	
	decrease	increase
Total Atmospheric Deposition	-100	+100
Soil Water Content	+73	-64
Solids-Water Partition Coefficient	+73	-41
Soil Reduction Rate Constant	+73	-41
Soil Enrichment Ratio	-64	+45
Pore Water Diffusion Coefficient	- 45	+53
Sediment-Pore Water Partition Coefficient	+64	-32
Soil Erosion Factors**	+50	-41
Sediment Methylation Rate Constant	-45	+45
Water Demethylation Rate Constant	+50	-32
Water Methylation Rate Constant	-32	+32
Sediment Demethylation Rate Constant	+ 36	-23
Soil Demethylation Rate Constant	+41	- 14
Watershed Surface Area	+27	-23
Benthic Solids Concentration	-23	+18
Water Reduction Rate Constant	+18	-14
Primary Productivity	+18	-14
Dilution Flow	+14	-14

* Sensitivity is expressed as relative change in total water column mercury concentration divided by the relative change in the model parameter, in percent.

**Erosion factors include rainfall erosivity, soil erodibility, the topographic factor, the cover factor, and the sediment delivery ratio.

sediment-pore water partition coefficient are strongly sensitive parameters affecting fish concentrations. Higher diffusion and lower sediment partitioning lead to increased diffusion of MHg to the water column and higher fish concentrations. The **sediment methylation and demethylation rate constants** are moderately sensitive parameters that control sediment MHg concentrations, and thus loading to the water column and fish concentrations.

MHg is lost from the water column through demethylation and settling, and is gained in the water column through methylation. An increase in the **solids-water partition coefficient** leads to moderately-increased settling loss of MHg, and thus moderately lower fish concentrations. The **water column methylation and demethylation rate constants** moderately influence the MHg concentrations, and thus the levels of mercury in fish. Increases in methylation and decreases in demethylation lead to higher fish mercury concentrations.

6.4.2 Variability and Parameter Sensitivity Analysis for R-MCM

Given constant atmospheric mercury deposition, in-lake processes can lead to significant variability in resulting mercury concentrations in water, sediment, and fish. To analyze the potential lake-to-lake variability of mercury levels, we conducted a series of sensitivity analyses with the Regional Mercury Cycling Model (R-MCM) (Harris, et al., 1996). R-MCM is a steady-state model that explicitly handles most of the factors affecting fish mercury levels in a mechanistic way. Funded by the Electric Power Research Institute (EPRI) and the Wisconsin Department of Natural Resources, R-MCM was designed to examine and explain variations in mercury levels among lakes. It is an extension of an earlier dynamic model developed for a set of seven oligotrophic seepage lakes in Wisconsin (Hudson et al., 1994). The fish bioaccumulation compartments are based on equations from the Fish Bioenergetics Model 2 (Hewett and Johnson, 1992). The R-MCM has been developed and calibrated to data from several lakes in Wisconsin, and can be considered descriptive of these and similar lakes. While it is presently being extended to lakes in other regions, it has not been validated for general nationwide use.

The Beta Version 1.0b (December 1996) version of the R-MCM was obtained from Tetra Tech, Inc., with permission from EPRI, and used in these analyses.

6.4.2.1 Overview of R-MCM

R-MCM is a compartment model that performs a steady-state mass balance for three mercury components -- elemental mercury (Hg^0), divalent mercury (HgII), and methyl mercury (MHg). The lake is divided into two or three physical compartments, including epilimnion, hypolimnion (optional), and surficial sediments. A simple food chain is simulated, including phytoplankton and benthos at its base, zooplankton, prey fish, and predator fish. Fish are divided into year classes to which a set of bioenergetics equations are applied. Specified atmospheric mercury concentrations and fluxes drive the simulations.

The model simulates a set of simple transport processes, including atmospheric wetfall and dryfall deposition, inflow and outflow through surface water or groundwater, sorption to biotic and abiotic solids, settling, resuspension, and burial of abiotic particles and sorbed mercury, volatile exchange of dissolved and vapor phase mercury at the air-water boundary, and pore water exchange of dissolved mercury at the sediment-water interface. A set of equilibrium reactions is solved to calculate the complexation of HgII and MHg with DOC and inorganic ligands. The resulting speciation depends on the specified environmental characteristics (i.e., pH, DOC, SO_4 , Cl, solids) and the equilibrium constants and partition coefficients in the model database.

Abiotic solids, phytoplankton, and zooplankton concentrations are specified as model input parameters, as are settling and burial velocities and benthic mineralization rate constants. Bulk density is calculated internally from specified porosity and solids density. Resuspension velocities are computed using a solids mass balance.

Next, R-MCM solves a set of transformation reactions, including reduction in the water column and methylation and demethylation in the water column and sediments. Reduction is modeled as a first-order rate applied to dissolved $\text{Hg}(\text{OH})_2$, and so is pH-dependent. Higher pH values favor this species, and so promote reduction. Water column and sediment methylation are modeled as second-order rates applied to all dissolved HgII species. The water column methylation rate constant is multiplied by the DOC concentration, while the sediment rate constant is multiplied by the sediment TOC concentration. The rates are further modified by a temperature correction function that is based on the maximum monthly temperature, and a Monod function that represents the stimulating effect of sulfate on methylation. The temperature function doubles the methylation rate for every 10°C increase above 15°C. The sulfate function is disabled as a default option in this version of R-MCM. Apparently, differences in sulfate concentrations among the set of Wisconsin lakes were not enough to require the use of this function to describe differences in lake methylation rates. Demethylation in the water column is modeled as a second-order rate applied to dissolved MHg species. The water surface demethylation rate constant is multiplied by the average sunlight, and then attenuated throughout the water column using a light extinction coefficient to obtain a depth-averaged rate. Demethylation in the sediments is modeled as a second-order rate applied to the dissolved MHg species in pore water. The rate constant is multiplied by the sediment TOC concentration, but is not temperature-corrected.

Finally, R-MCM solves a set of bioenergetics and biouptake equations to calculate the bioaccumulation of mercury in a 5-component food web containing phytoplankton, zooplankton, benthos, prey fish, and predatory fish. The fish bioenergetics equations are based on the Fish Bioenergetics Model 2. These are used to calculate the energy requirements for growth and metabolism, from which consumption, excretion, and gill exchange are derived. These rates are coupled with mercury concentrations in the water and the diet to calculate mercury food chain fluxes and concentrations. Up to 10 individual year-classes of prey and predator fish with different diets are simulated. The default fish species of yellow perch and walleye were used here. The model output reports mercury concentrations in 1-year old prey fish and in 5-year old predatory fish.

6.4.2.2 Analysis of In-Lake Variability in Mercury Levels

Representations of several Wisconsin lakes are available in the R-MCM database. To examine the effects of water body characteristics on mercury levels, we worked with four -- Palette Lake, Little Rock Lake, Crystal Lake, and Lake Muskellunge. The model default values for atmospheric deposition fluxes in this region were used -- $8.5 \mu\text{g}/\text{m}^2\text{-yr}$ for wetfall and $3 \mu\text{g}/\text{m}^2\text{-yr}$ for dryfall. In order to isolate the variability due to intrinsic lake properties, we set the volume, depth, and hydraulic residence time for these four lakes equal to the characteristic eastern lake analyzed with IEM-2M. The four lakes were designated as “drainage lakes.” For one set of simulations, the surrounding watersheds were removed so that the mercury levels respond to direct atmospheric deposition only. Another set of simulations was conducted with the standard eastern watershed draining to the four lakes. A final set of simulations was conducted in which the water columns of the four lakes were divided into epilimnion and hypolimnion, keeping the total lake volume the same. These simulations were run with no watershed in order to determine the effect of the hypolimnion on fish levels.

In order to study the effects of watershed characteristics on mercury levels, we conducted further simulations with the modified Palette Lake. The first was designated a perched lake, fed by rainwater only, with a surrounding watershed area equal to 10 percent of the lake surface area and no wetlands.

The second simulation represented a seepage lake, fed by groundwater, with a watershed area equal to the lake surface area and 30 percent wetlands. The third simulation represented a drainage lake with the same watershed properties. The fourth simulation represented a drainage lake with watershed area 5 times the lake surface area and 6 percent wetlands. The final simulation represented a drainage lake with watershed area 15 times the lake surface area and 2 percent wetlands. Note that the seepage lake and the drainage lakes all have the same wetland area, 30 percent of the lake surface area.

The general properties and forcing functions used in all four lakes are summarized in Table 6-15. The variable properties are given in Table 6-16. The effective partition coefficients and first-order rate constants calculated internally are summarized in Table 6-17, along with the values used in the IEM-2M eastern lake simulation. The calculated concentrations in the four R-MCM lakes and the IEM-2M eastern lake are presented in Table 6-18 (no watershed) and Table 6-19 (standard watershed). The calculated concentrations in the four R-MCM lakes with added hypolimnion are presented in Table 6-20. Finally, the calculated concentrations in the modified Palette Lake with the five different watershed/hydrology combinations are given in Table 6-21.

Variability due to in-lake processes -- The primary in-lake characteristics expected to influence mercury concentrations in water and fish are pH, DOC, and solids. While hypolimnetic anoxia should be important in deeper lakes, the four lakes represented here are all oligotrophic and shallow. Palette is characterized by higher pH, DOC, and sedimentary TOC. Crystal is lower in pH, DOC, and TOC. Little Rock and Muskellunge have intermediate DOC and TOC levels, with lower and higher pH, respectively. Palette and Little Rock have higher solids concentrations and resuspension velocities.

Predicted total mercury concentrations in the water column varied by a factor of 2 for each series of simulations. With no watershed, values varied from 0.67 ng/L in Muskellunge to 1.21 ng/L in Little Rock. With the watershed, values varied from 1.35 ng/L in Palette to 2.11 ng/L in Muskellunge. IEM-2M calculated total water column mercury levels at the low end of these ranges, predicting 1.49 ng/L and 0.63 ng/L with and without a watershed.

Total sediment mercury concentrations varied by a factor of 6 within each set of simulations. With no watershed, values varied from 35 ng/g in Palette to 205 ng/g in Crystal. With the watershed, the range was 61 to 359 ng/g. Again, the IEM-2M lake is at the low end of the ranges, with 50 and 116 ng/g, respectively. Predatory fish concentrations varied by just over a factor of 2. With no watershed, values varied from 200 ng/g in Palette to 463 ng/g in Little Rock. With the watershed, the range was 340 to 797 ng/g. With no watershed, IEM-2M predicted fish levels of 330 ng/g -- the middle of the range. With the watershed, IEM-2M predicted fish levels of 740 ng/g, which is at the high end of the range.

Adding a hypolimnion had the effect of decreasing the variability among the four lakes examined here. Total mercury varied between 0.75 and 0.81 ng/L in the epilimnion, and between 1.39 and 1.70 in the hypolimnion. Predatory fish varied between 240 and 366 ng/g. Mercury concentrations in the epilimnion and fish did not change systematically with the addition of a hypolimnion.

It should be stressed that R-MCM (version 1.0b) is currently parameterized for a limited set of lakes. Some key processes, such as the effect of anoxia on methylation, are not included in the model

Table 6-15
General Properties of the Four R-MCM Lakes

Property	Value and Units
Volume	$1.245 \times 10^7 \text{ m}^3$
Surface Area	$2.49 \times 10^6 \text{ m}^2$
Depth	5 m
Hydraulic Residence Time	314 days
Advective Flow	$0.46 \text{ m}^3/\text{sec}$
Upper Sediment Depth	0.02 m
Wet Deposition	$8 \mu\text{g}/\text{m}^2\text{-yr}$
Dry Deposition	$3.5 \mu\text{g}/\text{m}^2\text{-yr}$
Maximum Monthly Temperature	22°C
Average Sunlight	$318 \mu\text{Einsteins}/\text{m}^2\text{-sec}$
Fish Biomass	1 kg/ha
Benthic Biomass	$25 \text{ g}/\text{m}^2$
Solids Density	$1.5 \text{ g}/\text{mL}$
Benthic Porosity	0.95 - 0.90

Table 6-16
Variable Properties of the Four R-MCM Lakes

Variable	Palette	Little Rock	Crystal	Muskel-lunge	IEM-2M **
pH	7.2	6.0	6.3	7.2	-
DOC (water), mg/L	5.4	3.3	1.8	3.8	-
DOC (sediment), mg/L	16	10	5	11	-
TOC (sediment), g/m ²	800	500	275	550	-
SO ₄ , μeq/L	56	65	72	77	-
Cl, mg/L	.25	.28	.46	.30	-
DO, mg/L	8	8	8	8	-
Ca, mg/L	2.2	.94	1.14	5.8	-
light extinction coefficient, m ⁻¹	1.0	.75	.36	.76	-
phytoplankton, mg/L	.28	.2	.1	.1	0.4*
zooplankton, mg/L	.14	.1	.05	.05	
abiotic solids, mg/L	.9	.7	.35	.35	0.5*
settling velocity, m/day	.5	.5	.5	.5	2
burial velocity, mm/yr	.21	.15	.1	.1	.13*
resuspension velocity, mm/yr	2.02*	1.35*	0.49*	0.53*	3.7
sediment mineralization, yr ⁻¹	.01	.01	.013	.011	.05

*calculated internally ** revised solids parameters for comparison with Wisconsin lakes

Table 6-17
Partition Coefficients and First-order Rate Constants for Simulations

Coefficient	Palette	Little Rock	Crystal	Muskel-lunge	IEM-2M
Partition Coefficients, L/kg					
HgII - abiotic S	80,000	160,000	270,000	110,000	100,000
HgII - TSS	100,000	190,000	340,000	140,000	100,000
HgII - sediment	30,000	52,000	100,000	43,000	50,000
MHg - abiotic S	94,000	160,000	250,000	130,000	100,000
MHg - TSS	230,000	400,000	670,000	330,000	400,000
MHg - sediment	2,200	3,500	7,800	3,600	3,000
Rate Constants, day⁻¹					
reduction in water	.0046	.00059	.0021	.0065	.0075
methylation in water	.000044	.000027	.000015	.000031	.001
demethylation in water	.0063	.0083	.015	.0082	.015
methylation in sediment*	.000055	.000020	.0000057	.000026	.0001
demethylation in sediment*	.00048	.00018	.000048	.00019	.002

* applied to the total sediment mercury concentration

**Table 6-18
Simulation Results, No Watershed**

Compartment and Variable	Palette	Little Rock	Crystal	Muskel-lunge	IEM-2M*
WATER COLUMN					
Unfiltered Total, ng/L	0.78	1.21	0.90	0.67	0.63
Dissolved Methyl, ng/L	0.053	0.057	0.024	0.036	.051
Dissolved Elemental, ng/L	0.045	0.022	0.030	0.051	.047
SEDIMENT					
Particulate Total, ng/g	35	120	205	42	50
Dissolved Methyl, ng/L	0.45	0.58	0.26	0.23	0.43
BIOTA					
Prey Fish, ng/g	35	84	165	57	80
Predatory Fish, ng/g	200	463	336	278	330

*Adjusted watershed size, erosion to yield abiotic solids = 0.5 mg/L; no watershed Hg yield.

**Table 6-19
Simulation Results with Standard Watershed**

Compartment and Variable	Palette	Little Rock	Crystal	Muskel-lunge	IEM-2M*
WATER COLUMN					
Unfiltered Total, ng/L	1.35	2.11	1.57	1.68	1.49
Dissolved Methyl, ng/L	0.090	0.096	0.039	0.081	0.108
Dissolved Elemental, ng/L	0.071	0.030	0.044	0.113	0.099
SEDIMENT					
Particulate Total, ng/g	61	210	359	106	116
Dissolved Methyl, ng/L	0.77	0.99	0.44	0.56	1.10
BIOTA					
Prey Fish, ng/g	59	144	279	138	170
Predatory Fish, ng/g	340	797	572	668	740

* Adjusted watershed erosion by 0.4 to yield abiotic solids = 0.7 mg/L.

Table 6-20
Simulation Results with Hypolimnion, No Watershed

Compartment and Variable	Palette	Little Rock	Crystal	Muskel-lunge
WATER COLUMN				
Epilimnion Unfiltered Total, ng/L	0.78	0.81	0.75	0.78
Hypolimnion Unfiltered Total, ng/L	1.70	1.27	1.39	1.64
Epilimnion Dissolved Methyl, ng/L	0.057	0.036	0.016	0.037
Hypolimnion Dissolved Methyl, ng/L	0.245	0.159	0.029	0.089
SEDIMENT				
Epilimnion Particulate Total, ng/g	56	82	172	52
Hypolimnion Particulate Total, ng/g	36	76	111	21
BIOTA				
Prey Fish, ng/g	108	60	39	75
Predatory Fish, ng/g	270	345	240	366

*Same total water body volume as shallow lake.

Table 6-21
Simulation Results for 5 Combinations of Watershed and Hydrology

Compartment and Variable	Perched $0.1 \cdot A_w$	Seepage $1 \cdot A_w$	Drainage $1 \cdot A_w$	Drainage $5 \cdot A_w$	Drainage $15 \cdot A_w$
WATER COLUMN					
Unfiltered Total, ng/L	0.68	0.71	0.82	0.98	1.36
Dissolved Methyl, ng/L	0.02	0.03	0.06	0.07	0.10
Dissolved Elemental, ng/L	0.04	0.04	0.05	0.05	0.07
SEDIMENT					
Particulate Total, ng/g	26	27	37	44	61
Dissolved Methyl, ng/L	0.13	0.14	0.50	0.59	0.80
BIOTA					
Prey Fish, ng/g	12	14	40	46	62
Predatory Fish, ng/g	62	74	225	263	357

structure. Other key processes, such as the effect of sulfate on methylation, are not parameterized for these lakes. Consequently, the variability due to in-lake processes demonstrated here is somewhat less

than the actual variability among lakes.

Variability due to watershed and hydrology -- The primary watershed characteristics affecting the R-MCM predictions are the surface area, the presence of wetlands, and the nature of the hydrologic connection with the lake. Wetlands are expected to contribute more methyl mercury to the lake than other watershed elements. Larger watersheds connected by surface drainage are expected to contribute more total mercury loading than smaller watersheds and those connected through groundwater.

The five watershed hydrology combinations range from a perched lake with minimal watershed connection to a large drainage watershed. Total water column and sediment mercury varied by a factor of 2, from 0.68 ng/L and 26 ng/g in the perched lake to 1.36 ng/L and 61 ng/g in the drainage lake with the largest watershed. Predatory fish varied by a factor of 6, from 62 to 357 ng/g. The perched lake and the seepage lake had similar concentrations. There is a significant difference between the seepage lake and the drainage lake with the same watershed size. Although total mercury did not increase much between these two lakes, the sediment methyl mercury and fish mercury increased by a factor of 3.

6.4.2.3 Sensitivity of Water Column Mercury to Model Parameters

Following the base simulations for the reconstructed Palette and Crystal datasets, the major parameters were systematically varied and the changes in model output were noted. The relative sensitivity of total water column mercury to these parameters is summarized in Table 6-22. Total water column mercury is strongly sensitive to **wetfall concentration**, which represents two-thirds of the total loading in these simulations. **Dryfall loading** is a moderately sensitive parameter that represents about a third of the total loading. Increases in loading lead to increases in total mercury concentrations.

DOC is a moderately sensitive parameter that complexes mercury and increases its mobility from the sediments to the water column. Increases in DOC lead to increases in total water column mercury. **Hydraulic residence time** is inversely proportional to advective flow. Decreases in hydraulic residence time strongly dilute the loading and decrease total mercury levels. Increases in residence time moderately increase total mercury.

Particle density and **benthic porosity** are inversely related. Increases in particle density and decreases in porosity lead to higher benthic solids concentration, which in R-MCM results in lower resuspension rates and thus lower water column mercury concentrations. Increased **solids partitioning** causes more deposition of mercury from the water column, leading to lower water column concentrations and higher sediment concentrations. Increased **sediment burial velocity** is associated with lower resuspension rates and less transfer of sediment mercury to the water column. These effects are weakly sensitive for the Palette data set and moderately sensitive for the Crystal data set. Increases in **benthic mineralization** are associated with weak decreases in water column mercury. This is a consequence of how R-MCM calculates the resuspension velocity by balancing solids deposition, burial, and mineralization. Given a constant resuspension velocity, increases in benthic mineralization should actually cause decreases in burial and thus increased mercury concentrations in the sediments and water column.

Total mercury levels are moderately sensitive to $[H^+]$, which is calculated from specified pH levels. R-MCM applies the reduction rate constant only to dissolved $Hg(OH)_2$. As a result, increased pH (i.e., decreased $[H^+]$) strongly increases $Hg(OH)_2$ concentrations causing significantly more reduction of

Table 6-22
R-MCM Parameter Sensitivity for Total Water Column Mercury

Model Parameter	Palette		Crystal	
	decrease	increase	decrease	increase
Wetfall Concentration	-67	+67	-68	+68
DOC	-46	+34	-57	+40
Hydraulic Residence Time	-53	+27	-59	+33
Dryfall Load	-30	+30	-30	+30
Particle Density	+10	- 9	+37	-37
Porosity	- 9	+10	-37	+38
[H ⁺]	-55	+12	-43	- 6
Solids Partitioning	+ 9	- 9	+36	-28
Sediment Burial Velocity	+10	- 9	+30	-23
Benthic Mineralization	+ 1	- 1	+10	-13
Average Sunlight	+ 6	- 4	+ 4	- 2
Biotic Solids Concentration	- 4	+ 4	- 4	+ 4
Light Extinction Coefficient	- 5	+ 4	- 2	+ 2
Abiotic Solids Concentration	- 0	+ 2	- 6	+ 5
Abiotic Solids Settling Velocity	+ 4	- 2	- 1	+ 1
Sediment TOC	+ 3	- 1	+ 2	- 2

* Sensitivity is expressed as relative change in total water column mercury concentration divided by the relative change in the model parameter, in percent.

HgII to Hg⁰ with subsequent loss due to volatilization. The two datasets are only weakly sensitive to decreasing pH which causes a relatively small decline in reduction and volatilization.

Total mercury concentrations were only weakly sensitive to the other parameters tested, including **sunlight**, **light extinction**, biotic and abiotic **solids concentrations**, **settling velocity**, and **sediment TOC**. Total mercury levels were insensitive to **dissolved oxygen**, **sulfate**, **chloride** and **fish biomass**.

6.4.2.4 Sensitivity of Fish Mercury to Model Parameters

The relative sensitivity of mercury concentration in upper trophic level fish (5-years old) to the model parameters is summarized in Table 6-23. The most sensitive parameter for fish mercury is the **maximum monthly temperature**. The annual-average R-MCM adjusts the base methylation rate constant using the maximum monthly temperature (i.e., July) to account for the higher fish activity at this time of year. Demethylation rates are not temperature-corrected due to a lack of data. As a consequence, an increase in maximum temperature leads to an increase in net methylation, and a subsequent increase in fish concentrations. **Sediment TOC** concentrations directly affect methylation rates in the sediment. While increases in TOC cause proportional increases in both benthic methylation and demethylation rates, some of the extra MHg production diffuses to the water column leading to higher fish mercury levels.

Fish mercury levels are strongly sensitive to **solids partitioning**. The partition coefficients for HgII and MHg partitioning to abiotic solids and sediments were adjusted up and down as a group. Higher partitioning causes water column mercury levels to decline somewhat and benthic concentrations to increase strongly. The elevated mercury concentrations in benthic biota enter the food web, ultimately resulting in higher fish concentrations. The strong sensitivity of fish mercury to **DOC** operates in the opposite direction. Higher levels of DOC complex more mercury, leading to higher benthic fluxes and water column concentrations. The DOC-bound mercury concentrations, however, are not bioavailable, and thus fish mercury levels strongly decline.

Fish mercury concentrations, like total water column levels, are strongly sensitive to **wetfall concentration** and moderately sensitive to **dryfall loading**. Fish mercury is more sensitive than total water column mercury to **hydraulic residence time**. Increases in residence time associated with lower flow rates provide less dilution not only to external loading of HgII, but also to benthic fluxes of MHg, leading to significantly higher fish concentrations.

Average sunlight and the **light extinction coefficient** are moderately sensitive parameters that affect the water column reduction and demethylation rates. Increased light levels cause increased reduction and loss of HgII and increased demethylation of MHg, leading to lower MHg concentrations and thus lower fish mercury concentrations.

The **abiotic solids concentration** and **deposition velocity**, the **sediment mineralization rate**, and the **sediment burial velocity** are moderately to weakly sensitive parameters connected through the R-MCM solids balance. The resuspension velocity is calculated internally from these parameters, along with porosity and particle density using a solids mass balance. Increases in the abiotic solids concentration or deposition velocity increase the supply of solids to the sediment layer, which leads to higher calculated resuspension velocities given the fixed burial and mineralization rates. These higher resuspension velocities cause higher fluxes of MHg to the water column, and thus higher MHg and fish mercury concentrations.

Table 6-23
R-MCM Parameter Sensitivity for Upper Trophic Level Fish Mercury

Model Parameter	Palette		Crystal	
	decrease	increase	decrease	increase
Maximum Monthly Temperature	-160	+180	-160	+180
Solids Partitioning	- 91	+100	- 94	+ 88
DOC	+120	- 54	+120	- 54
Wetfall Concentration	- 59	+ 59	- 58	+ 57
Hydraulic Residence Time	- 70	+ 40	- 65	+ 37
Sediment TOC	- 50	+ 45	- 74	+ 62
Average Sunlight	+ 46	- 27	- 27	_ 26
[H ⁺]	- 64	+ 15	- 53	+ 19
Light Extinction Coefficient	- 41	+ 27	- 27	+ 27
Dryfall Deposition	- 28	+ 27	- 27	+ 26
Abiotic Solids Settling Velocity	- 40	+ 29	- 18	+ 17
Abiotic Solids Concentration	- 37	+ 26	- 15	+ 13
Sediment Burial Velocity	+ 10	- 9	+ 27	- 21
Sediment Mineralization Rate	- 6	+ 5	- 22	+ 29
Benthic Porosity	- 10	+ 5	- 3	+ 3
Biotic Solids Concentration	+ 5	- 5	+ 5	- 5

* Sensitivity is expressed as relative change in level 4 fish mercury concentration divided by the relative change in the model parameter, in percent.

Sediment burial velocity affects mercury in a similar way. Decreases in burial lead to increases in calculated resuspension and thus increased MHg flux to the water column and higher fish mercury levels. On the other hand, an increase in the sediment remineralization rate causes a lower calculated resuspension rate, but also causes increased concentration of sediment mercury levels. The net effect is to increase MHg diffusion flux to the water column leading to higher levels of MHg and fish mercury. The burial and remineralization effects are more pronounced in the Crystal data set than in the Palette data set.

The model was not parameterized to simulate the effects of **dissolved oxygen** and **sulfate** on methylation rates. These parameters are expected to affect fish bioaccumulation significantly in some lakes.

6.4.3 Summary and Conclusions

For a particular atmospheric deposition rate, mercury concentrations in watersheds and water bodies can vary significantly. Several intrinsic and extrinsic watershed and water body characteristics influence the mercury concentrations in soil, water, and fish. These should cause significant variability in mercury concentrations between regions and among individual lakes within a region.

Mercury concentrations in watershed soils are strongly influenced by atmospheric loading and soil loss processes. The influence of plant canopy and roots in mediating both the loading to the soil and the loss from the soil is not well characterized at present, although published studies indicate its potential importance. Reduction of HgII in the upper soil layer appears to control the volatile loss of mercury, and variations in this reaction can cause significant variations in soil mercury levels. The factors controlling mercury reduction are not well characterized at present. Soil erosion from a watershed can vary more than 3 orders of magnitude depending on rainfall patterns, soil type, topography, and plant cover. High levels of soil erosion should significantly diminish soil mercury concentrations. Runoff and leaching are not expected to affect soil mercury concentrations significantly.

Total mercury concentrations in a water body are strongly influenced by atmospheric loading and, for drainage lakes, by watershed loading. Variations in watershed size and erosion rates can cause significant variability in lake mercury levels. Hydraulic residence time, the water body volume divided by total flow, affects the maximum possible level of total water column mercury for a given loading rate. Parameters controlling mercury loss through volatilization and net settling can also cause significant variations among lakes. Mercury loss through settling is affected by *in-situ* productivity, by the supply of solids from the watershed, and by the solids-water partition coefficient. DOC concentrations can significantly affect partitioning, and thus overall mercury levels. Mercury loss through volatilization is controlled by the reduction rate, which is a function of sunlight and water clarity. Reduction may also be controlled by pH, with lower values inhibiting this reduction and leading to higher total mercury levels.

Fish mercury levels are strongly influenced by the same factors that control total mercury levels. In addition, fish concentrations are sensitive to methylation and demethylation in the water column and sediments. A set of water body characteristics appears to affect these reactions, including DOC, sediment TOC, sunlight, and water clarity. Variations in these properties can cause significant variations in fish concentrations among lakes. Other factors not examined here, such as anoxia and sulfate concentrations, can stimulate methylation and lead to elevated fish concentrations. Fish mercury levels are sensitive to factors that promote methyl mercury mobility from the sediments to the water column; these factors include sediment DOC and sediment-pore water partition coefficients.

The IEM-2M has not been validated with site-specific data. Here the model is benchmarked against the independently-derived R-MCM, which itself is calibrated to several Wisconsin lakes. When driven by the same atmospheric loading and solids concentrations, IEM-2M predictions of mercury concentrations compare well with those calculated by R-MCM for a set of Wisconsin lakes.

The R-MCM is a useful research model that has been set up to describe mercury dynamics in a set of Wisconsin lakes. Current work is extending the model to lakes in other regions. This model shows promise for use as a more general management tool, especially as it is applied and tested in diverse water bodies around the nation. As of this writing it remains a scientific work in progress.

Based on the variability and sensitivity analyses with IEM-2M and R-MCM, predictions of average mercury concentrations in particular watersheds and waterbodies should vary about an order of magnitude based on variable environmental characteristics. Total mercury concentration in a water body is a function of atmospheric deposition, watershed soil retention, solids erosion, water body flow, suspended solids partitioning and deposition, and water column reduction and volatilization loss. Fish mercury concentrations depend upon total mercury concentrations along with net water column and sediment methylation rates, uptake at the base of the food web, and fish bioaccumulation. To predict mercury levels in particular water bodies, these environmental factors must be properly parameterized. Site-specific calibration data would allow more accurate predictions.

In the analysis relating mercury emissions to water body and fish concentrations, the IEM-2M model was parameterized for an average shallow lake using data collected from studies across a number of water bodies. This analysis of general response to atmospheric loadings is national in scope and appears to be an appropriate application of the model. The variability and sensitivity analyses conducted here provide a context in which to interpret the predicted average loading response.

7. CONCLUSIONS

Summary Conclusions

- The present study in conjunction with available scientific knowledge supports a plausible link between mercury emissions from anthropogenic combustion and industrial sources and mercury concentrations in air, soil, water and sediments. The critical variables contributing to this linkage are these:
 - a) the species of mercury that are emitted from the sources;
 - b) the overall amount of mercury emitted from a combustion source;
 - c) atmospheric and climatic conditions;
 - d) reduction rates in the soil and water body;
 - e) erosion rates within the watershed; and
 - f) solids deposition and burial in the water body.
- The present study, in conjunction with available scientific knowledge, supports a plausible link between mercury emissions from anthropogenic combustion and industrial sources and methylmercury concentrations in freshwater fish. The additional critical variables contributing to this linkage are the following:
 - a) the extent (magnitude) of mercury methylation and demethylation in the water body; and
 - b) the degree of complexation of mercury with DOC and solids.
- Mercury is a natural constituent of the environment; concentrations of mercury in many environmental media appear to have increased over the last 500 years.
- There is a lack of adequate mercury measurement data near the anthropogenic atmospheric mercury sources considered in this report. Measurement data are needed to assess how well the modeled data predict actual mercury concentrations in different environmental media at a variety of geographic locations. The lack of such measured data preclude a comparison of the modeling results with measured data around these sources. Missing data includes measured mercury deposition rates as well as measured concentrations in the local atmosphere, soils, water bodies, and biota.
- From the atmospheric modeling analyses of mercury deposition and on a comparative basis, a facility located in a humid climate has a higher annual rate of mercury deposition than a facility located in an arid climate. The critical variables are the estimated washout ratios of elemental and divalent mercury as well as the annual amount of precipitation. Precipitation removes various forms of mercury from the atmosphere and deposits mercury to the surface of the earth. Of the species of mercury that are emitted, divalent mercury is predicted to generally deposit to local environments near sources. Elemental mercury is predicted to generally remain in the

atmosphere until atmospheric conversion to divalent species or uptake and retention by plant leaves and the subsequent deposition as divalent species in litter fall.

- On a national scale, an apportionment between specific sources of mercury and mercury in environmental media and biota at particular locations cannot be described in quantitative terms with the current scientific understanding of the environmental fate of mercury.
- From the modeling analysis and a review of field measurement studies, it is concluded that mercury deposition appears to be ubiquitous across the continental U.S. and at, or above, detection limits when measured with current analytic methods.
- Based on the RELMAP modeling analysis and a review of recent measurement data published in peer-reviewed scientific literature, there is predicted to be a wide range of mercury deposition rates across the continental U.S. The highest predicted rates (i.e., above 90th percentile) are about 20 times higher than the lowest predicted rates (i.e., below the 10th percentile). Three principal factors contribute to these modeled and observed deposition patterns:
 - a) emission source locations;
 - b) amount of divalent and particulate mercury emitted or formed in the atmosphere; and
 - c) climate and meteorology.
- Based on the modeling analysis of the transport and deposition of stationary point source and area source air emissions of mercury from the continental U.S., it is concluded that the following geographical areas have the highest annual rate of deposition of mercury in all forms (above the levels predicted at the 90th percentile):
 - a) the southern Great Lakes and Ohio River Valley;
 - b) the Northeast and southern New England; and
 - c) scattered areas in the South with the most elevated deposition occurring in the Miami and Tampa areas.

Measured deposition estimates are limited, but are available for certain geographic regions. The data that are available corroborate the RELMAP modeling results for specific areas.

- Based on modeling analysis of the transport and deposition of stationary point source and area source air emissions of mercury from the continental U.S., it is concluded that the following geographical areas have the lowest annual rate of deposition of *mercury in all forms* (below the levels predicted at the 10th percentile):
 - a) the less populated areas of the Great Basin, including southern Idaho, southeastern Oregon, most of southern and western Utah, most of Nevada, and portions of western New Mexico; and
 - b) western Texas other than near El Paso, and most of northeastern Montana.

- Based on limited monitoring data, the RELMAP model predictions of atmospheric mercury concentrations and wet deposition across the U.S. are comparable with typically measured data.
- A number of factors appear to affect the local-scale atmospheric fate of mercury emitted by/from major anthropogenic sources as well as the quantity of mercury predicted to deposit. These factors include the following:
 - a) the amounts of divalent and particulate mercury emitted;
 - b) parameters that influence the plume height, primarily the stack height and stack exit gas velocity;
 - c) meteorology; and
 - d) terrain.
- From the analysis of deposition and on a comparative basis, the deposition of divalent mercury close to an emission source is greater for receptors in elevated terrain (i.e., terrain above the elevation of the stack base) than for receptors located in flat terrain (i.e., terrain below the elevation of the stack base). The critical variables are parameters that influence the plume height, primarily the stack height and stack exit gas velocity.
- Modeling estimates of the transport and deposition of stationary point source and area source air emissions of mercury from the continental U.S. have revealed the following partial mass balance.
 - Of the total amount of elemental mercury vapor that is emitted, about 1 percent (0.9 metric tons/yr) may be atmospherically transformed into divalent mercury by tropospheric ozone and adsorbed to particulate soot in the air and subsequently deposited in rainfall and snowfall to the surface of the continental U.S. The vast majority of emitted elemental mercury does not readily deposit and is transported outside the U.S. or vertically diffused to the free atmosphere to become part of the global cycle.
 - Nearly all of the elemental mercury vapor emitted from other sources around the globe also enters the global cycle and can be deposited slowly to the U.S. Over 30 times as much elemental mercury vapor is deposited from these other sources than from stationary point sources and area sources within the continental U.S.
 - Of the total amount of divalent mercury vapor that is emitted, about 70 percent (36.8 metric tons/year) deposits to the surface through wet or dry processes within the continental U.S. The remaining 30 percent is transported outside the U.S. or is vertically diffused to the free atmosphere to become part of the global cycle.
 - Of the total amount of particulate mercury that is emitted, about 38 percent (10.0 metric tons/year) deposits to the surface through wet or dry processes within the continental U.S. The remaining 62 percent is transported outside the U.S. or is vertically diffused to the free atmosphere to become part of the global cycle.

- Given the simulated deposition efficiencies for each form of mercury air emission (namely; elemental mercury - 1 percent, divalent mercury vapor - 70 percent, and particulate mercury - 38 percent) the relative source contributions to the total anthropogenic mercury deposited to the continental U.S. are strongly and positively correlated to the mass of emissions in oxidized form. This oxidized mercury occurs in both gaseous (Hg^{2+}) and particulate (Hg_p) forms. While coal combustion is responsible for more than half of all emissions of mercury in the inventory of U.S. anthropogenic sources, the fraction of coal combustion emissions in oxidized form is thought to be less than that from waste incineration and combustion. The true speciation of mercury emissions from the various source types modeled is still uncertain and is thought to vary, not only among source types, but also for individual plants as feed stock and operating conditions change. With further research, it may be possible to make a confident ranking of relative source contributions to mercury deposition in the continental U.S. However, no such confident ranking is possible at this time. Given the total mass of mercury thought by EPA to be emitted from all anthropogenic sources and EPA's modeling of the atmospheric transport of emitted mercury, coal combustion and waste disposal most likely bear the greatest responsibility for direct anthropogenic mercury deposition to the continental U.S.
- Based on the local scale atmospheric modeling results in flat terrain, at least 75 percent of the emitted mercury from each facility is predicted to be transported more than 50 km from the facility.
- The models used in the analysis as well as the assumptions implemented concerning the species of mercury emitted and the wet and dry deposition velocities associated with atmospheric mercury species indicate that deposition within 10 km of a facility is may be dominated by emissions from the local source rather than from emissions transported from regional mercury emissions sources, with some exceptions. Specifically, the models predict that in the Eastern U.S., individual large anthropogenic sources dominate predicted mercury deposition within 2.5 km; chlor-alkali facilities are predicted to dominate up to 10 km from the source. In the western site, the models predict that the dominance of local source mercury deposition in emissions extends beyond the predicted range of the eastern site.
- Of the mercury deposited to watershed soils, a small fraction is ultimately transported to the water body. Deposition to and evasion from soils as well as the amount of reduction in upper soil layers are important factors in the determining soil concentration of mercury. In forested watersheds canopy interactions can provide significant fluxes both to and from the atmosphere. Mercury from litter fall may be an important source of mercury to some soils and water bodies, but the magnitude of the contribution from this source is uncertain at this time.
- The net mercury methylation rate (the net result of methylation and demethylation) for most soils appears to be quite low with much of the measured methylmercury in soils potentially resulting from wet fall. A significant and important exception to this appears to be wetlands. Wetlands appear to convert a small but significant fraction of the deposited mercury into methylmercury; which can be exported to nearby water bodies and potentially bioaccumulated in the aquatic food chain.
- Both watershed erosion and direct atmospheric deposition can be important sources of mercury to the water body depending on the relative sizes of the water body and the watershed.

- There appears to be a great deal of variability in the processing of mercury among bodies of water. This variability extends to water bodies that have similar and dissimilar physical characteristics. Important properties influencing the levels of total mercury and methylmercury in a water body include: pH, anoxia, DOC, productivity, turbidity, and the presence of wetlands.
- Some of the mercury entering a water body is methylated predominately through biotic processes forming methylmercury (predominately monomethylmercury). Methylmercury is accumulated and retained by aquatic organisms. Important factors influencing bioavailability of methylmercury to aquatic organisms include DOC and solids, which complex methylmercury and reduce the bioavailable pool.
- Methylmercury is bioaccumulated in predatory species of the aquatic food chain. The concentrations of methylmercury in fish muscle tissue are highly variable across water bodies. Within a given body of water methylmercury concentrations generally increase with fish size and position within the trophic structure.

To improve the quantitative environmental fate component of the risk assessment for mercury and mercury compounds, U.S. EPA would need more and better mercury emissions data and measured mercury data near sources of concern, as well as a better quantitative understanding of mercury chemistry in the emissions plume, the atmosphere, soils, water bodies and biota. Specific needs include these.

Mercury in the Atmosphere

- aqueous oxidation-reduction kinetics in atmospheric water droplets
- physical adsorption and condensation of divalent mercury gas to ambient particulate matter
- photolytic reduction of particle-bound divalent mercury by sunlight
- convincing evidence that gas-phase oxidation of mercury is insignificant

Mercury in Soils and Water Bodies

- uptake and release kinetics of mercury from terrestrial and aquatic plants
- biogeochemical mercury transport and transformation kinetics in benthic sediments
- methylation, demethylation, and reduction kinetics in water bodies
- sorption coefficients to soils, suspended solids, and benthic solids
- complexation to organic matter in water bodies
- more data to better discern seasonal trends
- reduction kinetics in soils

- mercury mass balance studies in wetlands

Information Leading to an Improved Quantitative Understanding of Aquatic Bioaccumulation Processes and Kinetics

- uptake kinetics by aquatic plants and phytoplankton
- partitioning and binding behavior of mercury species within organisms
- metabolic transformations of mercury, and the effect on uptake, internal distribution, and excretion
- more measurements of methylmercury concentrations in fish for better identification of the range in fish species.
- more measurements of methylmercury concentrations in other biotic components of the aquatic environment such as benthic and macro invertebrates and aquatic macrophytes

8. RESEARCH NEEDS

During the development of the mercury fate and transport assessment, many areas of uncertainty and significant data gaps were identified. Many of these have been identified in the document, and several are presented in the following list.

1. Improved analytical techniques for measuring speciated mercury air emissions as well as total mercury emissions from major point sources. Laboratory evidence suggests that divalent mercury gas emissions will wet and dry deposit much more readily than elemental mercury gas. Particle-bound mercury is also likely to deposit relatively quickly. Current stack sampling methods do not provide sound information about the fraction of mercury emissions that are in oxidized form. While filters are used to determine particulate mercury fractions, high temperature stack samples may not be indicative of the fraction of mercury that is bound to particles after dilution and cooling in the first few seconds after emission to the atmosphere. Methods for determination of the chemical and physical forms of mercury air emissions after dilution and cooling need to be developed and used to characterize all known major point sources.
2. Evaluated Local and Regional Atmospheric Fate and Transport Models are needed. These models should treat all important chemical and physical transformations which take place in the atmosphere. The development of these models will require comprehensive field investigations to determine the important atmospheric transformation pathways (e.g., aqueous cloud chemistry, gas-phase chemistry, particle attachment, photolytic reduction) for various climatic regions. The evaluation of these models will require long-term national (possibly international) monitoring networks to quantify the actual air concentrations and surface deposition rates for the various chemical and physical forms of mercury.
3. Better understanding of mercury transport from watershed to water body including the soil chemistry of mercury, the temporal aspects of the soil equilibrium, the impact of low levels of volatile mercury species in surface soils and water bodies on total mercury concentrations and equilibrium.
4. Better understanding of foliar uptake of mercury and plant/mercury chemistry. (The most important questions: Do plants convert elemental or divalent mercury into forms of mercury that are more readily bioaccumulated? Do plants then emit these different forms to the air?) A better understanding of the condensation point for mercury is needed.
5. Better understanding of mercury movement from plant into soil (detritus). May need to refine the models used to account for movement of mercury in leaf litter to soil.
6. The impact of anthropogenic mercury on the "natural," existing mercury levels and species formed in soil, water, and sediments needs better understanding. How does the addition of anthropogenic mercury affect "natural" soil and water mercury cycles? Natural emission sources need to be studied better and their impacts better evaluated.
7. Improved understanding of mercury flux in water bodies and impact of plant and animal biomass are needed. Unlike many other pollutants, most of the methylmercury in a water body appears to be in the biological compartment. The sedimentation rate as well as benthic sediment:water

partition coefficient require field evaluation. Important to consider rivers and other larger water bodies in these flux analyses.

8. The BAF contains a substantial level of uncertainty. A more appropriate BAF can probably be developed when the data base upon which the estimate is based is enlarged; i.e., need data from more than four studies. The availability of more data would enable the possible development of lake-type adjustment factors for the mercury BAF possibly based on color, acidification susceptibility, etc., or species-specific BAF adjustment factors for freshwater species most commonly consumed. Also need a time analysis of fish mercury uptake which could lead to the development of a dynamic fish model. A mercury BAF for saltwater fish is needed.
9. Need to improve the biotransfer factors for mercury from soil and plants to beef.

9. REFERENCES

- Anderson, W. L. and K.E. Smith (1977) Dynamic of mercury at coal-fired utility power plant and adjacent cooling lake. *Environ. Sci and Technol.* 11:75.
- Bache, E., W. Gutenmann, M. Rutzke, G. Chu, D. Elfving and D. Lisk (1991) Concentrations of Metals in Grasses in the Vicinity of a Municipal Refuse Incinerator. *Arch. Environ. Contam. Toxicol.* 20:538-542.
- Baes, C., R. Sharp, A. Sjoreen and R. Shor (1984) A Review and Analysis of parameters for assessing transport of environmentally released radionuclides through agriculture. Prepared under contract No. DE-AC05-84OR21400. U.S. Department of Energy, Washington, D.C.
- Bahnick, D., C.Sauer, B. Butterworth and D. Kuehl (1994) A National Study of Mercury Contamination of Fish. *Chemosphere* 29(3):537-546.
- Benoit, J.M., W.F. Fitzgerald and A.W.H. Damman (1994) Historical Atmospheric Mercury Deposition in the Mid-Continental U.S. as Recorded in an Ombrotrophic Peat Bog. Pp. 187-202 in Watras, C.J. and J.W. Huckabee eds. Mercury Pollution Integration and Synthesis.
- Bloom, N. and W. F. Fitzgerald (1988) Determination of Volatile Mercury Species at the Picogram level by Low-Temperature Gas Chromatography with Cold-Vapor Atomic Fluorescence Detection. *Analytica Chimica Acta*, 208:151-161.
- Bloom, N. S. and C. J. Watras (1989) Observations of Methylmercury in Precipitation. *The Sci. Tot. Environ.* 87/88:191-207.
- Bloom, N. S., C. J. Watras, and J. P. Hurley (1991) Impact of Acidification on the Methylmercury Cycle of Remote Seepage Lakes. *Water, Air and Soil Poll.* 56:477-491.
- Bloom, N. S. (1992) On the Chemical Form of Mercury in Edible Fish and Marine Invertebrate Tissue. *Can. J. Fisher. Aq. Sci.* 49:1010-1017.
- Bloom, N.S. and E. Kuhn (1994) Mercury speciation in meat products, personal communication, October 1, 1994.
- Briggs, G.A. (1973) *Diffusion Estimation for Small Emissions*, ATDL Contribution File No. 79, Atmospheric Turbulence and Diffusion Laboratory.
- Briggs, G.A. (1973) *Diffusion Estimates for Small Emissions*, Atmospheric Turbulence and Diffusion Laboratory, Contribution No. 70 (Draft), Oak Ridge, Tennessee.
- Briggs, G.A. (1975) Plume Rise Predications, in *Lectures on Air Pollution and Environmental Impact Analysis*, Americal Meteorological Society, Boston, Massachusetts.
- Brosset, C. (1981) The Mercury Cycle. *Water, Air and Soil Poll.* 16:253-255.

- Brosset, C. and E. Lord (1991) Mercury in Precipitation and Ambient Air: A new Scenario. *Water, Air and Soil Poll.* 56:493-506.
- Bullock, Jr., O. R. (1994) A computationally efficient method for the characterization of sub-grid-scale precipitation variability for sulfur wet removal estimates. *Atmos. Env.*28:555-566.
- Bullock, Jr., O. R., W. G. Benjey and M. H. Keating (1997a) Modeling of regional scale atmospheric mercury transport and deposition using RELMAP. *Atmospheric Deposition of Contaminants to the Great Lakes and Coastal Waters: Joel E. Baker, Ed.* pp.323-347. SETAC Press, Pensacola, Florida.
- Bullock, Jr., O. R., K. A. Brehme and G. R. Mapp (1997b) Lagrangian modeling of mercury airmass emission, transport and deposition: An analysis of model sensitivity to emissions uncertainty. *Special Issue on Mercury as a Global Pollutant: Science of the Total Environment*, in press.
- Burke, J., M. Hoyer, G. Keeler and T. Scherbatskoy (1995) Wet Deposition of Mercury and Ambient Mercury Concentrations at a Site in the Lake Champlain Basin. *Water, Air and Soil Pollution* 80:353-362.
- Cappon, C.J. (1981) Mercury and Selenium Content and Chemical Form in Vegetable Crops Grown on Sludge-Amended Soil. *Arch. Environm. Contam. Toxicol.* 10: 673-689.
- Cappon, C. J. (1987) Uptake and Speciation of Mercury and Selenium in Vegetable Crops Grown on Compost-Treated Soil. *Water, Air and Soil Poll.* 34:353-361.
- Carpi, A., L. Weinstein and D. Ditz (1994) Bioaccumulation of Mercury by Sphagnum Moss near a Municipal Solid Waste Incinerator. *Air and Waste* 44:669-672.
- Carpi, A., and S.E. Lindberg (1997) Sunlight-Mediated Emission of Elemental Mercury from Soil Amended with Municipal Sewage Sludge. *Environmental Science and Technology*, 31(7):2085-2091.
- CARB (1986) Subroutines for calculating dry deposition velocities using Sehmel's curves. Prepared by Bart Croes, California Air Resources Board.
- CARB (1987) Subroutines for calculating dry deposition velocities using Sehmel's curves. Prepared by Bart Croes, California Air Resources Board.
- Clark, T.L., P. Blakely, G. Mapp (1992) Model calculations for the annual atmospheric deposition of toxic metals to Lake Michigan. 85th Annual Meeting for the Air and Water Management Assoc., Kansas City, MO, June 23-27.
- Cleckner, L. B., E. S. Esseks, P. G. Meier, and G. J. Keeler (1995) Mercury Concentrations in Two "Great Waters". Accepted for Publication in *Water, Air and Soil Pollution*.
- Cossa, D. M. Coquery, C. Gobeil, and J. Martin (1996) Mercury Fluxes at the Ocean margins. In: Global and Regional Mercury Cycles: Sources, Fluxes and Mass Balances. Edited by: W. Baeyens, R. Ebinghaus, and O. Vasiliev. Kluwer Academic Publishers, (Netherlands). 229-248.
- Cramer, G.M. (1992) Interoffice memorandum, April 21, 1992.

- Crockett, A. and R. Kinnison (1979) Mercury residues in soil around a coal-fired power-plant. *Envir. Sci. Technol.* 13:712-715.
- Cunningham, P. S. Smith, J. Tippet and A. Greene (1994) A National Fish Consumption Advisory Data Base: A Step Toward Consistency. *Fisheries.* 19(5):14-23.
- Dooley, J. H. (1992) Natural Sources of Mercury in the Kirkwood-Cohansey Aquifer System of the New Jersey Coastal Plain. New Jersey Geological Survey, Report 27.
- Driscoll, C. T., C. Yan, C. L. Schofield, R. Munson, and J. Holsapple (1994) The Mercury Cycle and Fish in the Adirondack Lakes. *ES+T.*
- Dvonch, J.T., A.F. Vette, G.J. Keeler, G. Evans and R. Stevens (1995) An intensive Multi-site Pilot Study Investigating Atmospheric Mercury in Broward County, Florida. *Water, Air, and Soil Pollution* 80: 169-178.
- Ebinghaus, R., and O. Kruger (1996) Emission and Local Deposition Estimates of Atmospheric Mercury in North-Western and Central Europe. Pp. 135-159 in Baeyens, W., R. Ebinghaus, and O. Vasiliev, eds., Global and Regional Mercury Cycles: Sources, Fluxes and Mass Balances.
- Eder, B. K., D. H. Coventry, T. L. Clark, and C. E. Bollinger (1986) RELMAP: A regional Lagrangian model of air pollution - users guide. Project Report, EPA/600/8-86/013, U.S. Environmental Protection Agency, Research Triangle Park, NC.
- Egan, B.A. (1975) Turbulent Diffusion in Complex Terrain, in *Lectures on Air Pollution and Environmental Impacts Analysis*, pp.112-135, D. Haugen (Ed.), American Meteorological Society, Boston, Mass.
- Engstrom D.R., E.B. Swain, T.A. Henning, M.E. Brigham and P.L. Brezonick (1994) Atmospheric Mercury Deposition to Lakes and Watersheds: A Quantitative Reconstruction from Multiple Sediment Cores. Pp. 33-66 in L.A. Baker (ed). Environmental Chemistry of Lakes and Reservoirs. American Chemical Society.
- Engstrom, D. R., and E. B. Swain (1997) Recent Declines in Atmospheric Mercury Deposition in the Upper Midwest. *Environmental Science and Technology* **31**: 960-967.
- Evans, R.D. (1986) Sources of mercury contamination in the sediments of small headwater lakes in south-central Ontario, Canada. *Arch. Environ. Contam. Toxicol.* 15:505-512.
- Expert Panel on Mercury Atmospheric Processes (1994) *Mercury Atmospheric Processes: A Synthesis Report.* Report No. TR-104214.
- Fitzgerald, W. F., R. P. Mason and G. M. Vandal (1991) Atmospheric Cycling and Air-Water Exchange of Mercury over Mid-Continental Lacustrine Regions. *Water, Air and Soil Poll.* 56:745-767.
- Fitzgerald, W. F. and T. W. Clarkson (1991) Mercury and Methylmercury: Present and Future Concerns. *Envir. Health Perspec.* 96:159-166.

Fitzgerald, W. F. (1994) Global Biogeochemical Cycling of Mercury. Presented at the DOE/FDA/EPA Workshop on Methylmercury and Human Health, Bethesda, MD March 22-23 1994.

Fitzgerald, W. F. (1995) Is Mercury Increasing in the Atmosphere? The Need for an Atmospheric Mercury Network (AMNET). *Water, Air, and Soil Pollution* **80**: 245-254.

Fitzgerald, W. F., and R. P. Mason (1996) The Global Mercury Cycle: Oceanic and Anthropogenic Aspects. Pp. 85-108 in Baeyens, W., R. Ebinghaus, and O. Vasiliev, eds., Global and Regional Mercury Cycles: Sources, Fluxes and Mass Balances.

Florida Department of Environmental Regulation (1990) Mercury, Largemouth Bass and Water Quality: A Preliminary Report.

Fortmann, L. C., D. D. Gay, and K. O. Wirtz (1978) Ethylmercury: Formation in Plant Tissues and Relation to Methylmercury Formation. U.S. EPA Ecological Research Series, EPA-600/3-78-037.

Gerstsenberger, S., J. Pratt-Shelley, M. Beattie and J. Dellinger (1993) Mercury Concentrations of Walleye (*Stizostedion vitreum vitreum*) in 34 Northern Wisconsin Lakes. *Bull. Environ. Contam. Toxicol.* **50**:612-617.

Giesy, J., D. Verbrugge, R. Othout, W. Bowerman, M. Mora, et. al. (1994) Contaminants in Fishes from Great Lakes-influenced Sections and above dams of three Michigan Rivers. I. Concentrations of organochlorine insecticides, polychlorinated biphenyls, dioxin equivalents and mercury. *Arch. Environ. Contam. Toxicol.* **27**:202-212.

Glass, G.E., J.A. Sorensen, K.W. Schmidt and G.R. Rapp (1990) New Source Identification of Mercury Contamination in the Great Lakes. *Environ. Sci. Technol.* **24** (7):1059-1069.

Glass, G., J. Sorensen, K. Schmidt, G. Rapp, D. Yap, and D. Fraser (1991) Mercury Deposition and sources for the Upper Great Lakes Region. *Water, Air and Soil Pollution.* **56**:235-249.

Glass, G.E., J.A. Sorensen, K.W. Schmidt, G.R. Rapp, D. Yap and D. Fraser (1992) Mercury Sources and Distribution in Minnesota's Aquatic Resources: Deposition. Part 1 of Chapter 4 (Mercury Washout from Precipitation: Atmospheric Sources) in Mercury in the St. Louis River, Mississippi River, Crane Lake and Sand Point Lake: Cycling, Distribution and Sources. Report to the Legislative Commission on Minnesota Resources. April, 1992. Water Quality Division Minnesota Pollution Control Agency St. Paul, MN.

Gloss, S. P., T. M. Grieb, C. T. Driscoll, C. L. Scholfield, J. P. Baker, D. H. Landers, and D. B. Porcella (1990) Mercury levels in fish from the Upper Peninsula of Michigan (ELS Subregion 2B) in Relation to Lake Acidity. USEPA Corvallis Env. Res. Lab. Corvallis.

Greenberg, A., I Wojtenko, H. Chen, S. Krivanek, J. Butler, J. Held, P. Weis and N. Reiss (1992) Mercury in Air and Rainwater in the Vicinity of a Municipal Resource Recovery Facility in Western New Jersey. Presented at International Symposium on Measurement of Toxic and Related Pollutants, Durham, NC. May 8.

Grieb, T., C. Driscoll, S. Gloss, C. Schofield, G. Bowie and D. Porcella (1990) Factors Affecting Mercury Accumulation in Fish in the Upper Michigan Peninsula. *Environ. Tox. Chem.* **9**:919-930.

- Hakanson, A. T. Andersson and A. Nilsson (1990) Mercury in Fish in Swedish Lakes-Linkages to Domestic and European Sources. *Water, Air and Soil Poll.* 50:171-191.
- Hakanson, L. A. Nilsson and T. Anderson (1988) Mercury in Fish in Swedish Lakes. *Environmental Pollution.* 49:145-162.
- Hanson, P.J., S.E. Lindberg, K.H. Kim, J.G. Owens and T.A. Tabberer (1994) Air/Surface Exchange of Mercury Vapor in the Forest Canopy I. Laboratory Studies of Foliar Hg Vapor Exchange. 3rd International Conference on Mercury as a Global Pollutant. Whistler, BC, Canada (July 10-14, 1994)
- Hanson, P.J., S.E. Lindberg, T.A. Tabberer, J.G. Owens and K.-H. Kim (1995) Foliar exchange of mercury vapor: Evidence for a compensation point. *Water, Air and Soil Pollution* 80:373-382.
- Harris, R., Gherini, S.A., and Hudson, R. (1996) Regional Mercury Cycling Model (R-MCM): A Model for Mercury Cycling in Lakes, Draft User's Guide and Technical Reference. Prepared for The Electric Power Research Institute, Palo Alto, CA and Wisconsin Department of Natural Resources, Monona, WI.
- Hatch, W. and W. Ott. (1968) Determination of submicrogram quantities of mercury by atomic absorption spectrophotometry. *Anal. Chem.* 40:2085 - 2087.
- Hewett and Johnson (1992) Fish Bioenergetics Model 2. University of Wisconsin Sea Grant Institute (WIS-SG-91-250).
- Hicks, B.B., D.D. Baldocchi, T.P Meyers, R.P. Hosker, Jr., and D.R. Matt (1987) A preliminary multiple resistance routine for deriving dry deposition velocities from measured quantities. *Water, Air, and Soil Pollution* 36: 311-330.
- Hovart, M., N. S. Bloom, L. Liang (1993a) Comparison of distillation with other current isolation methods for the determination of methylmercury compounds in low level environmental samples. Part I: Sediments. *Analytica Chimica Acta*, 281:135-152.
- Hovart, M., L. Liang, N. S. Bloom (1993b) Comparison of distillation with other current isolation methods for the determination of methylmercury compounds in low level environmental samples. Part II: Water. *Analytica Chimica Acta*, 282:153-168.
- Hoyer, M., J. Burke and G. Keeler (1995) Atmospheric sources, transport and deposition of mercury in Michigan: Two years of event precipitation. *Water, Air and Soil Pollution* 80:199-208.
- Hudson, R.J.M., Gherini, S.A., Watras, C.J., and Porcella, D.P. (1993) "Modeling the Biogeochemical Cycle of Mercury in Lakes: the Mercury Cycling Model (Mcm) and its Application to the Mtl Study Lakes." *Mercury as a Global Pollutant: Toward Integration and Synthesis*, W.J. Watras and J.W. Huckabee, Eds, Lewis Publishers.
- Hudson, R., S. Gherini, W. Fitzgerald, and D. Porcella (1995) Anthropogenic influences on the global mercury cycle: a model-based analysis. *Water, Air, and Soil Pollution* 80:265-272.
- Hurley, J.P., Benoit, J.M., Babiarz, C.L., Shafer, M.M., Andren, A.W., Sullivan, J.R., Hammond, R., and Webb, D. (1995) Influences of Watershed Characteristics on Mercury Levels in Wisconsin Rivers. *Environmental Science and Technology*, 29(7):1867-1875.

Iverfeldt, A., and O. Lindqvist (1986) Atmospheric oxidation of elemental mercury by ozone in the aqueous phase. *Atmospheric Environment* 20:1567-1573.

Iverfeldt, Å. (1991) Occupance and turnover of atmospheric mercury over the nordic countries. *Water, Air and Soil Pollution* 56:251-265.

Jensen, A. and A. Jensen (1991) Historical Deposition Rates of Mercury in Scandinavia Estimated by Dating and Measurement in Cores of Peat Bogs. *Water, Air and Soil Poll.* 56:769-777.

Jensen, A., and A. Iverfeldt (1994) Atmospheric Bulk Deposition of Mercury to the Southern Baltic Sea Area. Pp. 221-229 in Watras, C. J., and J. W. Huckabee eds. Mercury Pollution: Integration and Synthesis.

Johansson, K., M. Aastrup, A. Andersson, L. Bringmark and A Iverfeldt (1991) Mercury in Swedish Forest Soils and Waters-Assessment of Critical Load. *Water, Air and Soil Pollution.*56:267-281.

John, M.K. (1972) Mercury Uptake from Soil by Various Plant Species. *Bull. Environ. Contam. Toxicol.* 8(2): 77-80.

Jernelov, A. and T. Wallin (1973) Air-borne Mercury Fallout on Snow around five Swedish Chlor-alkali Plants. *Atmos. Environ.* 7:209-214.

Keeler, G., M. Hoyer, and C. Lamborg (1994) Measurements of Atmospheric Mercury in the Great Lakes Basin. Pp. 231-241 in Watras, C.J. and J.W. Huckabee eds. Mercury Pollution Integration and Synthesis.

Keeler, G., G. Glinsorn and N. Pirrone (1995) Particulate Mercury in the Atmosphere: Its Significance, Transport, Transformation and Sources. *Water, Air and Soil Pollution* 80:159-168.

Keeler, G. J. (1997) Lake Michigan mass balance study atmospheric mercury data report. Submitted to the U. S. Environmental Protection Agency, Great Lakes National Program Office, Chicago, Illinois, for Grant No. GL995569-01

Lambourg, C., W. Fitzgerald, G. Vandal, and K. Rolfhus (1995) Atmospheric Mercury in Northern Wisconsin: Sources and Species. *Water Air Soil Pollut.* 80:189-198.

Lambourg, C.H., M.E. Hoyer, G.J. Keeler, I. Olmez and X. Huang (1994) Particulate-Phase Mercury in the Atmosphere: Collection/Analysis Method Development and Applications. Pp. 251-259 in Watras, C.J. and J.W. Huckabee eds. Mercury Pollution Integration and Synthesis.

Lange, T. R., H. R. Royals, and L. L. Conner (1993) Influence of Water Chemistry on Mercury Concentrations in Largemouth Bass from Florida Lakes. *Trans. Amer. Fish. Soc.* 122:74-84.

Lathrop, R. C., K. C. Noonan, P. M. Guenther, T. L. Grasino, and P. W. Rasmussen (1989) Mercury Levels in Walleyes from Wisconsin Lakes of different Water and Sediment Chemistry Characteristics. Tech. Bull. No. 163. DNR, State of Wisconsin, Madison.

Lenka, M., K. K. Panda, and B. B. Panda (1992) Monitoring and Assessment of Mercury Pollution in the Vicinity of a Chloralkali Plant. IV. Bioconcentration of Mercury in *In Situ* Aquatic and Terrestrial Plants at Ganjam, India. *Arch. Environ. Contam. Toxicol.* 22:195-202.

Lee, Y. and A. Iverfeldt (1991) Measurement of Methylmercury and Mercury in Run-off, Lake and Rain Waters. *Water, Air and Soil Poll.* 56:309-321.

Lindberg, S. E., D. R. Jackson, J. W. Huckabee, S. A. Janzen, M. J. Levin, and J. R. Lund (1979) Atmospheric Emission and Plant Uptake of Mercury from Agricultural Soils near the Almaden Mercury Mine. *J. Environ. Qual.* 8(4):572-578.

Lindberg, S. E., R. R. Turner, T. P. Meyers, G. E. Taylor, and W. H. Schroeder (1991) Atmospheric Concentrations and Deposition of Hg to a Deciduous Forest at Walker Branch Watershed, Tennessee, USA. *Water, Air and Soil Poll.* 56:577-594.

Lindberg, S. E., T. P. Meyers, G. E. Taylor, R. R. Turner, and W. H. Schroeder (1992) Atmosphere-Surface Exchange of Mercury to a Forest: Results of Modelling and Gradient Approaches. *J. of Geophys. Res.* 97(D2):2519-2528.

Lindberg, S. and S. Vermette (1995) Workshop on sampling mercury in precipitation for the National Atmospheric Deposition Program. *Atmospheric Environment* 29:1219-1220.

Lindberg, S.E. (1996) Forests and the Global Biogeochemical Cycle of Mercury: The Importance of Understanding Air/Vegetation Exchange Processes. W. Baeyens et al. (Eds.), *Global and Regional Mercury Cycles: Sources, Fluxes, and Mass Balances*, 359-380.

Lindqvist, O. and H. Rodhe (1985) Atmospheric Mercury-a review. *Tellus.* 37B:136-159.

Lindqvist, O., K. Johansson, M. Aastrup, A. Andersson, L. Bringmark, G. Hovsenius, L. Hakanson, A. Iverfeldt, M. Meili, and B. Timm (1991) Mercury in the Swedish Environment - Recent Research on Causes, Consequences and Corrective Methods. *Water, Air and Soil Poll.* 55:(all chapters)

Lowe TP, May TW, Brumbaugh WG, and Kane DA (1985) National Contaminant Biomonitoring Program: Concentrations of seven elements in fresh-water fish, 1978-1981. *Arch. Environ. Contamin. Toxicol.* 14: 363-388.

Lucotte, M., A. Mucci, C. Hillaire-Marcel, P. Pichet, and A. Grondin (1995) Anthropogenic Mercury Enrichment in Remote Lakes of Northern Quebec (Canada). *Water, Air, and Soil Pollution* 80: 467-476.

MacCrimmon, H. R., C. D. Wren, and B. L. Gots (1983) Mercury Uptake by Lake Trout, *Salvelinus namaycush*, relative to age, growth and diet in Tadenac Lake with comparative data from other Precambrian Shield lakes. *Can. J. Fisher. Aq. Sci.* 40:114-120.

Mason, R., and W. Fitzgerald (1993) The distribution and biogeochemical cycling of mercury in the equatorial Pacific Ocean. *Deep Sea Resch.* 40(9):1897-1924.

Mason, R., and W. Fitzgerald (1996) Sources, Sinks and Biogeochemical Cycling of Mercury in the Ocean. In: *Global and Regional Mercury Cycles: Sources, Fluxes and Mass Balances*. Edited by: W. Baeyens, R. Ebinghaus, and O. Vasiliev. Kluwer Academic Publishers, (Netherlands). 249-272.

- Mason, R.P., W.F. Fitzgerald and F.M.M. Morel (1994) The Biogeochemical Cycling of Elemental Mercury: Anthropogenic Influences. *Geochimica et Cosmochimica Acta*. 58(15):3191-3198.
- Mason, R., F. Morel and H. Egmond (1995) The role of microorganisms in elemental mercury formation in natural waters. *Water Air Soil Pollut* 80:775-787.
- McIntyre, J.W., J.T. Hickey, K. Karwowski, C.L. Holmquist, and K. Carr (1993) In *Proceedings fo the 1992 Conference on the Loon and its Ecosystem Status*. Edited by L. Morse and M. Pokras. Concord, NH. U.S. Fish and Wildlife Service, pp. 73-91.
- Meili, M., A. Iverfeldt and L. Hakanson (1991) Mercury in the Surface Water of Swedish Forest Lakes - Concentrations, Speciation and Controlling Factors, *Water, Air, and Soil Pollution* 56: 439-453.
- Michigan Environmental Science Board (1993) Mercury in Michigan's Environment: Environmental and Human Health Concerns. Report to Gov. John Engler.
- Mierle, G. and R. Ingram (1991) The Role of Humic Substances in the Mobilization of Mercury from Watersheds. *Water, Air and Soil Poll.* 56:349-357.
- Mills, E.L., W.H. Gutenmann, and D.J. Lisk (1994) Mercury content of small pan fish from New York State Waters, *Chemosphere*, Vol. 29, No. 6, pp. 1357-1359.
- Mills, W.B., D.B. Porcella, M.J. Unga, S.A. Gherini, K.V. Summers, Lingfung Mok, G.L. Rupp and G.L. Bowie (1985) Water Quality Assessment: A Screening Procedure for Toxic and Conventional Pollutants in Surface and Ground Waters (Revised 1985), EPA-600/6-85-002a and b. Volumes I and II. U.S. Environmental Protection Agency. Athens, GA.
- Mitra, S. (1986) Mercury in the Ecosystem. Trans Tech Publications Ltd. Switzerland.
- Mosbaek, H., J. C. Tjell, and T. Sevel (1988) Plant Uptake of Mercury in Background Areas. *Chemosphere* 17(6):1227-1236.
- Munthe, J., Z.F. Xiao, and O. Lindqvist (1991) The aqueous reduction of divalent mercury by sulfite. *Water Air Soil Pollut.* 56:621-630.
- Munthe, J. (1992) The aqueous oxidation of elemental mercury by ozone. *Atmospheric Environment* 26A:1461-1468.
- Munthe, J., and W. McElroy (1992) Some aqueous reactions of potential importance in the atmospheric chemistry of mercury. *Atmospheric Environment* 26A:553-557.
- Nagase, H., Y. Ose, T. Sato, and T. Ishikawa. (1982) Methylation of Mercury by Humic Substances in an Aquatic Environment. *Sci. Total Environ.* 32:147-156.
- NAS (National Academy of Science) (1977) An Assessment of Mercury in the Environment. Safe Drinking Water Committee, National Research Council.
- Nater, E. and D. Grigal (1992) Regional Trends in Mercury Distribution across the Great Lakes States, north central USA. *Nature* 358:139-141.

New Jersey Department of Environmental Protection and Energy (1993) Final Report on Municipal Solid Waste Incineration. Volume II: Environmental and Health Issues.

New Jersey Department of Environmental Protection and Energy Division of Science and Research (1994) Preliminary Assessment of Total Mercury Concentrations in Fishes from Rivers, Lakes and Reservoirs of New Jersey. 93-15F.

New York State Department of Environmental Conservation (1990) Chemical Contaminants in Fish from the St. Lawrence River Drainage on Lands of the Mohawk Nation at Akwesasne and Near the General Motors Corporation /Central Foundry Division Massena, New York Plant. Technical Report 90-1.

Newton, I., I. Wyllie, and A. Asher (1993) Long-term trends in organochlorine and mercury residues in some predatory birds in Britain. *Environ. Pollut.* 79:143-151.

NOAA (1978) as described in the NMFS data base.

Nriagu, J. O. (1979) The Biogeochemistry of Mercury in the Environment. Elsevier/North Holland. Biomedical Press: New York.

O'Conner, T.P. and B. Beliaeff (1995) Recent Trends in Coastal Environmental Quality: Results from the Mussel Watch Project. 1986 to 1993. U.S. Department of Commerce, National Oceanic and Atmospheric Administration, National Ocean Service, Office of Ocean Resources Conservation and Assessment, Silver Spring, MD.

Olmez, I., G. Keeler and P. Hopke (1994) Interim Data Interpretation Report of MIT/ALSC Data Set (MIT Report No. MITNRL-060).

Parks, J. W., A. Lutz, and J. A. Sutton (1989) Water Column Methylmercury in the Wabigoon/English River-Lake System: Factors Controlling Concentrations, Speciation, and Net Production. *Can. J. Fisher. Aq. Sci.* 46:2184-2202.

Pauling, L. (1963) College Chemistry, 3rd Edition. Freeman Press, NY., p. 505.

PEI Associates, Inc and H.E. Cramer Company, Inc. (1986) Air quality modeling analysis of municipal waste combustors. Prepared for Monitoring and Data Analysis Division, Office of Air Quality Planning and Standards, Research Triangle Park, North Carolina 27711.

Penner, J. E., H. Eddleman, and T. Novakov (1993) Towards the development of a global inventory for black carbon emissions. *Atmospheric Environment* 27A:1277-1295.

Petersen, G., Å. Iverfeldt and J. Munthe, (1995) Atmospheric mercury species over Central and Northern Europe. Model calculations and comparison with observations from the Nordic Air and Precipitation Network for 1987 and 1988. *Atmospheric Environment* 29:47-68.

Pollman, C. D., G. A. Gill, W. M. Landing, D. A. Bare, J. Guentzel, D. Porcella, E. Zillioux, and T. Atkeson. (1994) Overview of the Florida Atmospheric Mercury Study (FAMS).

- Porcella, D.B. (1994) Mercury in the Environment: Biogeochemistry. Pp. 3-19 in Watras, C.J. and J.W. Huckabee eds. Mercury Pollution Integration and Synthesis.
- Porcella, D. B., P. Chu, and M. A. Allan (1996) Inventory of North American Hg Emissions to the Atmosphere: Relationship to the Global Mercury Cycle. Pp. 179-190 in Baeyens, W., R. Ebinghaus, and O. Vasiliev, eds., Global and Regional Mercury Cycles: Sources, Fluxes and Mass Balances.
- Rada, R., J Wiener, M. Winfrey, and D. Powell (1989) Recent increases in atmospheric deposition of mercury to north-central Wisconsin Lakes inferred from sediment Analysis. *Arch. Environ. Contam. Toxicol.* 18:175-181.
- Revis, N. W., T. R. Osborne, G. Holdsworth, and C. Hadden (1990) Mercury in Soil: A Method for Assessing Acceptable Limits. *Arch. Environ. Contam. Toxicol.*, 19:221-226.
- Rolfus, K., and W. Fitzgerald (1995) Linkages between atmospheric mercury deposition and the methylmercury content of marine fish. *Water Air Soil Pollution* 80:291-297
- Sanemasa, I. (1975) The solubility of elemental mercury vapor in water. *Bulletin of the Chemical Society of Japan*, 48:1795-1798.
- Schuster, E (1991) The Behavior of Mercury in the Soil with special emphasis on Complexation and Adsorption processes- A Review of the Literature. *Water, Air and Soil Poll.* 56:667-680.
- Schofield, C.L., Driscoll, C.T., Munson, R.K., Yan C., and Holsapple, J.G. (1994) The Mercury Cycle and Fish in the Adirondack Lakes. *Environmental Science and Technology*, 28(3):136A-143A.
- Schroeder, W. H. and R. A. Jackson (1987) Environmental Measurements with an Atmospheric Mercury Monitor having Specific Capabilities. *Chemosphere*, 16:183-199.
- Schroeder, W., G. Yarwood, and H. Niki (1991) Transformation processes involving mercury species in the atmosphere: Results from a literature survey. *Water, Air, and Soil Pollution.* 56:653-666.
- Seinfeld, J. H. (1986) *Atmospheric Chemistry and Physics of Air Pollution*, John Wiley and Sons, New York, p. 198-200.
- Seritti, A., A. Petrosino, E. Morelli, R. Ferrara, and C. Barghigiani (1982) The biogeochemical cycling of mercury in the Mediterranean. Part I: Particulate and dissolved forms of mercury in the northern Tyrrhenian Sea. *Environ. Tech. Lett.* 3:251-256.
- Shannon, J. D., and E. C. Voldner (1994) Modelling Atmospheric Concentrations and Deposition of Mercury to the Great Lakes. Presented at the DOE/FDA/EPA Workshop on Methylmercury and Human Health, Bethesda, MD March 22-23 1994.
- Shitara, K., and A. Yasumasa (1976) *Hokkaidoritzu Eigel kenkyushoho Hokkaidorita* 26:73-78.
- Simonin, H. A., S. P. Gloss, C. T. Driscoll, C. L. Schofield, W. A. Kretser, R. W. Karcher, and J. Symula (1994) Mercury in Yellow Perch from Adirondack Drainage Lakes (New York, U.S.), soon to be published in: (1994) Watras, C. J. and J. W. Huckabee [eds], Mercury Pollution: Integration and Synthesis, Lewis Publishers, Boca Raton, FL (in press).

Skinner, L.C., S.J. Jackling, G. Kimber, J. Waldman, J. Shastay, and A.J. Newell (1996) Chemicals in Fish, Shellfish and Crustaceans from the New York-New Jersey Harbor Estuary: PCB, Organochlorine Pesticides, and Mercury. New York State Department of Environmental Conservation, Division of Fish, Wildlife and Marine Resources, Albany, NY.

Slemr, F. (1996) Trends in Atmospheric Mercury Concentrations over the Atlantic Ocean and at the Wank Summit, and the Resulting Constraints on the Budget of Atmospheric Mercury. Pp. 33-84 in Baeyens, W., R. Ebinghaus, and O. Vasiliev, eds., Global and Regional Mercury Cycles: Sources, Fluxes and Mass Balances.

Slinn, W.G.N. (1984) Precipitation Scavenging, in *Atmospheric Science and Power Production*, D. Randerson, ed. DOE/TIC-27601.

Sloan, R. (1990) Trends in Mercury Concentrations of the Fish of Onondaga Lake, in Proceedings of the Onondaga Lake Remediation Conference, Bolton Landing, NY, February 5-8 1990.

Sorensen, J., G. Glass, K. Schmidt, J. Huber and G. Rapp (1990) Airborne Mercury Deposition and Watershed Characteristics in Relation to Mercury Concentrations in Water, Sediments, Plankton and Fish of Eighty Northern Minnesota Lakes. *Environ. Sci. Technol.* 24:1716-1727.

Sorensen, J., G. Glass, K. Schmidt, and G. Rapp (1991) Mercury Concentrations in Fish from the St. Louis River Near the Fond Du Lac-Indian Reservation (Below the Cloquet and White Pine Rivers). First Year Report on the St. Louis River Water Resources Project.

Sorensen, J.A., G.E. Glass and K.W. Schmidt (1992) Regional Patterns of Mercury Wet Deposition and Major Ions. Part 2 of Chapter 4 in Mercury in the St. Louis River, Mississippi River, Crane Lake and Sand Point Lake: Cycling, Distribution and Sources. Report to the Legislative Commission on Minnesota Resources. April, 1992. Water Quality Division Minnesota Pollution Control Agency St. Paul, MN.

Sorensen, J.A., G.E. Glass and K.W. Schmidt (1994) Regional Patterns of Mercury Wet Deposition. *Environ. Sci. Tech.* 28:2025-2032.

St. Louis, V.L., Rudd, J.W., Kelly, C.A., Beaty, K.G., Flett, R.J.K., and Roulet, N.T. (1996) Production and Loss of Methylmercury and Loss of Total Mercury from Boreal Forest Catchments Containing Different Types of Wetlands. *Environmental Science and Technology*, 30(9):2719-2729.

Stafford, C. P. (1994) Mercury Concentrations in Maine Predatory Fishes. Masters Thesis, University of Maine.

Stevens, R. K., R. Zweidinger, E. Edgerton, W. Mayhew, R. Kellog and G. Keeler (1996) Source characterization in support of modeling the transport of mercury emissions in south Florida. *4th International Conference on Mercury as a Global Pollutant*, August 4-8, 1996, Hamburg, Germany.

Strobel, C.J., S.J. Benyi, D.J. Keith, H.W. Buffum, E.A. Petrocelli, N.I. Rubinstein, and B. Melzian. (1994) Statistical Summary: EMAP-Estuaries Virginia Province - 1992. United States Environmental Protection Agency, Environmental Research Laboratory, Narragansett, RI. EPA/620/R-94/019.

Somu, E., B.R. Singh, A.R. Selmer-Olsen, and K. Steenburg (1985) Uptake of ²⁰³Hg-labeled Mercury compounds by Wheat and Beans Grown on an oxisol. *Plant and Soil* 85: 347-355.

Sukhenko, S. A., and O. F. Vasiliev (1996) A Regional Mercury Budget for Siberia and the Role of the Region in Global Cycling of the Metal. Pp. 123-133 in Baeyens, W., R. Ebinghaus, and O. Vasiliev, eds., Global and Regional Mercury Cycles: Sources, Fluxes and Mass Balances.

Swain, E. B., and D. D. Helwig (1989) Mercury in Fish from Northeastern Minnesota Lakes: Historical Trends, Environmental Correlates, and Potential Sources. *Journal of the Minnesota Academy of Science* 55:103-109.

Swain, E. B., D. A. Engstrom, M. E. Brigham, T. A. Henning, and P. L. Brezonik. (1992) Increasing Rates of Atmospheric Mercury Deposition in Midcontinental North America. *Science* 257:784-787.

Swedish EPA (1991) Mercury in the Environment: Problems and Remedial Measures in Sweden. ISBN 91-620-1105-7.

Szymczak, J. and H. Grajeta.(1992) Mercury Concentrations in Soil and Plant Material, *Pol. J. Food Nutr. Sci.*, Vol 1/42, No.2, pp.31-39.

Tamura, R., M. Fukuzaki, Y. Hirano, and Y. Mitzushima (1985) Evaluation of Mercury Contamination using Plant Leaves and Humus as Indicators. *Chemosphere* 14(11/12):1687-1693.

Temmerman, L. R., R. Vandeputte, and M. Guns (1986) Biological Monitoring and Accumulation of Airborne Mercury in Vegetables. *Environ. Poll.*, 41:139-151.

Temple, P. J. and S. N. Linzon (1977) Contamination of Vegetation, Soil, Snow and Garden Crops by Atmospheric Deposition of Mercury from a Chlor-Alkali Plant, in (1977) D. D. Hemphill [ed] Trace Substances in Environmental Health - XI, Univ Missouri, Columbia. p. 389-398.

U.S. Department of Commerce (1978) Report on the chance of U.S. seafood consumers exceeding the current acceptable daily of mercury and on recommended regulatory controls. National Oceanic and Atmospheric Administration, Washington, DC.

U.S. EPA (1975) Control of Water Pollution from Cropland: Volume I, A Manual for Guideline Development. EPA-600/2-75-026a. Office of Research and Development.

U.S. EPA (1976) Control of Water Pollution from Cropland: Volume I, An Overview. EPA-600/2-75-026b. Office of Research and Development.

U.S. EPA (1985) *Water Quality Assessment: A Screening Procedure for Toxic and Conventional Pollutants in Surface and Ground Water (Part 1)*. Washington, D.C. EPA/600/6-85/002-A.

U.S. EPA (1988) Drinking Water Criteria Document for Inorganic Mercury. ECAO-CIN-025

U.S. EPA (1990) Methodology for Assessing Health Risks Associated with Indirect Exposure to Combustor Emission. Interim Final. EPA/600/6-90/003.

U.S. EPA (1990) Addendum to: 1990 External review draft of Methodology for Assessing Health Risks Associated with Indirect Exposure to Combustor Emission. Interim Final. EPA/600/6-90/003.

U.S. EPA (1991) Feasibility of Environmental Monitoring and Exposure Assessment for a Municipal Waste Combustor: Rutland, Vermont Pilot Study. EPA/600/8-91/007.

U.S. EPA (1992a) Assessment and Remediation of Contaminated Sediments (ARCS) Program. EPA 905-R92-007.

U.S. EPA (1992b) Assessment and Remediation of Contaminated Sediments (ARCS) Program. EPA 905-R92-008.

U.S. EPA (1992c) National Study of Chemical Residues in Fish. EPA 823-R-92-008a.

U.S. EPA (1993) Summary Review of Health Effects Associated with Mercuric Chloride. Office of Health and Environmental Assessment, Washington, D.C. EPA/600/R-92/1993. September 1993.

U.S. EPA (1997) Locating and Estimating Air Emissions from Sources of Mercury and Mercury Compounds. Final Draft Report. Research Triangle Park, NC.

Vandal, G. and W. Fitzgerald (1995) A Preliminary Mercury budget for Narragansett Bay (Rhode Island, USA). *Water, Air and Soil Pollut.* 80:679-682.

Vanoni, V.A. (Ed.) (1975) Sedimentation Engineering. American Society of Civil Engineers, New York.

Vermette, S., S. Lindberg and N. Bloom (1995) Field tests for a Regional Mercury Deposition Network - Sampling design and preliminary test results. *Atmospheric Environment* 29:1247-1251.

Verta, M., and Matilainen, T. (1995) Methylmercury Distribution and Partitioning in Stratified Finnish Forest Lakes. *Water, Air and Soil Pollution*, 80:585-588.

Vreman, K., N.J. van der Veen, E.J. van der Molen and W.G. de Ruig (1986) Transfer of cadmium, lead, mercury and arsenic from feed into milk and various tissues of dairy cows: chemical and pathological data. *Netherlands Journal of Agricultural Science* 34:129-144.

Walcek, C.J., R.A. Brost, J.S. Chang, and M.L. Wesely (1985) SO₂, sulfate, and HNO₃ deposition velocities computed using regional land use and meteorological data. *Atmospheric Environment* 20:949-964.

Watras, C. J. and N. S. Bloom (1992) Mercury and Methylmercury in Individual Zooplankton: Implications for bioaccumulation. *Limnol. Oceanogr.*, 37(6):1313-1318.

Watras, C.J., N. S. Bloom, R.J.M. Hudson, S. Gherini, R. Munson, S.A. Claas, K. A. Morrison, J. Hurley, J.G. Wiener, W.F. Fitzgerald, R. Mason, G. Vandal, D. Powell, R. Rada, L. Rislov, M. Winfrey, J. Elder, D. Krabbenhoft, A.W. Andren, C. Babiarz, D.B. Porcella, and J.W. Huckabee (1994) Sources and Fates of Mercury and Methylmercury in Wisconsin Lakes. In *Mercury Pollution: Integration and Synthesis*, C.J. Watras and J.W. Huckabee, eds. Lewis Publishers, Boca Raton.

Watras, C.J., Morrison, K.A., and Host, J.S. (1995) Concentration of Mercury Species in Relationship to Other Site-Specific Factors in the Surface Waters of Northern Wisconsin Lakes. *Limnology and Oceanography*, 40(3): 556-565.

- Weber, J. (1993) Review of possible paths for abiotic methylation of mercury(II) in the aquatic environment. *Chemosphere* 26(11):2063-2077.
- Wesely, M.L. (1986) On the parameterization of dry deposition of acidifying substances for regional models. Internal Report (Nov. 1986): Interagency Agreement DW89930060-01 to the U.S. Department of Energy, U.S. Environmental Protection Agency, Atmospheric Sciences Research Laboratory, Research Triangle Park, NC, 23 pp.
- Westling, O. (1991) Mercury in runoff from drained and undrained peatlands in Sweden. *Water Air Soil Pollut.* 56:251.
- Whitby, K. (1978) The physical characteristics of sulfur aerosols. *Atmosph. Env.* 12:135-159.
- Wiener, J., W. Fitzgerald, C. Watras and R. Rada. (1990) Partitioning and Bioavailability of Mercury in an Experimentally Acidified Wisconsin Lake. *Environ. Toxicol. Chem.* 9:909-918.
- Wiersma, D., B. J. van Goor, and N. G. van der Veen (1986) Cadmium, Lead, Mercury, and Arsenic Concentrations in Crops and Corresponding Soils in the Netherlands. *J. Agric. Food Chem.*, 34:1067-1074.
- Wilken, R. D. and H. Hintelmann (1991) Mercury and Methylmercury in Sediments and Suspended particles from the River Elbe, North Germany. *Water, Air and Soil Poll.* 56:427-437.
- Winfrey, M. R. and J. W. M. Rudd (1990) Environmental Factors Affecting the Formation of Methylmercury in Low pH Lakes. *Environ. Toxicol. and Chem.*, 9:853-869.
- World Health Organization (1976) Environmental Health Criteria I, Mercury. Geneva.
- World Health Organization (1989) Environmental Health Criteria 86: Mercury Environmental Aspects. Geneva.
- World Health Organization (1990) Environmental Health Criteria 101: Methylmercury. Geneva.
- Wren, C. D., W. A. Scheinder, D. L. Wales, B. M. Muncaster, and I. M. Gray (1991) Relation Between Mercury Concentrations in Walleye (*Sitizostedion vitreum vitreum*) and Northern Pike (*Esox lucius*) in Ontario Lakes and Influence of Environmental Factors. *Can. J. Fisher. Aq. Sci.* 44:750-757.
- Xiao, Z., D. Stromberg, and O. Lindqvist (1995) Influence of Humic Substances on photolysis of divalent mercury in aqueous solution. *WASP* 80:789-798.
- Xun, L., N. Campbell and J.W. Rudd (1987) Measurements of Specific Rates of Net Methyl Mercury Production in the Water Column and Surface Sediments of Acidified and Circumneutral Lakes. *Can. J. Fish Aquat. Sci.* 44:750-757.

APPENDIX A

ATMOSPHERIC MODELING PARAMETERS

TABLE OF CONTENTS

	<u>Page</u>
A. ATMOSPHERIC MODELING PARAMETERS	A-1
A.1 Phase and Oxidation State of Emitted Mercury	A-1
A.2 Modeling the Deposition of Mercury	A-2
A.3 References	A-6

LIST OF TABLES AND FIGURES

<u>Tables</u>	<u>Page</u>
A-1 Representative Particle Sizes and Size Distribution Assumed for Divalent Mercury Particulate Emissions	A-2
A-2 Parameter Values Assumed for Calculation of Dry Deposition Velocities for Divalent Mercury Vapor	A-3
A-3 Air Modeling Parameter Values Used in the Exposure Assessment: Generic Parameters ...	A-5

<u>Figures</u>	<u>Page</u>
A-1 Wet Deposition Scavenging Ratios Used in Local Scale Air Modeling for Particulate-Bound Mercury (Jindal and Heinold 1991)	A-4

A. ATMOSPHERIC MODELING PARAMETERS

In this appendix, a summary is provided of the local scale air modeling performed. The program used to model the transport of the anthropogenic mercury with 50 km was the ISC3 gas deposition model, obtained from USEPA's Support Center for Regulatory Air Models (SCRAM) website (the program is called GDISCDFT). This model has a gas dry deposition model that was applied in this study.

A.1 Phase and Oxidation State of Emitted Mercury

Reports describe several forms of mercury detected in the emissions from the selected sources. Primarily, these include elemental mercury (Hg^0) and inorganic mercuric (Hg^{2+}). Generally, only total mercury has been measured in emission analyses. The reports of MHg in emissions are imprecise. It is believed that, if MHg is emitted from industrial processes and combustion sources, the quantities emitted are much smaller than emissions of Hg^0 and Hg^{+2} . Only Hg^0 and Hg^{+2} were considered in the air dispersion modeling.

The two types of mercury species considered in the emissions are expected to behave quite differently once emitted from the stack. Hg^0 , due to its high vapor pressure and low water solubility, is not expected to deposit close to the facility. In contrast, Hg^{2+} , because of differences in these properties, is expected to deposit in greater quantities closer to the emission sources.

At the point of stack emission and during atmospheric transport, the contaminant is partitioned between two physical phases: vapor and particle-bound. The mechanisms of transport of these two phases are quite different. Particle-bound contaminants can be removed from the atmosphere by both wet deposition (precipitation scavenging) and dry deposition (gravitational settling, Brownian diffusion). Vapor phase contaminants may also be depleted by these processes, although historically their main impacts were considered to be through absorption into plant tissues (air-to-leaf transfer) and human exposure (which may occur through inhalation).

For the present analysis, the vapor/particle (V/P) ratio was assumed to be equal to the V/P ratio as it would exist in stack emissions. It is recognized that this is a simplification of actual conditions, as the ratio when emitted from the stack is likely to change as the distance from the stack increases. The air concentration used for inhalation was taken as the sum of the vapor and particle air concentrations.

The particle-size distribution may differ from one combustion process to another, depending on the type of furnace and design of combustion chamber, composition of feed/fuel, particulate matter removal efficiency and design of air pollution control equipment, and amount of air in excess of stoichiometric amounts that is used to sustain the temperature of combustion. The particle size distribution used is an estimate of the distribution within an ambient air aerosol mass and not at stack tip. Based on this assumption, an aerosol particle distribution based on data collected by Whitby (1978) was used. This distribution is split between two modes: accumulation and coarse particles. The geometric mean diameter of several hundred measurements indicates that the accumulation mode dominates particle size, and a representative particle diameter for this mode is 0.3 microns. The coarse particles are formed largely from mechanical processes that suspend dust, sea spray and soil particles in the air. A representative diameter for coarse particles is 5.7 microns. The fraction of particle emissions assigned to each particle class is approximated based on the determination of the density of surface area of each representative particle size relative to total surface area of the aerosol mass. Using this method, approximately 93% and 7% of the total surface area is estimated to be in the 0.3 and 5.7 micron diameter particles, respectively (Table A-1).

Table A-1
Representative Particle Sizes and Size Distribution
Assumed for Divalent Mercury Particulate Emissions

Representative Particle Size (microns)*	Assumed Fraction of Particle Emissions in Size Category
0.3	0.93
5.7	0.07

*These values are based on the geometric means of aerosol particle distribution measurements as described in Whitby (1978).

The speciation estimates for the model plants were made from thermal-chemical modeling of mercury compounds in flue gas, from the interpretation of bench and pilot scale combustor experiments, and from interpretation of available field test results. The amount of uncertainty surrounding the emission rates data varies for each source. There is also a great deal of uncertainty with respect to the species of mercury emitted.

Although the speciation may change with distance from the local source, it was assumed for this analysis that there were no plume reactions that significantly modified the speciation at the local source. Because of the differences in deposition characteristics of the two forms of mercury considered, the assumption of no plume chemistry is a particularly important source of uncertainty.

A.2 Modeling the Deposition of Mercury

Once emitted from a source, the mercury may be deposited to the ground via two main processes: wet and dry deposition. Wet deposition refers to the mass transfer of dissolved gaseous or suspended particulate mercury species from the atmosphere to the earth's surface by precipitation, while dry deposition refers to such mass transfer in the absence of precipitation.

The deposition properties of the two species of mercury addressed in stack emissions, elemental and divalent mercury, are considered to be quite different. Due to its higher solubility, divalent mercury vapor is thought to deposit much more rapidly than elemental mercury. However, at this time no conclusive data exist to support accurate quantification of the deposition rate of divalent mercury vapor. In this analysis, nitric acid vapor is used as a surrogate for Hg⁺⁺ vapor based on their similar solubilities in water. Whether a pollutant is in the vapor form or particle-bound is also important for estimating deposition, and each is treated separately.

Dry deposition is estimated by multiplying the predicted air concentration at ground level by a deposition velocity. For particles, the dry deposition velocity is estimated using the CARB algorithms (CARB 1986) that represent empirical relationships for transfer resistances as a function of particle size, density, surface area, and friction velocity. For the vapor phase fraction for elemental mercury, a single dry deposition velocity of 0.06 cm/s is assumed. This is based on the average of the winter and summer deposition velocities presented in Lindberg et al. (1992) for forests. Although it is generally acknowledged

that elemental mercury dry deposits with a (net) rate much lower than divalent mercury vapor, the precise value is uncertain, and there can be considerable variability with season and time of day. A further issue is that dry deposition of elemental mercury may not occur at all unless the air concentration is sufficiently high. Preliminary research (Hanson et al. 1995) indicates that under some experimental conditions no dry deposition occurs unless the air concentration is at least about 10 ng/m³. The value at which dry deposition would begin to occur (the compensation point) is expected to depend on many factors, including time of year and flora type. These preliminary results were not specifically addressed in the current study; however, sensitivity analyses were conducted in order to determine the possible impact that such a compensation point might have on the predicted dry deposition of elemental mercury.

In ISC-GAS, the dry deposition of divalent mercury vapor was modeled by calculating a dry deposition velocity for each hour using the assumptions usually made for nitric acid for the input parameters (see EPA 1996; User's Guide for the Gas Dry Deposition Model, page inserts to the User's Guide for the Industrial Source Complex (ISC3) Dispersion Models). The values assumed are provided in Table A-2 below. Ultimately, using these assumptions, the average predicted dry deposition velocity was about 2.9 cm/s for divalent mercury vapor, which is essentially the average of the values used in the RELMAP modeling for coniferous forests.

Table A-2
Parameter Values Assumed for Calculation of Dry Deposition
Velocities for Divalent Mercury Vapor

Parameter	Value
Molecular diffusivity (cm ² /sec)	0.1628
Solubility enhancement factor	10 ⁹
Pollutant reactivity	800
Mesophyll resistance	0
Henry's law coefficient	2.7e ⁻⁷

Wet deposition is estimated assuming that the wet deposition rate is characterized by a scavenging coefficient that depends on precipitation intensity and particle size. For particles, the scavenging ratios used are from Jindal and Heinold (1991) (see Figure A-1). For the vapor phase fraction, a scavenging coefficient is also used, but it is calculated using estimates for the washout ratio, which is the ratio of the concentration of the chemical in surface-level precipitation to the concentration in surface-level air. Because of its higher solubility, divalent mercury vapor is assumed to be washed out at significantly higher rates than elemental mercury vapor. The washout ratio for divalent mercury vapor was selected based on an assumed similarity between scavenging for divalent mercury and gaseous nitric acid. This is based on Peterson et al. (1995), and the value used for the washout ratio for divalent vapor was 1.6 x 10⁶. The washout ratio for elemental mercury vapor was assumed to be 1200. This is a calculated value based on the model of Peterson et al. (1995), with a soot concentration zero.

Other options utilized in the local air modeling of mercury are summarized in Table A-3.

Figure A-1
Wet Deposition Scavenging Ratios Used in Local Scale Air Modeling for Particulate-Bound Mercury (Jindal and Heinold 1991)

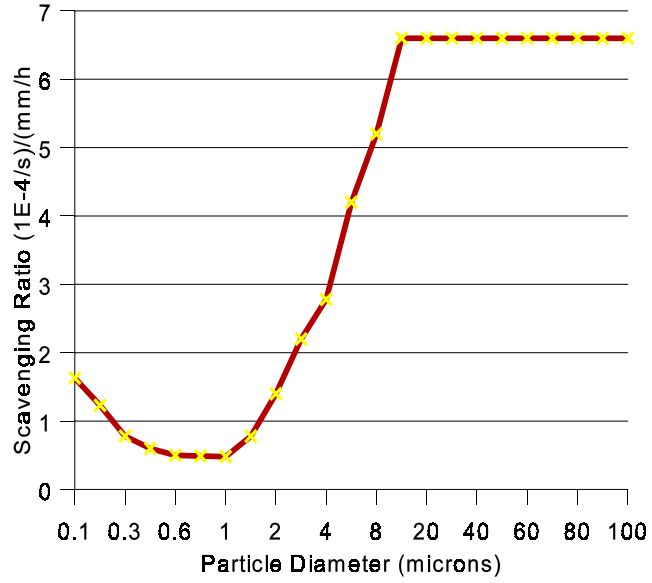


Table A-3
Air Modeling Parameter Values Used in the
Exposure Assessment: Generic Parameters

Parameter	Value Used in Study
Particle Density (g/cm ³)	1.8
Surface Roughness Length (m)	0.30
Anemometer Height (m)	10
Values used for options:	
Final plume rise	Default
Stack-tip downwash	Default
Buoyancy-induced dispersion	Default
Calms processing routine	Used
Missing data processing routine	Not used
Wind profile exponents	Default
Vertical potential temperature gradients	Default
Values for supersquat buildings	“Upper Bound”
Rural mode setting	No exponential decay
State of vegetation	Active and Unstressed
Type of Dispersion	Rural
Dry depletion setting	True
Wet depletion setting	True
Type of terrain	Flat

A.3 References

CARB (1986). Subroutines for calculating dry deposition velocities using Sehmel's curves. Prepared by Bart Croes, California Air Resources Board.

Lindberg, S. E., T. P. Meyers, G. E. Taylor, R. R. Turner, and W. H. Schroeder (1992). Atmosphere-Surface Exchange of Mercury to a Forest: Results of Modeling and Gradient Approaches. *J. of Geophys. Res.* 97(D2):2519-2528.

Petersen, G., Å. Iverfeldt and J. Munthe, 1995. Atmospheric mercury species over Central and Northern Europe. Model calculations and comparison with observations from the Nordic Air and Precipitation Network for 1987 and 1988. *Atmospheric Environment* 29:47-68.

Whitby, K. (1978). The physical characteristics of sulfur aerosols. *Atmosph. Env.* 12:135-159.

APPENDIX B

WATERSHED AND WATERBODY MODELING PARAMETERS

TABLE OF CONTENTS

	<u>Page</u>
LIST OF TABLES	B-iii
DISTRIBUTION NOTATION	B-iv
B. WATERSHED AND WATERBODY MODELING PARAMETERS	
B.1 SCENARIO INDEPENDENT PARAMETERS	B-1
B.1.1 Chemical Independent Parameters	B-1
B.1.1.1 <u>Basic Constants</u>	B-1
B.1.1.2 <u>Receptor Parameters</u>	B-1
B.1.1.2.1 Body Weight	B-1
B.1.1.2.2 Exposure Duration	B-2
B.1.1.3 <u>Agricultural Parameters</u>	B-3
B.1.1.3.1 Interception Fraction	B-3
B.1.1.3.2 Length of Plant Exposure	B-4
B.1.1.3.3 Plant Yield	B-5
B.1.1.3.4 Plant Ingestion by Animals	B-6
B.1.1.3.5 Soil Ingestion by Animals	B-7
B.1.1.4 <u>Exposure Parameters</u>	B-8
B.1.1.4.1 Inhalation Rate	B-8
B.1.1.4.2 Consumption Rates	B-9
B.1.1.4.3 Soil Ingestion Rate	B-10
B.1.1.4.4 Groundwater Ingestion Rate	B-11
B.1.1.4.5 Fish Ingestion Rate	B-12
B.1.1.4.6 Contact Fractions	B-14
B.1.2 Chemical Dependent Parameters	B-15
B.1.2.1 <u>Basic Chemical Properties</u>	B-15
B.1.2.1.1 Molecular Weight	B-15
B.1.2.1.2 Henry's Law Constant	B-15
B.1.2.1.3 Soil-Water Partition Coefficient	B-16
B.1.2.1.4 Sediment-to-Water Partition Coefficient	B-16
B.1.2.1.5 Suspended Sediment-Water Partition Coefficient	B-17
B.1.2.1.6 Suspended Biotic Solids-Water Partition Coefficient	B-17
B.1.2.1.7 Chemical Diffusivity in Air	B-18
B.1.2.1.8 Chemical Transformation Rate Constants	B-18
Reduction in Water Column	B-18
Reduction in Sediments	B-19
Reduction in Soil	B-19
Methylation in Water Column	B-20
Methylation in Sediments	B-21
Methylation in Soil	B-21
Demethylation in Water Column	B-21
Demethylation in Sediments	B-22
Demethylation in Soil	B-22
B.1.2.2 <u>Biotransfer Factors</u>	B-22
B.1.2.2.1 Plant-Soil BCF	B-24

	B.1.2.2.2 Air-Plant BCF	B-27
	B.1.2.2.3 Animal BTF	B-31
	B.1.2.2.4 Fish Bioaccumulation Factor	B-34
	B.1.2.2.5 Plant Surface Loss Coefficient	B-34
	B.1.2.2.6 Fraction of Wet Deposition Adhering	B-35
B.2	SCENARIO DEPENDENT PARAMETERS	B-36
	B.2.1 Time of Concentration	B-37
	B.2.2 Average Air Temperature	B-37
	B.2.3 Watershed Area	B-38
	B.2.4 Average Annual Precipitation	B-38
	B.2.5 Average Annual Irrigation	B-38
	B.2.6 Average Annual Runoff	B-39
	B.2.7 Average Annual Evapotranspiration	B-39
	B.2.8 Wind Speed	B-40
	B.2.9 Soil Density	B-40
	B.2.10 Mixing Depth in Watershed Area	B-41
	B.2.11 Mixing Depth for Soil Tillage	B-41
	B.2.12 Soil Volumetric Water Content	B-41
	B.2.13 Soil Erosivity Factor	B-43
	B.2.14 Soil Erodability Factor	B-43
	B.2.15 Topographic Factor	B-43
	B.2.16 Cover Management Factor	B-44
	B.2.17 Sediment Delivery Ratio to Water Body	B-45
	B.2.18 Pollutant Enrichment Factor	B-46
	B.2.19 Water Body Surface Area	B-46
	B.2.20 Water Body Volume	B-47
	B.2.21 Long-Term Dilution Flow	B-47
	B.2.22 Abiotic Solids Deposition Velocity	B-48
	B.2.23 Biotic Solids Production Rate	B-48
	B.2.24 Phytoplankton Mortality	B-48
	B.2.25 Biotic Solids Deposition Velocity	B-49
	B.2.26 Surficial Sediment Particle Density and Dry Density (Sediment Concentration) ...	B-49
	B.2.27 Upper Benthic Sediment Depth	B-50
	B.2.28 Resuspension Velocity	B-50
B.3	REFERENCES	B-51

LIST OF TABLES

B-1	Chemical Independent Constants	B-1
B-2	Chemical Transformation Rate Constants	B-18
B-3	Soil-to-Plant Transfer Coefficients for Mercury	B-25
B-4	Other Values for Soil-to-Plant Transfer Coefficients for Hg^{2+}	B-26
B-5	Relative Concentration of Mercury in Different Parts of Edible Plants	B-28
B-6	Mercury Speciation in Various Plants	B-30
B-7	Mercury Concentrations in Specific Beef Tissue Media Per Test Group and Dose	B-32
B-8	Animal Biotransfer Factors Derived from Vreman et al. (1986)	B-32
B-9	Mercury Concentrations and Resulting BTFs in Lamb Muscle Tissue Per Test Group and Dose	B-33
B-10	Values From Hoffman et al. (1992) and the Values of F_w Estimated Using Those Values ..	B-36
B-11	Water Content Per Soil Type	B-42
B-12	Representative Soil Types For Each Site	B-42
B-13	Cover Factor Values of Undisturbed Forest Land	B-45
B-14	Long-Term Dilution Flow In In/Yr	B-47

DISTRIBUTION NOTATION

A comprehensive uncertainty analysis was not conducted as part of this study. Initially, preliminary parameter probability distributions were developed. These are listed in this appendix. These were not utilized in the generation of quantitative exposure estimates. They are provided as a matter of interest for the reader.

Unless noted otherwise in the text, distribution notations are presented as follows.

Distribution	Description
Log (A,B)	Lognormal distribution with mean A and standard deviation B
Log*(A,B)	Lognormal distribution, but A and B are mean and standard deviation of underlying normal distribution.
Norm (A,B)	Normal distribution with mean A and standard deviation B
U (A,B)	Uniform distribution over the range (A,B)
T (A,B,C)	Triangular distribution over the range (A,C) with mode of B

B.1 SCENARIO INDEPENDENT PARAMETERS

This part of Appendix B describes the scenario-independent parameters used in the exposure modeling for the Mercury Study Report to Congress. Scenario independent parameters are variables whose values are independent of a particular site and are constant among various site-specific situations. Examples of scenario independent parameters are air density, the average height of an adult, or the average crop yield of a particular food item. These scenario independent parameters may be either chemical independent or chemical dependent. The following sections present the chemical independent and chemical dependent parameters used in this study.

B.1.1 Chemical Independent Parameters

Chemical independent parameters are variables that remain constant despite the specific contaminant being evaluated. The chemical independent variables used in this study are described in the following sections.

B.1.1.1 Basic Constants

Table B-1 lists the chemical independent constants used in the study, their definitions, and values.

Table B-1
Chemical Independent Constants

Parameter	Description	Value
R	ideal gas constant	8.21E-5 m ³ -atm/mole-K
pa	air density	1.19E-3 g/cm ³
ua	viscosity of air	1.84E-4 g/cm-second
ρ_{pa}	abiotic solids density	2.7 g/cm ³
Cdrag	drag coefficient	1.1E-3
κ	Von Karman's coefficient	7.40E-1
λ_2	boundary thickness	4.0

B.1.1.2 Receptor Parameters

Receptor parameters are variables that reflect information about potential receptors modeled in the study. These parameters include body weight, exposure duration, and other characteristics of potential receptors.

B.1.1.2.1 Body Weight

Parameter: BWa, BWc

Definition: Body weights (or masses) of individual human receptors

Units: kg

Receptor	Default Value (kg)
Child	17
Adult	70

Technical Basis:

The default values for children and adults are those assumed in U.S. EPA, 1990.

B.1.1.2.2 Exposure Duration

Parameter: ED

Definition: Length of time that exposure occurs.

Units: years

Receptor	Default Value (years)	Distribution	Range (years)
Child	18	U(1,18)	1-18
Adult	30	U(7,70)	7-70

Technical Basis:

The 18-year exposure duration for the child is based on U.S. EPA guidance for this study. For adults, the 30-year duration is the assumed lifetime of the facility (U.S. EPA, 1990). It should be noted for noncarcinogenic chemicals the exposure duration is not used in the calculations. The range and distribution are arbitrary to determine the relative sensitivity of this variable, when appropriate.

B.1.1.3 Agricultural Parameters

B.1.1.3.1 Interception Fraction

Parameter: RPi

Definition: The fraction of the total deposition within a unit area that is initially intercepted by vegetation.

Units: unitless

Crop	Default Value	Distribution	Range
Leafy vegetables	0.15	Log (0.16, 0.10)	0.08 - 0.38
Legume vegetables	0.008	Log(0.008, 0.004)	0.005 - 0.01
Fruiting vegetables	0.05	Log(0.05, 0.05)	0.004 - 0.08
Rooting vegetables	0	N/A	N/A
Grains and cereals	0	N/A	N/A
Forage	0.47	Norm(0.47, 0.3)	0.02 - 0.89
Silage	0.44	Log (0.44, 0.3)	
Fruits	0.05	Log (0.05, 0.05)	0.004 - 0.08
Potatoes	0	N/A	N/A

Technical Basis:

For leafy vegetables, Baes et al. (1984) obtained an average interception fraction of 0.15 where it was emphasized that this value represents a theoretical average over the United States. This value was calculated assuming a logistic growth pattern for leafy vegetables and taking into account a distribution of field spacings (for details see Baes et al., p.68). The associated distribution and ranges shown in the previous table were calculated based on Baes's analyses by Belcher and Travis (1989).

For legumes and fruits, Belcher and Travis (1989) used the exposed produce equation that relates the interception fraction to the standing crop biomass (also called productivity) and crop biomass values from Shor et al. (1982) to obtain the range of values given in the previous table. The values for fruiting vegetables are assumed to be the same as for fruits.

The distribution for forage is based on the work of Hoffman and Baes (1979), who determined that the values are normally distributed with the parameters presented in the previous table.

The value for silage was calculated in Baes et al. (1984) and is based essentially on sorghum and corn plantings (Knott, 1957; Rutledge, 1979).

Potatoes, root vegetables and grains are assumed to equal zero since the edible portion of the plant is protected from direct deposition (grains have a protective husk).

B.1.1.3.2 Length of Plant Exposure

Parameter: TPi

Definition: The amount of time that the edible part of an exposed plant is exposed to direct deposition.

Units: years

Plant Type	Default Value (years)	Distribution	Range (years)
Leafy vegetables	0.157	U(0.082,0.247)	0.082- 0.247
Legume vegetables	0.123	U(0.082,0.247)	0.082- 0.247
Fruiting vegetables	0.123	U(0.082,0.247)	0.082 - 0.247
Forage	0.123	U(0.082,0.247)	0.082 - 0.247
Silage	0.123	U(0.082,0.247)	0.082 - 0.247
Fruits	0.123	U(0.082,0.247)	0.082 - 0.247

Technical Basis:

Bounding estimates were obtained by assuming an average time between successive harvests of 30 and 90 days. This range is based on the values in Baes et al. (1984) of 60 to 90 days and the reported values by the South Coast Air Quality Management District (SCAQMD) (1988) of 45 days for tomatoes and 30-85 days for lettuce.

The default value for leafy vegetables is the midpoint of the range for lettuce. The values for legumes, fruits and fruiting vegetables are based on the value of 45 days for tomatoes. The value for forage and silage is the average time between successive hay harvests and successive grazings by cattle (Baes et al., 1984).

B.1.1.3.3 Plant Yield

Parameter: YPi

Definition: Yield of the *i*th plant per unit area.

Units: kg (dry weight)/m²

Type of Crop	Default Value (kg (dry weight)/m²)	Range (kg (dry weight)/m²)	Distribution
Leafy vegetables	0.177	0.091 - 0.353	Log (0.177, 0.086)
Legume vegetables	0.104	0.077 - 0.130	Log (0.104, 0.038)
Fruiting vegetables	0.107	0.012 - 0.253	Log(0.107, 0.093)
Rooting vegetables	0.334	0.090 - 0.434	Log(0.334, 0.142)
Grains and cereals	0.3	0.14 - 0.45	Log (0.30, 0.09)
Forage	0.31	0.02- 0.75	0.84482993969
Fruits	0.107	0.012 - 0.253	Log(0.107, 0.093)
Potatoes	0.48	0.405 - 0.555	Log (0.48, 0.106)
Silage	0.84	0.3- 1.34	Log(0.84,0.26)

Technical Basis:

The distributions and ranges shown for all but the silage values are those used in Belcher and Travis (1989). The distributions selected were chosen based on a probability plot for leafy vegetables with data in Shor et al. (1982). The default values are the means of the distributions. Silage was not considered in Belcher and Travis (1989), but the same method by which the default values and distributions were calculated there were replicated using data from Shor et al. (1982) for the purpose of this assessment.

B.1.1.3.4 Plant Ingestion by Animals

Parameter: QPij

Definition: The daily consumption of plants by livestock.

Units: kg dry weight/day

Livestock Consumption of Plants	Default Value (kg dry weight/day)	Distribution	Range (kg dry weight/day)
Beef/Beef Liver			
grain	0.97	U(0.5,6.5)	0.5-6.5
forage	8.80	U(2.0,9.0)	2.0-9.0
silage	2.50	U(1,5)	1.0-5.0
Dairy			
grain	2.60	U(0.5,6.5)	0.5 - 6.5
forage	11.0	U(7,15)	7.0-15.0
silage	3.30	U(1,5)	1.0-5.0
Pork			
grain	3.0	U(2,4)	2.0-4.0
silage	1.3	U(0.5,3)	0.5-3.0
Sheep (lamb)			
forage	1.1	U(0,2)	0.0 - 2.0
Poultry/Eggs			
grain	0.08	U(0.04,0.10)	0.04-0.10

Technical Basis:

With the exception of the beef liver, egg and lamb-forage values, the default values are from U.S. EPA (1990). The value for beef liver is assumed to be the same as for cattle, and the value for eggs is assumed to be the same as for poultry. The value for lamb-forage is from the National Academy of Sciences (NAS,1987).

The ranges shown are based on a combination of the ranges determined by Belcher and Travis (1989), the U.S. EPA (1990) values, and the objective of capturing all of the most likely values.

Although lognormal distributions were chosen in Belcher and Travis (1989), this was not based on the actual distribution of the available data; that is, no probability plots were done. For that reason, uniform distributions are suggested here.

B.1.1.3.5 Soil Ingestion by Animals

Parameter: QSj

Definition: Quantity of soil ingested daily by the a specific animal.

Units: kg/day

Livestock	Default Value (kg/day)	Range (kg/day)
Beef/beef liver	0.39	0.1 - 0.72
Dairy	0.41	0.1 - 0.72
Pork	0.034	0.0 - 0.0688
Sheep (lamb)	0.05	0.01 - 0.15
Poultry/eggs	0.009	0.006 - 0.012

Technical Basis:

The values for beef cattle and dairy cattle are from McKone and Ryan (1989). The value for beef liver is assumed to be the same as for beef. The value for pork is the mean of the distributions used in Belcher and Travis (1989) and are based on values in Fries (1987). The sheep value is from Fries (1982). The value for poultry is the mean of the distribution used in the Hanford Environmental Dose Reconstruction Project (HEDR, 1992) and is based on values for free-ranging chickens. The range is that used in HEDR (1992).

For beef, dairy and pork, the ranges are from Belcher and Travis (1989).

The range for sheep is based on the values reported in Fries (1982). The lower end of the range is for sheep that are fed in a lot, in which case they eat little soil. The upper end is based on sheep grazing on poor pasture land.

B.1.1.4 Exposure Parameters

Exposure parameters are variables that directly affect an individual's dose or intake of a contaminant. Such parameters include inhalation and ingestion rates of air, water and crops and the surface area of skin for the purposes of dermal contact scenarios.

B.1.1.4.1 Inhalation Rate

Parameter: INH

Definition: Rate of inhalation of air containing contaminants.

Units: m³/day

Receptor	Default Value (m³/day)	Distribution
Infant	5.14	T(1.7,5.14,15.4)
Child	16	T(2.9,16,53.9)
Adult	20	T(6,20,60)

Technical Basis:

The default value for infants is the central value of the distribution used for 1 year olds in Hanford Environmental Dose Reconstruction Project (HEDR) (1992) and is from Roy and Courtay (1991). The default value for children is based on U.S. EPA (1990). The default value for adults is that recommended in U.S. EPA (1989b), which states that this value represents a reasonable upper bound for individuals that spend a majority of time at home.

The range for infants is that used for 1 year olds in HEDR (1992) and was determined by scaling the value 5.14 by 0.3 and 3.0, respectively. The range for children is the smallest range containing the values used for 5-, 10-, and 15-year-old children in HEDR (1992). The range for the adult was obtained by scaling the default value by the same numbers used for infants of 0.3 and 3.0 (we note that HEDR, 1992 used a slightly higher central value of 22 m³/day).

To prevent a bias towards upper-end inhalation rates, triangular distributions were considered more appropriate than more arbitrary uniform distributions, with a most likely value equal to the default value.

B.1.1.4.2 Consumption Rates

Parameter: CPi, CAj

Definition: Consumption rate of food product per kg of body weight per day.

Units: g dry weight/kg BW/day

Food Type	Child (gDW/kgBW/day)	Adult (g DW/kg BW/day)
Leafy Vegetables	0.008	0.0281
Grains and cereals	3.77	1.87
Legumes	0.666	0.381
Potatoes	0.274	0.170
Fruits	0.223	0.570
Fruiting vegetables	0.120	0.064
Rooting Vegetables	0.036	0.024
Beef, excluding liver	0.553	0.341
Beef liver ^a	0.025	0.066
Dairy (milk)	2.04	0.599
Pork	0.236	0.169
Poultry	0.214	0.111
Eggs	0.093	0.073
Lamb ^a	0.061	0.057

^a Only the 95-100 percentile of the data from TAS (1991) was nonzero.

Technical Basis:

All of the values reported above are given on a gram dry weight per kg of body weight per day basis. With the exception of the ingestion rates for adults for leafy vegetables and fruits, the values are either the 50-55 percentile (or the 95-100 percentile if the median was zero) of the data from Technical Assessment Systems, Inc. (TAS). The values for the percentiles were reported in g DW/kg of body weight per day.

TAS conducted this analysis of food consumption habits of the total population and five population subgroups in the United States. The data used were the results of the Nationwide Food Consumption Survey (NFCS) of 1987-88 conducted by the United States Department of Agriculture. The information in the NFCS was collected during home visits by trained interviewers using one-day interviewer-recorded recall and a two-day self-administered record. A stratified area-probability sample of households was drawn in the 48 contiguous states from April 1987 to 1988. More than 10,000 individuals provided information for the basic survey.

Each individual's intake of food was averaged across the 3 days of the original NFCS survey, and food consumption for each food group was determined for each individual. Percentiles were then computed for six population subgroups:

- U.S. population
- males \geq 13 years
- females \geq 13 years
- children 1-6 years
- children 7-12 years
- infants $<$ 1 year.

The values for children in the previous table are based on the data for children between 7 and 12 year of age, while the adult values are for males older than 12 years of age. The males older than 12 years of age were chosen to represent the adult since rates for females are lower; this is recognized to be somewhat conservative. The United States population rates include the rates of children which were considered inappropriate for the hypothetical adult receptors modeled in this analysis.

The values for leafy vegetables and fruits for adults are from U.S. EPA (1989b).

B.1.1.4.3 Soil Ingestion Rate

Parameter: Cs

Definition: Amount of soil ingested daily.

Units: g/day

Receptor	Default Value (g/day)	Distribution	Range (g/day)
Pica Child	7.5	U(5,10)	5-10
Child	0.2	U(0.016,0.2)	0.016-0.2
Adult	0.1	U(0.016,0.1)	0.016-0.1

Technical Basis:

Soil ingestion may occur inadvertently through hand-to-mouth contact or intentionally in the case of a child who engages in pica. The default values for adults and non-pica children are those suggested for use in U.S. EPA (1989b). More recent studies have found that these values are rather conservative. For example, Calabrese and Stanek (1991) found that average soil intake by children was found to range from 0.016 to 0.055 g/day. This range, in conjunction with the suggested U.S. EPA values, was used to obtain the ranges shown.

Several studies suggest that a pica child may ingest up to 5 to 10 g/day (LaGoy, 1987, U.S. EPA, 1989b). This range was selected, and the midpoint was chosen as the default value.

B.1.1.4.4 Groundwater Ingestion Rate

Parameter: Cw

Definition: The amount of water consumed each day.

Units: L/day

Receptor	Default Values (L/day)	Distribution
Child	1.0	Log*(0.378; 0.079)
Adult	2.0	Log*(0.1; 0.007)

Technical Basis:

The default values for children and adult are those also suggested in U.S. EPA (1989b) and were first published by the Safe Drinking Water Committee of the National Academy of Sciences (NAS, 1977).

The distributions are those computed in Roseberry and Burmaster (1992). In that paper, lognormal distributions were fit to data collected in a national survey for both total water intake and tap water intake by children and adults. These data were originally gathered in the 1977-1978 Nationwide Food Consumption Survey of the United States Department of Agriculture and were analyzed by Ershow and Cantor (1989).

In Roseberry and Burmaster (1992), distributions were fit to the intake rates for humans ages 0-1 year, 1-11 years, 11-20 years, 20-65 years and older than 65 years. The distribution for children ages 1-11 was chosen for the child's distribution given in the previous table and the distribution for adults ages 20-65 was used for the adult. For the purpose of the present analysis, the tap water intake was deemed more appropriate than total water intake. The total water intake included water intrinsic in foods that are accounted for in the agricultural pathways, while the tap water intake was the sum of water consumed directly as a beverage and water added to foods and beverages during preparation.

The minima and maxima were selected as the 2.5 and 97.5 percentiles, respectively.

B.1.1.4.5 Fish Ingestion Rate

Parameter: Cf

Definition: Quantity of locally - caught fish ingested per day.

Units: g/day

Receptor	Default Value (g/day)
High End Fisher	60
Child of high end fisher	20
Recreational Angler	30

Technical Basis:

Because of the bioaccumulation of methylmercury in fish, the fish ingestion rate is an important parameter for modeling mercury exposure. Fish consumption rates are difficult to determine for a general population study because individual fish ingestion rates vary widely across the United States. This animal protein source may be readily consumed or avoided on a seasonal, social, economic or demographic basis. Ideally, for an actual site, specific surveys identifying the type, source, and quantity of fish consumed by area residents would be used. Within the context of this study, it is not possible to characterize this variability completely. (Please see Chapter 4 of Volume IV of this Report for a more complete discussion of reported fish consumption rate variability.)

For this part of the assessment, individuals in three broad groups of exposed populations will be considered: high end fishers, recreational anglers and the general population. For the general population, no commercial distribution of locally caught fish was assumed. All consumers of locally-caught fish were assumed to be recreational anglers or subsistence fishers.

In U.S. EPA's 1989 Exposure Factors Handbook, fish consumption data from Puffer (1981) and Pierce et al. (1981) are suggested as most appropriate for fish consumption of recreational anglers from large water bodies. The median of this subpopulation is 30 g/day with a 90th percentile of 140 g/day (340 meals/year). The median was used as the surrogate value for recreational anglers.

For subsistence fishers, human fish consumption data were obtained from the report of the Columbia River Inter-Tribal Fish Commission (1994), which estimated fish consumption rates for members of four tribes inhabiting the Columbia River Basin. The estimated fish consumption rates were based on interviews with 513 adult tribe members who lived on or near the reservation. The participants had been selected from patient registration lists provided by the Indian Health Service. Adults interviewed provided information on fish consumption for themselves and for 204 children under 5 years of age.

During the study fish were consumed by over 90% of the population with only 9% of the respondents reporting no fish consumption. Monthly variations in consumption rates were reported. The average daily consumption rate during the two highest intake months was 107.8 grams/day, and the daily consumption rate during the two lowest consumption months was 30.7 grams/day. Members who were aged 60 years and older had an average daily consumption rate of 74.4 grams/day. During the past two decades, a decrease in fish consumption was generally noted among respondents in this survey. The maximum daily consumption rate for fish reported for this group was 972 grams/day.

The mean daily fish consumption rate for the total adult population (aged 18 years and older) was reported to be 59 grams/day. The mean daily fish consumption rate for the adult females surveyed was 56 g/day and the mean daily fish consumption rate for the adult males surveyed was 63 grams. A value of 60 grams of fish per day was selected for the subsistence angler modeled in this report.

Other fish consumption rate studies for specific subpopulations (i.e., anglers and subsistence consumers) have been conducted. These studies are briefly described in Chapter 4 of Volume IV of this Report. These studies demonstrate the wide range of fish consumption rates exhibited across the U.S. population. They also tend to corroborate the estimates to be used in this analysis. These analyses also illustrate the difficulty in determining average and high-end consumption rates for subpopulations considered to be more likely to consume more fish.

In the lacustrine scenarios of this assessment, all fish were assumed to originate from the lakes, which are considered to represent several small lakes that may be present in a hypothetical location.

The effects of fish preparation for food on extant mercury levels in fish have also been evaluated (Morgan et al., 1994). Total mercury levels in walleye were found to be constant before and after preparation; however, mercury concentrations in the cooked fish were increased 1.3 to 2.0 times when compared to mercury levels in the raw fish. It was suggested that this increase was probably due to water and fat loss during cooking and fish skin removal. A preparation factor adjustment was noted but not implemented in this analysis because human consumption levels were measured on uncooked fish. (For more information see Chapter 4 of Volume IV of this Report.)

B.1.1.4.6 Contact Fractions

Parameter: FPi, Faj

Definition: That fraction of the food type grown or raised on contaminated land

Units: Unitless

Food	Subsistence Farmer	Rural Home Gardener/ Subsistence Fisher	Urban Gardener	Comment
Grains	1	0.667	0.195	Values are for corn from Table 2-7 in U.S. EPA (1989b)
Legumes	1	0.8	0.5	Values are for peas from Table 2-7 in U.S. EPA (1989b).
Potatoes	1	0.225	0.031	Values are for total fresh potatoes from Table 2-7 in U.S. EPA (1989b).
Root Vegetables	1	0.268	0.073	Values are for carrots from Table 2-7 in U.S. EPA (1989b).
Fruits	1	0.233	0.076	Values are for Total non-citrus fruit from Table 2-7 in (1989b).
Fruiting Vegetables	1	0.623	0.317	Values are for tomatoes from Table 2-7 in U.S. EPA (1989b).
Leafy Vegetables	1	0.058	0.026	Values are for lettuce from U.S. EPA (1989b).
Beef	1	0	0	
Beef liver	1	0	0	
Dairy	1	0	0	
Pork	1	0	0	
Poultry	1	0	0	
Eggs	1	0	0	
Lamb	1	0	0	

Technical Basis:

The values for the subsistence farmer are consistent with the assumptions regarding this scenario. The values for the gardeners are from U.S. EPA (1989b), per U.S. EPA guidance. Because it is assumed that only the subsistence farmers will consume contaminated animal products, the contact fractions for gardeners is zero for consumption of local animal products.

B.1.2 Chemical Dependent Parameters

Chemical dependent parameters are variables that change depending on the specific contaminant being evaluated. The chemical dependent variables used in this study are described in the following sections.

B.1.2.1 Basic Chemical Properties

The following sections list the chemical properties used in the study, their definitions, and values.

B.1.2.1.1 Molecular Weight

Parameter: MW

Definition: The mass in grams of one mole of molecules of a compound.

Units: g/mole

Chemical	Default Value (g/mole)
Hg ⁰ , Hg ²⁺	201
Methylmercury	216
Methyl mercuric chloride	251
Mercuric chloride	272

B.1.2.1.2 Henry's Law Constant

Parameter: H

Definition: Provides a measure of the extent of chemical partitioning between air and water at equilibrium.

Units: atm-m³/mole

Chemical	Default Value (atm-m³/mole)
Hg ⁰	7.1x10 ⁻³
HgII (HgCl ₂)	7.1x10 ⁻¹⁰
Methylmercury	4.7x10 ⁻⁷

Technical Basis:

The Henry's Law constant is set to 0.0071 atm-m³/mole for Hg⁰ (Iverfeldt and Persson, 1985) and 4.7x10⁻⁷ atm-m³/mole for MHg (Lindquist and Rodhe, 1985).

B.1.2.1.3 Soil-Water Partition Coefficient

Parameter: K_d

Definition: Equilibrium concentration in soil particulates divided by concentration in soil water.

Units: mL/g

Chemical	Default Value (mL/g)	Range
Hg ⁰	1000	--
HgII	58,000	24,000-270,000
Methylmercury	7,000	2,700-31,000

Technical Basis:

Calculated soil-water partition coefficients for HgII in the upper soil layer are reported to range between 24,000 and 270,000 mL/g, with a mean value of about 60,000 mL/g (Lyon, et al., 1997). For MHg, values range between 2,700 and 31,000 mL/g, with a mean value of about 6,700 mL/g.

B.1.2.1.4 Sediment-to-Water Partition Coefficient

Parameter: K_{db}

Definition: Equilibrium concentration in sediment solid divided by concentration in pore water.

Units: mL/g

Chemical	Default Value (mL/g)	Range
Hg ⁰	3000	--
HgII	50,000	16,000-990,000
Methylmercury	3000	2,200-7,800

Technical Basis:

Calculated benthic sediment partition coefficients for HgII are reported to range between 16,000 and 990,000 mL/g, with median values between 54,000 and 79,000 mL/g (Lyon, et al., 1997). For MHg, values range between 650 and 110,000 mL/g, with median values between 6100 and 9000 mL/g. In the R-MCM model (Harris, et al, 1996) the partitioning of HgII to benthic solids in four lakes ranges from 30,000 to 100,000 mL/g, while the partitioning of MHg ranges from 2,200 to 7,800 mL/g. (see Table 6-17, in Chapter 6 of Volume III). The values chosen here are at the lower mid-range of the reported values.

B.1.2.1.5 Suspended Sediment-Water Partition Coefficient

Parameter: K_{dw}

Definition: Suspended sediment-water partition coefficient.

Units: L/kg

Chemical	Default Value (L/kg)	Range
Hg ⁰	1000	--
HgII	100,000	1,380-270,000
Methylmercury	100,000	94,000-250,000

Technical Basis:

The estimated value for both Hg(II) and MHg is consistent with available literature on suspended sediment partition coefficients, with reported values of 1380-188,000 (Moore and Ramamoduray, 1980), 118,000 (Glass et al. 1990), and 86,800-113,000 (Robinson and Shuman, 1989). In the R-MCM model (Harris, et al, 1996) the partitioning of HgII to abiotic suspended solids in four lakes ranges from 80,000 to 270,000 L/kg, while the partitioning of MHg ranges from 94,000 to 250,000 L/kg. (see Table 6-17, in Chapter 6 of Volume III).

B.1.2.1.6 Suspended Biotic Solids-Water Partition Coefficient

Parameter: K_{Bio}

Definition: Suspended biotic solids-water partition coefficient.

Units: L/kg

Chemical	Default Value (L/kg)
Hg ⁰	1000
HgII	200,000
Methylmercury	500,000

Technical Basis:

Because of higher organic matter content, partitioning to biotic solids should be similar to, but slightly higher than partitioning to abiotic solids. In the R-MCM model (Harris, et al, 1996) the partitioning of HgII to total (abiotic plus biotic) suspended solids is calculated to be 20-25% higher than partitioning to abiotic solids (see Table 6-17, in Chapter 6 of Volume III). Given the low ratio of biotic to total solids, the effective partition coefficients of HgII to biotic solids should be about a factor of 1.5 - 2 higher than the partition coefficients to abiotic solids. Likewise, the partitioning of MHg to total suspended solids is about 2.5 times higher than partitioning to abiotic solids, giving an effective partition coefficient of MHg to biotic solids about 5 to 8 times higher than the partition coefficient to abiotic solids.

B.1.2.1.7 Chemical Diffusivity in Air

Volatilization of gas phase Hg⁰ and MHg is calculated using a diffusion coefficient of 4700 cm²/day, based upon a general formula for air diffusivity as a function of molecular weight (Schnoor, et al., 1987):

$$D_{a,i} = \frac{1.9}{MW_i^{2/3}}$$

where D_{a,i} is the atmospheric diffusivity of component “i”, cm²/sec, and MW_i is the molecular weight of component “i”, in g/mole.

B.1.2.1.8 Chemical Transformation Rate Constants

Fifteen transformation rate constants must be specified or calculated for the soil, water column, and benthic sediment equations -- oxidation of Hg⁰ (k_{s_o}, k_{w_o}, k_{b_o}); reduction of HgII (k_{s_r}, k_{w_r}, k_{b_r}); methylation of HgII (k_{s_m}, k_{w_m}, k_{b_m}); demethylation of MHg to HgII (k_{s_{dm}}, k_{w_{dm}}, k_{b_{dm}}); and mer cleavage demethylation of MHg to Hg⁰ (k_{s_{md}}, k_{w_{md}}, k_{b_{md}}). Values (in day⁻¹) are summarized in Table B-2 and discussed below. Calculated volatilization rate constants are included in the table for comparison.

Table B-2
Chemical Transformation Rate Constants

Rate Constants, day ⁻¹	Watershed Soil	Water Column	Benthic Sediments
volatilization of Hg ⁰	0.082*	0.10*	0
oxidation	0	0	0
reduction	0.000025*	0.0075	0.000001
methylation	0.00005	0.001	0.0001
demethylation to HgII	0.0025	0.015	0.002
mer demethylation to Hg ⁰	0	0	0

* Calculated internally for specified conditions.

Reduction in Water Column -- The reduction rate constant in the water column, k_{w_r}, was set to 0.0075 day⁻¹.

Technical Basis:

Recent literature has addressed reduction of divalent mercury in the water column due to the presence of sunlight, heterotrophic bacteria, and some species of phytoplankton. Reduction of aqueous Hg(II) solutions in the presence of simulated sunlight was observed, with rate constants of 3.5 day⁻¹ and 0.05 day⁻¹ for 20% and 80% of the mercury when normalized to sunlight in Stockholm, Sweden (Xiao, et al., 1995). Mason et al. (1994) calculated reduction rate constants between 0.005 and 0.1 day⁻¹ from mass balances in the equatorial Pacific and in Wisconsin seepage lakes. Mason et al. (1995) give

reduction rate constants in the epilimnion of Mystic Lake between 0.02 and 0.04 day⁻¹; this reaction is attributed primarily to heterotrophic bacteria. Rate constants declined to 0.01 day⁻¹ at 9 meters depth, and less than 0.005 day⁻¹ at 17 meters depth. Amyot et al. (1997a) report reduction rate constants of 0.14 day⁻¹ in high Arctic lakes during a 24-hour sunlight period. Under low DOC conditions, these rate constants reached 0.2 to 0.4 day⁻¹, whereas under high DOC conditions, rate constants varied between 0.02 to 0.14 day⁻¹. Amyot et al. (1997b) report rapid DGM production in the epilimnion of temperate lakes, driven mainly by sunlight. The most likely limiting factor was thought to be the reactive HgII pool itself; the nature of the photoreducible complexes is unknown. Lower DGM production is observed in high DOC lakes due to reduced light penetration and increased complexation of HgII. In Palette Lake, Vandal et al. (1995) report reduction rate constants in July-August 1993 averaging 0.10 day⁻¹ in the upper 3 meters and 0.05 day⁻¹ at 9 meters. In May 1994, observed reduction rate constants increased to 0.22 day⁻¹ in the upper 6 meters. High levels of DGM supersaturation, which indicates significant reduction, exist from mid-May to mid-September.

Maximum surficial reduction rate constants must be adjusted to reflect the attenuation of light with depth in water bodies with significant light attenuation. In addition, cool temperatures and reduced sunlight should lead to significantly lower reduction rates during winter months. A yearly-average water column rate constant of 0.075 day⁻¹ was selected for this study.

Reduction in Sediments -- The reduction rate constant in sediments, $k_{b,r}$, was set to 10⁻⁶ day⁻¹.

Less literature is available for reduction in sediments. Amyot et al. (1994) report an increase in DGM concentrations near the bottom of Ranger Lake and speculate that this is caused by aerobic and facultative bacteria reducing HgII in the sediments. Vandal et al. (1995) report porewater Hg⁰ concentrations of 65 pg/L, or 10% of the total mercury, indicating the presence of reduction in sediments. A whole-sediment reduction rate constant of 10⁻⁶ day⁻¹ along with the pore water diffusion and solids resuspension rates used in this model produces pore water Hg⁰ concentrations of about 50 pg/L given a partition coefficient of 1000 L/kg for Hg⁰.

A benthic rate constant of 10⁻⁶ day⁻¹ was selected based on model calibration to general observations of Hg⁰ concentration in pore water.

Reduction in Soil -- The reduction rate constant in the upper 5 mm soil layer of the watershed, normalized to water content, is set to 0.0005 L/L_w-day. The reduction rate constant in the upper 5 mm soil layer of the field site, normalized to water content, is set to 0.0013 L/L_w-day. For water content of 0.1, and depths of 1 and 20 cm, the watershed and field site rate constants are 2.5×10⁻⁵ and 3.25×10⁻⁶ day⁻¹, respectively.

Technical Basis:

Assuming that the net flux of Hg⁰ is driven by the reduction of HgII, reduction rate constants can be derived from evasion flux measurements over soil:

$$F_r = k_{rs} \cdot C_{2T} \cdot \rho_B \cdot \theta_w \cdot z_r$$

where F_r is the net evasion flux in $\mu\text{g}/\text{m}^2\text{-year}$, k_{rs} is the reference reduction rate constant normalized to soil water content, C_{2T} is the volumetric concentration of HgII in soil in mg/L, L/L_w-yr, ρ_B is the soil bulk density in kg/L, θ_w is the soil water content in L_w/L, and z_r is the soil layer thickness over which reduction occurs, in mm. This equation normalizes the reduction rate constant to the soil water in the surficial 5 mm layer, following observations presented in Carpi and Lindberg (1997). To derive the reduction rate constant $k_{s,r}$ used in the model, k_{rs} must be multiplied by the soil water content and averaged over the entire soil depth (ie, by multiplying k_{rs} by 0.5 cm and dividing by either 2 or 20 cm for the nontilled and tilled soils, respectively).

From data presented in Lindberg (1996) and Carpi and Lindberg (1997), values for k_{rs} can be calculated for fields exposed to sunlight and for forests with canopy. These rate constants represent diurnal and seasonal averages. First, the observed fluxes must be modified to represent annual averages. Following the diurnal pattern observed for sludge-amended soils, the summer mid-day fluxes in background field sites were multiplied by 0.25 to obtain a diurnal average. For the shaded forest site, the summer daylight flux is multiplied by 0.6 to obtain a diurnal average. Assuming that winter rates are about half of summer rates, the summer diurnal average fluxes were multiplied by 0.75 to obtain annual average fluxes. Applying these factors, both field sites yield a value of 0.0013 L/L_w-day for k_p , while the forest site yielded a value of 0.0001 L/L_w-day. Presumably the difference in rate constants is due to the significant shading under the forest canopy. Any given watershed should experience average rate constants somewhere between these estimates, depending on the landscape pattern. A value of 0.0005 L/L_w-day is recommended. The field k_{rs} , 0.0013 L/L_w-day, should be used for calculating concentrations in tilled soil. For water content of 0.1 L_w/L and depths of 2 cm and 20 cm for the watershed and field, the soil reduction rate constants are calculated to be $1.25 \times 10^{-5} \text{ day}^{-1}$ and $3.3 \times 10^{-6} \text{ day}^{-1}$, respectively.

Methylation in Water Column -- The water column methylation rate constant, $k_{w,m}$, was set to 0.001 day⁻¹.

Technical Basis:

Using radiolabelled mercury, maximum potential methylation rates have been measured in a number of water bodies. Gilmour and Henry (1991) report maximum potential methylation rate constants between 0.0001 and 0.003 day⁻¹ in the water column of fresh water bodies. Henry et al. (1995) report net methylation rates in Onondaga Lake, New York between April and November, 1992; a net production of 0.003 ng/L-day at 3 m depth, and 0.03 ng/L-day at 9 m was calculated. Given divalent Hg concentrations averaging about 5 ng/L at these depths (Jacobs, et al., 1995), these production rates would correspond to net methylation rate constants of about 0.0006 day⁻¹ and 0.006 day⁻¹, respectively. For the surficial water layers where photodegradation of methyl mercury is significant, the net methylation rate constant should be adjusted to yield the gross methylation rate constant:

$$k_{w,m} = k_{w,m,net} + k_{w,d} \times \frac{C_{MeHg}}{C_{HgII}}$$

Assuming a demethylation rate constant at 3 m depth of about 0.013 day⁻¹ (see discussion below) and a ratio of MHg to HgII of about 10%, the gross methylation rate constant at 3 m should have been about 0.002 day⁻¹. At the seasonally-anoxic 15 m depth, the reported net methylation rate of 0.11 ng/L-day yields rate constants between 0.01 and 0.03 day⁻¹. Matilainen (1995) reports low but detectable non-microbial methylation rate constants of 0.0005 to 0.001 day⁻¹ in the oxic portions of four forest lakes in Finland. Higher rate constants of 0.004 to 0.01 day⁻¹ were observed in deeper, anaerobic layers of the hypolimnion. For Palette Lake, Wisconsin, Watras et al. (1995) report high methylation rates within a layer of bacterioplankton near the top of the anoxic hypolimnion. This 0.5 to 1 meter layer exhibited rate constants of about 0.01 to 0.04 day⁻¹. The methylation rates are linked to sulfate reduction “within anoxic microbial layers, whether in hypolimnetic waters or in sediments underlying oxic water.”

For this case study representing a shallow lake with little or no anoxia, the average water column methylation rate constant was set to 0.001 day⁻¹, reflecting observed non-microbial rate constants in oxic waters. For case studies representing deeper lakes with seasonal anoxia, the methylation rate constant in the hypolimnion should be increased to account for a higher microbial rate constant of 0.01 day⁻¹ within the oxic/anoxic boundary layer.

Methylation in Sediments -- The methylation rate constant in the upper sediment layer, $k_{b,m}$, was set to 0.0001 day⁻¹.

Technical Basis:

In freshwater sediments, Gilmour and Henry (1991) report maximum potential methylation rate constants between 10^{-5} and 10^{-1} day⁻¹. In studies of Quabbin Reservoir, MA, Gilmour et al. (1992) found that the highest rates of methylation occur at the sediment surface, and conclude that sulfate-reducing bacteria are important mediators of this reaction. Stordal and Gill (1995) report methylation rate constants above intact sediment cores of 0.0008 to 0.025 day⁻¹, reflecting both net methylation and sediment exchange. Gilmour and Riedel (1995) report methylation rates of 0.29 and 0.09 $\mu\text{g}/\text{m}^2\text{-day}$ in the upper 4 cm of Little Rock Lake sediments. Although rate constants were not reported, the sediment concentrations can be combined with an assumed dry density of 1.2 g/cm³ to yield rate constants of 8×10^{-5} and 2×10^{-5} day⁻¹.

As a bacterial reaction, sediment methylation should proceed more slowly in the winter months, giving a yearly-average rate about half of the summer rate due to temperature alone. Gilmour and Henry (1991) and Henry et al. (1995) report up to 40 times higher methyl mercury production rates from sediments under anoxic/sulfidic waters than under oxic waters. More oxygenated waters during the winter are expected to result in significantly lowered methylation rates than those observed during the summer months. Here, the yearly-average methylation rate constant in the upper sediment layer was set to 0.0001 day⁻¹ on a whole-sediment basis.

Methylation in Soil -- The soil methylation rate constant, k_{s_m} , was set to 5×10^{-5} day⁻¹.

Technical Basis:

Beckert et al. (1974) provide qualitative evidence showing methylation of mercuric salts in agricultural soils in Nevada due, presumably, to methanogenic bacteria. Abiotic methylation may also occur in soils, either by transmethylation from other organometals at contaminated sites or by humic substances in uncontaminated soils (Gilmour and Henry, 1991). Porvari and Verta (1995) report a laboratory study of potential methylation and demethylation in flooded soils using radiolabelled mercury. While rates varied during the 120-day experiment, maximum potential methylation rate constants in humus and peat averaged about 10^{-3} day⁻¹ under anaerobic conditions and 2×10^{-4} day⁻¹ under aerobic conditions.

For this study, a soil methylation rate constant of 5×10^{-5} day⁻¹ was chosen. This value is 25% of the potential aerobic rate constants measured by Porvari and Verta (1995) and lies at the lower end of the range for sediments reported by Gilmour and Henry (1991).

Demethylation in Water Column -- The water column demethylation rate constant, $k_{w_{dm}}$ was set to 0.015 day⁻¹.

Technical Basis:

Gilmour and Henry (1991) report maximum potential demethylation rate constants in the water column between 0.001 and 0.025 day⁻¹. From *in-situ* incubations in the Ontario Experimental Lakes area, Sellers et al. (1996) derive rate constants for abiotic photodegradation of methyl mercury that are first-order with respect to light levels and with concentration. From data presented in this report, the rate equation is $k_{dm} = 0.0017 \times \text{PAR}$ (photosynthetically-active radiation, in E/m²-day). Zepp (1980) gives a mean annual daytime PAR of 95 E/m²-day for clear skies at 40°N latitude. Kirk, 1994 reports a cloud reduction factor for Europe in the summer of 0.5 to 0.8. Assuming an average cloud reduction factor of 0.65, a surface reflectance of 5%, and a light attenuation factor of 0.75 m⁻¹ through a 5-meter deep lake, an average demethylation rate constant is calculated to be 0.013 day⁻¹. This rate, of course, would be highest in the epilimnion and during the summer months. For this study, the water column demethylation

rate constant was set to 0.015 day^{-1} , producing a MHg fraction close to the observed epilimnetic average of 6%.

Demethylation in Sediments -- The demethylation rate constant in upper sediments, $k_{b_{dm}}$ was set to 0.002 day^{-1} .

Technical Basis:

In freshwater sediments, maximum potential demethylation rate constants are generally higher than corresponding methylation rate constants, with observations between 2×10^{-4} and 10^{-1} day^{-1} (Gilmour and Henry 1991). Gilmour et al. (1992) report that demethylation is maximal at the sediment-water interface. While direct measurements of demethylation rates in sediments are lacking in the literature, rate constants in sediments can be calculated from methylation rate constants and the percent methyl mercury (%MHg). This percentage is generally lower than the water column. Verta and Matilainen (1995) report %MHg between 0.03% and 6% in the sediments of four lakes in Finland. Consistent with reported observations, the demethylation rate constant in upper sediments was set to 0.002 day^{-1} , producing a sediment MHg fraction of 3%.

Demethylation in Soil -- The soil demethylation rate constant, $k_{s_{dm}}$ was set to 0.0025 day^{-1} .

Technical Basis:

Porvari and Verta (1995) report potential demethylation in flooded soils using radiolabelled mercury. Maximum potential demethylation rate constants in humus averaged about 0.06 day^{-1} under anaerobic conditions and 0.03 day^{-1} under aerobic conditions.

For this study, a soil demethylation rate constant of 0.0025 day^{-1} was chosen. This value is 10% of the potential aerobic rate constants measured by Porvari and Verta (1995), and is a factor of 50 higher than the methylation rate constant chosen for this study.

B.1.2.2 Biotransfer Factors

Biotransfer factors reflect the extent of chemical partitioning between a biological medium (plants, meats or fish) and an external medium (air, soil or water). The following sections describe the BCFs used in this study.

It is necessary to note the uncertainty inherent in determining BCFs for mercury species with regard to plant uptake. In general, there seems to be no consensus in the literature on plant bioconcentration factors for mercury, as values for each crop vary widely among studies. Further, in many studies the mercury speciation is not determined. In deriving BCFs for plant absorption of mercury species from the air and soil, it was, therefore sometimes necessary to make assumptions about certain behaviors of mercury based on whatever information was at hand, as opposed to established scientific knowledge, which was lacking. These assumptions are described in each Technical Basis section that follows, but it is useful at this time to identify some of the general uncertainties regarding plant uptake of mercury.

- (1) Plants both absorb and release mercury to the environment. Hanson et al. (1994) demonstrates clearly that at ambient air concentrations forest foliage usually acts as a source of elemental mercury to the atmosphere; deposition (plant absorption) only occurs above a "compensation concentration" at air mercury levels well above background. It is not yet known from where the mercury released by the plants originates (air uptake during periods of high mercury air concentrations, root uptake, Hg(II) absorption, etc.). Similarly, Mosbaek (1988) found that for a given period of time more elemental mercury

was released from a plant-soil system than was absorbed by the plant. These cases, however, in no way indicate that mercury is not bioconcentrated in plants; the above behaviors are consistent with mercury being collected by plants only to certain levels, after which any mercury absorbed is simply released.

- (2) It is usually not known from where the mercury that is found in plants originated (air vs. soil). Only one study determined the fractions of total mercury in plants which came from air and soil (Mosbaek, 1988); in this study, soil was isotopically labeled with ^{203}Hg . After some time the specific activity in the plant was compared to that in the soil to ascertain how much of the mercury in the plant came from the soil. Although the experiment worked well, isotopic equilibrium in the soil was never achieved, and the number of plants studied was limited.
- (3) The speciation of mercury in plants is often not known. If it is known, it is still very unclear as to how the speciation occurred. The plant speciation may be simply a result of direct uptake of different mercury species from the environment (but from air or soil?). It has been shown, however, that a few plants have the ability to change the species of mercury initially taken up from the environment (Fortmann et al., 1978). Such behavior may have to be accounted for regarding plant uptake of mercury.

B.1.2.2.1 Plant-Soil BCF

Parameter: BRi

Definition: The ratio of the contaminant concentration in plants (based on dry weight) to that in the soil.

Units: Unitless

Crop	Hg ²⁺		Methylmercury	
	Default Value	Distribution	Default Value	Distribution
Leafy vegetables	0	None	0	None
Legume vegetables	0.015	U(0.00026, 0.157)	0.031	U(0.0, 0.090)
Fruiting vegetables	0.018	U(0.007,0.059)	0.024	U(0.0,0.11)
Rooting vegetables	0.036	U(0.011, 0.073)	0.099	U(0.013,0.29)
Grains and cereals	0.0093	U(0.0024,0.057)	0.019 ^a	U(0.0048,0.11) ^a
Forage	0	None	0	None
Fruits	0.018	U(0.007-0.059)	0.024	U(0.0,0.11)
Potatoes	0.1	U(0.05,0.2)	0.2 ^a	U(0.1,0.4) ^a
Silage	0	None	0	None

^a Hg²⁺ values multiplied by 2

Technical Basis:

Mosbaek (1988) convincingly showed that for leafy, above-ground parts of plants virtually all of the mercury uptake was from air; therefore, for leafy vegetables, forage and silage no root uptake was modeled.

Values in Cappon (1987) and Cappon (1981) were the only data located which measured methylmercury concentrations in plants, and methylmercury plant-soil BCF's were determined for rooting vegetables, fruiting vegetables, and legumes. Values were determined for crops grown on compost (Cappon 1987) and sludge-treated soils (Cappon 1981), and those values considering edible portions of plants are shown in Table B-3.

Table B-3
Soil-to-Plant Transfer Coefficients for Mercury
(from Cappon, 1987 and Cappon, 1981)

Crop	1987 Values		1981 Values	
	Hg ²⁺	Methylmercury	Hg ²⁺	Methylmercury
<i>Rooting Vegetables</i>				
Beet	.055	.227	.017	.11
Carrot	.026	.118	.014	.048
Onion, Yellow	.073	.288	.053	.042
Onion, Spanish	-	-	.047	.030
Red Radish	.056	.092	.018	.066
White Radish	-	-	.011	.060
Turnip	.026	.013	-	-
<i>Fruiting Vegetables</i>				
Cucumber, slicing	-	-	.015	0
Cucumber, pickle	.007	0	.015	.006
Pepper	.019	.022	.016	.042
Zucchini	.021	0	.014	.018
Summer Squash	-	-	.007	0
Acorn Squash	-	-	.016	.012
Spaghetti Squash	-	-	.016	.024
Pumpkin	-	-	.008	.006
Tomato	.059	.105	.020	.072
<i>Legumes</i>				
Green Bush Beans	.011	0	.014	.020
Yellow Bush Beans	-	-	.017	.015
Lima Beans	-	-	.017	.090

It has been shown, however, that mercury taken up into plants from the environment can be transformed into other mercury species, especially to organomercuric forms such as methylmercury (Fortmann et al., 1978). The methylmercury in plants, therefore, may not have been directly absorbed from the environment. For the purposes of this study, considering root uptake, methylmercury concentrations in plants were treated as though they originated from the soil. It is also important to note that air-to-plant transfer may have occurred, but the Cappon (1981, 1987) studies were not designed to measure air-uptake.

Table B-4 shows additional soil-to-plant transfer coefficients for Hg²⁺ species (it was assumed that all the mercury in the soil is Hg²⁺, which at worst would result in an error of a few percent in the Hg²⁺ soil-to-plant transfer coefficients) determined from a number of studies. Temple and Linzon (1977) sampled garden produce in the vicinity of a chlor-alkali plant. Lenka et al. (1992) also measured mercury concentrations in soil and plants near a chlor-alkali plant. Somu et al. (1985) determined

mercury uptake in wheat and beans grown on HgCl₂ contaminated soil. John (1972) determined mercury concentrations in plants grown on soil artificially contaminated with HgCl₂. Wiersma et al. (1986) measured soil and plant total mercury concentrations from major growing areas in the Netherlands. Belcher and Travis (1989) compiled data from EPA (1985). Mosbaek (1988) studied plant concentrations from soil and air uptake under background conditions. For studies reporting wet weight plant concentrations, wet weight to dry weight conversion factors in Baes et al. (1984) were used to convert to dry weight based concentrations.

Table B-4
Other Values for Soil-to-Plant Transfer Coefficients for Hg²⁺

Crop	Values	References
Legume vegetables	0.157-1.79, 0.00026-0.0003, 0.0005, 0.003-0.03	Lenka et al. (1992), Somu et al. (1985), John (1972), Belcher and Travis (1989).
Fruiting vegetables	0.013-0.33, 0.127-1.36, 0.0078-0.028	Temple and Linzon (1977), Lenka et al. (1992), Belcher and Travis (1989).
Rooting vegetables	0.09-0.33, 0.090-0.149, 0.0065-0.013, 0.05-0.2, 1.6-1.9	Temple and Linzon (1977), Lenka et al. (1992), John (1972), Belcher and Travis (1989), Mosbaek (1988)
Grains and cereals	0.0024-0.0093, 0.0033, 0.00038-0.057	Somu et al. (1985), John (1972), Belcher and Travis (1989).
Fruits	0.0078-0.028	Belcher and Travis (1989).
Potatoes	0.05-0.2	Belcher and Travis (1989).

When possible, default values were chosen based on experiments under reasonable or background conditions, as opposed to experiments where the soil was "spiked" with large amounts of mercury or measurements were taken from severely polluted areas. This is actually a conservative approach; although plants from mercury polluted areas will have greater contaminate levels, the efficiency of accumulation (quantified in the transfer coefficients) tends to decrease with increasing contaminate concentrations. Values from Cappon (1987) and Cappon (1981) were used when possible, since these experiments were conducted under reasonable garden conditions, edible portions of plants were analyzed separately, and different mercury species were measured. Cappon (1981) analyzed plants grown in control soil (total mercury soil content of 120 ng/g with 4.2% methylmercury) in addition to the sludged soil (330 ng/g with 5.1% methylmercury, which is comparable to the 1987 soil levels of 430 ng/g with 5.3% methylmercury). The control soil data were not used since the methylmercury levels were often undetectable. Note that the compost and sludge-amended soils, although elevated in mercury, are nonetheless at reasonable concentrations. For fruiting vegetables, rooting vegetables and legumes values from Cappon (1987) and values derived from the edible portions of plants grown on sludged soil from Cappon (1981) were pooled and averaged; the results were used as the defaults for these plant types.

Default Hg²⁺ values for grains and cereals are from Somu (1985); the methylmercury values were assumed to be twice as great in accordance with the overall average trend noted in plants from the pooled Cappon data. The default values for fruits were assumed to be the same as for fruiting vegetables. The default Hg²⁺ value for potatoes was taken from Belcher and Travis (1989); the methylmercury value for potatoes was assumed to be twice the Hg²⁺ value.

B.1.2.2.2 Air-Plant BCF

Parameter: BI

Definition: The ratio of the contaminant concentration in plants (based on dry weight) to that in the air.

Units: Unitless

Crop	Hg ^{2+a}		Methylmercury ^a	
	Default Value	Distribution	Default Value	Distribution
Leafy vegetables	18000	U[12000,24000]	5000	U[3300,6800]
Legume vegetables	1050	U[700,1400]	100	U[65,130]
Fruiting vegetables	22000	U[14000,29000]	1200	U[780,1600]
Rooting vegetables	0	NA	0	NA
Grains and cereals	1050	U[700,1400]	100	U[65,130]
Forage	18000	U[12000,24000]	5000	U[3300,6800]
Fruits	22000	U[14000,29000]	1200	U[780,1600]
Potatoes	0	NA	0	NA
Silage	18000	U[12000,24000]	5000	U[3300,6800]

^a Based on elemental mercury air concentration, and speciation of divalent and methylmercury species based on Cappon (1981,1987).

Technical Basis:

Mosbaek (1988) determined that mercury concentration in the above-ground, leafy parts of plants is almost entirely the result of air-to-plant transfer of mercury. Cappon (1987,1981), however, found only divalent and methylmercury in these types of plants. Fitzgerald (1986) noted that up to 99% of the total airborne mercury is Hg⁰ vapor (Fitzgerald, 1986). It was assumed that any atmospheric elemental mercury taken up by the plant is converted into Hg²⁺ and methylmercury in the plant tissue. This is not unreasonable: it has been shown that mercury taken up into plants from the environment can be transformed into other mercury species (Fortmann et al., 1978).

A strong correlation between mercury soil concentration and concentration in rooting vegetables has been established (John, 1972; Lenka et al., 1992; Lindberg et al., 1979), and the Mosbaek study (1988) demonstrated that much of the mercury in rooting vegetables was from the soil. As a result, air-to-plant uptake of mercury was not modeled for rooting vegetables and potatoes.

For grains, fruits, legumes and fruiting vegetables, little correlation between mercury plant concentrations and either air or soil concentrations has been found; however, non-negligible concentrations of mercury species in these plants are routinely observed. For this reason, both air-to-plant and soil-to-plant uptake was modeled for these plants. Using a conservative approach, the transfer factors for each accumulation pathway were calculated as if all of the mercury in the plant came only from that pathway. This has the effect of possibly double-counting the amount of mercury in the plant tissue. There is a great deal of uncertainty due to the lack of applicable data.

The range of air-plant bioconcentration factors based on Mosbaek et al. (1988) was found to be 15,000 - 31,000, based on total mercury concentration in the plant tissue. Mosbeak et al. (1988) determined average mercury concentrations due to air uptake in lettuce, radish tops, and grass. Concentrations were converted to dry weight according to Baes et al. (1984), and the overall range of air-plant bioconcentration factors based on total mercury in the plant tissue was found to be 15,000 - 31,000. Air to plant bioconcentration factors can be derived from other studies only indirectly (by making a reasonable estimate of the air concentration and assuming all the mercury in plant tissue comes from air), and the values arrived at for various plant species generally fall into the previous range. Due to the limited data, it was decided to use the midpoint of the Mosbeak et al. (1988) bioconcentration values (23,000) as the starting default for all plant species assumed to accumulate mercury from the air.

This approach was adjusted for the consideration of portions of grains and legumes that are not directly exposed to the atmosphere. Although atmospherically absorbed mercury can translocate throughout different portions of the plant, data indicate internal portions of grains and legumes (the edible portions) do not appear to accumulate mercury to the same degree as plant leaves or vines. Somu et al. (1985), John (1972), and Cappon (1981) determined mercury concentrations from different portions of the same plants. Table B-5 below shows the relative concentrations of total mercury found in plant parts from the portions of these studies representative of noncontaminated conditions.

**Table B-5
Relative Concentration of Mercury in Different Parts of Edible Plants**

Legumes	Beans (Somu et al. 1985)	Peas (John 1972)	Beans (Cappon 1981)
vines		1.0	
stalks	1.0		
Pods		0.045	1.0
seeds	0.060	0.0091	0.028 - 0.089
Grains	Wheat (Somu et al. 1985)	Oats (John 1972)	
leaves		1.0	
stalks	1.0	0.063	
husks		0.61	
grain	0.14	0.051	

A clear trend of decreasing mercury concentrations is seen proceeding from leafy to seed portions of the plants. Based on these data, it was decided to decrease the default air-to-plant bioconcentration factor of 23,000 by a factor of 20 (to 1200) to account for the decreasing accumulation

of airborne mercury for the edible portions of these plants as compared to the leafy portions (for which the bioconcentration factor of 23,000 is applicable). Airborne mercury uptake by fruits may also be overestimated with the default bioconcentration factor. However, no data are available to explore this possibility.

The product of the bioconcentration factors and the atmospheric mercury concentration is the total mercury in the plant tissue resulting from accumulation of airborne elemental mercury. Plant-specific speciation estimates from Cappon (1981,1987) were used to partition the total mercury bioconcentration factor (and corresponding range) in order to model the relative fractions of methylmercury and Hg^{2+} found in the plant; these are shown in Table B-6; note that the rest of the mercury was found to be divalent mercury.

Thus, for leafy, fruiting and legume vegetables, the default values for the bioconcentration of methylmercury based on the elemental mercury concentration in air were assumed to be 23,000 or 1200 multiplied by the average methylmercury percentages in Table B-5; the Hg^{2+} values were derived similarly (Hg^{2+} fraction x 23,000). The values for fruits were assumed to be the same as for fruiting vegetables. The values for forage and silage were assumed the same as for leafy vegetables, and the values for grains were assumed to be the same as for legumes (beans).

Table B-6
Mercury Speciation in Various Plants

Plant Type	% Methylmercury Cappon (1981)	% Methylmercury Cappon (1987)
Leafy vegetables		
Head lettuce	8.8	21.4
Leaf lettuce	16.5	18
Spinach	19.8	23.1
Swiss chard, Fordhook	30.2	14.8
Swiss chard, Ruby Red	28.6	-
Broccoli ^a	33.1	17.8
Late Cabbage	28.8	-
Red Cabbage	22.4	-
Savoy King Cabbage	25.2	-
Jersey Wakefield Cabbage ^a	-	18
Cauliflower	21.2	-
Collards	22.8	-
Average		21.8
Legume vegetables		
Green Bush Beans	0	7.2
Yellow Bush Beans	-	4.3
Lima Beans	-	22.4
Average		8.5
Fruiting vegetables		
Cucumber, slicing	0	-
Cucumber, pickle	2.1	0
Pepper	12.5	6.1
Zucchini	6.7	0
Summer Squash	0	-
Acorn Squash	4.1	-
Spaghetti Squash	7.4	-
Pumpkin	4.0	-
Tomato	16.0	9.1
Average		5.2

^a These were classified as "cole" in Cappon (1987).

B.1.2.2.3 Animal BTF

Parameter: BA_j

Definition: The equilibrium concentration of a pollutant in an animal divided by the average daily intake of the pollutant.

Units: day/kg DW

Livestock	Default Value (day/kg DW)	Distribution
beef	0.02	U(0.0008,0.04)
beef liver	0.05	U(0.02,0.1)
dairy	0.02	U(0.003,0.09)
pork	0.00013	U(0.00005,0.00026)
poultry	0.11	U(0.094,0.13)
eggs	0.11	U(0.094,0.13)
lamb	0.09	U(0.009,0.3)

Technical Basis:

Biotransfer factors measure pollutant transfer from the environment to animal tissues and products. They are defined as the ratio of pollutant concentration in animal tissue to the daily pollutant intake of an animal. The biotransfer factors for mercury to cattle tissues were estimated based on data found in Vreman et al. (1986), and biotransfer factors for mercury to lamb were based on data found in van der Veen and Vreman (1986).

The data collected from Vreman et al. (1986) and van der Veen and Vreman (1986) are not from single pollutant and single route ingestion studies; rather, the animals in these studies were generally dosed with elevated levels of several metals in a single wafer. This is not the ideal set of studies for assessing the transfer of mercury primarily from ingested grass and soil. These studies, however are multiple dose and long-term experiments which should provide data more representative of the desired equilibrium situation than a single, very large dose experiment.

In two experiments, Vreman et al. (1986) measured transfer of mercury from diet to tissues and milk of dairy cattle. In the first experiment 12 lactating cows/group were placed on pasture in 2 groups for 3 months. The control group was fed uncontaminated wafers and, based on mercury levels in the pasture grass, were estimated to ingest 0.2 mg mercury/day. The exposed group received wafers treated with a solution of mercury acetate, lead, cadmium and arsenic pentoxide; the daily mercury ingestion rate for the exposed group was 1.7 mg/day. During the experiment mercury levels in milk were measured. After three months on test, four cows/group were slaughtered, and mercury levels were measured in liver, kidney and muscle samples. In the second study, lactating cows were kept indoors and divided into 4 groups of 8 for up to 28 months. In addition to the control group, the diets of 3 other groups were supplemented with the following: wafers containing the same metals (1.7 mg mercury/day), sludge delivering dietary levels of 3.1 mg mercury/day, and sludge delivering dietary levels of 1.2 mg mercury/day. Two cows from each group were slaughtered at study termination (except for the group receiving 3.1 mg mercury/day from sludge in which only one cow was sacrificed). Mean milk mercury

concentrations in the groups were reported, and mercury levels in the slaughtered cows were measured in liver, kidney and muscle samples.

Shown in Table B-7 are data from Vreman et al. (1986) that are relevant to deriving beef and dairy biotransfer factors. The tissue mercury concentrations presented are in wet weight.

Table B-7
Mercury Concentrations in Specific Beef Tissue
Media Per Test Group and Dose (from Vreman et al, 1986)

Test Group	Dose (mg mercury/day)	Mercury in Milk (ug/Kg WW ^A)	Mercury in Muscle (ug/Kg WW ^A)	Mercury in Liver (ug/Kg WW ^A)
Pasture Control	0.2	2.3	3	7
Pasture Treated	1.7	0.9	4	10
Indoor Control	0.2	<0.5	2	3
Indoor Wafer	1.7	0.6	2	26
Indoor High-Level Sludge	3.1	2.4	1	14
Indoor Low-Level Sludge	1.2	1.3	2	9

^A Wet weight

The data in Table B-7 can be easily converted into milk, beef and liver biotransfer factors by converting the tissue concentrations to dry weight and dividing the tissue concentrations by the daily intake of mercury (after converting the intake from mg/day to ug/day). The moisture content of the above tissues are reported in Baes et al. (1984): 0.87 for whole milk, 0.615 for beef and 0.70 for liver. The biotransfer factors derived are shown in Table B-8.

Table B-8
Animal Biotransfer Factors Derived from Vreman et al. (1986)

Test Group	Biotransfer Factor (day/kg DW)		
	Dairy	Beef	Beef Liver
Pasture Control	0.09	0.04	0.1
Pasture Treated	0.004	0.006	0.02
Indoor Control	0.02	0.03	0.05
Indoor Wafer	0.003	0.003	0.05
Indoor High-Level Sludge	0.006	0.0008	0.02
Indoor Low-Level Sludge	0.008	0.004	0.03

Using the number of animals sampled for each value in Table B-8, weighted averages for the Dairy, Beef and Beef Liver Biotransfer factors can be derived. These are chosen as the default values, with the ranges taken from Table B-8.

In a experiment very similar to Vreman et al. (1986), van der Veen and Vreman (1986) measured transfer of mercury from diet to tissues of 10 week old fattening lambs. Two groups of 8 lambs were placed on pasture for 3 months. The control group was fed uncontaminated feed concentrate and based on mercury levels in the pasture grass and uncontaminated feed were estimated to ingest <0.02 mg mercury/Kg dry feed-day. The exposed group received feed concentrate treated with a solution of mercury acetate, lead, cadmium and arsenic pentoxide; the daily mercury ingestion rate for the exposed group was 0.08 mg/Kg dry feed. Another four groups of 8 lambs were kept indoors and were fed hay and feed concentrate. A control group was fed uncontaminated feed concentrate, and were estimated to ingest <0.02 mg mercury/Kg dry feed-day. The 3 other groups were fed feed concentrate contaminated with, respectively, a soluble solution of the metals, harbor sludge and sewage sludge. Daily mercury ingestion rates for these groups ranged from 0.14 - 0.27 mg/Kg dry feed. After three months all lambs were slaughtered and mercury levels were measured in liver, kidney, brain and muscle samples.

Shown in Table B-9 are data from van der Veen and Vreman et al. (1986) and the biotransfer factors derived from these data.

Table B-9
Mercury Concentrations and Resulting BTFs in Lamb Muscle Tissue
Per Test Group and Dose (from van der Veen and Vreman 1986)

Test Group	Dose (mg mercury/Kg dry feed-day)	Feed Amount (Kg DW/day)	mercury in Muscle (ug/Kg WW)	Muscle Dry %	BTF ^A (day/Kg DW)
Pasture Control	<0.02	1.36	1	32.3	0.2
Pasture Treated	0.08	1.36	3	32.8	0.08
Indoor Control	<0.02	1.3	2	30.5	0.3
Indoor Wafer	0.14	1.28	1	29.5	0.02
Indoor High-Level Sludge	0.27	1.39	1	30.5	0.009
Indoor Low-Level Sludge	0.17	1.38	1	29.1	0.02

^A Biotransfer Factor (BTF)

To calculate the biotransfer factors listed from the data in Table B-9, the daily mercury intake was calculated from the mercury concentration in dry feed and daily intake of dry feed. van der Veen and Vreman (1986) reported the dry weight fractions of the muscle samples, and the mercury concentration in muscle was calculated on a dry weight basis. The biotransfer factor for each group of lambs was then determined. The average over all groups was chosen as the default value, with the ranges taken from Table B-9.

In U.S. EPA (1993b), uptake slopes were developed for a number of pollutants found in sludge including mercury. For pork and poultry, U.S. EPA (1993b) reviewed the literature on concentrations of metals in meat from studies in which livestock were fed known concentrations of the metals in feed. These values were used to obtain the default values (after converting wet-weight values to dry-weight).

B.1.2.2.4 Fish Bioaccumulation Factor

Parameter: Tier 3 Fish BAF (BAF₃)
Tier 4 Fish BAF (BAF₄)

Definition: The concentration of the methylmercury in fish divided by the concentration of total dissolved methylmercury in water

Units: L/kg

Fish Type	Percentiles (L/kg)			
	Default Value (L/kg)	5th Percentile	Median	95th Percentile
Trophic Level 3 Fish	1.6E6			
Trophic Level 4 Fish	6.8E6			

Technical Basis:

For a discussion of these values, the reader is referred to Appendix D of this volume.

B.1.2.2.5 Plant Surface Loss Coefficient

Parameter: kp

Definition: A measure of the loss of contaminants deposited on plant surfaces over time as a result of environmental processes.

Units: /yr

Chemical	Default Value (per year)	Distribution	Range
Hg ⁰	40.41	Log(40.41,17.39)	28.11 - 52.7
Hg ²⁺	40.41	Log(40.41,17.39)	28.11-52.7
Methylmercury	40.41	Log(40.41,17.39)	28.11-52.7

Technical Basis:

The values in the previous table were taken from Belcher and Travis (1989), although no speciation was provided. The values for all species were assumed to be the same. The default value is the mean of the lognormal distribution used in Belcher and Travis (1989). The choice of a lognormal distribution was based on the work of Miller and Hoffman (1983).

B.1.2.2.6 Fraction of Wet Deposition Adhering

Parameter: Fw

Definition: Fraction of wet deposition that adheres to plant (i.e., is not washed off).

Units: unitless

Default Value	Distribution	Range
0.6	T(0.1,0.6,0.8)	0.1-0.8

Technical Basis:

The unitless parameter F_w represents the fraction of the pollutant in wet deposition that adheres to the plant, is not washed off by precipitation and is used to estimate plant pollutant levels. A value of 1 is the most conservative; this implies that all of the pollutant which deposits onto the plant via wet deposition will adhere to the plant. U.S. EPA (1990) originally used a value of 0.02, which significantly diminishes the impact of this pathway. A more recent study by Hoffman et al. (1992) suggests an answer between these extremes for both dissolved pollutants and suspended particulates in simulated rain drops.

Hoffman et al. (1992) attempted to quantify the amount of radiolabeled beryllium (Be) and Iodine (I) as well as particles of sizes 3, 9, and 25 μm that adhered to three plant types (fescue, clover, and a typical weeded plot). The radiolabeled pollutants were dissolved or suspended in water, which was then showered upon the different types of vegetation to simulate precipitation. Two precipitation intensities were modeled in the experiment: moderate (1-4 cm/hour) and high (4-12 cm/hour). Due to experimental complications, total deposition and pollutant retention upon the vegetation were estimated by the authors; these estimates were termed the interception fraction in the Hoffman report. For example, in the experiment. Beryllium in the form of BeCl_2 was dissolved in the water and then showered upon the vegetation. For the moderate and high intensity precipitation events simulated, the mean interception fractions were estimated to be 0.28 and 0.15, respectively.

The 1993 Addendum to the Indirection Exposure Methodology (U.S. EPA, 1993a) models deposition and retention as the product of the interception fraction (R_p) and F_w . In terms of the U.S. EPA model, the Hoffman report estimates the product $R_p \times F_w$. To obtain estimates for F_w , the values reported in Hoffman et al. (1992) were divided by the interception fraction for forage used in this assessment (0.47; Baes et al., 1984). This provides estimates of 0.60 and 0.32 for F_w for the moderate and high precipitation intensities, respectively (see Table B-10).

Table B-10 shows the Hoffman et al. (1992) estimates for the interception and adhesion of dissolved pollutants and suspended particles in simulated moderate and high intensity precipitation. Based on the Hoffman estimates and the assumption of an interception fraction for forage of 0.47, the F_w for the two pollutants and three particle sizes were estimated for the precipitation intensities studied, and the means were calculated. No attempt has been made to adjust the final estimate for frequency of the two precipitation intensities; however, since moderate precipitation intensities are more common, the unadjusted means are probably an underestimate.

Table B-10
Values From Hoffman et al. (1992)
and the Values of *F_w* Estimated Using Those Values

Compound	R _p x <i>F_w</i> for Moderate Intensity	R _p x <i>F_w</i> for High Intensity	<i>F_w</i> Estimate for Moderate Intensity	<i>F_w</i> Estimate for High Intensity	<i>F_w</i> Mean
I	0.08	0.05	0.17	0.11	0.14
Beryllium	0.28	0.15	0.60	0.32	0.46
3 μm	0.30	0.24	0.64	0.51	0.58
9 μm	0.33	0.26	0.70	0.55	0.63
25 μm	0.37	0.31	0.79	0.66	0.72

The *F_w* estimated for beryllium was used as a surrogate for mercury. Be²⁺, as a cation, is assumed to behave in a manner similar to Hg²⁺ during deposition. Because the moderate intensity is expected to be more common than the heavy intensity, an *F_w* of 0.60 is assumed to be a reasonable estimate of *F_w* for divalent mercury. This value is higher than the range of 0.1-0.3 presented in McKone and Ryan (1989). For beryllium, Hoffman noted the appearance of a strong attraction between the cation and the plant surface, which was assumed to be negatively charged. Beryllium is believed to adsorb to cation exchange sites in the leaf cuticle. Once dried on the plant surface, beryllium was not easily removed by subsequent precipitation events. Divalent mercury is assumed to exhibit a similar behavior. The range of 0.1-0.8 was used to estimate the sensitivity of this parameter.

The adjusted Hoffman data indicate that the greater the intensity of the precipitation, the smaller the *F_w* estimate for both dissolved pollutants and suspended particles. This is intuitively appealing given the understanding of the physical process. Hoffman et al. (1992) noted that the intensity and amount of rainfall had approximately the same impact on the estimated values. It should also be noted that the data indicate that the value of *F_w* for pollutants that deposit as anions (e.g., I) may be significantly lower than cations.

B.2 SCENARIO DEPENDENT PARAMETERS

This section of Appendix B describes the scenario dependent parameters used in the exposure modeling for the Mercury Study Report to Congress. Scenario dependent parameters are variables whose values are dependent on a particular site and may differ among various site-specific situations. For this assessment, three settings are being evaluated: (1) rural, (2) lacustrine, and (3) urban. The receptors differ for each of these scenarios, as do the parameters. These scenario dependent parameters may be either chemical independent or chemical dependent. The following sections present the chemical independent and chemical dependent parameters used in this assessment.

Chemical independent parameters are variables that remain constant despite the specific contaminant being evaluated. The chemical independent variables used in this assessment are described in the following sections.

Site physical data include information such as the environmental setting, vegetative cover, presence of surface water or groundwater, area of source and meteorological and climatological data. These parameters are described in the following sections.

B.2.1 Time of Concentration

Parameter: Tc

Definition: Number of years that the air concentration at the above level persists; equal to the facility lifetime for calculations from anthropogenic sources

Units: yrs

Scenario	Default Value(s) (years)	Distribution
All	30	None

Technical Basis:

The time of concentration is the same as the assumed facility lifetime. The generic value is 30 years.

B.2.2 Average Air Temperature

Parameter: Ta

Definition: Average air temperature of microscale area

Units: °C

Location	Default Value (Years value is based upon) (°C)	Distribution
Eastern Location	11.9 (25)	U (8,16)
Western Location	13.4 (47)	U (9,17)

Technical Basis:

The values for local airports are reported in the section "U.S. Local Climatological Data Summaries for 288 Primary Stations throughout the U.S." on CDROM by WeatherDisc Associates (1992). The distributions are arbitrary to explore the sensitivity of this parameter.

B.2.3 Watershed Area

Parameter: A_s

Definition: Area of contamination which drains into a water body

Units: Km²

Location	Default Value (Km²)
Eastern Location	37.3
Western Location	37.3

Technical Basis:

The values for the fish ingestion pathways are based on hypothetical watershed/waterbody surface area ratio of 15 and a lake diameter of 1.78 km. This parameter was used only to calculate the erosion and runoff load to the water body.

B.2.4 Average Annual Precipitation

Parameter: P

Definition: Average annual precipitation

Units: cm/yr

Location	Default Value (cm/yr)	Distribution
Eastern Location	102	T(82,102,122)
Western Location	21	T(1,21,41)

Technical Basis:

All values are for local airports as reported in the section "U.S. Local Climatological Data Summaries for 288 Primary Stations throughout the U.S." on CDROM by WeatherDisc Associates (1992). These were considered the "best estimates" of a triangular distribution, with a range of 20 cm/yr above and below the mode.

B.2.5 Average Annual Irrigation

Parameter: I

Definition: Average annual irrigation of plants

Units: cm/yr

Location	Default Value (cm/yr)	Distribution
Eastern Location	12.5	U(0,25)
Western Location	57.5	U(50,65)

Technical Basis:

The ranges were approximated from Figure 4.25 in Baes et al. (1984). The tentative default values are the midpoint of this range. It was assumed that both the farmer and home gardener will irrigate the same amount if they are in the same area of the country (i.e., irrigation rate does not depend on size of plot).

B.2.6 Average Annual Runoff

Parameter: Ro

Definition: Average annual runoff

Units: cm/yr

Location	Default Value (cm/yr)	Distribution
Eastern Location	18	U(9,27)
Western Location	1	U(0,2)

Technical Basis:

The default values for the eastern location are from Geraghty et al. (1973). The total runoff values given in that report include groundwater recharge, direct runoff, and shallow interflow. Following U.S. EPA (1993c), this number was reduced by one-half to represent surface runoff. Because of the difficulty of hydrologic modeling in the western location, the PRZM-2 model (Carsel, 1984) was used to estimate the runoff for this area. The estimated value was 1 cm/yr. The distributions are arbitrary to determine the sensitivity of this parameter.

B.2.7 Average Annual Evapotranspiration

Parameter: Ev

Definition: Average annual loss of water due to evaporation

Units: cm/yr

Location	Default Value (cm/yr)	Distribution
Eastern Location	65	U(60,70)
Western Location	13	U(8,18)

Technical Basis:

For the eastern location, the ranges are based on estimates from isopleths given in Figure 4.24 in Baes et al. (1984). The values presented there were estimated based on local data (average temperature and precipitation) as well as the maximum possible sunshine for the area. The default value is the

midpoint of this range. For the western location, the model PRZM-2 was used to estimate the values given previously.

B.2.8 Wind Speed

Parameter: W

Definition: Wind speed

Units: m/s

Location	Default Value (m/s)	Distribution
Eastern Location	4.3	U(1,7)
Western Location	4.0	U(1,7)

Technical Basis:

All values were collected for local airports and reported in the section "U.S. Local Climatological Data Summaries for 288 Primary Stations throughout the U.S." on CDROM by WeatherDisc Associates (1992). The primary use of this parameter is for estimating volatilization from soil and water bodies. The distributions are arbitrary to explore the sensitivity of this parameter.

B.2.9 Soil Density

Parameter: BD

Definition: Soil density

Units: g/cm³

Location	Default Value (g/cm ³)	Distribution	Range
All Sites	1.4	Log(1.4,0.15)	0.93-1.84

Technical Basis:

The distribution is from Belcher and Travis (1989) and is based on a probability plot using data from Hoffman and Baes (1979). There is little variation in the parameter, despite the fact that more than 200 data points were used. The default value is the mean of the distribution.

B.2.10 Mixing Depth in Watershed Area

Parameter: Zd

Definition: The depth that contaminants are incorporated into soil (no tillage)

Units: cm

Location	Default Value (cm)	Distribution
All Sites	1.0	U(0.5,5)

Technical Basis:

The default value is based on U.S. EPA (1990). The distribution is arbitrary to determine the relative sensitivity of the parameter.

B.2.11 Mixing Depth for Soil Tillage

Parameter: Ztill

Definition: The depth that contaminants are incorporated into tilled soil

Units: cm

Location	Default Value (cm)	Distribution
All Sites	20	U(10,30)

Technical Basis:

The default value is based on U.S. EPA (1990). The distribution is arbitrary to determine the sensitivity of this parameter.

B.2.12 Soil Volumetric Water Content

Parameter: Θ_w

Definition: Amount of water that a given volume of soil can hold

Units: ml/cm³

Location	Default Value (ml/cm³)	Distribution
Eastern Location	0.30	U(0.15,0.42)
Western Location	0.36	U(0.15,0.42)

Technical Basis:

Values for water content can range from 0.003 to 0.40 ml/cm³ depending on the type of soil (Hoffman and Baes, 1979). Table B-11 demonstrates the dependency of values on the hydrologic soil type. These values were derived from the PATRIOT software system (Imhoff et al., 1994), which can be obtained from the Center for Exposure Assessment Modeling at the U.S. Environmental Protection Agency, Athens, Georgia.

Table B-11
Water Content Per Soil Type

Soil Type	Water Content
A	0.15
B	0.22
C	0.30
D	0.42

Representative soil types for both sites are shown in Table B-12 and were determined from Carsel (1984). The soil types were used in conjunction with the previous table to determine the default value for the soil water content, with the value for the western location being the average of the values for types C and D.

Table B-12
Representative Soil Types For Each Site

Location	Soil Type
Eastern Location	C
Western Location	C/D

The distribution for all sites is a uniform distribution over the range over all soil types.

B.2.13 Soil Erosivity Factor

Parameter: R

Definition: Quantifies local rainfall's ability to cause erosion

Units: kg/km²-yr

Location	Default Value (kg/km ² -yr)	Distribution
Eastern Location	200	U(100,300)
Western Location	53	U(30,75)

Technical Basis:

The ranges were determined based on an isopleth map for the region in USDA (1978). The upper and lower bounds were determined from this map by finding extremes within a 300-mile radius.

B.2.14 Soil Erodability Factor

Parameter: K

Definition: Quantifies soil's susceptibility to erosion

Units: tons/acre per unit of R

Location	Default Value (tons/acre)	Distribution
Eastern Location	0.30	U(0.12,0.48)
Western Location	0.28	U(0.08,0.48)

Technical Basis:

Based on similar soil near the eastern location (loamy sand, loam, and silt loam) and using Table A2-2 in U.S. EPA (1989a), a range of 0.12 to 0.48 was obtained. A similar analyses has not been performed for the other sites, but the ranges listed in the previous table are apparently the maximum range possible based on Table A2-2 in U.S. EPA (1989a); therefore, these ranges encompass all likely values and can be used for sensitivity analyses. The default values are the midpoint of these ranges.

B.2.15 Topographic Factor

Parameter: LS

Definition: Provides a measure of the length and steepness of the land slope

Units: unitless

Location	Default Value	Distribution
Eastern Location	2.5	U(0.25,5)
Western Location	0.4	U(0.1,1.2)

Technical Basis:

The length and steepness of the land slope substantially affect the rate of soil erosion. Table A2-3 in U.S. EPA (1989a) contains LS values for various slopes and slope lengths and was used in conjunction with United States Geological Survey (USGS) maps to obtain the ranges given in the previous table. A 1:24000 map was available for the humid/east/complex I site while only a 1:250000 USGS map was available for all other sites. The default value was chosen as representative of the most common slope and length in the area.

B.2.16 Cover Management Factor

Parameter: C

Definition: The ratio of soil loss from land cropped under local conditions to the corresponding loss from clean tilled fallow

Units: unitless

Location	Default Value
Eastern Location	0.006
Western Location	0.1

Technical Basis:

The lower end of the range for areas having forests (0.001) is the lower of two values suggested for woodlands in U.S. EPA (1988). For those areas lacking forests (i.e., western site), the value of 0.1 given for grass in U.S. EPA (1993b) was used.

For the watershed, it was decided to use a cover fraction representative of undisturbed grass or forested areas, although high-end values were used. It was noted that the cover fraction can vary by several orders of magnitude, depending on the land use type and soil type. Table B-13 shows estimates of cover factor values for undisturbed forest land (Wischmeier and Smith, 1978).

Table B-13
Cover Factor Values of Undisturbed Forest Land
 (from WQAM, 1985; original citation Wischmeier and Smith, 1978)

Percent of Area Covered by Canopy of Trees and Undergrowth	Percent of Area Covered by Duff (litter) at least 5 cm deep	Cover Management Factor Value
75-100	90-100	0.0001-0.001
45-70	75-85	0.002-0.004
20-40	40-70	0.003-0.009

Based on the above values and the objectives of this exposure assessment, it was decided that the high-end values (of those above) would be appropriate; a nominal value of 0.006 (the midpoint of the high-end range) was chosen.

B.2.17 Sediment Delivery Ratio to Water Body

Parameter: Sdel

Definition: Sediment delivery ratio to water body

Units: unitless

Location	Default Value	Distribution
Both Locations	0.2	U(0.14,0.23)

Technical Basis:

The sediment delivery ratio is the fraction of soil eroded from the watershed that reaches the water body. It can be calculated based on the watershed surface area using an approach proposed by Vanoni (1975):

$$Sdel = a WA_L^{-b}$$

where WA_L is watershed area in m^2 , b is an empirical slope coefficient (-0.125) and a is an empirical intercept coefficient that varies with watershed area. A graph of the sediment delivery ratio as a function of watershed area is given in the Water Quality Assessment Manual (Mills et al. 1985, pp. 177,178).

B.2.18 Pollutant Enrichment Factor

Parameter: EF

Definition: The pollutant enrichment factor accounts for the fact that the lighter particles susceptible to erosion tend to have a greater concentration of pollutants attached per mass than what the average soil concentration may suggest.

Units: unitless

Location	Default Value	Distribution
Both Locations	2	U(1.5,2.6)

Technical Basis:

Enrichment refers to the fact that erosion favors the lighter soil particles, which have higher surface area to volume ratios and are higher in organic matter content. Concentrations of hydrophobic pollutants would be expected to be higher in eroded soil as compared to in-situ soil. While enrichment is best ascertained with sampling or site-specific expertise, generally it has been assigned values in the range of 1 to 5 for organic matter, phosphorus, and other soil-bound constituents of concern. Mullins et al. (1993, p.6-22) describe the following equation for calculating enrichment ratio for storm events:

$$EF = 2 + 0.2 \ln(X_e/A_w)$$

where X_e is the mass of soil eroded, in metric tons (1 metric ton = 1000 kg), and A_w is watershed area, in hectares (1 hectare = 10,000 m²). Experience suggests that typical values range from 1.5 to 2.0, reflecting erosion events from 0.08 to 1.0 tonnes per hectare. A very large erosion event of 20 tonnes per hectare would have a predicted enrichment ratio of 2.6. The default value assumed here is 2.

B.2.19 Water Body Surface Area

Parameter: A_w

Definition: Water body surface area

Units: km²

Location	Default Value	Distribution
Both Locations	2.49	U(1.5,3)

Technical Basis:

For the purpose of this assessment, it was assumed that the hypothetical water body has a diameter of 1.78 km, from which the default surface area is calculated.

B.2.20 Water Body Volume

Parameter: V_w

Definition: Water body volume

Units: m^3

Location	Default Value	Distribution
Both Locations	1.24×10^7	Constant

Technical Basis:

For the purpose of this assessment, it was assumed that the hypothetical water body has a diameter of 1.78 km and mean depth of 5 m. The corresponding volume is $1.24 \times 10^7 m^3$ (using the formula $volume = \pi r^2 h$).

B.2.21 Long-Term Dilution Flow

Parameter: Vf_x

Definition: Long term dilution flow

Units: m^3/yr

Location	Default Value (m^3/yr)
Eastern Location	1.44×10^7
Western Location	1.44×10^5

Technical Basis:

The long-term dilution flow can be estimated from Tables in Mills et al. (1985). The values in in/yr are given in Table B-14. These were multiplied by the watershed area of $3.3 \times 10^7 m^2$ to obtain the default values.

Table B-14
Long-Term Dilution Flow In In/Yr

Location	Value (in/yr)
Eastern Location	15
Western Location	0.15

B.2.22 Abiotic Solids Deposition Velocity

The settling velocity for abiotic solids, v_s , is represented in the spreadsheet by variable SSDEP. The default value is set to 730 m/year (2 m/day).

Technical Basis:

Stoke's equation can be used to calculate the terminal velocity of a particle settling through the water column:

$$V_s = \frac{g}{18\mu} (\rho_{pa} - \rho_w) d_p^2 \cdot 3.15 \cdot 10^7 \cdot 10^{-4}$$

where V_s is Stoke's velocity, m/year, for abiotic particles with diameter d_p , mm, and density ρ_{pa} , g/cm³; g is the acceleration of gravity, 981 cm/sec²; μ is the absolute viscosity of water, 0.01 poise (g/cm-sec) at 20°C; and ρ_w is the density of water, 1.0 g/cm³ at 20°C.

Values of V_s for particle density of 2.7 and diameters representative of clay, very fine silt, fine silt, and medium silt are 30, 120, 730, and 2900 m/year, respectively. Settling velocities should be set at or below Stoke's velocity corresponding to the median suspended particle size, keeping in mind that pollutants tend to sorb more to the smaller silts and clays than to large silt and sand particles. The value chosen here is the calculated Stoke's velocity for fine silt ($d_p = 0.005$ mm), and represents settling of fine to medium silts.

B.2.23 Biotic Solids Production Rate

The internal production of biotic solids, L_{Bio} , in g/m²-year, is set to a default value of 100.

Technical Basis:

The production of phytoplankton carbon, in mg-C/m²-day, has been linked to trophic status as follows (Wetzel, 1975):

ultra-oligotrophic:	< 50
oligotrophic:	50 - 300
mesotrophic:	25 - 1000
eutrophic:	>1000

The phytoplankton production is multiplied by 2.7 to get mg-solids/m²-day (Mills, et al., 1985, p. 62) and by 0.365 to get g-solids/m²-year (since the product of 2.7 and 0.365 is 0.99, the phytoplankton production in mg-C/m²-day is numerically equal to the solids production in g-solids/m²-year). A value representative of oligotrophic water bodies was chosen.

B.2.24 Phytoplankton Mortality

The phytoplankton mortality rate constant k_{mort} is set to a value of 11 yr⁻¹.

Technical Basis:

In calculating biotic solids, the net primary productivity incorporates phytoplankton growth and respiration. Grazing transfers phytoplankton solids to zooplankton solids, both of which are considered biotic solids. Settling removes phytoplankton solids from the water column, and is accounted for with a specific settling velocity. Nonpredatory mortality accounts for phytoplankton loss processes that are not

accounted for in the grazing, respiration, and settling loss. This loss term includes processes such as senescence, bacterial decomposition of cells, and stress-induced mortality, and is generally modeled using a first-order rate constant (Bowie, et al., 1985). Values for rate constants cited in Bowie, et al, 1985 range from 0.003 to 0.17 day⁻¹. A rate constant of 0.03 day⁻¹ (11 yr⁻¹) was chosen here as a representative mid-range value. Applying a typical oligotrophic production rate of 100 g/m²-year, a settling rate constant of 73 m/yr, and a mortality rate constant of 11 yr⁻¹ to the shallow lake parameterized here, biotic solids are predicted to be 0.75 mg/L. Assuming that about 75% are phytoplankton, this corresponds with chlorophyll *a* levels averaging less than 7 μg/L, which is reasonable for an oligotrophic lake.

B.2.25 Biotic Solids Deposition Velocity

The settling velocity of biotic solids, v_{sB} , is set to a default value of 73 m/year (0.2 m/day).

Technical Basis:

The settling of phytoplankton solids depends on several factors, including the density, size, shape, and physiological state of the cells and the turbulence of the flow (Bowie, et al., 1985). Phytoplankton settling is a calibration parameter in most modeling exercises. Most values cited in Bowie et al. (1985) fall between 0.02 and 2 m/day. A value of 0.2 m/day (73 m/year) is close to mid-range.

B.2.26 Surficial Sediment Particle Density and Dry Density (Sediment Concentration)

Upper benthic sediment particle density, ρ_p , is set to a default value of 1.5 g/cm³. The corresponding upper benthic sediment concentration, S_B , in mg/L, is set to a default value of 75,000.

Technical Basis:

Benthic sediment concentration is equivalent to dry density (ρ_D , in g-sediment/cm³), which can be calculated from the particle density (ρ_p , in g-sediment/cm³-sediment) and sediment porosity (n , in cm³-water/cm³):

$$\rho_D = \rho_p (1 - n)$$

Sediment porosity can be calculated from bulk density (ρ_B , in g-sediment+water/cm³), along with particle density and the density of water (ρ_w , in g-water/cm³-water):

$$n = \frac{\rho_p - \rho_B}{\rho_p - \rho_w}$$

Dry density, then, can be related to bulk density, particle density, and water density:

$$\rho_D = \frac{\rho_p (\rho_B - \rho_w)}{\rho_p - \rho_w}$$

Typical particle densities in sediments range between 2.6 and 2.7 g/cm³. At 20°C, water density is close to 1.0 g/cm³. For these properties, a bulk density value of 1.6 g/cm³ corresponds to a dry density of 1.0 g/cm³ and a porosity of 0.65, which represents consolidated benthic sediment. An analysis of 1680 measured bulk densities in marine sediments exhibited a range from 1.25 to 1.8 g/cm³ and an average particle density of 2.7 (Richards et al., 1974). Some waterbodies contain an upper unconsolidated layer of sediment with bulk densities of 1.1 to 1.3, which correspond to porosities of 0.94 to 0.82 and dry

densities of 0.16 to 0.48 g/cm³. In this study, we represent pollutant storage in the unconsolidated upper bed layer where the porosity is 0.95 and the particle density is 1.5 g/cm³, which would represent a significant percentage of biotic solids. The corresponding bulk density of this layer is 1.025 g/cm³, and the dry density is 0.075 g/cm³.

B.2.27 Upper Benthic Sediment Depth

Parameter: z_b

Definition: Benthic sediment concentration

Units: m

Scenario	Default Value (m)	Distribution
Both Locations	0.02	U(0.01,0.03)

Technical Basis:

The total benthic sediment depth can vary from essentially zero in rocky streams to hundreds of meters in oceans. In the lake environments being modeled here, the total benthic sediment depth usually exceeds a few centimeters. Here we are modeling only the upper layer that is in partial contact with the water column through physical mixing and bioturbation; thus, a shallow depth of 2 cm was chosen.

B.2.28 Resuspension Velocity

Resuspension velocity, v_{rs} , is set to a default value of 0.0037 m/year. .

Technical Basis:

Resuspension from a sediment bed is caused by shear stress in the overlying water; the rate of sediment resuspension for a given shear stress is determined by the shear strength of the upper sediment layer. Shear stress in streams is caused primarily by flow velocity. In lakes, shear stress may be caused by wind-driven residual currents and waves. In addition, biotic activity can cause some resuspension. For a small lake 5 meters deep with a short fetch (approximately 100 m), wave-induced resuspension should be almost zero under most wind conditions.

An empirical approach to parameterizing resuspension velocity is to calculate a value that would be sufficient to maintain equilibrium suspended solids levels at a given level:

$$v_{rs} = v_s \cdot \frac{S_w}{S_B}$$

Given a settling velocity of 730 m/year, a benthic solids concentration of 75,000 mg/L, and an equilibrium suspended solids concentration of 0.4 mg/L, the resuspension velocity is calculated to be 4×10^{-3} m/year.

B.3 REFERENCES

- Akagi H., D.C. Mortimer, and D.R. Miller (1979). Mercury Methylation and Partition in Aquatic Systems. *Bull. Environ. Contam. Toxicol.* 23: 372-376.
- Alberts, J.J., J.E. Schindler, and R.W. Miller. (1974). Elemental mercury evolution mediated by humic acid.
- Albeuts, J.J., J.E. Schindler, and R.W. Miller (1974). Elemental Mercury Evolution Mediated by Humic Acid. *Science* 184: 895-897.
- Amyot, M., D. Lean, and G. Mierle (1997). Photochemical Formation of Volatile Mercury in High Arctic Lakes. *Environmental Toxicology and Chemistry*, 16(10):2054-2063.
- Amyot, M., G. Mierle, D. Lean, and D.J. McQueen (1997b). Effect of Solar Radiation on the Formation of Dissolved Gaseous Mercury in Temperate Lakes. *Geochimica et Cosmochimica Acta*, 61(5):975-987.
- Amyot, M., G.Mierle, D.R.S. Lean, and D.J. McQueen (1994a). Sunlight-Induced Formation of Dissolved Gaseous Mercury in Lake Waters. *Environmental Science and Technology*, 28(13):2366-2371.
- Anderson, A., N. Browne, S. Duletsky, J. Ramig, and T. Warn (1985). Development of Statistical Distributions or Ranges of Standard Factors Used in Exposure Assessments. EPA 600/8-85- 101, U.S. Environmental Protection Agency, Office of Health and Environmental Assessment, Washington, D.C.
- Baes, C.F. and R.D. Sharp. (1983). A proposal for estimation of soil leaching constants for use in assessment models. *J. Environ. Qual.* 12: 17-28.
- Baes, C.F., R.D. Sharp, A.L. Sjoreen, and R.W. Shor (1984). A Review and Analysis of Parameters for Assessing Transport of Environmentally Released Radionuclides Through Agriculture. Prepared under contract No. DE-AC05-84OR21400. U.S. Department of Energy, Washington, D.C.
- Baes, C.F., R.D. Sharp, A.L. Sjoreen, and R.W. Shor (1984). A Review and Analysis of Parameters for Assessing Transport of Environmentally Released Radionuclides through Agriculture. Oak Ridge National Laboratory, ORNL-5786.
- Beckert, W.F., A.A. Moohiissi, F.H.F. Au, E.W. Bretthauer, and J.C. McFarlane (1974). Formation of Methylmercury in a Terrestrial Environment. *Nature*, 249:674-675.
- Belcher, G.D. and C.C. Travis (1989). Modeling Support for the Rura and Municipal Waste Combustion Projects: Final Report on Sensitivity and Uncertainty Analysis for the Terrestrial Food Chain Model. Prepared for the U.S. EP1.
- Belcher, G.D. and C.C. Travis (1989). Modelling Support for the Rural and Municipal Waste Combustion Projects: Final Report on Sensitivity and Uncertainty Analysis for the Terrestrial Food Chain Model. Prepared for the U.S. EPA.
- Bloom, N. and S.W. Effler. (1990). *Water, Air, and Soil Poll.* 53:251-265.
- Bloom, N.S. and C.J. Watras (1989). Observations of Methylmercury in Precipitation. *The Sci. Tot. Environ.* 87/88: 199-207.

Bloom, N.S., C.J. Watras, and J.P. Hurley (1991). Impact of Acidification on the Methylmercury Cycle of Remote Seepage Lakes. *Water, Air, and Soil Poll.* 56: 477-491.

Bousset, C. (1981). The Mercury Cycle. *Water, Air and Soil Pollution* 16: 253-255.

Bowie, G.L. et al. (1985). Rates, Constants, and Kinetics Formulations in Surface Water Quality Modeling (Second Edition). EPA/600/3-85/040. U.S. EPA, Athens, GA.

Bowie, G.L., W.B. Mills, D.B. Porcella, C.L. Campbell, J.R. Pagenkopf, G.L. Rupp, K.M. Johnson, P.W.H. Chan, S.A. Gherini and C.E. Chamberlin (1985). Rates, Constants, and Kinetics Formulations in Surface Water Quality Modeling. Second Edition. EPA/600/3-85/040. U.S. Environmental Protection Agency Athens, GA. EPA

Butcher, B., B. Davidoff, M.C. Amacher, C. Hinz, I.K. Iskandar, and H.M. Selim (1989). Correlation of Freundlich Kd and retention parameters with soils and elements. *Soil Science* 148: 370-379.

Calabrese, E.J. and E.J. Stanek, III (1991). A Guide to Interpreting Soil Ingestion Studies. II. Qualitative and Quantitative Evidence of Soil Ingestion. *Regul. Toxicol. Pharmacol.* 13:278- 292.

Cappon, C. (1984). Content and Chemical Form of mercury and selenium in soil, sludge and fertilizer materials. *Water, Air, Soil Pollut* 22:95-104.

Cappon, C.J. (1981). Mercury and Selenium Content and Chemical Form in Vegetable Crops Grown on Sludge-Amended Soil. *Arch. Environm. Contam. Toxicol.* 10: 673-689.

Cappon, C.J. (1987). Uptake and Speciation of Mercury and Selenium in Vegetable Crops Grown on Compost-Treated Soil. *Water, Air, Soil Poll.* 34: 353-361.

Carpi, A., and S.E. Lindberg (1997). Sunlight-Mediated Emission of Elemental Mercury from Soil Amended with Municipal Sewage Sludge. *Environmental Science and Technology*, 31(7):2085-2091.

Carsel, R.F., C.N. Smith, L.I. Mulkey, J.D. Dean, and P. Jowise (1984). User's Manual for the Pesticide Root Zone Model (PRZM) Release 1. U.S. EPA, Athens, GA. EPA-600/3-84-109.

Carsel, R.F., C.N. Smith, L.A. Mulkey, J.D. Dean, and P. Jowise (1984). User's Manual for the Pesticide Root Zone Model (PRZM) Release 1. U.S. EPA, Athens, GA. EPA-600/3-84-109.

Ershow, A.G. and K.P. Cantor (1989). Total Water and Tapwater Intake in the United States: Population-based Estimates of Quantities and Sources. Life Sciences Research Office, Federation of American Societies for Experimental Biology. Bethesda, Maryland.

Fitzgerald, W. (1986). Cycling of mercury between the atmosphere and oceans, in: *The Role of Air-Sea Exchange in Geochemical Cycling*, NATO Advanced Science Institutes Series, P. Buat-Menard (Ed.), D. Reidel publishers, Dordrecht, pp 363-408.

Fitzgerald, W.F., R.P. Mason, and G.M. Vandal (1991). Atmospheric Cycling and Air-Water Exchange of Mercury over Mid-Continental Lacustrine Regions. *Water, Air, and Soil Pollution* 56: 745-767.

Fortmann, L. C., D. D. Gay, and K. O. Wirtz (1978). Ethylmercury: Formation in Plant Tissues and Relation to Methylmercury Formation. U.S. EPA Ecological Research Series, EPA-600/3-78- 037.

Fries, G.F. (1982). Potential Polychlorinated Biphenyl Residues in Animal Products from Application of Contaminated Sewage Sludge to Land. *J. Environ. Quality.* 11: 14-20.

- Fries, G.F. (1987). Assessment of Potential Residues in Food Derived from Animals Exposed to TCDD-Contaminated Soil. *Chemosphere* 16: 2123-2128.
- Geraghty, J. J., D. W. Miller, F. V. Der Leenden, and F. L. Troise (1973). *Water Atlas of the United States*. A Water Information Center Publication, Port Washington, N.Y.
- Gill, G. And K. Bruland (1990). Mercury Speciation in surface freshwaters systems in California and other areas. *Sci. Total Environ.* 24:1392.
- Gilmour, C.C, E.A. Henry, and R. Mitchell (1992). Sulfate Stimulation of Mercury Methylation in Freshwater Sediments. *Environmental Science and Technology*, 26(11):2281-2287.
- Gilmour, C.C. and E.A. Henry (1991). Mercury Methylation in Aquatic Systems Affected by Acid Deposition. *Environmental Pollution*, 71:131-169.
- Gilmour, C.C. and G.S. Riedel (1995). Measurement of Hg Methylation in Sediments Using High Specific Activity ²⁰³Hg and Ambient Incubation. *Water, Air, and Soil Pollution*, 80:747-756.
- Glass, G.E., J.I. Sorenson, K.W. Schmidt, and G.R. Rapp (1990). New Source Identification of Mercury Contamination in the Great Lakes. *Environmental Science and Technology* 24:1059- 1069.
- Hanford Environmental Dose Reconstruction Project (1992). Parameters Used in Environmental Pathways (DESCARTES) and Radiological Dose (CIDER) Modules of the Hanford Environmental Dose Reconstruction Integrated Codes (HEDRICF) for the Air Pathway, PNWD-2023 HEDR, Pacific Northwest Laboratories, September 1992.
- Harris, R., Gherini, S.A., and Hudson, R. (1996). Regional Mercury Cycling Model (R-MCM): A Model for Mercury Cycling in Lakes, Draft User's Guide and Technical Reference. Prepared for The Electric Power Research Institute, Palo Alto, CA and Wisconsin Department of Natural Resources, Monona, WI.
- Hattemer-Frey, H. and C.C. Travis (1989). An Overview of Food Chain Impacts from Municipal Waste Combustion. Prepared for U.S. EP1.
- Hawley, J.K. (1985). Assessment of Health Risk from Exposure to Contaminated Soil. *Risk Anal.* 5(4): 289-302.
- Henry, E.A., L.J. Dodge-Murphy, G.N. Bigham, S.M. Klein, and C.C. Gilmour (1995a). Total Mercury and Methylmercury Mass Balance in an Alkaline, Hypereutrophic Urban Lake (Onondaga Lake, NY). *Water, Air, and Soil Pollution*, 80:509-518.
- Henry, E.A., L.J. Dodge-Murphy, G.N. Bigham, and S.M. Klein (1995b). Modeling the Transport and Fate of Mercury in an Urban Lake (Onondaga Lake, NY). *Water, Air, and Soil Pollution*, 80:489- 498.
- Hildebrand, S.G., R.H. Strand, and J.W. Huckabee (1980). Mercury accumulation in fish and invertebrates of the North Fork Holston river, Virginia and Tennessee. *J. Environ. Quan.* 9:393-400.
- Hildebrand, S.G., S.E. Lindberg, R.R. Turner, J.W. Huckabee (1980). Biogeochemistry of Mercury in a River Reservoir System: Impact of an Inactive Chloralkali Plant on the Holston River. ORNL/TM-6141.
- Hoffman, F.O. and D.F. Baes (1979). A Statistical Analysis of Selected Parameters for Predicting Food Chain Transport and Internal Dose of Radionuclotides. ORNL/NUREG/TM-882.

Hoffman, F.O. and D.F. Baes (1979). A Statistical Analysis of Selected Parameters for Predicting Food Chain Transport and Internal Dose of Radionuclides. ORNL/NUREG/TM-882.

Hoffman, F.O., K.M. Thiessen, M.L. Frank and 2.G. Blaylock (1992). Quantification of the interception and initial retention of radioactive contaminants deposited on pasture grass by simulated rain. *Atmospheric Environment*, 26A (18): 3313-3321.

Imhoff, J.C., P.R. Hummel, J.L. Kittle, and R.F. Carsel. (1994). PATRIOT - A Methodology and Decision Support System for Evaluating the Leaching Potential of Pesticides. EPA/600/S-93/010. U.S. Environmental Protection Agency, Athens, Georgia.

Iverfeldt, Å. and Persson, J. (1985). The solvation thermodynamics of methylmercury (II) species derived from measurements of the heat of solvation and the Henry's law constant. *Inorg. Chim. Acta*, 103, 113-119.

Iverfeldt, A. and J. Persson (1985). The solvation thermodynamics of methylmercury (II) species derived from measurements of the heat of solvation and the Henry's Law constant. *Inorganic Chimica Acta*, 103: 113-119.

Jacobs, L.A., S.M. Klein, and E.A. Henry (1995). Mercury Cycling in the Water Column of A Seasonally Anoxic Urban Lake (Onondaga Lake, NY). *Water, Air, and Soil Pollution*, 80:553-562.

John, M.K. (1972). Mercury Uptake from Soil by Various Plant Species. *Bull. Environ. Contam. Toxicol.* 8(2): 77-80.

Knott, J.E. (1957). *Handbook for Vegetable Growers*. J. Wiley and Sons, Inc., New York.

LaGoy, L.K. (1987). Estimated Soil Ingestion Rates for Use in Risk Assessment. *Risk Anal.* 7(3): 355-359.

Lee, Y., and H. Hultburg (1990). Methylmercury in some Swedish Surface Waters. *Environ. Toxicol. Chem.* 9: 833-841.

Lenka, M., K. K. Panda, and 2. 2. Panda (1992) Monitoring and Assessment of Mercury Pollution in the Vicinity of a Chloralkali Plant. IV. Bioconcentration of Mercury in In Situ Aquatic and Terrestrial Plants at Ganjam, Indi1. *Arch. Environ. Contam. Toxicol.* 22:195-202.

Lenka, M., K.K. Panda, and 2.2. Panda (1992a). Monitoring and Assessment of Mercury Pollution in the Vicinity of a Chloralkali Plant. II. Plant Availability, Tissue Concentration and Genotoxicity of Mercury from Agricultural Soil Contaminated with Solid Waste Assessed in Barley. *Environ. Poll.* 0269-7491/92. pp. 33-42.

Lenka, M., K.K. Panda, and 2.2. Panda (1992b). Monitoring and Assessment of Mercury Pollution in the Vicinity of a Chlor-alkali Plant. IV. Bioconcentration of Mercury in In Situ Aquatic and Terrestrial Plants at Ganjam, Indi1. *Arch. Environ. Contam. Toxicol.* 22:195-202.

Lepow, M.L., L. Bruckman, M. Gillette, S. Markowitz, R. Robino, and J. Kapish (1975). Investigations into Sources of Lead in the Environment of Urban Children. *Environ. Res.* 10: 415-426.

Lindberg, S. E., D. R. Jackson, J. W. Huckabee, S. I. Janzen, M. J. Levin, and J. R. Lund (1979). Atmospheric Emission and Plant Uptake of Mercury from Agricultural Soils near the Almaden Mercury Mine. *J. Environ. Qual.* 8(4):572-578.

Lindberg, S.E., 1996. Forests and the Global Biogeochemical Cycle of Mercury: The Importance of Understanding Air/Vegetation Exchange Processes. W. Baeyans et al. (Eds.), *Global and Regional Mercury Cycles: Sources, Fluxes, and Mass Balances*, 359-380.

Lindquist, O. and H. Rodhe (1985). Atmospheric Mercury: A Review. *Tellus* 37B: 136-159.

Lindqvist, O., K. Johansson, M. Aastrup, A. Andersson, L. Bringmark, G. Hovsenius, L. Hakanson, A. Iverfeldt, M. Meili, and 2. Timm (1991). Mercury in the Swedish Environment - Recent Research on Causes, Consequences and Corrective Methods. *Water, Air and Soil Poll.* 55:(all chapters)

Lyman, W.J., W.F. Rheel, and D.H. Rosenblatt (1982). *Handbook of Chemical Property Estimation Methods*. New York: McGraw-Hill.

Lyon, B.F., G.A. Rice, R.A. Ambrose, and C.J. Maxwell (1997). Calculation of soil-water and benthic sediment partition coefficients for mercury. *Chemosphere*, 35(4): 791-808.

Mason, R.P., F.M.M. Morel, and H.F. Hemond (1995). The Role of Microorganisms in Elemental Mercury Formation in Natural Waters. *Water, Air, and Soil Pollution*, 80:775-787.

Mason, R.P., W.F. Fitzgerald, and F.M.M. Morel (1994). The Biogeochemical Cycling of Elemental Mercury: Anthropogenic Influences. *Geochimica et Cosmochimica Acta*, 58(15):3191-3198.

Matilainen, T. (1995). Involvement of Bacteria in Methylmercury Formation in Anaerobic Lake Waters. *Water, Air, and Soil Pollution*, 80:757-764.

McKone, T.E. and P.2. Ryan (1989). Human Exposure to Chemicals Through Food Chains: An Uncertainty Analysis. *Environ. Sci. Technol.* 23(9): 1154-1163.

Miller, C. And F. Hoffman. (1983). An examination of the environmental half-time for radionuclides deposited on vegetation. *Health Physics* 45:731.

Miller, C.W. and F.O. Hoffman (1981). An Examination of the Environmental Half-time for Radionuclides Deposited on Vegetation. *Health Phys.* 45:731-744.

Mills, W.B., D.B. Porcella, M.J. Unga, S.A. Gherini, K.V. Summers, Lingfung Mok, G.L. Rupp and G.L. Bowie (1985). *Water Quality Assessment: A Screening Procedure for Toxic and Conventional Pollutants in Surface and Ground Waters (Revised 1985)*, EPA-600/6-85-002a and b. Volumes I and II. U.S. Environmental Protection Agency. Athens, GA.

Miskimmin, B.M. (1991). Effect of Natural Levels of Dissolved Organic Carbon (DOC) on Methylmercury Formation and Sediment-Water Partitioning. *Bull. Environ. Contam. Toxicol.* 47: 743-750.

Moore, J.W. and S. Ramamoorthy (1984). *Heavy Metal in Natural Waters - Applied Monitoring in Impact Assessment*. New York, Springer-Verlag.

Morgan, J., M. Berry and R. Graves. (1994) Effects of Native American Cooking Practices on Total Mercury Concentrations in Walleye. Abstract presented at ISEE/ISEA Joint Conference. September 18-21, 1994.

Mosbaek, H., J. C. Tjell, and T. Sevel (1988). Plant Uptake of Mercury in Background Areas. *Chemosphere* 17(6):1227-1236.

Mullins, J.A., R.F. Carsel, J.E. Scarbrough, and A.M. Ivery. (1993). PRZM-2, A Model for Predicting Pesticide Fate in the Crop Root and Unsaturated Soil Zones: Users Manual for Release 2.0. EPA/600/R-93/046. U.S. Environmental Protection Agency, Athens, Georgia.

NAS (National Academy of Science) (1977). Safe Drinking Water Committee. An Assessment of Mercury in the Environment. National Research Council.

NAS (National Academy of Sciences). (1987). Predicting Feed Intake of Food-Producing Animals. National Research Council, Committee on Animal Nutrition, Washington, DC.

National Climatic Data Center. (1986). Local Climatological Data - Annual Summary with Comparative Data - Cincinnati, (Greater Cincinnati Airport) Ohio. ISSN 0198-3911, Asheville, North Carolina.

Nriagu, J.O. (1979). The Biogeochemistry of Mercury in the Environment. Elsevier/North Holland. Biomedical Press: New York.

Parks, J.W., A. Luitz, and J.I. Sutton (1989). Water Column Methylmercury in the Wabigoon/English River-lake System: Factors Controlling Concentrations, Speciation, and Net Production. Can. J. Fish. Aquat. Sci. 46: 2184-2202.

Pierce, R., D. Noviello and S. Rogers. (1981). Commencement Bay Seafood Consumption Report. Preliminary Report. Tacoma, WA: Tacoma-Pierce County Health Department. As cited in U.S. EPA (1991). Exposure Factors Handbook. EPA/600/8-89/043.

Porvari, P. and M. Verta (1995). Methylmercury Production in Flooded Soils: a Laboratory Study. Water, Air, and Soil Pollution, 80:765-773.

Puffer, H. (1981). Consumption rates of potentially hazardous marine fish caught in the metropolitan Los Angeles area. EPA Grant #R807 120010. As cited in U.S. EPA (1991). Exposure Factors Handbook. EPA/600/8-89/043.

Richards, A.F., T.J. Hirst, and J.M. Parks. (1974). Bulk Density-Water Content Relationship in Marine Silts and Clays. Journal of Sedimentary Petrology, Vol.44, No.4, p 1004-1009.

Robinson, K.G. and M.S. Shuman (1989). Determination of mercury in surface waters using an optimized cold vapor spectrophotometric technique. International Journal of Environmental Chemistry 36: 111-123.

Roels, H.I., J.P. Buchet, and R.R. Lauwerys (1980). Exposure to Lead by the Oral and Pulmonary Routes of Children Living in the Vicinity of a Primary Lead Smelter. Environ. Res. 22: 81-94.

Roseberry, A.M. and D.E. Burmaster (1992). Lognormal Distributions for Water Intake by Children and Adults. Risk Analysis 12: 65-72.

Roy, M. and C. Courtay (1991). Daily Activities and Breathing Parameters for Use in Respiratory Tract Dosimetry. Radiation Protection Dosimetry 35 (3): 179-186.

Rutledge, A.D. (1979). Vegetable Garden Guide. Publication 447 (Revised) University of Tennessee Agricultural Extension Service, The University of Tennessee.

Sanemasa, I. (1975). Solubility of Elemental Mercury Vapor in Water. Bull. Chem. Soc. Jpn. 48(6): 1795-1798.

Schnoor, J.L., C. Sato, D. McKechnie, and D. Sahoo (1987). Processes, Coefficients, and Models for Simulating Toxic Organics and Heavy Metals in Surface Waters. EPA/600/3-87/015. U.S. Environmental Protection Agency. Athens, GA.

Schroeder, W., G. Yarwood and H. Niki (1991). Transformation Processes involving Mercury Species in the Atmosphere-Results from a Literature Survey. *Water, Air and Soil Pollution* 56: 653-666.

Sellers, P., C.A. Kelly, J.W.M. Rudd, and A.R. MacHutchon (1996). Photodegradation of Methylmercury in Lakes. *Nature*, 380:694-697.

Shor, R.W. , C.F. Baes , and R.D. Sharp (1982). Agricultural Production in the United States by County: A Compilation of Information from the 1974 Census of Agriculture for Use in Terrestrial Food Chain Transport and Assessment Models. Oak Ridge National Laboratory, ORNL-5786.

South Coast Air Quality Management District (SCAQMD) (1988). Multi-pathway Health Risk Assessment Input parameters. Guidance Document.

Stordal, M.C. and G.A. Gill (1985). Determination of Mercury Methylation Rates Using a 203-Hg Radiotracer Technique. *Water, Air, and Soil Pollution*, 80:529-538.

Sumo, E., B.R. Singh, A.R. Selmer-Olsen, and K. Steenburg (1985). Uptake of 203Hg-labeled Mercury compounds by Wheat and Beans Grown on an oxisol. *Plant and Soil* 85: 347-355.

Technical Assessment Systems (TAS) (1991). Distribution of Intake of Foods in Sixteen Food Groupings: grains and cereals; potatoes including sweet potatoes and yams; leafy vegetables, excluding brassica; brassica vegetables; legume vegetables; fruiting vegetables, including cucurbits; root vegetables; other vegetables; beef excluding liver; beefliver; sheep; pork; poultry; eggs; milk; and fruits, excluding cucurbits. Prepared for U.S. EP1.

Temple, P. J. and S. N. Linzon (1977). Contamination of Vegetation, Soil, Snow and Garden Crops by Atmospheric Deposition of Mercury from a Chlor-Alkali Plant, in (1977) D. D. Hemphill [ed] Trace Substances in Environmental Health - XI, Univ Missouri, Columbia. p. 389-398.

Turner, R. (1994). Personal communication with Ralph Turner, Environmental Sciences Division, Oak Ridge National Laboratory.

U.S. Department of Commerce. (1977). 1974 Census of Agriculture. Bureau of the Census, Agriculture Division, Washington, D.C.

U.S. Department of Agriculture (USDA) (1978). Handbook No. 537: Predicting Rainfall Erosion Losses. U.S. Government Printing Office, Washington, D.C.

U.S. EPA (1984). Health Assessment Document for Mercury. Prepared by the Office of Health and Environmental Assessment, Environmental Criteria and Assessment Office, Cincinnati, OH for the Office of Emergency and Remedial Response, Washington, D.C.

U.S. EPA (1985). Environmental profiles and hazard indices for constituents of municipal sludge: Mercury. Washington, D.C.: Office of Water Regulations and Standards.

U.S. EPA. (1985). Water Quality Assessment: A Screening Procedure for Toxic and Conventional Pollutants in Surface and Ground Water (Part 1). Washington, D.C. EPA/600/6-85/002-A.

- U.S. EPA. (1988). Superfund Exposure Assessment Manual. Office of Remedial and Emergency Response, Washington, D.C. EPA/540/1086/060.
- U.S. EPA. (1989a). Development of Risk Assessment Methodology for Land Application and Distribution and Marketing of Municipal Sludge. Office of Health and Environmental Assessment, Washington, D.C. EPA/600/6-89/001.
- U.S. EPA (1989b). Exposure Factors Handbook. Office of Health and Environmental Assessment, Exposure Assessment Group, Washington, D.C. EPA 600/8-89-043. NTIS PB90-106774.
- U.S. EPA (1990). Methodology for Assessing Health Risks Associated with Indirect Exposure to Combustor Emissions. Office of Health and Environmental Assessment, Washington, D.C. EPA/600/6-90/003.
- U.S. EPA (1993a). Assessment of Mercury Occurrence in Pristine Freshwater Ecosystems, prepared by ABT Associates, Inc. Draft as of September 1993.
- U.S. EPA (1993b). Technical Support document on Land Application of Sewage Sludge. Federal Register. 40 CFR Part 257 et al. Standards for the Use or Disposal of Sewage sludge; Final Rules. February 19.
- U.S. EPA. (1993c). Addendum to the Methodology for Assessing Health Risks Associated with Indirect Exposure to Combustor Emissions. Office of Research and Development, Washington, D.C. EPA/600/AP-93/003.
- van der Veen, N.G. and K. Vreman (1986). Transfer of cadmium, lead, mercury and arsenic from feed into various organs and tissues of fattening lambs. *Netherlands Journal of Agricultural Science* 34: 145-153.
- Vandal, G.M., W.F. Fitzgerald, K.R. Rolfhus, and C.H.Lamborg, (1995). Modeling the Elemental Mercury Cycle in Pallette Lake, Wisconsin, USA. *Water, Air, and Soil Pollution*, 80:789-798.
- Vanoni, V.A. (1975). *Sedimentation Engineering*. American Society of Civil Engineers, New York, NY. pp. 460-463.
- Vreman, K., N.J. van der Veen, E.J. van der Molen and W.G. de Ruig (1986). Transfer of cadmium, lead, mercury and arsenic from feed into milk and various tissues of dairy cows: chemical and pathological data. *Netherlands Journal of Agricultural Science* 34: 129-144.
- Watras, C.J. and N.S. Bloom (1992). Mercury and Methylmercury in Individual Zooplankton: Implications for Bioaccumulation. *Limnol. Oceanogr.*37(6): 1313-1318.
- Watras, C.J., N.S. Bloom, S.A. Claas, K.A. Morrison, C.C. Gilmour, and S.R. Craig (1995). Methylmercury Production in the Anoxic Hypolimnion of a Dimictic Seepage Lake. *Water, Air, and Soil Pollution*, 80:745-745.
- WeatherDisc Associates (1992). U.S. Local Climatological Data Summaries for 288 Primary Stations throughout the U.S., on CDROM.
- Wetzel, R.G. (1975). *Limnology*. 1st. Edition. W.B. Saunders, Philadelphia, 743 pp.

Wiersma, D., B. J. van Goor, and N. G. van der Veen (1986). Cadmium, Lead, Mercury, and Arsenic Concentrations in Crops and Corresponding Soils in the Netherlands. *J. Agric. Food Chem.*, 34:1067-1074.

Wiessman, D., B.J. vanGoor, and N.G. van der Veen (1986). Cadmium, Lead, Mercury, and Arsenic Concentrations in Coops amd Corresponding Soils in the Netherlands. *J. Agric. Food Chem.* 34: 1067-1074.

Wilken, R.D. and H. Hintelmann (1991). Mercury and Methylmercury in Sediments and Suspended Particles from the River Elbe, North Germany. *Water, Air, and Soil Poll.* 56: 427-437.

Wischmeier, W. and D. Smith. (1978). Predicting Rainfall and Erosion Losses: A Guide to Conservation Planning. U.S. Department of Agriculture, Agriculture Handbook No. 537.

Xiao, Z.F., D. Stromberg, and O. Lindqvist (1995). Influence of Humic Substances on Photolysis of Divalent Mercury in Aqueous Solution. *Water, Air, and Soil Pollution*, 80:789-798.

APPENDIX C

DESCRIPTION OF MODEL PLANTS

TABLE OF CONTENTS

C.1	Introduction	C-1
C.2	Relationship of Plant Process Conditions to Emissions	C-1
C.2.1	Municipal Waste Combustors	C-3
C.2.1.1	Description of Source Category	C-3
C.2.1.2	Summary of Available Data on Emissions and Controls	C-4
C.2.1.3	Selection of MWC Model Plant Parameters	C-6
C.2.2	Medical Waste Incinerators	C-7
C.2.2.1	Description of Source Category	C-7
C.2.2.2	Summary of Available Data on Emissions and Controls	C-7
C.2.2.3	Selection of MWI Model Plant Parameters	C-8
C.2.3	Utility Boilers	C-8
C.2.3.1	Description of Source Category	C-8
C.2.3.2	Summary of Available Data on Emissions and Controls	C-9
C.2.3.3	Selection of Model Plant Parameters	C-11
C.2.4	Chlor-Alkali Production	C-11
C.2.4.1	Description of Source Category	C-11
C.2.4.2	Summary of Available Data on Emissions and Control	C-12
C.2.4.3	Selection of Model Plant Parameters	C-12
C.3	References	C-13

LIST OF TABLES

C-1 Process Parameters for Model Plants C-2
C-2 Scenarios for Sensitivity of Total Mercury Deposition Rate to Emissions Speciation
for Municipal Waste Combustors C-7
C-3 Mercury Removal Efficiencies C-10

LIST OF FIGURES

C-1 Distribution of Mercury in EPA Method 29 Sampling Train, Camden County and Stanislaus
County Carbon Injection Projects C-5

C.1 Introduction

Model plants representing six source categories were developed to represent a range of mercury emission parameters. The source categories were selected for the local impact analysis based on their estimated annual mercury emissions or their potential to be localized point sources of concern. The categories were municipal waste combustors (MWCs), medical waste incinerators (MWIs), utility boilers, and chlor-alkali plants.

Descriptive characteristics, or parameters for each model plant were selected after evaluating the characteristics of the entire source class. Important variables for mercury risk assessments include the following: mercury emission rates, mercury speciation, and mercury transport/deposition rates. Important model plant parameters included stack height, stack diameter, stack volumetric flow rate, stack gas temperature, plant capacity factor (relative average operating hours per year), stack concentration, and mercury speciation.

Table C-1 summarizes the model plant parameters modeled in this analysis. These parameters represent operating conditions associated with each source type's current mercury control. That is, mercury emissions reductions being achieved by the air pollution control devices presently in place were considered for each source category. These parameters are not meant to represent a "worst-case" emissions scenario; they are believed to be representative of the full range of sources (of a given category) across the United States. The amount of uncertainty surrounding the emission rates varies for each model plant. This uncertainty is reflected in Chapter 8 -- Research Needs -- of this Volume.

C.2 Relationship of Plant Process Conditions to Emissions

Mercury speciation estimates for elemental mercury (Hg^0) and divalent mercury (Hg^{2+}) were made using literature results of thermal-chemical modeling of mercury compounds in flue gas, interpretation of bench and pilot scale combustor experiments and interpretation of available field test results.

The amount and speciation of mercury emitted from high temperature process depends on the composition of the feed material, amount of mercury in the process feed material, process operating conditions, and process flue gas cleaning techniques (Lindqvist and Schager, 1990).

The inorganic mercury compounds that are considered important in high temperature processes are $\text{HgS}(s)$, $\text{HgO}(s,g)$, $\text{HgCl}_2(s,g)$, $\text{Hg}_2\text{Cl}_2(s)$ and $\text{HgSO}_4(s)$. Some organic compounds, such as methylmercury, CH_3HgCH_3 , and CH_3HgCl may also occur (Hall et al., 1991). Thermochemical calculations indicate that at combustion temperatures above 700°C nearly all mercury is vaporized to form gaseous Hg^0 . As the flue gas cools, changing equilibrium conditions favor oxidized forms of mercury. When there are significant levels of HCl , Cl_2 , O_2 and SO_2 in the flue gas, all of the above oxidized inorganic forms of mercury will tend to occur. In flue gas from coal and peat combustion at temperatures below 200°C , the dominant equilibrium species are HgO and Hg^0 . For combustion wastes containing relatively high levels of chlorine, HgCl_2 will be the dominant mercury compound (Hall et al., 1990; Hall 1991, Lindqvist and Schager, 1990).

**Table C-1
Process Parameters for Model Plants**

Model Plant	Plant Size	Capacity (% of year)	Stack Height (ft)	Stack Diameter (ft)	Hg Emission Rate (kg/yr)	Speciation Percent (Hg ⁰ /Hg ²⁺ /Hg ^p)	Exit Velocity (m/sec)	Exit Temp. (°F)
Large Municipal Waste Combustors	2,250 tons/day	90%	230	9.5	220	60/30/10	21.9	285
Small Municipal Waste Combustors	200 tons/day	90%	140	5	20	60/30/10	21.9	375
Large CommercialHMI Waste Incinerator (Wetscrubber)	1500 lb/hr capacity (1000 lb/hr actual)	88%	40	2.7	4.58	33/50/17	9.4	175
Large Hospital HMI Waste Incinerators (Good Combustion)	1000 lb/hr capacity (667 lb/hr actual)	39%	40	2.3	23.9	2/73/25	16	1500
Small Hospital HMI Waste Incinerators (1/4 sec.Combustion)	100 lb/hr capacity (67 lb/hr actual)	27%	40	0.9	1.34	2/73/27	10.4	1500
Large Hospital HMI Waste Incinerators (Wet Scrubber)	1000 lb/hr capacity (667 lb/hr actual)	39%	40	2.3	0.84	33/50/17	9.0	175
Small Hospital HMI Waste Incinerators (Wet Scrubber)	100 lb/hr capacity (67 lb/hr actual)	27%	40	0.9	0.05	33/50/17	5.6	175
Large Coal-fired Utility Boiler	975 Megawatts	65%	732	27	230	50/30/20	31.1	273
Medium Coal-fired Utility Boiler	375 Megawatts	65%	465	18	90	50/30/20	26.7	275
Small Coal-fired Utility Boiler	100 Megawatts	65%	266	12	10	50/30/20	6.6	295
Medium Oil-fired Utility Boiler	285 Megawatts	65%	290	14	2	50/30/20	20.7	322
Chlor-alkali plant	300 tons chlorine/day	90%	10	0.5	380	70/30/0	0.1	Ambient

^a Hg⁰ = Elemental Mercury

^b Hg²⁺ = Divalent Vapor Phase Mercury

^c Hg_p = Particle-Bound Mercury

Experimental evidence shows that the speciation of mercury is more complicated than indicated by thermochemical equilibrium calculations. For example SO₂, soot, activated carbon, CaO and iron may promote low temperature reactions that reduce oxidized forms of mercury to Hg⁰ (Hall et al., 1990; Hall 1991). The presence of trace gases and particulate in flue gas promote mercury reactions and provide surfaces for physical and chemical adsorption. Reaction kinetics can also be expected to play an important role under the changing thermodynamics conditions that exist in high temperature flue gas streams. Also, some gases such as HCl may not always be or reaction with mercury because of mixing limitations.

While thermochemical chemical calculations provide information on likely mercury compounds in flue gas, their presence and relative magnitude have not been confirmed with experimental data. This shortcoming is primarily the result of difficulties in the sampling and analysis for mercury compounds. One study of mercury speciation on a pilot combustor and a full scale municipal waste incinerator found that the flue gas contained mainly mercury chlorides, and that Hg⁰ mercury was present in insignificant amounts (Metzger and Braun, 1987). Another experimental study of mercury sampling methods concluded that total mercury and Hg⁰ can be adequately measured, that the results of the different sampling methods tested for ionic mercury differed significantly and that additional efforts must be devoted the development of mercury speciation methodologies (Lindqvist and Schager, 1990).

In a third study, conducted in the U.S., measurements with a sampling train designed to provide information on mercury speciation tentatively indicated the presence of methylmercury in the exhaust of coal and municipal waste combustors (Bloom, 1993). It was later reported that the methylmercury reported in that study were the result of artifacts associated with the laboratory analytical procedures. Based on these studies it is concluded that the results of tests providing information on total mercury, Hg⁰ and Hg²⁺ are probably valid, but results of tests for methylmercury and other compounds must be considered suspect until sampling and analysis protocols for those compounds are validated.

The capture of mercury in flue gas cleaning devices depends on the mercury form [e.g, speciation and phase (gas, liquid or solid)] and the control devices employed. Most metals condense to form solid particles as the flue gases are cooled so that the metals can be collected as particulate matter (PM). However, mercury specie such as Hg⁰ and HgCl₂ are vapors at flue gas temperatures and are difficult to control. Some mercury compounds such as HgCl₂ are soluble in water and can be controlled by wet scrubbers. Some specie such as HgCl₂ can be adsorbed onto activated carbon and fly ash carbon for subsequent collection as PM. Reagents can be used to produce mercury compounds that condense for collection as PM. Reagents can also be used to produce soluble mercury compounds for scrubber collection.

C.2.1 Municipal Waste Combustors

C.2.1.1 Description of Source Category

There are three major types of municipal waste combustors (MWC's): mass burn combustors, refuse-derived fuel (RDF) combustors and modular combustors. There are number of sub-categories of these three major types, plus some other types of MWCs, such as fluidized bed combustors. These other types of MWCs constitute a minor fraction of the total MWC population.

As of January 1995, there were over 160 MWC plants in the U.S. with aggregate capacities ranging from greater than 36 Mg/day (40 tons/day). Most large facilities contain from two to four mass burn or refuse-derived fuel (RDF) combustors. Approximately 50 percent of the MWC capacity in the

U.S. now employ spray dryers and fabric filters (SD/FFs) or SD and electrostatic precipitators (SD/ESPs) for emission control. The remaining large facilities do not have acid gas control equipment and generally use good combustion practice and electrostatic precipitators (ESPs) for emissions control. Few U.S. facilities use wet scrubbers. A number of facilities are planning to use activated carbon to control mercury emissions as mandated by siting permits. At least one MWC using activated carbon is in commercial operation.

C.2.1.2 Summary of Available Data on Emissions and Controls

Uncontrolled mercury emissions from MWC's range from less than 200 ug/dscm to more than 1500 ug/dscm depending on the mercury content of wastes being burned. Average uncontrolled flue gas concentrations in mass burn combustors are estimated to be in the range of 600 to 700 ug/dscm (U.S. EPA, 1993; White et al., 1992; Nebel et al., 1992; White et al., 1993). Uncontrolled flue gas concentrations in RDF combustors are somewhat lower since some mercury contained in batteries and other items is removed in the process that produces RDF.

For combustion sources, the degree of mercury control depends on the flue gas composition, the amount of fly ash carbon and the flue gas cleaning techniques employed. Well designed and operated mass burn combustors have little carbon in their fly ash; even when equipped with SD/FFs or SD/ESPs they exhibit mercury control levels that typically range from 0 to 50 percent (Nebel et al., 1992; White et al., 1992). When powdered activated carbon is injected into the flue gas upstream of the spray dryer in mass burn combustors, control levels exceeding 90 percent can be achieved for both SD/FF and SD/ESP systems (Brown and Felsvang, 1992; White et al., 1992; Nebel et al., 1992; White et al., 1993). However, SD/ESP systems require from 2 to 3 times more carbon than SD/FF systems (Kilgroe et al., 1993).

The RDF combustors contain a relatively high amounts of carbon in the fly ash and exhibit control efficiencies of approximately 80 percent when equipped with SD/ESPs and above 90 percent when equipped with SD/FFs (White et al., 1992). Injection of powdered activated carbon can also be used to augment mercury control in RDF combustion facilities.

Little information is available concerning the performance of flue gas cleaning techniques for controlling mercury in modular MWCs. It is expected that the performance of flue gas cleaning devices on modular units will be similar to the performance of comparable equipment installed on conventional mass burn combustors.

Electrostatic precipitators and wet scrubbers are commonly used to control emissions from European MWCs. Some European plants have installed activated carbon beds downstream of the primary air pollution control devices to act as polishing filters for control of metals, dioxins and acid gases. The use of activated carbon filter beds in combination with conventional control equipment have demonstrated mercury reductions exceeding 99 percent and mercury outlet concentrations of less than 1 ug/dscm (Hartenstein, 1993).

In conducting risk assessments, it is important to estimate the form and speciation of mercury emitted in the flue gas. Several studies estimate the speciation of mercury in MWC flue gases. Metzger and Braun (1987) estimate that nearly all mercury emitted from MWCs at flue gas cleaning temperatures is in the form of mercury chlorides. Lindqvist and Scagher (1990) estimate that the speciation of mercury emissions from European waste incinerators consist of 10 percent Hg^0 , 85 percent Hg^{2+} , and 5 percent mercury associated with PM (Hg (PM)). Pacyna (1991) estimates that mercury emissions from European waste incinerators consist of 10 percent Hg^0 , 85 percent Hg^{2+} , and 5 percent Hg (PM).

There is currently no validated U. S. EPA method for determining the speciation of mercury in stack gas. Information on the chemical behavior of mercury and the distribution of mercury in EPA's

multi-metal sampling train (Method 29) can be used to estimate the form and speciation of mercury in MWC stack gas. Mercury found in the probe and filter can be assumed to have been vapor-phase mercury adsorbed onto PM or be a solid-phase compound. Both phases are associated with PM. Mercuric chloride is soluble in water and mercury found in the $\text{KMnO}_4/\text{H}_2\text{SO}_4$ impingers is probably Hg^0 . The distribution of multi-metal train samples collected during the activated carbon injection tests at the Camden County MWC and Stanislaus County tests is shown in Figure C-1 (Nebel et al., 1992; White et al., 1993).

Figure C-1
Distribution of Mercury in EPA Method 29 Sampling Train,
Camden County and Stanislaus County Carbon Injection Projects

Tests showing mercury stack concentrations of greater than 100 $\mu\text{g}/\text{dscm}$ represent either low carbon injection feed rates or no carbon injection. For these tests, Hg^0 ranged from 2 to 26 percent of total mercury. As carbon injection rates and mercury capture increased, the percentage of Hg^0 as a fraction of total mercury increased. This implies that Hg^{2+} is more easily captured by activated carbon than Hg^0 . For mercury stack concentrations less than 50 $\mu\text{g}/\text{dscm}$, the fraction of Hg^0 ranged from approximately 14 to 72 percent. The fraction of $\text{Hg}(\text{PM})$ was generally below detection limits for most tests. It exceeded 10 percent for only one test and was below 10 percent for all other tests where it was detected.

At low levels of control, the stack concentration of mercury is probably 15 to 30 percent $\text{Hg}^0(\text{v})$ and the rest is $\text{Hg}^{2+}(\text{v})$. At high levels of control, $\text{Hg}^{2+}(\text{v})$ is selectively removed, increasing the relative concentration of $\text{Hg}^0(\text{v})$, and the relative concentration of $\text{Hg}^0(\text{v})$ may be 50 percent or higher.

For this analysis the speciation profiles for these course types were derived from Petersen et al., 1995. The profiles are shown below for each model plant.

C.2.1.3 Selection of MWC Model Plant Parameters

In this analysis, the range of MWC plant conditions are represented by a large 2250 tons/day model plant and a small 200 tons/day model plant. The large model plant consists of 3 conventional 750 tons/day mass burn combustors. The small MWC model plant was assumed to consist of two conventional 100 tons/day mass burn combustors.

Large MWC Model Plant

In October 1995, the U.S. EPA finalized emissions guidelines for existing MWCs and New Source Performance Standards (NSPS) for new facilities. These require new and existing MWCs that combust more than 39 tons of waste per day to reduce their mercury emissions to no more than 80 $\mu\text{g}/\text{dscm}$. To achieve this emission reduction it is likely that most facilities will use activated carbon injection as a control measure. Activated carbon injection effectively captures Hg^{2+} with the result that the percentage of Hg^0 as a fraction of total mercury increases. In addition, the fraction of mercury associated with particulate matter ($\text{Hg}(\text{PM})$) also decreases.

The model plants in this analysis reflected these requirements. In the analysis, the speciation profile utilized for the large MWC model was 60 percent Hg^0 , 30 percent Hg^{2+} , and 10 percent Hg^{P} (see Table C-1).

Small MWC Model Plant

The small MWC model plant was assumed to consist of two state-of-the-art 100 tons/day mass burn combustors. The waste composition and behavior of mercury in the combustor was assumed to be similar to that observed in large mass burn combustors. Since the 1995 emissions guidelines and NSPS apply to the small MWCs as well, it is again likely that most facilities will use activated carbon injection as a control measure. Stack emissions were therefore assumed to consist of mercury consisting of 60 percent Hg^0 , 30 percent Hg^{2+} , and 10 percent particulate mercury.

Sensitivity to Emissions Speciation

For the two municipal waste combustors, two additional emissions speciations were utilized to investigate the sensitivity of the deposition rates to the speciation. These scenarios are summarized in Table C-2.

Table C-2
Scenarios for Sensitivity of Total Mercury Deposition Rate to Emissions Speciation

for Municipal Waste Combustors

Mercury Emissions Scenario	% Hg0	% Hg2 Vapor	% Hg2 Particulate
LMWC_A	30	50	20
LMWC_B (used in analyses)	60	30	10
LMWC_C	90	10	0
SMWC_A	30	50	20
SMWC_B (used in analyses)	60	30	10
SMWC_C	90	10	0

C.2.2 Medical Waste Incinerators

C.2.2.1 Description of Source Category

Medical waste incinerators (MWIs) are small incinerators that burn from 1 ton/day (0.9 Mg/day) to 60 tons/day (55 Mg/day) of infectious and noninfectious wastes. These wastes are generated by various facilities including hospitals, clinics, medical and dental offices, veterinary clinics, nursing homes, medical laboratories, medical and veterinary schools and research laboratories and funeral homes.

Approximately 2,400 MWIs currently operate throughout the country; geographic distribution is relatively even. Of these units, most are hospital incinerators (U.S. EPA, 1996).

The primary function of MWIs is to render the waste biologically innocuous and to reduce the volume and mass of solids that must be landfilled (by combusting the organic material contained within the waste). Currently, three major types of MWI operate in the United States: continuous, intermittent, and batch. All three have two chambers that operate on a similar principle. Waste is fed to a primary chamber, where it is heated and volatilized. The volatiles and combustion gases are then sent to a secondary chamber, where combustion of the volatiles is completed by adding air and heat. All mercury in the waste is assumed to be volatilized during the combustion process and emitted with the combustion stack gases.

C.2.2.2 Summary of Available Data on Emissions and Controls

A number of air pollution control systems are used to control PM and acid gas emissions from MWI stacks. Most of these systems fall into the general classes of either wet or dry systems. Wet systems typically comprise a wet scrubber, designed for PM control (venturi scrubber or rotary atomizing scrubber), in series with a packed-bed scrubber for acid gas removal and a high efficiency mist elimination system. Most dry systems use a fabric filter for PM removal, but ESP's have been used on some of the larger MWIs. All of these systems have limited success in controlling mercury emissions. Recent EPA studies indicate that sorbent injection/fabric filtration systems can achieve improved mercury control by adding activated carbon to the sorbent material (U.S. EPA, 1994).

C.2.2.3 Selection of MWI Model Plant Parameters

To represent the MWI source category, three model plants were devised: a large commercial MWI, a large hospital MWI (with good combustion), and a small hospital MWI (with 1/4 sec. combustion). For the large and small hospital MWIs, two alternate scenarios were examined using the assumption that wet scrubbers were utilized as a control technology (in accordance with the final emissions guidelines for MWIs).

Large Commercial Facility

The large commercial MWI was assumed to have a capacity of 1500 lb/hr. This incinerator was modeled at a mercury emissions rate of 4.58 kg/yr with a speciation profile consisting of 33 percent Hg^0 , 50 percent Hg^{2+} , and 17 percent particulate mercury.

Hospital Facilities

Two hospital facilities were modeled: a large hospital MWI and a small hospital MWI. The larger facility was assumed to perform with good combustion and a capacity of 1000 lb/hr. It was modeled at a mercury emissions rate of 23.9 kg/yr with a speciation profile consisting of 2 percent Hg^0 , 73 percent Hg^{2+} , and 25 percent particulate mercury. The smaller hospital MWI, with 1/4 sec. combustion, was assumed to have a capacity of 100 lb/hr. It was modeled with a speciation profile consisting of 2 percent Hg^0 , 75 percent Hg^{2+} , and 23 percent particulate mercury.

In developing the alternate speciation profiles for the large and small hospital MWIs, it was assumed that the wet scrubber would remove 94 percent of the Hg^{2+} from the flue gas. The effect of this is that the large and small hospitals with wet scrubbers emit more elemental mercury relative to what they emit when they are uncontrolled (see Table C-1).

C.2.3 Utility Boilers

C.2.3.1 Description of Source Category

Utility boilers are large boilers used by public and private utilities to generate electricity. There are approximately 1800 utility boilers in the U.S. which burn coal, oil and natural gas. In 1990, utility boilers consumed fossil fuel at an annual level of 21×10^{15} British thermal units (Btu). About 80 percent of this total energy consumption resulted from coal combustion, 6 percent from oil and petroleum fuels and 14 percent from natural gas consumption. Ninety-five percent of the coal burned is bituminous and subbituminous; lignite accounts for 4 percent. Mercury emission estimates were not calculated for natural gas combustion because reliable test data necessary to calculate an emission factor do not exist. Given these factors, the indirect exposure analysis focused only on coal-fired units burning bituminous coal and residual oil-fired units.

C.2.3.2 Summary of Available Data on Emissions and Controls

About 80 percent of coal-fired utility boilers use ESPs for PM control. Scrubbers (or flue gas desulfurization units (FGDs)) are the most commonly used device for sulfur dioxide (SO₂) control. Spray dryer absorption (SDA), or dry scrubbing, followed by a PM control device may also be used. Mechanical collectors are used infrequently. Coal washing, which separates coal and impurities from crushed and screened coal by differences in specific gravity, is done routinely to meet customer specifications for heating value, ash and sulfur content. Advanced coal cleaning techniques may reduce the concentration of mercury contained in the mineral and organic phases of the coal, but the reliability and feasibility of these emerging techniques are unknown at this time.

Carbon filter beds are being used successfully in Europe for control of heavy metals, organic compounds and acid gases (Hartenstein, 1993). Five full-scale applications of carbon beds are currently in use for utilities, with future applications planned for hazardous waste incinerators and MWCs. Activated carbon injection has been used successfully in the U.S. for mercury removal from the stack gas of MWCs and MWIs. This technology has been tested on a pilot-scale basis in the U.S.. Table C-3 summarizes the control efficiencies for various control technologies for utility boilers, based on pilot-scale test data.

**Table C-3
Mercury Removal Efficiencies**

Control Technique	Range of Removal Efficiency (percent)	Median Removal Efficiency (percent)	Reference
Carbon bed	Unknown	99	Hartenstein (1993)
Fabric Filter + AC (Low temp. + Low C injection rate)	76-99	98	Volume VIII, App. A.
Fabric Filter + AC (High temp. + Low C injection rate)	14-47	29	Volume VIII, App. A
Fabric Filter + AC (Low temp. + High C injection rate)	95-99	98	Volume VIII, App. A
Fabric Filter + AC High temp. + High C injection rate)	69-91	73	Volume VIII, App. A
SDA/ESP + AC	75-91	86	Volume VIII, App. A
SDA/FF + AC	50- >99	NA	Volume VIII, App. A
Fabric filter	0 - 51	29	Volume II
Scrubber (FGd)	18 - 84	23	Volume II
Dry scrubber (SDa)	23 - 83	67	Volume II
ESP	0 - 22	15	Volume II
Mechanical collector	0	0	Volume II
Coal washing	-200 - 64	21 (average removal)	Volume II
Advanced coal washing	Unknown	-	Volume VII

Mercury emissions of mercury from utility boilers can vary depending on the mercury content of the fuel and the control technique used. Based on emissions test data (as described in the mercury emissions inventory, documented in a separate report), a mercury emission rate of 10 ug/dscm was chosen to represent emissions from a coal-fired utility with PM control. Two ug/dscm was chosen as the emission rate for mercury emissions from an uncontrolled residual oil-fired utility. This emission rate is a worse-case estimate for an oil-fired plant. This high estimate was selected for the modeling because the impacts from oil-fired boiler were expected to be very small even using the worst-case.

As discussed above, the chemical specie of mercury being emitted affects both the removal efficiency of the control device and the deposition of mercury from the atmosphere. Based on Petersen et al., 1995, it was assumed for the local impact analysis that the mercury emitted from the utility model plants (both coal- and oil-fired) consisted of 50 percent HgO and 30 percent Hg²⁺, and 20 percent Hg(PM).

C.2.3.3 Selection of Model Plant Parameters

The source of data for selecting the model plant sizes was the Utility Data Institute (UDI)/Edison Electric Institute (EEI) Power Statistics Database (1991 edition). This database provided information on fuel use, boiler sizes and stack parameters. The database had information on 1708 units, of which 795 were bituminous coal-fired and about 225 were oil-fired. The remainder were primarily fired with natural gas although there were some boilers burning lignite and anthracite coals. Given the predominance of bituminous coal-fired units, those were the units chosen for the indirect exposure analysis as well as one residual oil-fired unit.

The 795 coal-fired units were divided into 3 size classifications (by megawatt (MW)) according to 33rd percentiles. The size classes had approximately the same number of units in each. The "large" group which consisted of units greater than or equal to 575 MW had 262 units. The "medium" group which consisted of units between 199 MW and 575 MW had 256 units. The "small" group consisting of units greater than 25 MW but less than 200 MW had 277 units. The model plant parameters were chosen by evaluating each group separately and taking the average value for each parameter from each group (e.g., for representative MW, stack height and stack diameter).

Based on this analysis, three boiler sizes were chosen as the basis for the coal-fired model plants: 975 MW, 375 MW, and 100 MW. The same type of analysis for the oil-fired units led to the selection of a 285 MW residual-oil fired unit as a representative model plant size for the oilfired units.

Coal-Fired Utility Model Plants

All of the coal-fired utility model plants had a capacity factor of 65 percent, and were equipped with a cold-side ESP. The inlet mercury level (i.e., the amount of mercury entering the emission control device) was assumed to be $10 \mu\text{g}/\text{dscm}$ (4.4 gr/million dscf). For emissions, it was assumed that no mercury control across the ESP was achieved and that the mercury emissions were $10 \text{ug}/\text{dscm}$ (4.4 gr/million dscf).

Oil-Fired Utility Model Plant

The oil-fired utility model plant was a 285 MW boiler firing No. 6 fuel oil containing 1 percent sulfur and 300 ppm chlorine. It was assumed to have a capacity factor of 65 percent, and was not equipped with any particulate matter control device. The inlet mercury level associated with this model plant was assumed to be $2 \mu\text{g}/\text{dscm}$ (1 gr/million dscf). It was assumed that no mercury control was achieved and that the mercury emissions were $2 \text{ug}/\text{dscm}$ (1 gr/million dscf).

C.2.4 Chlor-Alkali Production

C.2.4.1 Description of Source Category

Chlor-alkali production using the mercury cell process, (which is the only chlor-alkali process that uses mercury), accounted for 14.7 percent of all U.S. chlorine production in 1993 (Dungan, 1994). The three primary sources of mercury air emissions from chlor-alkali plants are the byproduct hydrogen stream, the end box ventilation air and the cell room ventilation air. The byproduct hydrogen stream from the decomposer is saturated with mercury vapor and may also contain fine droplets of liquid mercury. The quantity of mercury emitted in the end box ventilation air depends on the degree of mercury saturation and the volumetric flow rate of the air. The amount of mercury in the cell room ventilation air is variable and comes from many sources, including end box sampling, removal of mercury butter from end boxes, maintenance operations, mercury spills, equipment leaks and cell failure (U.S. EPA, 1984).

C.2.4.2 Summary of Available Data on Emissions and Control

The most recent source of mercury emission data is from Clean Air Act section 114 survey questionnaires of the chlor-alkali industry (as referenced in section 4.2.1 of Volume II of this report). The industry survey data were reported for 1991; total annual mercury emissions were 6.5 Mg (7.1 tons) which includes 12 of 14 facilities that were operational in 1996. A previous report by the U.S. EPA was used to develop plant-specific parameters (U.S. EPA, 1973).

The control techniques that are typically used to reduce the level of mercury in the hydrogen streams and in the ventilation stream from the end boxes are the following: gas stream cooling, mist eliminators, scrubbers and adsorption on activated carbon or molecular sieves. Mercury emissions from the cell room air circulation are not subject to specific emission control measures. Concentrations are maintained at acceptable worker exposure levels through good housekeeping practices and equipment maintenance procedures (U.S. EPA, 1984).

Speciated emissions data for chlor-alkali plants are extremely limited. For this analysis was assumed that the emitted mercury was in the vapor phase and consisted of 70 percent Hg^0 and 30 percent Hg^{2+} (Peterson et al., 1995).

C.2.4.3 Selection of Model Plant Parameters

For the indirect exposure analysis, one chlor-alkali model plant, which produces 273 Mg (300 tons) of chlorine per day, was devised. This model plant represented the mid-range size of chlor-alkali plants in operation (U.S. EPA, 1984). The model plant had individual flow rates from the hydrogen and end-box streams of 4,080 dscm/hr (144,000 dscf/hr) each at 21 percent O_2 (combined to equal 8,160 dscm/hr [288,000 dscf/hr]) (U.S. EPA, 1973). A 90 percent capacity factor (operation for 7889 hr/yr) was assumed.

The typical emissions control scenario for both the hydrogen and end-box streams was assumed to consist of a heat exchanger to cool the effluent gas, followed by a knockout drum to separate the condensed mercury from the hydrogen and end-box streams. A mercury level of 1,040 g/day (2.3 lb/day) was assumed for the purpose of indirect exposure analysis to be consistent with the federally-mandated mercury standard for the hydrogen and end-box streams at all chlor-alkali plants (U.S. EPA, 1984).

C.3 References

Bloom, Nicolas S., Eric M. Prestbo, Vesna L. Miklavcic, "Flue Gas Mercury Emissions and Speciation from Fossil Fuel Combustion," Second International Conference on Managing Hazardous Air Pollutants, Washington, D.C. July 1993.

Brna, T. G. Toxic Metal Emissions from MWCs and their Control, In Proceedings: 1991 International Conference on Municipal Waste Combustion, Volume 3, EPA-600/R-92-209c (NTIS PB93-124196), pp 23-39, November 1992.

Brna, T.G., J.D. Kilgroe, and C.A. Miller, Reducing Mercury Emission from Municipal Waste Combustion with Carbon Injection into Flue Gas, ECO World '92 Conference, Washington, DC, June 1992.

Brown, B. and K.S. Felsvang, Control of Mercury and Dioxin Emissions from United States and European Municipal Solid Waste Incinerators by Spray Dryer Absorption Systems, In Proceedings, 1991 International Conference on Municipal Waste Combustion, Volume 3, EPA600/R-92-209c (NTIS PB93-124196), pp 287-317, November 1992.

Buonicore, A.J., and W.T. Davis, , 1992, eds. Air Pollution Engineering Manual. Van Nostrand Reinhold, New York. 1992.

Dungan, A., 1994. Chlorine Production Routes - U.S. and Canada. Facsimile to Ommen, Roy, Radian Corporation. April 1994.

Edlund. H., 1993, Boliden Contech, telefax to K. Nebel, Radian Corporation. August 17, 1993.

Hall, B. Reactions of Mercury with Flue Gas Components, Statens Energiverk, National Energy Administration, Sweden, (STEV-FBT-91-18), 1991.

Hall, B., O. Lindqvist, and D. Ljungstrom, Mercury Chemistry in Simulated Flue Gases Related to Waste Incineration Conditions, Environ. Sci. and Tech., 24 (1990), 108-111.

Hartenstein, H.U., 1993. Activated Carbon Filters for Flue Gas Polishing of MWI's. Presented at the International Conference on Municipal Waste Combustion, Williamsburg, Virginia, March 1993.

Hartenstein, H. U. Activated Carbon Filters for Flue Gas Polishing of MWI'S, In Proceedings 1993 Conference on Municipal Waste Combustion, Air & Waste Management Association (VIP32), Pittsburgh, PA, 1993, pp 87-105.

Kilgroe, J. D. et al., Camden County MWC Carbon Injection Test Results, Presented at the 1993 International Conference on Municipal Waste Combustion, Williamsburg, VA, March 30 to April 2, 1993.

Kiser, J. V. L. The IWSA Municipal Waste Combustion Directory: 1993 Update of U. S. Plants, Integrated Waste Services Association, Washington, DC, 1993.

Lerner, B.J., Beco Engineering Company, 1992. Mercury Emissions Control in Medical Waste Incineration. Presented at the 86th Annual Meeting, Air and Waste Management Association, Denver, Colorado. June 1992.

Lindqvist, O. and P. Schager, Continuous Measurements of Mercury in Flue Gases from Waste Incinerators and Combustion Plants, VDI Berichte, (NR. 838), 1990, pp. 401-421.

Metzger, M. and H. Braun, In-situ Mercury Speciation in Flue Gas by Liquid and Solid Sorption Systems, *Chemosphere*, 16 (1987), 821-832.

Midwest Research Institute, 1992. Medical Waste Incinerators -Background Information for Proposed Standards and Guidelines: Control Technology Performance Report for New and Existing Facilities. Draft Report. July 1992.

Nebel, K.L. et al., Emission Test Report: OMSS Field Test on Carbon Injection for Mercury Control, EPA-600/R-92-192 (NTIS PB93-105518), Air and Energy Engineering Research Laboratory, Research Triangle Park, NC, September 1992.

Pacyna, J. M. Anthropogenic Mercury Emission in Europe, *Water, Air and Soil Pollution*, 56 (1991), 51-61.

Peterson, G., A. Iverfeldt, J. Munthe, 1995. Atmospheric Mercury Species Over Central and Northern Europe, Model Calculations and Comparison with Observations from the Nordic Air and Precipitation Network for 1987 and 1988. GKSS Research Centre, Institute of Physics, Max-Planck-Str. 1, D-21502, Geesthacht, Germany.

TRC Environmental Corporation, 1992. Emission Characterization Program. Prepared for Copper Range Company, White Pine, Michigan. October 15, 1992.

U.S. Environmental Protection Agency, 1996. Standards of Performance for New Stationary Sources and Emissions Guidelines for Existing Sources: Medical Waste Incinerators, Proposed Rule, Federal Register, June 20, 1996.

U.S. Environmental Protection Agency, 1994. Medical Waste Incinerators - Background Information for Proposed Standards and Guidelines: Industry Profile Report for New and Existing Facilities. EPA-453/R-94-042a. Office of Air Quality Planning and Standards, Research Triangle Park, NC. July 1994.

U.S. Environmental Protection Agency, 1993. Locating and Estimating Air Emissions from Sources of Mercury and Mercury Compounds. EPA 454/R-93-023. Office of Air Quality Planning and Standards, Research Triangle Park, NC. September 1993.

U.S. Environmental Protection Agency, 1992a. Medical Waste Incinerators - Background Paper for New and Existing Facilities, Draft. U.S., Environmental Protection Agency, Research Triangle Park, NC. June 1992.

U.S. Environmental Protection Agency, 1992b. Medical Waste Incineration Emission Test Report -- Borgess Medical Center, Kalamazoo, Michigan. September 1992.

U.S. Environmental Protection Agency, 1991. Medical Waste Incineration Emission Test Report -- Morristown Memorial Hospital, Morristown, New Jersey. EMB Report 91-MWI-8. December 1991.

U.S. Environmental Protection Agency, 1989. Municipal Waste Combustors, Background Information for Proposed Standards, Post-Combustion Technology Performance, Volume 3, EPA450/-3-89-27c (NTIS PB90-154865), Research Triangle Park, NC, August 1989.

U.S. Environmental Protection Agency, 1988a. Compilation of Air Pollution Emission Factors, A,P-42, Fourth Edition, Supplement B. Office of Air Quality Planning and Standards, Research Triangle Park, NC.

U.S. Environmental Protection Agency, 1984. Review of National Emissions Standards for Mercury. EPA 450/3-84-014. Office of Air Quality Planning and Standards, Research Triangle Park, NC. December 1984.

U.S. Environmental Protection Agency, 1974. Background Information for New Source Performance Standards: Primary Copper, Zinc and Lead Smelters. EPA-450/2-74-002a. Office of Air Quality Planning and Standards, Research Triangle Park, NC. October 1974.

U.S. Environmental Protection Agency, 1973. Control Techniques for Mercury Emissions from Extraction and Chlor-Alkali Plants. Office of Air Quality Planning and Standards, Research Triangle Park, NC. February 1973.

White, D. M. et al., Field Test of Carbon Injection for Mercury Control, Camden County Municipal Waste Combustor, EPA-600/R-93-181 (NTIS PB94-101540), September 1993.

White, D.M., K.L. Nebel, and M.G. Johnston, Municipal Waste Combustors: A Survey of Mercury Emissions and Applicable Control Technologies , In Proceedings, 1991 International Conference on Municipal Waste Combustion, Volume 3, EPA-600/R-92-209c (NTIS PB93124196), pp 247-257, November 1992.

White, D.M., et al., Parametric Evaluation of Activated Carbon Injection for Control of Mercury Emissions from a Municipal Waste Combustor, Paper No. 92-40.06, 1992 Annual Meeting, Air & Waste Management Association, Kansas City, MO, June 1992.

APPENDIX D

**AQUATIC BIOACCUMULATION FACTOR DEVELOPMENT AND
UNCERTAINTY ANALYSIS**

TABLE OF CONTENTS

	<u>Page</u>
D. AQUATIC BIOACCUMULATION FACTOR DEVELOPMENT AND UNCERTAINTY ANALYSIS	D-1
D.1 Introduction	D-1
D.2 Probabilistic Uncertainty Analysis	D-1
D.2.1 Sources of Uncertainty and Their Treatment	D-1
D.2.2 Probabilistic Simulation	D-2
D.2.3 Selection of Distributions for Input Variables	D-2
D.2.4 Conventions for Representation of Distributions in This Appendix	D-3
D.3 Estimation of BAFs for Methylmercury	D-4
D.3.1 Data Quality Objectives	D-4
D.3.2 Estimation of BAFs For Mercury Using a Modified GLWQI Approach ...	D-5
D.3.2.1 BAFs Published in the Proposed Guidance	D-5
D.3.2.2 Inputs and Assumptions for the Present Analysis	D-6
D.3.2.3 Results of Probabilistic Analysis of the Modified GLWQI Methodology	D-13
D.3.3 Estimation of a BAF ₄ for Methylmercury Using Measured Values for Trophic Level 3 and a Field-Derived Food Chain Multiplier	D-13
D.3.3.1 Bioaccumulation Factors Directly Estimated From Field Data - Methylmercury in Forage Fish	D-13
D.3.3.2 Results of Probabilistic Simulation of ${}_{MD}BAF_4$ Using Field-Derived ${}_{MD}BAF_3$ and PPF ₄ Estimates	D-15
D.3.4 Specification of a Distribution for ${}_{MD}BAF_4$ Directly Derived from Field DataD-16	D-16
D.3.4.1 Bioaccumulation Factors Directly Estimated From Field Data - Methylmercury in Piscivorous Fish	D-16
D.3.5 Specification of BAF Distributions Based on Dissolved Total Mercury ...	D-18
D.3.5.1 Bioaccumulation Factors Directly Estimated From Field Data - Total Dissolved Mercury in Forage Fish	D-18
D.3.5.2 Bioaccumulation Factors Directly Estimated From Field Data - Total Dissolved Mercury in Piscivorous Fish	D-20
D.3.6 Estimation of Methylmercury BAF for Trophic Level 4 from Distributions Based on Total Mercury	D-21
D.3.6.1 Speciation of Mercury in the Water Column	D-22
D.3.6.2 Simulation of a Methylmercury BAF ₄	D-23
D.3.7 Sensitivity Analysis	D-25
D.3.8 Selection of Bioaccumulation Factors for Trophic Levels 3 and 4	D-26
D.3.9 Discussion of Uncertainty and Variability in the BAF	D-29
D.4 Other Variables Concerning the Form of Mercury in the Water Column	D-30
D.4.1 Fraction of Methylmercury in the Hypolimnion	D-30
D.4.2 Fraction of Dissolved Methylmercury in the Water Column	D-30

D.5	References	D-32
-----	------------------	------

LIST OF TABLES AND FIGURES

<u>Tables</u>	<u>Page</u>	
D-1	Bioconcentration Factor for Methylmercury in Phytoplankton	D-6
D-2	Predator-Prey Factor for Trophic Level 2	D-7
D-3	Predator-Prey Factor for Trophic Level 3	D-8
D-4	Predator-Prey Factor for Trophic Level 4	D-11
D-5	Statistics for BAFs Using the Modified GLWQI Methodology	D-13
D-6	Bioaccumulation Factor for Methylmercury in Trophic Level 3 Fish	D-15
D-7	Statistics for Methylmercury $_{MD}BAF_3$; Direct Estimate from Field Data	D-15
D-8	Statistics for Methylmercury $_{MD}BAF_4$ Estimated from $_{MD}BAF_3 \times PPF_4$	D-16
D-9	Bioaccumulation Factors for Methylmercury in Trophic Level 4 Fish	D-17
D-10	Statistics for Field-Derived $_{MD}BAF_4$	D-18
D-11	Bioaccumulation Factor for Dissolved Total Mercury in Trophic Level 3 Fish	D-19
D-12	Statistics for Field-Derived $_{TD}BAF_3$	D-20
D-13	Bioaccumulation Factor for Dissolved Total Mercury in Trophic Level 4 Fish	D-20
D-14	Statistics for Field-Derived $_{TD}BAF_4$	D-21
D-15	Methylmercury as a Fraction of Total Dissolved Mercury in the Epilimnion	D-22
D-16	Statistics for Methylmercury BAFs Estimated from Total Mercury BAFs	D-24
D-17	Comparison of Lognormal and Normal (Directly Estimated) $_{MD}BAF$ Distributions	D-26
D-18	Summary of Methylmercury Bioaccumulation Factors for Trophic Level 3	D-27
D-19	Summary of Methylmercury Bioaccumulation Factors for Trophic Level 4	D-28
D-20	Methylmercury as a Fraction of Total Dissolved Mercury in the Hypolimnion	D-30
D-21	Dissolved Methylmercury as a Fraction of Total Methylmercury in the Epilimnion	D-31

<u>Figures</u>	<u>Page</u>	
D-1	Input Distribution for PPF_4	D-12
D-2	Distribution for $fmmw_E$	D-23
D-3	$_{MD}BAF_4$ Distribution Based on $_{TD}BAF_4$	D-24
D-4	$_{MD}BAF_4$ Distribution Based on $_{TD}BAF_3$	D-25
D-5	$_{MD}BAF_4$ Distributions	D-28
D-6	Distribution for $fdmw$	D-31

D. AQUATIC BIOACCUMULATION FACTOR DEVELOPMENT AND UNCERTAINTY ANALYSIS

D.1 Introduction

This appendix describes efforts to estimate bioaccumulation factors (BAFs) for mercury in fish. Following the food chain structure described in Section 3.3 of Volume VI, BAFs are estimated for fish that occupy trophic levels 3 and 4. Respectively, these values are referred to as BAF_3 and BAF_4 . In this analysis, BAFs for mercury are derived for methylmercury and total mercury in filtered surface lake water (dissolved species in the epilimnion, only). The BAF for methylmercury is defined as the concentration of methylmercury in whole fish divided by the concentration of dissolved MeHg in the the epilimnion. The BAF for total mercury is defined as the concentration of total mercury in whole fish divided by the concentration of dissolved total mercury in the the epilimnion. As the primary focus is on the methylmercury species, several methods are used to estimate methylmercury BAFs. The BAFs serve as critical inputs to the calculation of wildlife criterion (WC) values and are also used to characterize human exposure from consumption of contaminated fish. Special emphasis is placed on evaluating uncertainties associated with these values.

Measures of mercury accumulation that are not treated in this appendix include: (1) BAFs for trophic levels 1 and 2; (2) biota-sediment bioaccumulation factors (BSAFs) for trophic levels 1 - 4; and (3) predator-prey factors (PPFs) for piscivorous wildlife (i.e., the concentration of mercury in piscivorous birds and mammals divided by that of their prey). Readers interested in information concerning these parameters, including summaries of field data from which estimated values can be derived, are referred to section 2.3.1 of Volume VI.

The wildlife criterion methodology used to derive BAFs in the Great Lakes Water Quality Initiative (GLWQI) served as a starting point for the present analysis. The analysis was then extended to include an examination of field data from which BAFs could be estimated directly. It was recognized that considerable natural variability exists with respect of the accumulation of mercury in aquatic food chains. An effort therefore, was made to incorporate this variability into the analysis. This was accomplished by using a probabilistic simulation approach. The probabilistic simulation method is described in Section D.2.2.

Two other variables are also presented in this appendix that are not directly used in the calculation of BAFs for methylmercury, but are necessary for other parts of Volume III. Those variables are 1) the fraction of total methylmercury in the epilimnion that is dissolved and 2) the fraction of total methylmercury in the hypolimnion that is dissolved.

D.2 Probabilistic Uncertainty Analysis

D.2.1 Sources of Uncertainty and Their Treatment

Models of environmental phenomena must deal with two basic sources of uncertainty. The first is uncertainty arising from natural variability, such as the size of individuals in a population or their differences in xenobiotic metabolism. The second is uncertainty of the value of a parameter or variable when it is known that there is a single value, such as measurement error in duplicate samples or lack of knowledge of the true variance of a process. These two sources of uncertainty are formally referred to as "variability" and "uncertainty", respectively. In the current analysis (this Appendix), variability and

uncertainty are aggregated in the probabilistic simulation output. That is, there is no attempt to fully separate variability and uncertainty, except to the extent that variability of within-lake processes are used to estimate the uncertainty in the means of the among-lake variables. Ideally, each parameter for each input distribution should be distributions, themselves. The distributions for the input distribution parameters are determined best by formal expert-elicitation techniques designed to assess subjective knowledge (Morgan and Henrion, 1990). In this appendix the term "variability" is used in a general context, comprising both variability and uncertainty. The term "variable" is used to describe model variables treated as random variates, while the term "parameter" refers to a fixed parameter of the mathematical form of a specific distribution.

In dealing with the issue of uncertainty, it is important to distinguish between qualitative and quantitative models. A qualitative analysis can only make descriptive value-judgement statements about the magnitude of the uncertainty or about the general confidence in the model output, such as "high", "medium" or "low" and cannot address the statistical properties of the model. A quantitative analysis allows for a more precise expression of the overall variability, is essential for comparing the results of different models and is necessary to determine which of the input parameters have the greatest effect on the model output. The latter procedure, called a sensitivity analysis, allows the model developers to focus future efforts on the most important aspects of the model and gives the risk assessor or risk manager valuable perspective for interpreting the results.

D.2.2 Probabilistic Simulation

There are a number of methods for expressing uncertainty in a quantitative fashion, the discussion of which is beyond the scope of this document. The reader is referred to Morgan and Henrion (1990) for a description of these techniques. Monte Carlo simulation is an approach that is commonly used as a means of explicitly treating the variability in the input variables. The Monte Carlo method is an iterative random sampling technique that mathematically combines prescribed distributions rather than single numbers and allows for the propagation of variability in each input variable throughout the model; that is, the variability in each input will be reflected in the output, which is also in the form of a distribution.

For models in which all variables are Gaussian ("normal") and all operations are addition or subtraction, a mathematical ("analytic") solution exists and Monte Carlo simulation is unnecessary (Aitchison and Brown, 1966). In the analytic solution, the output is a normal distribution with a mean equal to the sum (or difference) of the means of the inputs and a standard deviation equal to the square root of the sum of the variances of the input distributions. This solution is also applicable to lognormal distributions when the mathematical operations are carried out on the logarithms of the inputs (commonly referred to as "log space").

Calculation of a WC value requires that a single BAF value be established for each trophic level contributing to the analysis. The same is true for estimating human exposure due to ingestion of contaminated fish. It should be noted, however, that the probabilistic simulation approach yields both a mean and distribution of BAF values. Although mean values were used for the calculation of WC values, it is of interest to characterize the statistical variation about this estimate, since it may reflect actual variation in natural systems. The possible significance of these distributions is discussed in Volume VI.

D.2.3 Selection of Distributions for Input Variables

Input distributions are based on an analysis of published data and one unpublished report (see Sec. D.3.1., Data Quality Objectives). In general, an empirical distribution representing both the central tendency and the extremes of the given data is determined. For analytical convenience the actual input distributions are given in parametric form for this analysis. That is, formal analytic distributions that are expressed by a mathematical equation (with specific defining parameters) are assigned to the inputs rather than using the preliminary empirical forms (a collection of values). The choice of the mathematical form for each of the variables is somewhat a matter of judgement. The particular set of parameters chosen for each of the distributions is only one realization of a number of possible choices.

Lognormal distributions are used almost exclusively in this analysis, partly for analytical convenience but primarily because many of the factors contributing to the variability of the modeled processes are likely to be multiplicative rather than additive. Given the complexity and nonlinear nature of the underlying processes, the actual distribution of model variables is unlikely to follow any simple closed-form mathematical relationship. The lognormal form is judged to be the most appropriate, but values from the distribution far outside the range of observations do not necessarily have any real-world significance. A general rule-of-thumb is that the empirical observations span a fractile range of $0.5/n$ to $(n - 0.5)/n$, where n is the number of observations (Wilk and Gnanadesikan, 1968). That is, for a sample size of 5, the extreme observations would be considered to be at the 0.1 and 0.9 fractiles (10th and 90th percentiles). This approach allows for the possibility of more extreme values in larger samples and is used in this analysis to construct all empirical distributions. In this analysis, the 90% confidence interval (5th to 95th percentiles) is used extensively for comparisons of approaches. In many cases this interval is somewhat outside the spread of the empirical distribution. Therefore, no strong significance should be attached to these extreme values.

Distribution parameters are established by the method of moments, in which the sample mean and sample standard deviation, themselves, are used as estimates of the parameters. For the lognormal, the parameters are determined in log space (mean and standard deviation of the logs of the observations). The only other distribution used in this analysis is the beta. The beta is used for all values that are expressed as fractions of a whole, primarily because the beta has limits of 0 and 1 and can take on a wide range of shapes. The beta has two shape parameters (α and β), which, in this analysis, are indirectly determined by the method of moments. That is, the two equations for α and β in terms of the moments are solved simultaneously using the sample mean and standard deviation (Evans et al., 1993).

The fundamental data unit in all analyses was defined as the water body (lake). That is, each lake was treated as an independent unit. In some cases, when data from several lakes were aggregated in the published study or to avoid over-representation of a specific geographical area, data points were defined by the average across several lakes.

All simulations were performed on an Intel Pentium[®]/130 CPU in S-PLUS[®] (version 3.1) in the MS Windows[®] (version 3.11) environment.

D.2.4 Conventions for Representation of Distributions in This Appendix

Parameters of the lognormal distributions are expressed as the geometric mean (GM) and the geometric standard deviation (GSD). The geometric mean is defined as e^{μ} , where μ is the mean of the logarithms of the observations. The geometric standard deviation is defined as e^{σ} , where σ is the

standard deviation of the logarithms of the observations. The beta distribution is characterized by two shape parameters (α and β).

All of the distributions developed in this analysis represent the variability of the mean value of a specific variable across water bodies. As all of the variables in this analysis deal with estimates for a randomly-selected single water body, independent of any other water body, the central-tendency estimate will be given as the median. The arithmetic mean (average of the untransformed values) is given in some cases for purposes of comparison. The arithmetic mean would be useful only in the case when fish were consumed equally by a receptor from all of the lakes in the analysis. The arithmetic mean given in tables showing the output of analytic (lognormal) simulations is the analytic mean of the specified distribution, calculated directly from the distribution parameters (Evans et al., 1993). The spread of the distribution will be expressed as the interquartile range (25th to 75th percentiles) and the 90% confidence interval (5th to 95th percentiles). When possible, a distribution will be represented graphically by an empirical density histogram overlaid with the fitted probability density function (PDF).

D.3 Estimation of BAFs for Methylmercury

BAF values for methylmercury in aquatic food chains were calculated in three different ways. The first method of calculation was a modification of the method used to support WC development in the GLWQI (U.S. EPA, 1994) and involved multiplication of a weighted bioconcentration factor (BCF) by appropriate food chain multipliers (FCMs). This method (modified GLWQI method) yielded BAFs for trophic levels 3 and 4. The second method (direct method or field-derived method) involved direct estimation of a BAF for trophic level 3 from field data, which was then multiplied by a predatory-prey factor (PPF) for trophic level 4 to yield a BAF for trophic level 4. A BAF for trophic level 4 was also estimated directly from field data. The results of all three analyses were then compared. Final BAF values for trophic levels 3 and 4 were recommended for calculation of WC values and for estimation of human exposure from consumption of contaminated fish.

More detailed approaches have been proposed to estimate BAFs for mercury in aquatic food chains (e.g., the mercury cycling model (MCM), developed by the Electric Power Research Institute; Hudson et al., 1994). Such approaches were considered to be inappropriate, however, in view of the general lack of understanding of mercury accumulation and the broad geographical focus of this report. In particular, it was determined that models requiring calibration to specified food chains and lake water characteristics were unlikely to yield information that could be applied with confidence to a different food chain, or in a lake with different biogeochemical characteristics. Instead, the decision was made to accept that considerable variability exists with respect to mercury concentrations in fish, and to employ statistical methods that treat this variability quantitatively.

D.3.1 Data Quality Objectives

Preference was given to data published in the peer-reviewed literature. Data from one unpublished report was also included (Suchanek et al., 1993), which was notable for its scope, level of detail and quality; this study also provides the only data for a eutrophic water body in a more temperate climate. Also, because of recent advances in analytical techniques for measurement of methylmercury in natural waters, primary consideration was given to methylmercury values reported since 1990 (Bloom, 1989; Bloom, 1992). BAFs based on methylmercury from earlier literature tend to be lower due to higher (biased) reported water concentrations. This restriction does not apply to reported values for total mercury. An attempt was made to characterize the data as necessary to permit comparisons to be made between studies. For example, mean values were estimated even if the original authors did not do so. When possible BAFs were reported in terms of both the age or size of the fish involved and the mercury species measured in the fish.

D.3.2 Estimation of BAFs For Mercury Using a Modified GLWQI Approach

D.3.2.1 BAFs Published in the Proposed Guidance

BAFs for mercury were estimated to support the development of wildlife criteria values in the GLWQI (U.S. EPA, 1993). The approach and assumptions used in these calculations were subsequently modified to incorporate new information (U.S. EPA, 1994) and to provide BAFs for methylmercury rather than total mercury. The following is a description of the modified approach.

BAFs were calculated in support of wildlife criterion development to relate methylmercury concentrations in fish to dissolved methylmercury concentrations in water. The formula for the calculation of the BAF for a given trophic level is given in equation 1.

$$BAF_X = BCF_{MeHg} \times FCM_X \times fmmf \quad (1)$$

where

BAF_X is the bioaccumulation factor for trophic level X (L/kg),
 BCF_{MeHg} is the bioconcentration factor for methylmercury at trophic level 1,
 FCM_X is the food-chain multiplier representing the cumulative biomagnification of mercury from trophic level 2 to trophic level X and
 $fmmf$ is the fraction of total mercury in fish flesh that is in the methylated form.

The formula for FCM_4 is given in equation 2.

$$FCM_4 = PPF_2 \times PPF_3 \times PPF_4 \quad (2)$$

where

PPF_2 is the predator-prey factor at trophic level 2 representing the biomagnification of mercury in zooplankton as a result of feeding on contaminated phytoplankton,
 PPF_3 is the predator-prey factor for forage fish feeding on contaminated zooplankton, and
 PPF_4 is the predator-prey factor piscivorous fish feeding on forage fish.

The estimated inputs for equations 1 and 2 are as follows:

The BCF for methylmercury in aquatic biota is 33,000.
The predator-prey factors (PPFs) for trophic levels 2, 3 and 4 are 6.3, 6.2 and 4.9, respectively.
The FCM for trophic level 3 is 39 (6.3 x 6.2).
The FCM for trophic level 4 is 195 (6.3 x 6.2 x 5.0).

The estimated BAFs for trophic levels 3 and 4 are as follows:

BAF for trophic level 3 = 1.32×10^6 L/kg
BAF for trophic level 4 = 6.52×10^6 L/kg

Several key assumptions were made to permit estimation of these values. These assumptions include the following:

1. The mercury concentration at trophic level 1 is determined by the extent to which mercury bioconcentrates during an aqueous exposure,

2. BCFs and PPFs are lognormally distributed,
3. 100% of total mercury in fish exists as methylmercury,
4. Phytoplankton are 90% water by weight,
5. Zooplankton are 80% water by weight.

D.3.2.2 Inputs and Assumptions for the Present Analysis

Input variable distributions are presented individually along with the data from which they were derived.

Bioconcentration Factor for Methylmercury in Fish

Variable: BCF_{MHg}
 Definition: Total mercury concentration in fish divided by dissolved methylmercury in water
 Point Estimate: 33,000 (unitless)
 Distribution: lognormal (GM = 33,400; GSD = 4.888)

Technical Basis:

Bioconcentration factors (BCFs) for methylmercury in phytoplankton ranging from 3,400 to 133,000 were estimated from field data in the published literature and are presented in Table D-1. As phytoplankton analysis is done on a dry weight basis an assumption was made that phytoplankton were 90% water (Watras and Bloom, 1992). This assumption applies to all of the values in Table D-1. The lowest value of 3,400 estimated from Mason and Sullivan (1997) was a result of a very low percentage of methylmercury (2.3%) of the total mercury in the sample. The highest value of 133,000 for Little Rock Lake was converted from a BCF for total methylmercury of 88,900 calculated from data in Watras and Bloom (1992) by dividing by 0.667, the fraction of total methylmercury in the water column that is dissolved. The latter value was calculated from mercury speciation data reported in Bloom et al. (1991) for the same lake. The BCF from Hill et al. (1996) is an average of 4 locations in E. Fork Poplar Creek.

Table D-1
Bioconcentration Factor for Methylmercury in Phytoplankton

Value		Reference
3,400	Lake Michigan	Mason and Sullivan, 1997
38,400	E. Fork Poplar Cr., TN	Hill et al., 1996
107,000	Onondaga Lake, NY	Becker and Bigham, 1995
133,000	Little Rock Lake, WI	Watras and Bloom, 1992

Predator-Prey Factor for Trophic Level 2

Variable: PPF_2
 Definition: Factor by which methylmercury concentrations in trophic level 2 organisms exceed those in trophic level 1 organisms upon which they prey.
 Point Estimate: 6.3 (unitless)

Distribution: lognormal (GM = 6.34; GSD = 1.273)

Technical Basis:

Three studies were found in the literature for the estimation of PPF₂. The estimated values are listed in Table D-2. Concentrations of methylmercury in trophic level 1 organisms (phytoplankton) were estimated as for BCF_{MHg}. That is, phytoplankton were assumed to be 90% water. In addition, to convert from dry weight to wet weight, zooplankton were assumed to be 80% water (Watras and Bloom, 1992) for all of the values. The factors contributing to the variability in PPFs were assumed to be multiplicative and best represented by a lognormal distribution.

Table D-2
Predator-Prey Factor for Trophic Level 2

Value	Location	Reference
5.0	Little Rock Lake, WI	Watras and Bloom, 1992
6.3	L. Michigan	Mason and Sullivan, 1997
8.1	Onondaga L., NY	Becker and Bigham, 1995

Predator-Prey Factor for Trophic Level 3

Variable: PPF₃
Definition: Factor by which methylmercury concentrations in trophic level 3 organisms exceed those in trophic level 2 organisms upon which they prey.
Point Estimate: 6.2 (unitless)
Distribution: lognormal (GM = 6.22; GSD = 2.120)

Technical Basis:

Five studies were found in the literature for the estimation of PPF₃. The estimated values and trophic level 3 species are listed in Table D-3. Concentrations of methylmercury in trophic level 2 organisms (zooplankton) were estimated as for PPF₂. That is, zooplankton were assumed to be 80% water. Trophic level 3 species were reported only as “planktivorous fishes” in Plourde et al. (1997). The factors contributing to the variability in PPFs were assumed to be multiplicative and best represented by a lognormal distribution.

**Table D-3
Predator-Prey Factor for Trophic Level 3**

Value	Trophic Level 3 Species	Location	Reference
2.6	gizzard shad, white perch	Onondaga L., NY	Becker and Bigham, 1995
3.2	yellow perch	Little Rock Lake, WI	Watras and Bloom, 1992
7.5	bloater	L. Michigan	Mason and Sullivan, 1997
9.6	“planktivorous fishes”	LG2 Res., Quebec	Plourde et al., 1997
15.5	“planktivorous fishes”	4 lake aggregate, Quebec	Plourde et al., 1997

Predator-Prey Factor for Trophic Level 4

Variable: PPF₄
 Definition: Factor by which methylmercury concentrations in trophic level 4 organisms exceed those in trophic level 3 organisms upon which they prey.
 Point Estimate: 5.0 (unitless)
 Distribution: lognormal (GM = 4.95; GSD = 1.464)

Technical Basis:

PPF_{4s} on a total mercury basis ranging from 2.4 to 7.5 were estimated for "standardized" lake trout (60 cm) and rainbow smelt (15 cm) from nine Ontario lakes (MacCrimmon et al., 1983). Values from very old (20+ years) lake trout from Tadenac Lake exceeded those of age 2+ year-old rainbow smelt by a factor of 12.3. Levels in trout appeared to increase dramatically when they became large enough (about 6 years old) to switch from a diet of benthic invertebrates to smelt. The overall average PPF was 5.0.

PPF_{4s} (total mercury basis) ranging from 1.2 to 8.4 were calculated from data reported by Wren et al. (1983). These estimates were computed by dividing the average values for three predators (smallmouth bass, northern pike, and lake trout) by average values for two forage fish (bluntnose minnow and rainbow smelt). The maximum value was obtained by dividing the value for pike by that for minnows. The overall average PPF was 3.0.

Data presented by Mathers and Johansen (1985) were used to calculate PPF_{4s} of 5.9 and 4.9 for northern pike and walleye, respectively. Each value was calculated by dividing the total mercury residue in eight-year-old fish by the weighted average total mercury content of the diet for each species. Corresponding values for four-year-old fish were 2.8 and 2.2, respectively. Values for both species tended to increase with fish age and in some very old walleye exceeded 10. The overall average PPF was 4.0.

PPF_{4s} ranging from 2.7 to 4.5 were computed by dividing the average total mercury residues in two predators (northern pike and brown trout) by average values for two forage fish (whitefish and smelt) (Skurdal et al., 1985). The overall average PPF was 3.6.

A PPF of 5.22 was calculated from data presented by Cope et al. (1990). Data for age 5 walleye were regressed against data from age 2 yellow perch. All fish were collected from northern Wisconsin

seepage lakes. The PPF was calculated from the regression equation for a perch containing 0.1 micrograms/g of total mercury. It should be noted that in this study mercury levels in muscle from walleye were compared with whole-body levels in perch.

Residue data given by Jackson (1991) were used to calculate PPF₄s ranging from 5.5 to 14. Estimates were computed for four lakes in Manitoba by dividing the average values for two predators (northern pike and walleye) by average values for two forage fish (yellow perch and spottail shiners). The average value was 9.8.

A value of 6.8 was obtained by regressing total mercury data for 1 kg northern pike against that from 8 to 10 cm yellow perch (Lindqvist, 1991). The data are from 43 lakes and are remarkable for the consistency of the relationship.

A PPF₄ of 7.4 was calculated by comparing total mercury in 1 kg northern pike to total mercury in 5 to 10 g yellow perch (Meili et al., 1991).

Average concentrations of total mercury were calculated for largemouth bass and silversides in Clear Lake, California (Suchanek, 1993). The average PPF₄ estimated from these data was 7.1.

A PPF₄ of 2.75 was calculated from total mercury residues in lake trout (trophic level 4) and bloater (trophic level 3) in Lake Michigan (Mason and Sullivan, 1997).

A PPF₄ of 3.42 was estimated from data on total mercury levels in predatory fish (pescada and tucunaré) and planktivores (mapará) in the Tucuruí reservoir in Brazil (Porvari, 1995).

PPFs ranging from 3.52 to 6.72 were estimated for six Canadian Shield lakes from data on total mercury levels reported by Bodaly et al. (1993). The trophic level 4 fish were northern pike and walleye. The trophic level 3 fish were white sucker and cisco. The overall average BAF was 5.06.

A PPF₄ of 5.63 was estimated from data on methylmercury levels for walleye and smallmouth bass feeding on gizzard shad and bluegill in Onondaga Lake, NY (Becker and Bigham, 1995).

Summary:

Predator-prey factors reflecting the increase in mercury concentration between trophic levels 3 and 4 range from 1 to 20 considering one-to-one species comparisons only. The overall mean values from any given water body is more in the range of 3 to 10, with a median of about 5. Interpretation of predator-prey factors is complicated by the fact that piscivorous fish accumulate mercury throughout their lifetime; thus, calculation of this value for a given species and system depends to a large extent upon the age of the fish sampled. In addition, it is well known that the diet of a piscivorous fish changes with age, tending in many cases to be dominated by invertebrates until fish reach a critical size that allows them to prey efficiently upon small fish. In general, therefore, the mercury concentration in prey of a piscivorous fish can be expected to increase with the age or size of the predator. Additional considerations, including sexual reproduction, prey selection and availability and seasonal changes in bioenergetics due to changes in water temperature are also likely to be important determinants of bioaccumulation.

Overall, it can be shown that for most, if not all, piscivorous fish, mercury concentrations increase in a nearly linear fashion with age. The increase appears to be linear for younger fish but may be closer to exponential for older fish (Monteiro et al., 1991). The apparent exponential increase results in ever increasing BAFs as fish get older and larger. An exponential increase hypothesis is supported by

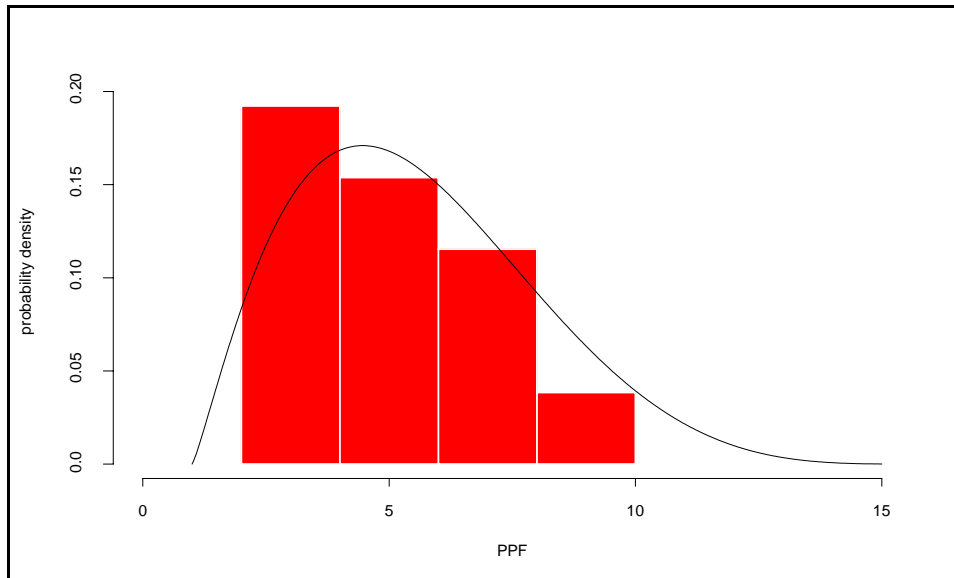
regression analyses of the association of mercury concentration in fish and fish age or size in the literature. For those regressions based on the log of the mercury concentrations (Wren and MacCrimmon, 1986; Monteiro et al., 1991; Kim, 1995; Monteiro et al., 1996), correlation coefficients averaged 0.84 ($r^2 = 0.7$). When the regression was based on the untransformed mercury concentrations (Grieb et al., 1990; Lange et al., 1994; Kim, 1995; Porvari, 1995; Hoover et al., 1997), the correlation coefficients averaged 0.54 ($r^2 = 0.3$). That is 70% of the variability in the logarithms of fish mercury concentrations for a given species is explained by the variability in fish age/size, while only 30% of the variability is explained on an untransformed mercury concentration basis. This result suggests a multiplicative or exponential relationship. For a given system, therefore, it is feasible to extrapolate data for small predators to larger members of the same species. The mix of species and size ranges in the diet of a given piscivore would still be required in order to construct a receptor-specific distribution for more accurate exposure estimation. Only one of the studies described in this section presented specific diets for piscivorous species (Mathers and Johansen, 1985).

The values defining the empirical distribution for PPF_4 are given in Table D-4. The GM and GSD of the values were 4.95 and 1.464, respectively. The arithmetic mean and standard deviation were 5.29 and 2.04, respectively. The lowest and highest values fall at the 4th and 96th percentiles, respectively, in the empirical distribution. The median of the empirical distribution is 5.06. The factors contributing to the variability in PPFs were assumed to be multiplicative and best represented by a lognormal distribution. The arithmetic mean of the resulting distribution was 5.32. The empirical distribution and PDF for PPF_4 is shown in Figure D-1.

**Table D-4
Predator-Prey Factor for Trophic Level 4**

Value	TL4 Species	TL3 Species	Location	Reference
2.75	lake trout	bloater	L. Michigan	Mason and Sullivan, 1997
3.0	smallmouth bass, lake trout, n. pike	bluntnose minnow, rainbow smelt	L. Tadenac, Ontario, Canada	Wren et al., 1983
3.42	pescada, tucunaré	mapará	Tucuruí Res., Brazil	Porvari, 1995
3.5	northern pike, largemouth bass	yellow perch, white sucker	35 lake aggregate, upper MI	Grieb et al., 1990
3.6	northern pike	rainbow smelt, whitefish	L. Tyrifjorden, Norway	Skurdal et al., 1985
4.0	n. pike, walleye	specific weighted diets	L. Simcoe, Canada	Mathers and Johansen, 1985
5.0	lake trout (60 cm)	rainbow smelt (15 cm)	9 lake aggregate, Ontario, Canada	MacCrimmon et al., 1983
5.06	n. pike, walleye	white sucker, cisco	average of 6 Canadian Shield lakes	Bodaly et al., 1993
5.22	walleye (age 5)	yellow perch (age 2)	10 lake aggregate, WI	Cope et al., 1990
5.63	smallmouth bass, walleye	gizzard shad, bluegill	Onondaga L., NY	Becker and Bigham, 1995
6.8	northern pike (1 kg)	y. perch (8-10 cm)	43 lake aggregate, Sweden	Lindqvist, 1991
7.1	largemouth bass	silversides	Clear L., CA	Suchanek et al., 1993
7.4	northern pike	yellow perch	25 lake aggregate, Sweden	Meili et al., 1991
9.8	n. pike, walleye	spottail shiner, yellow perch	4 lake average, Manitoba, Canada	Jackson, 1991

Figure D-1.
Input Distribution for PPF₄



Mercury Speciation in Fish Tissues

Variable: fmmf
Definition: Fraction of total mercury in fish tissues existing as the methylated form.
Point Estimate: 1
Distribution: none

Technical Basis:

Bloom (1992) reported that virtually all (>95%) of the mercury in muscle tissues from largemouth bass, yellow perch, northern pike and white suckers existed as methylmercury. In addition, the author suggested that lower values reported in earlier literature are probably erroneous due to inadequate sampling, analytical and reporting techniques. In particular, even with the best analytical methods, recovery of methylmercury is, at best, 95%, while recovery of total Hg can be virtually 100%. That is, any value greater than 0.9 is probably indistinguishable from 1. Subsequent studies support a value of >0.95 for this variable (Lasorsa and Allen-Gil, 1995; Akagi et al., 1995; Malm et al., 1995; Kim, 1995; Becker and Bigham, 1995).

Summary:

Because of continued refinement in mercury analysis methods, more confidence should be placed in recent values (see Bloom (1992) for a discussion of factors that can result in lower estimates than are actually present). Collectively, the most recent values suggest that the percentage of mercury in fish that exists as the methylated form exceeds 95%. Minor differences in reported values may be due the different types of samples evaluated (e.g., whole fish vs. skin-on fillets vs. skin-off fillets), but are unlikely to be important in the calculation of a BAF. fmmf was assigned a value of 1.0, as the contribution of this variable to both the mean and variance of the BAF output was judged to be negligible.

D.3.2.3 Results of Probabilistic Analysis of the Modified GLWQI Methodology

Selected statistics for the BAF₃ and BAF₄ distributions generated from the Modified GLWQI methodology are given in Table D-5. There was a large variability in the simulation output for both BAFs as evidenced by the large GSDs. The 90% confidence interval spans a 340-fold range for BAF₃ and a 390-fold range for BAF₄. The large variances also resulted in a large difference between the geometric and arithmetic means.

Table D-5
Statistics for BAFs Using the Modified GLWQI Methodology

Statistic	BAF ₃	BAF ₄
Geometric Mean	1,320,000	6,520,000
Arithmetic Mean	6,350,000	33,700,000
GSD	5.884	6.127
Percentiles:		
5th	71,500	331,000
25th	399,000	1,920,000
50th	1,320,000	6,520,000
75th	4,360,000	22,100,000
95th	24,400,000	129,000,000

D.3.3 Estimation of a BAF₄ for Methylmercury Using Measured Values for Trophic Level 3 and a Field-Derived Food Chain Multiplier

In this analysis a BAF for trophic level 4 was calculated using a field-derived BAF value for trophic level 3 and published predator-prey factors for trophic level 4. The distribution of BAFs for trophic level 3 is presented along with the data from which it was derived. The distribution of predator-prey factors for trophic level 4 was defined previously in Section D.3.2.2. All of the mercury in fish was assumed to be methylmercury (see Section D.3.2.2). Here, as is the case throughout the document, ${}_{MD}BAF_3$ and ${}_{MD}BAF_4$ refer to the concentrations of methylmercury in fish divided by the concentration of methylmercury in filtered water.

D.3.3.1 Bioaccumulation Factors Directly Estimated From Field Data - Methylmercury in Forage Fish

Variable: ${}_{MD}BAF_3$
 Definition: Average methylmercury concentrations in planktivorous fish (trophic level 3) divided by average dissolved methylmercury concentrations in water, accumulated by all possible routes of exposure.
 Point Estimate: 1.6×10^6 L/kg
 Distribution: lognormal (GM = 1.58×10^6 ; GSD = 2.115)

Technical Basis:

A $_{MD}BAF_3$ of 667,000 was estimated for gizzard shad from Onondaga Lake (NY) from data reported by Becker and Bigham (1995). The value was derived from an average concentration of 0.2 ppm methylmercury in shad (age classes 3-4 years) and 0.3 ng/L (3×10^{-7} ppm) dissolved methylmercury in the water. There is considerable uncertainty in this BAF estimate as water methylmercury concentrations were determined for a single season (summer) only.

A $_{MD}BAF_3$ of 1.46×10^6 for yellow perch from Lake Iso Valkjarvi in Finland was calculated from data reported by Rask and Verta (1995). Concentrations of total mercury in perch averaged 0.15 ppm over a 3-year period (1990-1993). The mean concentration of dissolved methylmercury in the epilimnion was 0.103 ng/L (1.03×10^{-7} ppm). The water concentrations were determined on a single day (8/24/93). All measurements were taken from the control basin of Iso Valkjarvi as the lake was partitioned for experimental liming to control pH.

$_{MD}BAF_3$ s for silversides and juvenile bass in Clear Lake (CA) were estimated from data tables providing cross-seasonal measurements for two years (Suchanek et al., 1993). $_{MD}BAF_3$ s were estimated from matched fish (total mercury) and water (dissolved surface methylmercury) concentrations for each measurement for this period across 4 lake areas and up to 5 sampling locations for each area. The average $_{MD}BAF_3$ for silversides was 1.13×10^6 and for juvenile bass was 1.93×10^6 , with an overall mean of 1.53×10^6 .

A $_{MD}BAF_3$ of 4.17×10^6 for bloater in Lake Michigan was calculated from data reported by Mason and Sullivan (1997). A two-seasonal average (August/October, 1994) of methylmercury in the surface waters was calculated to be 0.0104 ng/L or 1.04×10^{-8} ppm (all methylmercury assumed to be monomethylmercury). The average concentration of methylmercury in bloater was calculated to be 0.0434 ppm (assuming that all the mercury was monomethylmercury).

Summary:

Only two of the data points for $_{MD}BAF_3$ incorporated cross-seasonal variability for water methylmercury concentrations and the fish species/age/size range was limited or undeterminable for most of the studies. The geometric mean of 1.58×10^6 , however, was still considered to be the best (unbiased) estimate of central tendency. The values defining the empirical distribution for $_{MD}BAF_3$ are given in Table D-6. The GM and GSD of the values were 1.58×10^6 and 2.115, respectively. The arithmetic mean and standard deviation were 1.95×10^6 and 1.52×10^6 , respectively. The lowest and highest values fall at the 12.5th and 87.5th percentiles, respectively, in the empirical distribution. The median of the empirical distribution is 1.50×10^6 . The factors contributing to the variability in BAFs were assumed to be multiplicative and best represented by a lognormal distribution. Selected statistics for $_{MD}BAF_3$ are given in Table D-7.

Table D-6
Bioaccumulation Factor for Methylmercury in Trophic Level 3 Fish

Value	Species	Location	Reference
6.67 x 10 ⁵	gizzard shad	Onondaga L., NY	Becker and Bigham, 1995
1.46 x 10 ⁶	yellow perch	Iso Valkjarvi, Finland	Rask and Verta, 1995
1.53 x 10 ⁶	silversides, juvenile bass	Clear L., CA	Suchanek et al., 1993
4.17 x 10 ⁶	bloater	L. Michigan	Mason and Sullivan, 1997

Table D-7
Statistics for Methylmercury _{MD}BAF₃:
Direct Estimate from Field Data

Statistic	Value
Geometric Mean	1,580,000
Arithmetic Mean	2,090,000
GSD	2.115
Percentiles:	
5th	461,000
25th	953,000
50th	1,580,000
75th	2,662,000
95th	5,410,000

D.3.3.2 Results of Probabilistic Simulation of _{MD}BAF₄ Using Field-Derived _{MD}BAF₃ and PPF₄ Estimates

The formula for the calculation of _{MD}BAF₄ by this method is given in equation 3.

$$\text{MDBAF}_4 = \text{MDBAF}_3 \times \text{PPF}_4 \quad (3)$$

where

_{MD}BAF₃ is the field-derived distribution for the _{MD}BAF at trophic level 3

PPF₄ is the predator-prey factor at trophic level 4 representing the biomagnification of mercury in piscivorous fish feeding on forage fish

Selected percentiles from the distribution of BAFs calculated by the analytic solution of Equation 3 using lognormal distributions for field-derived _{MD}BAF₃ (§D.3.3.1) and PPF₄ (§D.3.2.2) estimates are given in Table D-8.

Table D-8
Statistics for Methylmercury $_{MD}BAF_4$
Estimated from $_{MD}BAF_3 \times PPF_4$

Statistic	Value
Geometric Mean	4,820,000
Arithmetic Mean	11,100,000
GSD	2.317
Percentiles:	
5th	1,960,000
25th	4,440,000
50th	7,820,000
75th	1,380,000
95th	31,100,000

D.3.4 Specification of a Distribution for $_{MD}BAF_4$ Directly Derived from Field Data

D.3.4.1 Bioaccumulation Factors Directly Estimated From Field Data - Methylmercury in Piscivorous Fish

Variable: $_{MD}BAF_4$
Definition: Average methylmercury concentrations in piscivorous fish (trophic level 4) divided by average dissolved methylmercury concentrations in water, accumulated by all possible routes of exposure.
Point Estimate: 6.8×10^6 L/kg
Distribution: lognormal (GM = 6.81×10^6 ; GSD = 1.564)

Technical Basis:

A $_{MD}BAF_4$ of 4×10^6 was reported by Becker and Bigham (1995) for methylmercury in piscivores from Onondaga Lake (NY). The piscivorous species included smallmouth bass (age classes 6-9 years) and walleye (age classes not given). There is considerable uncertainty in this BAF estimate as water methylmercury concentrations were determined for a single season (summer) only.

A $_{MD}BAF_4$ of 5.86×10^6 was estimated for walleye and northern pike from four lakes in the Manitoba Province of Canada from data reported by Jackson (1991). Fish and water methylmercury concentrations were estimated from Figures 2 and 3 (in Jackson, 1991). The BAF is an average of BAFs ranging from 4.0×10^6 to 7.0×10^6 across the four lakes. An average was used to avoid over representation of this one area outside the continental U.S. Mean lengths, only, were reported for walleye (37-46 cm) and northern pike (55-71 cm). Fish sample collection was in 1980 and dissolved methylmercury concentrations were determined in June, 1981. As a result, this $_{MD}BAF$ estimate should be considered to be a minimum value (downward bias arising from pre-1990 analytical methods) and highly uncertain (no cross-seasonal average).

A $_{MD}BAF_4$ for largemouth bass in Clear Lake (CA) was estimated from data reported by Suchanek et al. (1993). In this case, fish mercury concentrations (total mercury) were estimated from figures showing fish mercury levels versus fish weight for each of three lake areas. Mercury

concentrations were averaged for all fish of 450 grams or higher, ranging up to 4200 grams, suggesting that a broad range of year classes was represented. The average fish mercury levels in each lake area were divided by average dissolved methylmercury concentrations in the surface waters for the same area. The water methylmercury concentrations, in each case, were averaged across seasons over a two year period.

A $_{MD}BAF_3$ of 1.14×10^7 for lake trout in Lake Michigan was calculated from data reported by Mason and Sullivan (1997). A two-seasonal average (August/October, 1994) of methylmercury in the surface waters was calculated to be 0.0104 ng/L or 1.04×10^{-8} ppm (all methylmercury assumed to be monomethylmercury). The average concentration of methylmercury in lake trout was calculated to be 0.1186 ppm (assuming that all the mercury was monomethylmercury).

Summary:

Only two of the data points for $_{MD}BAF_4$ incorporated cross-seasonal variability for water methylmercury concentrations and the fish species/age/size range was limited or undeterminable for most of the studies. The geometric mean of 6.81×10^6 , however, was still considered to be the best (unbiased) estimate of central tendency. The values defining the empirical distribution for $_{MD}BAF_4$ are given in Table D-9. The GM and GSD of the values were 6.81×10^6 and 1.564, respectively. The arithmetic mean and standard deviation were 7.33×10^6 and 3.18×10^6 , respectively. The lowest and highest values fall at the 12.5th and 87.5th percentiles, respectively, in the empirical distribution. The median of the empirical distribution is 6.96×10^6 . The factors contributing to the variability in BAFs were assumed to be multiplicative and best represented by a lognormal distribution. Selected statistics for $_{MD}BAF_4$ are given in Table D-10.

**Table D-9
Bioaccumulation Factors for Methylmercury in Trophic Level 4 Fish**

Value	Species	Location	Reference
4.00×10^6	smallmouth bass, walleye	Onondaga L., NY	Becker and Bigham, 1995
5.86×10^6	northern pike, walleye	4 lake average, Manitoba, Can.	Jackson, 1991
8.06×10^6	largemouth bass	Clear L., CA	Suchanek et al., 1993
1.14×10^7	lake trout	L. Michigan	Mason and Sullivan, 1997

Table D-10
Statistics for Field-Derived $_{MD}BAF_4$

Statistic	Value
Geometric Mean	6,810,000
Arithmetic Mean	7,530,000
GSD	1.564
Percentiles:	
5th	3,260,000
25th	5,040,000
50th	6,810,000
75th	9,210,000
95th	14,200,000

D.3.5 Specification of BAF Distributions Based on Dissolved Total Mercury

D.3.5.1 Bioaccumulation Factors Directly Estimated From Field Data - Total Dissolved Mercury in Forage Fish

Variable: $_{TD}BAF_3$
 Definition: Average total mercury concentrations in forage fish (trophic level 3) divided by average dissolved total mercury concentrations in water, accumulated by all possible routes of exposure.
 Point Estimate: 1.2×10^5 L/kg
 Distribution: lognormal (GM = 1.19×10^5 ; GSD = 1.531)

Technical Basis:

$_{TD}BAF_3$ s for silversides and juvenile bass in Clear Lake (CA) were estimated from data tables providing cross-seasonal measurements for two years (Suchanek et al., 1993). $_{MD}BAF_3$ s were estimated from matched fish (total mercury) and water (dissolved surface total mercury) concentrations for each measurement for this period across two lake areas and up to five sampling locations for each area. The Oaks Arm total mercury measurements were excluded from the analysis as this area of the lake was the site of the point-source for mercury contamination (chlor-alkali plant); total mercury levels were anomalously high in this area (5 times that of other lake areas) and were judged not to be representative. The combined average $_{TD}BAF_3$ for silversides and juvenile bass was 76,000.

A $_{TD}BAF_3$ of 76,000 was estimated for gizzard shad from Onondaga Lake (NY) from data reported by Becker and Bigham (1995) and Henry et al. (1995). The value was derived from an average concentration of 0.2 ppm mercury in shad (age classes 3-4 years; Becker and Bigham, 1995) and 2.625 ng/L dissolved total mercury in the water (Henry et al., 1995). The water concentration represents an average across three seasons (spring, summer and fall) for an entire year.

A $_{TD}BAF_3$ of 113,000 for yellow perch from Lake Iso Valkjarvi (control basin) in Finland was calculated from data reported by Rask and Verta (1995). Concentrations of total mercury in perch

averaged 0.15 ppm over a 3-year period (1990-1993). The mean concentration of dissolved total mercury in the epilimnion was 1.33 ng/L. The water concentrations were based on three observations on a single day (8/24/93).

A $_{TD}BAF_3$ of 212,000 for bloater in Lake Michigan was calculated from data reported by Mason and Sullivan (1997). A two-year (1994, 1995) three-season (spring, summer, fall) average of dissolved total mercury in the surface waters was calculated to be 0.2 ng/L. The average concentration of total mercury in bloater was calculated to be 0.0434 ppm.

Summary:

All but one of the data points for $_{TD}BAF_3$ incorporated cross-seasonal variability for water mercury concentrations but the fish species/age/size ranges were somewhat limited. Overall, the data, although meager, were somewhat more representative of the definition for this variable than for $_{MD}BAF_3$. The values defining the empirical distribution for $_{MD}BAF_4$ are given in Table D-11. The GM and GSD of the values were 1.19×10^5 and 1.531, respectively. The arithmetic mean and standard deviation were 1.28×10^5 and 5.87×10^4 , respectively. The lowest and highest values fall at the 12.5th and 87.5th percentiles, respectively, in the empirical distribution. The median of the empirical distribution is 1.11×10^5 . The factors contributing to the variability in BAFs were assumed to be multiplicative and best represented by a lognormal distribution. Selected statistics for $_{TD}BAF_3$ are given in Table D-12.

Table D-11
Bioaccumulation Factor for Dissolved Total Mercury in Trophic Level 3 Fish

Value	Species	Location	Reference
7.60×10^4	gizzard shad	Onondaga L., NY	Becker and Bigham, 1995; Henry et al., 1995
1.09×10^5	silversides, juvenile bass	Clear L., CA	Suchanek et al., 1993
1.13×10^5	yellow perch	Iso Valkjarvi, Finland	Rask and Verta, 1995
2.12×10^5	bloater	L. Michigan	Mason and Sullivan, 1997

Table D-12
Statistics for Field-Derived $_{TD}BAF_3$

Statistic	Value
Geometric Mean	119,000
Arithmetic Mean	130,000
GSD	1.531
Percentiles:	
5th	59,100
25th	89,300
50th	119,000
75th	159,000
95th	240,000

D.3.5.2 Bioaccumulation Factors Directly Estimated From Field Data - Total Dissolved Mercury in Piscivorous Fish

Variable: $_{TD}BAF_4$
 Definition: Average total mercury concentrations in Piscivorous fish (trophic level 4) divided by average dissolved total mercury concentrations in water, accumulated by all possible routes of exposure.
 Point Estimate: 5.0×10^5 L/kg
 Distribution: lognormal (GM = 4.96×10^5 ; GSD = 1.181)

Technical Basis:

A $_{TD}BAF_4$ of 4.19×10^5 was estimated for piscivores (smallmouth bass and walleye) in Onondaga Lake (NY) from data reported by Becker and Bigham (1995) and Henry et al. (1995). The value was derived from an average concentration of 1.1 ppm mercury in piscivores (Becker and Bigham, 1995) and 2.625 ng/L dissolved total mercury in the water (Henry et al., 1995; see D.3.5.1).

A $_{TD}BAF_4$ of 5.0×10^5 for largemouth bass in Clear Lake (CA) was estimated from data reported by Suchanek et al. (1993). Estimation of fish mercury concentrations was described in D.3.4.1, previously. The average fish mercury levels in each of two lake areas were divided by average dissolved total mercury concentrations in the surface waters (see D.3.5.1) for the same area.

A $_{TD}BAF_4$ of 5.84×10^5 for lake trout in Lake Michigan was calculated from data reported by Mason and Sullivan (1997). A two-year (1994, 1995) three-season (spring, summer, fall) average of dissolved total mercury in the surface waters was calculated to be 0.2 ng/L. The average concentration of total mercury in trout was calculated to be 0.1186 ppm.

Summary:

Only three studies were available for the estimation of $_{TD}BAF_4$. All of the data points, however, incorporated cross-seasonal variability for water mercury concentrations. The fish species/age/size range was undeterminable for one study (Mason and Sullivan, 1997) but fairly representative for the other two.

Overall, the data, although meager, were more representative of the definition for this variable than for ${}_{MD}BAF_4$. The values defining the empirical distribution for ${}_{TD}BAF_4$ are given in Table D-13. The GM and GSD of the values were 4.96×10^5 and 1.181, respectively. The arithmetic mean and standard deviation were 5.01×10^5 and 8.25×10^4 , respectively. The lowest and highest values fall at the 16.7th and 83.3th percentiles, respectively, in the empirical distribution. The median of the empirical distribution is 5.00×10^5 . The factors contributing to the variability in BAFs were assumed to be multiplicative and best represented by a lognormal distribution. Selected statistics for ${}_{TD}BAF_4$ are given in Table D-14.

Table D-13
Bioaccumulation Factor for Dissolved Total Mercury in Trophic Level 4 Fish

Value	Species	Location	Reference
4.19×10^5	smallmouth bass, walleye	Onondaga L., NY	Becker and Bigham, 1995; Henry et al., 1995
5.00×10^5	largemouth bass	Clear L., CA	Suchanek et al., 1993
5.84×10^5	lake trout	L. Michigan	Mason and Sullivan, 1997

Table D-14
Statistics for Field-Derived ${}_{TD}BAF_4$

Statistic	Value
Geometric Mean	496,000
Arithmetic Mean	503,000
GSD	1.181
Percentiles:	
5th	377,000
25th	422,000
50th	496,000
75th	555,000
95th	652,000

D.3.6 Estimation of Methylmercury BAF for Trophic Level 4 from Distributions Based on Total Mercury

BAFs for methylmercury in piscivorous fish (trophic level 4) were estimated from the BAF_3 and BAF_4 distributions based on dissolved total mercury. The estimation of ${}_{MD}BAF_4$ from ${}_{TD}BAF_4$ required a second distribution that estimated the fraction of dissolved total mercury in the water column (epilimnion) that is in the methylated form (f_{mmw_E}). The estimation of ${}_{MD}BAF_4$ from ${}_{TD}BAF_3$ required the same additional distribution and a third distribution, PPF_4 . In both cases, ${}_{MD}BAF_4$ was estimated by means of a Monte Carlo simulation, as there was no analytical solution (f_{mmw_E} was defined as a beta distribution).

D.3.6.1 Speciation of Mercury in the Water Column

Mercury Speciation in the Epilimnion

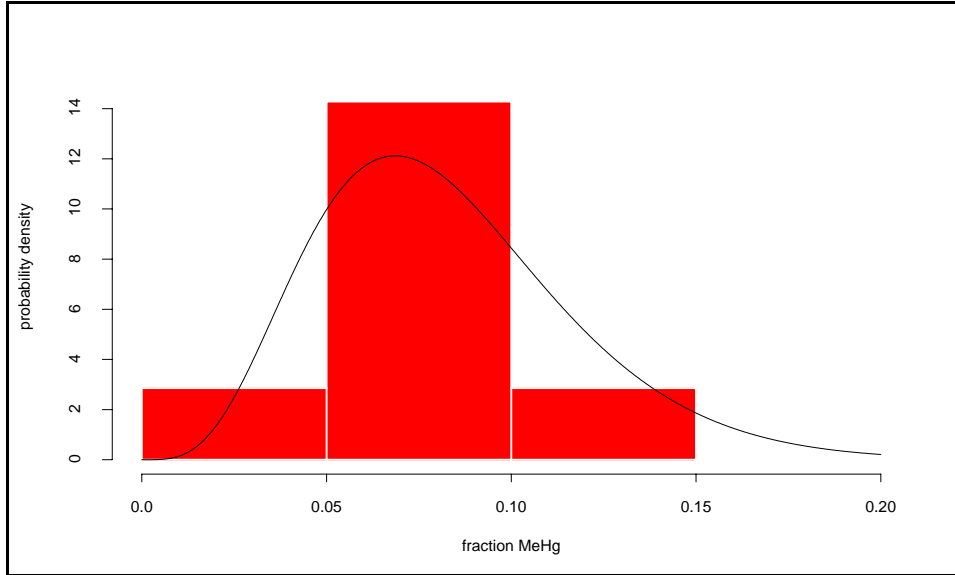
Variable: f_{mmw_E}
Definition: Fraction of total dissolved mercury in the epilimnion existing as the methylated species
Point Estimate: 0.078 (unitless)
Distribution: beta ($\alpha = 5.07$; $\beta = 56.3$)

The values defining the empirical distribution for f_{mmw_E} are given in Table D-15. The beta distribution was chosen as best representative of fractions. The distribution was fitted by the method of moments. The point estimate is the median of the resulting distribution. The empirical distribution and PDF for f_{mmw_E} is shown in Figure D-2

Table D-15
Methylmercury as a Fraction of Total Dissolved Mercury in the Epilimnion

Value	Location	Reference
0.046	Palette L., WI	Bloom et al., 1991
0.054	Oregon Pond, NY	Driscoll et al., 1995
0.059	Lake Michigan	Mason and Sullivan, 1997
0.089	Clear L., CA	Suchanek et al., 1993
0.089	Onondaga L., NY	Henry et al., 1995
0.092	Iso Valkjarvi, Finland	Rask and Verta, 1995
0.15	22 lake aggregate, WI	Watras et al., 1995a, 1995b

Figure D-2
Distribution for fmmw_E



D.3.6.2 Simulation of a Methylmercury BAF₄ from a Total Mercury BAF₄

The formula for the methylmercury BAF₄ based on $_{TD}BAF_4$ and $fmmw_E$ is given in Equation 4.

$$_{MD}BAF_4 = _{TD}BAF_4 \div fmmw_E \quad (4)$$

The formula for the methylmercury BAF₄ based on $_{TD}BAF_3$, PPF_4 and $fmmw_E$ is given in Equation 5.

$$_{MD}BAF_4 = _{TD}BAF_4 \times PPF_4 \div fmmw_E \quad (5)$$

Results of the Monte Carlo simulations (100,000 iterations) for these equations are shown in Table D-16. The $_{MD}BAF_4$ based on $_{TD}BAF_4$ (GSD = 1.614) was only slightly more variable than the directly estimated $_{MD}BAF_4$ (GSD = 1.564), largely because of the low variance of $_{TD}BAF_4$, itself. This result may reflect the greater uncertainty in the direct $_{MD}BAF_4$ estimate arising from the more uncertain methylmercury water concentrations, or it may just reflect the large variability in GSD estimates from such small sample sizes. The variability of $_{MD}BAF_4$ based on $_{TD}BAF_3$ (GSD = 2.067) was intermediate to the variabilities in the direct $_{MD}BAF_4$ estimate and $_{MD}BAF_4$ based on $_{MD}BAF_3 \times PPF_4$ (GSD = 2.317).

Table D-16
Statistics for Methylmercury BAFs Estimated from Total Mercury BAFs

Statistic ^a	Method	
	${}_{TD}BAF_4 \div fmmw_E$	${}_{TD}BAF_3 \times PPF_4 \div fmmw_E$
Geometric Mean	6,580,000	7,810,000
Arithmetic Mean	7,440,000	10,200,000
GSD	1.614	2.067
Percentiles:		
5th	3,180,000	2,430,000
25th	4,710,000	4,750,000
50th	6,370,000	7,700,000
75th	8,860,000	12,600,000
95th	15,200,000	26,400,000

^a statistics based on 100,000 iterations

Both of these output distributions were closely approximated by lognormal distributions, which were fitted by the method of moments. The Monte Carlo simulation output and the fitted distributions for methylmercury BAF₄s based on ${}_{TD}BAF_4$ and ${}_{TD}BAF_3$ are shown in Figures D-3 and D-4, respectively.

Figure D-3
 ${}_{MD}BAF_4$ Distribution Based on ${}_{TD}BAF_4$

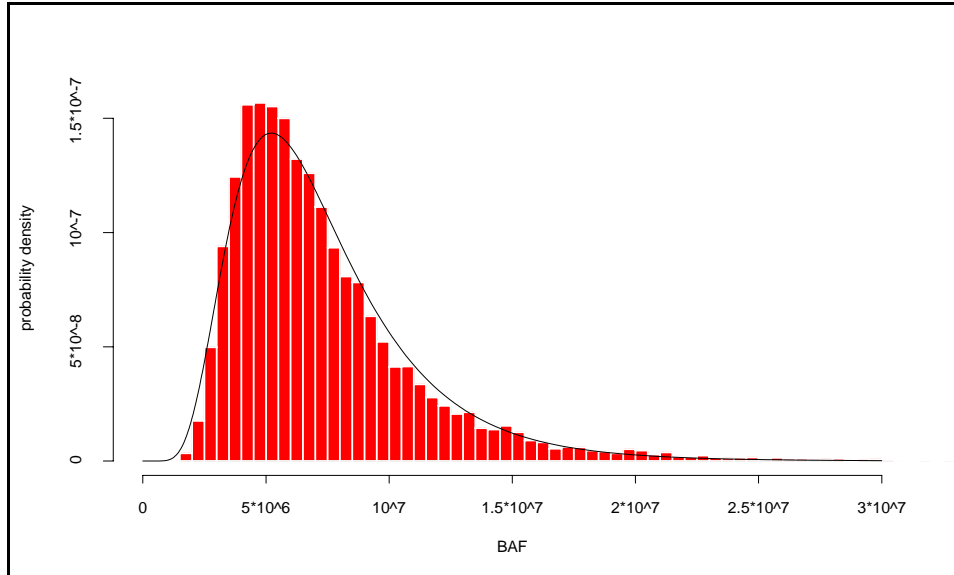
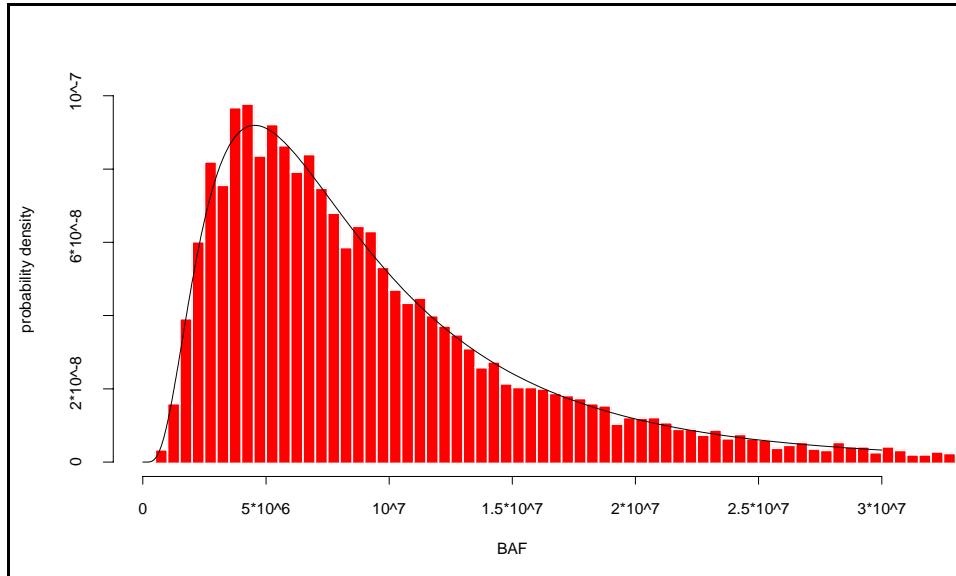


Figure D-4
 $_{MD}BAF_4$ Distribution Based on $_{TD}BAF_3$



D.3.7 Sensitivity Analysis

The focus of the sensitivity analysis was on the primary method for BAF estimation, that is, direct estimation from field data. The impact of the assumption that BAFs were lognormally distributed was examined by assigning normal (Gaussian) distributions to the variables and comparing the outputs. Normal distributions were fit to the $_{MD}BAF_3$ and $_{MD}BAF_4$ field data (Tables D-7 and D-10, respectively) by the method of moments. A comparison of the normal and lognormal distributions for each variable is given in Table D-11. BAF values for the percentiles at the empirical distribution extremes were also calculated for comparison to the actual observations. The normal distribution for $_{MD}BAF_4$ was similar to the lognormal; the primary difference was the slightly higher median for the distribution in normal form. The negative 5th percentile outcome for $_{MD}BAF_3$ illustrated a common problem when assigning normal distributions to variables that have a lower bound of zero; a truncated form of the distribution must be used to give meaningful results. Otherwise, the median and 95th percentile for the normal form of $_{MD}BAF_3$ were only slightly higher than for the lognormal form. The lognormal forms allow for slightly larger values in the upper tails of the distributions. The empirical extremes match the lognormal distributions slightly better than the normal forms.

Table D-17
Comparison of Lognormal and Normal (Directly Estimated) $_{MD}BAF$ Distributions

Percentile	$_{MD}BAF_3$		$_{MD}BAF_4$	
	lognormal ^a	normal ^b	lognormal ^c	normal ^d
5th	461,000	(-545,000)	3,260,000	2,100,000
12.5th ^e	667,000	205,000	4,070,000	3,670,000
50th	1,580,000	1,950,000	6,810,000	7,330,000
87.5th ^f	3,740,000	3,700,000	11,400,000	11,000,000
95th	5,410,000	4,450,000	14,200,000	12,600,000

^a GM = 1.58×10^6 , GSD = 2.115

^b mean = 1.95×10^6 , std. dev. = 1.517×10^6

^c GM = 6.81×10^6 , GSD = 1.564

^d mean = 7.33×10^6 , std. dev. = 3.181×10^6

^e $100 \times (1 - (n - 0.5)/n)$, n = 4

^f $100 \times (n - 0.5)/n$, n = 4

D.3.8 Selection of Bioaccumulation Factors for Trophic Levels 3 and 4

As all of the BAF distributions in this analysis dealt with estimates for a randomly-selected single water body, independent of any other water body, the central-tendency estimate was given as the median (equivalent to the geometric mean for lognormal distributions). That is, the median represents equal likelihood that the lake-specific BAF will be greater or less than the chosen value and is most appropriate when sampling only once from the distribution. The overall average (arithmetic mean) would be useful only in the case when fish were consumed equally by a receptor from all of the lakes in the analysis. That is, the mean value better reflects actual exposure when repeatedly sampling from the same distribution. If a similar analysis would be conducted for a narrowly-defined region, where fish consumption across several lakes would be a reasonable scenario, the average BAF across those water bodies would be more appropriate.

Bioaccumulation factors for trophic level 3 estimated using each of the two previously described methods are given in Table D-17. Bioaccumulation factors for trophic level 4 estimated using each of the five previously described methods are given in Table D-18. These factors are meant to be applied when appropriate local site data do not exist. **For a particular site of concern, BAFs derived from data collected at the site are preferred to the estimated values in Tables D-18 and D-19.** Median BAF estimates are within 20% irrespective of the method used. The similarity of the direct and GLWQI estimates is somewhat surprising, given the greater number of variables for the GLWQI approach and the relative independence of the data sets. The much greater variability of the results from the GLWQI approach than those from the direct BAF derivation, however, is expected. As an example, the GSD of 6.13 for the GLWQI $_{MD}BAF_4$ reflects a 17-fold greater variance than the GSD of 1.56 for the direct estimate of $_{MD}BAF_4$ from field data. The result is a 90% confidence interval for the GLWQI $_{MD}BAF_4$ that is 90 times wider than that for the direct estimate of $_{MD}BAF_4$. The $_{MD}BAF_4$ derived from $_{MD}BAF_3$ and PPF₄ estimates is also more variable, with a 90% confidence interval that is about three times wider than for the direct estimate of $_{MD}BAF_4$. A graphical representation of the $_{MD}BAF_4$ distributions for the direct

estimate and the two most divergent estimates is provided in Figure D-5. The vertical line represents the recommended value for ${}_{MD}BAF_4$.

Most of the data for estimating BAFs are from studies of northern oligotrophic water bodies. These freshwater systems are all similar, in that they are at risk due to acid deposition and that, by virtue of average temperature, etc., support similar fish assemblages (typically northern pike, walleye, yellow perch and spottail shiners). This has the potential to create two possible problems of interpretation.

- 1) Because data from such systems tend to look similar, it would be easy to overlook relationships that would be important under a different set of circumstances.
- 2) The relative abundance of these data introduce a regional bias into any type of analysis that is intended for nationwide application.

The one exception, Clear Lake, CA (Suchanek et al., 1993), however, provides ${}_{MD}BAF$ estimates for both trophic levels that are similar to the central tendency estimates for all lakes combined. Clear Lake is warm, highly eutrophic, and receives considerable agricultural runoff from nearby orchards and vineyards. Lacking any corroborating information, it is not possible to determine how representative the Clear Lake data are of warm water systems generally. Clearly, however, there is a need for additional residue data collected from a broader spectrum of freshwater systems.

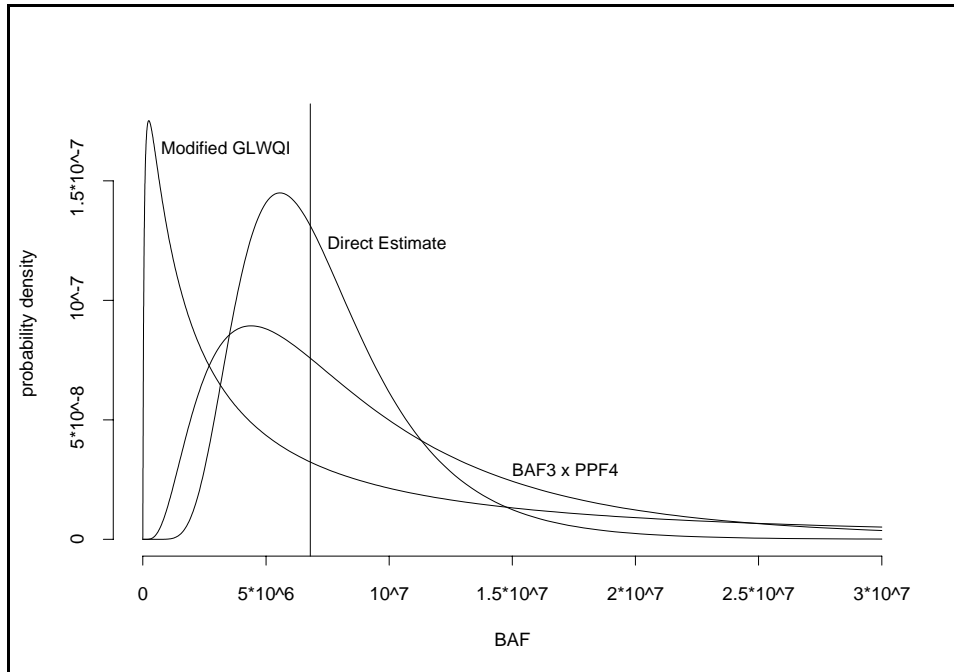
Table D-18
Summary of Methylmercury Bioaccumulation Factors for Trophic Level 3
(BAF values in units of L/kg)

Recommended Value	1,600,000	
Method	Direct Estimate	Modified GLWQI
5 th pctl	461,000	7,000
50 th pctl	1,580,000	1,320,000
95 th pctl	5,410,000	24,400,000
GSD	2.152	5.884

Table D-19
Summary of Methylmercury Bioaccumulation Factors for Trophic Level 4
(BAF values in units of L/kg)

Recommended Value	6,800,000				
Method	Direct Estimate	$\frac{TD BAF_4}{fmmw_F}$	$MD BAF_3 \times PPF_4$	$\frac{TD BAF_3 \times PPF_4}{fmmw_F}$	Modified GLWQI
5 th pctl	3,260,000	3,180,000	1,960,000	2,430,000	330,000
50 th pctl	6,810,000	6,370,000	7,820,000	7,700,000	6,520,000
95 th pctl	14,200,000	15,200,000	31,100,000	26,400,000	129,000,000
GSD	1.564	1.614	2.317	2.067	6.127

Figure D-5
 $MD BAF_4$ Distributions



As stated previously, BAFs derived from data collected at the site are preferred to the estimated values in Tables D-18 and D-19. Otherwise, given the large differences in the variances of the distributions, BAFs estimated by the direct method are preferred over BAFs calculated using the modified GLWQI methodology. The median $MD BAF$ values estimated using the direct approach are therefore recommended for subsequent calculation of a WC for methylmercury (Volume VI) and for an evaluation of human exposure due to consumption of contaminated fish (Volume IV). The recommended $MD BAF$ s for methylmercury are 1.6×10^6 L/kg for trophic level 3 and 6.8×10^6 L/kg for trophic level 4.

D.3.9 Discussion of Uncertainty and Variability in the BAF

The BAF distributions were designed to estimate an average concentration of methylmercury in fish of a given trophic level from an average concentration of dissolved methylmercury in the epilimnion for a (single) randomly-selected lake in the continental U.S. In the overall mercury fate and exposure model, the input (water concentrations) to this distribution represented an annual average, aggregating variability in methylmercury concentrations in the epilimnion over an entire year and the output (fish concentrations) represented the average methylmercury concentration in the diet of a specific receptor. Available data were inadequate to satisfy these representations fully. In most cases, water methylmercury concentrations incorporated limited or no cross-seasonal variability. Also, fish diets for specific receptors have not been determined. For this analysis a generic receptor was assumed and was approximated by including a large range of fish age or size classes whenever possible. Also, because of the general paucity of appropriate data, many studies on lakes in other countries were included in the analysis; biotic and abiotic processes in these lakes were assumed to be similar to lakes in the continental U.S. These limitations introduced additional uncertainty in the BAF output that was not quantified in this analysis.

Except as will be discussed, there were no distinctions in the BAF distributions as to size of fish, lake trophic status, lake pH, or relative methylmercury concentrations in the water column. The data, however, are heavily biased towards northern oligotrophic lakes and somewhat towards smaller (younger) fish. There was also no distinction made between variability and uncertainty in the BAF₃ and BAF₄ distributions; they are aggregated in the output. Thus, from this analysis, it cannot be determined where natural variability stops and uncertainty starts. The distributions do, however, provide a rough estimate of the total uncertainty in the aggregate processes and an idea of the precision (or lack thereof) of these types of estimates.

The large amount of variability evidenced by the data and reflected in the output distributions arises from several sources, which have not yet been quantified. A primary source of variability in both BAF₃ and PPF₄ is the dependence of methylmercury bioaccumulation on the age of the fish as discussed in Section D-3.2.2 (PPF₄). Reported BAF values for a given species will, therefore, vary as a function of the ages of the animals examined. As a result, some researchers have suggested that comparisons between lakes should be made using "standardized" fish values (i.e., a value for a hypothetical 1 kg northern pike), typically derived by linear regression of residue data collected from individuals of varying size and/or age (see discussion in Section D-3.2.2). The available data, however, are too limited to allow for this kind of analysis. The distributions derived in this appendix include both "standardized" comparisons and those based on "opportunity" (whatever you catch, you include).

Perhaps the greatest source of variability is that of model uncertainty, that is, uncertainty introduced by failure of the model to account for significant real-world processes. The simple linear BAF model relating methylmercury in fish to total mercury in water masks a number of nonlinear processes leading to the formation of bioavailable methylmercury in the water column. Much of the variability in field data applicable to the estimation of mercury BAFs can be attributed to differences between aquatic systems. As an example, in lake surveys conducted within a relatively restricted geographic region, large differences can exist between lakes with respect to mercury concentrations in a given species of fish (Cope et al., 1990; Grieb et al., 1990; Sorenson et al., 1990; Jackson, 1991; Lange et al., 1993). These observations have led to the suggestion that much of this variability is due to differences in within-lake processes that determine the percentage of total mercury that exists as the methylated form. Limited data also indicate that within a given water body concentrations of methylmercury are likely to vary with depth and season. Unfortunately, while the concentration of methylmercury in fish flesh is presumably a function of these varying concentrations, published BAFs

are generally estimated from a small number of measured water values, the representativeness of which is poorly known.

D.4 Other Variables Concerning the Form of Mercury in the Water Column

Two other variables are presented in this section that are not used in the calculation of mercury BAFs, but are referred to in other parts of Volume III. Those variables are 1) the fraction of dissolved total mercury in the hypolimnion that is methylmercury and 2) the fraction of total methylmercury in the water column that is dissolved.

D.4.1 Fraction of Methylmercury in the Hypolimnion

Mercury Speciation in the Hypolimnion

Variable: f_{mmw_H}
 Definition: Fraction of total dissolved mercury in the hypolimnion existing as the methylated species
 Point Estimate: 0.36 (unitless)
 Distribution: beta ($\alpha = 11.0$; $\beta = 19.6$)

The values defining the empirical distribution for f_{mmw_H} are given in Table D-20. The beta distribution was chosen as best representative of fractions. The distribution was fitted by the method of moments. The point estimate is the median of the resulting distribution.

Table D-20
Methylmercury as a Fraction of Total Dissolved Mercury in the Hypolimnion

Value	Location	Reference
0.27	Iso Valkjarvi, Finland	Rask and Verta, 1995
0.37	Palette L., WI	Bloom et al., 1991
0.44	Onondaga L., NY	Henry et al., 1995

D.4.2 Fraction of Dissolved Methylmercury in the Water Column

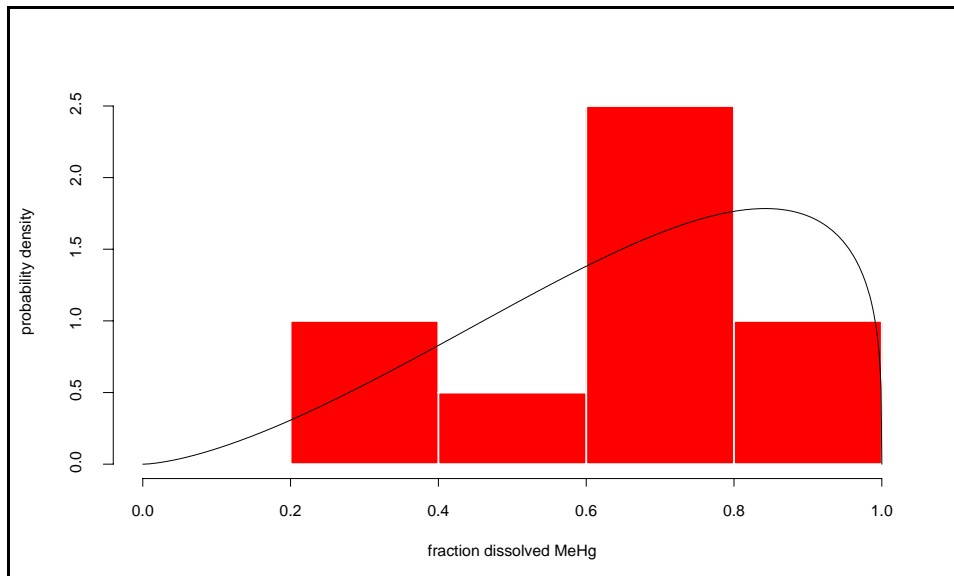
Variable: f_{dmw}
 Definition: Fraction of total methylmercury in the epilimnion that is dissolved
 Point Estimate: 0.69 (unitless)
 Distribution: beta ($\alpha = 2.55$; $\beta = 1.29$)

The values defining the empirical distribution for f_{dmw} are given in Table D-21. The beta distribution was chosen as best representative of fractions. The distribution was fitted by the method of moments. The point estimate is the median of the resulting distribution and is identical to the median of the empirical distribution. The empirical distribution and PDF for f_{dmw} is shown in Figure D-6

Table D-21
Dissolved Methylmercury as a Fraction of Total Methylmercury in the Epilimnion

Value	Location	Reference
0.303	Vandercook Lake, WI	Bloom et al., 1991
0.353	Onondaga Lake, NY	Henry et al., 1995
0.577	Palette Lake, WI	Bloom et al., 1991
0.60	Lake Hako, Finland	Verta and Matilainen, 1995
0.667	Little Rock Lake, WI	Bloom et al., 1991
0.72	Max Lake, WI	Bloom et al., 1991
0.762	Lake Michigan	Mason and Sullivan, 1997
0.79	Lake Iva, Finland	Verta and Matilainen, 1995
0.82	Lake Keha, Finland	Verta and Matilainen, 1995
1.02	Clear Lake, CA	Suchanek et al., 1993

Figure D-6
Distribution for fdmw



D.5 References

Aitchison, J. and J. A. C. Brown (1966). *The Lognormal Distribution*. University Press, Cambridge.

- Akagi, H., O. Malm, Y. Kinjo, M. Harada, F.J.P. Branches, W.C. Pfeiffer and H. Kato (1995). Methylmercury pollution in the Amazon, Brazil. *Sci. Total Environ.* 175:85-95.
- Becker, D. S. and G.N. Bigham (1995). Distribution of Mercury in the Aquatic Food Web of Onondaga Lake, New York. *Water Air Soil Pollu.* 80:563-571.
- Bloom, N.S. (1989). Determination of picogram levels of methylmercury by aqueous phase ethylation, followed by cryogenic gas chromatography with cold vapour atomic fluorescence detection. *Can. J. Fish. Aquat. Sci.* 46:1131-1140.
- Bloom, N.S. (1992). On the chemical form of mercury in edible fish and marine invertebrate tissue. *Can. J. Fish. Aquat. Sci.* 49:1010-1017.
- Bloom, N.S., C.J. Watras and J.P. Hurley (1991). Impact of Acidification on the methylmercury cycle of remote seepage lakes. *Water Air Soil Pollu.* 56:477-491.
- Bodaly, R.A., J.W.M. Rudd, R.J.P. Fudge and C.A. Kelly (1993). Mercury concentrations in fish related to size of remote Canadian Shield lakes. *Can. J. Fish. Aquat. Sci.* 50:980-987.
- Cope, W.G., J.G. Wiener and R.G. Rada (1990). Mercury accumulation in yellow perch in Wisconsin seepage lakes: Relation to lake characteristics. *Environ. Toxicol. Chem.* 9:931-940.
- Driscoll, C. T., V. Blette, C. Yan, C.L. Schofield, R. Munson and J. Holsapple (1995). The Role of Dissolved Organic Carbon in the Chemistry and Bioavailability of Mercury in Remote Adirondack Lakes. *Water Air Soil Pollu.* 80:499-508.
- Evans, M., N. Hastings and B. Peacock (1993). *Statistical Distributions*. 2nd Edition. John Wiley and Sons, Inc., New York, NY, pp. 42-44.
- Grieb, T.M., C.T. Driscoll, S.P. Gloss, C.L. Schofield, G.L. Bowie and D.B. Porcella (1990). Factors affecting mercury accumulation in fish in the upper Michigan peninsula. *Environ. Toxicol. Chem.* 9:919-930.
- Henry, E.A., L.J. Dodge-Murphy, G.N. Bigham and S.M. Klein (1995). Modeling the transport and fate of mercury in an urban lake (Onondaga Lake, NY). *Water Air Soil Pollu.* 80:489-498.
- Hill, W.R., A.J. Stewart and G.E. Napolitano (1996). Mercury Speciation and Bioaccumulation in Lotic Primary Producers and Primary Consumers. *Can. J. Fish. Aquat. Sci.* 53:812-819.
- Hoover, S.M., R.A. Hill and T.A. Watson (1997). Exposure of Aborigines in British Columbia to methylmercury in freshwater fish: a comparison to Reference Doses and estimated thresholds. *Hum. Ecol. Risk Assess.* 3:439-463.
- Hudson, R.J.M., S.A. Gherini, C.J. Watras and D.B. Porcella (1994). Modeling the biogeochemical cycle of mercury in lakes: the mercury cycling model (MCM) and its application to the MTL study lakes. In: *Mercury Pollution, Integration and Synthesis*. C.J. Watras and J.W. Huckabee (Eds.), Lewis Publishers, Boca Raton, FL, pp. 473-523.
- Jackson, T.A. (1991). Biological and environmental control of mercury accumulation by fish in lakes and reservoirs of northern Manitoba, Canada. *Can. J. Fish. Aquat. Sci.* 48:2449-2470.

- Kim, J.P. (1995). Methylmercury in rainbow trout (*Oncorhynchus mykiss*) from Lakes Okareka, Okaro, Rotmahana, Rotorua and Tarawera, North Island, New Zealand. *Sci. Total Environ.* 164:209-219.
- Lange, T.R., H.E. Royals and L.L. Connor (1993). Influence of water chemistry on mercury concentration in largemouth bass from Florida lakes. *Trans. Am. Fish. Soc.* 122:74-84.
- Lange, T.R., H.E. Royals and L.L. Connor (1994). Mercury accumulation in largemouth bass (*Micropterus salmoides*) in a Florida lake. *Arch. Environ. Contam. Toxicol.* 27:466-471.
- Lasorsa, B. and S. Allen-Gil (1995). The methylmercury to total mercury ratio in selected marine, freshwater, and terrestrial organisms. *Water Air Soil Pollu.* 80:905-913.
- Lindqvist, O. (1991). Mercury in forest lake ecosystems - Bioavailability, bioaccumulation and biomagnification. *Water Air Soil Pollu.* 55:131-157.
- MacCrimmon, H.R., C.D. Wren and B.L. Gots (1983). Mercury uptake by lake trout, *Salvelinus namaycush*, relative to age, growth, and diet in Tadenac Lake with comparative data from other precambrian shield lakes. *Can. J. Fish. Aquat. Sci.* 40:114-120.
- Malm, O., F.J.P. Branches, H. Akagi, M.B. Castro, W.C. Pfeiffer, M. Harada and W.R. Bastos (1995). Mercury and methylmercury in fish and human hair from the Tapajos River Basin, Brazil. *Sci. Total Environ.* 175:141-150.
- Mason, R.P. and K.A. Sullivan (1997). Mercury in Lake Michigan. *Environ. Sci. Technol.* 31:942-947.
- Mathers, R.A. and P.H. Johansen (1985). The effects of feeding ecology on mercury accumulation in walleye (*Stizostedion vitreum*) and pike (*Esox lucius*) in Lake Simcoe. *Can. J. Zool.* 63:2006-2012.
- Meili, M., A. Iverfeldt and L. Hakanson (1991). Mercury in the surface water of Swedish forest lakes - Concentrations, speciation, and controlling factors. *Water Air Soil Pollu.* 56:439-453.
- Monteiro, L.R., E.J. Isidro and H.D. Lopes (1991). Mercury content in relation to sex, size, age and growth in two scorpionfish (*Helicolenus dactylopterus*) and (*Pontinus kuhlii*) from Azorean waters. *Water Air Soil Pollu.* 56:359-367.
- Monteiro, L.R., V. Costa, R.W. Furness and R.S. Santos (1996). Mercury concentrations in prey fish indicate enhanced bioaccumulation in mesopelagic environments. *Mar. Ecol. Prog. Ser.* 141:21-25.
- Morgan, M.G. and M. Henrion (1990). *Uncertainty*. Cambridge University Press, Cambridge, England.
- Plourde, Y., M. Lucotte and P. Pichet (1997). Contribution of suspended particulate matter and zooplankton to MeHg contamination of the food chain in midnorthern Quebec (Canada). *Can. J. Fish. Aquat. Sci.* 54:821-831.
- Porvari, P. (1995). Mercury levels of fish in Tucuruí hydroelectric reservoir and in River Mojú in Amazonia, in the state of Pará, Brazil. *Sci. Total Environ.* 175:109-117.
- Rask, M. and M. Verta (1995). Concentrations and Amounts of Methylmercury in Water and Fish in the Limed and Acid Basins of a Small Lake. *Water Air Soil Pollu.* 80:577-580.

Skurdal, J., T. Qvenild and O.K. Skogheim (1985). Mercury accumulation in five species of freshwater fish in Lake Tyrifjorden, southeast Norway, with emphasis on their suitability as test organisms. *Environ. Biol. Fish.* 14:233-237.

Suchanek, T.H., P.J. Richerson, L.A. Woodward, D.G. Slotton, L.J. Holts and C.E.E. Woodmansee (1993). A survey and evaluation of mercury. In: Sediment, water, plankton, periphyton, benthic invertebrates and fishes within the aquatic ecosystem of Clear Lake, California. Preliminary lake study report prepared for the U.S. Environmental Protection Agency, Region 9, Superfund Program.

U.S. Environmental Protection Agency (1993). Water Quality Guidance for the Great Lakes System and Correction; Proposed Rules. *Fed. Regist.* 58(72):20802-21047 (April 16, 1993).

U.S. Environmental Protection Agency (1994). Great Lakes Water Quality Initiative Technical Support Document for the Procedure to Determine Bioaccumulation Factors - July 1994. EPA-822-R-94-002. U.S. EPA, Office of Science and Technology, Washington, D.C.

Verta, M. and T. Matilainen (1995). Methylmercury distribution and partitioning in stratified Finnish forest lakes. *Water Air Soil Pollu.* 80:585-588.

Watras, C.J. and N.S. Bloom (1992). Mercury and methylmercury in individual zooplankton: Implications for bioaccumulation. *Limnol. Oceanogr.* 37:1313-1318.

Watras, C.J., K.A. Morrison, J.S. Host, N.S. Bloom (1995a). Concentration of mercury species in relationship to other site-specific factors in the surface waters of northern Wisconsin lakes. *Limnol. Oceanogr.* 40:556-565

Watras, C.J., K.A. Morrison, J.S. Host, N.S. Bloom (1995b). Chemical correlates of Hg and methyl-Hg in northern Wisconsin lake waters under ice-cover. *Water Air Soil Pollu.* 84:253-267.

Wilk, M.B. and R. Gnanadesikan (1968). Probability plotting methods for the analysis of data. *Biometrika* 55:1-17.

Wren, C.D. and H.R. MacCrimmon (1986). Comparative bioaccumulation of mercury in two adjacent freshwater ecosystems. *Nat. Resour.* 20:763-769.

Wren, C.D., H.R. MacCrimmon and B.R. Loescher (1983). Examination of bioaccumulation and biomagnification of metals in a precambrian shield lake. *Water Air Soil Pollu.* 19:277-291.